National Research
Council Canada

Conseil national
de recherches Canada

NRC · CNRC

Canadian Journal of Fisheries and Aquatic Sciences

Journal canadien des sciences halieutiques et aquatiques

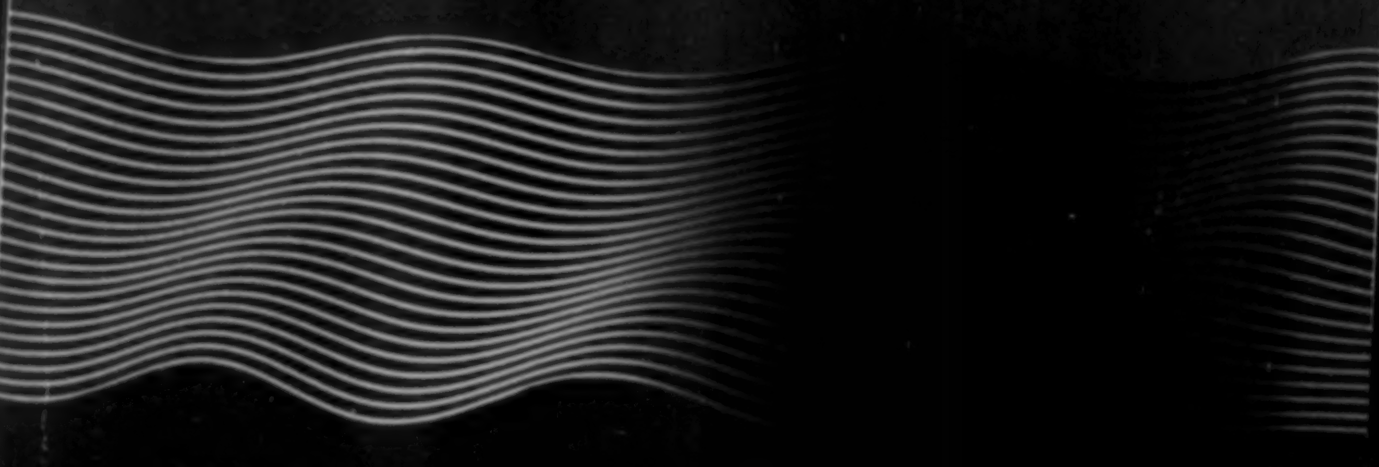

http://cjfas.nrc.ca

http://jcsha.cnrc.ca

ISSN 0706-652X / CJFSDX 61(10) 1807–2023 (2004)

The *Canadian Journal of Fisheries and Aquatic Sciences*, previously published as *Contributions to Canadian Biology* 1901–1925, *Contributions to Canadian Biology and Fisheries* 1926–1934, *Journal of the Biological Board of Canada* 1934–1937, and *Journal of the Fisheries Research Board of Canada* 1938–1979, is issued monthly to form annual volumes of 12 numbers plus supplements.

Editorial policy. The Journal publishes original research articles, perspectives (syntheses, critiques, re-evaluations), discussions (comment and reply), and rapid communications. Manuscripts may concern cells, organisms, populations, communities, ecosystems, or processes that affect aquatic systems. They may cover a range of disciplines including biology and ecology of marine and freshwater organisms, limnology, oceanography, physiology, toxicology, genetics, economics, disease, and management. Preference will be given to manuscripts that emphasize understanding of observed phenomena and interpretation of experimental results. The Journal encourages papers that lead from clearly stated purpose or rationale and from testable hypotheses, concepts, or questions to identifiable conclusions or syntheses. Such papers may amplify, modify, question, or redirect accumulated knowledge embodied in contemporary perceptions of a particular state of aquatic sciences. The Journal discourages papers that are essentially descriptive, except in emerging disciplines; have only site-specific or local applications (a certain year, place, taxon, chemical compound, etc.); only confirm previously established principles; or apply standard techniques without breaking new methodological ground.

Manuscripts for publication should be submitted to the Senior Editor, *Canadian Journal of Fisheries and Aquatic Sciences*, Department of Organismal Biology, Ecology and Evolution, University of Guelph, Guelph, ON N1G 2W1, Canada (519-824-4120 ext. 52646; fax: 519-767-9798; e-mail: cjfas@uoguelph.ca).

Submissions in either English or French are acceptable. The information must be original, that is, not copyrighted, published, or submitted elsewhere except in abstract form or unless by written consent of the Editor.

Correspondence concerning accepted manuscripts and corrected proofs should be sent to NRC Research Press, National Research Council of Canada, Ottawa, ON K1A 0R6, Canada (fax: 613-952-7656; e-mail: pubs@nrc-cnrc.gc.ca).

Instructions to Authors are published once a year in the first issue of each volume. Copies are available from NRC Research Press or at http://cjfas.nrc.ca. The **Publication Policy** of NRC Research Press is available at http://pubs.nrc-cnrc.gc.ca.

Microfilm. Issues from 1934 through the current volume can be purchased on 16- or 35-mm microfilm. Photocopies of individual articles or issues can be purchased from University Microfilms International, 330 North Zeeb Road, Ann Arbor, MI 48106, USA.

US periodical postage paid at Champlain, NY 12919, USA, and at additional mailing offices. Attention U.S. POSTMASTER: Send address changes to **Canadian Journal of Fisheries and Aquatic Sciences**, c/o USACAN Media Distribution Center, P.O. Box 2888, Plattsburgh, NY 12901, USA.

Publié sans interruption depuis 1901, le *Journal canadien des sciences halieutiques et aquatiques* a paru sous plusieurs titres : *Contributions to Canadian Biology* 1901–1925, *Contributions to Canadian Biology and Fisheries* 1926–1934, *Journal of the Biological Board of Canada* 1934–1937, et *Journal of the Fisheries Research Board of Canada* 1938–1979. Le Journal paraît tous les mois, formant ainsi un volume de 12 numéros, et offre en plus jusqu'à deux suppléments par année.

Politique éditoriale. On publie, dans le Journal, des articles rendant compte de recherche originale, des perspectives (synthèses, critiques et réévaluations), des discussions (commentaires et réponses) et des communications rapides. Les documents peuvent porter sur les cellules, organismes, populations, communautés, écosystèmes ou processus qui affectent les systèmes aquatiques. Ils peuvent relever de divers domaines y compris la biologie et l'écologie des organismes marins et d'eau douce, la limnologie, l'océanographie, la physiologie, la toxicologie, la génétique, l'économie, la pathologie et la gestion. On accorde la préséance aux articles qui contribuent à la compréhension de phénomènes observés et à l'interprétation de résultats expérimentaux. On invite les auteurs à soumettre des articles ayant des objectifs précis ou relevant d'hypothèses, de concepts ou de questions vérifiables et se terminant par de solides conclusions ou d'utiles synthèses. Ces articles enrichissent, changent, mettent en question ou réorientent les connaissances acquises sur divers aspects des sciences aquatiques. On décourage toutefois la soumission d'articles simplement descriptifs (à moins qu'il ne s'agisse de nouvelles disciplines), d'application très limitée (applicables à une seule année, une seule région ou un seul taxon, portant sur un unique composé chimique, etc.); d'articles qui ne font que reprendre les principes énoncés dans des articles précédents; et d'articles rendant compte de l'application de normes sans gain de méthodologie.

Les auteurs voudront adresser leurs **manuscrits** à la directrice scientifique principale, *Journal canadien des sciences halieutiques et aquatiques*, Department of Organismal Biology, Ecology and Evolution, University of Guelph, Guelph, ON N1G 2W1, Canada (519-824-4120 poste 52646; télécopieur : 519-767-9798; courriel : cjfas@uoguelph.ca).

Les contributions peuvent être en anglais ou en français. Elles doivent être originales, c.-à.-d. qu'elles ne doivent pas avoir fait l'objet d'un copyright, avoir été publiées ou soumises ailleurs, sauf sous forme abrégée ou avec le consentement du rédacteur. Le CNRC ne se tient en aucune façon responsable des opinions exprimées par un collaborateur ou des déclarations qui pourrait faire ce dernier.

La correspondance ayant trait aux manuscrits acceptés et les **épreuves corrigés** doivent être envoyées aux Presses scientifiques du CNRC, Conseil national de recherches du Canada, Ottawa, ON K1A 0R6, Canada (télécopieur : 613-952-7656; courriel : pubs@nrc-cnrc.gc.ca).

Les Recommandations aux auteurs sont publiées une fois par année dans le premier numéro de chaque volume. Des copies sont disponibles auprès du Bureau de la rédaction aux Presses scientifiques du CNRC ou au http://jcsha.cnrc.ca. **La Politique de publication** est disponible auprès des Presses scientifiques du CNRC ou au http://pubs.nrc-cnrc.gc.ca.

Microfilms. On peut acheter sur microfilms de 16 ou 35 mm tous les numéros depuis 1934. Des photocopies d'articles ou de numéros individuels sont aussi en vente auprès de University Microfilms International, 330 North Zeeb Road, Ann Arbor, MI 48106, É.-U.

This Journal is indexed or abstracted in / Cette revue est signalée ou résumée dans
ABSEARCH, Applied Science and Technology Index and Abstracts, Aquatic Sciences and Fisheries Abstracts, Biological Abstracts, Biological and Agricultural Abstracts, CAB Abstracts, Chemical Abstracts, Current Contents, Elsevier BIOBASE, Environmental Abstracts, ETDE Energy Database, General Science Index and Abstracts, GEOBASE, GeoRef, Life Sciences Collection, Meteorological and Geoastrophysical Abstracts, Oceanic Abstracts, PASCAL Database, and Science Citation Index.

Volume 61, Number 10, October 2004

Canadian Journal of Fisheries and Aquatic Sciences

Published by the National Research Council of Canada

Volume 61, numéro 10, octobre 2004

Journal canadien des sciences halieutiques et aquatiques

Publié par le Conseil national de recherches du Canada

Senior Editor / Directrice scientifique principale Moira M. Ferguson

Editors / Directeurs

Jeffrey A. Hutchings, *Dalhousie University, Halifax*
Pierre Pepin, *Northwest Atlantic Fisheries Centre, DFO/MPO, St. John's, Newfoundland*
W. Gary Sprules, *University of Toronto at Mississauga*
Assistant to the Editors / Adjointe aux directeurs scientifiques **Holly Foster**

Associate Editors / Directeurs scientifiques associés

D. Boisclair, *Université de Montréal*
U. Borgmann, *Environment Canada, Burlington*
M.J. Bradford, *DFO/MPO and Simon Fraser University*
S.E. Campana, *DFO/MPO, Dartmouth*
R. Carignan, *Université de Montréal*
J.J. Dodson, *Université Laval*
G.T. Evans, *DFO/MPO, St. John's, Newfoundland*
K.T. Frank, *DFO/MPO, Dartmouth*
J.W.A. Grant, *Concordia University*
M.M. Hansen, *Danish Institute for Fisheries Research, Silkeborg, Denmark*
R. Hilborn, *University of Washington*
A. Hontela, *Université du Québec à Montréal*
D.F. Houlihan, *University of Aberdeen*
F.A. Huntingford, *University of Glasgow*
G.S. Jamieson, *DFO/MPO, Nanaimo*
J.M. Jech, *NFSC/NOAA, Woods Hole, Mass.*
B. Jonsson, *Norwegian Institute for Nature Research, Oslo, Norway*
D.L. MacLatchy, *University of New Brunswick, Saint John*
P. Magnan, *Université du Québec à Trois Rivières*
C.T. Marshall, *University of Aberdeen*
R.B. Millar, *University of Auckland, New Zealand*
W.P. Patterson, *University of Saskatchewan*
Y.T. Prairie, *Université du Québec à Montréal*
T.J. Quinn II, *University of Alaska–Fairbanks, Juneau, Alaska*
T.P. Quinn, *University of Washington*
C.W. Ramcharan, *Laurentian University*
R.D. Roberts, *Environment Canada, Saskatoon*
B. Sainte-Marie, *DFO/MPO, Mont-Joli*
D.W. Schindler, *University of Alberta*
R.E.H. Smith, *University of Waterloo*
S.J. Smith, *DFO/MPO, Dartmouth*
W.F. Vincent, *Université Laval*
R.D. Vinebrooke, *University of Alberta*
C.J. Walters, *University of British Columbia*
R.D. Ward, *CSIRO Marine Research, Australia*
B. de Young, *Memorial University of Newfoundland*

NRC Research Press / Presses scientifiques du CNRC

Editor-in-Chief / Directeur scientifique en chef **Bruce P. Dancik**
Assistant Editor-in-Chief / Adjoint au directeur scientifique en chef **Iain E.P. Taylor**

Journals Program / Programme des revues

Fax / Télécopieur : 613-952-7656; e-mail / courriel : pubs@nrc-cnrc.gc.ca; URL / URL : pubs.nrc-cnrc.gc.ca
Director / Directeur **Cameron D. Macdonald**
Acting Business Manager / Gestionnaire des affaires par intérim **Mike Boroczki**
Manager, Journals Program / Gestionnaire, Programme des revues **Carolyn Brown**
Managing Editor / Rédactrice administrative **Cecily M. Pearson** (613-993-9099)
Publication Officers / Agents de publication **Jennifer McColl, Thad Costigan**
Advertising and reprints / Annonces publicitaires et tirés à part **Roxanne Landriault** (613-990-2254)
Subscriptions / Abonnements **Eileen Evans-Nantais** (613-990-7873)

The National Research Council of Canada accepts no responsibility for statements or opinions expressed by a contributor. Acceptance of an advertisement, announcement, or other material does not imply endorsement by either the Journal's Senior Editor or the National Research Council.

© National Research Council of Canada 2004. All rights reserved.

No part of this publication may be reproduced, stored, or transmitted in any form or by any means, without the written permission of the publisher, except as stated below.

The National Research Council of Canada grants **permission*** to individuals to make single copies of articles for personal use. Any person may reproduce short excerpts from articles in the journal for any purpose that respects the moral rights of authors, provided that the source is fully acknowledged. As a courtesy, the consent of authors of such material should be obtained directly from the author.

Authorization to reproduce items for other than personal use, as stated above, is granted by the National Research Council of Canada provided that the copyright fee of $7.00 per copy is paid directly to CANCOPY, One Yonge Street, Suite 1900, Toronto, ON M5E 1E5, Canada.

*The above permission does not extend to other kinds of copying, such as copying for general distribution, for advertising, or promotional purposes, for creating new collective works, or for resale. For such copying, arrangements must be made with the publisher, National Research Council of Canada, Ottawa, ON K1A 0R6, Canada.

Subscription information

The *Canadian Journal of Fisheries and Aquatic Sciences* (ISSN 0706-652X) is published monthly by the National Research Council of Canada. The 2005 annual subscription rates (second class postage) for Canada are $892CAN institutional and $276CAN personal, for US & foreign $892US institutional and $276US personal. For air mail add $175US to foreign rate. Canadian customers please include 7% GST (business no. 12149 1807 RT 0275). Subscriptions are entered for the calendar year. Remittances should be made payable to the Receiver General for Canada, credit NRC. Price for regular single issues: institutional, $110.00; personal, $35.00. Supplements will be priced separately. Special rates apply to members of Canadian scientific and engineering societies if they subscribe through their respective societies.

There are no refunds on cancelled subscriptions once delivery has begun. Claims for missing issues should be made within four months (N. America) or six months (outside N. America) following the date of publication. The publisher expects to supply missing issues only when losses have occurred in transit and when the reserve stock will permit. For change of address and subscription enquiries: Subscription Office, NRC Research Press, National Research Council of Canada, Ottawa, ON K1A 0R6, Canada; tel.: 613-993-9084; fax: 613-952-7656; e-mail: pubs@nrc-cnrc.gc.ca.

Microform backfiles are available from UMI, P.O. Box 1346, Ann Arbor, MI 48106-1346, USA, and Micromedia Ltd., 20 Victoria St., Toronto, ON M5C 2N8, Canada.

All issues of the *Canadian Journal of Fisheries and Aquatic Sciences* since 1996 are available on the Web. Pricing information can be found at http://pubs.nrc-cnrc.gc.ca.

Le Conseil national de recherches du Canada ne se tient en aucune façon responsable des opinions exprimées par un collaborateur ou des déclarations que pourrait faire ce dernier. La publication d'annonces publicitaires, d'avis et autres n'implique pas l'endossement de leur contenu par la directrice principale de la Revue ou le CNRC.

© Conseil national de recherches du Canada 2004. Tous droits réservés.

Il est interdit de reproduire, de sauvegarder ou de transmettre quelque partie de la présente publication dans quelque format ou de quelque façon sans le consentement écrit de l'éditeur, à l'exception des conditions suivantes.

Le Conseil national de recherches du Canada accorde aux particuliers le droit de faire des copies individuelles pour leur usage personnel. Toute personne peut reproduire de courts extraits des articles de la Revue pour autant que les droits moraux de l'auteur soient respectés et que la mention de provenance soit clairement indiquée. Il est de convenance de demander le consentement de l'auteur avant de faire mention de son travail.

On obtiendra l'autorisation de reproduire des articles à d'autres fins que l'usage personnel (tel qu'on l'a décrit ci-dessus) auprès du Conseil national de recherches du Canada pour autant que des redevances de droits d'auteurs de 7,00 $/copie soient versées au CANCOPY, 1, rue Yonge, bureau 1900, Toronto, ON M5E 1E5, Canada.

*La permission ci-dessus ne s'applique pas à la reproduction à grande échelle, telle que la reproduction aux fins de distribution générale, publicitaire ou promotionnelle, de compilation de nouveaux ouvrages collectifs ou de revente. Dans de tels cas, il faudra ratifier une entente particulière avec l'éditeur, le Conseil national de recherches du Canada, Ottawa, ON K1A 0R6, Canada.

Renseignements sur l'abonnement

Journal canadien des sciences halieutiques et aquatiques (ISSN 0706-652X) est une publication mensuelle du Conseil national de recherches du Canada. Le prix de l'abonnement annuel en 2005 au Canada (courrier de deuxième classe) est de 892 $CAN pour les organismes et de 276 $CAN pour les particuliers. À l'étranger (y compris les É.-U.), le prix de l'abonnement est de 892 $US pour les organismes et de 276 $US pour les particuliers. L'expédition par avion exige des frais de 175 $US en sus du prix d'abonnement à l'étranger. Les clients du Canada doivent ajouter la TPS de 7 % (numéro d'entreprise 12149 1807 RT 0275). Les abonnements sont pour l'année civile. Tout paiement doit être adressé au Receveur général du Canada, crédit du CNRC. Le prix par numéro est de 110 $ pour les organismes et de 35 $ pour les particuliers. Le prix des hors-série varie. Les membres des sociétés canadiennes de sciences et de génie bénéficient de taux préférentiels en s'abonnant via leurs sociétés respectives.

Aucun remboursement ne sera accordé ni aucune annulation acceptée une fois que les livraisons auront commencé. Les réclamations de numéros manquants devront être soumises dans les quatre mois (Amérique du Nord) ou dans les six mois (à l'extérieur de l'Amérique du Nord) suivant la date de publication. L'éditeur ne fournira de numéros manquants que si le document a été perdu pendant l'expédition et que si le stock le permet. Adressez tout changement d'adresse ou toute question quant à l'abonnement au : Bureau des abonnements, Presses scientifiques du CNRC, Conseil national de recherches Canada, Ottawa, ON K1A 0R6, Canada; téléphone : 613-993-9084; télécopieur : 613-952-7656; courriel : pubs@nrc-cnrc.gc.ca.

On peut obtenir les fichiers rétrospectifs sur **microforme** auprès de UMI, P.O. Box 1346, Ann Arbor, MI 48106-1346, É.-U., et auprès de Micromedia Ltée, 20, rue Victoria, Toronto, ON M5C 2N8, Canada.

À partir de 1996, tous les numéros de *Journal canadien des sciences halieutiques et aquatiques* sont accessibles sur le Web. On trouvera des renseignements sur les tarifs à http://pubs.nrc-cnrc.gc.ca.

A fossil record of colonization and response of lacustrine fish populations to climate change

Michael G. Newbrey and Allan C. Ashworth

Abstract: To study fish species colonization and the response of populations to climate change, we reexamined a well-preserved late Pleistocene to early Holocene fossil fish assemblage from lake deposits on the Missouri Coteau, North Dakota. The fossil fishes in the assemblage include complete specimens of yellow perch (*Perca flavescens*), brassy minnow (*Hybognathus hankinsoni*), blacknose shiner (*Notropis heterolepis*), banded killifish (*Fundulus diaphanus*), and brook stickleback (*Culaea inconstans*). The sequence of colonization is explained by individual thermal and relative water velocity tolerances for each species. There are six peaks in fish abundance during approximately 1000 years, indicating a response to environmental perturbations. Charcoal deposition from fires is inferred to represent episodic droughts during which nutrient levels were reduced and fish abundance declined. The fluctuations follow an overall trend of increased fish abundance during a time when lake-marginal vegetation changed from a spruce to a deciduous forest in response to climatic warming. This study provides insight into the complex effects of a changing climate on fish populations and demonstrates the potential of using fossils to examine the long-term abundance patterns of contemporary fish species.

Résumé : Nous avons examiné à nouveau une collection de poissons fossiles bien conservés datant de la fin du Pléistocène au début de l'Holocène et provenant de dépôts lacustres sur le coteau Missouri au Dakota du Nord afin d'étudier la colonization des espèces de poissons et la réaction des populations au changement climatique. Les poissons fossiles dans la collection comprennent des spécimens entiers de perchaudes (*Perca flavescens*), de ménés laiton (*Hybognathus hankinsoni*), de museaux noirs (*Notropis heterolepis*), de fondules barrés (*Fundulus diaphanus*) et d'épinoches à cinq épines (*Culaea inconstans*). La séquence de la colonization s'explique par les tolérances individuelles des espèces à la température et à la vitesse relative du courant. Il y a six maximums d'abondance des poissons sur une période d'environ 1000 ans qui correspondent à des réactions à des perturbations de l'environnement. Les dépôts de charbon de bois provenant de feux représentent, dans notre interprétation, des périodes de sécheresse répétées durant lesquelles les concentrations de nutriments et l'abondance des poissons diminuent. Les fluctuations suivent une tendance générale d'accroissement de l'abondance des poissons au moment où la végétation des rives lacustres a changé d'une forêt d'épinettes à une forêt décidue en réaction au réchauffement du climat. Notre étude fournit une perspective sur les effets complexes d'un climat changeant sur les populations de poissons et démontre le potentiel de l'étude des fossiles pour déterminer les patterns d'abondance de répartition à grande échelle des espèces contemporaines de poissons.

[Traduit par la Rédaction]

Introduction

We reexamined fossils and data from an exceptionally well-preserved late Pleistocene to early Holocene (i.e., 11 000 years ago) fish assemblage located on the Missouri Coteau, North Dakota. The fishes include blacknose shiner (*Notropis heterolepis*) (Cyprinidae), brassy minnow (*Hybognathus hankinsoni*) (Cyprinidae), banded killifish (*Fundulus diaphanous*) (Fundulidae), yellow perch (*Perca flavescens*) (Percidae), and brook stickleback (*Culaea inconstans*) (Gasterosteidae) (Bickley 1970; Cvancara et al. 1971). These species are also extant in North Dakota today (Power and Rychman 1998).

In this study we explore the relationships among species colonization and fish population responses to climate change using fire frequency, gastropod abundance, and plant pollen from a record that is approximately 1000 years in length. Our objectives are to examine the order of colonization of fishes with regard to life-history characteristics; describe the changes in fish abundance associated with charcoal deposition; describe fish abundance with a proxy for lacustrine nutrients that increase during a shift in terrestrial vegetation (i.e., climate change); and show that the proxy for lacustrine nutrients varies with the relative abundance of charcoal.

This fossil record permits us to examine freshwater-fishery data and its effects of climate change on fish populations.

Received 19 March 2004. Accepted 22 June 2004. Published on the NRC Research Press Web site at http://cjfas.nrc.ca on 4 December 2004.
J18028

Michael G. Newbrey.[1] Department of Biological Sciences, North Dakota State University, Fargo, ND 58105-5517, USA.
Allan C. Ashworth. Department of Geosciences, North Dakota State University, Fargo, ND 58105-5517, USA.

[1] Corresponding author (e-mail: michael.newbrey@ndsu.nodak.edu).

Can. J. Fish. Aquat. Sci. **61**: 1807–1816 (2004)

doi: 10.1139/F04-113

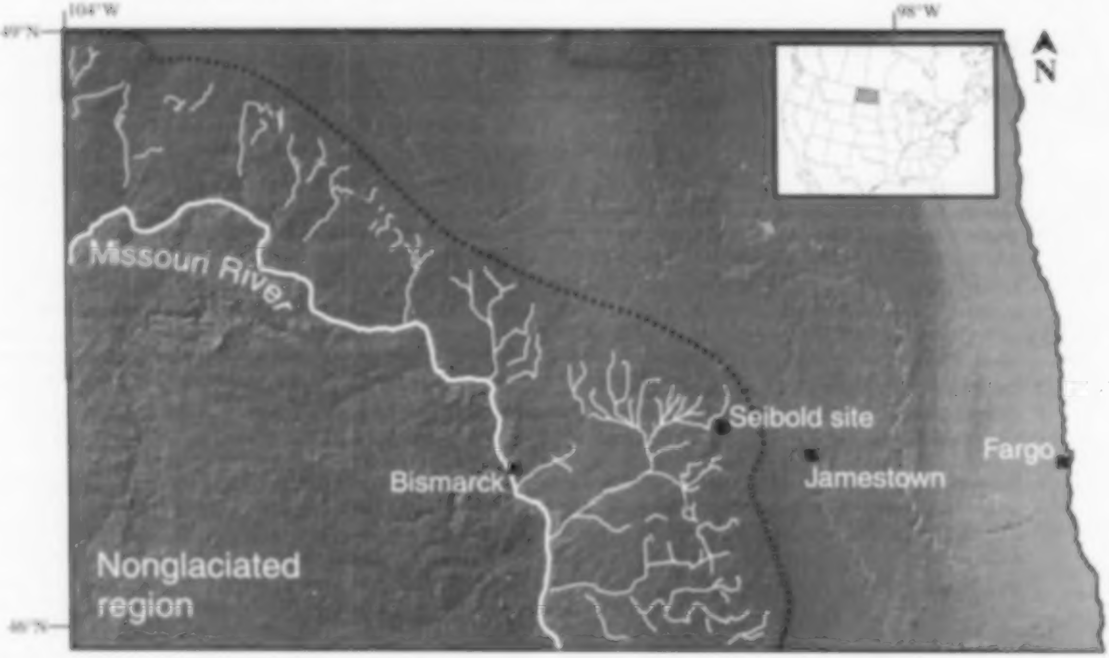

Fig. 1. Ancient tributaries (i.e., fine white lines) of the late Pleistocene to early Holocene Missouri River are based on the distribution of sand and gravel deposits mapped by Clayton et al. (1980). The black dotted line indicates the eastern edge of the Missouri Coteau. All of North Dakota except the southwest was glaciated (the location of North Dakota in the USA is shown in the inset map). The shaded relief map is modified from Sterner (1995).

These data allow us to effectively detect the response of fish to climate change because there are no confounding effects of anthropogenic harvest and other impacts such as are found in contemporary fish populations. Also the data permit us to describe ecological processes occurring on longer time scales than is possible from studies of living fish.

Materials and methods

Study site

The Seibold site (47.02°N, 99.18°W) is an ephemeral wetland on the Missouri Coteau, near Buchanan, North Dakota (Fig. 1). Cvancara et al. (1971) and Ashworth and Brophy (1972) described the geological and paleolimnological setting of the deposit. The site represents a small basin (100 m in diameter) that was probably part of larger lake complex which formed on an ice-cored moraine at the end of the late Wisconsinan glaciation.

The site has excellent preservation of terrestrial and aquatic plants and animals, which permits taxonomic assignments of many fossils to species. Near the base of the deposit is a continuous sequence of lacustrine sediments containing complete fish skeletons. The fossils come from a sedimentary unit composed of brown to green organic mud overlain by calcareous mud. Bickley (1970) referred to the deposit as the fish-bearing unit. A pollen profile from the fish-bearing unit indicated that the lake was initially surrounded by spruce, which was later replaced by a mixed assemblage of deciduous trees, shrubs, herbs, and grasses (Cvancara et al. 1971). The radiocarbon age of the decline of spruce pollen is 9750 ± 140 [I–4537] radiocarbon years before present. Converted to calendar years, this represents an age of 11 065 calendar years before present (BP) (CALIB 4.4; Stuiver and Reimer 1993; Stuiver et al. 1998*a*, 1998*b*). The age of decline of spruce pollen (Cvancara et al. 1971) is consistent with the age of decline of spruce pollen at Moon Lake 130 km southeast of the Seibold site (Laird et al. 1996; Grimm 2001) and at Spiritwood Lake 46 km east of the Seibold site (McAndrews 1970). The span of time represented by the fish-bearing unit is uncertain. However, based on comparison with the Moon Lake pollen record, the fish-bearing unit probably represents about 1000 years of deposition, from approximately 11 500 to 10 500 calendar years BP.

Paleoecological context

To understand the ecological patterns of the Seibold fish assemblage, information about the origin of the lake and its climatic history is briefly discussed. The Missouri Coteau is a broad band of low morainic hills that stretches from Saskatchewan to South Dakota (Clayton et al. 1980). The moraines, representing a complex of active and stagnant ice features, were deposited at the end of the Wisconsinan ice age. Large volumes of ice remained buried in the till and outwash deposits into the late Quaternary (Clayton 1967). The stagnant ice terrain had greater topographic relief than the morainic hills today (Clayton and Cherry 1967). The melting of buried ice formed kettle lake basins and also provided meltwater for the rivers. Soils formed on the adjacent

Table 1. Limiting environmental factors for the species recovered as fossils from the Seibold site.

	Sequence of colonization (observed)	Maximum water velocity		Northerly extent of geographic range		Minimum spawning water temperature	
		Flow rate	Citation	Latitude (°N)	MAT_{air} (°C)	°C	Citation
Yellow perch	1	Moderate	Otto and Rice 1974	62	–5.2	6.7	Weber 1975
Brassy minnow	1	Moderate	Becker 1983; Copes 1975	55	–0.3	10.0	Dobie et al. 1956
Blacknose shiner	2	Slow–moderate	Becker 1983	55	–3.5	?	—
Brook stickleback	3	Slow	Becker 1983	68	–9.5	4.5	Carlander 1969
Banded killifish	3	Slow	Becker 1983	49	2.0	21.0	Richardson 1939

Note: Fishes are arranged in chronological order of colonization, with yellow perch and brassy minnow found in the oldest sediments. Northern latitude represents the northerly extent of the range of each species. The mean annual air temperature (MAT_{air}) is from the northerly range of the species. The minimum spawning water temperature is the lowest spawning temperature noted in the literature.

ice-cored moraines and were colonized by vegetation, similar to those of the Klutlan Glacier in the Yukon Territory, Canada, today (Birks 1980).

The vegetation of the Missouri Coteau, based on pollen studies, changed around 11 000 calendar years BP from open spruce forest to a mosaic of deciduous woodland and prairie uplands (Grimm 2001). The short- to medium-grass prairie surrounding the Seibold wetland today is very different from forested habitats, which colonized the area following the retreat of the ice. Fritz et al. (1991) and Laird et al. (1996) reported increasing lake salinity in North Dakota between 11 000 and 9000 calendar years BP, a change that is consistent with the climate becoming warmer and drier. We interpret the greater frequency of deposits of charcoal in the upper part of the Seibold fish-bearing unit to be due to fires associated with the trend to warmer and drier climatic conditions.

The ecological ramifications for the fish populations are complex, owing to the landscape and climatic changes we have outlined. Climate change directly affects water temperature, evaporation rates, flow regimes, and water levels in lakes and rivers. As stagnant and buried ice melted, the gradient and flow regimes of rivers connecting the Seibold Paleolake to the Missouri River drainage changed dramatically. The faster flowing, colder water rivers of the late glacial system were replaced, after melt-out of stagnant ice, by sluggish warm-water streams and finally by a nonintegrated drainage during the early Holocene.

Data and sampling

Data for fish species richness and fish and gastropod abundance within the fish-bearing unit are taken from Bickley (1970, his Fig. 6). Bickley examined the fish-bearing unit (i.e., a 15 cm × 20 cm × 37 cm thick stratigraphic section) at 1-cm intervals and counted and reported fish and gastropods for every 2 cm of thickness (i.e., 1–2.9 cm). The species of fossil gastropods include *Gyraulus parvus* Say, *Helisoma anceps* Menke, *Helisoma campanulatum* Say, *Promenetus exacuous* Say, *Physa gyrina* Say, *Lymnaea stagnalis* L., *Amnicola limosa* Say, and *Valvata tricarinata* Say. Bickley (1970, his Figs. 7–9) also counted charcoal fragments derived from a 7.62-cm^2 area continuously throughout the fish-bearing unit. Although Bickley did not indicate the charcoal-sampling interval, we assume that he used a 1-cm sampling interval based on his sampling for fishes, invertebrates, and spruce needles. He filtered his samples through 63-μm mesh, but did not indicate the size of charcoal particles sampled. Pollen was sampled at depths of 50, 45, 40, 30, and 0 cm. Fish, charcoal, and pollen data were described from the same unit, but from different locations relative to the lake margin. Consequently, the thicknesses of all fish-bearing-unit samples for charcoal and pollen were standardized to Bickley's sediment-depth values (Bickley 1970, his Fig. 6).

Colonization

To explain colonization of fishes (i.e., the order of appearance of taxa) at the site and to provide paleoecological interpretations, we examined contemporary life-history characteristics to better understand the probable ecological affinities of the fossil fish taxa. We feel that colonization of the site can be best described by ranking each taxon according to its swimming abilities (e.g., tolerance for fast- or slow-moving meltwater) and thermal preferences. Either swimming abilities or thermal preferences could have prevented fish from migrating to the Missouri Coteau from the Missouri River. For example, fish that cannot tolerate relatively fast-moving meltwater should be the last to arrive after the meltwater has dissipated. Fish with higher spawning temperatures and generally warmer thermal life histories should also be the last to arrive. Conversely, fish with preferences for lower temperatures should be the first to arrive if they were able to negotiate faster moving water. We compiled information about water-velocity preferences and minimum water temperatures necessary for spawning for each species from the sources listed in Table 1. We also assumed that the minimum temperature limit for each species is correlated with the mean annual air temperature at the northern limit of its range today. Information about the geographic distributions of the species is from Lee et al. (1980) and mean annual air temperatures from Hoare (2003).

Temporal changes associated with climate

To describe the changes in the aquatic system in relation to climate, we examined the mean differences among the various fish measures, gastropod abundance, and charcoal concentration across the change in vegetation. We used the Mann–Whitney nonparametric *t* test to determine if the mean number of fish, species richness, diversity, and gastropod abundance differed among the 2-cm intervals between

Fig. 2. A profile of the fish-bearing layer from Seibold Lake showing fish species richness, total abundance, diversity (Shannon Index), and abundance of five species in relation to charcoal concentration and vegetation. Shaded lines indicate fire events. Fish abundance and charcoal concentration are derived from Bickley (1970). Vegetation interpretation is from Cvancara et al. (1971).

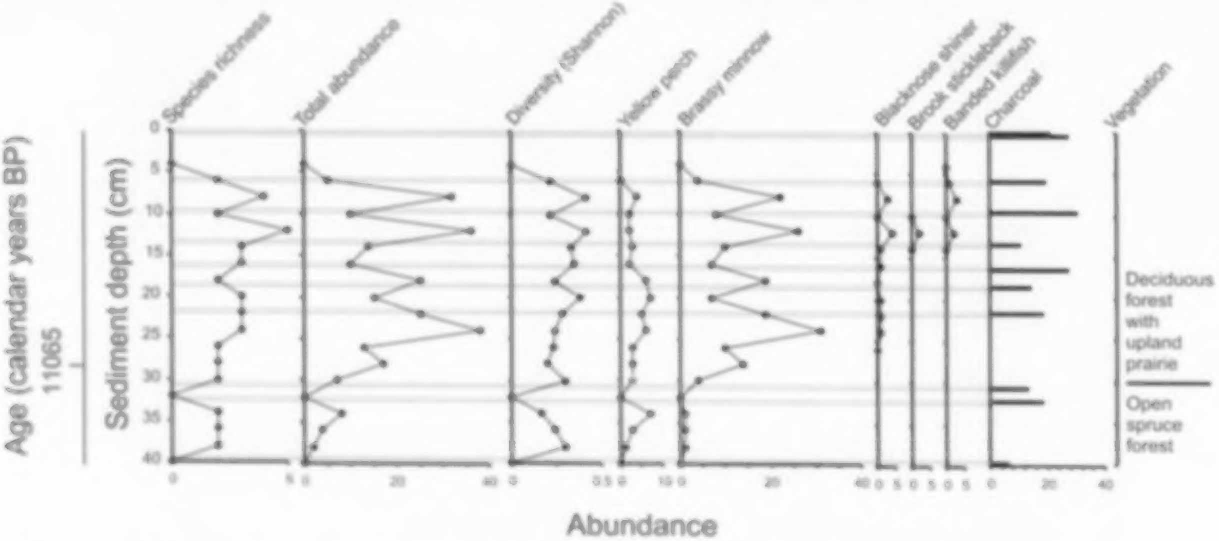

sediments with high concentrations of boreal forest pollen (38–32 cm in depth) and those with mainly deciduous pollen (30–0 cm in depth). We calculated fish diversity using the Shannon Diversity Index (Zar 1984). Total fish abundance was described using a polynomial regression because fish abundance would decrease to zero as the system converted to a wetland (Cvancara et al. 1971). All tests were performed with SYSTAT® version 10.0 (2002) and α was set at ≤0.05.

Impact of fire

The stratigraphic distribution of fossil fish and gastropod abundance was used to examine the effect of fire marked by charcoal deposition. The change in abundance (Δ) of the organisms for each stratigraphic sample was determined by subtraction, e.g., total of $\text{fish}_{38\text{-cm level}}$ – total of $\text{fish}_{36\text{-cm level}}$ = $\Delta\text{fish}_{36\text{-cm level}}$. The change in abundance was recorded for each group of organisms, one representing change before (i.e., calculated for levels from 36 to 4 cm in depth) and another representing change after (i.e., calculated for levels from 38 to 6 cm in depth) charcoal deposition. An example of how change before deposition was calculated is shown above. Change after deposition was calculated in a similar way, e.g., total of $\text{fish}_{36\text{-cm level}}$ – total of $\text{fish}_{34\text{-cm level}}$ = $\Delta\text{fish}_{36\text{-cm level}}$. Two-sample t tests were used to determine if there were significant differences in the mean changes of abundance between charcoal and noncharcoal layers.

Impact of changes in nutrients

To examine the effects of changes in nutrient levels in relation to environmental perturbations, we examined the relationships between charcoal concentration and gastropod and fish abundances. The relationship between gastropod and fish abundances from 4 to 38 cm in sediment depth was analyzed using linear regression. Gastropod abundance is assumed to be dependent on periphyton and thereby on the availability of nutrients, although we recognize that fish and gastropod abundances can also be limited by factors not quantifiable with the available Seibold data (e.g., water levels or salinity). Charcoal abundance in relation to fish or gastropod abundance was analyzed using linear regression to test whether environmental events correlated with charcoal concentration had a significant impact on gastropods and fishes. Data on fish and gastropod abundances and charcoal concentration were natural-log-transformed. Fish abundances and charcoal concentrations were summed with a value of 1 prior to transformation.

Results

Colonization

Fish species first appeared at different times in the stratigraphic column interpreted here as a pattern of colonization (Fig. 2). Yellow perch and brassy minnow were the first to appear, followed by blacknose shiner, and finally by brook stickleback and banded killifish (Fig. 2). When yellow perch and brassy minnow appeared in the fossil record, the vegetation was an open spruce forest, but by the time that blacknose shiner, brook stickleback, and banded killifish appeared, the vegetation had changed to open deciduous woodland.

The sequence of colonization corresponds to the descending order of relative water-velocity tolerances for each species (Table 1). Yellow perch and brassy minnow tolerate moderate water velocities and were the first to be recorded at the site. Blacknose shiner appears second and tolerates slow to medium water velocities, followed by brook stickleback and banded killifish, which prefer slow-moving water. The sequence of colonization does not correspond to increases in water temperatures. Brook stickleback have very

Table 2. A comparison of the means and standard errors for fish species richness, fish and gastropod abundances, and fish diversity by dominant vegetation type, spruce or deciduous trees.

Variable	Spruce (mean ± 1 SE)	Deciduous trees (mean ± 1 SE)	U	p
Species richness	1.6±0.40	2.8±0.27	14.5	0.055
Fish abundance	4.2±1.50	20.0±3.16	6.5	**0.010**
Diversity (Shannon Index)	0.20±0.06	0.30±0.02	24.5	0.430
Gastropod abundance	19.8±7.28	65.3±13.15	13.0	0.054

Note: Mann–Whitney U tests were used to determine significant differences (boldface p value; α was set at 0.05).

Fig. 3. (*a*) Relationship between total fish abundance and sediment depth ($y = -0.069x^2 + 2.582x - 2.091$, $r^2 = 0.386$, 95% confidence interval = –0.121 to –0.016, 0.317 to 4.848, –23.027 to 18.845). (*b*) Relationship between total gastropod abundance and depth of the fish-bearing-layer sediments. (*c*) Relationship of total gastropod abundance (line), total fish abundance (shaded bars), and charcoal concentration (solid bars) with sediment depth.

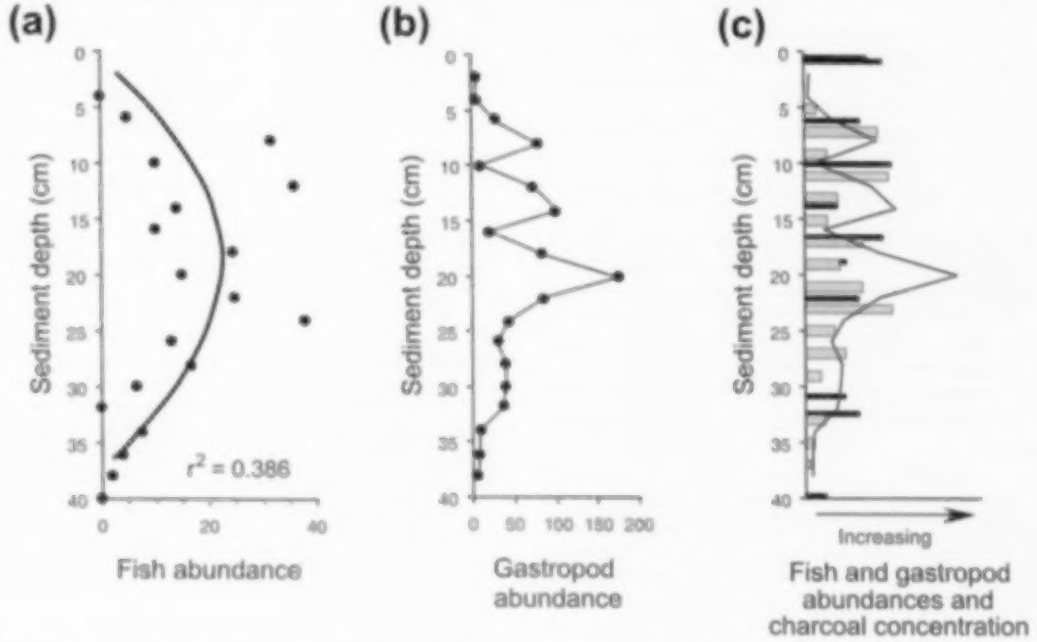

cool thermal tolerances but were third in the order of appearance, along with the banded killifish, which has warmer life-history characteristics.

We recognize that predator-sensitive fish such as brassy minnow, blacknose shiner, banded killifish, and brook stickleback may respond to abundance of yellow perch. We examined the fish-abundance data using regression analysis and found no significant relationships between the abundances of yellow perch and the prey species.

Temporal changes associated with climate

Species richness and diversity (Shannon Index) fluctuate as the lake ages, but there are no significant increases in either measure (Table 2). Species richness increased from two to five fish after the shift from boreal to deciduous vegetation. Total fish abundance increased following the shift from spruce to deciduous vegetation (Fig. 2). During the spruce-dominated period (i.e., sediment depths 38–32 cm), relative fish abundance is low (mean = 4.2; Table 2). However, during the time when the landscape was deciduous-dominated, relative fish abundance significantly increased to a mean of 20.0 from 30 to 0 cm sediment depth (Mann–Whitney U-test statistic = 6.5, $p = 0.010$). Total fish abundance increased significantly in a parabolic relation to sediment depth until senescence ($r^2 = 0.386$; 95% confidence interval = –0.121 to –0.016, 0.317 to 4.848, and –23.027 to 18.845; Fig. 3*a*). During the spruce-dominated period, relative gastropod abundance, our proxy for nutrients, was low (mean = 19.8; Table 2; Figs. 3*a*, 3*b*). Relative gastropod abundance increased to a mean of 65.3 during the time when the landscape was deciduous-dominated; however, the relationship was not significant ($p = 0.054$).

Impact of fire

Fish abundance fluctuated between 30% and 70% and was characterized by six peaks in total abundance, most of the variation being produced by changes in abundance of brassy minnow. Five of the six peaks in fish abundance occur be-

Fig. 4. Relationships between fish and gastropod abundances and charcoal concentration. (*a*) Regression analysis indicates a significant relationship between charcoal concentration and gastropod abundance (△); fish abundance (□) was summed with a value of one prior to transformation but was not found to be significant. (*b*) Total fish abundance and gastropod abundance (i.e., our proxy for nutrient levels); both variables were natural-log-transformed and a regression analysis indicates a significant relationship.

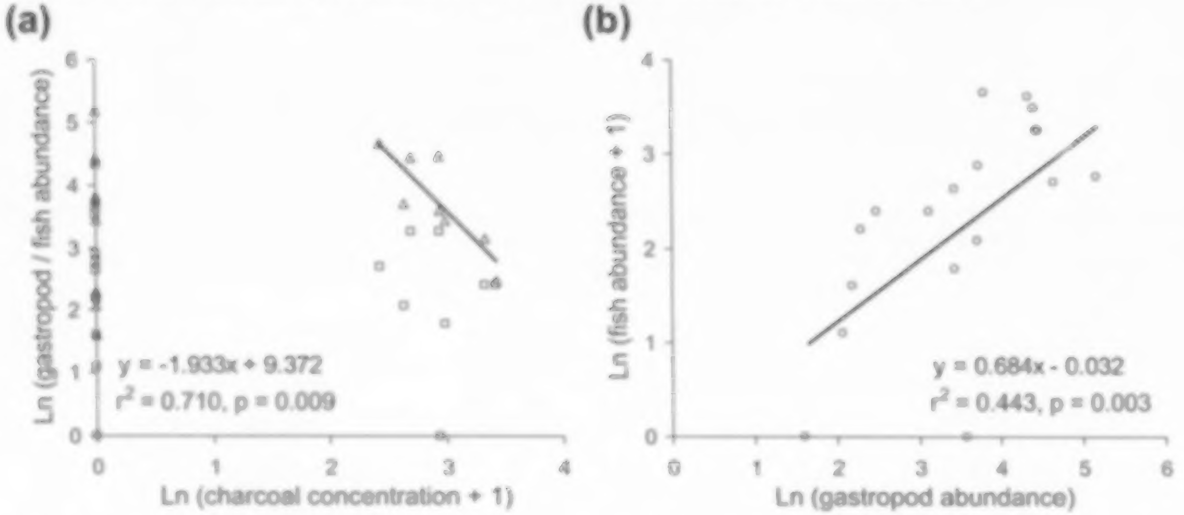

Table 3. Comparisons between the mean changes in fish and gastropod abundances before and after charcoal deposition.

	Charcoal (mean ± 1 SE)	No charcoal (mean ± 1 SE)	*t*	*p*
Gastropod abundance				
Δ before	−14.1±21.70	11.2±12.10	1.019	0.330
Δ after	16.3±20.08	−13.1±13.32	−1.218	0.246
Fish abundance				
Δ before	−8.5±5.09	7.3±4.36	2.4	**0.033**
Δ after	4.4±4.87	−4.1±5.59	−1.145	0.270

Note: Two-sample *t* tests were used to test for significant differences as indicated by the test statistic (*t*) and probability values (*p*); α was set at 0.05. The boldface *p* value indicates a significant relationship.

tween intervals with high concentrations of charcoal that are assumed to represent fire events (Fig. 2). In several, but not all, locations in the sediment column (i.e., 30–33.9, 13–16.9, 9, and 6 cm in depth), high charcoal concentrations occurred during intervals of relatively lower fish abundance. There was no significant correlation between the amount of charcoal and fish abundance (Fig. 4*a*). The mean change in fish abundance prior to charcoal deposition is –8.5, which is significantly lower than the mean change in abundance not associated with charcoal deposition (7.3; $p = 0.033$; Table 3). There are no significant changes in gastropod abundance before charcoal deposition and none in gastropod or fish abundance after it (Table 3).

Impact of changes in nutrients

Gastropod abundance fluctuated within the fish-bearing unit and was characterized by four distinct peaks (Figs. 3*b*, 3*c*). Gastropod abundance was negatively correlated with charcoal concentration ($r^2 = 0.710$, $p = 0.009$; Fig. 4*a*). Fish abundance significantly increased with gastropod abundance, which is our proxy for nutrients ($r^2 = 0.443$, $p = 0.003$; Fig. 4*b*).

Discussion

The data show three distinct types of patterns that are superimposed on one another. First, fish species colonized the lake in a sequence that may be explained in terms of their life-history characteristics. Second, total abundance of fish increased during a time of climatic transition as indicated by a vegetational shift from an open spruce to an open deciduous forest. Third, fish-abundance fluctuations and population declines are correlated with episodic droughts inferred from charcoal deposition.

Colonization

The change in climate from relatively cold and moist to warm and dry conditions resulted in changes in the landscape and fluvial systems that periodically allowed access for species with different autecologies. Access to the site for some fish was dependent on landscape subsidence resulting from the melting of stagnant ice and the reduction of fluvial gradients and water velocities. Additionally, the climate warmed and became drier as indicated by the vegetation and charcoal records. During the drier periods, discharge from rivers would be relatively decreased, allowing fish with preferences for slow-moving water to access the site.

Fish colonized Seibold Lake in a sequential manner. Yellow perch and brassy minnow have life-history characteristics that enable them to be early colonizers of the deglaciated landscape. They tolerate relatively low spawning and water temperatures (Dobie et al. 1956; Weber 1975) and are able to negotiate faster flowing water (Otto and Rice 1974; Copes 1975; Becker 1983), which is characteristic of cooler and wetter climates. The third species to colonize the lake was the blacknose shiner. This species has an ecology that allows it to cope with moderately low temperatures, but tolerates only slow to moderate water velocities compared with yellow perch and brassy minnow (Becker 1983). The brook stickleback and banded killifish were the last species to colonize the lake. The brook stickleback today tolerates a wide range of thermal regimes (Reisman and Cade 1967; Carlander 1969), but its ability to be an early colonizer is limited by relatively slow-flowing water (Becker 1983). The brook stickleback may be expected to have colonized the lake relatively early with yellow perch, given its tolerances for colder water. However, higher water velocities in rivers probably hampered brook stickleback colonization. Only as the current slowed could fish with preferences for lower water velocity colonize the lake. The banded killifish requires relatively low water velocities and warm water for spawning (Richardson 1939; Becker 1983).

The Missouri River drainage likely acted as a source (Stewart and Lindsey 1983), and perhaps a refugium, for fishes that colonized the Missouri Coteau, as is thought to be so for the brassy minnow (Burr and Page 1986). There is strong evidence that meltwater from the drainage of the ice-cored moraines was to the southwest, based on a dendritic pattern of sand and gravel fluvial deposits originating in the Missouri Coteau and trending to the southwest (Clayton et al. 1980). We interpret this pattern to represent a series of tributaries of the Missouri River. The presence of fossil bivalves at several locations in the sand and gravel fluvial deposits within the morainic deposits of North Dakota (Clayton 1961, 1967) provides further insight into fish colonization (Sherrod 1963). The reproduction and dispersal of many bivalves depend on fishes transporting glochidia in their gills.

The colonization of previously glaciated terrain has probably occurred numerous times, because major glaciations and interglaciations are known to have occurred about every 100 000 years during the past 1 million years of the Quaternary period (i.e., the last 2 million years) (Shackleton and Hall 1990). In the northern latitudes of North America and Europe, fish populations would have been forced to relocate as habitats were glaciated and deglaciated. Following each glaciation, the warming climate would expand the northern potential range of fish (e.g., Miller 1958; Cavender 1986; Robison 1986 and references therein).

Fluctuating abundance

Fluctuations in fish abundance can be explained in terms of either mass mortality (i.e., death assemblages) or increased abundance (i.e., productivity). We prefer the latter interpretation for the following reasons. The time scale of deposition of the fish-bearing unit is approximately 1000 years and encompasses shifts in vegetation from spruce to deciduous woodland, suggesting that increased fish fossil deposition (i.e., peak abundance) occurred over longer time periods with more individuals existing and dying in the system as opposed to potential annual events (e.g., winter-related fish kills). Population cycles of brassy minnow, blacknose shiner, brook stickleback, and banded killifish, which span, on the average, 160 years, would have ample time to recover from perturbations caused by annual events or fire. With respect to fire, studies on Minnesota lakes failed to show substantial effects on lake productivity (McColl and Grigal 1975; Wright 1976; Bradbury 1986), and a study of fish growth after the Yellowstone National Park fires also failed to show an effect (Gresswell 2004), suggesting that in Seibold Lake neither mass mortality nor fish abundance would be strongly affected by fire.

Fish abundance at the Seibold site varies in a manner that is independent of colonization of the species. We show that decreases in fish abundance are correlated with charcoal deposition and that fish abundance increased throughout the fish-bearing unit until 8 cm in depth. We suggest that fire events are related to drought cycles associated with warming climatic conditions, which influences fish abundance in three potentially interacting ways, by periodically limiting nutrient inputs, increasing eutrophication, or changing population structure and overall productivity.

First, nutrients may be limited by episodic drought, thereby periodically limiting system productivity. The changes in fish abundance associated directly with charcoal layers are significantly less than those associated interhorizons. This suggests to us that more change in abundance is associated with the onsets of droughts and not directly with fire events. Fire is linked to drought and it has been suggested that it is the drier conditions, rather than fire, that limit input of nitrogen and, ultimately, productivity (Kilham et al. 1996; Theriot et al. 1997; Gresswell 1999). Nutrients derived from the atmosphere tend to dominate annual trends in water quality before and after a fire event (Wright 1976; Lathrop 1994; Theriot et al. 1997). Drought conditions may reduce nutrients by limiting atmospheric inputs, temperature, water level, light penetration, lake productivity, vegetation around the lake, and also watershed nutrients being carried into the lake through precipitation runoff (Theriot et al. 1997; Gresswell 1999).

From the Seibold data, nutrients appear to play a role in the abundance of fish and gastropods. Fish abundance is positively correlated with gastropod abundance. We chose gastropods as a proxy for nutrients because of their dependence on periphyton, and thereby nutrients. However, the relative nutrient levels vary throughout the record and are punctuated with a series of droughts. We speculate that the amount of charcoal deposited in each of the layers would be positively correlated with the intensity of the drought associated with the charcoal layer. We hypothesize this relationship because fish abundance is lower prior to the charcoal layer being deposited and because gastropod abundance associated with charcoal layers negatively responds to the amount of charcoal deposited, which is inferred to be correlated with the intensity of the drought.

Second, nutrient input increased as the vegetation shifted from spruce to deciduous woodland as a result of climatic warming. As we previously discussed, gastropod abundance, as a proxy for system nutrient levels, is correlated with fish abundance. The greatest increases in fish abundance occurred after the vegetation in the riparian area had converted to a deciduous forest and fire frequency increased. As the climate warmed, drought, deciduous trees, and fire became more common, thereby changing the landscape. We have already discussed the potential effects of the limitation of nutrients due to drought, but we have not discussed the implications of allochthonous inputs from a deciduous-dominated riparian area on fish abundance. Nutrients from deciduous trees may have increased eutrophication by elevating nutrient levels in the lake higher than those of the spruce-dominated watershed, thereby permitting a trend of increasing total fish abundance until the system senesced. Enright (2001) found that nutrients (i.e., nitrogen and phosphorus) from deciduous litter were significantly higher than those from conifers, thus permitting increases in system productivity to support higher fish abundance. In addition, soil nutrients were found to be the highest among hardwoods and lowest among spruce in the boreal forests of North America (Pastor et al. 1987, 1988).

Only two of the five species occur in the uppermost lake sediments, brassy minnow and banded killifish. From the species richness and abundance data, we interpret that fish species richness and abundance declined in the system because the postglacial lake turned into an isolated wetland like many of the prairie potholes today. We speculate that the system ceased to support significant numbers of fish because the streams and rivers, which interconnected many of the prairie potholes, dried up from a lack of meltwater and rain. As a result, no more fish were able to colonize the system and fish populations declined because of a fall in lake levels due to evaporation.

Third, a warming climate may influence fish population structure and overall productivity through a complex series of biological and climate-related effects. Research conducted to examine the effects of a warming climate on fishes, using information from population dynamics and bioenergetics studies, has produced hypotheses concerning the effects of climatic warming on fishes. For example, Hill and Magnuson (1990) suggested that changes in bioenergetics due to climate change might modify yearling growth and prey consumption, thereby greatly influencing the food-web dynamics. Shuter and Post (1990) suggested that an increase of 4 °C may increase the northern distributional limit of yellow perch and, depending on lake morphometry and productivity, may also greatly influence survival, relative year-class strength, and system carrying capacity. Fossil fish deposited during a time of warming climate have the potential to be used to test Shuter and Post's (1990) hypotheses to examine fish growth and shifts in modal year classes.

Temperature probably has an influence on Seibold fish abundance cycles because temperature and other climate-related conditions could alter population dynamics and fishery productivity (Pauly 1980; Beamish and Bouillon 1993; Finney et al. 2002). Pauly (1980) examined many fish populations from polar to tropical regions and from fresh water to salt water, and he derived a mathematical relationship for mortality, growth, and temperature. Beamish and Bouillon (1993) identified similar trends between production of salmon and copepods with the pressure patterns of the Aleutian Low. Finney et al. (2002) used diatoms as a proxy for estimating sockeye salmon (*Oncorhynchus nerka*) productivity because they were correlated with climatic forcing. Nevertheless, there remains a need to consider the additional dynamic effects of temperature and drought on the dispersion and population dynamics of fishes in the light of climate change.

In summary, this research provides a snapshot of fish colonization and abundance patterns during a time of climatic warming. In this study, we conclude that appearances of fishes in the lake can be explained in terms of differences in life-history characteristics. Yellow perch and brassy minnow, species with tolerances for moderate water velocities, appeared early during a cool-climate period. Fishes with preferences for slow-moving and warmer water appeared later. In a dynamic landscape, like that of the Missouri Coteau at the end of the ice age, fish colonization was controlled by the dispersal potential of the species. Independent of colonization, changes in abundance were probably the result of changes of productivity rather than representing a series of mass fish kills. Further, changes in productivity appear to be linked to the occurrence of drought and climate change, but the relationships are uncertain.

From our perspective, climate change is complex in its effects on aquatic systems, which are more easily detectable in long-term data sets. We showed that fish colonization and populations could be affected by climate change by responding to factors such as changes in nutrients, changes in drought frequency and intensity, and changes in rivers incorporating various lacustrine systems. The resolution of our data is low, but our results provide a conceptual framework of the ecology based on observations, which is useful in developing testable hypotheses in other studies examining the effects of climate change on contemporary and fossil fishes. The complex relationships that we have outlined in our paleoecological study emphasize the need for study of longer data sets in examining the causal relationships between productivity, nutrient cycles, fire frequency, and climate change (Gresswell 1999).

Acknowledgements

We are appreciative of the comments provided to us by four anonymous reviewers. We thank C. Tom Shay at the University of Manitoba for providing us with pollen data and samples of fossil fish used in this study. We are grateful to Elroy Kadrmas of the North Dakota Geological Survey, who provided us with a digitized copy of Clayton's Surface Geology Map of North Dakota. We also thank the landowners, Vernon and Carol Seibold of Buchanan, N.D., for allowing access to the site and providing samples of the sediment. We are grateful to Cathy Whitlock, Department of Earth Sciences, Montana State University, and Robert Gresswell, United States Geological Survey, Northern Rocky Mountain Science Center, Montana State University, for their comments on an earlier version of the manuscript. Funding was provided to Michael Newbrey by the GraSUS program supported by National Science Foundation Project DGE-0086445, North Dakota State University, and the North Dakota Water Resources Research Institute, North Dakota State University, through its Fellowship program supported by the United States Geological Survey.

References

Ashworth, A.C., and Brophy, J.A. 1972. Late Quaternary fossil beetle assemblage from the Missouri Coteau, North Dakota. Geol. Soc. Am. Bull. **83**: 2981–2988.

Beamish, R.J., and Bouillon, D.R. 1993. Pacific salmon production trends in relation to climate. Can. J. Fish. Aquat. Sci. **50**: 1002–1016.

Becker, G.C. 1983. Fishes of Wisconsin. University of Wisconsin Press, Madison.

Bickley, W.B., Jr. 1970. Paleoenvironmental reconstruction of Late Quaternary lacustrine sediments (Seibold site) in southeastern North Dakota. M.S. thesis, University of North Dakota, Grand Forks.

Birks, H.J.B. 1980. Modern pollen assemblages and vegetation history of the moraines of the Klutlan Glacier and its surroundings, Yukon Territory, Canada. Quat. Res. **14**: 101–129.

Bradbury, J.P. 1986. Effects of forest fire and other disturbances on wilderness lakes in northeastern Minnesota II. Paleolimnol. Arch. Hydrobiol. **106**: 203–217.

Burr, B.M., and Page, L.M. 1986. Zoogeography of fishes of the lower Ohio – upper Mississippi basin. *In* The zoogeography of North American freshwater fishes. *Edited by* C.H. Hocutt and E.O. Wiley. John Wiley and Sons, New York. pp. 287–324.

Carlander, K.D. 1969. Handbook of freshwater fishery biology. Vol. 1. Iowa State University Press, Ames.

Cavender, T.M. 1986. Review of the fossil history of North American freshwater fishes. *In* The zoogeography of North American freshwater fishes. *Edited by* C.H. Hocutt and E.O. Wiley. John Wiley and Sons, New York. pp. 699–724.

Clayton, L. 1961. Late Wisconsin Mollusca from ice-contact deposits in Logan County, North Dakota. Proc. N.D. Acad. Sci. **15**: 11–18.

Clayton, L. 1967. Stagnant-glacial features of the Missouri Coteau in North Dakota. N.D. Geol. Surv. Misc. Ser. No. 30. pp. 25–46.

Clayton, L., and Cherry, J.A. 1967. Pleistocene superglacial and ice-walled lakes of west-central North America. N.D. Geol. Surv. Misc. Ser. No. 30. pp. 47–52.

Clayton, L., Moran, S.R., and Bluemle, J.P. 1980. Explanatory text to accompany the geologic map of North Dakota. N.D. Geol. Surv. Invest. Rep. No. 69.

Copes, F. 1975. Ecology of the brassy minnow, *Hybognathus hankinsoni* Hubbs. Fauna and flora of Wisconsin. Part III. Rep. No. 10. Museum of Natural History, University of Wisconsin, Stevens Point. pp. 46–72.

Cvancara, A.M., Clayton, L., Bickley, W.B., Jr., Jacob, A.F., Ashworth, A.C., Brophy, J.A., et al. 1971. Paleolimnology of Late Quaternary deposits: Seibold site, North Dakota. Science (Wash., D.C.), **171**: 269–306.

Dobie, J.R., Meehean, O.L., Snieszko, S.F., and Washburn, G.N. 1956. Raising bait fishes. U.S. Fish. Wildl. Serv. Circ. No. 35.

Enright, N.J. 2001. Nutrient accessions in a mixed conifer-angiosperm forest in northern New Zealand. Aust. Ecol. **26**: 618–629.

Finney, B.P., Gregory-Eaves, I., Douglas, M.S.V., and Smol, J.P. 2002. Fisheries productivity in the northeastern Pacific Ocean over the past 2,200 years. Nature (Lond.), **416**: 729–733.

Fritz, S.C., Juggins, S., Battarbee, R.W., and Engstrom, D.R. 1991. Reconstruction of past changes in salinity and climate using a diatom-based transfer function. Nature (Lond.), **352**: 705–706.

Gresswell, R.E. 1999. Fire and aquatic ecosystems in forested biomes of North America. Trans. Am. Fish. Soc. **128**: 193–221.

Gresswell, R.E. 2004. Effects of wildfire on growth of cutthroat trout in Yellowstone Lake. Chap. 7. *In* After the fires: the ecology of change in Yellowstone National Park. *Edited by* L. Wallace. Yale University Press, New Haven, Connecticut. pp. 143–164.

Grimm, E.C. 2001. Trends and palaeoecological problems in the vegetation and climate history of the Northern Great Plains, U.S.A. Proc. R. Irish Acad. Sect. B Biol. Environ. **101**: 47–64.

Hill, D.K., and Magnuson, J.J. 1990. Potential effects of global climate warming on the growth and prey consumption of Great Lakes fish. Trans. Am. Fish. Soc. **119**: 265–275.

Hoare, R. 2003. World climate [online]. Available from www.worldclimate.com.

Kilham, S.S., Theriot, E.C., and Fritz, S.C. 1996. Linking planktonic diatoms and climate change using resource theory in the large lakes of the Yellowstone ecosystem. Limnol. Oceanogr. **41**: 1052–1062.

Laird, K.R., Fritz, S.C., Grimm, E.C., and Mueller, P.G. 1996. Century-scale paleoclimatic reconstruction from Moon Lake, a closed basin lake in the northern Great Plains. Limnol. Oceanogr. **41**: 890–902.

Lathrop, R.G. 1994. Impacts of the 1988 wildfires on the water quality of Yellowstone and Lewis lakes, Wyoming. Int. J. Wildland Fire, **4**: 169–175.

Lee, D.S., Gilbert, C.R., Hocutt, C.H., Jenkins, R.E., McAllister, D.E., and Stauffer, J.R., Jr. 1980. Atlas of North American freshwater fishes. Publ. N. C. Biol. Surv. No. 1980-12.

McAndrews, J.H. 1970. Spiritwood Lake pollen record. *In* North American pollen database. *Edited by* E.C. Grimm et al. IGBP PAGES/World Data Center for Paleoclimatology. National Atmospheric and Oceanographic Administration National Geophysical Data Center Paleoclimatology Program, Boulder, Colo.

McColl, J.G., and Grigal, D.F. 1975. Forest fire: effects on phosphorus movement to lakes. Science (Wash., D.C.), **188**: 1109–1111.

Miller, R.R. 1958. Origin and affinities of the freshwater fish fauna of western North America. *In* Zoogeography. *Edited by* C.L. Hubbs. AAAS Publ. No. 51. pp. 187–222.

Otto, R.G., and Rice, J.O. 1974. Swimming speeds of yellow perch (*Perca flavescens*) following an abrupt change in environmental temperature. J. Fish. Res. Board. Can. **31**: 1731–1734.

Pastor, J., Naiman, R.J., and Dewey, B. 1987. A hypothesis of the effects of moose and beaver foraging on soil nitrogen and carbon dynamics, Isle Royale. Alces, **23**: 107–123.

Pastor, J., Naiman, R.J., Dewey, B., and McInnes, P. 1988. Moose, microbes, and the boreal forest. Bioscience, **38**: 770–777.

Pauly, D. 1980. On the interrelationships between natural mortality, growth parameters, and mean environmental temperature in 175 fish stocks. J. Cons. Cons. Int. Explor. Mer, **39**: 175–192.

Power, G.J., and Rychman, F. 1998. North Dakota fisheries investigations: status of North Dakota's Fishes. North Dakota Game and Fish Department Rep. No. 27.

Reisman, H.M., and Cade, M.E. 1967. Physiological and behavioral aspects of reproduction in the brook stickleback, *Culaea inconstans*. Am. Midl. Nat. **77**: 257–295.

Richardson, L.R. 1939. The spawning behavior of *Fundulus diaphanus* (LeSueur). Copeia, 1939: 156–167.

Robison, H.W. 1986. Zoogeographic implications of the Mississippi River basin. *In* The zoogeography of North American freshwater fishes. *Edited by* C.H. Hocutt and E.O. Wiley. John Wiley and Sons, New York. pp. 267–286.

Shackleton, N.J., and Hall, M.A. 1990. Stable isotope history of the Pleistocene at ODP Site 677. *In* Proceedings of the Ocean Drilling Program Scientific Results 111. *Edited by* K. Becker and H. Sakai. Ocean Drilling Program, College Station, Texas. pp. 295–316.

Sherrod, N.R. 1963. Late Pleistocene fish from lake sediments in Sheridan County, North Dakota. Proc. N.D. Acad. Sci. **17**: 32–36.

Shuter, B.J., and Post, J.R. 1990. Climate, population viability, and the zoogeography of temperate fishes. Trans. Am. Fish. Soc. **119**: 314–336.

Sterner, R. 1995. Surface relief map of North Dakota. *In* Color landform atlas of the USA. Applied Physics Laboratory, Johns

Hopkins University, Licensed by North Star Science and Technology, LLC, Baltimore, Md.

Stewart, K.W., and Lindsey, C.C. 1983. Post-glacial dispersal of lower vertebrates into the Lake Agassiz region. Geol. Assoc. Can. Spec. Pap. No. 26. pp. 391–419.

Stuiver, M., and Reimer, P.J. 1993. Extended ^{14}C data base and revised CALIB radiocarbon calibration program. Radiocarbon, **35**: 215–230.

Stuiver, M., Reimer, P.J., Bard, E., Beck, J.W., Burr, G.S., Hughen, K.A., et al. 1998*a*. INTCAL98 radiocarbon age calibration 24,000–0 cal BP. Radiocarbon, **40**: 1041–1083.

Stuiver, M., Reimer, P.J., and Braziunas, T.F. 1998*b*. High-precision radiocarbon age calibration from terrestrial and marine samples. Radiocarbon, **40**: 1127–1151.

Systat Software Inc. 2002. SYSTAT®: statistics. Version 10.0 [computer program]. Systat Software Inc., Richmond, Calif.

Theriot, E.C., Fritz, S.C., and Gresswell, R.E. 1997. Long-term limnological data from the larger lakes of Yellowstone National Park. Arct. Alp. Res. **29**: 304–314.

Weber, J.J. 1975. Golden strands. Wis. Conserv. Bull. **40**: 18–19.

Wright, R.F. 1976. The impact of forest fire on the nutrient influxes to small lakes in northeastern Minnesota. Ecology, **57**: 649–663.

Zar, J.H. 1984. Biostatistical analysis. Prentice-Hall, Inc., Englewood Cliffs, N.J.

Influence of nontrophic interactions between benthic invertebrates on river sediment processes: a microcosm study

Florian Mermillod-Blondin, Magali Gérino, Sabine Sauvage, and Michel Creuzé des Châtelliers

Abstract: The main objective of this study was to measure the impact of benthic invertebrate diversity on river sediment processes. We quantified the effects of interactions between three taxa (asellids, chironomid larvae, and tubificid worms). The impacts of different taxa richness treatments were measured on sediment reworking, O_2 concentrations, bacterial abundances, and numbers of active bacteria in slow filtration sand–gravel columns. The coefficients of sediment reworking measured in multitaxa treatments were lower than those predicted from one-taxon treatments. The interactions among invertebrates also significantly reduced O_2 concentrations in sediments. These results were probably due to interactions between the different sediment structures produced by each taxon (tubes, macropores, and fecal pellets) that modified water flow and associated microbial activities in the interstitial habitat. The stimulation of aerobic microbial processes with two- and three-taxa treatments, whereas one-taxon treatments could increase or decrease O_2 consumption in columns, indicates that interactions among invertebrates limited the variability of the system functioning. We suggest that, beyond a small number of detritivorous taxa, a threshold effect on bioturbation process and microbial activities was produced by animals in the experimental system. Finally, the interactions between taxa played a significant role in microbial processes in the system studied.

Résumé : Le but de cette étude était de mesurer l'impact de la diversité des invertébrés sur le fonctionnement d'un milieu sédimentaire de rivière. Nous avons quantifié les effets des interactions entre trois taxons (aselles, larves de chironomes et oligochètes tubificidés). Les effets produits par différents traitements en invertébrés ont été mesurés sur le remaniement sédimentaire, les concentrations en O_2, les abondances totales en bactéries et le nombre de bactéries actives dans des colonnes filtrantes remplies de sables et graviers. Les coefficients de remaniement sédimentaire mesurés dans les traitements avec plusieurs taxons étaient plus faibles que ceux estimés à partir des effets individuels produits par chaque taxon. Les interactions entre les taxons ont aussi produit une diminution significative des concentrations en O_2 dans les sédiments. Ces résultats étaient probablement liés à des interactions entre les structures sédimentaires produites par chaque taxon (tubes, macropores et pelotes fécales), lesquelles modifient les flux d'eau et les activités microbiennes dans l'habitat interstitiel. La stimulation des processus microbiens aérobies dans les traitements avec deux et trois taxons alors que les traitements avec un seul taxon peuvent stimuler mais aussi réduire la consommation en O_2 dans les colonnes indique que les interactions entre invertébrés limitent la variabilité dans le fonctionnement du système. Nous supposons que, au delà d'un nombre faible de taxons, un effet seuil est observé sur le processus de bioturbation et les activités microbiennes dans le système expérimental. En définitive, les interactions entre les taxons jouent un rôle significatif sur les processus microbiens dans le système étudié.

Introduction

In the last 10 years, an increasing number of studies have focussed on the effect of species diversity on ecosystem properties (Naeem et al. 1994; Loreau et al. 2002; Jonsson and Malmqvist 2003). The impact of biodiversity on ecosystem processes depends on the functional characteristics of each species but also on the interactions among species present in the community (Wardle et al. 1997; van der Heijden et al. 1998; Loreau et al. 2001).

Received 14 May 2003. Accepted 13 April 2004. Published on the NRC Research Press Web site at http://cjfas.nrc.ca on 2 December 2004.
J17527

F. Mermillod-Blondin[1] and M. Creuzé des Châtelliers. UMR–CNRS 5023, Laboratoire d'Écologie des Hydrosystèmes Fluviaux, French National Centre for Scientific Research and University Claude Bernard Lyon I, Domaine Scientifique de la Doua, 69622 Villeurbanne cedex, France.
M. Gérino and S. Sauvage. FRE CNRS–UPS 2630, Laboratoire d'Écologie des Hydrosystèmes, French National Centre for Scientific Research and University Paul Sabatier, 29 rue Jeanne Marvig, 31055 Toulouse, France.

[1] Corresponding author (e-mail: mermillo@univ-lyon1.fr).

Can. J. Fish. Aquat. Sci. **61**: 1817–1831 (2004) doi: 10.1139/F04-114

At the water–sediment interface in marine and lake systems, the effects of various benthic invertebrates on the bioturbation process and their influences on biogeochemical cycling have been widely studied (Fukuhara and Sakamoto 1987; Hansen and Kristensen 1998; Stief and de Beer 2002). However, the impacts of assemblages of benthic invertebrates on nutrient fluxes have been analysed only very recently in marine sediments (Emmerson and Raffaelli 2000; Emmerson et al. 2001; Raffaelli et al. 2003). These studies demonstrated that the diversity of functional traits (e.g., mode of bioturbation) strongly affects the ecosystem processes.

In rivers, the exchange between the surface and the riverbed sediments (hyporheic zone) plays a key role in organic matter processing and nutrient cycling (Grimm and Fisher 1984; Boulton et al. 1998; Morrice et al. 2000). Battin et al. (2003) showed that hyporheic respiration accounts for 41% of whole-ecosystem respiration in White Clay Creek (Pennsylvania). Triska et al. (1993) demonstrated that the nitrogen cycle in rivers was dependent on microbial processes occurring in bed sediments. Marmonier et al. (1995) also reported high efficiency of interstitial habitats in organic matter processing. Despite such functional importance of these sedimentary systems in organic matter processing and nutrient cycling in the hydrosystems, the impact of invertebrate diversity on biogeochemical processes occurring in river sediments (characterized by course particles and an advective flux of water) has been poorly studied (Danielopol 1989; Boulton 2000).

It has, however, been demonstrated that benthic invertebrates may significantly affect physical, chemical, and microbial processes occurring in such river sediment habitats (Danielopol 1989; Torreiter et al. 1994; Mermillod-Blondin et al. 2000*a*, 2003). In a previous study (Mermillod-Blondin et al. 2002), three invertebrate taxa typically associated with river sediment systems (asellids, chironomids, and tubificid worms) were described as three distinct ecosystem engineers (sensu Jones et al. 1994). Their activities in sediments were tested separately. They corresponded to three specific modes of bioturbation, producing different effects on sediment structure and microbial activities.

The aim of the present study was to test the influence of interactions among taxa (assemblages of the three taxa) on sediment properties and processes (sediment reworking, O_2 concentrations, and microbial characteristics). We used experimental microcosms with several treatments of different taxa richness combinations and measured the resulting processes. We predicted that the three benthic taxa would strongly interact in sediments by modifying the same physical habitat in different ways. Therefore, system functioning tested with a mixture of taxa was predicted to be different from that calculated by the summation of the individual roles of each taxon forming the mixture. To measure the impact of interactions between taxa, we used sediment reworking as an indication of the effect of taxa assemblages on the physical structure of sediments and dissolved O_2 concentration as an indicator of respiration in river sediments (with a constant flow rate, dissolved O_2 in pore water is determined by the distance from the O_2 source and the rate of O_2 consumption by microorganisms, Malard and Hervant 1999). The abundances of bacteria and electron transport system (ETS) active bacteria were measured to estimate the impact of invertebrates on biofilm characteristics.

Materials and methods

Experimental design

Experiments took place in gravel–sand filtration columns (50 cm high, 10 cm in diameter) (Fig. 1) modified from Torreiter et al. (1994) and Griebler (1996). Each column was filled with sand (60–630 μm) previously incubated during 4 days with bacteria and cellulose powder (0.5% of sediment mass) as source of particulate organic matter at a final concentration equivalent to that measured in secondary channels of the Rhône River (Mermillod-Blondin et al. 2000*b*) and with calcinated (550 °C) fine gravel (4–5 mm) to a height of 40 cm. Constant masses of gravel (590 g) and incubated sand (210 g) were alternately added to obtain a heterogeneous interface with presence of zones where sand was trapped and zones with macropores. A water column (6–10 cm) was maintained at the surface of the sediment to simulate the overlying river water. Openings in the column at different depths permitted the collection of water and fine sediments with a syringe. Further details of the columns are given in Mermillod-Blondin et al. (2000*a*).

The experiments were performed in a constant-temperature room at 15 ± 0.5 °C with a 12 h light : 12 h dark cycle. The sediment of the column was kept in the dark for suppressing photoautotrophic growth. Dechlorinated drinking water, permanently aerated to maintain high O_2 concentrations, was continuously fed into the columns with a peristaltic pump. Before entering into the columns, the water was enriched with nitrate (to a nitrate concentration of 20 mg·L^{-1}) and dissolved organic carbon (2 mg potassium acetate·L^{-1}) with another peristaltic pump to support biofilm activity (Fig. 1). These concentrations of carbon and nitrate were equivalent to those measured in secondary channels of the Rhône River (Mermillod-Blondin et al. 2000*b*). The resulting infiltration rate was 2.0 ± 0.1 mL·min^{-1} (Darcy velocity 1.53 cm·h^{-1}), which generated an interstitial water velocity of 3.75 cm·h^{-1}. This velocity corresponded to values measured in the hyporheic zone of streams (Triska et al. 1993; Morrice et al. 2000). The first measurements were made 3 days after the beginning of the water flow after the hydraulic properties had stabilized.

As in previous studies (Mermillod-Blondin et al. 2000*a*, 2002), one experimental set consisted of four columns: three columns (animal columns) with the same combination of taxa and one column (without animals) acting as a control. In the present study, we used seven experimental sets, giving eight treatments: (1) control without animals (seven columns), (2) 25 asellids (*Asellus aquaticus*, A treatment, three columns), (3) 50 chironomids (*Prodiamesa* sp., C treatment, three columns), (4) 100 tubificid worms (50 *Limnodrilus* spp. and 50 *Tubifex* sp., T treatment, three columns), (5) 25 asellids and 50 chironomids (A+C treatment, three columns), (6) 25 asellids and 100 tubificid worms (A+T treatment, three columns), (7) 50 chironomids and 100 tubificid worms (C+T treatment, three columns), and (8) 25 asellids, 50 chironomids, and 100 tubificid worms (A+C+T treatment, three columns). The tested densities were equivalent to 3250,

Fig. 1. Schematic diagram of an experimental unit. DOC, dissolved organic carbon, ETS, electron transport system.

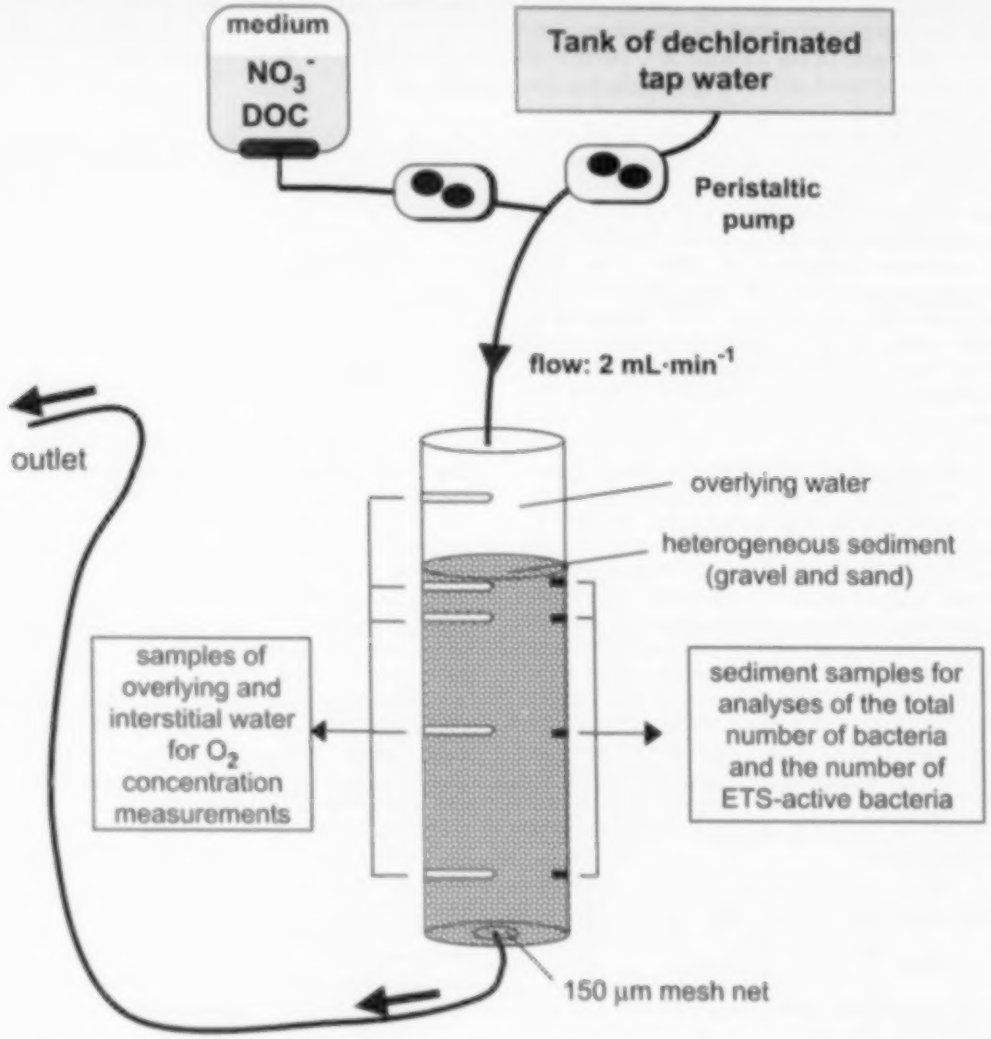
medium
NO_3^-
DOC
Tank of dechlorinated tap water
Peristaltic pump
flow: 2 mL·min^{-1}
outlet
overlying water
heterogeneous sediment (gravel and sand)
samples of overlying and interstitial water for O_2 concentration measurements
sediment samples for analyses of the total number of bacteria and the number of ETS-active bacteria
150 µm mesh net

6500, and 13 000 individuals·m^{-2} for asellids, chironomids and tubificid worms, respectively. These densities approached those observed in natural gravel–sand sediments of braided channels of the Rhône River (Fruget 1989; Martinet 1993). The organisms were collected at three sites: a dead arm of the Rhône River about 20 km upstream of Lyon, the Semène River, and the Ardière River. For acclimation to the experimental conditions (sediment grain sizes and food), animals were maintained in the laboratory for more than 30 days before introduction into the microcosms. The first measurements (day 0) confirmed consistency in conditions among the four columns of each experiment before introduction of the invertebrates. After this, invertebrates were introduced in the overlying water of the columns.

Sediment reworking was estimated after 20 days of experimentation. O_2 concentrations and bacterial parameters were also measured on day 20. Dissolved O_2 concentrations were measured at five depths (5 cm above the sediment surface and 1, 5, 15, and 35 cm below the sediment surface), and bacterial parameters (bacterial abundance and numbers of ETS-active bacteria on fine sediment) were evaluated at four depths in the sediment (1, 5, 15, and 35 cm below the sediment surface).

Methods of analysis

Sediment reworking in the columns was quantified by the luminophore tracer technique (Gérino 1990). To reproduce the grain size heterogeneity of the sand present in the columns, we used two size fractions of luminophores (natural sediment particles dyed with fluorescent paint): 63- to 100-µm particles (pink) and 100- to 350-µm particles (yellow). On day 0 of each experiment, a mixture of the two fractions (0.5 grams per fraction) was deposited at the surface of the sediment of the four columns before invertebrate introduction. After a 20-

day period, water was removed from all columns and columns were opened to allow sampling of sediment and luminophores. The top 2 cm of sediment was collected at 0.5-cm intervals and the next 18 cm collected at 1-cm intervals. Each layer was homogenized and a 1-g subsample was dried at 50 °C for luminophore counting. The number of luminophores in each subsample was estimated using an ultraviolet light microscope and converted into grams of tracers per gram of dry sediment.

The effect of invertebrates on particle transport was estimated using the diffusion–advection–nonlocal model in non-steady-state conditions (Mugnai et al. 2003). This model links a nonlocal component to a diffusion–advection model (Officer and Lynch 1982; Gérino et al. 1994). Biological diffusive transport (diffusion (D), square centimetres per year) was defined as omnidirectional transport in the sediment column and is analogous to molecular diffusion in water. Biodiffusion spreads tracers in the sediment column (Guinasso and Schink 1975) by the exchange of small amounts of material with adjacent parcels of sediment. Most deposit-feeding activities result in the vertical transport of material, which cannot be fitted with diffusional models. Biologically mediated vertical transports account for advective transport and nonlocal transport. Bioadvection (V, centimetres per year) is created by head-down deposit-feeders like worms that feed in the deeper sediment and egest fecal pellets at the surface (conveyor belt organisms). This feeding mode causes an accelerated rate of sediment and pore water burial within the feeding zone. Nonlocal transport results from largely open burrows into which surface particles may fall, and this type of vertical transport is much more rapid than bioadvection. This nonlocal mixing is modeled as a removal function that simulates the deposition of surface material (expressed in grams of transported tracer per day) in a deposition zone. The basic equation is

$$(1)\qquad \frac{\partial C(z,t)}{\partial t} = D\frac{\partial^2 C(z,t)}{\partial z^2} - V\frac{\partial C(z,t)}{\partial z} + K(z,t) - R(z,t)$$

where C is the normalized tracer concentration, t is time (years), z is depth (centimetres), D is the diffusive mixing rate (square centimetres per year), V is the advective transport rate (centimetres per year), R is the removal function that determines the mass of tracer (grams per day) removed from the surface and K is the injection function of the nonlocal transport that simulates tracer inputs (grams per day) into the injection zone of the sediment column; K_e is a constant parameter (per day) estimated from the model, and depths $Z_{\min}$ and $Z_{\max}$ represent the upper and lower limits of the injection zone, respectively. The nonlocal transport is thus quantified by a flux of sediment removed from the surface. In this case, $R(z,t) = 0$ for $z > 0$ and $R(z,t) = K(z,t)$ $(Z_{\max} - Z_{\min})$ for $z = 0$ and $K(z,t) = K_e$ for $z \in Z_{\min},Z_{\max}]$ and $K(z,t) = 0$ for $z \notin [Z_{\min},Z_{\max}]$.

Luminophores were added as pulse input at the surface of the sediment at the beginning of each experiment so that the model was applied under non-steady-state conditions. Thus, model eq. 1 was used with the upper boundary condition of an instantaneous source of unit strength (maximal C of tracer) at $z = 0$ at $t = 0$, a lower boundary $C \rightarrow 0$ at $z \rightarrow \infty$, and initial condition $C = 0$ at $z > 0$. The general solution was given by Officer and Lynch (1982) as

$$(2)\qquad C(z,t) = \frac{1}{\sqrt{\pi Dt}}\exp\left[-\frac{(z-Vt)^2}{4Dt}\right] - \frac{V}{2D}\exp\left(\frac{Vz}{2D}\right)erfc\left(\frac{z+Vt}{\sqrt{4Dt}}\right) - R_e t + K_e t$$

with

$$R_e = K_e(Z_{\max} - Z_{\min})$$

and

$$erfc(x) = 1 - \frac{2}{\sqrt{\pi}}\int_0^x e^{-t^2}\,dt$$

where c is a normalized concentration relative to unit input. The model allows the calculation of the theoretical tracer concentration given suitable values of the parameters D, V, $Z_{\min}$, $Z_{\max}$, and K_e. These parameters were obtained from profiles that produced the best fit with the experimental data using the least squares method.

O_2 concentration was measured with the technique developed by Mermillod-Blondin et al. (2000*a*). At each depth, 30 mL of water was collected in a N_2 sparged bottle. This water circulated at a rate of 20 mL·min^{-1} through an Orbisphere-type respirometer chamber equipped with a Clarke-type electrode connected to an Orbisphere oxymeter (model 3600). This procedure allowed the measurement of dissolved O_2 concentrations in the samples without contact with atmospheric O_2.

The total number of bacteria was estimated by epifluorescence after 4′,6-diamidino-2-phenylindole (DAPI) staining (Porter and Feig 1980). Wet sediment (0.3–0.5 g) was suspended in 40 mL of filtered (on a 0.2-µm acetate membrane) distilled water and 10 mL of a solution of pyrophosphate (0.002 mol·L^{-1} final concentration) by sonication (Bioblock Vibracell 72041; for 180 s, power 2, duty cycle 50%). One millilitre of the suspension was filtered through a GF/D Whatman filter (mean pore size 2.7 µm) to eliminate the coarsest particles. Staining was performed by addition of 0.1 mL of DAPI solution (100 µg·L^{-1}) to 1 mL of the filtrate. After 10 min of incubation, the suspension was filtered on a GTBP Millipore membrane (mean pore size 0.2 µm), which was then washed, air-dried, and mounted in low-fluorescence immersion oil on a microscope glass slide. Bacterial counts were performed using an epifluorescence microscope (Zeiss microscope fitted with a 200-W mercury burner and a Zeiss 365-nm excitation filter). At least 30 randomly selected fields were counted per slide. Results were expressed as numbers of bacteria per gram of dry sediment.

The number of bacteria with an active ETS (ETS-active bacteria) was measured using 5-cyano-2,3-ditolyltetrazolium chloride staining (Rodríguez et al. 1992). Wet sediment (0.3–0.5 g) was incubated with a 1.38 mg 5-cyano-2,3-ditolyltetrazolium chloride·L^{-1} solution (final concentration) for 3 h at 20 °C and then sonicated using the same procedure as for DAPI with a dilution in 20 mL of pyrophosphate solution. Five millilitres of the suspension was processed and slides pre-

Fig. 2. Depth profiles (means ± SD) of luminophores (circles) in the eight treatments and calculated profiles (diamonds) obtained with the advection–diffusion–nonlocal model and the average coefficients of transport. Animal treatments: A, 25 asellids; C, 50 chironomids; T, 100 tubificid worms; A+C, 25 asellids + 50 chironomids; A+T; 25 asellids + 100 tubificid worms; C+T, 50 chironomids + 100 tubificid worms; A+C+T, 25 asellids + 50 chironomids + 100 tubificid worms.

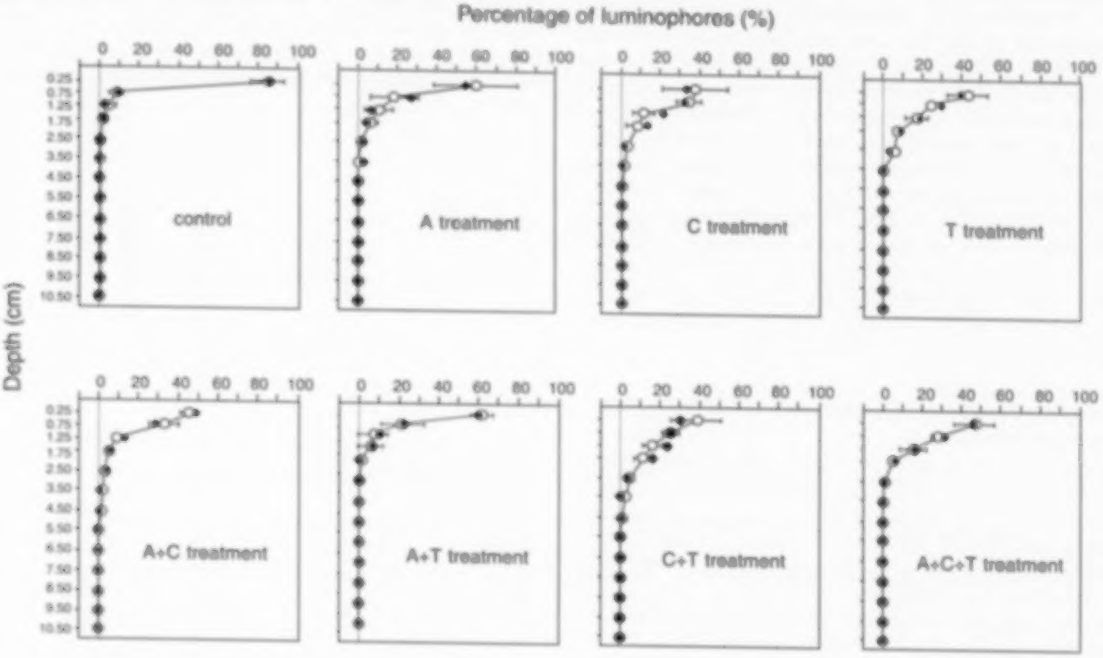

Table 1. Mixing rates of sediment estimated in the eight treatments.

Treatment	Advection (cm·year^{-1})	Diffusion (cm^2·year^{-1})	Nonlocal transport (g·day^{-1})	Z_{min} (cm)	Z_{max} (cm)
Control	0 (0)	1.06 (0.26)	0.013 (0.011)	0.875 (0.48)	1.875 (0.25)
A	0 (0)	3.3 (2.3)	0.043 (0.020)	1.27 (0.46)	3.73 (1.27)
C	0 (0)	8.23 (6.82)	0.068 (0.035)	0.67 (0.29)	2.33 (1.53)
T	0 (0)	7.8 (5.4)	0.023 (0.002)	0.83 (0.29)	3 (0)
A+C	0 (0)	4.23 (0.25)	0.047 (0.012)	0.83 (2.9)	3.33 (2.08)
A+T	0 (0)	2.4 (0.85)	0.040 (0.057)	1 (0)	2 (0)
C+T	0 (0)	13.13 (14.66)	0.036 (0.029)	1 (0.5)	2.17 (0.76)
A+C+T	0 (0)	6.0 (2.16)	0.011 (0.001)	1 (0)	2.17 (0.76)

Note: Advective, diffusive, and nonlocal transport coefficients are presented as means (SD) (n = 7 for control and n = 3 for animal treatments). Z_{min} and Z_{max} are the respective upper and lower limits of the sediment layer influenced by nonlocal transport. Animal treatments: A, 25 asellids; C, 50 chironomids; T, 100 tubificid worms; A+C, 25 asellids + 50 chironomids; A+T; 25 asellids + 100 tubificid worms; C+T, 50 chironomids + 100 tubificid worms; A+C+T, 25 asellids + 50 chironomids + 100 tubificid worms.

pared using the procedure for DAPI samples. Bacteria were counted with an epifluorescence microscope fitted with a 200-W mercury burner, a blue 420-nm excitation filter (Zeiss model BP 390-420), and a 540-nm barrier filter (Zeiss model LP 540). At least 30 randomly selected fields were counted per slide. Results were expressed as numbers of bacteria per gram of dry sediment.

At the end of each experiment, the living invertebrates were enumerated at three layers (0–10, 10–20, and 20–40 cm depth) of each column. The numbers of collected invertebrates were used to estimate the animal mortality and to provide information about the vertical distribution of invertebrates in columns.

Data treatment

Effect of each animal treatment

The data obtained in control columns of the seven experiments were combined in the statistical analyses. The sediment reworking coefficients obtained from the eight treatments were $\ln(x + 1)$ transformed to homogenize variances. Differences in transformed reworking coefficients were tested using a one-way analysis of variance (ANOVA). Bonferroni–Dunn post hoc tests were performed if significance was detected to determine which treatments differed. For each column, the O_2 concentrations measured in sediments were expressed as percentages of the value measured in the overlying water (= dissolved O_2 in water supplied to the column, mean values ± SD: 5.92 ± 0.24 mg·L^{-1}). In the analyses, the total number of bacteria and the number of ETS-active bacteria were log transformed. The effects of animals on O_2 concentrations and numbers of bacteria measured on day 20 were compared using a two-way ANOVA with treatment and depth as main effects (Statistica 5^{TM}; Statsoft, Tulsa, Oklahoma). Bonferroni–Dunn post hoc tests were performed to determine which treatments differed. Numbers of living invertebrates found at the end of the experiments were expressed as percentages. We compared the percentages of living animals between animal treatments using a one-way ANOVA. The numbers of animals found at the three sampling layers were also expressed as percentages. We tested the taxa and depth effects on invertebrate distributions using a two-way ANOVA with taxa and depth as main effects. Variables expressed as percentages (microbial variables) were arcsine transformed (Sokal and Rohlf 1995).

Impact of mixture in comparison with individual effects (measure of interactions)

Comparisons of effects of two- or three-taxa mixtures with effects of invertebrates in isolation were made by comparing sediment reworking coefficients, O_2 concentrations, and microbial variables in animal and control columns. Using single-taxon effects, we used an additive model similar to those described by Raffaelli et al. (2003, p. 137) against which we compared observed multitaxa effects. The interactions were measured as the differences between the observed effects with two- or three-taxa mixtures and the predicted effects of mixtures calculated by all combinations of the effects of the taxon in isolation (individual effects). For example, in the case of the A+C treatment, values calculated using the additive model (n = 9, 3 columns × 3 columns) = $E(\mathrm{A})_{n=3}$ + $E(\mathrm{C})_{n=3}$ were compared with observed values (n = 3) = $E(\mathrm{A+C})_{n=3}$, where E(A) and E(C) are asellid effect and chironomid effects in one-taxon experiments and E(A+C) is the value measured in the A+C experiment. With this method, we expected that, in the absence of interactions, the effects of 50 chironomids and the effects of 25 asellids would be simply added in the treatment with 50 chironomids + 25 asellids. Using this additive model, we assumed that effects measured in mixtures were linked to interactions between taxa rather than a simple effect of animal density. Because the impact of each invertebrate taxon in sediment was linked to its life mode (Mermillod-Blondin et al. 2002), the type of effect (production of tubes or galleries, sediment reworking mode) produced by a taxon in sediment was not expected to be strongly affected by its density. For O_2 concentrations and microbial variables, observed and predicted values were compared using a two-way ANOVA with observed–predicted and depth as main effects. For coefficients of sediment reworking, observed and predicted values were compared using Student t tests. A significant (negative or positive) difference indicates that interactions between taxa modified the system functioning because the effects of the two or three taxa were not reported in mixture treatments. In addition, it could be observed that the dominant effect of one taxon in mixtures can lead to the detection of significant interactions. Thus, the effects of mixtures were compared with the effects of each taxon forming the mixture to determine if one taxon present in the mixture drove the system functioning. Statistical tests used to compare mixture effects and one-taxon effects were the same as those used for observed–predicted comparisons.

Fig. 3. Coefficients (means ± SD) of (*a*) biodiffusion and (*b*) nonlocal transport (expressed as ln(x + 1)) measured in the eight treatments (open bars). Predicted coefficients (shaded bars) are indicated for the two- and three-taxa treatments. Animal treatments: A, 25 asellids; C, 50 chironomids; T, 100 tubificid worms; A+C, 25 asellids + 50 chironomids; A+T, 25 asellids + 100 tubificid worms; C+T, 50 chironomids + 100 tubificid worms; A+C+T, 25 asellids + 50 chironomids + 100 tubificid worms.

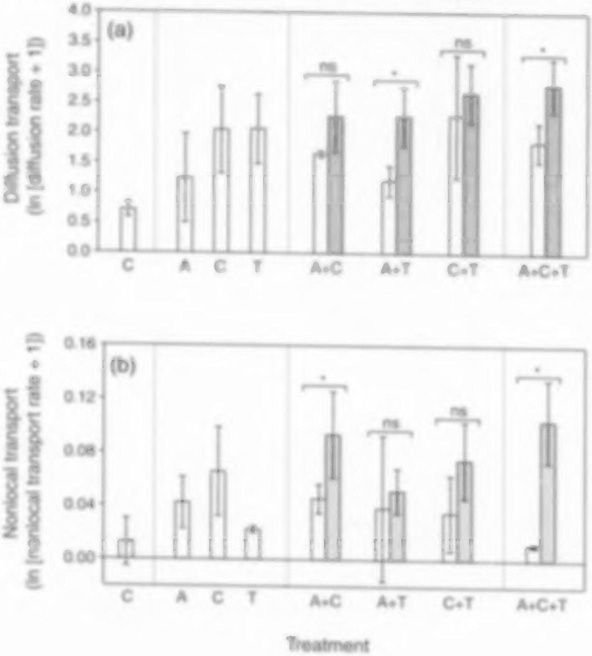

Results

Effects of animal treatments

The luminophore profiles obtained at the end of the experiments showed that the average percentage of tracer measured at the sediment surface (0–0.5 cm layer) was the highest in the control columns (87%) and varied from 62% to 38% in invertebrate treatments (Fig. 2). With the exception of chironomid treatment, the profiles were characterized by a rapid decrease of tracer with depth, indicating a biodiffusive reworking of sediment. With chironomids, similar concentrations of luminophore were measured in the 0–0.5 and 0.5–1 cm layers. This result was attributed to a nonlocal transport of the tracer from the surface to the 0.5–1 cm layer. Model data fit experimental data well (Fig. 2). The coefficients of sediment reworking from model simulations are shown in Table 1. No bioadvection was observed in the treatments. The biodiffusion coefficient varied significantly among treatments (Fig. 3; Table 2). With the exception of

Table 2. ANOVAs for the comparison among treatments (and depth for two-way ANOVA) on coefficients of sediment reworking, O_2 concentrations, and microbial parameters.

Variable	Source	df	*F*	*p*
One-way ANOVA				
Biodiffusion of surface particles	Treatment	7	4.6	<0.05
	Error	19		
Nonlocal transport of surface particles	Treatment	7	2.4	>0.05
	Error	19		
Two-way ANOVA				
O_2	Treatment	7	19.7	<0.001
	Depth	3	306.3	<0.001
	Treatment × depth	21	3.8	<0.001
	Error	80		
Total number of bacteria	Treatment	7	4	<0.001
	Depth	3	257.1	<0.001
	Treatment × depth	21	4.3	<0.001
	Error	80		
Number of ETS-active bacteria	Treatment	7	12.1	<0.001
	Depth	3	408.2	<0.001
	Treatment × depth	21	3.5	<0.001
	Error	80		

Table 3. Effects of each animal treatment on coefficients of sediment reworking, O_2 concentrations, and microbial characteristics (comparison with the control treatment).

	Animal treatment						
Variable	A	C	T	A+C	A+T	C+T	A+C+T
Biodiffusion	0	+	+	+	0	+	+
Nonlocal transport	0	+	0	+	0	0	0
Effect on O_2 concentrations	+	+	–	–	–	–	–
Effect on total number of bacteria	0	0	+	0	+	0	+
Effect on ETS-active bacteria	0	–	+	+	+	+	+

Note: Bonferroni–Dunn test with $n = 3$ for invertebrate treatments and $n = 7$ for the control. 0, no significant difference; +, significant increase; –, significant decrease owing to the invertebrates. Animal treatments: A, 25 asellids; C, 50 chironomids; T, 100 tubificid worms; A+C, 25 asellids + 50 chironomids; A+T; 25 asellids + 100 tubificid worms; C+T, 50 chironomids + 100 tubificid worms; A+C+T, 25 asellids + 50 chironomids + 100 tubificid worms.

the A and the A+T treatments, all invertebrate assemblages significantly increased the diffusion of surface sediment within the porous media (Table 3). No significant difference in nonlocal transport was measured among the different treatments (Table 2). However, C and A+C treatments had significantly higher nonlocal transport rates than the control (Table 3).

Whatever the treatment, O_2 concentration decreased with depth in all columns and this decrease was the highest in the top 5 cm of sediment (Fig. 4; Table 2). Significant decreases in total number of bacteria and number of ETS-active bacteria with depth were also observed in columns (Figs. 5 and 6; Table 2). For all variables, significant differences were measured among treatments. The A and the C treatments significantly increased the O_2 concentrations (Table 3). In contrast, the other animal treatments significantly reduced O_2 concentrations in the sediment. These significant differences depended on depth (two-way ANOVA, interaction taxa–depths) (Table 2), as most animal treatments had significantly higher effects in the top 5 cm of sediments. The same patterns were observed in number of ETS-active bacteria: all animal treatments significantly increased the number of active bacteria except the A treatment, which had no significant effect, and the C treatment, which reduced this bacterial variable in sediments. Like ETS-active bacteria, the total abundance of bacteria significantly decreased with depth and was different among treatments. The A treatment and C treatments had no significant effect on this variable. However, unlike results obtained with O_2 measurements and abundances of ETS-active bacteria, all of the other treatments did not increase the number of bacteria in the sediment (A+C and C+T treatments had no significant effects on this variable (Table 3)).

The results also showed that the variabilities among the effects of one-taxon treatments were higher than those obtained among multitaxa treatments (Table 3). For O_2 concentrations, the three one-taxon treatments did not have the same effect (increase or decrease of O_2 concentrations), whereas the same response of the system (a decrease of O_2 concentrations) was measured in all two- and three-taxa treatments. All two- and three-taxa treatments also produced a significant increase in the number of ETS-active bacteria. In contrast, with one taxon, increases or decreases in ETS-

Fig. 4. Depth profiles (means ± SD) of O_2 concentrations in the eight treatments. The depth profile of the control treatment (open circles) is reported on all graphs with each animal treatment (solid circles). Animal treatments: A, 25 asellids; C, 50 chironomids; T, 100 tubificid worms; A+C, 25 asellids + 50 chironomids; A+T; 25 asellids + 100 tubificid worms; C+T, 50 chironomids + 100 tubificid worms; A+C+T, 25 asellids + 50 chironomids + 100 tubificid worms.

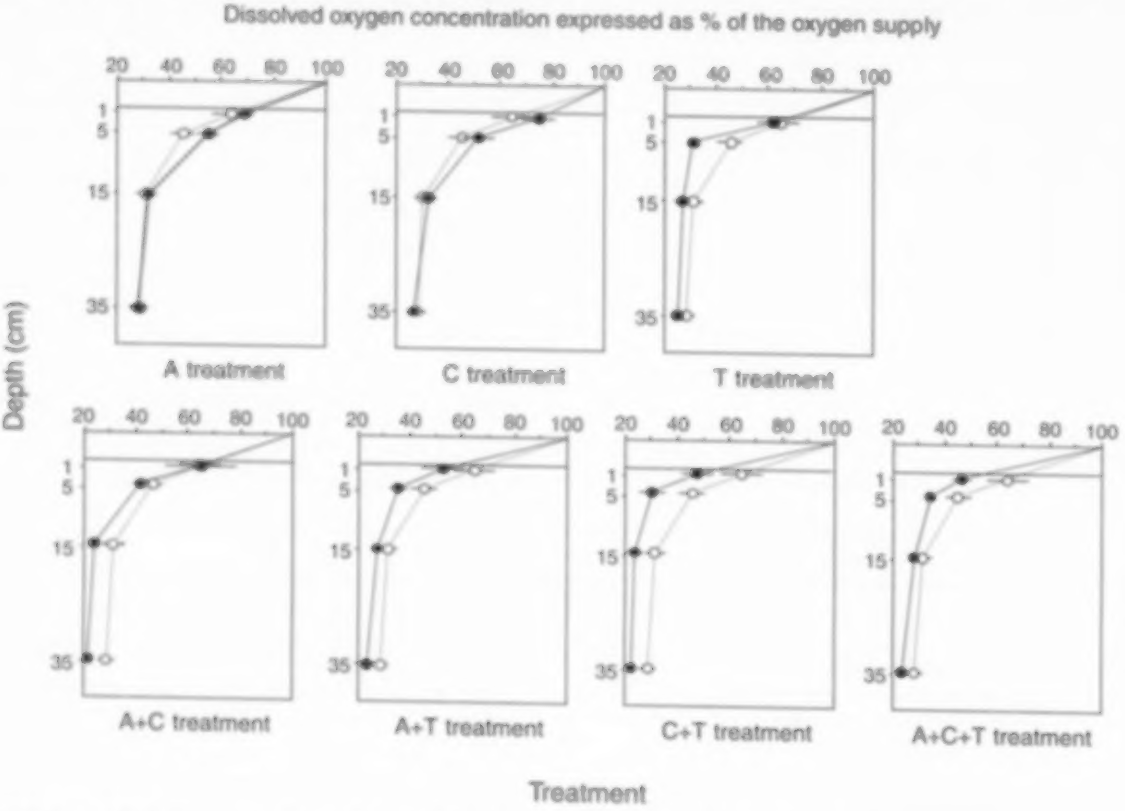

active bacteria abundances were observed depending on the taxon tested.

Estimation of the interactions between taxa

For both diffusion and nonlocal transport, the reworking coefficients measured in mixtures were in the range of values measured in one-taxon treatments (Fig. 3). However, the measured coefficients in mixtures tended to be lower than the predicted coefficients calculated from individual effects of the taxa. Significantly lower coefficients of biodiffusion were measured in A+T and A+C+T treatments in comparison with predictions. The nonlocal transports of surface sediment measured in the A+C and A+C+T treatments were significantly lower than those predicted.

Whatever the invertebrate mixture, all treatments produced significantly higher decreases in O_2 concentration than those predicted with the additive model (Fig. 7*a*). The effects of the A+C treatment decreased O_2 concentrations in columns, whereas A and C treatments had the opposite effect. Therefore, the mixture of asellids and chironomids created a significantly different effect than expected and the single-taxon effects (two-way ANOVA, measured data in mixture versus measured data in one-taxon treatments, $p < 0.01$). For the mixtures with tubificid worms, the O_2 concentrations were always lower at 1 cm depth in the mixture than in one-taxon treatments (two-way ANOVA, measured data versus calculated data and measured data in one-taxon treatments, $p < 0.01$) and significant differences between predicted and observed values in mixtures were detected (Fig. 7*a*).

In contrast, the interaction between taxa did not provide significant differences in bacterial abundances (total numbers and numbers of ETS-active bacteria) (Figs. 7*b* and 7*c*), except the interaction between chironomids and tubificids, which significantly increased the number of ETS-active bacteria in sediments (two-way ANOVA, measured data versus calculated data, $p < 0.05$). High variability in bacterial counting clearly limited statistical power. For instance, although the A+C treatment tended to increase the number of ETS-active bacteria at 5 and 15 cm depth, while calculated values showed the opposite trend, no significant difference between measured and predicted values was observed.

Estimated mortality and distribution of invertebrates at the end of the experiments

Whatever the invertebrate assemblage tested, the percentage of living invertebrates varied from 77% to 92% and was not significantly different among treatments (one-way ANOVA, $p = 0.11$) (Table 4). The number of invertebrates found at

Fig. 5. Depth profiles (means ± SD) of $\log_{10}$(total number of bacteria) in the eight treatments. The depth profile of the control treatment (open bars) is reported on all graphs with each animal treatment (solid bars). Animal treatments: A, 25 asellids; C, 50 chironomids; T, 100 tubificid worms; A+C, 25 asellids + 50 chironomids; A+T; 25 asellids + 100 tubificid worms; C+T, 50 chironomids + 100 tubificid worms; A+C+T, 25 asellids + 50 chironomids + 100 tubificid worms.

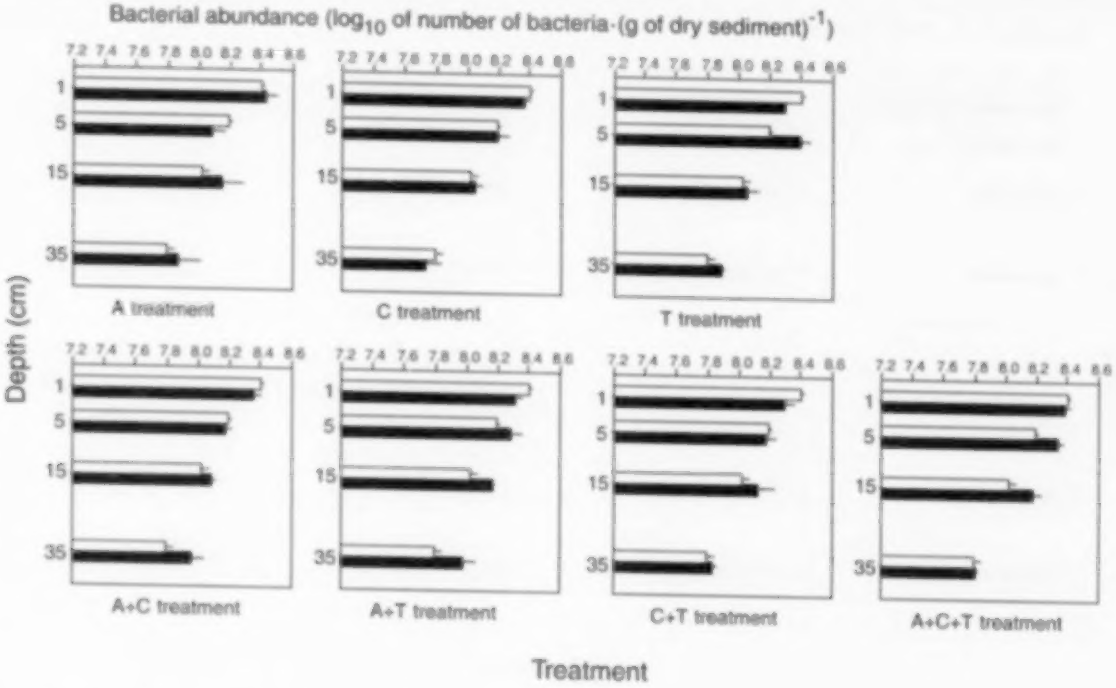

each layer of sediment showed that most animals (>90%) were observed in the first 10 cm of sediment (two-way ANOVA, depth effect, $p < 0.001$). Furthermore, no significant differences were measured in the vertical distribution of each taxon among treatments.

Discussion

Individual effects of the three taxa

In the river sediments, the three taxa showed significantly different bioturbation activities: asellids had no significant effect on surface sediment distribution, tubificid worms increased the biodiffusion of surface particles, and chironomids enhanced both biodiffusion and nonlocal transport of surface sediment in the porous media. As described in a previous study (Mermillod-Blondin et al. 2003), the pore water flow in sediment columns was characterized by a 50% mobile water phase in macropores (where water flow took place by advection), a 50% immobile phase in sandy zones (where water flow took place by diffusion), and an exchange coefficient of $0.15 \cdot h^{-1}$ between the mobile and immobile phases. Several studies (Molz et al. 1986; Murphy et al. 1997; Thullner et al. 2002) have shown that microbial activities are linked to O_2 and nutrient transport in porous media. Thus, the modification of hydrodynamics by bioturbation was expected to affect microbial characteristics in the experimental system. As a consequence, the distinct bioturbation processes performed by the three taxa may have modified hydrodynamics and nutrients availability for microorganisms in sediments (Mermillod-Blondin et al. 2002). The nonlocal transport of surface sediment produced by chironomids was due to the presence of tubes inserted into the sediments. The O_2 measurements showed that these tubes opened macropores through the sediment, which favoured a rapid transfer of O_2 to the deeper layers by concentrating the flow through pores (reducing the contact between mobile and immobile phases of water flow). This effect on water transport reduced the nutrient availability for bacteria in sandy zones and decreased microbial activity outside these pores, as indicated by the decrease in the number of ETS-active bacteria in chironomid treatment. The lack of surface sediment reworking by asellids was probably linked to their use of sediments restricted to the subsurface zone (1–3 cm), as demonstrated by Mermillod-Blondin et al. (2002). Despite a low redistribution of surface sediment by asellids, the sediment reworking in subsurface might have created macropores that concentrated the downward flow of water. As supposed for chironomid action, this change in hydrodynamics would reduce the contact time between water and the sandy zone and lead to the increase in O_2 concentrations measured in the foraging zone of asellids (0–5 cm below the sediment surface). In one-taxon experiments, the effect of tubificid worms on O_2 concentration was the opposite of that of the other two taxa. In contrast with asellids and chironomid larvae, which created macropores that limited the exchange of infiltrated water with sandy zones, tubificid worms built a dense network of galleries and ejected fecal pellets at the sediment surface (Mermillod-Blondin et al. 2001), producing increased

Fig. 6. Depth profiles (means ± SD) of $\log_{10}$(number electron transport system (ETS)-active bacteria) in the eight treatments. The depth profile of the control treatment (open bars) is reported on all graphs with each animal treatment (solid bars). Animal treatments: A, 25 asellids; C, 50 chironomids; T, 100 tubificid worms; A+C, 25 asellids + 50 chironomids; A+T, 25 asellids + 100 tubificid worms; C+T, 50 chironomids + 100 tubificid worms; A+C+T, 25 asellids + 50 chironomids + 100 tubificid worms.

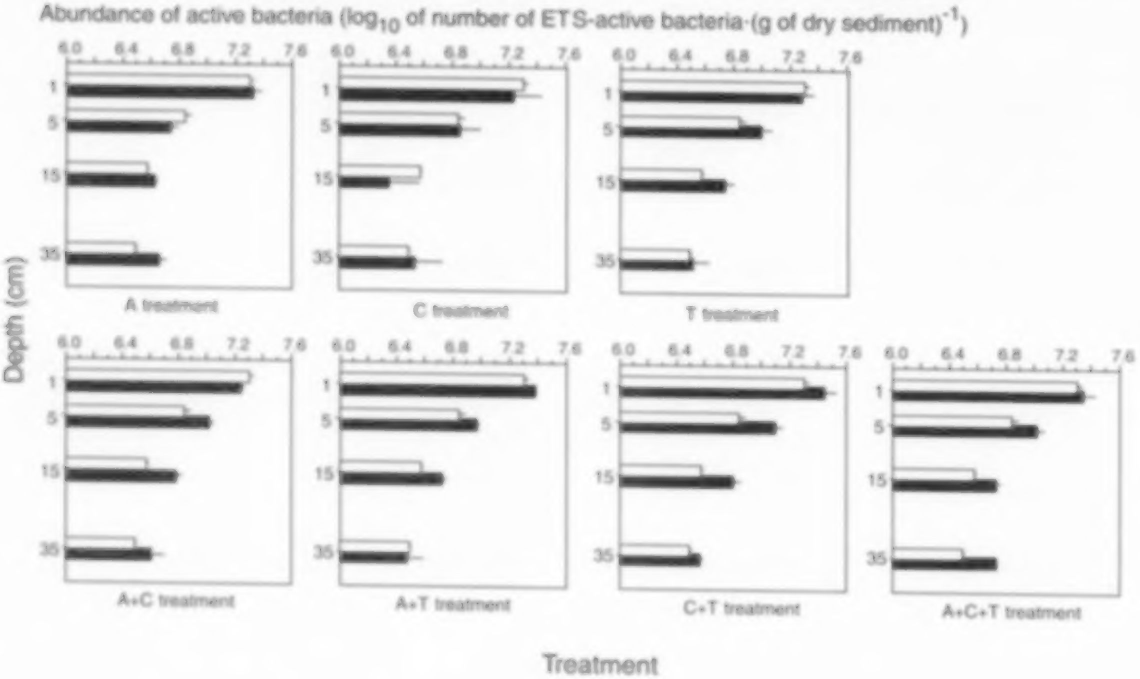

exchanges between mobile and immobile phases of water, which stimulated microbial activities in the sediment.

Effect of interactions on system functioning

The results of sediment reworking and O_2 measurements support the hypothesis that the mixture effect was not the sum of the individual effects of the taxa tested in the mixture. This lack of additive process was not due to the dominance of certain taxon in mixtures because mixture treatments always produced lower O_2 concentrations than predicted and observed in one-taxon treatments. These results suggest that interactions between taxa have strong effects on the functioning of the water–sediment interface. The sediment reworking induced by the assemblage of two taxa was mostly lower than the predicted one calculated with the additive model. These significant interactions measured between taxa on bioturbation processes probably resulted from a spatial competition among the three taxa, which lived and foraged in the same habitat (>90% of animals were found in the first 10 cm of sediment). As a consequence, these modifications of sediment reworking affected water transport and associated microbial activities. For example, O_2 concentration, which is an indicator of aerobic microbial activity in the controlled system, showed that interaction in bioturbation processes affected microbial respiration.

The interaction between asellids and chironomid larvae (A+C treatment) strongly affected microbial respiration. The association of the two taxa produced an opposite effect (O_2 decrease in sediments) compared with the A and C treatments (O_2 increase). The sediment reworking experiments showed that nonlocal transport was significantly lower in the assemblage than expected with the additive model. As chironomid tubes were responsible for nonlocal transport, this result suggests that burrowing by asellids destroyed the tubes produced by chironomids (Fig. 8). Therefore, this interaction may have limited the occurrence of continuous macropores in the sediment matrix, which was observed when each taxon was tested separately. The bioturbated zone produced by the assemblage of chironomids and asellids acted as a fine-sediment filter, increasing the dispersion of the water in the heterogeneous sediment and stimulating O_2 utilization by bacteria in the top 5 cm of sediment (according to O_2 decreases). The opposite effects observed in the A+C treatment in comparison with the A and the C treatments indicate that interactions between taxa can mask the specific role of each taxon. As a consequence, the assessment of the interaction between taxa is necessary to determine the role of invertebrate assemblages in river sediment processes.

As in the A+C treatment, the interactions between chironomids and tubificid worms strongly increased the aerobic microbial respiration (decrease in O_2) in the first centimetre of sediment. At this depth, O_2 concentration and ETS-active bacteria were the opposite of the effects observed with C and T treatments and the effects predicted by the additive model. Although there were no significant differences in sediment reworking between observed and predicted effects

Fig. 7. Measured (open circles and bars) and predicted (shaded circles and bars) effects (means ± SD, $n = 3$) of the two- and three-taxa assemblages on depth profiles of (*a*) O_2 concentrations, (*b*) total number of bacteria, and (*c*) numbers of electron transport system (ETS)-active bacteria. The results of the statistical comparison between observed and predicted values are indicated on the graphs (observed–predicted: **, significant difference; ns, no significant difference). Animal treatments: A+C, 25 asellids + 50 chironomids; A+T; 25 asellids + 100 tubificid worms; C+T, 50 chironomids + 100 tubificid worms; A+C+T, 25 asellids + 50 chironomids + 100 tubificid worms.

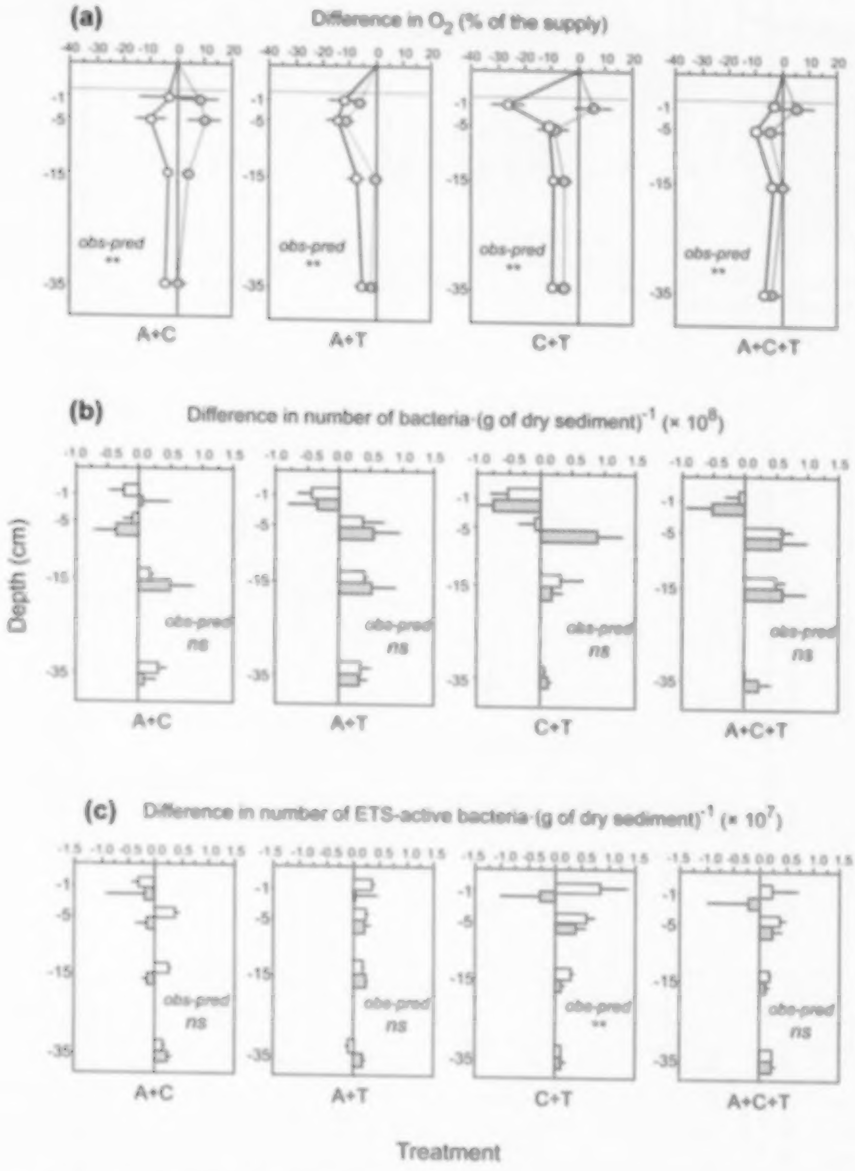

of the C+T treatment, the mean coefficient of nonlocal transport was twofold lower than the measured coefficient with chironomids and the predicted value. Tubificids produce fecal pellets at the water–sediment interface and we speculate that, in assemblages, fecal pellets deposited by worms filled the macropores produced by chironomid larvae, limiting the continuity of tubes. Therefore, the transport of surface particles within sediments and the rapid downward transfer of O_2 through macropores were reduced. The colonization of the fecal pellet surface by bacteria (Yingst and Rhoads 1980) may also have stimulated aerobic respiration in the top 5 cm of sediment.

The A+T and A+C+T treatments also indicated that interaction between taxa affected the bioturbation process (measured coefficients of surface sediment reworking were lower than those predicted) and resulted in increased O_2 respiration.

Table 4. Numbers of living invertebrates found on day 20 in the three animal columns of each animal treatment at three sediment layers.

	Animal treatment											
	One-taxon treatments			A+C		A+T		C+T		A+C+T		
	Asellids	Chironomids	Tubificids	Asellids	Chironomids	Asellids	Tubificids	Chironomids	Tubificids	Chironomids	Asellids	Tubificids
Column 1												
0–10 cm	21	43	79	19	40	20	79	40	80	39	21	70
10–20 cm	1	0	3	2	1	1	3	0	3	1	1	6
20–40 cm	0	0	0	0	0	0	0	0	0	0	0	0
% of living invertebrates	88	86	82	84	82	84	82	80	83	80	88	76
Total (%)	88	86	82	82.7		82.4		82.0			78.9	
Column 2												
0–10 cm	19	44	80	21	39	18	78	38	73	45	17	77
10–20 cm	1	0	2	1	0	2	2	1	5	0	1	2
20–40 cm	0	0	0	0	0	0	0	0	0	0	0	0
% of living invertebrates	80	88	82	88	78	80	80	78	78	90	72	79
Total (%)	80	88	82	81.3		80.0		78.0			81.1	
Column 3												
0–10 cm	23	41	74	20	40	18	74	37	80	39	22	82
10–20 cm	0	0	4	0	0	1	4	0	2	0	1	4
20–40 cm	0	0	0	0	0	0	0	0	0	0	0	0
% of living invertebrates	92	82	78	80	80	76	78	74	82	78	92	86
Total (%)	92	82	78	80.0		77.6		79.3			84.6	

Note: Estimated percentages of living invertebrates were indicated for each taxon. Animal treatments: A+C, 25 asellids + 50 chironomids; A+T; 25 asellids + 100 tubificid worms; C+T, 50 chironomids + 100 tubificid worms; A+C+T, 25 asellids + 50 chironomids + 100 tubificid worms.

Fig. 8. Schematic representation of the presumed interactions between invertebrates in the two-taxa treatments. This representation does not take into account a possible modification of the behaviour of the taxa when they were associated.

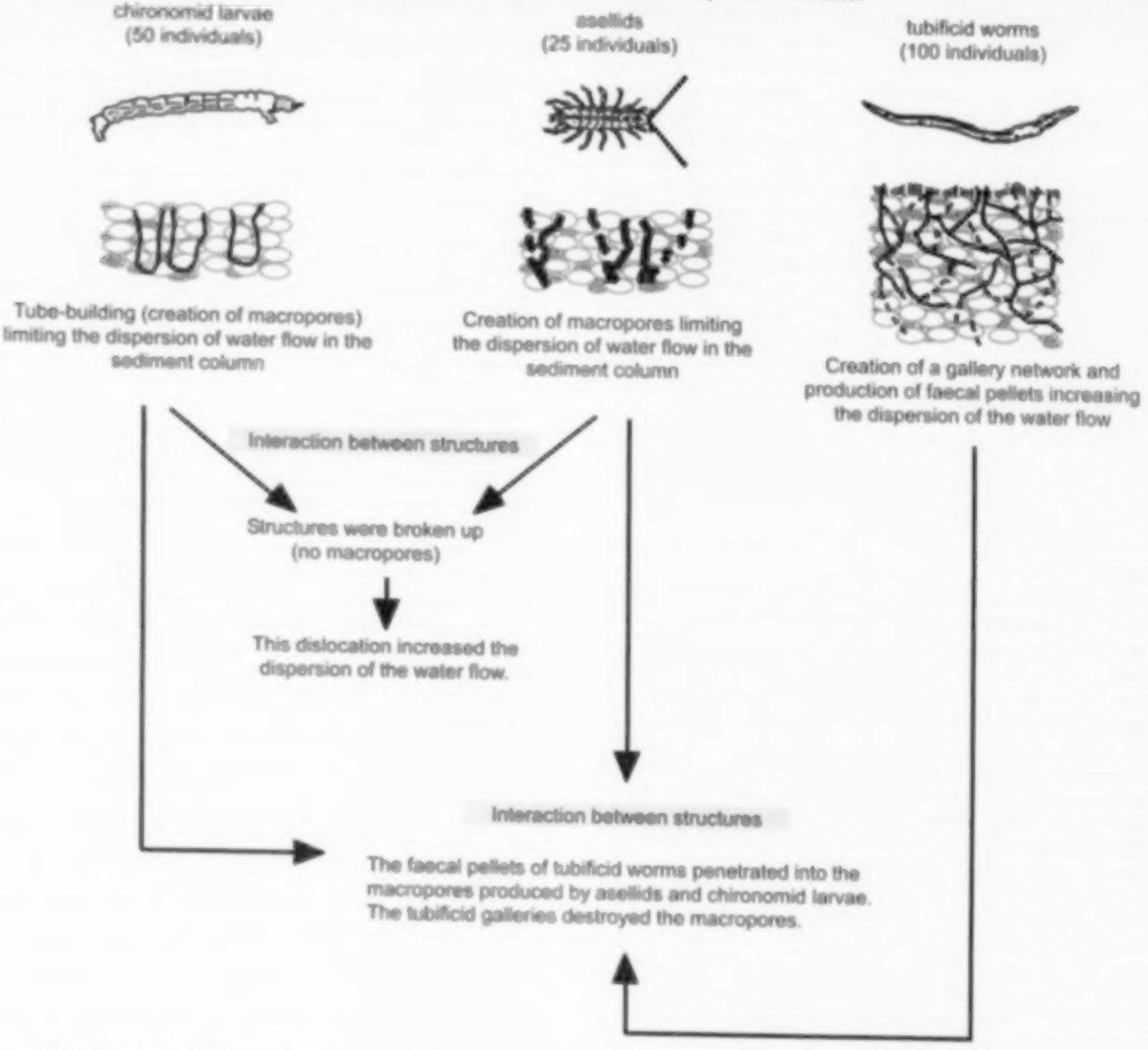
chironomid larvae
(50 individuals)
asellids
(25 individuals)
tubificid worms
(100 individuals)
Tube-building (creation of macropores) limiting the dispersion of water flow in the sediment column
Creation of macropores limiting the dispersion of water flow in the sediment column
Creation of a gallery network and production of faecal pellets increasing the dispersion of the water flow
Interaction between structures
Structures were broken up
(no macropores)
This dislocation increased the dispersion of the water flow.
Interaction between structures
The faecal pellets of tubificid worms penetrated into the macropores produced by asellids and chironomid larvae.
The tubificid galleries destroyed the macropores.

As explained previously, interactions between built structures (tubes, macropores, galleries, and fecal pellets) may explain the functioning of river sediments (Fig. 8). However, biogenic structure interaction may not be the only explanation. Despite the fact that the distribution of each taxon was not strongly modified by the presence of another taxon, the behaviour of one taxon (type and intensity of bioturbation) may be affected by another taxon and could also modify system processes.

In contrast with coefficients of sediment reworking and O_2 measurements, few significant interactions were measured among taxa on microbial variables. This result is probably linked to the high variability in bacterial counting but may also reflect the competing effects of invertebrates on bacteria (Riisgard and Banta 1998): the fauna grazes on biofilm and reduces the bacteria number but also stimulates bacterial growth rates, increasing the bacterial biomass (gardening effect) and the respiration rate of the microbial community.

Impact of taxa addition on system functioning

The results indicated that one-taxon treatments might increase (A and C treatments) or decrease (T treatment) O_2 concentrations in the sediment as a result of the different activities of fauna (burrowing and moving) in the porous media. In contrast, all two- and three-taxa treatments decreased O_2 concentration and stimulated the number of ETS-active bacteria in the sediment. This lower variability measured among two-taxa than among one-taxon treatments was mostly due to the interaction between asellids and chironomids, which created a complete shift in respiration process. Therefore, the fact that interactions between taxa can reduce the variability in several processes supports the assumption that functioning variability decreases with taxa number (Naeem and Li 1997). The similar modifications of microbial processes observed with two and three taxa can also be of great importance for the stability of ecosystem functioning. This result suggests that addition of a new taxon did not significantly modify the functioning of a system with two taxa (whatever the characteristics of the added taxon). Because each taxon can tolerate only a limited range of physico-chemical and biotic conditions (Tachet et al. 2000), any change in environment (e.g., pollution) beyond these conditions leads to its extinction. Therefore, in the case of environmental changes, the occurrence of three taxa rather than two taxa in the community should provide "insurance" (Chapin et al. 1992; Yachi and Loreau 1999) for the functioning of the sediment–water interface. In other words, a higher number of detritivorous taxa should enhance the probability that the river sediment system will provide a consistent level of performance over a given unit of time. This similar effect of two-taxa and three-taxa treatments also suggests that, beyond a given number of taxa, the physical modification of the system was limited to a threshold level of modification of system functioning (sediment reworking, stimulation of bacteria, and O_2 consumption).

Perspectives

Although our results demonstrated the significant impact that bioturbator interactions have on several river sediment processes, our study used a simplified experimental system with average natural density of each taxon and a limited number of taxa. For example, the impact of density of each taxon and assemblages of taxa on ecosystem functioning has not been tested for all treatments (except for tubificid worms; Mermillod-Blondin et al. 2001) because our additive model supposed that animal density did not strongly affect the impact of asellids or chironomids. The opposite effect of A+C treatment on O_2 concentration in the top 5 cm of sediment in comparison with the A and C treatments supports our assumption because it is very improbable that bioturbation activities of chironomids and asellids (tube building and reworking of fine sediment) leading to O_2 increases would be affected by animal density. However, further investigations using variable densities of each taxon in assemblages should be developed to analyse the possible density-dependent impact on system functioning. Extending the experimental approach developed here to assemblages with much higher species richness is also needed to better understand the links between invertebrate diversity and river sediment functioning.

Acknowledgments

This work was a part of the programme entitled "Rôle de la diversité des invertébrés à l'interface sédimentaire eaux de surface – eaux souterraines" supported by the French National Centre for Scientific Research (CNRS) (No. 98N62/0144, "Programme Environnement Vie et Sociétés") within the programme "Biodiversité et Fonctionnement des Ecosystèmes (Programme National Dynamique de la Biodiversité et Environnement)". We thank G. Fauvet for his assistance in microbial analyses; J.-L. Reygrobellet and L. Mauclaire for their assistance in collecting invertebrates; and C.P. Henry, F. Malard, and M.-J. Olivier for reviewing a previous draft of this manuscript.

References

Battin, T.J., Kaplan, L.A., Newbold, J.D., and Hendricks, S.P. 2003. A mixing model analysis of stream solute dynamics and the contribution of hyporheic zone to ecosystem function. Freshw. Biol. **48**: 995–1014.

Boulton, A.J. 2000. The functional role of the hyporheos. Verh. Int. Ver. Limnol. **27**: 51–63.

Boulton, A.J., Findlay, S., Marmonier, P., Stanley, E.H., and Valett, H.M. 1998. The functional significance of the hyporheic zone in streams and rivers. Annu. Rev. Ecol. Syst. **29**: 59–81.

Chapin, F.S., Schulze, E.-D., and Mooney, H.A. 1992. Biodiversity and ecosystem processes. Trends Ecol. Evol. **7**: 107–108.

Danielopol, D.L. 1989. Groundwater fauna associated with riverine aquifers. J. North Am. Benthol. Soc. **8**: 18–35.

Emmerson, M.C., and Raffaelli, D.G. 2000. Detecting the effects of diversity on measures of ecosystem function: experimental design, null models and empirical observation. Oikos, **91**: 195–203.

Emmerson, M.C., Solan, M., Emes, C., Paterson, D.M., and Raffaelli, D. 2001. Consistent patterns and the idiosyncratic effects of biodiversity in marine ecosystems. Nature (London), **411**: 73–77.

Fruget, J.-F. 1989. L'aménagement du bas-Rhône. Évolution du fleuve et influence sur les peuplements de macro-invertébrés benthiques. Ph.D. thesis, University Lyon-I, France.

Fukuhara, H., and Sakamoto, M. 1987. Enhancement of inorganic nitrogen and phosphate release from lake sediment by tubificid worms and chironomid larvae. Oikos, **48**: 312–320.

Gérino, M. 1990. The effects of bioturbation on particle redistribution in Mediterranean coastal sediment — preliminary results. Hydrobiologia, **207**: 251–258.

Gérino, M., Stora, G., and Durbec, J.P. 1994. Quantitative estimation of biodiffusive and bioadvective sediment mixing: in situ experimental approach. Oceanol. Acta, **17**: 547–554.

Griebler, C. 1996. Some applications for the DMSO-reduction method as a new tool to determine the microbial activity in water-saturated sediments. Arch. Hydrobiol. Suppl. **113**: 405–410.

Grimm, N.B., and Fisher, S.G. 1984. Exchange between interstitial and surface water: implication for stream metabolism and nutrient cycling. Hydrobiologia, **111**: 219–228.

Guinasso, N.L., and Schink, D.R. 1975. Quantitative estimates of biological mixing rates in abyssal sediments. J. Geophys. Res. **80**: 3032–3043.

Hansen, K., and Kristensen, E. 1998. The impact of the polychaete *Nereis diversicolor* and enrichment with macroalgal (*Chaetomorpha linum*) detritus on benthic metabolism and nutrient dynamics in organic-poor and organic-rich sediment. J. Exp. Mar. Biol. Ecol. **231**: 201– 223.

Jones, C.G., Lawton, J.H., and Shachak, M. 1994. Organisms as ecosystem engineers. Oikos, **69**: 373–386.

Jonsson, M., and Malmqvist, B. 2003. Mechanisms behind positive diversity effects on ecosystem functioning: testing the facilitation and interference hypotheses. Oecologia, **134**: 554–559.

Loreau, M., Naeem, S., Inchausti, P., Bengtsson, J., Grime, J.P., Hector, A., Hooper, D.U., Huston, M.A., Raffaelli, D., Schmid, B., Tilman, D., and Wardle, D.A. 2001. Biodiversity and ecosystem functioning: current knowledge and future challenges. Science (Washington, D.C.), **294**: 804–808.

Loreau, M., Naeem, S., and Inchausti, P. (*Editors*). 2002. Biodiversity and ecosystem functioning. Oxford University Press, Oxford, UK.

Malard, F., and Hervant, F. 1999. Oxygen supply and the adaptations of animals in groundwater. Freshw. Biol. **41**: 1–30.

Marmonier, P., Fontvieille, D., Gibert, J., and Vanek, V. 1995. Distribution of dissolved organic carbon and bacteria at the interface between the Rhône River and its alluvial aquifer. J. North Am. Benthol. Soc. **14**: 382–392.

Martinet, F. 1993. Le macrobenthos limnivore, descripteur des flux organiques liés aux sédiments : exemples dans diverses annexes fluviales du Rhône. Ph.D. thesis, University Lyon-I, France.

Mermillod-Blondin, F., Creuzé des Châtelliers, M., Gérino, M., and Gaudet, J.-P. 2000*a*. Testing the effect of *Limnodrilus* sp. (Oligochaeta, Tubificidae) on organic matter and nutrient processing in the hyporheic zone: a microcosm method. Arch. Hydrobiol. **149**: 467–487.

Mermillod-Blondin, F., Creuzé des Châtelliers, M., Marmonier, P., and Dole-Olivier, M.-J. 2000*b*. Distribution of solutes, microbes and invertebrates in river sediments along a riffle–pool–riffle sequence. Freshw. Biol. **44**: 255–269.

Mermillod-Blondin, F., Gérino, M., Degrange, V., Lensi, R., Chassé, J.-L., Rard, M., and Creuzé des Châtelliers, M. 2001. Testing the functional redundancy of *Limnodrilus* and *Tubifex* (Oligochaeta, Tubificidae) in hyporheic sediments: an experimental study in microcosms. Can. J. Fish. Aquat. Sci. **58**: 1747–1759.

Mermillod-Blondin, F., Gérino, M., Degrange, V., and Creuzé des Châtelliers, M. 2002. Functional diversity of bioturbation by three detritivorous hyporheic invertebrates: an experimental study in microcosms. J. North Am. Benthol. Soc. **21**: 132–149.

Mermillod-Blondin, F., Gaudet, J.-P., Gérino, M., Desrosiers, G., and Creuzé des Châtelliers, M. 2003. Influence of macroinvertebrates on physico-chemical and microbial processes in hyporheic sediments. Hydrol. Processes, **17**: 779–794.

Molz, F.J., Widdowson, M.A., and Benefield, L.D. 1986. Simulation of microbial growth dynamics coupled to nutrient and oxygen transport in porous media. Water Resour. Res. **22**: 1207–1216.

Morrice, J.A., Dahm, N.D., Valett, H.M., Unnikrishna, P.V., and Campana, M.E. 2000. Terminal electron accepting processes in the alluvial sediments of a headwater stream. J. North Am. Benthol. Soc. **19**: 593–608.

Mugnai, C., Gérino, M., Frignani, M., Sauvage, S., and Bellucci, L.G. 2003. Bioturbation experiments in the Venice lagoon. Hydrobiologia, **494**: 245–250.

Murphy, E.M., Ginn, T.R., Chilakapati, A., Resch, C.T., Phillips, J.L., Wietsma, T.W., and Spadoni, C.M. 1997. The influence of physical heterogeneity on microbial degradation and distribution in porous media. Water Resour. Res. **33**: 1087–1103.

Naeem, S., and Li, S. 1997. Biodiversity enhances ecosystem reliability. Nature (London), **390**: 507–509.

Naeem, S., Thompson, L.J., Lawler, S.P., Lawton, J.H., and Woodfin, R.M. 1994. Declining biodiversity can alter the performance of ecosystems. Nature (London), **368**: 734–737.

Officer, C.B., and Lynch, D.R. 1982. Interpretation procedures for the determination of sediment parameters from time-dependent flux inputs. Earth Planet. Sci. Lett. **61**: 55–62.

Porter, K.G., and Feig, Y.S. 1980. The use of DAPI for identifying and counting aquatic microflora. Limnol. Oceanogr. **25**: 943–948.

Raffaelli, D., Emmerson, M., Solan, M., Biles, C., and Paterson, D. 2003. Biodiversity and ecosystem processes in shallow coastal waters: and experimental approach. J. Sea Res. **49**: 133–141.

Riisgard, H.U., and Banta, G.T. 1998. Irrigation and deposit feeding by the lugworm *Arenicola marina*, characteristics and secondary effects on the environment — a review of current knowledge. Vie Milieu, **48**: 243–257.

Rodriguez, G.G., Phipps, D., Ishiguro, K., and Ridgway, H.F. 1992. Use of a fluorescent redox probe for direct visualization of actively respiring bacteria. Appl. Environ. Microbiol. **58**: 1801–1808.

Sokal, R.R., and Rohlf, J. 1995. Biometry. 3rd ed. W.H. Freeman and Co., New York.

Stief, P., and de Beer, D. 2002. Bioturbation effects of *Chironomus riparius* on the benthic N-cycle as measured using microsensors and microbiological assays. Aquat. Microb. Ecol. **27**: 175–185.

Tachet, H., Richoux, P., Bournaud, M., and Usseglio-Polatera, P. 2000. Invertébrés d'eau douce : systématique, biologie, écologie. CNRS Editions, Paris.

Thullner, M., Mauclaire, L., Schroth, M.H., Kinzelbach, W., and Zeyer, J. 2002. Interaction between water flow and spatial distribution of microbial growth in a two-dimensional flow field in saturated porous media. J. Contam. Hydrol. **58**: 169–189.

Torreiter, P., Pitaksintorn-Watanamahart, P., and Danielopol, D.L. 1994. The activity of oligochaetes in relation to their ecological role in slow filtration columns. *In* Second International Conference on Groundwater Ecology, 27–30 March, Atlanta, USA. Environmental Protectin Agency, AWRA, Herndon, Va. pp. 85–94.

Triska, F.J., Duff, J.H., and Avanzino, R.J. 1993. The role of water exchange between a stream channel and its hyporheic zone in nitrogen cycling at the terrestrial–aquatic interface. Hydrobiologia, **251**: 167–184.

van der Heijden, M.G.A., Klironomos, J.N., Ursic, M., Moutoglis, P., Streitwolf-Engel, R., Boller, T., Wiemken, A., and Sanders, I.R. 1998. Mycorrhizal fungal diversity determines plant biodiversity, ecosystem variability and productivity. Nature (London), **396**: 69–72.

Wardle, D.A., Bonner, K.I., and Nicholson, K.S. 1997. Biodiversity and plant litter: experimental evidence which does not support the view that enhanced species richness improves ecosystem function. Oikos, **79**: 247–258.

Yachi, S., and Loreau, M. 1999. Biodiversity and ecosystem productivity in a fluctuating environment: the insurance hypothesis. Proc. Natl Acad. Sci. USA, **96**: 1463–1468.

Yingst, J.Y., and Rhoads, D.C. 1980. The role of bioturbation in the enhancement of microbial turnover rates in marine sediments. *In* Marine benthic dynamics. *Edited by* K.R. Tenore and B.C. Coull. University of South Carolina Press, Columbia, S.C. pp. 407–422.

Interpopulation variation in early growth of threespine sticklebacks (*Gasterosteus aculeatus*) under laboratory conditions

Hazel A. Wright, Robert J. Wootton, and Iain Barber

Abstract: Logistical difficulties associated with accurately measuring juvenile stages have contributed to a lack of detailed information on population-level variation in the early growth of fish. In this study, we used computerised image analysis to determine the trajectories of early growth, from hatching to 126 days posthatch, of replicated, laboratory-bred, full-sibling groups of threespine stickleback (*Gasterosteus aculeatus*) from five resident freshwater populations. Sibling groups were held under controlled "common garden" conditions and fed ad libitum, to excess, and standard lengths (SL) of all individuals in each sibling group were recorded at regular intervals over four separate time periods (0–6, 6–38, 38–70, and 70–126 days). Although there was no significant population-level variation in SL at hatching, we detected significant population-level differences in growth trajectory after 38 days and population differences in mean SL of up to 6.8 mm (16.6%) by 126 days. Our results suggest that population-level variation in the intrinsic growth rates of juvenile sticklebacks has a strong genetic component.

Résumé : Des problèmes logistiques reliés à la mesure exacte des jeunes stades de poissons expliquent en partie le manque d'information détaillée sur la variation de la croissance initiale à l'échelle de la population. Au cours de notre étude, nous avons utilisé un système d'analyse d'images par ordinateur pour déterminer les trajectoires de la croissance initiale, de l'éclosion à l'âge de 126 jours après l'éclosion, chez des groupes dédoublés d'épinoches à trois épines (*Gasterosteus aculeatus*) issus de mêmes parents, élevés en laboratoire et provenant de cinq populations établies d'eau douce. Les groupes de frères et soeurs ont été maintenus dans des conditions contrôlées de « jardin commun » et nourris à volonté à l'excès; nous avons mesuré la longueur standard (SL) de tous les individus de chaque groupe de frères et soeurs à intervalles réguliers durant quatre périodes (0–6, 6–38, 38–70 et 70–126 jours). Bien qu'il n'y ait pas de variation significative de SL à l'échelle de la population à l'éclosion, nous avons décelé des différences significatives à l'échelle de la population dans la trajectoire de croissance après 38 jours et des différences de SL moyenne pouvant atteindre 6,8 mm (16,6 %) au jour 126. Nos résultats laissent croire que la variation à l'échelle de la population des taux intrinsèques de croissance chez les jeunes épinoches a une forte composante génétique.

[Traduit par la Rédaction]

Introduction

For species with widespread geographical ranges, adult body size is often the most diverse of all physical characters (Mayr 1963) and this is true of many fishes (e.g., McPhail 1977). For ectothermic organisms, which show indeterminate growth, environmental factors such as water temperature regimes are central in determining maximum achievable growth rates (Mills 1988; Jensen et al. 2000). Genetic variation in growth between populations of the same species may reflect local adaptation to such environmental factors (Jensen et al. 2000). Such genetic differences may persist for several generations even if organisms are reared under identical conditions (e.g., Levinton 1983; Conover 1990).

Genetically based interpopulation variation in maximum attainable growth rates has been widely demonstrated in ectotherms (e.g., Travis 1981; Stearns 1983; Schultz and Conover 1997) and has been associated with differences in provenance, linked to latitude (e.g., Conover and Present 1990; Schultz et al. 1998) and altitude (e.g., Cavalli et al. 2002). Genetic variation in growth rate suggests that body size (or growth rate itself) may be an important adaptive trait, as the physiological efficiencies of a population should be maximised by natural selection (Slobodkin and Rapoport 1972) and this argument that there should be selection for rapid growth is often supported by early life history studies (e.g., Miller et al. 1988; Pepin 1991). For example, faster-growing larvae have a better chance of survival and avoid starvation and predation better than smaller larvae (Jones 2002). In the later stages, faster growth rates, leading to larger body size at age, are thought to confer benefits such as refuge from competitors (Arendt 1997) and certain predators (e.g., Power 1987 but see Billerbeck et al. 2001; Lankford et al. 2001), earlier maturation (Morita and Morita 2002), increased fecundity (Wootton 1976), and the increased capacity to endure food deprivation. The latter is known to be

Received 17 October 2003. Accepted 24 April 2004. Published on the NRC Research Press Web site at http://cjfas.nrc.ca on 16 December 2004.
J17798

H.A. Wright,[1] R.J. Wootton, and I. Barber. Institute of Biological Sciences, University of Wales Aberystwyth, Edward Llwyd Building, Aberystwyth, Ceredigion, Wales SY23 3DA, UK.

[1] Corresponding author (email: haw00@aber.ac.uk).

Can. J. Fish. Aquat. Sci. **61**: 1832–1838 (2004) doi: 10.1139/F04-119

especially important where size-dependent winter mortality occurs (Conover and Present 1990; Schultz and Conover 1997; Schultz et al. 1998). However, the benefits of rapid growth may be countered by associated costs, such as increased fluctuating asymmetry (Robinson and Wardrop 2002), reduced scale strength (Arendt et al. 2001), decreased cranial ossification (Arendt and Wilson 1999), reduced immune capacity, and reduced ability to respond to environmental stress (Arendt and Wilson 1997). Observed maximum growth rates may therefore reflect an adaptive trade-off between the benefits and costs of fast growth.

To separate genetic and environmental aspects of growth rate variation, "common garden" experiments are often required. However, because of logistic difficulties associated with measuring small fish, few such experiments have examined early growth in small fishes (but see Schultz et al. 1996; Barfoot et al. 1999 for notable exceptions). In addition, most studies have been concerned with commercially relevant, hatchery-reared fish (e.g., Krisfalusi and Cloud 1996; Svåsand et al. 1996). Consequently, there is a lack of information on population-level variation in early growth of small fishes from natural populations.

Field studies on one widely distributed, noncommercial species, the threespine stickleback, *Gasterosteus aculeatus*, have demonstrated differences in life history traits (Snyder 1989; Snyder and Dingle 1989; Baker and Foster 2002) that are attributable to provenance. For example, Snyder (1989) found differences in length-at-age in three populations of stickleback from northern California, differing in their degree of migration. These differences were demonstrated under common garden conditions and thus implicated genetic variation in this life history trait. Furthermore, migratory behaviour in stickleback was correlated with delayed reproduction, increased size at first reproduction, and increased fecundity such that migratory estuarine stickleback showed a delay in reproduction, were larger at first reproduction, and had larger clutch sizes than upstream, nonmigratory stickleback (Snyder and Dingle 1989). However, the timing of growth rates during ontogeny that generate such differences in adult size is still poorly described.

In the present study, the early growth (from hatching to 126 days posthatch (ph)) for five populations of *G. aculeatus* was followed under common garden conditions. Only early growth was examined to minimise diversion of somatic growth into sexual maturation. This is especially important as Trivers (1972) argues that selective factors affecting life history traits operate differently on males and females. Computerised image analyses reduced the difficulties associated with the measurement of size of the delicate larval and early juvenile fish and allowed a description of the temporal dynamics of growth in length. The aim of the study was to determine whether there were intrinsic differences in growth rates between the five populations and to identify when, during ontogeny, the differences occurred.

Materials and methods

Fish collection and husbandry

Sexually immature threespine sticklebacks from five geographically isolated stickleback populations (Aurs Burn, 55°47′59″N, 4°22′54″W, 40 m altitude; River Endrick, 56°03′34″N, 4°22′48″W, 40 m altitude; Llyn Frongoch, 52°21′41″N, 3°52′46″W, 290 m altitude; Hogganfield loch, 55°52′50″N, 4°10′15″W, 80 m altitude; River Kelvin, 55°54′03″N, 4°19′03″W, 40 m altitude) were housed under laboratory conditions in separate 72-L stock tanks. All fish were low plated morphs (leiurus form, sensu Wootton 1976) from resident (nonmigratory) populations. Fish were housed in the aquarium for 3 months before the start of the breeding programme to standardise any potential maternal effects (Svåsand et al. 1996) and fed ad libitum with *Artemia* nauplii and frozen bloodworm (Chironomid larvae). Light regimes (light (L) – dark (D)) and water temperature were maintained at levels to facilitate fish entering the breeding phase (16 h L – 8 h D, 19 ± 1 °C). A breeding programme was implemented from April to July 2001. Males developing nuptial colouration were removed from stock tanks, housed in individual 16-L aquaria (220 mm × 200 mm × 350 mm), and given daily visual access to gravid females from their own population until a nest was constructed. Receptive males were then allocated a gravid female and allowed to spawn. After a successful spawning, fertilised broods were removed and incubated artificially (see Barber and Arnott 2000 for details) until hatching occurred. Eggs from different spawnings were housed in separate incubators. All fish used in this study were, therefore, F1 progeny of wild caught parents, and all fry used were obtained in June 2001. No deaths occurred during the study period.

Growth study

On the day of hatching, six full-sibling fry (a "kin group") were removed from the incubator and transferred to a 16-L aquarium. Three kin groups were obtained from each population; none of the kin groups shared the same parents. Aquaria were assigned random positions within a temperature-controlled room and maintained at 18 ± 0.5 °C under 14 h L – 10 h D.

Unused fry were transferred to population-specific stock tanks. All fry were provided with 5 mL of concentrated protozoan culture ("infusoria", obtained by soaking hay in rainwater for several weeks) per day until 3 days ph. All other food was provided to excess. All tanks were checked twice daily, and no tank was without food through the duration of the study, allowing fish to feed to satiation. Freshly hatched *Artemia* nauplii were then provided until day 70; thereafter, all fish were fed bloodworm. On days 8 ph and 12 ph, 5 mL of infusoria was also provided in addition to the *Artemia*.

Fry measurement

The small size and fragility of young fry meant that early growth could not be accurately or safely measured using standard techniques for larger fish. Instead, fry were filmed on digital videotape and the images were analysed using computerised image-analysis software (Scion Image™, Adobe Photoshop™, and Image Tool™). Fry were filmed on the day of hatching (day 0) and then every 2 days until day 8 ph. Fry were then filmed every 4 days until day 38 ph. From this point, fish were filmed every 7 days until day 70 ph, after which fry were filmed once every 4 weeks for 3 months (total study period: 126 days). Kin groups were placed in a small glass crystallising dish (18 cm diameter) with a standardised water depth of 50 mm and were illuminated from beneath using a fluorescent light table (Barber and Svensson 2003). All fish were filmed when they touched the bottom of the crystallising dish. A 1-mm calibration grid, photocopied onto an acetate sheet, was placed underneath the crystallising dish to allow calibration of the analysis software. The total length (TL) of all fish was measured until the caudal peduncle could be observed clearly enough to use standard length (SL, at a total length of approximately 12.5 mm). To convert TL to SL, the relationship between TL and SL was calculated for fish (TL range 13–37 mm) from each population. Analysis of covariance (ANCOVA) was used to determine that there was no effect of provenance on either slope (ANCOVA, $F_{[4,124]} = 0.21$, $p = 0.93$) or elevation ($F_{[4,124]} = 1.18$, $p = 0.33$) of the relationships between SL and TL of sticklebacks, so data from all fish were combined to generate a single regression equation ($SL = 0.906TL + 0.200$, $r^2 = 0.996$), which was used to make standard length conversions.

Statistical analysis

All lengths were log-transformed before analysis to stabilise variances. A one-way analysis of variance (ANOVA) was used to compare within- and between-population variation in initial length at hatching (SL_0) and final length at the end of the study (SL_{126}). Post hoc Fisher's pairwise comparisons were used to identify between populations in which differences occurred, with the basic $\alpha = 0.05$. ANCOVA was used to determine the effect of initial length on final length. The growth in length was analysed by a repeated-measures ANOVA. Separate repeated-measures ANOVA of specific growth rates were carried out for periods 0–8, 8–38, 38–70, and 70–126 days ph (which corresponds to measurement intervals of 2, 4, 8, and 28 days, respectively. A Bonferroni correction was applied to determine the significance of the F ratios, with the basic $\alpha = 0.05$.

Results

Significant within-provenance differences in SL_0 were found among kin groups from the Aurs Burn (AB), River Kelvin (RK), and River Endrick (RE) sibling groups (AB, $F_{[2,17]} = 25.91$, $p < 0.001$; RK, $F_{[2,17]} = 28.48$, $p < 0.001$; RE, $F_{[2,17]} = 16.74$, $p < 0.001$), with only marginal differences between SL_0 of replicate groups from Llyn Frongoch (LF) and Hogganfield Loch (HL) provenances (LF, $F_{[2,17]} = 2.85$, $p = 0.089$; HL, $F_{[2,17]} = 3.59$, $p = 0.052$). However, there was no consistent effect of provenance on the mean SL_0 of kin groups ($F_{[4,14]} = 1.43$, $p = 0.294$).

ANCOVA showed that SL_0 had no significant effect on final length, SL_{126}. At the end of the study, there was no significant within-population variation in mean SL_{126} among sibling groups from the Kelvin ($F_{[2,17]} = 0.04$, $p = 0.956$), Hogganfield ($F_{[2,17]} = 1.89$, $p = 0.186$), Frongoch ($F_{[2,17]} = 3.39$, $p = 0.061$), and Endrick ($F_{[2,17]} = 0.86$, $p = 0.444$) populations, with sibling groups from Aurs Burn exhibiting only marginally significant differences in mean SL_{126} ($F_{[2,17]} = 3.87$, $p = 0.044$). However, there were significant differences in mean SL_{126} between populations ($F_{[4,14]} = 8.28$, $p = 0.003$). Fisher's pairwise comparison showed that kin groups from the Kelvin population (mean $SL_{126} = 40.88$ mm) had significantly higher mean SL_{126} than both the Endrick (mean $SL_{126} = 34.57$ mm) and Frongoch (mean $SL_{126} = 34.59$) populations. The mean SL_{126} for the River Endrick population was also significantly lower than the mean SL_{126} for the Aurs Burn population (mean $SL_{126} = 38.23$) (Fig. 1).

Growth in length continued throughout the experiment, but the rate of growth slowed as the fish got older (Figs. 2*a*, 2*b*). Repeated-measures ANOVA of length for the entire experimental period identified a marginally significant population × time interaction ($F_{[68,170]} = 1.509$, $p = 0.018$), suggesting there were some interpopulation differences in the trajectories of the increase in length.

In a more detailed analysis of the trajectories of increase in length, repeated-measures ANOVA for the period from hatching to day 6 ph (2 days between measurements) showed that length increased significantly ($F_{[3,30]} = 236.7$, $p < 0.000\,001$), but neither the population effect nor the population × time interaction was significant. Over the period day 6 ph to day 38 ph (4 days between measurements), there

Fig. 1. Interpopulation differences in mean standard length on day 0 (open bars) and on the final day (day 126, shaded bars). Final mean standard length (SL, mm) for River Endrick (RE) = 34.57, Llyn Frongoch (LF) = 34.59, Hogganfield Loch (HL) = 36.78, Aurs Burn (AB) = 38.23, and River Kelvin (RK) = 40.89. *, $p < 0.05$ after post hoc pairwise testing.

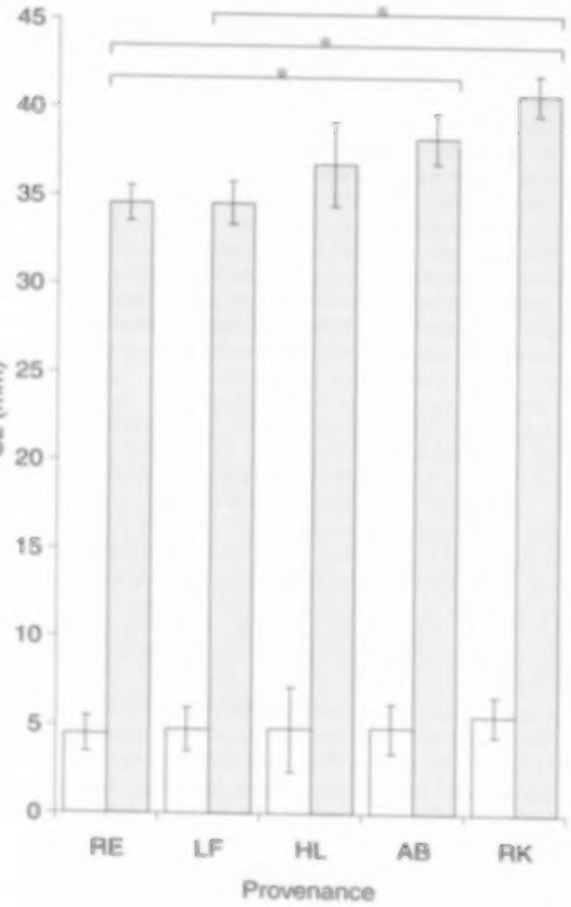

Fig. 2 (*a*) Growth trajectories (SL) and (*b*) log growth trajectories of the five populations over the 126-day study period. Changes in food items (ad libitum feeding) over the study period are shown. Analysis of growth trajectories was undertaken in four separate time periods (blocks I–IV). Significant interpopulation differences emerged from day 38 onwards (block III, $F_{[4,10]} = 4.842$, $p = 0.02$; block IV, $F_{[8,20]} = 4.230$, $p = 0.004$).

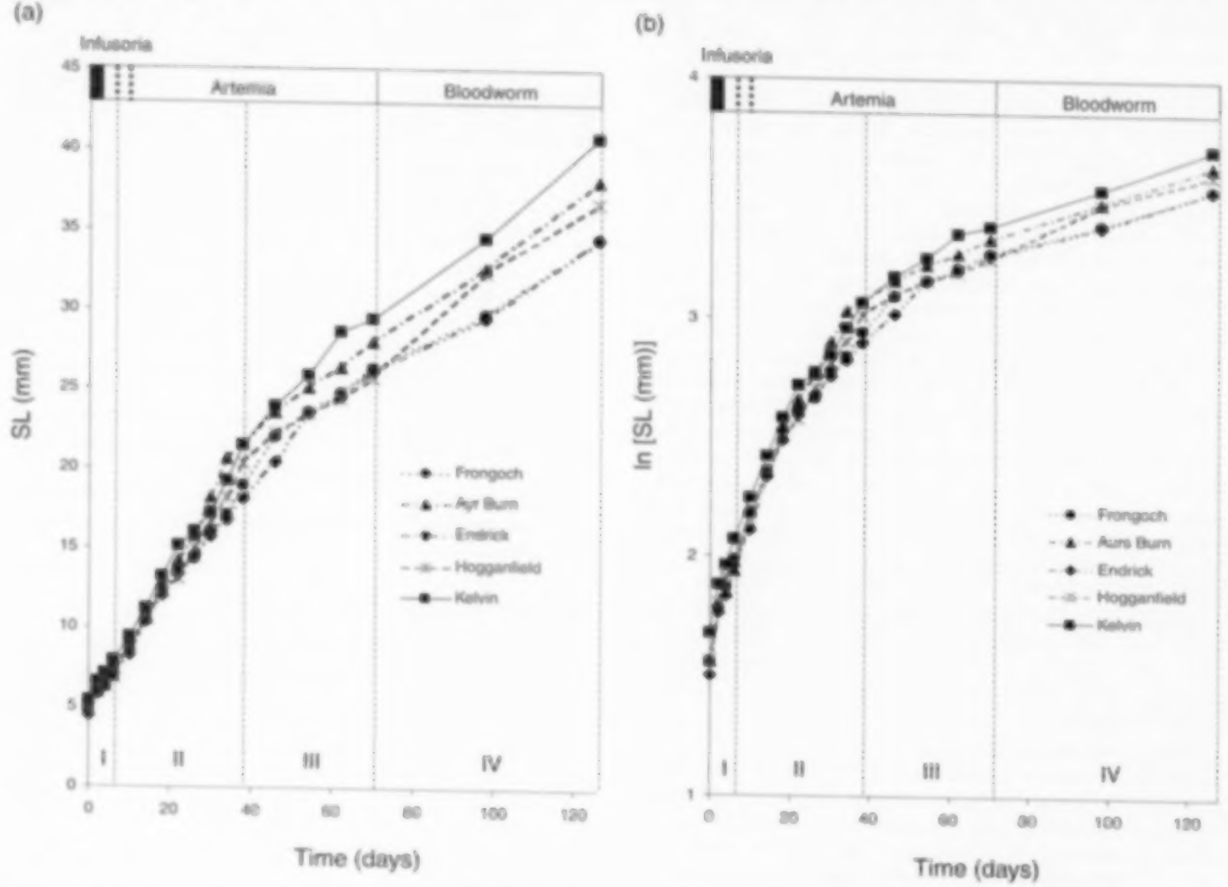

was a highly significant increase in length ($F_{[8,80]} = 1116$, $p < 0.000\,001$) and a significant population × time interaction ($F_{[32,80]} = 2.318$, $p = 0.001$) but no significant population effect. For the period, day 38 ph to day 70 ph (8 days between measurements), the time effect ($F_{[4,40]} = 521.4$, $p < 0.000\,001$) and the population × time interaction ($F_{[16,40]} = 5.064$, $p = 0.000\,02$) were highly significant, and the population effect approached Bonferroni-corrected significance ($F_{[4,10]} = 4.842$, $p = 0.02$). Over the final time period, day 70 ph to day 126 ph (28 days between measurements), the increase in length ($F_{[2,20]} = 865.1$, $p < 0.000\,01$) and the population × time interaction ($F_{[8,20]} = 4.203$, $p = 0.004$) were significant, as was the population effect ($F_{[4,10]} = 6.3586$, $p = 0.008$).

Thus, the interpopulation differences in length only started to emerge in the later phase of the experiment, although population differences in the trajectories of the increase in length were detected from the period starting 6 days ph.

Discussion

The study demonstrated that interpopulation variation in early growth rate in the threespine stickleback could be at least partly attributed to provenance. Even under common garden conditions, the mean standard length of stickleback from different populations, after 126 days growth, varied by as much as 6.79 mm (Kelvin vs. Endrick populations), which was equivalent to 16.6% of the final length of fish from the fastest growing population. Interestingly, initial growth trajectories (days 0–6) did not differ significantly between these study populations, suggesting that interpopulation maternal provisions were not sufficiently variable to cause immediate detectable growth differences. No population level differences in growth trajectories were found before day 38, suggesting that fish growth may be consistent between groups until this stage, but during the period days 38–70 ph, population differences in SL were found. Population size-at-age can be a highly variable characteristic in ecotherms (e.g., Quinn and Unwin 1993; Adams and Huntingford 1997; Rikardson and Elliot 2000). In some populations, natural selection will maximise growth rates (Slobodkin and Rapoport 1972) because of the advantages conferred by larger body size. The observed variation in growth after 38 days in the present study may reflect differences in the importance of a particular size-at-age between the populations under study.

Larger population size-at-age can be achieved through a number of mechanisms, especially by increasing the length of time available for growth (Neat et al. 1995) and by increasing initial size (e.g., Reznick 1982; Elliott 1989). Selection pressures that alter population level growth rates include mortality rates, migratory behaviour (Snyder 1989), resource abundance (Winemiller and Rose 1992), and predator abundance (McPhail 1977). For example, in 25 populations of stickleback in British Columbia, predation by salmonids is thought to select extremes (small or large sizes) (McPhail 1977). Birds and fish are likely to be major predators of adult sticklebacks in some of the populations in the present study, but there may also be a significant invertebrate predation on juvenile stickleback (Reimchen 1994; Houde 2002). Salmonids are known to be present in the River Endrick, Llyn Frongoch, and Hogganfield Loch. No data are available on the fish fauna of the Aurs Burn, but the River Kelvin was free from fish predators until approximately 20 years ago, when the river was cleaned and predatory salmonids reentered. All populations are subject to avian predation. McPhail (1977) suggested that in areas where large predators are abundant, a size refuge may be unattainable and individuals should breed as close to the physiological minimum as possible, giving a smaller size-at-age. For populations without a serious predation threat, larger size may be more advantageous because of all conferred benefits of large body size, and individuals may therefore have faster growth rates and mature at a larger size. The larger size of Kelvin fish may partly reflect a previous absence of large predators in this population.

The growth data in this study are comparable to those obtained in a common garden experiment on stickleback from the Navarro River, California (Snyder 1989). The mean SL of fish from Snyder's estuary, upstream, and inland populations of *Gasterosteus aculeatus*, at day 120 was 34.1, 34.3, and 32.5 mm, respectively. This was related to migratory behaviour, with the slowest growing being a nonmigratory population. In the present study, mean SL_{126} of resident populations ranged from 34.56 mm (Endrick) to 40.89 mm (Kelvin). Interestingly, the mean SL_{126} of Kelvin fish in this study was greater than that of the Snyder's estuary (migratory) population, even at 150 days (estuary mean SL = 39.1 mm).

In the wild, anadromous stickleback are usually larger than freshwater forms (Wootton 1976). This is true of many fishes (Dingle 1980) and is thought to reflect the fact that the relative energetic cost of migration decreases markedly with increasing body size (Roff 1984). The common garden experiment by Snyder (1989) showed that these population level differences have a genetic basis. The fast-growing Kelvin population used in this study may have recently diverged from a migratory form of stickleback, as the Kelvin is a tributary of the Clyde estuary, and this may also partly explain the higher growth trajectories observed in this population. Genetic studies would be needed to investigate this further.

In some cases, faster growth rates can be attributed to higher digestive performance (Nicieza et al. 1994), higher growth efficiencies, and (or) increased food consumption (Conover 1992). In the present study, the small size and particulate nature of the food types provided for fry (*Artemia* and infusoria) meant that daily food intake could not be measured accurately and all fish were thus fed ad libitum ration. Differences in growth rates could, therefore, reflect differences in consumption (willingness to feed), food conversion efficiency, or energetic expenditure. Although the demonstration of genetic differences in growth rate in the threespine stickleback related to provenance is clear, to what extent this growth variation is due to food intake alone has not yet been determined. The development of techniques to allow the quantification of the amount of food provided to fry and juvenile fish is essential to extricate the causes of the observed population-level variation in early growth rates.

In conclusion, this study has provided one of the first demonstrations of population-level genetic variation in early growth rates of threespine stickleback. Given our current limited knowledge of the evolution of growth rates (Arendt 1997), it is interesting and important to demonstrate that population-level variation exists, even without an a priori reason for expecting differences. There are few documented cases of such population differentiation. The use of novel image-analysis techniques, developed in this paper, enable early growth of juvenile stages to be tracked, and this technique can be applied in cases where standard measurements are inappropriate.

Acknowledgements

We are very grateful to Prof. F.A Huntingford (University of Glasgow) for providing the parental sticklebacks from the four Scottish populations. We thank J. Arendt and an anonymous referee for valuable comments on the manuscript. HAW acknowledges the support of a University of Wales Aberystwyth studentship. IB acknowledges fellowship funding from the UK Natural Environmental Research Council (GT/5/98/6/FS and NER/I/S/2000/00971).

References

Adams, C.E., and Huntingford, F.A. 1997. Growth, maturation and reproductive investment in arctic charr. J. Fish Biol. **51**: 750–759.

Arendt, J.D. 1997. Adaptive intrinsic growth rates: an integration across taxa. Q. Rev. Biol. **72**: 149–177.

Arendt, J.D., and Wilson, D.S. 1997. Optimistic growth: competition and an ontogenetic niche-shift select for rapid growth in pumpkinseed sunfish (*Lepomis gibbosus*). Evolution, **51**: 1946–1954.

Arendt, J.D., and Wilson, D.S. 1999. Countergradient selection for rapid growth in pumpkinseed sunfish: disentangling ecological and evolutionary effects. Ecology, **80**: 2793–2798.

Arendt, J.D, Wilson, D.S., and Stark, E. 2001. Scale strength as a cost of rapid growth in sunfish. Oikos, **93**: 95–100.

Baker, J.A., and Foster, S.A. 2002. Phenotypic plasticity for life history traits in a stream population of the threespine stickleback, *Gasterosteus aculeatus* L. Ecol. Freshw. Fish **11**: 20–29.

Barber, I., and Arnott, S.A. 2000. Split-clutch IVF: a technique to examine indirect fitness consequences of mate choice preferences in sticklebacks. Behaviour, **137**: 1129–1140.

Barber, I., and Svensson, P.A. 2003. Effects of experimental *Schistocephalus solidus* infections on growth, morphology and sexual development of female three-spined sticklebacks, *Gasterosteus aculeatus*. Parasitology, **126**: 359–367.

Barfoot, C.A., Gadomski, D.M., and Wertheimer, R.H. 1999. Growth and mortality of age-0 northern squawfish, *Ptychocheilus oregonensis*, rearing in shoreline habitats of a Columbia River reservoir. Environ. Biol. Fishes, **54**: 107–115.

Billerbeck, J.M., Lankford, T.E., and Conover, D.O. 2001. Evolution of intrinsic growth and energy acquisition rates. I. Trade-offs with swimming performance in *Menidia menidia*. Evolution, **55**: 1863–1872.

Cavalli, L., Pech, N., Tron, L., and Chappaz, R. 2002. Growth patterns of Arctic charr in five high altitude lakes in a French alpine massif. J. Fish Biol. **60**: 453–465.

Conover, D.O. 1990. The relationship between capacity for growth and length of growing-season — evidence for and implications of countergradient variation. Trans. Am. Fish. Soc. **119**: 416–430.

Conover, D.O. 1992. Seasonality and the scheduling of life history at different latitudes. J. Fish Biol. **41**: 161–178.

Conover, D.O., and Present, T.M. 1990. Countergradient variation in growth rate: compensation for length of the growing season among Atlantic silversides from different latitudes. Oceologica, **83**: 316–324.

Dingle, H. 1980. Ecology and evolution of migration. *In* Animal migration, orientation and navigation. *Edited by* S.A. Gauthreaux, Jr. Academic Press, New York. pp. 75–101.

Elliott, J.M. 1989. Growth and size variation in contrasting populations of trout *Salmo trutta*: an experimental study on the role of natural selection. J. Anim. Ecol. **58**: 45–58.

Houde, E.D. 2002. Mortality. *In* Fishery science: the unique contributions of early life stages. *Edited by* L.A. Fuiman and R.G. Werner. Blackwell Science Ltd., Oxford. pp. 64–87.

Jensen, A.J., Forseth, T., and Johnsen, B.O. 2000. Latitudinal variation in growth of young brown trout, *Salmo trutta*. J. Anim. Ecol. **69**: 167–177.

Jones, C.M. 2002. Age and growth. *In* Fishery science: the unique contributions of early life stages. *Edited by* L.A. Fuiman and R.G. Werner. Blackwell Science Ltd., Oxford. pp. 33–63.

Krisfalusi, M., and Cloud, J.G. 1996. Effects of exogenous estradiol-17 beta on early growth and gonadal development of diploid and triploid female rainbow trout (*Oncorhyncus mykiss*). Dev. Genet. **19**: 302–308.

Lankford, T.E., Billerbeck, J.M., and Conover, D.O. 2001. Evolution of intrinsic growth and energy acquisition rates. ii. Trade-offs with vulnerability to predation in *Menidia menidia*. Evolution, **55**: 1873–1881.

Levinton, J.S. 1983. The latitudinal compensation hypothesis — growth data and a model of latitudinal growth-differentiation based upon energy budgets. 1. Interspecific comparison of *Ophryotrocha* (Polychaeta, Dorvilleidae). Biol. Bull. **165**: 686–698.

Mayr, E. 1963. Animal species and evolution. Harvard University Press, Cambridge, Mass.

McPhail, J.D. 1977. Inherited interpopulation differences in size at first reproduction in threespine stickleback, *Gasterosteus aculeatus* L. Heredity, **38**: 53–60.

Miller, T.J., Crowder, L.B., Rice, J.A., and Marschall, E.A. 1988. Larval size and recruitment mechanism in fishes: toward a conceptual framework. Can. J. Fish Aquat. Sci. **45**: 1657–1670.

Mills, C.A. 1988. The effect of extreme northerly climatic conditions on the life history of the minnow, *Phoxinus phoxinus* (L.). Fish Biol. **33**: 545–561.

Morita, K., and. Morita, S.H. 2002. Rule of age and size at maturity: individual variation in the maturation history of resident white-spotted charr. J. Fish Biol. **61**: 1230–1238.

Neat, F., Fowler, K., and Partridge, L. 1995. Thermal evolution of growth efficiency in *Drosophila melanogaser*. Proc. R. Soc. Lond. B Biol. Sci. **260**: 73–78.

Nicieza, A.G., Reyes-Gavilan, F.G., and Brana, F. 1994. Differentiation in juvenile growth and bimodality patterns between northern and southern populations of Atlantic salmon (*Salmo salar* L.). Can. J. Zool. **72**: 1603–1610.

Pepin, P. 1991. Effect of temperature and size on development, mortality, and survival rates of the pelagic early life history stages of marine fish. Can. J. Fish. Aquat. Sci. **48**: 503–518.

Power, M. 1987. Predator avoidance by grazing fishes in temperate and tropical streams: importance of stream depth and prey size. *In* Predation: direct and indirect effects on aquatic communities. *Edited by* W.C. Kerfoot and A. Sih. University Press of New England, Hanover. pp. 333–351.

Quinn, T.P., and Unwin, M.J. 1993. Variation in life-history patterns among New Zealand chinook salmon (*Oncorhynchus tshawytscha*) populations. Can. J. Fish. Aquat. Sci. **50**: 1414–1421.

Reimchen. T.E. 1994. Predators and morphological evolution in threespine stickleback. *In* The evolutionary biology of the threespine stickleback. *Edited by* M.A. Bell and S.A. Foster. Oxford University Press, Oxford, UK. pp. 240–276.

Reznick, D. 1982. Genetic determination of offspring size in the guppy (*Poecilia reticulata*). Am. Nat. **120**: 181–188.

Rikardson, A.H., and Elliot, J.M. 2000. Variations in juvenile growth, energy allocation and life history startegies of two populations of Arctic charr in north Norway. J. Fish Biol. **56**: 328–346.

Robinson, B.W., and Wardrop, S.L. 2002. Experimentally manipulated growth rate in threespine sticklebacks: assessing trade offs with developmental stability. Environ. Biol. Fishes, **63**: 67–78.

Roff, D.A. 1984. The evolution of life history parameters in teleosts. Can J. Fish. Aquat. Sci. **41**: 989–1000.

Schultz, E.T., and Conover, D.O. 1997. Latitudinal differences in somatic energy storage: adaptive responses to seasonality in an estuarine fish (Atherinidae: *Menidia menidia*). Oecologia, **109**: 516–529.

Schultz, E.T., Reynolds, K.E., and Conover, D.O. 1996. Countergradient variation in growth among newly hatched *Fundulus heteroclitus*: geographic differences revealed by common-environment experiments. Funct. Ecol. **10**: 366–374.

Schultz, E.T., Conover, D.O., and Ehtisham, A. 1998. The dead of winter: size-dependent variation and genetic differences in seasonal mortality among Atlantic silverside (Atherinidae: *Menidia menidia*) from different latitudes. Can. J. Fish. Aquat. Sci. **55**: 1149–1157.

Slobodkin, L.B., and Rapoport, A. 1972. An optimal strategy of evolution. Q. Rev. Biol. **49**: 181–200.

Snyder, R.J. 1989. Migration and life histories of the threespine stickleback: evidence for adaptive variation in growth rate between populations. Environ. Biol. Fishes, **31**: 381–388.

Snyder, R.J., and Dingle, H. 1989. Adaptive, genetically based differences in life history between estuary and freshwater threespine sticklebacks (*Gasterosteus aculeatus* L.). Can. J. Zool. **67**: 2448–2454.

Stearns, S.C. 1983. The genetic-basis of differences in life-history traits among 6 populations of mosquitofish (*Gambusia affinis*) that shared ancestors in 1905. Evolution, **37**: 618–627.

Svåsand, T., Jørstad, K.E., Otterå, H., and Kjesbu, O.S. 1996. Differences in growth performance between arcto-Norwegian and Norwegian coastal cod reared under identical conditions. J. Fish Biol. **49**: 108–119.

Travis, J. 1981. Control of larval growth variation in a population of *Pseudacris triseriata* (Anura, Hylidae). Evolution, **35**: 423–432.

Trivers, R.L. 1972. Parental investment and sexual selection. *In* Sexual selection and the descent of man, 1871–1971. *Edited by* B.H. Campbell. Aldine Publishing Co., Chicago. pp. 136–179.

Winemiller, K.O., and Rose, K.A. 1992. Patterns of life history diversification in North American fishes: implications for population regulation. Can. J. Fish. Aquat. Sci. **49**: 2196–2218.

Wootton, R.J. 1976. The biology of the sticklebacks. Academic Press, London.

Acoustic characteristics of forage fish species in the Gulf of Alaska and Bering Sea based on Kirchhoff-approximation models

Stéphane Gauthier and John K. Horne

Abstract: Acoustic surveys are routinely used to assess fish abundance. To ensure accurate population estimates, the characteristics of echoes from constituent species must be quantified. Kirchhoff-ray mode (KRM) backscatter models were used to quantify acoustic characteristics of Bering Sea and Gulf of Alaska pelagic fish species: capelin (*Mallotus villosus*), Pacific herring (*Clupea pallasii*), walleye pollock (*Theragra chalcogramma*), Atka mackerel (*Pleurogrammus monopterygius*), and eulachon (*Thaleichthys pacificus*). Atka mackerel and eulachon do not have swimbladders. Acoustic backscatter was estimated as a function of insonifying frequency, fish length, and body orientation relative to the incident wave front. Backscatter intensity and variance estimates were compared to examine the potential to discriminate among species. Based on relative intensity differences, species could be separated in two major groups: fish with gas-filled swimbladders and fish without swimbladders. The effects of length and tilt angle on echo intensity depended on frequency. Variability in target strength (TS) resulting from morphometric differences was high for species without swimbladders. Based on our model predictions, a series of TS to length equations were developed for each species at the common frequencies used by fisheries acousticians.

Résumé : Les inventaires acoustiques sont utilisés régulièrement pour estimer l'abondance des poissons. Pour obtenir des estimations précises, les caractéristiques des échos provenant des différentes espèces doivent être quantifiées. Des modèles de réflexion acoustique fondées sur l'approximation de Kirchhoff ont été utilisés pour mesurer les propriétés acoustiques de plusieurs espèces dans le Golf de l'Alaska et la Mer de Béring : le capelan (*Mallotus villosus*), le hareng du Pacifique (*Clupea pallasii*), la goberge de l'Alaska (*Theragra chalcogramma*), le maquereau Atka (*Pleurogrammus monopterygius*) et l'eulakane (*Thaleichthys pacificus*). Le maquereau Atka et l'eulakane n'ont pas de vessies natatoires. La rétro-diffusion acoustique a été estimée en fonction de la fréquence sonore, de la taille et de l'orientation des poissons. L'intensité des échos et leur variance ont été comparées pour examiner la possibilité de discerner les espèces. Nous avons découvert que les espèces peuvent être séparées en deux groupes selon la présence ou l'absence de vessie natatoire. L'incidence de la taille et de l'orientation sur l'intensité des échos dépendaient de la fréquence sonore. La variabilité de l'indice de réflexion (IR) due aux différences morphométriques était élevée pour les espèces sans vessie. Des équations mettant en rapport la taille des poissons et l'IR ont été élaborées pour chaque espèce en fonction des fréquences sonores les plus couramment utilisées.

Introduction

Acoustic surveys are used to monitor the distribution, abundance, and habitat use of fish within ecosystems. These surveys are appealing for assessment purposes as large volumes of water are rapidly sampled at high spatial and temporal resolutions. To convert acoustic signals to estimates of fish abundance, species must be properly partitioned within survey areas and the echo energy of constituent species must be known. The intensity of an echo is generally expressed on a logarithmic scale as the target strength (TS). Acoustic properties of fish are species-specific and change over time. In addition to physical characteristics such as frequency (Foote 1982), TS depends on fish size (Nakken and Olsen 1977), anatomical features (e.g., presence of a swimbladder; Foote 1980*a*), morphology (e.g., swimbladder shape; McClatchie et al. 1996*a*), and physiological state (e.g., gonadal maturation and gut fullness; Ona 1990). Fish behavior can also significantly alter TS through changes in fish orientation relative to the wave front (Nakken and Olsen 1977; Foote 1980*b*; Blaxter and Blatty 1990) and vertical movement within the water column, which changes swimbladder volume (Ona 1990; Mukai and Iida 1996; Rose and Porter 1996). Ideally, TS should be measured under the same conditions as those encountered when populations are surveyed. Suitable in situ conditions for the measurement of TS can be difficult to ob-

Received 2 October 2003. Accepted 16 April 2004. Published on the NRC Research Press Web site at http://cjfas.nrc.ca on 11 December 2004.
J17772

S. Gauthier[1] and J.K. Horne. University of Washington, School of Aquatic and Fishery Sciences, Box 355020, Seattle, WA 98195-5020, USA.

[1]Corresponding author (e-mail: sgau@u.washington.edu).

doi: 10.1139/F04-117

tain, especially in mixed species aggregations or within dense schools of fish.

A modeling approach provides a practical alternative to measurements and can be used to examine the amplitude and variability of acoustic backscatter as a function of single or multiple variables. Modeling exercises can also be used to compare and contrast acoustic properties among species and identify potential metrics for species discrimination and identification. The Kirchhoff-ray mode (KRM) model uses low-mode solutions and Kirchhoff-ray approximations to estimate resonant and geometric backscatter using planar images of the fish body and swimbladder (Clay and Horne 1994). KRM model predictions have been successfully matched to empirical measures (Jech et al. 1995; Horne et al. 2000; Horne 2003). Matches of KRM model predictions to empirical backscatter measurements of pollack (*Pollachius pollachius*) and saithe (*Pollachius virens*) were comparable to those obtained using the boundary element model (BEM) over a frequency range of 38.1 to 120.4 kHz (Foote and Francis 2002). In the present study, KRM models are used to characterize acoustic properties of forage fish in the Gulf of Alaska and the Bering Sea. Five abundant and widely distributed species are considered: capelin (*Mallotus villosus*), Pacific herring (*Clupea pallasii*), walleye pollock (*Theragra chalcogramma*), Atka mackerel (*Pleurogrammus monopterygius*), and eulachon (*Thaleichthys pacificus*). Atka mackerel and eulachon do not possess swimbladders. Capelin and Pacific herring are physostomous (open swimbladder), whereas walleye pollock is physoclistous (closed swimbladder).

These fish species are important to the diet of many apex predators such as Steller sea lions (*Eumetopias jubatus*). Recent declines in western Steller sea lion populations in the Gulf of Alaska and the Bering Sea have increased interest in the assessment of forage fish species (Alverson 1992). It has been hypothesized that changes in the composition, distribution, and availability of fish in Steller sea lion habitat are in part responsible for their decline and lack of recovery (Rosen and Trites 2000; Stickney 2000; Trites and Donnelly 2003). Some of the challenges associated with the acoustic assessment of forage fish around Steller sea lion rookeries, haulouts, and feeding grounds include accurate conversion of acoustic energy to fish biomass and species discrimination in mixed fish aggregations. Our work examines acoustic characteristics of these forage species and identifies possible steps in the ongoing effort to develop acoustic discrimination techniques.

Materials and methods

Radiographs and digital pictures were used to image fish bodies and swimbladders used in KRM modeling (Fig. 1). Fish were captured using hand lines or midwater trawls and were kept in aerated tanks. When possible, a period of at least 12 h was allowed for fish with swimbladders captured at depth to acclimate to surface pressure. Fish were subsequently anesthetized for a period of 30–60 s in a 10-L basin of water containing 5 mL of a 9:1 mixture of ethanol to clove oil. Once immobilized, fish were placed individually on a flat surface for lateral and dorsal imaging. Fish with a swimbladder were radiographed using a portable veterinary x-ray unit (XTEC Laseray 90P; XTEC Inc., Columbia City, Indiana). The fish were placed at a focal distance of 40–45 cm on cassettes or redipaks containing rare earth film. Fish lateral and dorsal planes were exposed at 15 mA for 2 s at 95 kVp on the redipaks (generally used for <25-cm fish) or for 0.18 s at 70 kVp on cassettes with intensifying screens (generally used for >25-cm fish). Fish without swimbladders were photographed using a 3.3-megapixel digital camera (photoPC 3000z; Epson America Inc., Long Beach, Calif.). Lateral and dorsal images of the fish body and swimbladder (when present) were traced on acetate sheets, scanned, and then digitized at 1-mm resolution. Fins and tail were not included in the trace. Orientation of the swimbladder relative to the body was maintained, and the body parts were scaled to their true size using maximum and minimum body and swimbladder measurements. When necessary, trace lines were smoothed and rotated so that the sagittal axis of the fish body was horizontal. The resulting dorsal and lateral images were elliptically interpolated into 1-mm-thick cylinders to give a three-dimensional (3D) representation of the fish body and swimbladder (Fig. 2). A series of morphometric descriptors (including swimbladder volume and area) were estimated using these 3D fish representations. Species were partitioned into groups of similar-sized individuals (10-cm length groups). The ratio of the major to minor axes of the body and swimbladder (maximum length and width) were measured on the lateral traces as an index of elongation. The eccentricity (e) of the fish body or swimbladder was also measured as the ratio of the distance between the foci and the vertices of an ellipse having the same major and minor axes as the fish trace. Eccentricity varies between 0 and 1 ($0 \le e < 1$, where 0 is a circle).

Swimbladders were modeled as a series of gas-filled cylinders, and fish bodies were modeled as a series of fluid-filled cylinders. The energy backscattered by the fish body and swimbladder was obtained by estimating the scattering from each cylinder (for details see Clay and Horne 1994). The scattered sound pressure (P_{scat} at time t and range R) of an object insonified by a plane incident wave (of amplitude P_{inc} at the object) is

$$(1)\qquad P_{\mathrm{scat}}(t,R) = (P_{\mathrm{inc}}/R)\,e^{i(kR-2\pi ft)}\mathcal{F}(t)$$

where k is the wave number (m^{-1}), f is the frequency (Hz) for the convolution of the sound wave, and $\mathcal{F}(t)$ is the scattering length (m) of the object in the time domain. Scattering amplitudes from the fish body and swimbladder were added coherently to obtain the total scattering length of the fish. The absolute square of the scattering length is equivalent to the backscattering cross section of an insonified object (σ_{bs}, m^2):

$$(2)\qquad \sigma_{\mathrm{bs}} = |\mathcal{F}|^2$$

where $\mathcal{F}$ is a function of the insonifying frequency and length (L, m) of the object. Our model combines these variables as a nondimensional reduced scattering length (RSL):

$$(3)\qquad \mathrm{RSL} = \mathcal{F}(L/\lambda)/L$$

where λ is the acoustic wavelength (m). RSLs obtained in the frequency domain can be converted to target strength (TS, dB) at any specified length:

$$(4)\qquad \mathrm{TS} = 20\log(\mathrm{RSL}) + 20\log(L)$$

Fig. 1. Illustrations of the modeled species with corresponding lateral and dorsal radiographs (traces shown for species that do not possess a swimbladder). The air-filled swimbladder can be seen as a dark shape within the fish body, and the different shades of gray represent structures of different densities within the fish body (lighter shade = densest, as a result of high x-ray absorption).

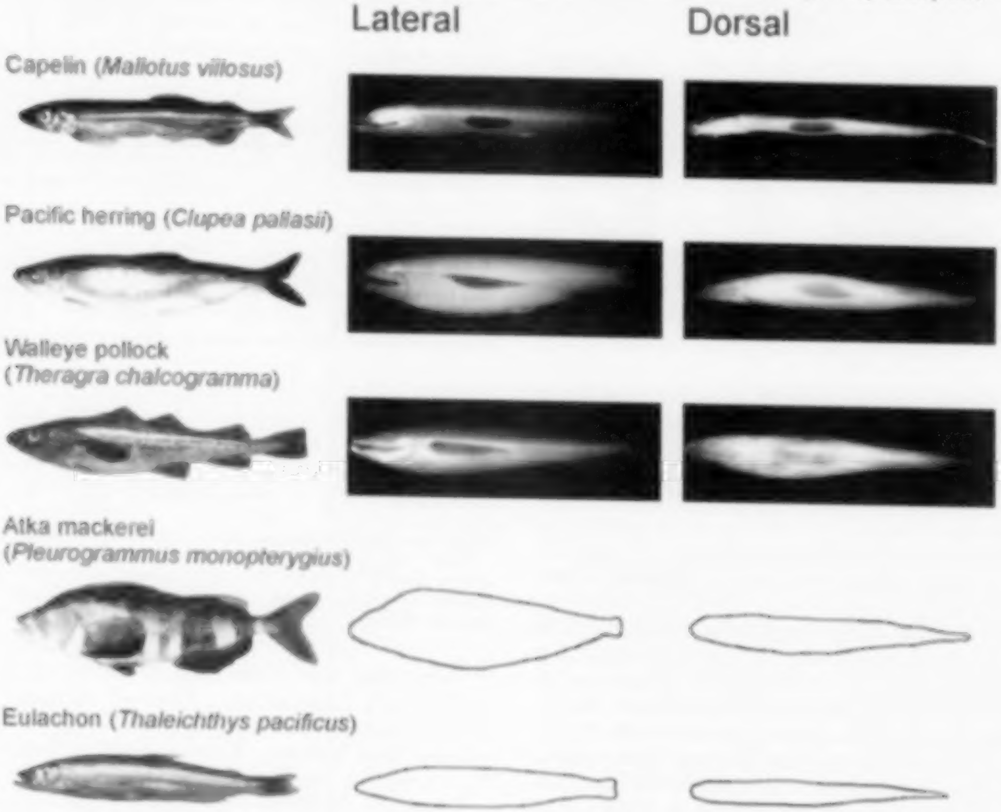
Lateral
Dorsal
Capelin (*Mallotus villosus*)
Pacific herring (*Clupea pallasii*)
Walleye pollock
(*Theragra chalcogramma*)
Atka mackerel
(*Pleurogrammus monopterygius*)
Eulachon (*Thaleichthys pacificus*)

We list the parameters used in KRM modeling (Table 1). Eulachon (an anadromous species) was modeled for both marine and freshwater environments.

For each species, TS was estimated as a function of length, carrier frequency, and tilt angle. The effect of one variable (e.g., length) was modeled for each fish over an arbitrary range by controlling for the other factors (e.g., fixed frequency and tilt angle in this case). Predicted RSL values were compiled for all digitized fish to obtain a mean and standard deviation of the acoustic backscatter for each species and size group. When representing the average value for a group of individuals, TS was denoted as $\overline{\mathrm{TS}}$. To estimate backscatter over a common length range, fish were linearly scaled in each dimension to all lengths within the modeled range. Length ranges (at 2-mm increments) were centered on the average length of collected specimens. The effect of frequency was modeled from 12 to 420 kHz. Tilt angles were modeled at increments of 1° over a range of 45° to 135°, where 90° represents a normal aspect (i.e., lateral axis of the fish body perpendicular to the incident wave front). The effects of length and frequency were modeled at dorsal incidence (normal aspect). Frequency and tilt angle effects were modeled at various scaled fish lengths.

Model results were used to estimate tilt-averaged target strength (TS_θ) to total length (L_T) relationships for the five studied species. To estimate TS_θ, reduced scattering lengths (RSL) were generated for each individual at their actual length over a range of 45° to 135° at 1° increments. A normal distribution of tilt angles having a known mean and standard deviation (based on in situ measurements when available) was randomly sampled to provide 1000 tilt values (Table 2). Echo-intensity values were tabulated from this tilt-angle distribution and corresponding model predictions. The resulting TS_θ of individual fish were subsequently used to estimate the regression parameters for each of the five species. The models were generated as

$$(5)\qquad \mathrm{TS}_\theta = a\log(L_\mathrm{T}\ (\mathrm{cm})) + b_a$$

$$(6)\qquad \mathrm{TS}_\theta = 20\log(L_\mathrm{T}\ (\mathrm{cm})) + b_{20}$$

where a is the slope and b_a (or b_{20}) is the intercept of the regression. The regression parameters were calculated at the five frequencies most commonly used in fisheries acoustics (12, 38, 70, 120, and 200 kHz). KRM predicts TS using fish caudal lengths (length from tip of snout to end of caudal peduncle). Total lengths were estimated based on regressions between caudal lengths and total lengths from the sampled fish (Table 2).

Fig. 2. Three-dimensional representation of a fish body or swimbladder with 1-mm cylinders (slabs) used in Kirchhoff-ray mode backscatter models.

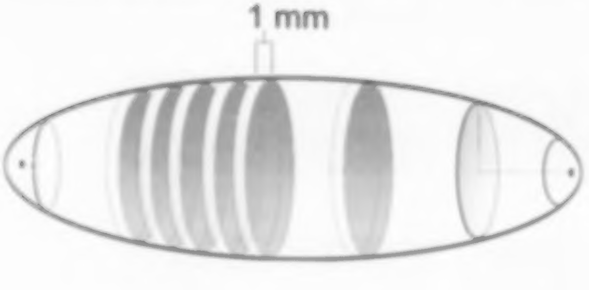

Table 1. Acoustic parameters used in Kirchhoff-ray mode models.

Parameter	Freshwater	Marine
Speed of sound in water ($m \cdot s^{-1}$)	1430	1470
Speed of sound in fish body ($m \cdot s^{-1}$)	1570	1570
Speed of sound in swimbladder ($m \cdot s^{-1}$)	—	335
Density of water ($kg \cdot m^{-3}$)	1000	1026
Density of fish body ($kg \cdot m^{-3}$)	1070	1070
Density of swimbladder ($kg \cdot m^{-3}$)	—	7.44

Note: Parameters for the fish body were taken from Clay and Horne (1994). Density of gas within the swimbladder was modeled at a depth of 50 m (607.95 $kN \cdot m^{-2}$).

Table 2. Tilt-angle distribution used for the TS_{θ}–L_T regressions and equations used to estimate fish total length from the modeled caudal length results (all $r^2 > 0.9$).

Species	Total length	Tilt-angle distribution (mean, SD)
Capelin	1.12CL + 1.43	(93.3, 18.4)[1]
Pacific herring	1.06CL + 0.55	(86.9, 14.2)[2]
Walleye pollock	1.06CL + 1.98	(85.6, 16.2)[3]
Atka mackerel	1.14CL + 0.88	(90, 15)[4]
Eulachon	1.08CL	(90, 15)[4]

Note: [1] Carscadden and Miller (1980); [2] Ona (2001), measurements on Atlantic herring ; [3] Olsen (1971), measurements on Atlantic cod (a related gadoid); [4] conservative values (no published data). CL, caudal length; SD, standard deviation.

Results

Nine fish groups were modeled. Each group consisted of at least 10 individuals of similar length. The average estimated dorsal swimbladder area varied from 6.4% to 11.3% of the total dorsal body area. Swimbladder volume varied from 2.6% to 3.7% of the total fish volume (Table 3). Capelin had the lowest values in both cases. This species also had the smallest swimbladder angle (mean of 3.9°) and the lowest swimbladder elongation (with corresponding eccentricity).

The effect of length on the mean target strength ($\overline{TS}$) of each species is illustrated at four different frequencies: 12, 38, 120, and 200 kHz (Fig. 3). Among fish of similar lengths, species with a swimbladder had much larger $\overline{TS}$ than species without a swimbladder (differences of up to 15 dB). Differences were also observed among the $\overline{TS}$ of any given species at various carrier frequencies. For example, the $\overline{TS}$ of Pacific herring (Fig. 3*b*) at 12 kHz was consistently 5–10 dB higher than the $\overline{TS}$ at 120 or 200 kHz. Intercepts, shapes, and slopes of the TS to length regressions were also dependent on frequency. At 12 kHz, the increase in $\overline{TS}$ with length was steep and relatively constant. At higher frequencies, successive TS peaks and troughs were observed with increasing length. This variability in the $\overline{TS}$ to L_T relationship was particularly marked in species without swimbladders. For example, the TS of eulachon peaks and dips twice, spanning more than 10 dB over a 20-cm length range. Variability in TS is attributed to constructive and destructive interference of reflected pressure waves within the fish body.

Intraspecific TS variability was high for species without swimbladders (as illustrated by the standard deviations in Fig. 4). Walleye pollock, a species with a swimbladder, also had high intraspecific TS variability at lengths greater than 40 cm. Capelin and Pacific herring had the smallest range in fish size and intraspecific TS variability. TS of fish modeled at their actual size often differed from the $\overline{TS}$ curve obtained by scaling the lengths of all fish (Fig. 4).

Frequency-dependent backscatter at a specified length and tilt are shown (Fig. 5). Pacific herring and walleye pollock TS values were higher at low frequencies, peaking at approximately 20 kHz. The $\overline{TS}$ of these species dropped sharply between 20 and 100 kHz and was relatively constant in the higher frequency range. This sharp decrease in $\overline{TS}$ was not observed for capelin, which exhibited more irregular patterns at lower frequencies. Echo-intensity variance of all fish with swimbladders dramatically increased between 12 and 100 kHz and remained relatively high thereafter. For species without swimbladders, $\overline{TS}$ and standard deviation were highly variable across all frequencies.

Effects of orientation on TS among species with swimbladders were pronounced at high frequencies (Fig. 6). At 12 kHz, the $\overline{TS}$ of a 16-cm capelin or walleye pollock varied by less than 6 dB over a tilt-angle range of 45° to 135°. Pacific herring $\overline{TS}$ decreased by more than 10 dB with increasing tilt angle, but the changes were relatively gradual. In contrast, the $\overline{TS}$ of fish with swimbladders changed sharply with tilt angle at 120 and 200 kHz, especially with orientations approaching swimbladder dorsal incidence (sagittal axis perpendicular to the wave front). Changes in amplitude with orientation were also important at 38 kHz, but the sharp decreases in $\overline{TS}$ occurred at greater tilt angles. It is also noteworthy that the maximum TS for these species with swimbladders did not occur exactly at normal aspect, but at a lower head-down tilt angle (between 80° and 90°). The $\overline{TS}$ of 16-cm Atka mackerel and eulachon varied by more than 30 dB over the range of the tilt angles modeled. The overall pattern (or shape) of the TS – tilt angle relationship for these species without swimbladders was not affected by frequency. At 38 kHz, TS of these fish displayed more variation over small tilt-angle ranges than at 200 or 12 kHz. Changes in $\overline{TS}$ with tilt angle are not symmetrical and depend on the orientation of the individual relative to the wave front (head-down versus head-up) (Fig. 6).

In most cases, TS_{θ} values were lower than the TS for the same individuals modeled at a 90° tilt (Fig. 4). Differences between these two values were highest for capelin and

Table 3. Mean and standard deviation (in parentheses) for morphological characteristics of the five fish species used in the Kirchhoff-ray mode (KRM) modeling.

Species	*n*	L_T (cm)	L_{KRM}	Sb area (cm^2)	Sb volume (mL)	Area %	Volume %	Sb angle	Body *x*/*y*	Body *e*	Sb *x*/*y*	Sb *e*
Capelin	34	14.2 (1.2)	10–20	1.5 (0.5)	0.3 (0.1)	6.4 (1.3)	2.6 (0.7)	3.9 (2.0)	7.1 (1.1)	0.99	3.9 (0.6)	0.96
Pacific herring	30	23.7 (1.7)	10–30	12.8 (2.5)	6.7 (2.2)	11.3 (1.4)	3.6 (0.8)	7.8 (1.0)	4.1 (0.2)	0.97	5.3 (0.5)	0.98
Walleye pollock	15	15.4 (1.2)	10–20	3.0 (0.8)	0.9 (0.4)	8.4 (0.9)	2.7 (0.6)	6.7 (3.0)	4.9 (0.2)	0.98	4.9 (0.7)	0.98
	10	27.4 (2.5)	20–35	9.6 (1.9)	4.8 (1.2)	9.0 (1.3)	3.0 (0.8)	6.5 (2.3)	5.0 (0.4)	0.98	5.4 (0.7)	0.98
	25	45.1 (4.7)	35–60	39.0 (6.8)	42.9 (12.1)	10.9 (1.3)	3.7 (0.7)	8.5 (2.7)	4.1 (0.4)	0.97	4.3 (0.7)	0.97
Atka mackerel	10	20.5 (2.0)	10–30	—	—	—	—	—	4.1 (1.0)	0.97	—	—
	10	47.4 (3.0)	30–50	—	—	—	—	—	4.6 (0.4)	0.98	—	—
Eulachon	30	17.9 (2.0)	10–20	—	—	—	—	—	5.8 (0.8)	0.98	—	—
	13	24.8 (1.5)	20–30	—	—	—	—	—	5.4 (0.2)	0.98	—	—

Note: All lengths are in centimetres. L_T, the mean total length of the collected specimens; L_{KRM}, the (caudal) length range used in the model; Sb, swimbladder, swimbladder areas were measured in the dorsal plane; Area % and Volume %, the proportion of the swimbladder area or volume to fish body area or volume; Sb angle, the angle of the swimbladder major axis relative to the sagittal axis of the fish body (positive values indicate that the anterior of the swimbladder is above the sagittal axis); *x*/*y*, ratio of major to minor axes as measured on the lateral traces; *e*, eccentricity for corresponding ellipse.

eulachon. The parameters of the TS_θ–L_T regressions obtained from the KRM model results are listed for all species at the five frequencies (*f*) most commonly used in fisheries acoustics (Table 4). The goodness of fit of the TS_θ–L_T relationships was often poor due to high variability in backscatter response. Values of the slope in the log-linear model often differed from 20, and the use of a 20log regression (forced slope) had, in some cases, considerable effect on the resulting goodness of fit (r^2). For fish with swimbladders, the b_{20} values generally decreased with increasing frequency. Capelin had the lowest b_{20} values, followed by walleye pollock and Pacific herring. Walleye pollock had the best-fit regressions (all $r^2 >$ 0.9) and the closest agreement between the log-linear and forced-slope (20log) models for the five tested frequencies, with the exception of Atka mackerel at 120 kHz. As expected, the intercepts of the 20log regressions were much lower for fish without swimbladders. Atka mackerel and eulachon had similar b_{20} values. The estimated regression intercepts of eulachon modeled in freshwater were 2–4 dB lower than those modeled in marine conditions.

Discussion

Agreement between KRM model predictions and published TS values was species-dependent. Values obtained from our model on capelin TS were much higher (4–5 dB for the tilt-averaged TS) than in other studies (O'Driscoll and Rose 2001; Jørgensen and Olsen 2002). Reasons for these differences are not clear. Jørgensen (2003) noted differences in the TS of capelin according to condition factor (based on weight–length relationships) and swimbladder length. TS predictions for Pacific herring are in good agreement with documented TS values for this species in fall ($TS = 20\log L_T - 66$ at 120 kHz; Thomas et al. 2002). However, herring used in our study were collected from large spawning aggregations during March 2002 (Sitka Bay, Alaska). Thomas et al. (2002) found that during spring, the b_{20} was 3.2 dB lower than during the fall. Because individuals used for the x-ray imaging were not sacrificed, it was impossible to determine if they had spawned. Herring gonad may modify the shape and size of the swimbladder and increase TS resulting from lipid content. Such characteristics would change once eggs or milt are released from the body cavity. Ona et al. (2001) noted that seasonal variation in the TS of a closely related herring species (*Clupea harengus*) could be as high as 4–8 dB and incorporated a gonadosomatic index (GSI) to improve the TS–length relationship for this species. In situ TS values obtained on stocks of Atlantic herring are typically 4–6 dB lower than our estimates for Pacific herring (Halldorsson and Reynisson 1983; Misund and Øvredal 1988; Rudstam et al. 1988). Walleye pollock TS–length predictions were comparable with documented TS values at 38 kHz (Traynor and Williamson 1983; Foote and Traynor 1988; Traynor 1996). Our estimated b_{20} intercept value was 1.2 dB lower than in the equation currently used for the conversion of acoustic size to fish length in annual surveys in the Gulf of Alaska and the Bering Sea (Foote and Traynor 1988; Guttormsen et al. 2001). Using ex situ measurements of walleye pollock and deformed cylinder models, Sawada et al. (1999) also found predicted TS values 1–3 dB lower than the Foote and Traynor (1988) equation. To our knowledge,

Fig. 3. Mean target strength ($\overline{TS}$) as a function of fish total length for (*a*) capelin (*Mallotus villosus*), (*b*) Pacific herring (*Clupea pallasii*), (*c*) walleye pollock (*Theragra chalcogramma*), (*d*) Atka mackerel (*Pleurogrammus monopterygius*), and (*e*) eulachon (*Thaleichthys pacificus*). Dotted line, 12 kHz; bold unbroken line, 38 kHz; thin unbroken line, 120 kHz; shaded line, 200 kHz. Averaging was done in the linear domain before logarithmic transformation.

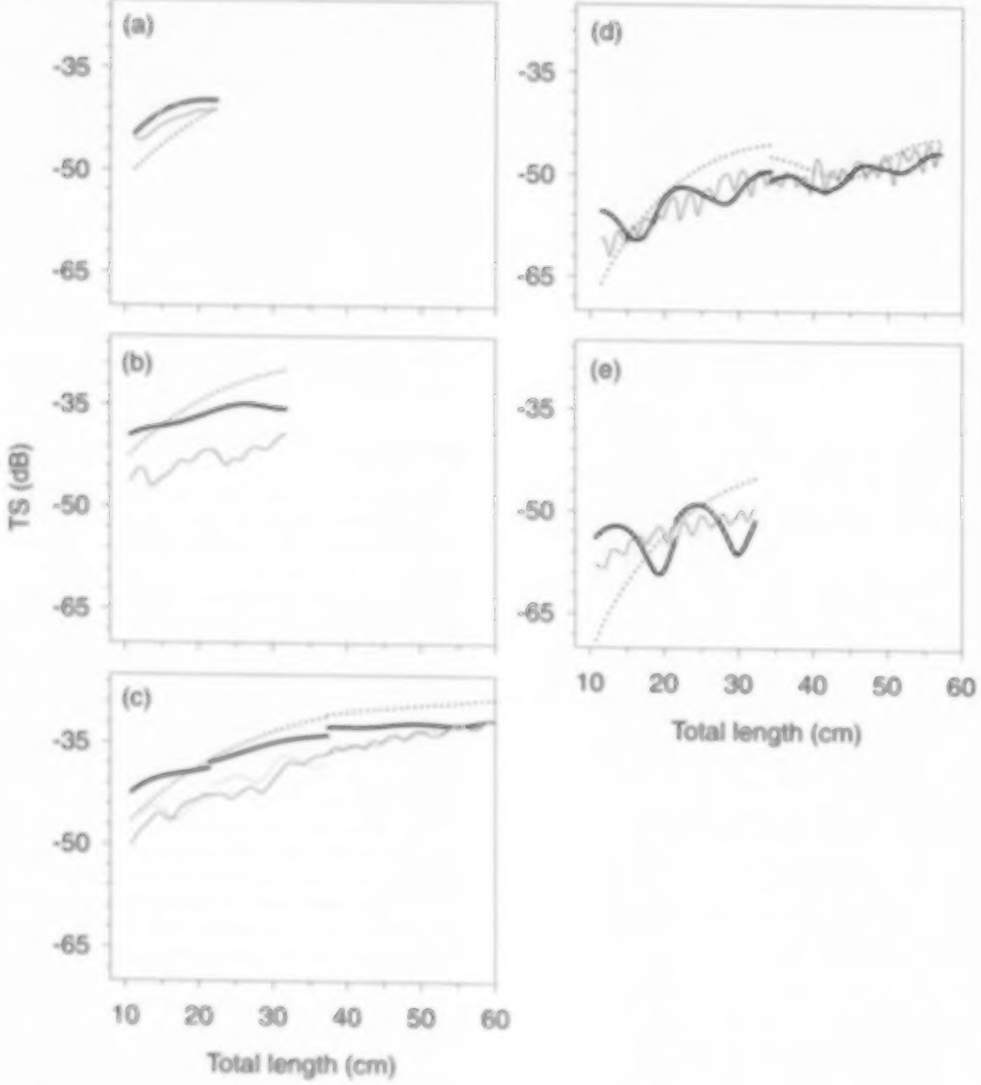

no published data exist on target strengths of Atka mackerel. Experiments on encaged mackerel (*Scomber scombus*) in the Atlantic suggest a b_{20} 1.7–5.7 dB lower (Edwards et al. 1984) than those found in our study. TS estimates for eulachon modeled in marine conditions were similar to those obtained for Atka mackerel of the same length. Predicted eulachon TS from KRM tilt-averaged models adjusted for freshwater were similar to in situ TS measurements of eulachon at 123 kHz (tilt-averaged model = –54.5 dB; mean in situ = –53.5 dB; mean fork length = 18.1 cm) and 208 kHz (tilt-averaged model = –54.9 dB; mean in situ = –50.3 dB; mean fork length = 17.1 cm) in the lower Fraser River, British Columbia (B. Stables, Shuksan Fisheries Consulting, P.O. Box 485, Sumas, WA 98295, USA, personal communication). Even though the 4.6 dB difference at 208 kHz appears large, predicted eulachon backscatter can differ by up to 4 dB within a 1-cm change in length.

Because of the large density and sound speed contrasts of gas and water, the echo intensity of a fish primarily depends on the presence or absence of a gas-filled swimbladder (Haslett 1962; Foote 1980*a*). Contributions of fish flesh and other organs to the total backscatter of a fish are minimal compared with the contributions from the swimbladder. Density and sound speed within the swimbladder will change with gas composition, depth, and temperature. Air is highly compressible compared with water and fish flesh. Its

Fig. 4. Target strength (TS) at 38 kHz as a function of fish total length (L_T) for (*a*) capelin (*Mallotus villosus*), (*b*) Pacific herring (*Clupea pallasii*), (*c*) walleye pollock (*Theragra chalcogramma*), (*d*) Atka mackerel (*Pleurogrammus monopterygius*), and (*e*) eulachon (*Thaleichthys pacificus*). Shaded lines, mean and standard deviation of all fish modeled over a range of scaled length and a tilt angle of 90° (normal aspect); ●, TS of individuals modeled at their default length and a tilt angle of 90°; △, TS of individuals modeled at their default length and averaged over a normal distribution of tilt angles; unbroken line, best fit log-linear regression for TS_θ ($TS_\theta = a\log(L_T) + b_0$); dotted line, best-fit 20log regression for the TS_θ ($TS_\theta = 20\log(L_T) + b_{20}$).

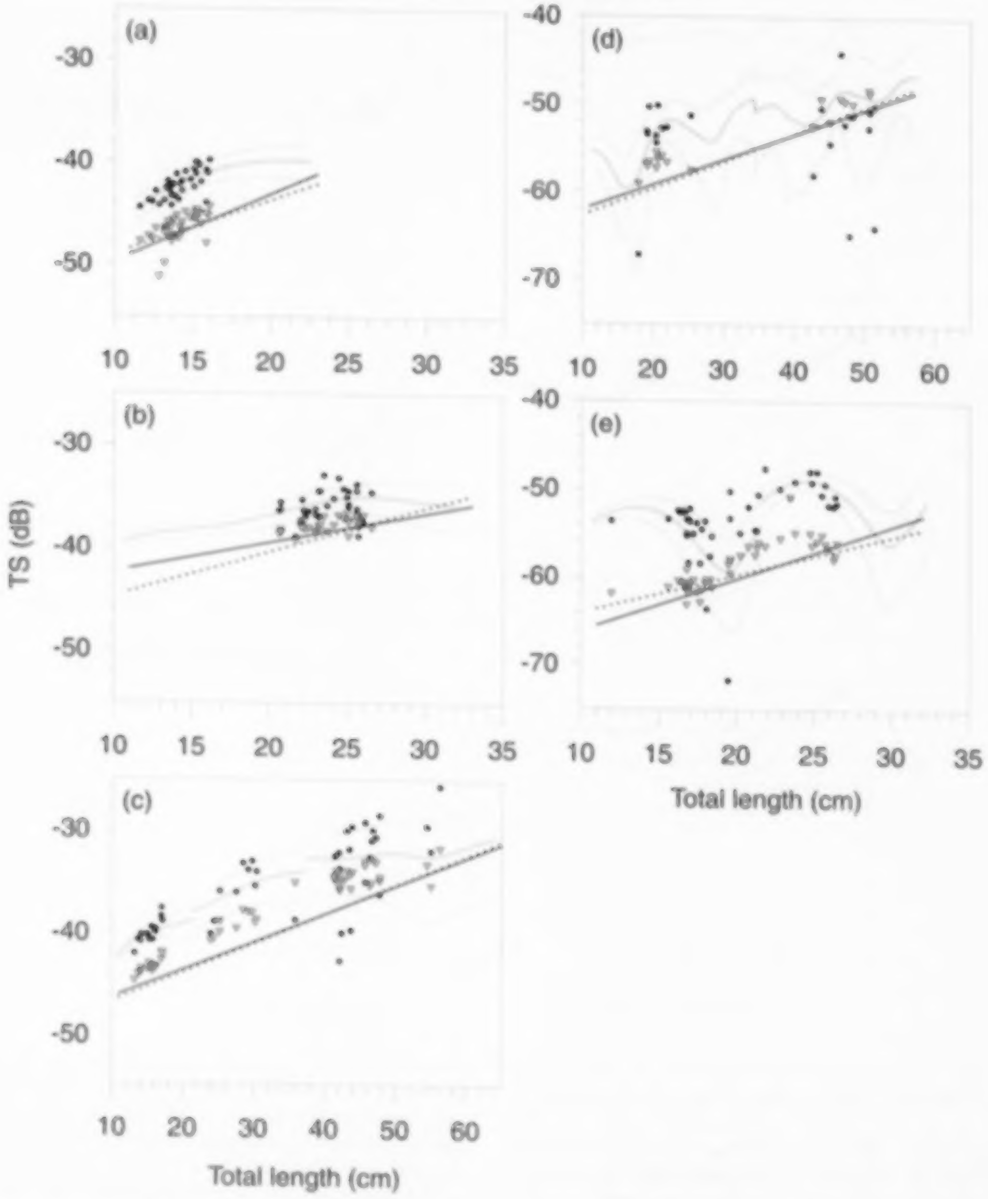

density increases proportionally to pressure (air density = 122.76 kg·m^{-3} at 1000 m). Changes in swimbladder volume as fish change depth according to Boyle's law can have a much more drastic effect on resulting backscatter intensity than density of sound speed contrasts (e.g., Mukai and Iida 1996; Gorska and Ona 2003). Changes in density and sound speed of water also influence KRM model predictions. As an example, TS of eulachon in freshwater were on average 3–4 dB higher than in seawater. Density and sound speed of water are easily calculated using ambient temperature, salinity, and depth (e.g., Mackenzie 1981; UNESCO 1983). Density and sound speed contrasts at interfaces will greatly affect the acoustic scattering of non-gas-bearing organisms (Stanton et al. 2000). Density and sound speeds of fish flesh

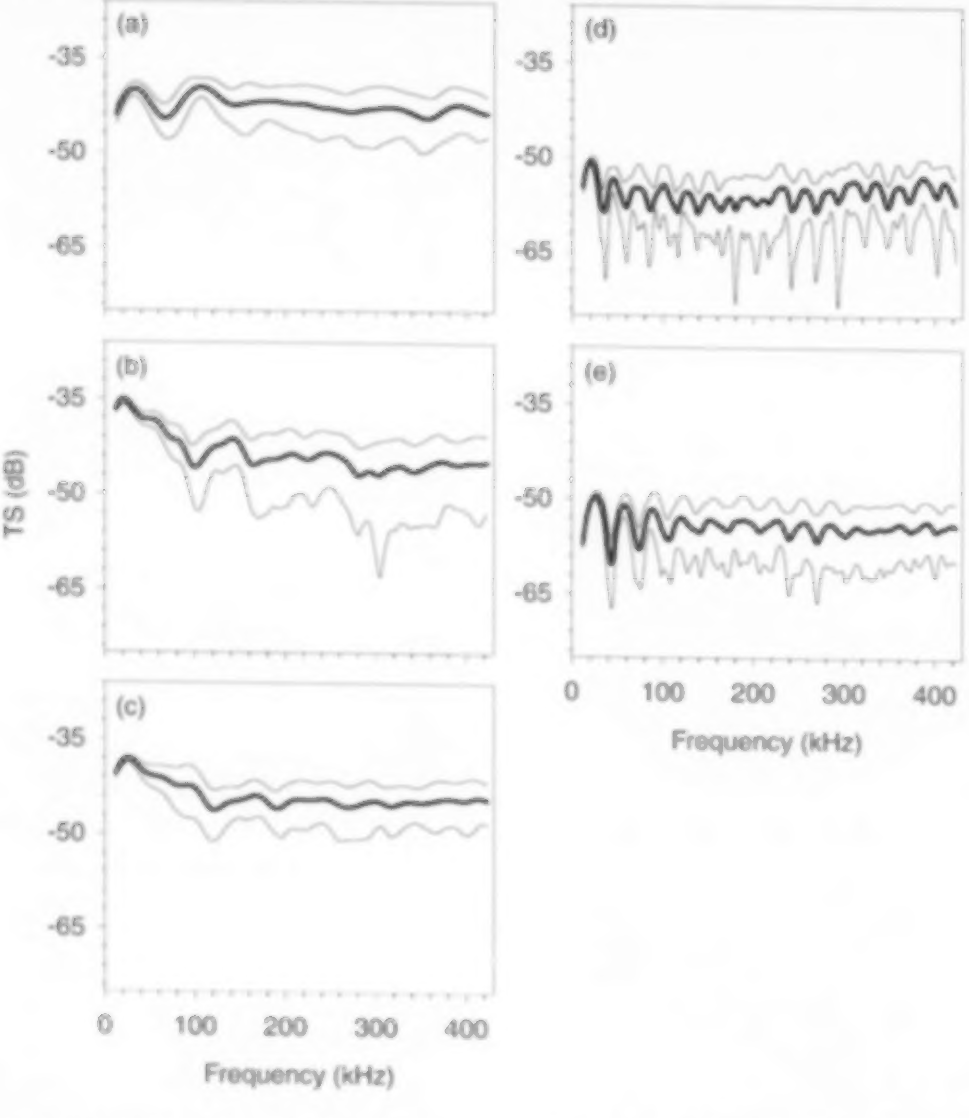

Fig. 5. Mean target strength ($\overline{TS}$, bounded by the standard deviation) as a function of frequency for fish scaled to 16 cm: (*a*) capelin (*Mallotus villosus*), (*b*) Pacific herring (*Clupea pallasii*), (*c*) walleye pollock (*Theragra chalcogramma*), (*d*) Atka mackerel (*Pleurogrammus monopterygius*), and (*e*) eulachon (*Thaleichthys pacificus*).

have been documented for a limited number of species (Qiu et al. 1999; McClatchie and Ye 2000; Barr 2001). Changing the sound speed (1548–1570 $m \cdot s^{-1}$) and density (1030–1070 $kg \cdot m^{-3}$) of fish flesh for eulachon and Atka mackerel altered the intercept values from the regressions by as much as 10 dB, but generally not the slopes or shapes of the curves (Gauthier and Horne, unpublished data).

TS of a species depends on several factors that potentially interact. These include the shape and length of the fish, the orientation (i.e., tilt, roll), and the insonyfing frequency. Morphometric (i.e., shape) differences within a species result in variable TS from fish of the same length, especially for species without swimbladders. The extent of this variability, as well as the effects of length on TS, depends on frequency. At 12 kHz, the increase in TS with increasing fish length was relatively constant. At higher frequencies, interactions of the wavelength within the fish body created more constructive and destructive interference. This typically results in more variable TS responses with increasing fish length. The effect of orientation on TS also depends on the presence or absence of a swimbladder and frequency. At 12 kHz, tilt angle has little effect on the TS of fish with swimbladders because of the small ratio of swimbladder length to acoustic wavelength. At any single frequency, the effects are more pronounced as fish size and corresponding swimbladder size increases. Maximum TS occurs at a tilt an-

Fig. 6. Mean target strength ($\overline{\mathrm{TS}}$) as a function of fish tilt angle for fish scaled to 16 cm: (*a*) capelin (*Mallotus villosus*), (*b*) Pacific herring (*Clupea pallasii*), (*c*) walleye pollock (*Theragra chalcogramma*), (*d*) Atka mackerel (*Pleurogrammus monopterygius*), and (*e*) eulachon (*Thaleichthys pacificus*). Bold line, 12 kHz; thin line, 38 kHz; shaded line, 200 kHz. Values at 120 kHz were similar to those at 200 kHz and are not plotted.

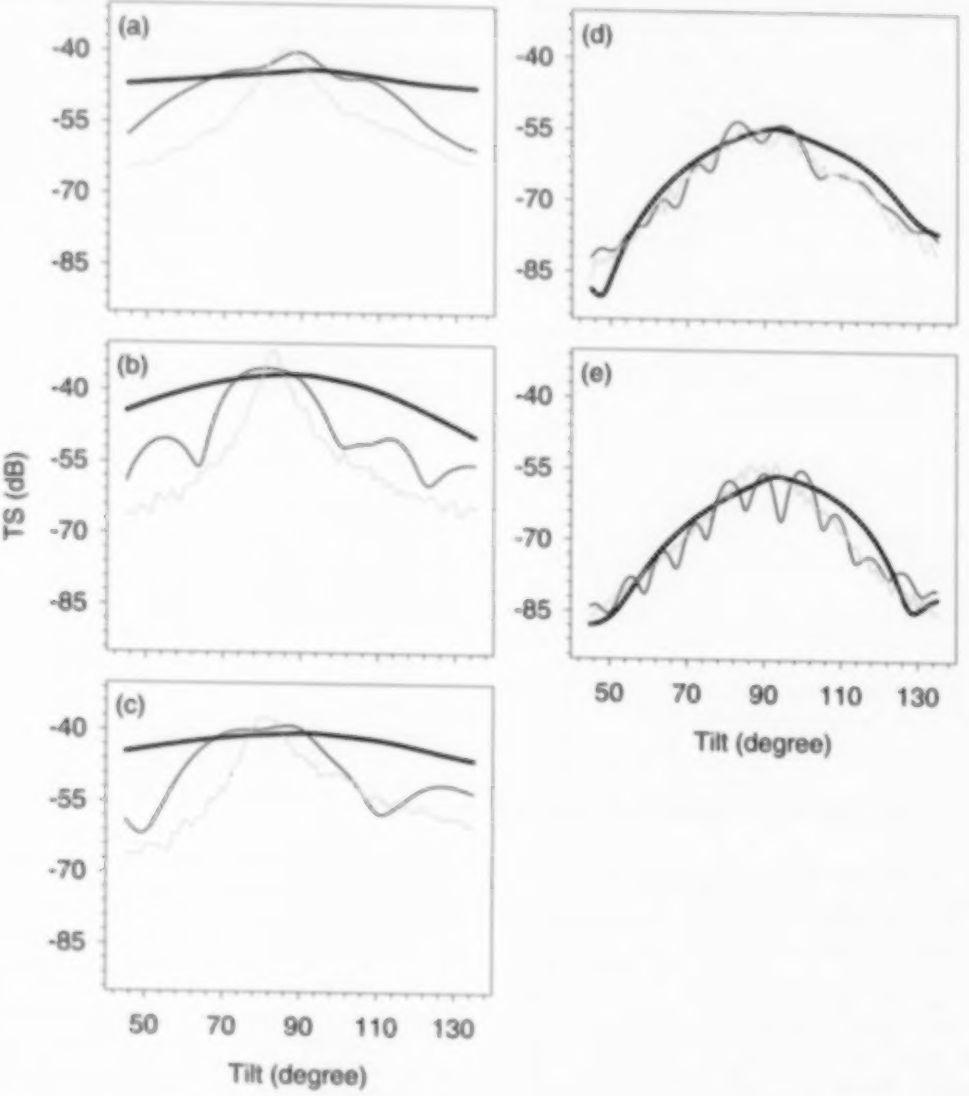

gle lower than normal aspect because of the angle of the swimbladder within the body. The swimbladder in teleost fish typically angles 5° to 10° posterior (Horne and Clay 1998). As the fish body is tilted downward, the swimbladder reaches normal aspect, maximizing the area exposed to the incident wave front. At high frequency (200 kHz), TS decreased sharply as tilt angle deviated from this maxima. Capelin had the lowest swimbladder elongation (and corresponding eccentricity) and showed the least TS variation with tilt angle at any frequency. Capelin also had the lowest proportional swimbladder volume and dorsal area. For species without swimbladders, maximum TS occurred at 90° and decreased gradually. Tilt–TS functions for these species were not as affected by frequency as fish with swimbladders. TS was more sensitive to small changes in tilt angle at higher frequencies.

We used tilt-averaged TS for the TS–length regressions to represent natural variations of tilt angles within fish populations. Among species with swimbladders, the largest difference between TS at normal incidence (90°) and tilt-averaged TS was observed for capelin. This was a surprising result as capelin TS were least affected by tilt angle. The standard deviation of the tilt distribution was higher than that of Pacific herring or walleye pollock. The average tilt angle was head-up for capelin (Carscadden and Miller 1980) versus the head-down orientation for Pacific herring and walleye

Table 4. Slope and intercept regression parameters for tilt-averaged target strength (TS_{θ}) based on total length (L_T) at five frequencies (f) based on the Kirchhoff-ray mode predictions.

Species	f (kHz)	Slope (a)	b_a	r^2	b_{20}	r^2
Capelin	12	40.0	–93.7	0.54	–70.8	0.41
	38	24.9	–75.0	0.35	–69.3	0.36
	70	11.1	–61.2	0.12	–71.3	0.05
	120	28.4	–81.8	0.62	–72.2	0.57
	200	22.3	–75.9	0.51	–73.2	0.52
Pacific herring	12	21.2	–64.1	0.01	–62.4	0.04
	38	13.3	–55.9	0.34	–65.1	0.27
	70	19.5	–66.1	0.35	–66.8	0.37
	120	21.0	–69.0	0.29	–67.6	0.31
	200	24.2	–74.3	0.32	–68.5	0.33
Walleye pollock	12	21.7	–68.1	0.96	–65.5	0.96
	38	19.2	–66.0	0.96	–67.2	0.96
	70	20.0	–68.2	0.96	–68.2	0.96
	120	21.1	–70.5	0.95	–68.9	0.94
	200	22.5	–73.1	0.96	–69.4	0.95
Atka mackerel	12	17.9	–79.1	0.86	–82.3	0.85
	38	18.5	–81.0	0.91	–83.2	0.91
	70	22.6	–87.6	0.92	–83.7	0.91
	120	19.9	–83.4	0.97	–83.6	0.97
	200	19.6	–83.1	0.93	–83.6	0.93
Eulachon						
Marine	12	40.3	–109.7	0.90	–83.4	0.68
	38	27.3	–94.0	0.66	–84.5	0.62
	70	25.0	–90.9	0.79	–84.4	0.76
	120	15.3	–77.6	0.51	–83.7	0.47
	200	21.5	–86.0	0.80	–84.0	0.80
Freshwater	12	39.8	–104.6	0.92	–80.1	0.70
	38	26.5	–89.5	0.74	–81.1	0.70
	70	23.5	–85.6	0.78	–81.1	0.77
	120	15.0	–73.8	0.61	–80.3	0.55
	200	20.5	–81.3	0.84	–80.7	0.84

pollock. The swimbladder angle for capelin was closer to horizontal, and the response of TS to tilt had a sharper peak at 38 kHz. The combination of tilt range, fish orientation, and tilt-dependent backscatter resulted in lower tilt-averaged TS for capelin than for the other species with swimbladders.

It is noteworthy that the log-linear regressions for walleye pollock and Atka mackerel had slopes near 20. Slopes of TS_{θ}–L_T regressions often differed from 20 for other species, especially capelin and eulachon. Given the relatively small length range available for these species, it is difficult to ascertain definitive values for the regression parameters. The large differences in goodness of fit (r^2) observed between the log-linear and 20log models suggest that it may not always be appropriate to express TS results using a 20log regression (cf. McClatchie et al. 1996*b*, 2003). Our modeled data also illustrate that regression parameters depend on frequency (especially for species with swimbladders) and that frequency-dependent scattering may be useful for species discrimination.

From our modeling results, we conclude that backscatter characteristics differ among the five species. As expected, the greatest differences were between fish with and without swimbladders. Variability in TS resulting from morphometric differences was high, especially for species without swimbladders. Tilt angle affected backscatter responses. TS–tilt functions also depended on the presence or absence of a swimbladder and its orientation within the fish body. Effects of fish length and tilt angle on TS were frequency-dependent. The slopes of TS_{θ}–L_T regressions were in many cases different than 20. Based on these results, the next logical step in this work is to examine potential discriminatory metrics using species-specific acoustic properties. Future efforts should also be directed at comparing model predictions with in situ measurements of monospecific and mixed aggregations of fish.

Acknowledgements

We would like to thank Jason Sweet and Rick Towler for their assistance in the field and with the analyses. Funding for this project was provided by the NMFS Steller Sea Lion Research Initiative (award number NA17FX1407), the North Pacific Universities Marine Mammal Consortium (award number NA16FX2629), the Office of Naval Research (N00014-00-1-0180), and the Alaska Fisheries Science Center (NA17RJ1232-AM01).

References

Alverson, D.L. 1992. A review of commercial fisheries and the Steller sea lion (*Eumetopias jubatus*): the conflict arena. Rev. Aquat. Sci. **6**: 203–256.

Barr, R. 2001. A design study of an acoustic system suitable for differentiating between orange roughy and other New Zealand deep-water species. J. Acoust. Soc. Am. **109**: 164–178.

Blaxter, J.H.S., and Batty, R.S. 1990. Swimbladder "behaviour" and target strength. Rapp. P.-V. Réun. Comm. Int. Explor. Mer, **189**: 233–244.

Carscadden, J.E., and Miller, D.S. 1980. Estimates of tilt angle of capelin using underwater photographs. ICES CM 1980/H:50.

Clay, C.S., and Horne, J.K. 1994. Acoustic models of fish: the Atlantic cod (*Gadus morhua*). J. Acoust. Soc. Am. **96**: 1661–1668.

Edwards, J.I., Armstrong, F., Magurran, A.E., and Pitcher, T.J. 1984. Herring, mackerel, and sprat target strength experiments with behavioral observations. ICES CM 1984/B:34.

Foote, K.G. 1980*a*. Importance of the swimbladder in acoustic scattering fish: a comparison of gadoid and mackerel target strengths. J. Acoust. Soc. Am. **67**: 2084–2089.

Foote, K.G. 1980*b*. Effect of fish behaviour on echo energy: the need for measurements of orientation distributions. J. Cons. Int. Explor. Mer, **39**: 193–201.

Foote, K.G. 1982. Optimizing copper spheres for precision calibration of hydroacoustic equipment. J. Plankton Res. **71**: 742–747.

Foote, K.G., and Francis, D.T.I. 2002. Comparing Kirchhoff-approximation and boundary-element models for computing gadoid target strengths. J. Acoust. Soc. Am. **111**: 1644–1654.

Foote, K.G., and Traynor, J.J. 1988. Comparison of walleye pollock target strength estimates determined from *in situ* measurements and calculations based on swimbladder form. J. Plankton Res. **83**: 9–17.

Gorska, N., and Ona, E. 2003. Modelling the effect of swimbladder compression on the acoustic backscattering from herring at normal or near-normal dorsal incidences. ICES J. Mar. Sci. **60**: 1381–1391.

Guttormsen, M.A., Wilson, C.D., and Stienessen, S. 2001. Echo integration-trawl survey results for walleye pollock in the Gulf of Alaska during 2001. *In* Stock Assessment and Fishery Evaluation Report for the Groundfish Resources of the Gulf of Alaska, November 2001. Prepared by the Gulf of Alaska Groundfish Plan Team, North Pacific Fishery Management Council, P.O. Box 103136, Anchorage, AK 99510.

Halldorsson, O., and Reynisson, P. 1983. Target strength measurement of herring and capelin in-situ at Iceland. FAO Fish. Rep. No. 300.

Haslett, R.W.G. 1962. The back-scattering of acoustic waves in water by an obstacle. II. Determination of the reflectivities of solids using small specimens. Proc. Phys. Soc. Lond. **79**: 559–571.

Horne, J.K. 2003. The influence of ontogeny, physiology, and behaviour on the target strength of walleye pollock (*Theragra chalcogramma*). ICES J. Mar. Sci. **60**: 1063–1074.

Horne, J.K., and Clay, C.S. 1998. Sonar systems and aquatic organisms: matching equipment and model parameters. Can. J. Fish. Aquat. Sci. **55**: 1296–1306.

Horne, J.K., Walline, P.D., and Jech, J.M. 2000. Comparing acoustic model predictions to *in situ* backscatter measurements of fish with dual-chambered swimbladders. J. Fish Biol. **57**: 1105–1121.

Jech, J.M., Schael, D.M., and Clay, C.S. 1995. Application of three sound scattering models to threadfin shad (*Dorosoma petenense*). J. Acoust. Soc. Am. **98**: 2262–2269.

Jørgensen, R. 2003. The effects of swimbladder size, condition and gonads on the acoustic target strength of mature capelin. ICES J. Mar. Sci. **60**: 1056–1062.

Jørgensen, R., and Olsen, K. 2002. Acoustic target strength of capelin measured by single-target tracking in a controlled cage experiment. ICES J. Mar. Sci. **59**: 1081–1085.

Mackenzie, K.V. 1981. Nine-term equation for sound speed in the oceans. J. Acoust. Soc. Am. **70**: 807–812.

McClatchie, S., and Ye, Z. 2000. Target strength of an oily deep-water fish, orange roughy (*Hoplostethus atlanticus*). II. Modeling. J. Acoust. Soc. Am. **197**: 1280–1285.

McClatchie, S., Alsop, J., Ye, Z., and Coombs, R.F. 1996*a*. Consequence of swimbladder model choice and fish orientation to target strength of three New Zealand fish species. ICES J. Mar. Sci. **53**: 847–862.

McClatchie, S., Alsop, J., and Coombs, R.F. 1996*b*. A re-evaluation of relationships between fish size, acoustic frequency, and target strength. ICES J. Mar. Sci. **53**: 780–791.

McClatchie, S., Macaulay, G.J., and Coombs, R.F. 2003. A requiem for the use of $20\log_{10}$length for acoustic target strength with special reference to deep-sea fishes. ICES J. Mar. Sci. **60**: 419–428.

Misund, O.A., and Øvredal, J.T. 1988. Acoustic measurements of schooling herring: estimation of school biomass and target strength. ICES CM 1988/B:26.

Mukai, T., and Iida, K. 1996. Depth dependence of target strength of live kokanee salmon in accordance with Boyle's law. ICES J. Mar. Sci. **53**: 245–248.

Nakken, O., and Olsen, K. 1977. Target strength measurements of fish. Rapp. P.-V. Réun. Comm. Int. Explor. Mer, **170**: 52–69.

O'Driscoll, R.L., and Rose, G.A. 2001. *In situ* acoustic target strength of juvenile capelin. ICES J. Mar. Sci. **58**: 342–345.

Olsen, K. 1971. Orientation measurements of cod in Lofoten obtained from underwater photographs and their relation to target strength. ICES CM 1971/B:17.

Ona, E. 1990. Physiological factors causing natural variations in acoustic target strength of fish. J. Mar. Biol. Assoc. U.K. **70**: 107–127.

Ona, E. 2001. Herring tilt angles measured through target tracking. *In* Herring: expectations for a new millenium. *Edited by* F. Funk, J. Blackburn, D. Hay, A.J. Paul, R. Stephenson, R. Toresen, and D. Witherell. Lowell Wakefield Fisheries Symposia Series, Fairbanks, Alaska. pp. 509–519.

Ona, E., Zhao, X., Svellingen, I., and Fosseidengen, J. E. 2001. Seasonal variation in herring target strength. *In* Herring: expectations for a new millenium. *Edited by* F. Funk, J. Blackburn, D. Hay, A.J. Paul, R. Stephenson, R. Toresen, and D. Witherell. Lowell Wakefield Fisheries Symposia Series, Fairbanks, Alaska. pp. 461–487.

Qiu, X.F., Zhang, R.H., Li, W.H., Jin, G.L., and Zhu, B.X. 1999. Frequency-selective attenuation of sound propagation and reverberation in the Yellow Sea. J. Sound Vib. **220**: 331–342.

Rose, G.A., and Porter, D.R. 1996. Target-strength studies on Atlantic cod (*Gadus morhua*) in Newfoundland waters. ICES J. Mar. Sci. **53**: 259–265.

Rosen, D.A.S., and Trites, A.W. 2000. Pollock and the decline of Steller sea lions: testing the junk-food hypothesis. Can. J. Zool. **78**: 1243–1250.

Rudstam, L.G., Lindem, T., and Hansson, S. 1988. Density and *in situ* target strength of herring and sprat: a comparison between two methods of analyzing single-beam sonar data. Fish. Res. **6**: 305–315.

Sawada, K., Ye, Z., Kieser, R., Mcfarlane, G.A., Miyanohana, Y., and Furusawa, M. 1999. Target strength measurements and modeling of walleye pollock and Pacific hake. Fish. Sci. **65**: 193–205.

Stanton, T.K., Chu, D., Wiebe, P.H., Eastwood, R.L., and Warren, J.D. 2000. Acoustic scattering by benthic and planktonic shelled animals. J. Acoust. Soc. Am. **108**: 535–550.

Stickney, R.R. 2000. Responses of pinniped populations to directed harvest, climate variability, and commercial fishery activity: a comparative analysis. Res. Fish. Sci. **8**: 89–124.

Thomas, G.L., Kirsh, J., and Thorne, R.E. 2002. *Ex situ* target strength measurements of Pacific herring and Pacific sand lance. N. Am. J. Fish. Manag. **22**: 1136–1145.

Traynor, J.J. 1996. Target-strength measurements of walleye pollock (*Theragra chalcogramma*) and Pacific whiting (*Merluccius productus*). ICES J. Mar. Sci. **53**: 253–258.

Traynor, J.J., and Williamson, N.J. 1983. Target strength measurements of walleye pollock (*Theragra chalcogramma*) and a simulation study of the dual beam method. FAO Fish. Rep. No. 300.

Trites, A.W., and Donnelly, P.L. 2003. The decline of Steller sea lions in Alaska: a review of the nutritional stress hypothesis. Mammal Rev. **33**: 3–28.

United Nations Educational, Scientific and Cultural Organization (UNESCO). 1983. Algorithms for computations of fundamental properties of seawater. UNESCO Tech. Pap. Mar. Sci. **44**: 1–53.

Multivariate analysis of stable-isotope ratios to infer movements and utilization of estuarine organic matter by juvenile weakfish (*Cynoscion regalis*)

Steven Y. Litvin and Michael P. Weinstein

Abstract: Canonical discriminant analysis of the natural carbon, nitrogen, and sulfur stable isotopes in tissues of young weakfish (*Cynoscion regalis*) captured in Delaware Bay was used to infer movements of juveniles and to estimate the utilization of estuarine organic matter in this marine transient species. Two gradients emerged in the data. The first was associated with contributions from tidal salt marsh macrophytes, *Spartina alterniflora* in the polyhaline lower Bay and *Phragmites australis* in the brackish upper Bay. The second was associated with the expected change in phytoplankton carbon-isotope values along the salinity gradient in addition to the availability of macrophyte-derived organic matter within the Bay. The separation of the gradients reflected differences in the relative contribution of phytoplankton to weakfish secondary production in open waters versus marsh habitats. As they grew, discrepancies between the anticipated isotopic signatures of juvenile weakfish collected in a specific habitat and their actual signatures were interpreted as down-bay movements based on known life-history patterns. The size-specific differences in the isotopic signatures of weakfish suggested that stable-isotope data can be used to gauge the relative magnitude of marsh-derived organic matter exported from Delaware Bay via movements of juveniles out of the estuary.

Résumé : Une analyse discriminante canonique des isotopes stables naturels de carbone, d'azote et de soufre dans les tissus de jeunes acoupas royaux (*Cynoscion regalis*) capturés dans la baie de la Delaware nous a servi à retracer les déplacements des jeunes et à estimer l'utilisation de la matière organique estuarienne chez cette espèce marine de passage. Deux gradients apparaissent dans les données, un premier associé aux contributions des macrophytes des marais salés affectés par la marée, *Spartina alternifolia*, dans la baie inférieure polyhaline et *Phragmites australis*, dans la baie supérieure saumâtre. Le second gradient est associé au changement attendu des values isotopiques du carbone phytoplanctonique en fonction du gradient de salinité, en plus de la disponibilité de la matière organique provenant des macrophytes à l'intérieur de la baie. La séparation des gradients est le reflet de différences dans les contributions relatives du phytoplancton à la production secondaire des acoupas dans les eaux du large et dans les habitats de marais. Durant la croissance, les écarts entre les signatures isotopiques anticipées des jeunes acoupas récoltés dans un habitat particulier et les signatures réelles s'interprètent comme des déplacements vers la baie inférieure basés sur des patterns connus du cycle biologique. Les différences de signatures isotopiques des acoupas reliées à la taille indiquent que les données sur les isotopes stables pourraient servir à évaluer l'importance relative de la matière organique provenant des marais qui est exportée de la baie de la Delaware par les déplacements des acoupas hors de l'estuaire.

[Traduit par la Rédaction]

Introduction

Among the taxa thought to benefit from the primary production of tidal salt marshes are marine transients, nekton adapted to life on a "coastal conveyor belt", often spawning far out on the continental shelf and producing estuary-dependent young that are recruited into coastal embayments year-round (Deegan et al. 2000). The life cycle of marine transients is completed when juveniles (young-of-the-year) accompany the adults offshore during their migration to wintering areas, which is sometimes repeated over several years until maturation.

Though salt marshes are believed to contribute to the success of juvenile marine transient finfishes (Boesch and Turner 1984), the extent to which they fuel the high rate of secondary production in these habitats, and in the greater estuary, has been a source of conjecture for more than four decades (Weinstein and Kreeger 2000). In the 1960s several investigators suggested that organic matter derived from salt-marsh macrophytes, especially *Spartina* spp., drives much of the secondary production of nearshore waters (Teal 1962; Darnell 1967; Odum 1968). However, as demonstrated in subsequent research, the relative rates of production and the availability of organic matter in estuaries are often mediated

Received 1 April 2003. Accepted 8 April 2004. Published on the NRC Research Press Web site at http://cjfas.nrc.ca on 16 December 2004.
J17440

S.Y. Litvin and M.P. Weinstein.[1,2] Institute of Marine and Coastal Sciences, Rutgers University, 71 Dudley Road, New Brunswick, NJ 08901-8521, USA.

[1] Corresponding author (e-mail: mweinstein@njmsc.org).
[2] Present address: New Jersey Marine Sciences Consortium, Sandy Hook Field Station, Building 22, Fort Hancock, NJ 07732, USA.

Can. J. Fish. Aquat. Sci. **61**: 1851–1861 (2004)   doi: 10.1139/F04-121

by geomorphology, spatial complexity, tidal magnitude, freshwater input, and the intermediate compounds through which organic matter is transferred to higher trophic levels (Deegan et al. 2000). In an attempt to unravel this complexity, Childers et al. (2000) posited a framework of estuarine subsystems — tidal marsh, macrofaunal beds, seagrass meadows, subtidal flats, and adjacent uplands — linked by an overlying water column that mediates and integrates processes across all subsystems. Nutrient and organic-matter flux associated with the movements of animals, especially marine transients, was also recognized as an important vector transcending system boundaries. However, attempts to link life-history stages and movements of marine transients to the nexus between primary and secondary production becomes problematic because their behavior and habitat preferences are often very flexible (Deegan et al. 2000).

Here we use stable-isotope analysis ($\delta^{13}C$, $\delta^{15}N$, and $\delta^{34}S$) to trace the movements of juveniles of a marine transient, the weakfish (*Cynoscion regalis*), in Delaware Bay, USA, and to gauge the extent of marsh primary production supporting their secondary production. The use of stable isotopes to determine the relative contribution of nutrient sources is predicated upon the observation that stable-isotope ratios of consumers reflect their diet at specific locales (Peterson and Fry 1987; Deegan and Garritt 1997). Contribution is inferred from a comparison of consumer stable-isotope signatures with those of isotopically distinct local organic matter sources while accounting for isotopic shifts associated with trophic fractionation (Peterson et al. 1986; Peterson and Fry 1987; Deegan and Garritt 1997). Spatial variability in sources of organic matter within habitats along the estuarine salinity gradient and geochemical influences (Fry 2002) create a mosaic of isotopic signatures that are characteristic of the local food webs. Nekton that move among habitat patches within the mosaic will retain the isotopic signatures commensurate with their most recent period of residency in a specific habitat, for a period that will be determined largely by growth (i.e., dilution; Hesslein et al. 1993; Herzka and Holt 2000; MacAvoy et al. 2001). Thus, movements and site fidelity can also be inferred by comparing stable-isotopic signatures of nekton captured in a specific habitat patch with the expected range of isotope values at that location (Fry 1983; Hesslein et al. 1991; Klein et al. 1998).

Previously, Litvin and Weinstein (2003) described the distribution of stable isotopes of carbon, nitrogen, and sulfur in post-settlement weakfish collected from open water and tidal-marsh creeks in Delaware Bay. The isotope content of young weakfish (<60 mm standard length (SL)) varied significantly with collection location as a function of (*i*) the change in dominant marsh vegetation from *Spartina* spp. to *Phragmites australis* along the estuarine salinity gradient; (*ii*) differences in the relative contributions of phytoplankton-derived organic matter between open-Bay and tidal-marsh habitats; and (*iii*) the anticipated change in phytoplankton $\delta^{13}C$ values with salinity (Fry 2002). By examining the stable-isotope content of larger juvenile weakfish (>60 mm SL) collected throughout the saline portion of Delaware Bay, including additional sites not reported on previously, we expand upon the previous study by (*i*) examining the spatial variability in the isotopic signatures of young-of-the-year weakfish and the corresponding contribution of estuarine organic sources using a multivariate approach (canonical discriminant analysis); (*ii*) utilizing the classification functions derived from the isotopic signatures of post-settlement individuals to assign larger, more mobile juveniles to habitats based on their isotopic signatures in order to infer movement patterns (Hobson 1999); and (*iii*) estimating the interaction of movements and the local availability of organic matter to gauge the relative magnitude of marsh-derived organic matter exported from Delaware Bay via movements of juveniles out of the estuary.

Materials and methods

Study area and sample collection

Tidal salt marsh composes about 73 000 ha of the Delaware Bay shorefront, but a substantial portion of brackish wetlands, at least 16 000 ha in Delaware and probably an area of similar magnitude on the New Jersey side, has been invaded by an aggressive variety of *P. australis* (Fig. 1). Sampling was conducted within three regions designated lower, mid-, and upper (Delaware) Bay, respectively (Fig. 1). Within each region fish were collected from open waters and adjacent tidal creeks: *P. australis*-dominated Alloway Creek, a 1253-ha meso-oligohaline marsh, and Mad Horse Creek, a relatively undisturbed 1558-ha mesohaline marsh, in the upper Bay and mid-Bay regions, respectively, and Dennis Creek, an undisturbed 1100-ha marsh, and West Creek, a nearby 234-ha formerly diked salt-hay farm, were located in polyhaline waters adjacent to the lower Bay (Fig. 1). In contrast to the virtual monocultures of *P. australis* in Alloway Creek, the intertidal marsh surface at both Mad Horse Creek and Dennis Creek was dominated by a more than 90% coverage of smooth cordgrass (*Spartina alterniflora*), but big cordgrass (*Spartina cynosuroides*) was also common on creek banks at Mad Horse Creek (Weinstein et al. 1997). Details of vegetation-sample collection and isotopic analysis (macrophytes, benthic microalgae, and phytoplankton measured as suspended particulate matter (SPM)) appear in Wainright et al. (2000), Weinstein et al. (2000), and Litvin and Weinstein (2003) and are not repeated here. Because whole water samples collected in tidal creeks may contain substantial pyrite, isotope values from the literature for SPM sulfur (Peterson et al. 1986) were substituted (Chanton and Lewis 1999; for a detailed discussion see Wainright et al. 2000).

Juvenile weakfish were collected from June through early October of 1998 and 1999 in tidal salt marsh creeks and the upper, middle, and lower reaches of the Bay (Fig. 1) with otter trawls towed near low tide for 10 min during daytime and (or) nighttime hours ($n = 450$). Fish were measured for SL to the nearest millimetre and preserved on dry ice for transport to storage at –80 °C. On each sampling date and location we attempted to collect individuals from three size classes: post-settlement <60 mm SL ("small"), 60–100 mm SL ("medium"), and >100 mm SL ("large"). These size classes reflect ontogenetic shifts in the juvenile weakfish diet from specialization on *Neomysis americana* when small, to an increasing proportion of fish when medium-sized, to roughly equal proportions of crustaceans and fish when large (Chao and Musick 1977; Nemerson 2001). In addition, juvenile weakfish were collected at the mouth of Delaware Bay prior

Fig. 1. Locations of the three subregions and affiliated marsh creeks that formed part of this study in Delaware Bay, USA (lower, mid- and upper Bay, Alloway Creek, Mad Horse Creek, West Creek, and Dennis Creek) and the extent of tidal salt marshes dominated by *Spartina alterniflora* and *Phragmites australis*.

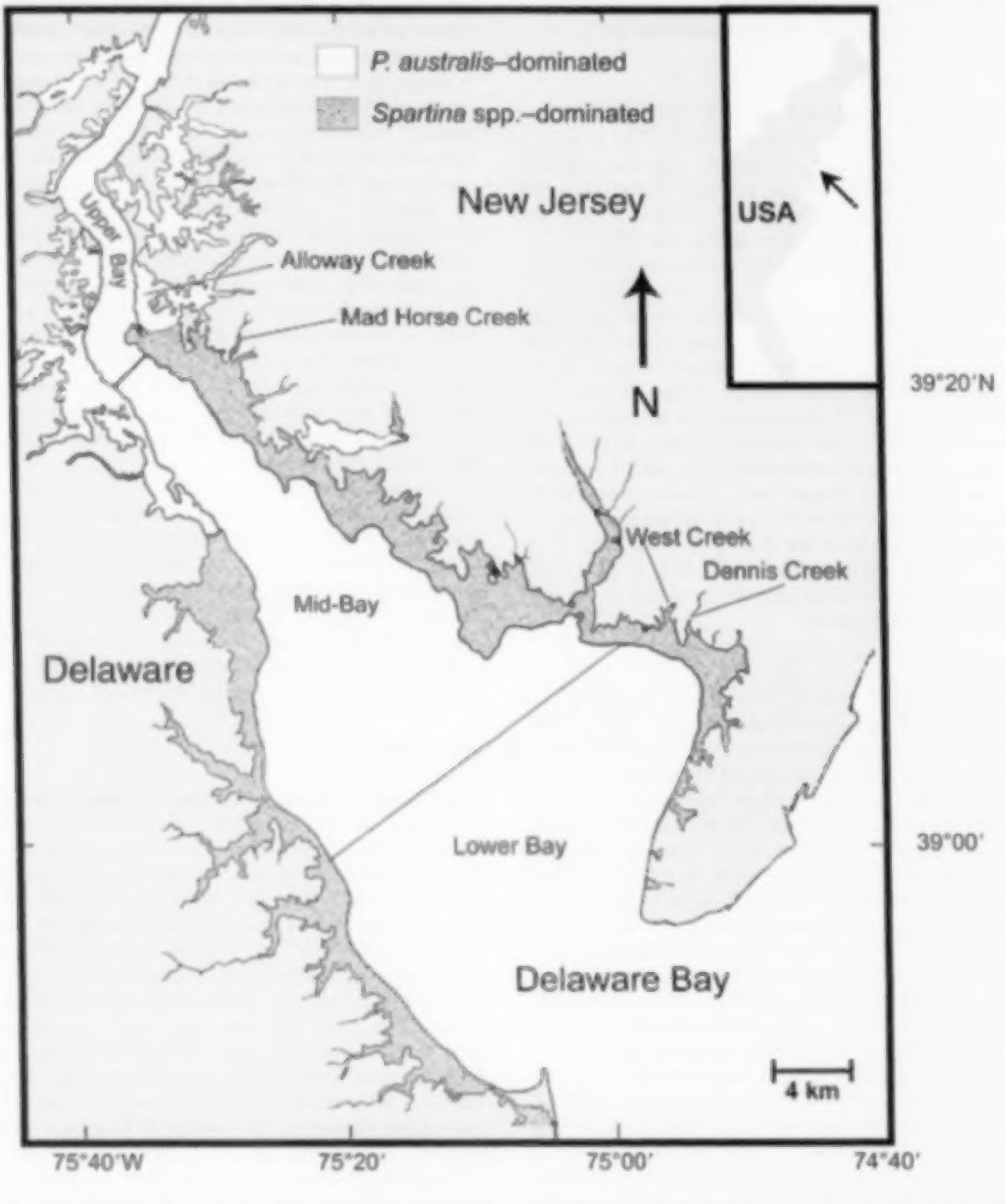
P. australis–dominated
Spartina spp.–dominated
New Jersey
USA
Upper Bay
Alloway Creek
Mad Horse Creek
N
39°20′N
West Creek
Dennis Creek
Mid-Bay
Delaware
Lower Bay
39°00′
Delaware Bay
4 km
75°40′W
75°20′
75°00′
74°40′

to emigration in late October and early November of 1998 and 1999 ($n = 141$).

Sample processing and isotope determination

In 1998, samples of muscle tissue were excised from weakfish >100 mm SL after skin and scales were removed, while smaller fish were used whole. Samples were dried to constant weight at 60 °C, then ground to a fine powder in a Spex/CertiPrep 5100 mill. In 1999, all fish were freeze-dried whole subsequent to removal of gut contents. Freeze-drying facilitated the simultaneous analysis of lipids and protein for a concurrent biochemical condition study (S.Y. Litvin, M.P. Weinstein, and V. Guida, unpublished data). In 1998, fish tissue samples were analyzed at both the Institute of Marine and Coastal Sciences, Rutgers University, New Brunswick, N.J., USA, on a Europa Scientific continuous-flow elemental analyzer (ANCA-GSL) – mass-spectrometer stable-isotope system and at the Environmental Isotope Laboratory, University of Waterloo, Ontario, Canada, on a Micromass Isochrom Continuous Flow Stable Isotope Mass Spectrometer coupled to a Carla Erba Elemental Analyzer (CHNS-O EA1 108). All fish sampled in 1999 were analyzed at the University of Waterloo. Isotopic composition is expressed in δ notation that indicates depletion (–) or enrichment (+) of the heavy isotope relative to the lighter isotope as

$$\delta X = [(R_{\text{sample}} \cdot R_{\text{standard}}^{-1}) - 1] \times 10^3$$

where X is ^{13}C, ^{34}S, or ^{15}N and R is $^{13}\mathrm{C}\cdot{}^{12}\mathrm{C}^{-1}$, $^{34}\mathrm{S}\cdot{}^{32}\mathrm{S}^{-1}$, or $^{15}\mathrm{N}\cdot{}^{14}\mathrm{N}^{-1}$ for the samples and the standards. The standards were Peedee Belemnite for carbon, air for nitrogen, and Canyon Diablo triolites for sulfur. Instrument precision was ±0.1–0.2‰ for δ^{13}C and δ^{15}N and ±0.5‰ for δ^{34}S at the Rutgers University laboratory and ±0.2‰ for δ^{13}C, ±0.3‰ for δ^{15}N, and ±0.5‰ for δ^{34}S at the University of Waterloo laboratory.

Prior to statistical comparison of stable-isotope signatures among juvenile weakfish from different size classes, normalization for ontogenetic shifts was required because of the expected enrichment of stable-isotope values, 1.0‰ δ^{13}C, 3.4‰ δ^{15}N, and 0.5‰ δ^{34}S, associated with trophic transfer (Peterson and Fry 1987). The estimated trophic level for the smallest size class was approximately 0.15 and 0.30 lower than the medium and larger size classes, respectively (Nemerson 2001). To account for these differences, stable-isotope values were reduced by 0.15‰ δ^{13}C, 0.51‰ δ^{15}N, and 0.08‰ δ^{34}S for medium-sized and 0.30‰ δ^{13}C, 1.02‰ δ^{15}N, and 0.15‰ δ^{34}S for large juvenile weakfish in the subsequent statistical comparisons.

Data analysis

We used small (least mobile; Grecay and Targett 1996) weakfish to establish a post-settlement baseline for isotopic comparisons with larger juveniles captured throughout Delaware Bay. To minimize the confounding effects of collection location and recent movements of individuals, we conjectured that small fish would exhibit the greatest site fidelity and this would be reflected in their tissue isotopic signatures (Deegan and Garritt 1997). This was true in all cases except one (Litvin and Weinstein 2003): the isotopic signatures of small weakfish collected in Alloway Creek were not readily distinguishable from those of individuals captured in open waters of the nearby mid-Bay. We anticipated that these fish would be depleted in both δ^{13}C and δ^{34}S; this is typical of individuals captured in *P. australis*-dominated systems. However, the majority of these fish exhibited the isotopic signatures, intermediate δ^{13}C values, and enriched δ^{34}S values that are typical of individuals collected in the open reach of the Bay (see Results; Weinstein et al. 2000; Litvin and Weinstein 2003).

Because small fish from Alloway Creek were collected on a single date, and may have been recent recruits (not having had sufficient time to take on the characteristic isotopic signatures of this habitat), they were removed from the pool of fish used to establish the post-settlement baseline and replaced by medium-sized fish from Alloway Creek that exhibited the anticipated isotopic signatures (Litvin and Weinstein 2003). These fish (<60 mm SL from all sites with the exception of medium-sized fish from Alloway Creek; n = 282) were analyzed by multiple analysis of variance (MANOVA) with δ^{13}C, δ^{15}N, and δ^{34}S as dependent variables and capture location as the independent factor (McGarigal et al. 2000). Canonical discriminant analysis was also employed to extract patterns of isotopic signatures as a function of capture location. The ability of the functions to correctly classify post-settlement-baseline weakfish (hereinafter referred to as baseline weakfish) to their collection location was tested by reclassification and jackknife validation where a single fish was removed from the total constituting the baseline, the classification results were re-derived, and the omitted fish were classified to a location, with the process repeated for each remaining fish. Jackknife classification results were then compared with the reclassification results to measure the reliability of the canonical functions (McGarigal et al. 2000). To discern their recent habitat-utilization patterns, we predicted the collection location of the remaining medium-sized and large weakfish (n = 299) by applying the classification functions to their isotopic signatures. We reasoned that the discrepancy between the isotopic signature of a medium-sized or large juvenile and the range of values expected for the particular area in which the individual was collected (i.e., the post-settlement baseline) indicated recent utilization of an alternative habitat within the estuary (Hobson 1999).

The lack of normality in the δ^{34}S data of the baseline weakfish (Kolmogorov–Smirnov one-sample tests; $\alpha = 0.05$) and lack of homogeneity within covariance matrices ($p <$ 0.001; Morrison 1976) in the MANOVA resulted in the use of untransformed data and a nonparametric K – nearest neighbor ($K = 10$; $n_{\min} - 1$; SAS Institute Inc. 2000) approach for the canonical discriminant analysis. SYSTAT® (SPSS Inc. 1998) and SAS® (SAS Institute Inc. 2000) for Windows® were used for all statistical comparisons.

Results

Weakfish constituting the post-settlement baseline

Overall, the isotopic signatures of baseline weakfish varied widely across the estuary but were generally bounded by the δ^{13}C and δ^{34}S values of primary producers (Fig. 2). In lower Delaware Bay, fish from open waters and *Spartina* spp.-dominated tidal creeks displayed overlapping stable-isotope signatures, with δ^{13}C intermediate between *Spartina* spp. and SPM and δ^{34}S intermediate between benthic microalgae and SPM (Figs. 2*a* and 2*b*). Fish collected in the mid-Bay, where a transition from *Spartina* spp. to *P. australis*-dominated tidal marshes occurred, had δ^{13}C and δ^{34}S values intermediate to those of the four organic sources (Fig. 2*c*). The δ^{13}C values of fish collected in this region and lower Bay habitats overlapped; however, the lowest δ^{13}C values exhibited by mid-Bay fish showed that they were depleted relative to fish collected in the lower Bay. The δ^{34}S contents of fish collected in mid-Bay open waters varied little and were slightly depleted relative to SPM, while the widest range of δ^{34}S values in post-settlement individuals was displayed by those in Mad Horse Creek. The δ^{15}N values of fish varied widely in the mid-Bay, becoming either enriched, in Mad Horse Creek, or depleted, in the open Bay, with decreasing δ^{13}C (Fig. 2*d*). The δ^{13}C values of fish collected in the upper Bay (Fig. 2*e*), where *P. australis* dominated the tidal-marsh macrophyte community, overlapped little with those from the lower Bay and included the most depleted values in baseline individuals. In fish from both Alloway Creek and upper Bay open

Fig. 2. Dual-isotope plots of $\delta^{15}N$ on $\delta^{13}C$ and $\delta^{34}S$ on $\delta^{13}C$ comparing weakfish, *Cynoscion regalis*, constituting the post-settlement baseline (<60 mm standard length (SL) except those in Alloway Creek, 60–100 mm SL; see the text) collected in lower Bay creeks (□) (*a*), lower Bay open waters (▷) (*b*), Mad Horse Creek (◇) (*b*), mid-Bay open waters (△) (*d*), Alloway Creek (○) (*e*), and upper Bay open waters (◁) (*f*), with those of primary producers (phytoplankton measured as suspended particulate matter (SPM), benthic microalgae (BMA), *Phragmites australis* (*Pa*), and *Spartina alterniflora* (*Sa*)). Ellipses represent mean values ±1 standard deviation.

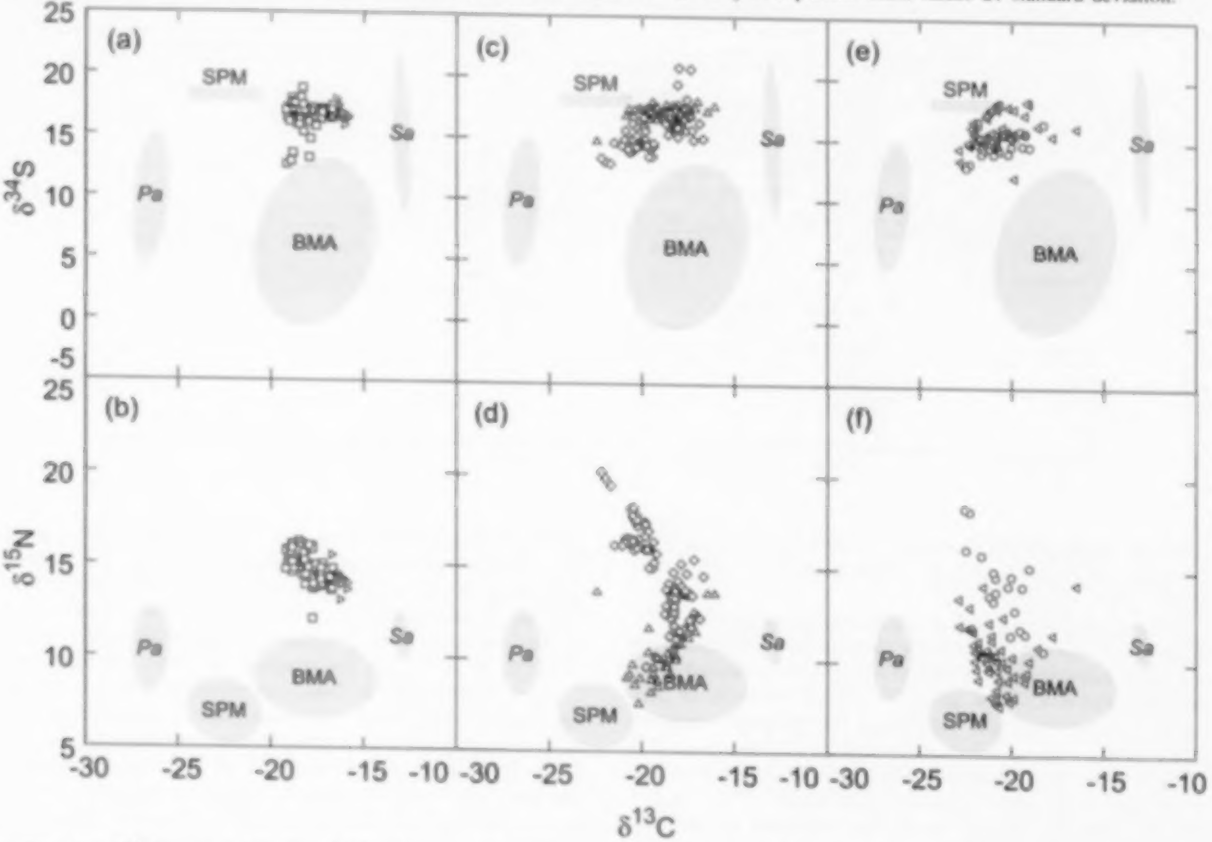

waters, the $\delta^{34}S$ content became depleted (Fig. 2*e*) and the $\delta^{15}N$ content became enriched (Fig. 2*f*) with decreasing $\delta^{13}C$. In addition, fish collected in Alloway Creek were generally depleted in $\delta^{34}S$ and enriched in $\delta^{15}N$ relative to individuals collected in the adjacent open Bay.

Multivariate analysis

The isotopic signatures of weakfish constituting the post-settlement baseline were significant for capture location, with $\delta^{13}C$, $\delta^{15}N$, and $\delta^{34}S$ all contributing to the differences among groups (MANOVA; Table 1A). The associated canonical discriminant analysis produced two significant canonical functions (Table 1B), the first accounting for 88% and the second for 11% of the variation among isotopic signatures of fish captured at different locations. Contributions by $\delta^{13}C$ and $\delta^{15}N$ to the first canonical function were dominant and approximately equal (Table 1B). Although the magnitude of the contribution of the stable isotopes was roughly equal to the second canonical function, the contribution of $\delta^{15}N$ was negative relative to that of $\delta^{13}C$ and $\delta^{34}S$ (Table 1B).

Two gradients emerged in the canonical plot comparisons (Fig. 3*a*). Both originated in fish from the lower Bay that exhibited enriched $\delta^{13}C$ values combined with intermediate $\delta^{15}N$ and $\delta^{34}S$ values (Fig. 2*a*). In open waters of the lower and mid-Bay, $\delta^{13}C$ and $\delta^{15}N$ values declined, while $\delta^{34}S$ values remained constant as distance from the Bay mouth increased. Similarly, $\delta^{13}C$ was further depleted at the transition from mid to upper Bay, while $\delta^{15}N$ ratios began to increase and $\delta^{34}S$ ratios to decrease (Fig. 2). This open-water gradient was reflected in the canonical function scores as a steady decrease in the values of the first function coupled with slightly decreasing values of the second function through the mid-Bay, followed by a pronounced decrease in the second function proceeding from mid- to upper Bay (Fig. 3*a*). A similar pattern emerged for tidal creeks in the form of decreases in $\delta^{13}C$ values with distance from the Bay mouth coupled with enriched $\delta^{15}N$ and depleted $\delta^{34}S$ in fish from the upper (Alloway Creek) and mid-Bay (Mad Horse Creek) marshes relative to those in the lower Bay tidal creeks (Fig. 2). The tidal-marsh gradient resulted in canonical function scores that approached a 1:1 ratio (Fig. 3*a*).

The canonical functions classified baseline weakfish to their location of collection at an average rate of 85% (reclassification; Table 2). All locations exhibited reclassification rates >79% with the exception of Mad Horse Creek. The

Table 1. Results from the multiple analysis of variance (A) and canonical discriminant analysis (B) utilizing a nonparametric *K* – nearest neighbor (n_{min} – 1) approach for the effect of collection location on the carbon, nitrogen, and sulfur isotopic signatures of juvenile weakfish, *Cynoscion regalis*, constituting the post-settlement baseline (<60 mm standard length (SL), except those in Alloway Creek, 60–100 mm SL).

(A) Multiple analysis of variance: contribution of individual isotopes to group differences.[a]

Isotope	$F_{[3,278]}$	p
$\delta^{13}C$	57.32	<0.0001
$\delta^{15}N$	83.32	<0.0001
$\delta^{34}S$	15.52	<0.0001

(B) Canonical discriminant analysis.

	Squared canonical correlation	Porportion of variance explained	Eigenvalue	F	p
Canonical function 1	0.78	0.88	3.04	$F_{[15,757]}$ = 50.25	<0.0001
Canonical function 2	0.30	0.11	0.44	$F_{[8,550]}$ = 15.62	<0.0001

	Canonical structure	
Isotope	Function 1	Function 2
$\delta^{13}C$	0.68	0.69
$\delta^{15}N$	0.80	–0.60
$\delta^{34}S$	0.02	0.82

[a] Overall effect of collection location on isotopic signature: Wilks' λ = 0.14839, $F_{[15,757]}$ = 50.25, $p < 0.0001$.

jackknife validation success rate was 80% and differed from the reclassification rate for the same location by 9% or less (Table 2).

By applying the canonical functions developed for post-settlement weakfish constituting the baseline, medium-sized and large individuals were classified to location according to their adjusted $\delta^{13}C$, $\delta^{15}N$, and $\delta^{34}S$ values (Table 3). In general, the stable-isotope signatures of juvenile weakfish >60 mm SL, and therefore their position on the canonical function plots, fell within the previously reported boundaries of the open-water and marsh-habitat gradients (Figs. 3*b*, 3*c*, and 3*d*). The majority of small fish collected in Alloway Creek (n = 10), which were not used to construct the post-settlement baseline, were classified to the mid-Bay (Table 3), supporting the earlier conclusion that they were recent arrivals from other habitats. At most locations large fish displayed a greater range of canonical-function scores than medium-sized fish (Figs. 3*b* and 3*c*), with larger individuals from the lower Bay and the Bay mouth exhibiting the widest range (Fig. 3*d*). However, 102 of 141 fish collected at the Bay mouth were classified into the lower Bay category (Fig. 4).

Discussion

Isotopic gradients in post-settlement weakfish

The tidal-marsh and open-water gradients depicted by canonical discriminant analysis underscore the importance of locally produced organic matter in the trophic spectrum of Delaware Bay (Wainright et al. 2000; Weinstein et al. 2000; Litvin and Weinstein 2003) and other estuarine systems (Peterson et al. 1986; Deegan and Garritt 1997; Deegan et al. 2000). Moreover, the stable-isotope composition and resulting canonical scores of juvenile weakfish captured in tidal salt marshes of Delaware Bay reflected their underlying dependence on phytoplankton and the local dominant vegetation, either *P. australis* or *S. alterniflora*. Together, the isotopic signatures of the macrophytes defined the end-members of what we described earlier as the marsh gradient. Baseline juveniles collected from polyhaline lower Bay marsh creeks displayed $\delta^{13}C$ values intermediate to those of SPM and *S. alterniflora* and $\delta^{34}S$ values intermediate to those of SPM and benthic microalgae, suggesting that *S. alterniflora* was an important source of organic matter. At the opposite end of the gradient, weakfish collected in Alloway Creek were characterized by $\delta^{13}C$ isotopic signatures intermediate to those of SPM and *P. australis* and $\delta^{34}S$ signatures intermediate to those of SPM and benthic microalgae, both characteristic of reliance on *P. australis* organic matter, and perhaps a proximate source of anthropogenic nitrogen as indicated by enriched $\delta^{15}N$ (McClelland and Valiela 1998; Weinstein et al. 2000; Litvin and Weinstein 2003). Although Mad Horse Creek is *Spartina* spp.-dominated (>90% coverage of the marsh plain), it is located in the *Spartina* spp. – *P. australis* transition zone in Delaware Bay. The canonical scores of young weakfish captured here, which were intermediate to those of individuals from tidal marshes in the upper and lower Bay, appeared to reflect the availability of both dominant macrophytes, which suggests that tidal action and (or) the local movements of individuals were responsible for the observed pattern. The overlap of canonical scores with those of individuals collected in Alloway and the lower Bay creeks was likely a result of the availability of organic matter from both marsh macrophytes in Mad Horse Creek. Interestingly, few post-settlement weakfish captured in tidal marshes exhibited stable-isotope signatures that were consistent with those of organic matter derived from benthic microalgae (intermediate $\delta^{13}C$ values coupled with depleted $\delta^{15}N$ and $\delta^{34}S$). This does not preclude a role for benthic microalgae as an organic matter source; rather it suggests that benthic micro-

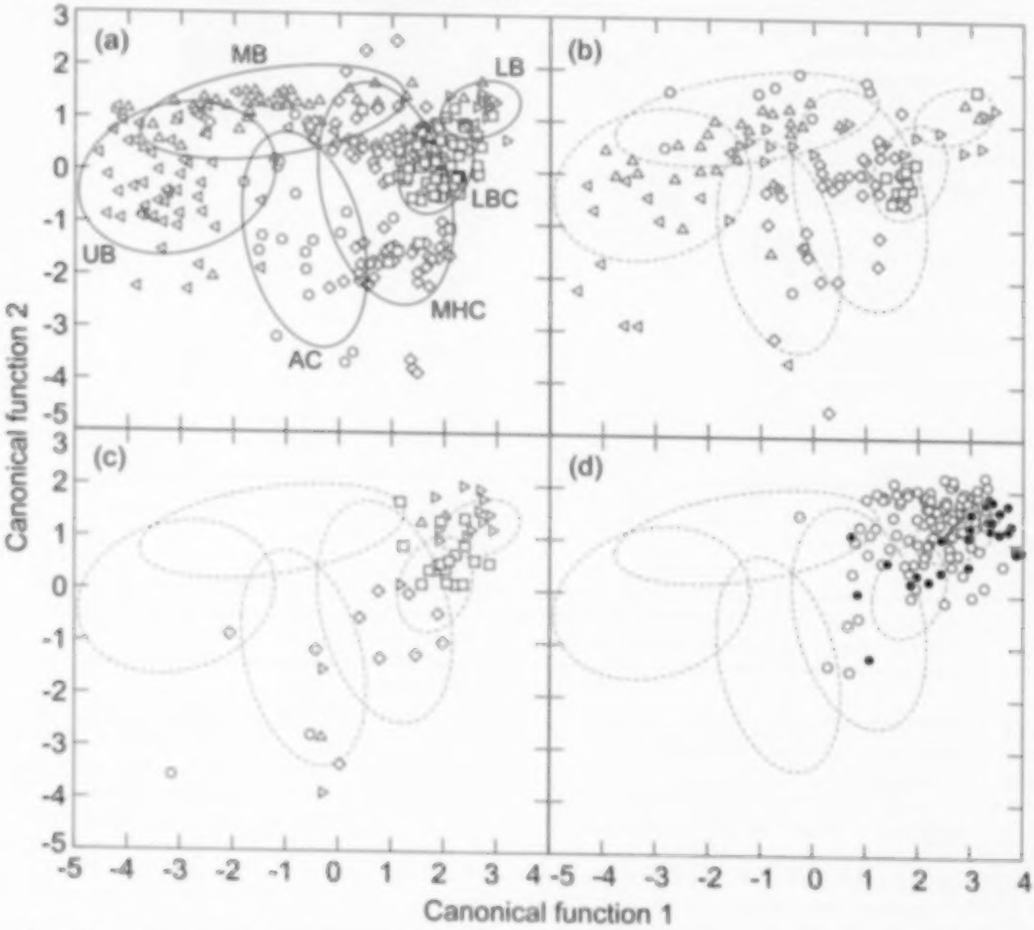

Fig. 3. Plot of standardized canonical function scores based on the carbon, nitrogen, and sulfur isotopic signatures of weakfish collected in Alloway Creek (AC: ○), Mad Horse Creek (MHC: ◇), lower Bay creeks (LBC: □), upper Bay open waters (UB: ◁), mid-Bay open waters (MB: △), and lower Bay open waters (LB: ▷). (*a*) Fish constituting the post-settlement baseline (<60 mm SL, except those in Alloway Creek, 60–100 mm SL; see the text). (*b*) Fish 60–100 mm SL (except those in Alloway Creek, <60 mm SL; see the text). (*c*) Fish >100 mm SL. (*d*) Fish 60–100 mm SL (●) and >100 mm SL (○) collected at the mouth of Delaware Bay prior to emigration. Ellipses represent mean values ±1 standard deviation of the standardized canonical function scores for fish constituting the post-settlement baseline and are repeated in *b*, *c*, and *d* for reference.

algae may be of less importance than phytoplankton and marsh macrophytes in contributing to the nutrition of this semipelagic species (Litvin and Weinstein 2003).

A similar pattern of spatial heterogeneity was observed in the open-water gradient, where, as in the marsh gradient, the isotopic signatures of the macrophytes defined end-members of the trophic spectrum. However, enriched S and depleted N isotopes reflected the increased reliance on phytoplankton that is represented in the separation of the two gradients on the second canonical axis.

The enriched carbon-isotope values (and the highest mean value for the first canonical function) of small weakfish collected in lower Delaware Bay compared with those found in other collection locations implies that organic matter derived from *S. alterniflora* was a substantial contributor to weakfish nutrition. While the decrease in scores for the first canonical function with distance from the Bay mouth could be solely attributed to the anticipated change in phytoplankton $\delta^{13}C$ values with salinity (Fry 2002), the depleted $\delta^{34}S$ values relative to SPM values observed in most small weakfish captured in the open Bay (combined with the significant change in $\delta^{34}S$ values with collection location; Litvin and Weinstein 2003) suggest that organic matter from marsh macrophytes was being exported to the open Bay. Additionally, the decrease in the first canonical function also suggests a change in contribution from *S. alterniflora* to *P. australis* organic matter along the estuarine salinity gradient, mirroring the changes seen in the marsh gradient.

Stable-isotope signatures as a measure of juvenile weakfish movements

The ability of canonical discriminant analysis to correctly identify the collection location of post-settlement weakfish validated the pattern of unique isotopic signatures associated

Table 2. Canonical discriminant function classification results for juvenile weakfish constituting the post-settlement baseline (<60 mm SL, except those in Alloway Creek, 60–100 mm SL), based on their carbon, nitrogen, and sulfur isotope signatures.

	Number of fish classified as:						
Collection location	AC	MHC	LBC	UB	MB	LB	Correctly classified (%)
Alloway Creek (AC) (*n* = 18)							
Reclassification	**17**	0	0	0	1	0	94
Jackknife	**16**	1	0	0	1	0	89
Mad Horse Creek (MHC) (*n* = 86)							
Reclassification	10	**51**	12	0	6	7	59
Jackknife	10	**50**	13	0	6	7	58
Lower Bay creeks (LBC) (*n* = 69)							
Reclassification	0	2	**62**	0	1	4	90
Jackknife	0	2	**60**	0	1	6	87
Upper Bay (UB) (*n* = 53)							
Reclassification	4	1	0	**42**	5	1	79
Jackknife	4	1	0	**41**	6	1	77
Mid-Bay (MB) (*n* = 45)							
Reclassification	1	0	0	1	**40**	3	89
Jackknife	1	1	0	4	**36**	3	80
Lower Bay (LB) (*n* = 11)							
Reclassification	0	0	0	0	0	**11**	100
Jackknife	0	0	1	0	0	**10**	91

Note: The number of individuals correctly classified to their collection location via the canonical discriminant function is indicated in boldface font (the percentage correctly classified is also shown); *n* is the number of individuals.

Table 3. Canonical discriminant function classification results for medium-sized (60–100 mm SL) and large (>100 mm SL) juvenile weakfish, and small (<60 mm SL) individuals collected in Alloway Creek, based on their carbon, nitrogen, and sulfur isotope signatures.

		Number of fish classified as:					
Collection location	*n*	AC	MHC	LBC	UB	MB	LB
Alloway Creek (AC)							
<60 mm SL	10	1	0	1	0	8	0
>100 mm SL	2	1	0	0	1	0	0
Mad Horse Creek (MHC)							
60–100 mm SL	38	11	16	10	0	0	1
>100 mm SL	10	4	4	2	0	0	0
Lower Bay creeks (LBC)							
60–100 mm SL	12	0	1	10	0	0	1
>100 mm SL	18	0	1	11	0	1	5
Upper Bay (UB)							
60–100 mm SL	13	2	1	0	10	0	0
>100 mm SL	0	—	—	—	—	—	—
Mid-Bay (MB)							
60–100 mm SL	27	3	3	0	6	13	2
>100 mm SL	3	1	0	1	0	0	1
Lower Bay (LB)							
60–100 mm SL	20	2	3	4	0	5	6
>100 mm SL	15	2	0	2	0	0	11
Bay mouth (BM)							
60–100 mm SL	29	0	2	7	0	0	20
>100 mm SL	112	2	3	17	0	8	82

Note: *n* is the number of individuals.

Fig. 4. Canonical discriminant function classification results based on the carbon, nitrogen, and sulfur isotopic signatures of small (<60 mm SL), medium-sized (60–100 mm SL), and large (>100 mm SL) weakfish collected in the open waters and at the mouth of Delaware Bay prior to emigration.

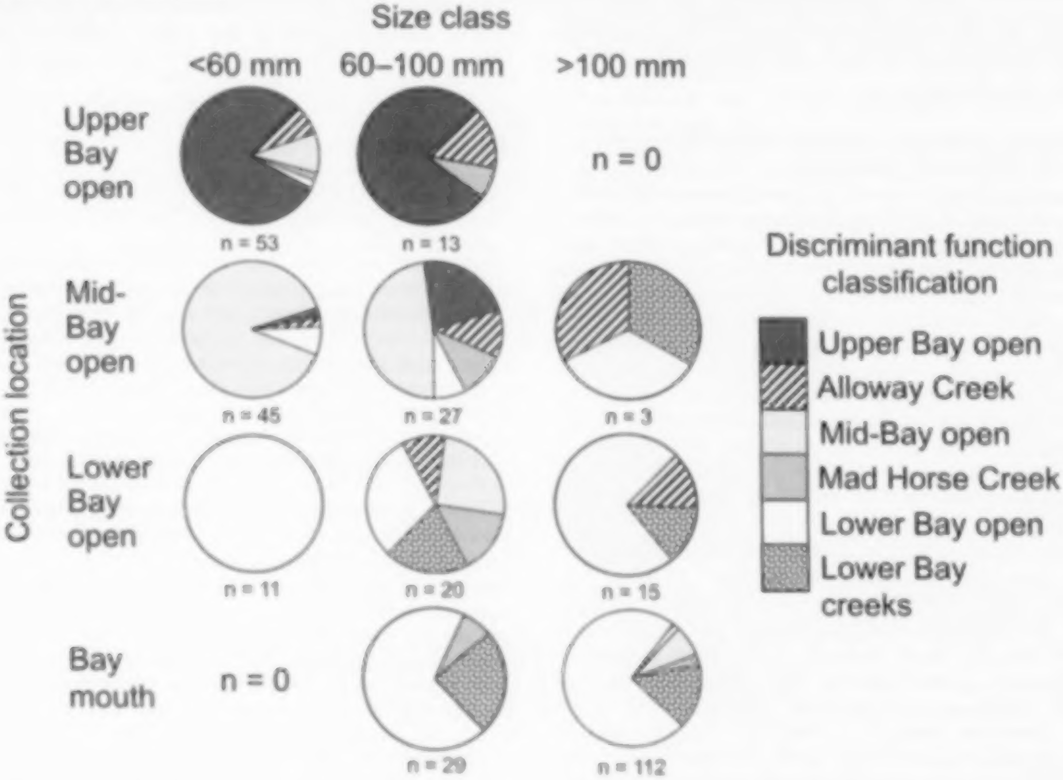

with short-term residency in open-water and tidal-marsh habitats and allowed us to infer the movements of larger, more mobile individuals within Delaware Bay (Hobson 1999). The classification results for medium-sized fish collected in the open waters of the upper Bay implied the same pattern of site fidelity found in small individuals. Conversely, for mid- and lower Bay open waters, greater than half of medium-sized individuals collected appeared to be recent arrivals from up-Bay habitats or adjacent tidal marshes, while in tidal marshes there was little evidence of emigration. With the exception of Mad Horse Creek, we collected few large juveniles in the mid- and upper Bay, indicating that they had previously emigrated from these habitats. Large juveniles collected in the lower Bay open waters, like medium-sized individuals, appeared to be a mixture of lower Bay residents and recent arrivals from other habitats, although a higher proportion of large individuals, 73% versus 30%, exhibited the stable-isotope signatures characteristic of extended residency in the lower Bay. These results indicate that a proportion of the large juveniles classified as "lower Bay open" arrived as medium-sized individuals and acquired the stable-isotope signature of the lower Bay as they grew. Our premise is further supported by the high growth rates exhibited by juvenile weakfish in Delaware Bay. An individual arriving in the lower Bay at 75 mm SL will increase its biomass by a factor of nearly 5 at 125 mm SL (S.Y. Litvin, unpublished data). At this new biomass, fish will have an isotopic signature that reflects in-situ trophic transfers and will dilute any previously acquired isotopic signature even in the absence of metabolic turnover (Hesslein et al. 1993; Herzka and Holt 2000; MacAvoy et al. 2001). A similar proportion of weakfish collected at the mouth of Delaware Bay in late October and early November accumulated the bulk of their biomass in lower Bay open waters, leading us to conclude that movements from up-bay habitats and the adjacent tidal marshes followed by continued growth in the lower Bay continued through the time of emigration. Of note were the few (6 of 176) medium-sized or large juveniles collected in the lower Bay open waters or at the mouth that had directly emigrated from upper Bay habitats.

Our observations are consistent with the expected behavior of young marine transients (Chao and Musick 1977; Weinstein and Brooks 1983; Szedlmayer et al. 1990); small juveniles recruit throughout the estuary early in the season and spend sufficient time in a given open-water region or marsh creek to acquire a distinct isotopic signature, i.e., they exhibit substantial site fidelity (Deegan and Garritt 1997). As they grow, they begin to move out of the marsh creeks and (or) upper Delaware Bay, sometimes moving directly to lower Bay habitats, but more often exhibiting "saltatory" behavior, i.e., moving partially down-Bay while spending sufficient time in the intermediate regions to acquire the dominant isotopic signature of that locality. Juvenile weakfish ultimately arrive in lower Delaware Bay, though apparently not in unison. Early arrivals are resident for a period that allows accumulation of sufficient biomass in the lower Bay to be reclassified as having originated there, while others retain the signature of other locations until the time they emigrate from Delaware Bay.

Implications of juvenile weakfish movements on the export of tidal-marsh production

Although early investigators proposed important modifications to the role of tidal-marsh organic matter in estuarine secondary production, changes to Teal's (1962) original model have largely been refinements rather than outright rejection or dismissal. Organic matter from tidal salt marshes is being made available to juvenile marine transients in open waters of the estuary, and probably in the coastal zone (Turner et al. 1979), through the movement of organisms (Haines 1979; Deegan 1993), phytoplankton and benthic microalgal production (Haines 1979; Sullivan and Montcrieff 1990), trophic relays (Kneib 1997), pulsed events (Odum 2000), export of dissolved organic matter (Eldridge and Cifuentes 2000), or microbial processing (Newell and Porter 2000), or by some as yet undefined route(s).

The isotopic signatures of juvenile weakfish collected just prior to emigration are telling in two ways. First, as suggested by Haines (1979), the presence of juvenile weakfish that are classified as recent inhabitants of salt marshes indicates not only that marsh macrophyte production is exported for utilization in open-estuary food webs (Eldridge and Cifuentes 2000) but that additional export occurs via the juvenile weakfish themselves. Secondly, the majority of juvenile weakfish collected just prior to emigration are reclassified as being from either marsh creeks or the open lower Bay (133 of 141), all locations where marsh macrophytes account for a significant proportion of the organic matter entering the food web. Therefore, a large proportion of the organic matter exported from Delaware Bay via juvenile weakfish in 1998 and 1999 had its origins in salt-marsh macrophyte production.

While it is clear that the most appropriate interpretation of the stable-isotope data requires an understanding of the seasonal movements of larger and more mobile weakfish, ultimately Delaware Bay salt marshes function as important sources of organic matter driving a significant portion of the production of juvenile weakfish both in the marsh and in the Bay as a whole (Litvin and Weinstein 2003). Furthermore, juvenile weakfish emigrating from the estuary in fall leave with a significant proportion of their biomass derived from salt-marsh organic-matter sources. Though our results do not quantify the various pathways that make nutrients available to consumers, including young weakfish, they support the notion that marine transients act as conduits of organic-matter export in estuaries.

Acknowledgements

Funding for this project was provided by grants NA 86FD0109 (National Oceanic and Atmospheric Administration (NOAA) Saltonstall–Kennedy (SK)) and NA 17RG1396 (NOAA Aquatic Nuisance Species (ANS)), the Marsh Ecology Research Program, and the Estuary Enhancement Program (EEP). We thank J. Balletto of the EEP for his support and Dr. Peter Morin for his statistical advice. This paper was submitted in partial fulfillment of the doctoral candidacy of S.Y.L. and is recorded as Sea Grant contribution NJSG-04-560 for the New Jersey Marine Sciences Consortium.

References

Boesch, D.F., and Turner, R.E. 1984. Dependence of fishery species on salt marshes: the role of food and refuge. Estuaries, **7**: 460–468.

Chanton, J.P., and Lewis, F.G. 1999. Plankton and dissolved inorganic carbon isotopic composition in a river-dominated estuary: Apalachicola Bay, Florida. Estuaries, **22**: 575–583.

Chao, L.N., and Musick, J.A. 1977. Life history, feeding habits and functional morphology of juvenile sciaenid fishes in the York River estuary, Virginia. Fish. Bull. **75**: 657–702.

Childers, D.L., Day, J.W., Jr., and McKellar, H.N., Jr. 2000. Twenty more years of marsh and estuarine flux studies: revisiting Nixon (1980). *In* Concepts and controversies in tidal marsh ecology. *Edited by* M.P. Weinstein and D.A. Kreeger. Kluwer Academic Publishers, Dordrecht, the Netherlands. pp. 391–424.

Darnell, R.M. 1967. The organic detritus problem. AAAS Publ. No. 83. pp. 374–375.

Deegan, L.A. 1993. Nutrient and energy transport between estuaries and coastal marine ecosystems by fish migration. Can. J. Fish. Aquat. Sci. **50**: 74–79.

Deegan, L.A., and Garritt, R.H. 1997. Evidence for spatial variability in estuarine food webs. Mar. Ecol. Prog. Ser. **147**: 31–47.

Deegan, L.A., Hughes, J.E., and Rountree, R.A. 2000. Salt marsh ecosystem support of marine transient species. *In* Concepts and controversies in tidal marsh ecology. *Edited by* M.P. Weinstein and D.A. Kreeger. Kluwer Academic Publishers, Dordrecht, the Netherlands. pp. 333–368.

Eldridge, P.M., and Cifuentes, L.A. 2000. A stable isotope model approach to estimating the contribution of organic matter from marshes to estuaries. *In* Concepts and controversies in tidal marsh ecology. *Edited by* M.P. Weinstein and D.A. Kreeger. Kluwer Academic Publishers, Dordrecht, the Netherlands. pp. 495–514.

Fry, B. 1983. Fish and shrimp migrations in the northern Gulf of Mexico analyzed using stable C, N, and S isotope ratios. Fish. Bull. **81**: 789–801.

Fry, B. 2002. Conservative mixing of stable isotopes across estuarine salinity gradients: a conceptual framework for monitoring watershed influences on downstream fisheries production. Estuaries, **25**: 264–271.

Grecay, P.A., and Targett, T.E. 1996. Spatial patterns in condition and feeding of juvenile weakfish in Delaware Bay. Trans. Am. Fish. Soc. **125**: 803–808.

Haines, E.B. 1979. Interactions between Georgia salt marshes and coastal waters: a changing paradigm. *In* Ecological processes in coastal and marine systems. *Edited by* R.J. Livingston. Plenum Press, New York. pp. 35–46.

Herzka, S.Z., and Holt, G.J. 2000. Changes in isotopic composition of red drum (*Sciaenops ocellatus*) larvae in response to dietary shifts: potential applications to settlement studies. Can. J. Fish. Aquat. Sci. **57**: 137–147.

Hesslein, R.H., Capel, M.J., Fox, D.E., and Hallard, K.A. 1991. Stable isotopes of sulfur, carbon, and nitrogen as indicators of trophic level and fish migration in the Lower Mackenzie River Basin, Canada. Can. J. Fish. Aquat. Sci. **48**: 2258–2261.

Hesslein, R.H., Hallard, K.A., and Ramlal, P. 1993. Replacement of sulfur, carbon, and nitrogen in tissue of growing broad whitefish (*Coregonus nasus*) in response to a change in diet traced by δ^{34}S, δ^{13}C, and δ^{15}N. Can. J. Fish. Aquat. Sci. **50**: 2071–2076.

Hobson, K.A. 1999. Tracing origins and migration of wildlife using stable isotopes: a review. Oecologia, **120**: 314–326.

Klein, T.C., Wilson, W.J., and Goering, J.J. 1998. Natural isotope indicators of fish migration at Prudhoe Bay, Alaska. Can. J. Fish. Aquat. Sci. **55**: 1494–1502.

Kneib, R.T. 1997. The role of tidal marshes in the ecology of estuarine nekton. Oceanogr. Mar. Biol. Annu. Rev. **35**: 163–220.

Litvin, S.Y., and Weinstein, M.P. 2003. Life history strategies of estuarine nekton: the role of marsh macrophytes, benthic microalgae and phytoplankton in the trophic spectrum. Estuaries, **26**(2B): 552–556.

MacAvoy, S.E., Macko, S.A., and Garman, G.C. 2001. Isotopic turnover in aquatic predators: quantifying the exploitation of migratory prey. Can. J. Fish. Aquat. Sci. **58**: 923–932.

McClelland, J.W., and Valiela, I. 1998. Changes in food web structure under the influence of increased anthropogenic nitrogen inputs to estuaries. Mar. Ecol. Prog. Ser. **168**: 259–271.

McGarigal, K., Cushman, S., and Stafford, S. 2000. Multivariate statistics for wildlife and ecology research. Springer-Verlag, New York.

Morrison, D.F. 1976. Multivariate statistical methods. 3rd ed. McGraw–Hill, New York.

Nemerson, D.A. 2001. Geographic, seasonal and ontogenetic patterns in the trophic dynamics of five fish species of Delaware Bay, USA. Ph.D. thesis, Rutgers University, New Brunswick, N.J.

Newell, S.Y., and Porter, D. 2000. Microbial secondary production from salt marsh-grass shoots, and its known and potential fates. *In* Concepts and controversies in tidal marsh ecology. *Edited by* M.P. Weinstein and D.A. Kreeger. Kluwer Academic Publishers, Dordrecht, the Netherlands. pp. 159–186.

Odum, E.P. 1968. A research challenge: evaluating the productivity of coastal and estuarine water. *In* Proceedings of the 2nd Sea Grant Conference, University of Rhode Island, Kingston, R.I. Graduate School of Oceanography, University of Rhode Island, Kingston, R.I. pp. 63–64.

Odum, E.P. 2000. Tidal marshes as outwelling/pulsing systems. *In* Concepts and controversies in tidal marsh ecology. *Edited by* M.P. Weinstein and D.A. Kreeger. Kluwer Academic Publishers, Dordrecht, the Netherlands. pp. 3–8.

Peterson, B.J., and Fry, B. 1987. Stable isotopes in ecosystem studies. Annu. Rev. Ecol. Syst. **18**: 293–320.

Peterson, B.J., Howarth, R.W., and Garritt, R.W. 1986. Sulfur and carbon isotopes as tracers of salt-marsh organic matter flow. Ecology, **67**: 865–874.

SAS Institute Inc. 2000. SAS procedures guide. Version 8. SAS Institute Inc. Cary, N.C.

SPSS Inc.. 1998. SPSS®. Version 8.0 for Windows® (SYSTAT) [computer program]. SPSS Inc., Chicago.

Sullivan, M.J., and Montcrieff, C.A. 1990. Edaphic algae are an important component of salt marsh food webs: evidence from multiple stable isotope analysis. Mar. Ecol. Prog. Ser. **62**: 149–159.

Szedlmayer, S.T., Weinstein, M.P., and Musick, J.A. 1990. Differential growth among cohorts of age-0 weakfish, *Cynoscion regalis*, in Chesapeake Bay. Fish. Bull. **88**: 45–752.

Teal, J.M. 1962. Energy flow in the salt marsh ecosystem of Georgia. Ecology, **43**: 614–624.

Turner, R.E.S., Woo, W., and Jitts, H.R. 1979. Estuarine influences on a continental shelf plankton community. Science (Wash., D.C.), **206**: 218–220.

Wainright, S.A., Weinstein, M.P., Able, K.W., and Currin, C.A. 2000. Relative importance of benthic microalgae, phytoplankton and detritus of smooth cordgrass (*Spartina*) and the common reed (*Phragmites*) to brackish marsh food webs. Mar. Ecol. Prog. Ser. **200**: 77–91.

Weinstein, M.P., and Brooks, H.A. 1983. Comparative ecology of nekton residing in a tidal creek and adjacent seagrass meadow: community composition and structure. Mar. Ecol. Prog. Ser. **12**: 15–27.

Weinstein, M.P., and Kreeger, D.A. 2000. Concepts and controversies in tidal marsh ecology. Kluwer Academic Publishers, Dordrecht, the Netherlands.

Weinstein, M.P., Balletto, J.H., Teal, J.M., and Ludwig, D.F. 1997. Success criteria and adaptive management for a large-scale wetland restoration project. Wetlands Ecol. Manag. **4**: 111–127.

Weinstein, M.P., Litvin, S.Y., Bosley, K.L., Fuller, C.M., and Wainright, S.C. 2000. The role of tidal salt marsh as an energy source for juvenile marine transient finfishes: a stable isotope approach. Trans. Am. Fish. Soc. **129**: 797–810.

Effects of clay turbidity and light on the predator–prey interaction between smelts and chaoborids

Jukka Horppila, Anne Liljendahl-Nurminen, and Tommi Malinen

Abstract: The effects of clay turbidity and light on the predator–prey interaction between planktivorous smelts (*Osmerus eperlanus*) and phantom midge (*Chaoborus flavicans*) larvae were studied by means of laboratory experiments. Irrespective of light intensity, fish-mediated mortality of chaoborid larvae was highest at intermediate turbidity (20 nephelometric turbidity units (NTU)). Increases in light intensity enhanced the feeding rate of smelts at very low light intensities. A regression model describing the dependence of smelt-mediated mortality of chaoborids on light intensity and turbidity was fitted to the data. The model suggested that turbidity exceeding 30 NTU combined with light intensity below 0.1 μE·m^{-2}·s^{-1} provides an efficient daytime refuge for chaoborids even in the presence of planktivorous smelts. In the field studies, the depth distribution of chaoborids followed the predictions of the model. The depth at which chaoborid density was highest depended on the existence and location of the thermocline, the densest swarms occurring beneath the turbidity maximum in the metalimnion. The smelts occupied water layers above the chaoborids, suggesting that the chaoborids used the steep turbidity gradient in the thermocline as a shelter against predation.

Résumé : Des expériences de laboratoire nous ont permis d'étudier les effets de la turbidité due à l'argile ainsi que de la lumière sur les interactions prédateurs–proies entre les éperlans (*Osmerus eperlanus*) planctonophages et les larves de chaoboridés (*Chaoborus flavicans*). Dans les expériences, quelle que soit l'intensité lumineuse, la mortalité des larves de chaoboridés due aux poissons est maximale au niveau intermédiaire de turbidité (20 unités néphélométriques de turbidité (NTU)). Aux intensités lumineuses très faibles, un accroissement de l'intensité lumineuse accroît le taux d'alimentation des éperlans. Nous avons ajusté aux données un modèle de régression qui décrit la dépendance entre la mortalité des chaoboridés due aux éperlans, d'une part, et la lumière et la turbidité, d'autre part. Le modèle indique qu'une turbidité supérieure à 30 NTU combinée à une intensité lumineuse inférieure à 0,1 μE·m^{-2}·s^{-1} procure aux chaoboridés un refuge de jour efficace, même en présence d'éperlans consommateurs de plancton. Dans les études sur le terrain, la répartition des chaoboridés en fonction de la profondeur suit les prédictions du modèle. La profondeur présentant la plus forte densité de chaoboridés dépend de l'existence et de la position de la thermocline; les regroupements les plus denses se retrouvent sous la profondeur de turbidité maximale dans le métalimnion. Les éperlans vivent dans les couches d'eau supérieures à celles où sont les chaoboridés, ce qui laisse croire que les chaoboridés utilisent le fort gradient de turbidité dans la thermocline comme un refuge contre la prédation.

[Traduit par la Rédaction]

Introduction

Increasing water turbidity may greatly affect the foraging efficiency of particulate-feeding planktivorous fish by decreasing their reactive distance. The effect is due to both decreased light intensity and light scattering, the latter having more pronounced effects (Vinyard and O'Brien 1976; Bruton 1985; Hinshaw 1985). Light scattering from suspended particles is harmful, since it interferes with the background light level, reduces contrast, and damages the transport of the prey image (Hinshaw 1985; Giske et al. 1994). The effects of turbidity on the feeding efficiency of planktivorous fish have been demonstrated with numerous fish species (Vinyard and O'Brien 1976; Sigler et al. 1984; Utne-Palm 1999). However, most studies have been carried out with fish feeding on herbivorous crustacean zooplankton. Studies on fish foraging on pelagic invertebrate predators have been rare. This is a shortcoming, since invertebrate predators are important regulators of herbivorous zooplankton and they may negate the effects of fish reductions conducted to enhance the consumption of phytoplankton biomass by herbivorous zooplankton (Benndorf 1995; Wissel and Benndorf 1998). For instance, chaoborid larvae are voracious predators and may weaken the effects of food-web management that relies on increasing the rate of grazing by zooplankton after the reductions of zooplanktivorous fish (Wissel and Benndorf 1998). Invertebrate predators are important food items for many fish species and their density often fluctuates reciprocally with the density of planktivorous fish (Pope et al. 1973; Benndorf et al. 1988). It has been concluded that invertebrate predators can significantly regulate zooplankton only if the density of planktivorous fish is very low, and that their negative effects can be prevented by allowing a moderate density of planktivorous fish (Benndorf 1995; Scheffer 1998). Results from Lake Hiidenvesi in southwestern Finland have demonstrated, however, that such an assumption

Received 10 October 2003. Accepted 4 May 2004. Published on the NRC Research Press Web site at http://cjfas.nrc.ca on 16 December 2004.
J17789

J. Horppila,[1] A. Liljendahl-Nurminen, and T. Malinen. Department of Biological and Environmental Sciences/Limnology, P.O. Box 65 (Viikinkaari 1), FIN 00014, University of Helsinki, Finland.

[1] Corresponding author (e-mail: jukka.horppila@helsinki.fi).

Can. J. Fish. Aquat. Sci. **61**: 1862–1870 (2004)

doi: 10.1139/F04-123

may not hold for all lakes. In Lake Hiidenvesi, the density of phantom midge (*Chaoborus flavicans*) larvae is several thousands of individuals per square metre (Liljendahl-Nurminen et al. 2002). The density of planktivorous fish (mainly smelt, *Osmerus eperlanus*), which forage on chaoborids, is also high (20 000–40 000 individuals·ha^{-1}) (Horppila et al. 2003). During daytime, chaoborids occupy depths of 12–15 m, the vertical distance between the densest swarms of chaoborids and smelts being only a few metres (Horppila et al. 2000). During the night, chaoborids migrate to the uppermost 5 m and forage mainly on cladocerans (Horppila et al. 2000). The rate of food consumption by *C. flavicans* clearly exceeds the production rate of cladocerans, and chaoborids are the main regulators of zooplankton biomass (Liljendahl-Nurminen et al. 2003).

A previous study suggested that the close coexistence of chaoborids with fish is facilitated by the metalimnetic oxygen minimum, which is situated just above the daytime depth of chaoborids and restricts the downward movements of smelts (Horppila et al. 2000). Another possibility is that clay turbidity, which originates from agricultural runoff and varies in the range of 10–50 nephelometric turbidity units (NTU), protects chaoborids from fish predation. Numerous studies have demonstrated that a distinct reduction in the feeding efficiency of fish may take place when turbidity increases from 10 to 30 NTU (Vinyard and O'Brien 1976; Sigler et al. 1984). Cuker (1993) showed that suspended clay (12 NTU) weakened fish predation on chaoborid larvae, which strengthened the effect of chaoborid predation on zooplankton. On the other hand, many studies have shown that moderate turbidity may enhance the feeding success of planktivorous fish by providing contrast between the background and the prey (Boehlert and Morgan 1985; Bristow et al. 1996; Utne-Palm 1999). Thus, based on earlier studies with other fish species, it is difficult to decide how turbidity of the water ranging from 10 to 50 NTU might affect the feeding efficiency of smelts. It is known that smelts avoid brightly illuminated waters (Dembinski 1971; Appenzeller and Leggett 1995), but the effects of turbidity on the feeding efficiency of adult smelts have not been experimentally quantified.

The objective of this study was to experimentally determine the effects of water turbidity on the feeding success of adult smelts foraging on chaoborid larvae. Our hypothesis was that chaoborids would be most severely threatened by smelts at some intermediate level of turbidity. The hypothesis was based on the fact that the positive effect of moderate turbidity on feeding success of fish is most pronounced for transparent prey such as *C. flavicans* (Utne-Palm 1999). In addition, the effects of varying absolute light intensities were studied. It was expected that the importance of light intensity would decrease with increasing clay turbidity (Benfield and Minello 1996). A regression model describing the dependence of smelt-mediated mortality of chaoborids on light intensity and turbidity was fitted to the data. Field surveys were conducted to explore whether the vertical distribution of chaoborids in the lake followed the predictions of the model.

Materials and methods

The effects of clay turbidity on the predator–prey interaction between smelts and *C. flavicans* were studied by determining the rate at which smelts were able to feed on *C. flavicans* at various water turbidities and light intensities. The experiments were conducted with smelts captured from Lake Hiidenvesi with a seine net and acclimated in laboratory conditions for 2 months. The fourth-instar larvae of *C. flavicans* used in the experiments were collected from Lake Hiidenvesi with net hauls and bottom sampling. The experiments were conducted in transparent plastic bags, which were placed in 450-L aquaria filled with water at 9 ± 1 °C. The temperature was thus held at the optimum for consumption by smelts (Lantry and Stewart 1993). The water volume in each bag was 45 L and water depth 60 cm.

After starvation for 2 days, three smelts (total length 68–105 mm, fresh mass 1.2–4.6 g) were placed in the bag 8–10 h before each experiment. At the beginning of the experiment, 100 fourth-instar *C. flavicans* larvae were released into the bag and fish were allowed to forage on them freely. The density of larvae in the bag corresponded to the circumstances in Lake Hiidenvesi, where most of the chaoborid population is often aggregated in a 2- to 3-m layer in the metalimnion (Horppila et al. 2000; Liljendahl-Nurminen et al. 2002, 2003). After 2 h, the smelts were captured from the bag, weighed to the nearest gram, measured to the nearest millimetre (total length), and analysed for swallowed *C. flavicans* larvae. Experiments were conducted at turbidity levels of 0, 10, 20, 40, and 50 NTU (±10%), thus covering the turbidity range in Lake Hiidenvesi. Turbidity was created before the addition of fish by adding a dose of clayish bottom sediment from Lake Hiidenvesi. Turbidity of 0 NTU, which was not found in the lake was used to clarify the effects of reduced light scattering on fish feeding. At the highest turbidity used (50 NTU), the concentration of suspended solids was 28 mg·L^{-1}, which is clearly below the upper tolerance level of fish (Bruton 1985; Lind 2003). Acute direct harmful effects on fish due to the suspendoids during the experiments were thus not likely to have occurred. At each turbidity level, experiments were carried out at 8–10 different light levels, irradiance at the bottom of the bag varying from total darkness to 3 μE·m^{-2}·s^{-1}, which is the light level in Lake Hiidenvesi at 2–5 m depth during a bright summer day. Irradiance (wavelength 400–700 nm) in the air and at the bottom of the bag during the experiments was monitored with a LI-1400 datalogger equipped with quantum sensors. Water temperature, turbidity, and dissolved-oxygen concentration were monitored 20 cm below the water surface with a YSI-6600 sonde. Slight air bubbling was used to prevent sedimentation of the suspended material during the experiment. Nonlinear regression analysis was used to describe the dependence of the smelts' feeding rate on light intensity and turbidity.

In the field, the daytime vertical distribution of smelts and *C. flavicans* in relation to temperature, dissolved-oxygen concentration, and turbidity profiles was studied on 4 June and 26 August 2001 in the deepest part of Lake Hiidenvesi (water depth 30 m). The first sampling took place before the formation of summer stratification, and the second sampling during stratication. The vertical distribution of smelts and *C. flavicans* was studied with simultaneous echosounding along four transects near the sampling station. Echosoundings were conducted with a SIMRAD EY-500 echosounder equipped with a split-beam transducer ES120-7F (operating

Fig. 1. Percentages of air irradiance (±95% confidence limits) left at the bottom of the experimental bags at the various turbidity levels.

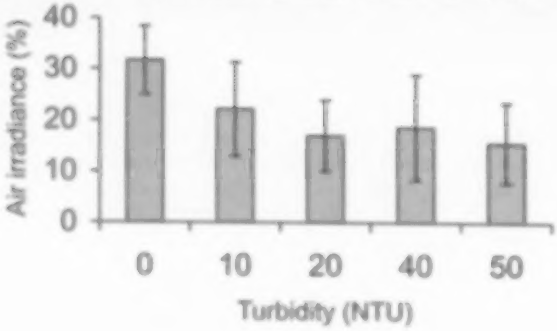

frequency 120 kHz and beam opening angle 7° at the –3 dB level). The transducer was mounted on a towed body, which was lowered to a depth of 0.6 m. Vertical analysis of hydroacoustic data was conducted with EP 500 software with time-varied gain 20 log *R* and integration threshold of –100 dB. For each sampling occasion, a vertical profile of echo-integral values (areal backscattering strength, s_a ($m^2 \cdot ha^{-1}$)), which is proportional to density, was computed in 20-cm layers. Because of high *C. flavicans* densities in some water layers, it was impossible to divide echo-integral values from *C. flavicans* and from smelts by thresholding (Eckmann 1998). However, it was possible to divide integral concentrations into those containing mainly fish and those containing mainly *C. flavicans* (Horppila et al. 2000). Smelt density in the epilimnion was computed by dividing the s_a value (threshold –60 dB) by the mean acoustic cross section for smelts. The total *C. flavicans* density in the water column was determined using a plankton net (diameter 50 cm, mesh size 183 µm). Three replicate vertical net hauls were conducted from the bottom to the surface. Water temperature, turbidity, and dissolved-oxygen concentration at different depths were measured with a YSI-6600 sonde. Light intensity at different depths was recorded with a LI-1400 datalogger and quantum sensors.

Results

At 0 NTU turbidity, 32% of the air irradiance, on average, reached the bottom of the bag (Fig. 1). At turbidities of 10 and 20 NTU, 22% and 17% of the air irradiance, on average, was left at the bottom, respectively. Further increases in water turbidity had only minor effects.

At 0 NTU turbidity, the consumption of chaoborids by smelts increased rapidly when light intensity was increased from total darkness. At 0.7 $\mu E \cdot m^{-2} \cdot s^{-1}$ irradiance, smelts captured a maximum 29 chaoborids per fish (Fig. 2). When irradiance exceeded 1.0 $\mu E \cdot m^{-2} \cdot s^{-1}$, the feeding rate declined rapidly and fell below 10 larvae per fish at 1.5–2.0 $\mu E \cdot m^{-2} \cdot s^{-1}$. When irradiance was further increased, the feeding rate was enhanced and exceeded 20 larvae per fish at irradiances >2.5 $\mu E \cdot m^{-2} \cdot s^{-1}$. At 10 NTU, the change in feeding rate along the irradiance gradient was also bimodal, but the variations were much smaller than at 0 NTU and the highest feeding rate (27 larvae per fish) was achieved at a high light level. At 20 NTU, no bimodality was observed. At light in-

Fig. 2. Effects of water turbidity and light intensity on the feeding efficiency of smelts (*Osmerus eperlanus*) foraging on fourth-instar larvae of *Chaoborus flavicans* at 0 nephelometric turbidity units (NTU) (*a*), 10 NTU (*b*), 20 NTU (*c*), 40 NTU (*d*), and 50 NTU (*e*). Each data point shows the average feeding rate of three smelts in one 2-h experiment. Vertical bars show the standard deviation.

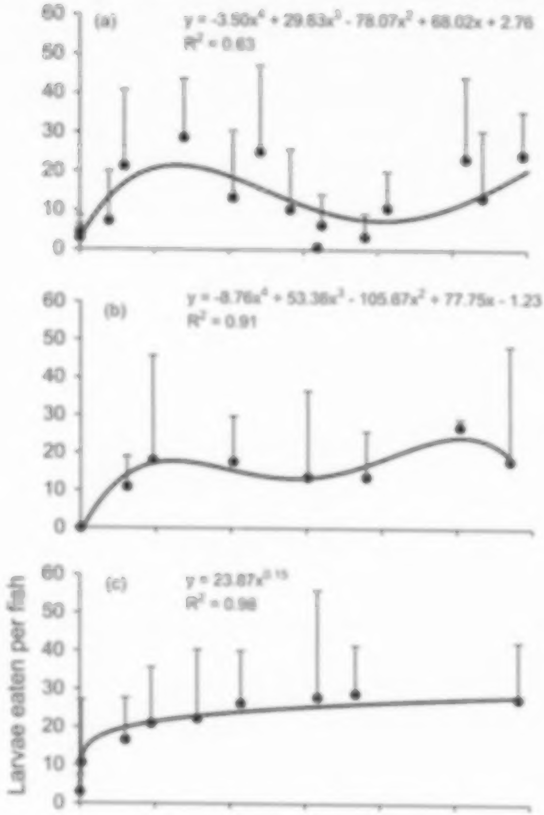

Fig. 3. Coefficients of variation of the number of chaoborid larvae eaten by individual smelts at different turbidities (*a*) and light intensities (*b*).

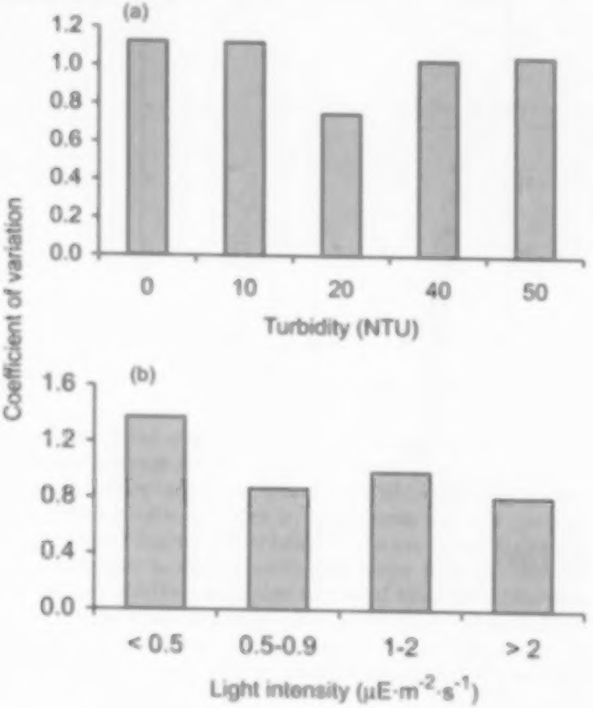

tensities <0.5 µE·m^{-2}·s^{-1}, an increase of even 0.1 µE·m^{-2}·s^{-1} in light intensity caused a substantial increase in the feeding rate of smelts, while at >0.5 µE·m^{-2}·s^{-1}, the feeding rate showed only a moderate response to increasing light level. At 3 µE·m^{-2}·s^{-1}, a maximum feeding rate of 26 larvae per fish was reached. At turbidities of 40 and 50 NTU, the feeding rate remained practically constant at light intensities >0.5 µE·m^{-2}·s^{-1}. At 40 NTU, the feeding rate varied mostly between 15 and 20 larvae per fish and at 50 NTU between 10 and 15 larvae per fish.

The coefficient of variation in feeding efficiency of smelts (calculated for individual fish within one experiment) was relatively constant at different turbidity levels, with the exception of experiments performed at 20 NTU, where between-fish variation was lower than at other turbidities (Fig. 3*a*). When the different light levels are considered, variation was highest at light intensities <0.5 µE·m^{-2}·s^{-1}, whereas the lowest between-fish variation occurred at light levels of 0.5–0.9 and >2 µE·m^{-2}·s^{-1} (Fig. 3*b*).

A nonlinear regression model was fitted to the data (Fig. 4). To improve the applicability of the model to the depths occupied by chaoborids in Lake Hiidenvesi, experiments conducted with a turbidity of 0 NTU and (or) light intensity of >2 µE·m^{-2}·s^{-1} were excluded from the model. Based on the laboratory experiments, a parabolic function was used to describe the relationship between turbidity and chaoborid mortality, while the effects of light were described by a power function. The model including the effects of both turbidity and light intensity was given the form

Fig. 4. Nonlinear regression model describing the effects of light and turbidity on the mortality of *C. flavicans* (number of larvae eaten per experiment) due to smelt predation.

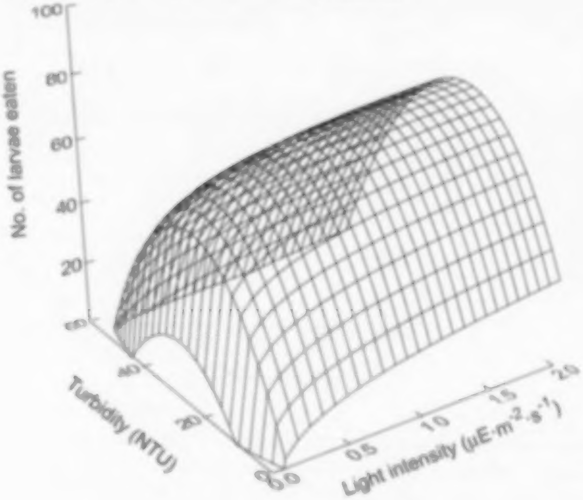

$$\begin{aligned}\text{number of larvae eaten} = &\\ -29.207 + 50.490 \cdot \text{light}^{0.179}&\\ + 3.518 \cdot \text{turbidity} - 0.065 \cdot \text{turbidity}^2&\end{aligned}$$

The model is applicable at water turbidities ≥10 NTU. All the parameters of the model ($R^2 = 0.817$) were statistically significant ($p < 0.05$) and model residuals showed no trend along turbidity and light-intensity gradients (Fig. 5). The interaction of turbidity and light intensity was excluded from the model, since it was insignificant ($p > 0.05$) and did not increase the R^2 value of the model. While the results of the laboratory experiments had suggested that the optimum turbidity for feeding efficiency of smelts was somewhere between 20 and 40 NTU, the optimum predicted by the model was 27 NTU.

In the field, on 4 June following spring circulation, the water-temperature gradient from the surface to the deepest water layers was only 2 °C and the dissolved-oxygen concentration was >8 mg·L^{-1} throughout the water column (Fig. 6). Turbidity was 20–23 NTU in the uppermost 5 m and increased steadily towards deeper layers. Light intensity was above 1 µE·m^{-2}·s^{-1} only in the uppermost 3 m, while in water layers below 5 m it remained below 0.1 µE·m^{-2}·s^{-1}. Smelts (density 18 600 individuals·ha^{-1}) were aggregated in the uppermost 5 m, the highest density occurring at 2.9 m depth, whereas *C. flavicans* (density in the water column 2675 individuals·m^{-2}) were distributed evenly in water layers below 10 m with no aggregation at any particular depth (Fig. 7). On 26 August, the dissolved-oxygen concentration decreased clearly in the metalimnion; however, it was >4 mg·L^{-1} at 15 m depth (Fig. 6). A distinct turbidity peak occurred in the metalimnion. From 8 to 14 m depth, turbidity jumped from 10 to 39 NTU, but decreased again at depths below 20 m. Owing to the lower turbidity in the epilimnion compared with June measurements, light penetrated somewhat deeper than during the previous sampling occasion and was approximately 1 µE·m^{-2}·s^{-1} at 5 m depth. Young-of-

Fig. 5. Residuals of the regression model along turbidity (*a*) and light-intensity (*b*) gradients.

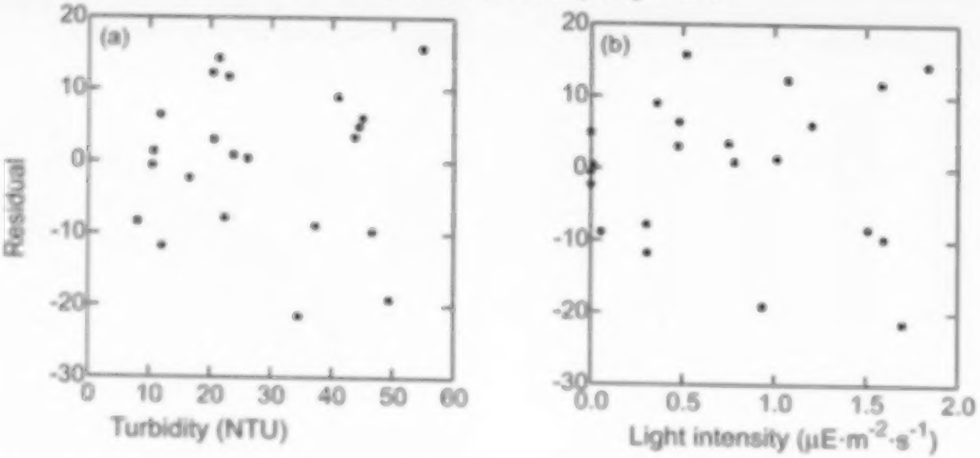

the-year (YOY) smelts (total density 12 300 individuals·ha^{-1}) mainly inhabited the 4- to 6-m depth, while the highest density of older smelts (total density 8500 individuals·ha^{-1}) was observed at 6 m depth (Fig. 7). A sharp peak of echo-integral values from chaoborids (total density 4354 individuals·m^{-2}) was recorded at 13 m depth.

Discussion

The prey-capture rate attained by smelts decreased when turbidity increased from 0 to 50 NTU, which was in accordance with the results of earlier studies on fish hunting planktonic prey (Gardner 1981; Cuker 1993). Such an effect of turbidity is usually attributed to the reduced reactive distance of fish (Vinyard and O'Brien 1976; Confer et al. 1978). Fish may partly compensate for their reduced ability to detect prey by increasing their swimming speed (Gardner 1981). Probably such compensation took place also in our experiments. A fivefold increase of turbidity (from 10 to 50 NTU) caused a 50% reduction in the maximum feeding rate attained by smelts, while the effect of turbidity on reactive distance is usually hyperbolic (Vinyard and O'Brien 1976; Aksnes and Giske 1993). Water turbidity also affected the fluctuations of the feeding rate along a light-intensity gradient. At low water turbidity, the effect of light was bimodal, and this is explained by the behavioral responses of chaoborids and fish. Numerous studies have shown that smelts avoid high light intensities (Dembinski 1971; Heist and Swenson 1983; Appenzeller and Leggett 1995). Dembinski (1971) reported that *O. eperlanus* avoids light levels above 20 μW·m^{-2}·s^{-1}, which corresponds to 0.8–0.9 μE·m^{-2}·s^{-1} (Morel and Smith 1974; McCree 1981). These results agree well with our finding that at low water turbidity the rate of feeding by smelts decreased as the light level approached 1 μE·m^{-2}·s^{-1}. On the other hand, the light intensity that represents the upper tolerance limit for *C. flavicans* is approximately 100 lx (Teraguchi and Northcote 1966; Wagner-Döbler 1988), which corresponds to approximately 1.8 μE·m^{-2}·s^{-1} (McCree 1981). Thus, at light intensities >2 μE·m^{-2}·s^{-1}, the rate of feeding by smelts increased because the chaoborids had to move to the bottom of the bag, away from the intolerably high irradiance level, and were exposed to predation. Such a phenomenon may not occur in natural conditions, but was due to the experimental circumstances. On the other hand, it explains why fourth-instar chaoborid larvae are never found in the surface layers during daytime. At high water turbidities, except at very low light intensities, the light level had only minor effects on the rate of feeding by smelts. This was expected, since above some threshold light intensity, reactive distance usually becomes constant (Vinyard and O'Brien 1976; Confer et al. 1978; Utne 1997).

Irrespective of the light level, the smelts' feeding rate was highest at 20 NTU turbidity. At the highest light intensities used in the experiments, the phenomenon was probably attributable to the combined effects of absolute light intensity and light scattering. Owing to the smelts' light sensitivity, their feeding rate was reduced as a result of the too-high absolute light level when this was combined with low turbidity (0–10 NTU). When the absolute light level is considered, whether the turbidity was 20, 40, or 50 NTU made no difference for smelts, since the effects of these turbidities on light extinction were practically the same. Light scattering, which is most harmful for the feeding success of fish, increases linearly with water turbidity measured in NTU (Kirk 1981). Hence, a turbidity of 20 NTU obviously offered the the most profitable combination of light scattering and absolute light intensity, i.e., a tolerable light intensity with the least possible light scattering. At low light intensities, the profitability of 20 NTU turbidity for smelts was probably connected to changes in prey contrast, which is of importance, especially at low light intensities, but does not affect prey mortality in brightly illuminated waters so much (Giske et al. 1994). Moderate turbidity may enhance feeding by providing visual contrast and enabling faster detection of planktonic prey (Boehlert and Morgan 1985; Gregory and Northcote 1993).

Between-fish variation in the feeding rate was lowest at 20 NTU, supporting the conclusion that such turbidity was profitable for the feeding efficiency of smelts. When food availability is low, a few individuals often dominate, while in favorable conditions, resources are more evenly used by different individuals (e.g., Symons 1968). Similarly, at the

Fig. 6. Profiles of temperature (○), dissolved-oxygen concentration (DO; ●), water turbidity (thick line), and light intensity (thin line) in Lake Hiidenvesi on 4 June (*a*) and 26 August 2001 (*b*).

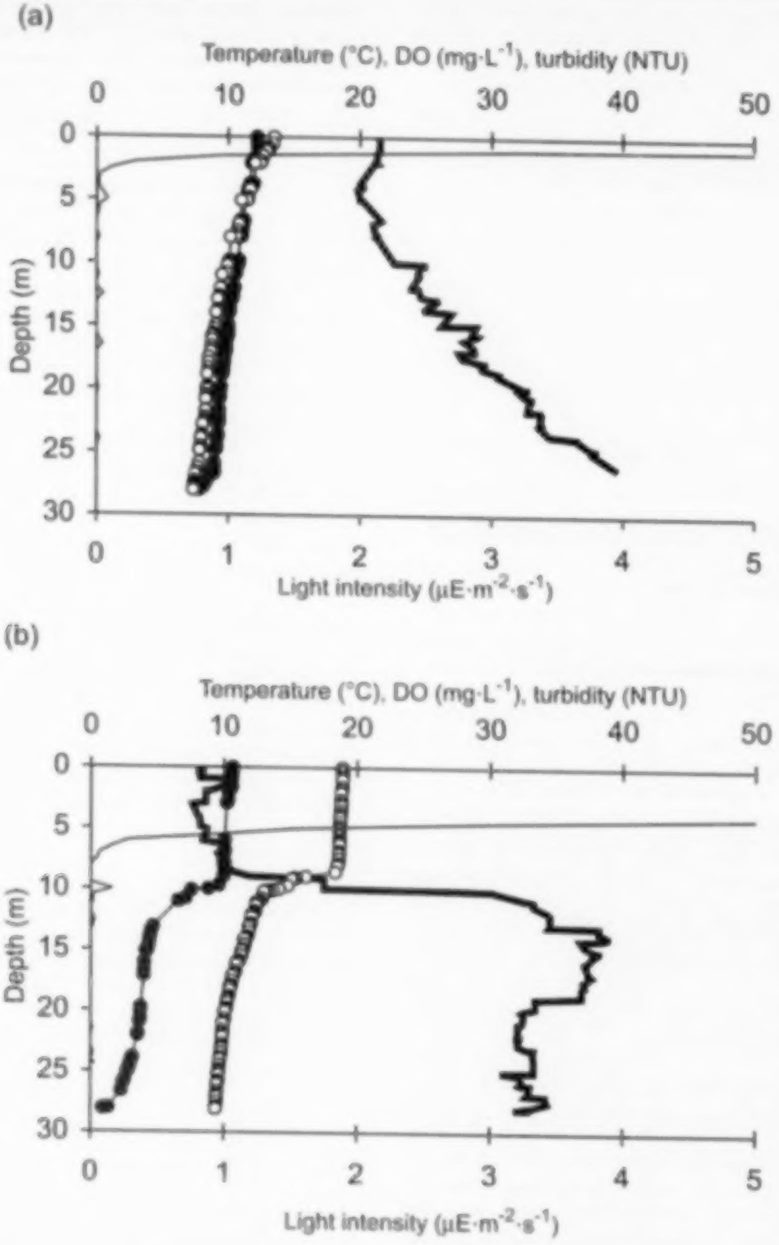

most profitable light intensities, between-fish variation in feeding efficiency was also lowest. It must be considered that in the most favorable feeding conditions for smelts, the density of chaoborids decreased below one-fifth of the initial level. Such a reduction in prey density probably reduced the feeding rate of smelts. In the lake, such an abrupt short-term decrease in prey density does not take place. Thus, in the laboratory experiments, the feeding efficiency of smelts in the most favorable conditions was probably underestimated.

In the field, adult smelts avoided the illuminated surface layers, their highest density being at light intensities <1 $\mu E \cdot m^{-2} \cdot s^{-1}$, which supports earlier findings on the light sensitivity of smelts (Dembinski 1971; Appenzeller and Leggett 1995). On 4 June, when the water temperature was suitable for smelts throughout the water column, the highest smelt density was found at 20 NTU turbidity, corroborating the results of the laboratory experiments. The highest densities of chaoborids were found in dark and turbid water layers

Fig. 7. Vertical daytime distribution of echo integrals in Lake Hiidenvesi on 4 June (*a*) and 26 August 2001 (*b*). The shaded area indicates the "blind" zone of the echosounder (YOY, young-of-the-year).

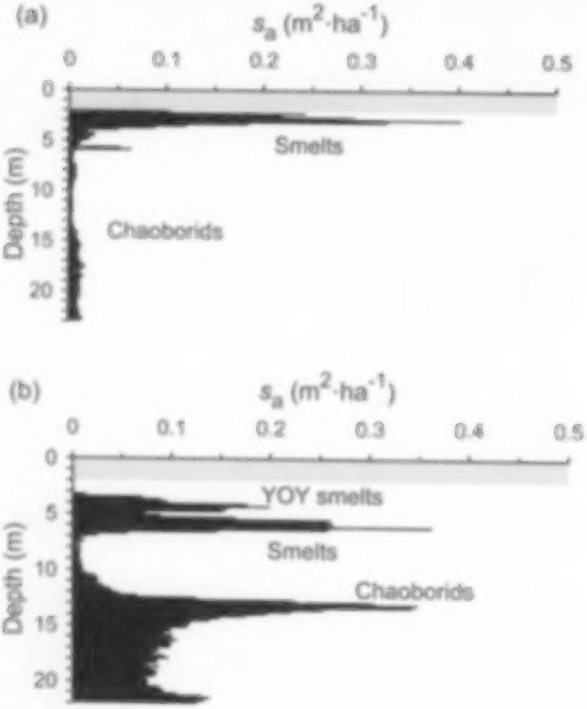

near the bottom, where the effectivity of smelt predation is low. In August, smelts were again aggregated in the epilimnion, which was unexpected, since the water temperature was >18 °C, and smelts (excluding YOY) usually have an upper temperature tolerance limit of 16–18 °C (Appenzeller and Leggett 1995 and references therein). The dissolved-oxygen concentration in the metalimnion was not low enough to form a strict boundary for fish. At 13 m depth with the highest chaoborid density, the dissolved-oxygen concentration was 5 mg·L^{-1}. The most likely explanation for the behavior of smelts was thus the steeply increasing water turbidity in the metalimnion. At 8 m depth, the turbidity was 10 NTU, but at 10 m depth it already exceeded 30 NTU, forming an effective refuge for chaoborids. Additionally, an important factor affecting the behavior of the smelts was probably the availability of zooplanktonic food. In Lake Hiidenvesi, the biomass of zooplankton declines rapidly with increasing depth. At 5–10 m depth, the biomass of crustacean zooplankton is more than twice that at 10–15 m (Tallberg et al. 1999). The uppermost 5 m being too warm, the 5- to 10-m layer thus offered the best environment for planktivorous feeding.

Fig. 8. Schematic presentation showing relative refuge availability (—) for *C. flavicans* at different depths in lakes having various turbidity profiles (····) and maximum depths. (*a*) A deep lake showing a turbidity maximum in the metalimnion. (*b*) A deep lake with turbidity increasing constantly towards the bottom. (*c*) A nonstratifying shallow lake with a homogeneous turbidity profile.

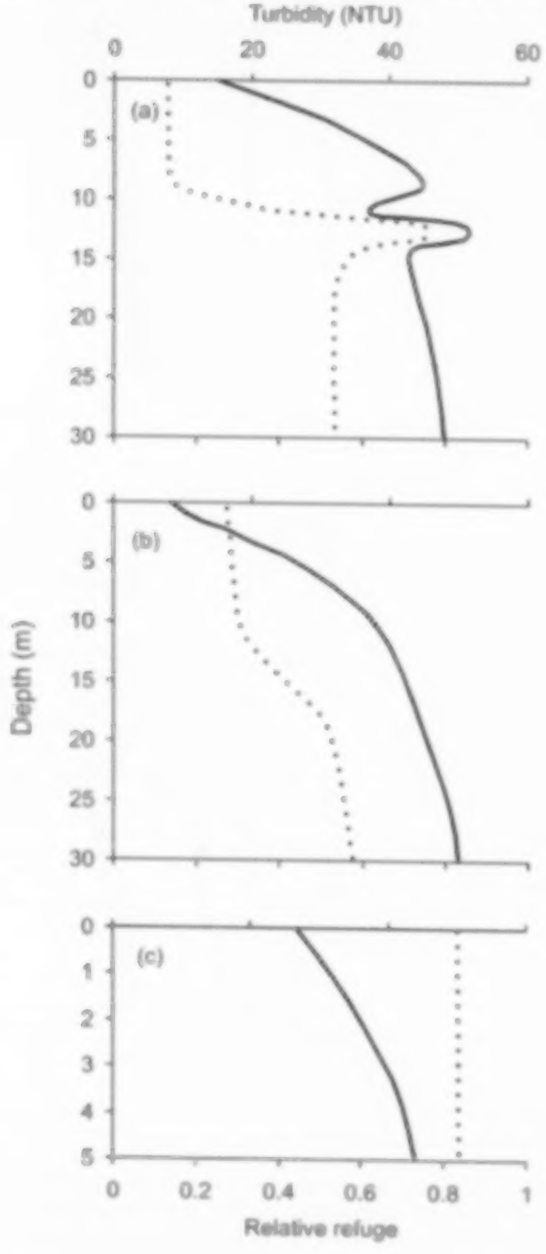

With the regression model, refuge availability in lakes with different turbidity profiles could be predicted. Using the turbidity measurements taken in Lake Hiidenvesi in August, and light intensities on a bright day at different depths (Horppila et al. 2000), the model results in a heterograde refuge profile, refuge being best at 10–12 m depth (Fig. 8*a*). Water layers just above this refuge are dangerous because the water turbidity is 20–30 NTU and thus profitable for fish feeding. The prediction fits well the independently observed depth distribution of chaoborids in Lake Hiidenvesi in August. In a situation where there is no metalimnetic turbidity maximum, but turbidity in the hypolimnion increases constantly towards the bottom (e.g., Lake Hiidenvesi in early June), the best refuge can be found in near-bottom layers (Fig. 8*b*). Accordingly, on 4 June in Lake Hiidenvesi, chaoborids mostly occupied the water layers below 15 m depth. In a nonstratifying shallow lake, refuge efficiency increases steadily downwards and is determined by the light intensity, since turbidity is homogeneous throughout the water column. The model prediction shows that at 3 m depth with 50 NTU turbidity, refuge is weaker than with 40 NTU in the metalimnion of a deep lake (Fig. 8*c*). This is because light-attenuation properties at 40 NTU do not differ from those at 50 NTU, but at such low light levels even a small decrease in light intensity (through movement downwards) increases the refuge effect considerably. In a shallow lake, however, the water depth limits downward movements and chaoborids often choose to burrow into the sediment to escape fish predation. Even such behavior may not be enough to protect the larvae if the lake is inhabited by dense populations of benthivorous fish. Such a situation occurs in Lake Hiidenvesi, where chaoborids are absent from the nonstratifying shallow basins where water turbidity is much higher than in the deep parts inhabited by a dense chaoborid population (Liljendahl-Nurminen et al. 2002).

In conclusion, the study suggests that clay turbidity strongly contributes to the co-existence of chaoborids and smelts at high densities. Turbidity exceeding 30 NTU combined with light intensity below 0.1 $\mu E \cdot m^{-2} \cdot s^{-1}$ provides an efficient daytime refuge for chaoborids. In lakes, where such an environment occurs high in the water column, chaoborids are able to stay a short distance from their zooplanktonic prey and maintain high predation pressure on the zooplankton.

Acknowledgements

The study was financially supported by the Academy of Finland (project 50320) and the Finnish Ministry of Agriculture and Forestry. Uusimaa Regional Environment Centre provided fish for the laboratory experiments. Jyrki Lappalainen and Hannu Rita helped with the modeling approach. Antti Tuomaala and numerous other persons helped in the echosounding surveys.

References

Aksnes, D.L., and Giske, J. 1993. A theoretical model of aquatic visual feeding. Ecol. Modell. **67**: 233–250.

Appenzeller, A.R., and Leggett, W.C. 1995. An evaluation of light-mediated vertical migration of fish based on hydroacoustic analysis of the diel vertical movements of rainbow smelt (*Osmerus mordax*). Can. J. Fish. Aquat. Sci. **52**: 504–511.

Benfield, M.C., and Minello, T.J. 1996. Relative effects of turbidity and light intensity on reactive distance and feeding of an estuarine fish. Environ. Biol. Fishes, **46**: 211–216.

Benndorf, J. 1995. Possibilities and limits for controlling eutrophication by biomanipulation. Int. Rev. Ges. Hydrobiol. **80**: 519–534.

Benndorf, J., Schultz, H., Benndorf, A., Unger, R., Penz, E., Kneschke, H., et al. 1988. Food-web manipulation by enhancement of piscivorous fish stocks: long-term effects in the hypertrophic Bautzen Reservoir. Limnologica (Berl.), **19**: 97–110.

Boehlert, G.W., and Morgan, J.B. 1985. Turbidity enhances feeding abilities of larval pacific herring, *Clupea harengus pallasi*. Hydrobiologia, **123**: 161–170.

Bristow, B.T., Summerfelt, R.C., and Clayton, R.D. 1996. Comparative performance of intensively cultured larval walleye in clear, turbid and coloured water. Prog. Fish-Cult. **58**: 1–10.

Bruton, M.N. 1985. The effects of suspendoids on fish. Hydrobiologia, **125**: 221–241.

Confer, J.L., Howick, G.L., Corzette, M.H., Kramer, S.L., Fitzgibbon, S., and Landesberg, R. 1978. Visual predation by planktivores. Oikos, **31**: 27–37.

Cuker, B.E. 1993. Suspended clays alter trophic interactions in the plankton. Ecology, **74**: 944–953.

Dembinski, W. 1971. Vertical distribution of vendace *Coregonus albula* L., and many other fish species in some Polish lakes. J. Fish Biol. **3**: 341–357.

Eckmann, R. 1998. Allocation of echo integrator output to small larval insect (*Chaoborus* sp.) and medium-sized (juvenile fish) targets. Fish. Res. (Amst.), **35**: 107–113.

Gardner, M.B. 1981. Mechanisms of size-selectivity by planktivorous fish: a test of hypotheses. Ecology, **62**: 571–578.

Giske, J., Aksnes, D.L., and Fiksen, Ø. 1994. Visual predators, environmental variables and zooplankton mortality risk. Vie Milieu, **44**: 1–9.

Gregory, R.S., and Northcote, T.G. 1993. Surface, planktonic, and benthic foraging by juvenile chinook salmon (*Oncorhynchus tshawytscha*) in turbid laboratory conditions. Can. J. Fish. Aquat. Sci. **50**: 233–240.

Heist, B.G., and Swenson, W.A. 1983. Distribution and abundance of rainbow smelt in western Lake Superior as determined from acoustic sampling. J. Gt. Lakes Res. **9**: 343–353.

Hinshaw, J.M. 1985. Effects of illumination and prey contrast on survival and growth of larval yellow perch *Perca flavescens*. Trans. Am. Fish. Soc. **114**: 540–545.

Horppila, J., Malinen, T., Nurminen, L., Tallberg, P., and Vinni, M. 2000. A metalimnetic oxygen minimum indirectly contributing to the low biomass of cladocerans in Lake Hiidenvesi — a diurnal study on the refuge effect. Hydrobiologia, **436**: 81–90.

Horppila, J., Liljendahl-Nurminen, A., Malinen, T., Salonen, M., Tuomaala, A., Uusitalo, L., and Vinni, M. 2003. *Mysis relicta* in a eutrophic lake — consequences of obligatory habitat shifts. Limnol. Oceanogr. **48**: 1214–1222.

Kirk, J.T.O. 1981. Estimation of the scattering coefficient of natural waters using underwater irradiance measurements. Aust. J. Mar. Freshw. Res. **32**: 533–539.

Lantry, B.F., and Stewart, D.J. 1993. Ecological energetics of rainbow smelt in the Laurentian Great Lakes — an interlake comparison. Trans. Am. Fish. Soc. **122**: 951–976.

Liljendahl-Nurminen, A., Horppila, J., Eloranta, P., Malinen, T., and Uusitalo, L. 2002. The seasonal dynamics and distribution of *Chaoborus flavicans* in adjacent lake basins of different morphometry and degree of eutrophication. Freshw. Biol. **47**: 1283–1295.

Liljendahl-Nurminen, A, Horppila, J., Malinen, T., Eloranta, P., Vinni, M., Alajärvi, E., and Valtonen, S. 2003. The supremacy of invertebrate predators over fish — factors behind the unconventional seasonal dynamics of cladocerans in Lake Hiidenvesi. Arch. Hydrobiol. **158**: 75–96.

Lind, O.T. 2003. Suspended clay's effect on lake and reservoir limnology. Arch. Hydrobiol. Suppl. **139**: 327–360.

McCree, K.J. 1981. Photosynthetically active radiation. *In* Encyclopedia of plant physiology (new series). Vol. 12A. Physiological plant ecology. *Edited by* O.L. Lange, P. Nobel, B. Osmond, and H. Ziegler. Springer-Verlag, Berlin, Heidelberg, and New York. pp. 41–55.

Morel, A., and Smith, R.C. 1974. Relation between total quanta and total energy for aquatic photosynthesis. Limnol. Oceanogr. **19**: 591–600.

Pope, G.F., Carter, J.C.H., and Power, G. 1973. The influence of fish on the distribution of *Chaoborus* spp. (Diptera) and density of larvae in the Matamek River System, Québec. Trans. Am. Fish. Soc. **102**: 707–722.

Scheffer, M. 1998. Ecology of shallow lakes. Chapman and Hall, London.

Sigler, J.W., Bjornn, T.C., and Everest, F.H. 1984. Effects of chronic turbidity on density and growth of steelheads and coho salmon. Trans. Am. Fish. Soc. **113**: 142–150.

Symons, P.E.K. 1968. Increase in aggression and in strength of the social hierarchy among juvenile atlantic salmon deprived of food. J. Fish. Res. Board Can. **25**: 2387–2401.

Tallberg, P., Horppila, J., Väisänen, A., and Nurminen, L. 1999. Seasonal succession of phytoplankton and zooplankton along a trophic gradient in a eutrophic lake — implications for food web management. Hydrobiologia, **412**: 81–94.

Teraguchi, M., and Northcote, T.G. 1966. Vertical distribution and migration of *Chaoborus flavicans* larvae in Corbett Lake, British Columbia. Limnol. Oceanogr. **11**: 164–176.

Utne, A.C.W. 1997. The effect of turbidity and illumination in the reaction distance and search time of the marine planktivore *Gobiusculus flavescens*. J. Fish Biol. **50**: 926–938.

Utne-Palm, A.C. 1999. The effect of prey mobility, prey contrast, turbidity and spectral composition on the reaction distance of *Gobiusculus flavescens* to its planktonic prey. J. Fish Biol. **54**: 1244–1258.

Vinyard, G.L., and O'Brien, J. 1976. Effects of light and turbidity on the reactive distance of bluegill (*Lepomis macrochirus*). J. Fish. Res. Board Can. **33**: 2845–2849.

Wagner-Döbler, I. 1988. Vertical migration of *Chaoborus flavicans* (Diptera, Chaoboridae): the control of day and night depth by environmental parameters. Arch. Hydrobiol. **114**: 251–274.

Wissel, B., and Benndorf, J. 1998. Contrasting effects of the invertebrate predator *Chaoborus obscuripes* and planktivorous fish on plankton communities of a long term biomanipulation experiment. Arch. Hydrobiol. **143**: 129–146.

Copper inhibition of phytoplankton in Saginaw Bay, Lake Huron

John T. Lehman, Ali Bazzi, Todd Nosher, and Jerome O. Nriagu

Abstract: Field surveys and bioassays during 1999 and 2000 demonstrated trace metal effects on the phytoplankton of inner and outer regions of Saginaw Bay, Lake Huron. Addition of as little as 1 $\mu g \cdot L^{-1}$ copper suppressed algal biomass, measured as particulate chlorophyll *a*, compared with control treatments, additions of ethylenediaminetetraacetic acid, or additions of carrier water alone. Suppression effects of copper, added alone or in combination with cadmium, lead, and thallium, were evident in inner and outer regions of Saginaw Bay during both spring and summer when phytoplankton communities were composed alternatively of diatoms and cyanobacteria. Experimental treatments were conducted in parallel with measurements of metal concentrations and metal complexation capacities of lake water collected by ultraclean trace metal techniques. Despite apparent overchelation of dissolved copper by organic ligands in Saginaw Bay, additions of a few tens of nanomoles of copper per litre strongly reduces algal biomass compared with control treatments. These results suggest that metal concentrations in some Great Lakes waters in equilibrium with natural chelators may be above the essential requirements and potentially at levels of incipient toxicity to the native phytoplankton communities.

Résumé : Des inventaires de terrain et des essais biologiques en 1999 et 2000 ont démontré les effets des métaux en traces sur le phytoplancton des régions intérieure et extérieure de la baie de Saginaw au lac Huron. L'addition d'une quantité aussi faible que 1 $\mu g \cdot L^{-1}$ de cuivre supprime la biomasse des algues, mesurée en tant que chlorophylle *a* particulaire par comparaison avec les témoins qui ont reçu des additions d'acide éthylènediamine tétra-acétique ou des additions de l'eau de dilution seule. Les effets de suppression du cuivre, ajouté seul ou en combinaison avec du cadmium, du plomb et du thallium, sont apparents dans les régions intérieure et extérieure de la baie de Saginaw, tant au printemps qu'à l'été, à des moments où les communautés phytoplanctoniques sont composées respectivement de diatomées et de cyanobactéries. Les expériences ont été réalisées en parallèle à des dosages des concentrations de métaux et des mesures du pouvoir de complexation des métaux de l'eau du lac récoltée par des techniques ultra-propres pour l'analyse des métaux en traces. Malgré une chélation excessive du cuivre dissous par les ligands organiques dans la baie de Saginaw, l'addition de quelques dixs de nanomoles de cuivre par litre réduit considérablement la biomasse des algues, par comparaison avec les témoins. Ces résultats indiquent que les concentrations de métaux dans certaines eaux des Grands Lacs en équilibre avec les agents de chélation naturels peuvent dépasser les besoins essentiels des communautés indigènes de phytoplancton et se situer potentiellement à des concentrations correspondant à un début de toxicité.

[Traduit par la Rédaction]

Introduction

Ecological and human health effects from metals and anthropogenic chlorinated organic compounds released into the St. Lawrence Great Lakes are an established concern of science and environmental policy in North America (International Joint Commission 1985). The metals that are targets of this concern are derived continuously from both natural and anthropogenic sources, and they can exhibit complex biogeochemical cycles in lakes.

Trace metals evoke diverse responses from aquatic communities. Some trace metals are essential nutrient resources for aquatic biota. Copper (Cu), for example, serves as a cofactor in redox reactions catalyzed by enzymes associated

Received 10 February 2003. Accepted 6 April 2004. Published on the NRC Research Press Web site at http://cjfas.nrc.ca on 15 December 2004.
J17328

J.T. Lehman.[1] Department of Ecology and Evolutionary Biology, Natural Science Building, University of Michigan, Ann Arbor, MI 48109-1048, USA.
A. Bazzi. Department of Natural Sciences, University of Michigan–Dearborn, Dearborn, MI 48128-1491, USA.
T. Nosher. Department of Ecology and Evolutionary Biology, Natural Science Building, University of Michigan, Ann Arbor, MI 48109-1048, and Department of Environmental Health Science, School of Public Health, University of Michigan, Ann Arbor, MI 48109-2029, USA.
J.O. Nriagu. Department of Environmental Health Science, School of Public Health, University of Michigan, Ann Arbor, MI 48109-2029, USA.

[1] Corresponding author (e-mail: jtlehman@umich.edu).

Can. J. Fish. Aquat. Sci. **61**: 1871–1880 (2004)

doi: 10.1139/F04-129

with photosynthesis (Raven et al. 1999). Copper has been implicated as a limiting resource for algae in eutrophic lakes (Knauer et al. 1997), but it is also a well-known algicide (Lustigman 1986; Luederitz et al. 1989) that has been purposely applied to some lakes to suppress algal nuisance blooms (McKnight 1981; Edmondson 1991). Experimental studies have documented stimulatory effects of copper at low concentrations, but inhibitory effects at higher levels (Lewis and Cave 1982; Wurtsbaugh and Horne 1982). Detrimental effects of copper on aquatic microbes are well known and are the basis for using copper as an antifouling agent. The metal can compete for binding sites of enzymes such as urease, acid phosphatase, and adenosine triphosphatase (ATPase) and can inhibit other enzymes of nitrogen metabolism and photosynthesis (Rai and Rai 1997). Bioassay experiments have documented copper inhibition of phytoplankton species (Graneli et al. 1986). Copper thus represents a vital physiological resource that can become toxic when present in excess.

The levels of copper that begin to cause inhibitory effects cannot be inferred from total concentrations. Effects have been shown to be species-specific (Wong et al. 1978; Hart et al. 1983; Nor 1987). As is true of other metals, copper can exist in aqueous solution at more than one oxidation state, either as free ions, in ion pairs, or in chelated form with various organic ligands. The chelated metals are typically not directly available to algae, and bioavailability tends to be based on free metal ion or kinetically labile inorganic species (Verweij et al. 1992; Campbell 1995; Sunda and Huntsman 1998). This complex chemical speciation of the metal makes it possible for the same total concentration to elicit different biological effects depending on the proportion of total metal that is free or bound.

The complexity of interaction between algae and metals has been studied in marine environments, but freshwater ecosystems have received less attention. Horne and Goldman (1974) demonstrated that nitrogen fixation by cyanobacteria in Clear Lake, California, was reduced by addition of as little as 5 μg·L^{-1} Cu, and they ascribed the response to possible saturation of natural chelators in the lake water by metal ions. Most work has involved laboratory experiments rather than field studies, and comparatively little is known about the complexation capacities and metal-binding specificities of natural ligands in freshwater ecosystems generally or the North American Great Lakes in particular. Pioneering work in this respect was conducted originally by Chau et al. (1970) and Gächter et al. (1973). The latter authors demonstrated that despite apparent excess complexing capacity for Cu of several hundred nanomoles per litre in waters from Lake Ontario, the Niagara River, and Hamilton Harbor, additions of as little as 100 nmol·L^{-1} Cu reduced carbon fixation substantially. They concluded that excess complexing capacity does not guarantee that equivalent amounts of copper can be tolerated without adverse effects.

We investigated metal concentrations, complexation characteristics of natural ligands, and the effect of copper addition on algal communities of Saginaw Bay, Lake Huron, during 1999 and 2000. Saginaw Bay has been an area of environmental concern regarding metal pollution because of industrial effects from the cities of Bay City and Saginaw, Michigan, as well as from intensive agriculture, petroleum production, and industrial waste disposal near the lakeshore. Saginaw Bay exhibits a longitudinal gradient in water quality indices. Inner bay stations have higher concentrations of total phosphorus (TP) and total nitrogen (TN), higher chlorophyll, higher specific conductance, and lower water transparency compared with upper bay stations. We presumed that the evident trophic gradient might present instructive gradients in trace metals and organic ligands and their relationships to the biota.

Table 1. Sampling dates and station characteristics for Saginaw Bay sites.

Date	Station	Latitude, N	Longitude, W	Z_{max}, m
19 May 1999	1	43°43.9′	83°46.0′	6
	3	43°48.2′	83°44.0′	8
	6S	43°53.8′	83°32.9′	5
	6	43°55.4′	83°35.9′	10
	6N	43°57.9′	83°39.0′	10
	8	44°00.0′	83°31.8′	10
28 June 1999	1	43°43.9′	83°46.0′	6
	8	44°00.0′	83°31.8′	10
4 Aug. 1999	1	43°43.9′	83°46.0′	6
	8	44°00.0′	83°31.8′	10
29 May 2000	1	43°43.9′	83°46.0′	6
30 May 2000	8	44°00.0′	83°31.8′	10
	6	43°55.4′	83°35.9′	9
	5	43°53.2′	83°37.9′	11
	3	43°48.2′	83°44.0′	7
	1	43°43.9′	83°46.0′	6
16 Sept. 2000	7	43°57.0′	83°36.9′	14
	5W	43°52.8′	83°47.0′	6
	3W	43°48.6′	83°50.6′	7
	1W	43°44.6′	83°52.4′	6

Methods

Field sites

We report results from sampling cruises in May, June, and August of 1999 and from May and September of 2000. Station locations are identified in Table 1, as well as in Fig. 1. In June and August 1999 and in May 2000, we collected lake water for experiments at stations selected as representative of inner and outer sections of the bay. Station 1 (inner bay) and station 8 (outer bay) were sampled for experiments in 1999 and in May 2000; stations 1W and 5W were sampled for experiments in September 2000 owing to unfavorable weather preventing sampling at more outer bay sites.

Field and laboratory methods

Station properties included water temperature and dissolved oxygen measured by YSI 55 meter (Yellow Springs Instruments, Yellow Springs, Ohio). Oxygen concentrations inferred by polarographic electrode were calibrated by Winkler titration at selected depths. Photosynthetically active radiance (PAR) was determined by cosine-corrected sensors (LiCor). Secchi disk transparency (20-cm plain white disk) and vertical zooplankton hauls (130-μm net aperture) were also taken

Fig. 1. Sampling stations for Saginaw Bay, Lake Huron, in 1999 and 2000. Site location is denoted on the inset map of the St. Lawrence River – Great Lakes.

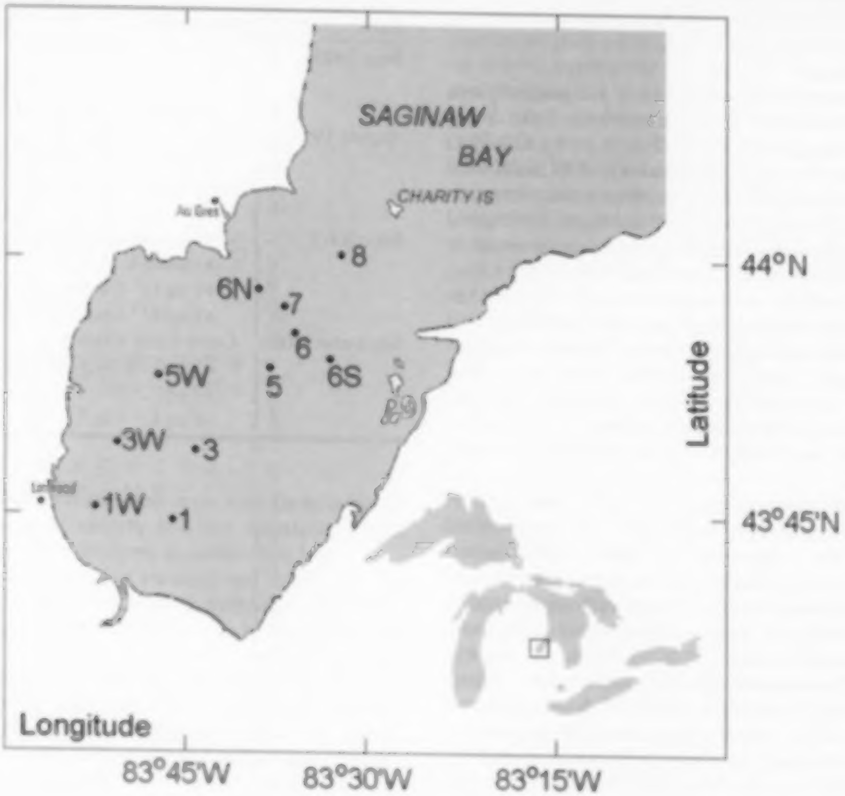

at each station. Post-cruise chemical analyses included specific conductance, pH, acid-neutralizing capacity (ANC) by Gran titration, calcium by titration with ethylenediaminetetraacetic acid (sodium salt, Na-EDTA) to a colorimetric endpoint, nitrate (NO_3) by ion chromatography or by flow injection colorimetric analysis following cadmium column reduction, soluble reactive silicon (SRSi) by acid molybdate reaction, total and dissolved phosphorus (TP and DP) by acid persulfate oxidation and acid molybdate reaction, and TN and total dissolved nitrogen (DN) by alkaline persulfate oxidation to NO_3. Chlorophyll *a* (Chl *a*) was measured as extracted florescence using 90% (by volume) acetone and a fluorometer (model TD-700, Turner Designs, Inc., Sunnyvale, Calif.) with an optical kit (model 10-040R) specific for Chl *a*. Colored dissolved organic matter (CDOM) was measured with a fluorometer (model 10, Turner Designs) equipped with an optical kit (model 10-303).

Because the existence of gradients in limnological properties within Saginaw Bay implies a degree of spatial autocorrelation among nearby sample stations, we adopted a simple statistical means of assessing similarity and differences among stations based on the suite of properties we measured. Stations were arranged in rank order by 10 measured limnological properties for each cruise period: temperature, specific conductance, ANC, Ca, SO_4, NO_3, TP, DP, Chl *a*, and CDOM. Then stations were scored according to whether they fell above or below the median values recorded for each property on each given cruise. Chi-squared analysis (df = 1) was used to identify significant differences or similarities between stations based on the aggregate rankings (i.e., total counts of station-specific cases above and below median values) and thereby to ascertain the degree of independence of the sampling sites.

Trace metal sampling and analysis

Sample bottles were meticulously cleaned with trace metal grade nitric acid, repeatedly rinsed with Milli-Q water, and finally filled with Milli-Q water and wrapped in three consecutive layers of Ziploc® polyethylene bags for transport to the field inside insulated plastic coolers. Trace metal samples were collected by GO-FLO Niskin (General Oceanics Inc., Miami, Fla.) sampler, using ultraclean techniques and field blanks as described by Bazzi et al. (2002). On station with the vessel at anchor and engines off, Milli-Q water in the sample bottles was discarded, and the bottles were first rinsed once and then filled with lake water. The sample bottles were returned to their polyethylene bags and their coolers for transport to the laboratory.

Measurements of total dissolved Cu, ligand-bound metal fractions, total ligand concentrations, and metal–ligand stability constants were conducted by square-wave anodic stripping voltammetry and have been described by Bazzi et al. (2002).

Bioassay experiments

Bioassay experiments were conducted in 1-L polyethylene bottles held under simulated in situ conditions. Lake water was collected from depths of either 2 or 3 m by GO-FLO Niskin sampler using the same precautions and methods used to collect trace metal samples. Bottle contents were immediately amended by trace metal or other additions, rewrapped in their original layered polyethylene bags, and returned to their cooler for transport to the shore-side laboratory. (Specific sample treatments for each experiment are identified in Table 2.) The method adopted for trace metal additions had the advantage of offering minimal disruption to the phytoplankton assemblage, but it also meant that cells were exposed to metal amendments directly, without any preincubation period for equilibration of metal–ligand complex formation. Possible implications of this procedure are discussed below.

Experimental bottles were incubated under simulated in situ conditions of temperature, light level, and photoperiod for 48-h duration. Field measurements were used to adjust incubation temperature and light levels to represent the sampling depth. Upon termination of each incubation experiment, two 250-mL aliquots were removed from each bottle for pigment determination as Chl *a* by extracted fluorescence, and final pH measurements were performed. Statistical differences among treatments within each experimental series were assessed by first applying one-way analysis of variance (ANOVA) to final Chl *a* concentrations grouped by treatment (Excel 2000 version 9.0.2720). When ANOVA detected statistically significant differences among treatments ($\alpha = 0.05$), pairwise comparisons were conducted using Dunnett adjusted probabilities (SYSTAT 5.01, Systat Inc., Evanston, Ill.) in one-sided tests to evaluate the a priori hypothesis that metal additions reduced chlorophyll biomass compared with control (no addition). Two-sided tests were used to evaluate the effects of mock additions (Milli-Q carrier water only) or chelator (EDTA) addition.

To ascertain the expected degree to which our experimental additions may have saturated the chelation capacity of natural ligands and also to investigate expected sensitivity of labile metal concentrations to our experimental treatments, we used the metal speciation model of Bazzi et al. (2002) to calculate labile Cu concentrations in our experiments using median values of total dissolved Cu and chelation capacity for minimum, median, and maximum values of the conditional stability constant (K') measured simultaneously in Saginaw Bay by Bazzi et al. (2002).

Results

Field measurements

Net phytoplankton collected during May cruises was dominated by diatom species of *Aulacoseira* and *Tabellaria*, but cyanobacteria were also present, including colonies of *Microcystis* and trichomes of *Oscillatoria* and *Lyngbya*. Cyanobacteria were relatively more abundant at inner bay sites than in the outer bay. June, August, and September samples at all sites were dominated by *Microcystis*; the green alga *Pediastrum* was also present at lesser abundance.

Table 2. Experimental treatments for trace metal bioassay experiments.

Date	Treatments
June 1999	Control (no additions)
	+5 $\mu g \cdot L^{-1}$ Cu as $Cu(NO_3)_2$
	+500 $\mu g \cdot L^{-1}$ Cu as $Cu(NO_3)_2$
August 1999	Control (no additions)
	+2 $\mu g \cdot L^{-1}$ Cu as $Cu(Cl)_2$
	+5 $\mu g \cdot L^{-1}$ Cu as $Cu(Cl)_2$
	+10 $\mu g \cdot L^{-1}$ Cu as $Cu(Cl)_2$
May 2000	Control (no additions)
	+1 $\mu mol \cdot L^{-1}$ EDTA
	+1 $\mu g \cdot L^{-1}$ Cu, Pb, Cd, and Tl as Cl salts
	+5 $\mu g \cdot L^{-1}$ Cu, Pb, Cd, and Tl as Cl salts
September 2000	Control (no additions)
	+5 mL Milli-Q water (mock metal addition)
	+5 $\mu g \cdot L^{-1}$ Cu as $Cu(Cl)_2$
	+5 $\mu g \cdot L^{-1}$ Cu, Pb, Cd, and Tl as Cl salts

Physical and chemical properties differed between the inner and outer bay stations selected for experimental study (Table 3). Sampling at multiple stations (Fig. 1) confirmed the existence of strong gradients in Saginaw Bay so that many properties co-vary along the axis of the bay and over time. Comparisons of epilimnetic conditions at the multiple stations sampled in 1999 and 2000 ($n = 20$) demonstrated strong correlations among bulk chemical properties such as specific conductance with bicarbonate ($R = 0.86$), calcium ($R = 0.84$), and sulfate ($R = 0.96$), but also with nitrate ($R = 0.84$) and CDOM ($R = 0.88$).

Objective assessment of gradient patterns (Table 4) revealed that inner bay stations consistently scored above the median with respect to all limnological properties examined. Outer bay stations were consistently below the medians for the same properties; intermediate locations were intermediate in their properties. Chi-squared analysis revealed that experimental stations 1 and 8 were dramatically different ($P = 10^{-11}$) and thus presumably largely independent of spatial autocorrelation; stations 1W and 5W, however, which were the sites used in September 2000 experiments, were not significantly different.

Secchi disk transparency proved to be an excellent predictor of PAR vertical attenuation, with reciprocal Secchi transparency depth (m^{-1}) predicting 98% of the variability in light attenuation ($r^2 = 0.977$, $n = 19$). Both dissolved and particulate matter evidently contributed significantly to light attenuation; linear regression relationships for TP, CDOM, and Chl *a* with PAR attenuation were highly significant in a statistical sense ($P < 0.005$ in every case).

Chelation capacity, or the capacity for complexation of Cu by organic ligands, in natural waters of Saginaw Bay was most strongly correlated ($R = 0.79$, $P = 0.035$) with CDOM fluorescence (Fig. 2). Total dissolved Cu was inversely correlated ($R = -0.77$, $P = 0.044$) with TP (Fig. 3). No other significant correlations were identified among limnological properties and either Cu concentrations or chelation capacity.

Table 3. Epilimnetic properties at sampling depths for experiments conducted in 1999 and 2000.

Date	Station	*T*, °C	K_{25}, µS	pH	ANC, mequiv.·L^{-1}	Ca, mmol·L^{-1}	NO$_3$, µmol·L^{-1}	Chl *a*, mg·m^{-3}	TP, µmol·L^{-1}	DP, µmol·L^{-1}	SO$_4$, µmol·L^{-1}	CDOM, relative units
28 June 1999	SB1	22.8	240	8.52	1.91	0.84	28.8	2.01	0.40	0.19	n/a	n/a
	SB8	22.6	220	8.61	1.78	0.77	23.6	1.25	0.24	0.13	n/a	n/a
4 August 1999	SB1	24.2	n/a	8.80	1.79	0.75	n/a	10.22	0.57	0.21	n/a	n/a
	SB8	22.1	n/a	8.76	1.69	0.71	n/a	2.76	0.16	0.09	n/a	n/a
29 May 2000	SB1	16.2	384	8.07	2.43	1.68	310	4.81	1.98	0.86	320	210
30 May 2000	SB8	14.7	272	8.36	1.91	1.03	36	5.89	0.80	0.69	225	28
16 September 2000	SB1W	17.7	271	8.46	1.73	0.83	14.1	17.4	0.79	0.17	231	54
	SB5W	16.6	289	8.71	1.54	0.75	11.0	17.5	0.70	0.19	265	72

Note: Colored dissolved organic matter (CDOM) in fluorescence units relative to quinine fluorescence standard; n/a, analyte was not measured; *T*, temperature; K_{25} denotes specific conductance referenced to 25 °C; ANC, acid-neutralizing capacity; TP, total phosphorus; DP, dissolved phosphorus.

Laboratory experiments

Experiments were conducted with uniform methods, but the specific details of trace metal additions changed through time as we took advantage of the information gained by each successive experiment. In general, this resulted in progressive decreases in the levels of added metal and various tests to rule out potential sources of artifact. We report final concentrations of Chl *a* in the various bioassay experiments of 1999 and 2000 (Table 5).

Experimental addition of Cu to natural plankton communities from Saginaw Bay produced striking declines in algal biomass with respect to control treatments as measured by particulate Chl *a* in June 1999 (Table 6). Effects were evident at both inner and outer Bay stations, with additions of 500 µg·L^{-1} Cu reducing the algae 10-fold below control levels; mean final Chl *a* levels at both stations were 11% of control levels after 48 h. Additions of 5 µg·L^{-1} Cu likewise caused statistically significant declines in biomass compared with control at both sites, corresponding with similar mean biomass reductions at each station: 20% reduction compared with control at station 1 and 21% reduction at station 8.

In August 1999, we tried to resolve more precisely the levels at which Cu addition produced inhibition. Moreover, we added the Cu as its Cl salt rather than as nitrate to avoid the confounding effect of adding N, a potentially limiting micronutrient. The experiment suffered from variability among the control replicates such that the coefficient of variation (CV) at station 1 was 23% versus 11% at station 8. Although mean biomass levels declined with respect to control at every addition treatment, there was insufficient statistical power to establish the significance of individual treatments. Nonetheless, a strong statistical effect of Cu at inner bay station 1 emerged when all Cu addition treatment levels were pooled to increase statistical power and then were contrasted with control by one-way ANOVA ($P = 0.017$).

At outer bay station 8, the inhibitory effects of Cu addition were statistically significant at all treatment levels, including 2 µg·L^{-1} Cu ($P = 0.03$; Table 6). The effects of adding 2 and 5 µg·L^{-1} Cu were statistically indistinguishable, but 10 µg·L^{-1} Cu reduced algal biomass more than either 2 or 5 µg·L^{-1} Cu.

In May 2000, we investigated the possibility that addition of EDTA, a metal chelator, would affect algal biomass by altering metal availability. We also explored the effects of adding a trace metal mixture consisting of equal mass concentrations of Cu, Cd, Pb, and Tl at either 1 or 5 µg·L^{-1} of each metal. Variation among replicates was relatively low (CV ≤ 10% in all treatments), so power to detect treatment effects was good. There was no statistically detectable effect of EDTA addition at either station 1 or station 8 (Table 6).

Additions of trace metals produced striking results at both stations. Additions of 1 µg·L^{-1} of the four metals reduced algal biomass after 48 h by 21% at station 1 and by 15% at station 8 with respect to control treatments. At additions of 5 µg·L^{-1}, biomass measured as Chl *a* was reduced by 43% versus control at station 1 and by 22% at station 8. Additions of 5 µg·L^{-1} were significantly more inhibitory than additions of 1 µg·L^{-1} at station 1, but effects of the two addition levels were statistically indistinguishable at station 8.

In September 2000, we supplemented the control treatment with a separate mock addition control in which we

Table 4. Physical and chemical similarities among Saginaw Bay sampling sites as revealed by chi-square analysis applied to quantitative rankings of limnological property values.

Station	*N* cases < median	*N* cases> median	Similarity index				
3	0	18	1				
1	3	29	1	2			
3W	2	8		2	3		
5W	5	5			3	4	
6	4	4			3	4	
6N	4	4			3	4	
1W	6	4			3	4	
7	7	3				4	
6S	6	2				4	5
6	14	4				4	5
5	8	2				4	5
8	30	2					5

Note: Comparisons included all properties listed in Table 3 except pH. Stations were scored by property according to whether they fell above or below the median value measured during each cruise period. Common values for similarity index indicate that the station rankings do not differ significantly by chi-square analysis, $\alpha = 0.05$.

Fig. 2. Relationship between total chelation capacity for copper (Cu) by natural organic ligands and colored dissolved organic matter (CDOM) content (relative units) of Saginaw Bay water samples.

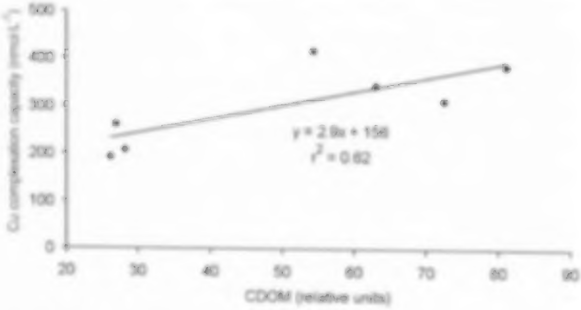

Fig. 3. Relationship between total dissolved copper (Cu) and total phosphorus (P) at multiple stations.

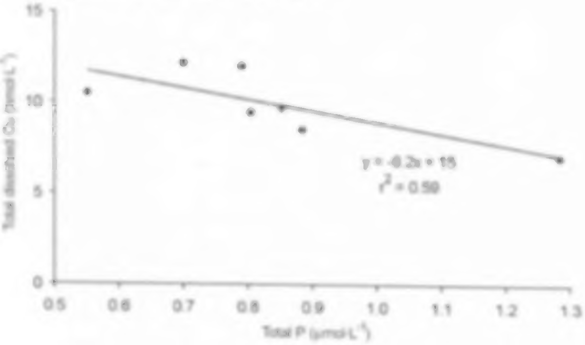

added 5 mL of the Milli-Q water that was the carrier solution and diluting medium for all metal additions. Results of this mock addition were statistically indistinguishable from control (no additions) treatments at both stations (Table 6).

In parallel treatments, we added Cu alone at 5 $\mu g \cdot L^{-1}$ Cu and Cu in combination with Pb, Cd, and Tl at 5 $\mu g \cdot L^{-1}$ for each individual metal. The inhibitory effects of Cu with respect to control were apparent at both stations, corresponding to mean biomass reductions of 15% and 10%, respectively. The effects of Cu in combination with other metals was even more striking. Biomass was reduced by 24% at station 1W and by 18% at station 5W compared with control treatments. The metal mixture proved significantly more inhibitory than Cu alone at both stations.

Based on the approach of Bazzi et al. (2002) to calculate labile Cu concentrations (Table 7), experimental additions of 1 $\mu g \cdot L^{-1}$ Cu increased labile Cu concentrations by a factor of 3 with respect to control across the full range of *K′* values measured in Saginaw Bay. Additions of 2 $\mu g \cdot L^{-1}$ Cu increased labile Cu by a factor of 5, and additions of 5 $\mu g \cdot L^{-1}$ Cu increased labile Cu by about 14-fold versus control. At higher addition levels, the stability constant of Cu–ligand formation exerts some influence on the amount of increase over control, but the binding sites were completely saturated by additions exceeding 15 $\mu g \cdot L^{-1}$ Cu.

Discussion

Phytoplankton communities in the Great Lakes may already be experiencing incipient inhibition by trace metals including Cu, based on consistent results from 2 years during different months and at different sites. Addition of as little as 2 $\mu g \cdot L^{-1}$ Cu alone, or a mixture containing 1 $\mu g \cdot L^{-1}$ each of Cu, Cd, Pb, and Tl, reduced algal biomass. Higher additions produced stronger inhibition. Every metal concentration that we tried resulted in depressed algal biomass with respect to control treatments, an observation that supports an earlier contention by Gächter et al. (1973) that even ambient levels may be at or near the threshold for inhibition in some Great Lakes waters.

The metal concentrations at which we observed experimental depression of algal biomass were lower than those used in previous studies with Great Lakes algae (Munawar et al. 1983, 1988*a*, 1988*b*), but they are consistent with the earlier work in the sense that we likewise observed depression of algal production at the higher metal additions we used.

Table 5. Results from bioassay experiments.

June 1999	Control (no additions)	+5 $\mu g \cdot L^{-1}$ Cu	+500 $\mu g \cdot L^{-1}$ Cu	
Station 1 (inner bay)	2.0	1.4	0.1	
	1.7	1.5	0.2	
	1.6	1.4	0.3	
	1.8	1.4	0.2	
Station 8 (outer bay)	1.4	1.0	0.2	
	1.2	1.1	0.1	
	1.0	1.0	0.2	
	1.6	1.0		
August 1999	Control (no additions)	+2 $\mu g \cdot L^{-1}$ Cu	+5 $\mu g \cdot L^{-1}$ Cu	+10 $\mu g \cdot L^{-1}$ Cu
Station 1 (inner bay)	11.8	8.9	7.5	6.2
	7.3	10.9	6.8	6.9
	8.8	6.6	8.2	7.1
	12.0	7.2		6.7
		5.2		
Station 8 (outer bay)	2.9	2.8	2.2	
	2.9	2.1	2.0	0.8
	3.4	1.6	1.9	1.2
	2.6	2.5	1.6	
May 2000	Control (no additions)	+1 $\mu mol \cdot L^{-1}$ EDTA	+1 $\mu g \cdot L^{-1}$	+5 $\mu g \cdot L^{-1}$
Station 1 (inner bay)	13.8	13.3	10.8	7.1
	14.1	15.6	9.9	7.9
	12.4	13.8	11.5	7.4
	13.9	13.0		8.5
Station 8 (outer bay)	3.2	2.8	2.7	2.3
	2.9	2.7	2.9	2.4
	2.7	3.0	2.4	2.3
	2.9	2.8	2.3	2.4
	3.3			
September 2000	Control (no additions)	+Milli-Q	+Cu	+metals
Station 1W (inner bay)	23.1	20.7	18.9	16.4
	22.2	22.6	19.8	19.4
	23.0	21.0	19.0	16.7
			19.8	16.5
Station 5W (outer bay)	20.0		17.2	16.0
	21.0	20.5	18.3	16.5
	19.5	20.5	18.8	17.1
	20.1		18.1	16.8

Note: Chl *a* at $t = 48$ h expressed as $mg \cdot m^{-3}$. Initial Chl concentrations ($t = 0$) are reported in Table 2.

Chelation dynamics involving metal mixtures and natural organic ligands are complex, and so one cannot be sure that inhibition from addition of Cu is caused directly by Cu itself. It may indeed be that Cu levels in the Great Lakes are toxic to the native communities, but there may be other root causes, as well. Added Cu displaces Cd from binding sites with natural ligands in Saginaw Bay, thus releasing free Cd into solution (Bazzi et al. 2002). Synergistic inhibitory effects of Cu and Cd on algal growth have in fact been demonstrated in laboratory cultures (Rachlin and Grosso 1993; Visviki and Rachlin 1994). One added metal can thus indirectly enhance the toxicity of another.

Another important caveat to consider is that the reaction kinetics of added Cu with natural ligands in Saginaw Bay are presently unknown. Implicit in the experimental design was an assumption that owing to the excess chelation capacity, a rapid equilibrium would be established between added Cu and ligands. If this assumption were false, algal cells may have been exposed initially to much higher levels of free ionic Cu than our measurements and model calculations imply. Anderson and Morel (1978) have in fact demonstrated differences in reaction time between Cu and the synthetic chelators EDTA and Tris with resulting differences in effective toxicity to a marine dinoflagellate upon initial introduction. Ma et al. (1999) demonstrated not only that Cu complexation equilibrium with a commercial humic acid source could take several hours, but also that ion exchange by Cu for Ca on humic acid ligands could take even longer. This means that there is a chance that Cu toxicity was somewhat exaggerated in our experiments by introducing the

Table 6. Summary of statistical contrasts among treatments for the bioassay experiments reported in Table 5.

June 1999	Control (no additions)	+5 µg·L^{-1} Cu	+500 µg·L^{-1} Cu	
Station 1 (inner bay), mean	1.78	1.42	0.20	
Exp. vs. control, *P*		0.0016	1.1×10^{-8}	
Station 8 (outer bay), mean	1.30	1.02	0.17	
Exp. vs. control, *P*		0.040	1.6×10^{-5}	
August 1999	**Control (no additions)**	**+2 µg·L^{-1} Cu**	**+5 µg·L^{-1} Cu**	**+10 µg·L^{-1} Cu**
Station 1 (inner bay), mean	9.98	7.76	7.50	6.72
One-way ANOVA: ns				
Station 8 (outer bay), mean	2.95	2.25	1.92	1.00
Exp. vs. control, *P*		0.03	0.004	0.0002
Exp. vs. +2 µg·L^{-1} Cu, *P*			ns	0.004
+10 vs. +5 µg·L^{-1} Cu, *P*				0.022
May 2000	**Control (no additions)**	**+1 µmol·L^{-1} EDTA**	**+1 µg·L^{-1}**	**+5 µg·L^{-1}**
Station 1 (inner bay), mean	13.6	13.9	10.7	7.7
Exp. vs. control, two-sided *P*		ns		
Exp. vs. control, *P*			0.0018	1.7×10^{-6}
+1 vs. +5 µg·L^{-1} Cu, *P*				0.001
Station 8 (outer bay), mean	3.0	2.8	2.6	2.4
Exp. vs. control, two-sided *P*		ns		
Exp. vs. control, *P*			0.010	0.00047
+1 vs. +5 µg·L^{-1} Cu, *P*				ns
Septempber 2000	**Control (no additions)**	**+ Milli-Q**	**+ Cu**	**+ metals**
Station 1W, mean	22.8	21.4	19.4	17.3
Exp. vs. control, two-sided *P*		ns		
Exp. vs. control, *P*			0.0014	0.00003
Cu vs. metals, *P*				0.014
Station 5W, mean	20.2	20.5	18.1	16.6
Exp. vs. control, two-sided *P*		ns		
Exp. vs. control, *P*			0.0006	6.3×10^{-6}
Cu vs. metals, *P*				0.005

Note: Mean Chl *a* expressed as mg·m^{-3}. Treatment contrasts are Dunnett one-sided pairwise contrasts unless stated otherwise; ns, not statistically significant at $\alpha = 0.05$; ANOVA, analysis of variance; Exp., experiment.

metals in their ionic state rather than in their long-term steady state equilibrium speciation.

When we supplemented Cu addition with other metals (September 2000), the resulting inhibition was significantly greater from the mixture than with Cu alone. The results lend credibility to the notion that metals in addition to Cu are involved at the physiological level to produce the experimental results that we recorded. Although we know that Cd is displaced from ligands by addition of Cu (Bazzi et al. 2002), other metals may be released as well, so we cannot conclude that the results we obtained were caused by Cu toxicity per se.

There were no clear or consistent differences between inner bay and outer bay sites in terms of the levels of metal addition required to depress algal biomass. Both sites seemed equally sensitive. When differences did emerge, they were more reasonably ascribed to loss of statistical power caused by poor replication than to diverging mean response levels. In every experiment at every site, trace metal treatments resulted in reduced algal biomass compared with corresponding control treatments.

Bazzi et al. (2002) report that Cu chelation capacity in Saginaw Bay varies by roughly a factor of two among our sampling sites (192–417 nmol·L^{-1}). The same is true for total dissolved Cu (7–13 nmol·L^{-1}). Data in their table 5 reveal that Cu levels do not correlate with the concentration of complexing ligands ($R = 0.044$, $n = 21$), which is consistent with the evidence for overchelation. Bazzi et al. (2002) demonstrated that between 93.1% and 99.9% of the total Cu in solution is tightly bound to organic ligands and that only 1% (median value) of the Cu is labile. The conditional stability constant (K'') for the Cu–ligand complex (Cu–L) varied from 3.3×10^7 to 4.3×10^9 where K'' is defined as either

$$(1) \qquad K'' = [\text{Cu–L}]/([\text{Cu}_{\text{labile}}] \times [\text{free ligand}])$$

or

$$(2) \qquad K'' = [\text{Cu–L}]/(([\text{Cu}_{\text{total}}] - [\text{CuL}]) \times ([\text{total ligand}] - [\text{Cu–L}]))$$

Equation 2 can be algebraically rearranged and solved as a quadratic formula for Cu–L in terms of the empirical measurements of K'', total Cu, and total ligand (Bazzi et al. 2002).

Measured variation in the conditional stability constant far surpasses the variation in either complexation capacity or to-

Table 7. Calculated levels of Cu–ligand complex (Cu–L) and labile Cu resulting from experimental Cu additions during 1999 and 2000.

Treatment	Total Cu, nmol·L^{-1}	K', mol^{-1}	Cu–L, nmol·L^{-1}	Labile Cu, nmol·L^{-1}	Relative increase versus control
Minimum K'					
Control	9.3	3.3×10^7	8.3	1.05	
+1 µg·L^{-1} Cu	25.1	3.3×10^7	22.1	2.99	2.8
+2 µg·L^{-1} Cu	40.8	3.3×10^7	35.7	5.15	4.9
+5 µg·L^{-1} Cu	88.1	3.3×10^7	74.8	13.28	12.6
+10 µg·L^{-1} Cu	167	3.3×10^7	131.7	35.12	33.3
+500 µg·L^{-1} Cu	7883	3.3×10^7	243.9	7639	7 242
Median K'					
Control	9.3	4.9×10^8	9.2	0.08	
+1 µg·L^{-1} Cu	25.1	4.9×10^8	24.8	0.23	2.9
+2 µg·L^{-1} Cu	40.8	4.9×10^8	40.4	0.40	5.0
+5 µg·L^{-1} Cu	88.1	4.9×10^8	86.9	1.12	14.0
+10 µg·L^{-1} Cu	167	4.9×10^8	162.8	4.05	50.5
+500 µg·L^{-1} Cu	7883	4.9×10^8	244.8	7639	95 417
Maximum K'					
Control	9.3	4.3×10^9	9.3	0.009	
+1 µg·L^{-1} Cu	25.1	4.3×10^9	25.0	0.03	2.9
+2 µg·L^{-1} Cu	40.8	4.3×10^9	40.8	0.05	5.1
+5 µg·L^{-1} Cu	88.1	4.3×10^9	87.9	0.13	14.2
+10 µg·L^{-1} Cu	167	4.3×10^9	166.3	0.50	53.5
+500 µg·L^{-1} Cu	7883	4.3×10^9	244.9	7638	824 473

Note: Ambient concentrations of total dissolved Cu (9.3 nmol·L^{-1}) and total ligand (245 nmol·L^{-1}) used in these calculations are the median values measured for Saginaw Bay.

tal Cu concentration. This implies the existence of multiple ligand types with different metal affinities and that they exhibit variation in time and space. We found CDOM measured by in vivo fluorescence to be a convenient predictor of chelation capacity. However, we did not find any convenient empirical predictors of the more important conditional stability constant K''. Values for log(K'') reported by Bazzi et al. (2002) do not exhibit significant seasonal variation among cruises (one-way analysis of variance, $P = 0.28$), which might have reflected changes in organic material released by different algal assemblages, but values do correlate negatively with total chelation capacity ($R = -0.45$, $n = 21$, $P = 0.042$). Because K'' is a weighted mean of multiple ligand types, some of which may have high affinity and others low affinity for the metal, the negative correlation with total ligand quantity may mean that the most variable organic ligands in Saginaw Bay are the ones least specific (low K'') for binding with copper.

In all of our metal addition experiments with the exception of May 1999 when we added 500 µg·L^{-1} Cu, there is no doubt that most of the added metal was complexed by organic ligands present naturally in the lake water. Nonetheless, even additions of 1 µg·L^{-1} Cu tripled labile concentrations of the metal and inhibited growth by the native algae. One µg·L^{-1} Cu equals 16 nmol·L^{-1} Cu, which is within the range of natural concentrations reported for Lakes Erie and Ontario (table 3 in Bazzi et al. (2002) and references therein), and is only slightly greater than the natural range of concentrations that we found in Saginaw Bay. Some metals may thus already be present at levels that are incipiently inhibitory to the planktonic algae at the base of the food webs.

Acknowledgments

We thank Dr. G. Meadows and Mr. H. Van Sumeren, Department of Naval Architecture and Marine Engineering, University of Michigan, for ship operations support, as well as Ms. D. Hollandsworth, and Mr. N. Irish for help collecting lake water and initiating experiments in 1999. We appreciate the helpful suggestions of the referees. This research was funded in part by Michigan Sea Grant.

References

Anderson, D.M., and Morel, F.M.M. 1978. Copper sensitivitiy of *Gonyaulax tamarensis*. Limnol. Oceanogr. **23**: 283–295.

Bazzi, A., Lehman, J.T., Nriagu, J.O., Hollandsworth, D., Irish, N., and Nosher, T. 2002. Chemical speciation of dissolved copper in Lake Huron with square wave anodic stripping voltammetry. J. Gt. Lakes Res. **28**: 466–478.

Campbell, P.G.C. 1995. Interactions between trace metals and aquatic organisms: a critique of the free ion activity model. *In* Metal speciation and bioavailability in aquatic systems. IUPAC series on analytical and physical chemistry of environmental systems. Vol. 3. *Edited by* A. Tessier and D.R. Turner. John Wiley and Sons, New York. pp. 47–102..

Chau, Y.K., Chawla, V.K., Nicholson, H.F., and Vollenweider, R.A. 1970. Distribution of trace metals and chlorophyll *a* in Lake Ontario. *In* Proceedings of the 13th Conference of Great Lakes Research, State College, Buffalo, N.Y. International Association for Great Lakes Research, Ann Arbor, Mich. pp. 659–671.

Edmondson, W.T. 1991. The uses of ecology. University of Washington Press, Seattle.

Gächter, R., Lum-Shue-Chan, K., and Chau, Y.K. 1973. Complexing capacity of the nutrient medium and its relation to inhibition of algal photosynthesis by copper. Schweiz. Z. Hydrol. **35**: 252–261.

Graneli, E., Persson, H., and Edler, L. 1986. Connection between trace metals, chelators and red tide blooms in the Laholm Bay, SE Kattegat — an experimental approach. Mar. Environ. Res. **18**: 61–78.

Hart, C.J., Duthie, H.C., and Wong, P.T.S. 1983. Effects of metal mixtures on natural phytoplankton communities in lake column simulators. *In* Proceedings of the 26th Conference of Great Lakes Research, SUNY, Oswego, N.Y. International Association for Great Lakes Research, Ann Arbor, Mich. p. 9.

Horne, A.J., and Goldman, C.R. 1974. Suppression of nitrogen fixation by blue-green algae in a eutrophic lake with trace addition of copper. Science (Wash., D.C.), **183**: 409–411.

International Joint Commission. 1985. Report on Great Lakes water quality. Great Lakes Water Quality Board. Report to the International Joint Commission, Windsor, Ontario.

Knauer, K., Behra, R., and Sigg, L. 1997. Effects of free Cu^{2+} and Zn^{2+} ions on growth and metal accumulation in freshwater algae. Environ. Toxicol. Chem. **16**: 220–229.

Lewis, A.G., and Cave, W.R. 1982. The biological importance of copper in oceans and estuaries. Oceanogr. Mar. Biol. Annu. Rev. **20**: 471–695.

Luederitz, V., Nicklisch, A., and Roloff, B. 1989. Copper toxicity for blue-green algae with reference to their physiological status. Arch. Hydrobiol. **82**(Suppl.): 449–459.

Lustigman, B.K. 1986. Enhancement of pigment concentrations in *Dunaliella tertiolecta* as a result of copper toxicity. Bull. Environ. Contam. Toxicol. **37**: 710–713.

Ma, H., Kim, S.D., Cha, D.K., and Allen, H.E. 1999. Effect of kinetics of complexation by humic acid on the toxicity of copper to *Ceriodaphnia dubia*. Environ. Toxicol. Chem. **18**: 828–837.

McKnight, D. 1981. Chemical and biological processes controlling the response of a freshwater ecosystem to copper stress: a field study of the $CuSO_4$ treatment of Mill Pond Reservoir, Burlington, Massachusetts. Limnol. Oceanogr. **26**: 518–531.

Munawar, M., Mudroch, A., Munawar, I.F., and Thomas, R.L. 1983. The impact of sediment-associated contaminants from the Niagara River mouth on various size assemblages of phytoplankton. J. Gt. Lakes Res. **9**: 303–313.

Munawar, M., Munawar, I.F., and McCarthy, L.H. 1988*a*. Seasonal succession of phytoplankton size assemblages and its ecological implications to the North American Great Lakes. Verh. Int. Verein. Limnol. **23**: 659–671.

Munawar, M., Munawar, I.F., McCarthy, L.H., and Duthie, H.C. 1988*b*. Phycological studies in the North Channel, Lake Huron. Hydrobiologia, **163**: 119–134.

Nor, Y.M. 1987. Ecotoxicity of copper to aquatic biota: a review. Environ. Res. **43**: 274–282.

Rachlin, J.W., and Grosso, A. 1993. The growth response of the green alga *Chlorella vulgaris* to combined divalent cation exposure. Arch. Environ. Contam. Toxicol. **24**: 16–20.

Rai, P.K., and Rai, L.C. 1997. Interactive effects of UV-B and Cu on photosynthesis, uptake and metabolism of nutrients in a green alga *Chlorella vulgaris* under simulated ozone column. J. Gen. Appl. Microbiol. **43**: 281–288.

Raven J., Evans, M., and Korb, R. 1999. The role of trace metals in photosynthetic electron transport in O_2-evolving organisms. Photosynth. Res. **60**: 111–149.

Sunda, W.G., and Huntsman, S.A. 1998. Processes regulating cellular metal accumulation and physiological effects: phytoplankton as model systems. Sci. Total Environ. **219**: 165–181.

Verweij, W., Glazewski, R., and DeHaan, H. 1992. Speciation of copper in relation to its bioavailability. Chem. Speciat. Bioavailab. **4**: 43–51.

Visviki, I., and Rachlin, J.W. 1994. Acute and chronic exposure of *Dunaliella salina* and *Chlamydomonas bullosa* to copper and cadmium: effects on growth. Arch. Environ. Contam. Toxicol. **26**: 149–153.

Wong, P.T.S., Chau, Y.K., and Luxon, P.L. 1978. Toxicity of a mixture of metals on freshwater algae. J. Fish. Res. Board Can. **35**: 479–481.

Wurtsbaugh, W.A., and Horne, A.J. 1982. Effects of copper on nitrogen fixation and growth of blue-green algae in natural plankton associations. Can. J. Fish. Aquat. Sci. **39**: 1636–1641.

Nonparametric estimates of age misclassification from paired readings

William G. Clark

Abstract: With a large enough sample, age misclassification probabilities can be estimated nonparametrically by fitting the observed distribution of differences between paired readings. Application of this procedure to Pacific halibut data reveals that the unsigned deviations of single readings from the mode follow a geometric distribution, leading to a simple specification of misclassification probabilities. The potential for bias in this and other published procedures is discussed.

Résumé : Dans un échantillon assez grand, on peut estimer par des méthodes non paramétriques les probabilités de classification erronée des âges en ajustant les distributions observées des différences entre des lectures appariées. L'application de cette procédure à des données sur le flétan du Pacifique indique que les déviations (sans signe) de lectures uniques tirées du mode suivent une distribution géométrique, ce qui mène à une simple spécification des probabilités de classification erronée. Les probabilités d'erreur dans cette procédure et dans d'autres présentées dans la littérature font l'objet d'une discussion.

[Traduit par la Rédaction]

Introduction

Most stock assessments are done by fitting an age-structured model to a series of age-structured fishery and survey data, the latter obtained by collecting samples of fish from commercial and survey catches and determining their ages by counting the annuli (annual rings) formed on a chosen structure, in most cases the sagittal otolith or earstone. Forsberg (2001) provides a detailed account of how otoliths are processed and read at the International Pacific Halibut Commission (IPHC) to estimate the age composition of catches. Campana (2001) reviews methods used to validate age readings and measure precision.

Age readers strive to follow consistent and objective rules for distinguishing annuli from other marks on an otolith, but there is still some judgement involved and, as a result, some variability in readings of a single otolith, both within and among readers (Kimura and Lyons 1991). A single age reading can therefore be regarded as a random variable drawn from a probability distribution. The mode of this distribution occurs at the age that would be chosen most often if the same otolith were read many times by experienced readers following the established protocol, and it is therefore by definition the correct age. It may or may not be the true age of the fish — that depends on whether the protocol is in fact accurate — but it is the correct result of applying the protocol. For clarity, in this paper, this modal age will be called the "canonical age" to stress the point that it is correct relative to the rules in use, not relative to the true age of a fish. When a different age is assigned, the otolith is said to be misclassified.

Otoliths are generally read only once, with a fraction read twice or more for quality control. Estimated age compositions therefore consist of a mixture of correct ages and misclassifications, and that leads to errors in estimates of abundance at age when a stock assessment is done, even if the age-reading protocol is accurate (Reeves 2003). If the misclassification probabilities are known, however, the assessment model can be so constructed that it will predict their effect on the observed age compositions and thereby correctly estimate the true underlying abundance at age.

For various reasons, it is not practical to assemble a large number of independent readings for each of even a small sample of otoliths, so one cannot directly observe the form of the distribution of readings or determine empirically what is the canonical age of a given otolith. What is usually available instead is a small number of readings for each of a large sample of otoliths, often the paired quality control readings done on some proportion of the total. It is common practice to estimate misclassification probabilities by fitting one or another assumed parametric model to data of this sort (e.g., Richards et al. 1992), but as explained below, some of the usual model fits can be misleading. This paper describes a nonparametric estimation method based on the observable distribution of differences between paired readings and its application to data on Pacific halibut (*Hippoglossus stenolepis*).

Materials and methods

Until the early 1990s, Pacific halibut otoliths were aged by surface reading wherein whole otoliths are examined at 5–50× under reflected light. It is now known that this method underestimates the age of older fish and so has been replaced by the break-and-burn method (Forsberg 2001). The canonical age of an otolith read by the surface method is

Received 12 August 2003. Accepted 20 July 2004. Published on the NRC Research Press Web site at http://cjfas.nrc.ca on 15 December 2004.
J17701

W.G. Clark. International Pacific Halibut Commission, P.O. Box 95009, Seattle, WA 98145, USA (e-mail: bill@iphc.washington.edu).

Can. J. Fish. Aquat. Sci. **61**: 1881–1889 (2004) doi: 10.1139/F04-122

therefore biased, but it is still the canonical surface age in that it is the modal age assigned by experienced readers following that protocol. The stock assessment model can be written to account for both bias and misclassification when predicting the age compositions estimated by surface readings.

The data available for estimating the misclassification probabilities consist of a large number (80 963) of paired surface readings, because in many years, all otoliths were read twice. The assigned ages range from 4 to 36, but the first age with a substantial number of readings is 6, and after 20, the numbers are small (Fig. 1).

The approach in this paper will be to derive and test a nonparametric method of estimating the misclassification probabilities from paired readings and then report the nonparametric estimates for the Pacific halibut surface readings. Some comparisons between this procedure and the usual parametric fits will be reported in the discussion section.

Derivation of the estimation method

Let $f_A(a)$ denote the probability distribution of a single reading of an otolith of canonical age A, and let $v = a - A$ denote the deviation of a single reading from the canonical age. The distribution of v is therefore the same as that of a, but with the mode at zero rather than at A. Let $f_A(v)$ denote this shifted distribution.

Suppose we have two independent readings (a_1, a_2) of every otolith in a large sample of otoliths of a given canonical age A. Such a sample could never be assembled in practice because the canonical age of an otolith cannot be observed, but the notion of such a sample will facilitate the derivation. Let d denote the signed difference between the paired readings, or $d = a_1 - a_2 = v_1 - v_2$, and let $g_A(d)$ denote the distribution of d. This distribution is determined by $f_A(v)$, and the elements of $f_A(v)$ can be estimated by predicting and fitting the sample distribution of d. For example, consider the probability of observing a difference $d = -2$ between the first and second readings of a particular otolith. If the deviation v of a single reading from the mode ranges from $v_{\min}$ (a negative number) to $v_{\max}$, then this probability is

$$g_A(-2) = P_A(v_2 = v_1 + 2) = \sum_{v_{\min}}^{v_{\max}-2} f_A(v) f_A(v+2)$$

The probability of observing $d = +2$ is the sum of the products of the same pairs, and likewise for other $d \neq 0$, so $g_A(d)$ is symmetric even if $f_A(v)$ is not. The frequency distribution of the absolute differences therefore contains all of the information in the sample, and the expected frequencies are

$$g_A(0) = \sum_{v_{\min}}^{v_{\max}} [f_A(v)]^2$$

and

$$g_A(|d|) = 2 \sum_{v_{\min}}^{v_{\max}-d} f_A(v) f_A(v+d) \quad \text{for } |d| > 0$$

In mathematical terms, $g_A(d)$ is the autocorrelation function of $f_A(v)$ (Press et al. 1988). Estimating the latter from the former is therefore a matter of inverting an autocorrelation function. There appears to be no discussion of this problem in the literature, but in extensive trials with randomly generated test distributions $f_A(v)$ and the corresponding computed distributions $g_A(d)$, it was always possible to locate the inverse numerically. The only restriction placed on the test distributions was that they decrease monotonically on either side of the mode.

Fig. 1. Joint distribution of the paired readings. The size of each point is proportional to the logarithm of the number of readings.

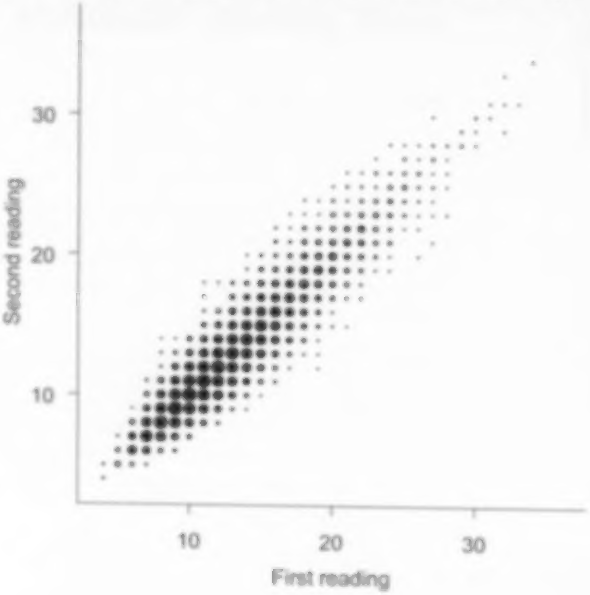

The trials showed that with deterministic data it is possible to recover any distribution of deviations $f_A(v)$ by numerically fitting the equations above to the observed frequencies of unsigned sample differences $g_A(d)$. However, there are two serious drawbacks to this procedure. The first is that any given $f_A(v)$ and its reverse will generate the same $g_A(d)$. If $f_A(v)$ is asymmetric, the search algorithm will locate one or the other isomer of $f_A(v)$, depending on the starting value of the parameter vector. The second drawback is that the estimates become quite variable in the presence of even moderate sampling error.

As a practical matter, therefore, it is only possible to obtain unique estimates if $f_A(v)$ is assumed to be symmetric. The symmetric estimates are also more stable. If $f_A(v)$ is not symmetric, the estimates obtained in this way are approximate averages, e.g., $\hat{f}_A(-2) = \hat{f}_A(+2)$ is approximately the average of $f_A(-2)$ and $f_A(+2)$. The same fitting procedure can be used, with obvious differences in how the parameter vector is specified. (Detailed instructions for the symmetric case are provided in Appendix A.)

Up to this point, the derivation has referred to a hypothetical sample of paired readings of otoliths of the same canonical age. Real data always consist of an unknown mixture of canonical ages, so they cannot be grouped by canonical age to estimate $f_A(v)$ for each A. Instead they can be grouped by mean assigned age, i.e., the mean of the two actual readings of each otolith. (The mean assigned age of the two readings is a sample value, and it can be higher or lower than the ca-

Fig. 2. Results of 100 simulation trials of the nonparametric estimates, computed with the readings grouped by canonical age and by mean assigned age. The total sample size was 80 000 in each trial.

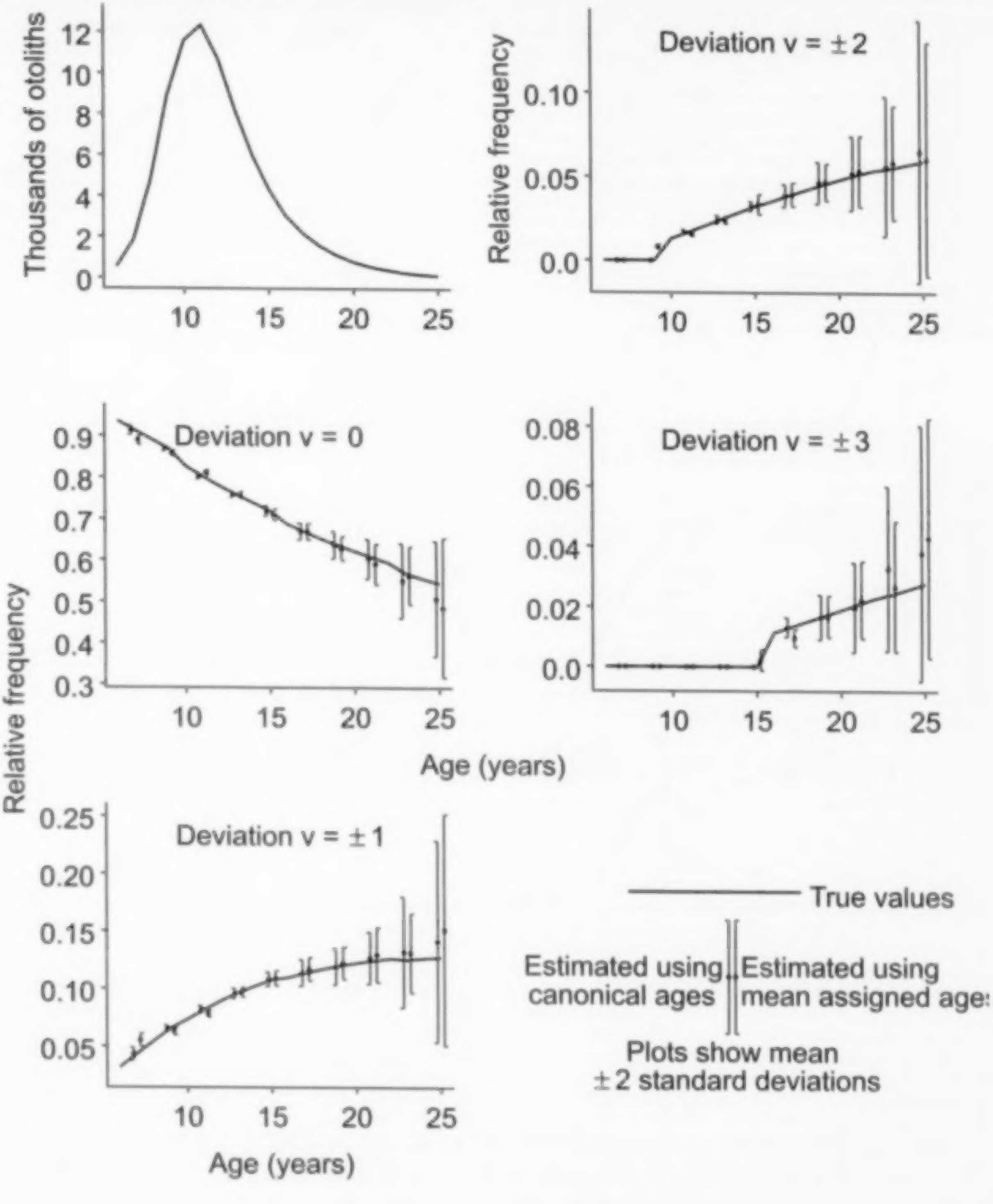

Fig. 3. Observed (points) and predicted (lines) distributions of differences between paired readings of Pacific halibut (*Hippoglossus stenolepis*) otoliths, plotted by mean assigned age.

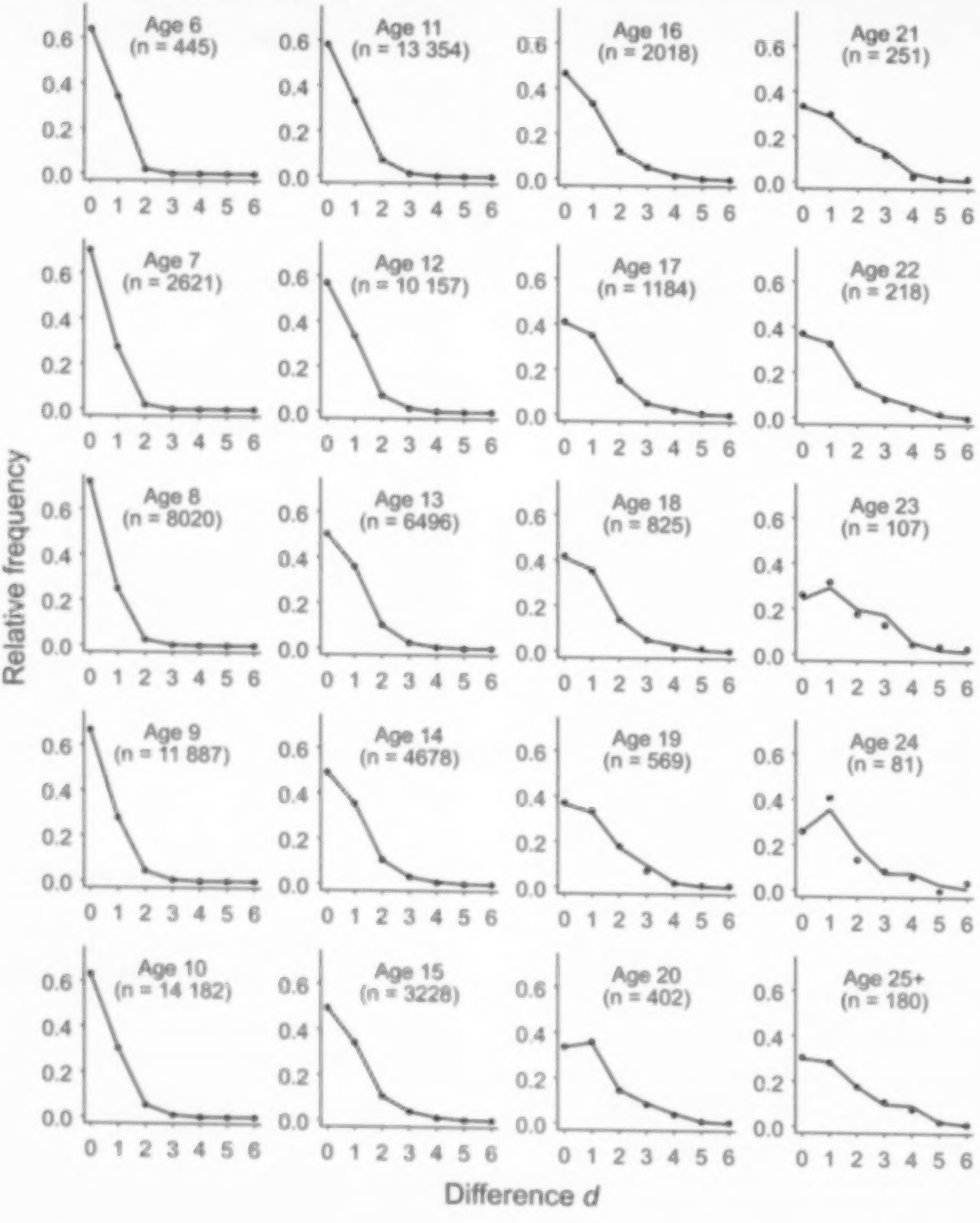

Fig. 4. Estimates of the relative frequencies of deviations of individual readings from the canonical age $f_A(v)$ computed from the Pacific halibut (*Hippoglossus stenolepis*) data, plotted against mean assigned age. The lines are data smoothers.

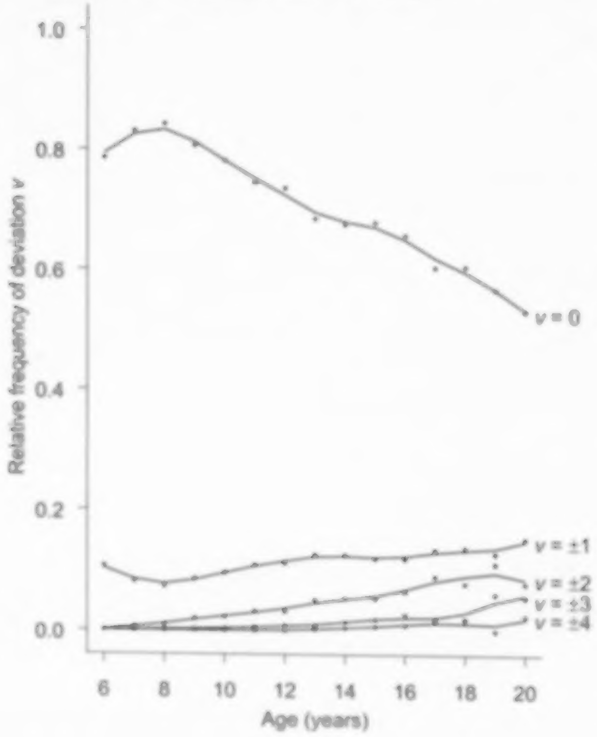

nonical age of the otolith, which is the mode that would be observed if the otolith were read many times.) In real data, the otoliths of mean assigned age $\bar{a} = A$ will consist of a mixture of canonical ages in the vicinity of A. It seems reasonable to suspect that the distribution of differences $g_a(d)$ would be very similar to $g_A(d)$, so $\hat{f}_a(v)$ would be a good estimate of $f_A(v)$, but that needs to be demonstrated. Simulations were conducted for that purpose.

Simulation tests

There were two questions to be investigated by simulation. First, what are the inherent bias and variance of the estimates when computed with paired readings grouped by canonical age (as can be done with simulated but not real data)? Second, what is the effect of grouping the data by mean assigned age?

A simulation model for this purpose was constructed with mortality and selectivity parameters appropriate to Pacific halibut. No attempt was made to model the effect of variable year-class strength on the estimates because the real Pacific halibut data come from several years, so the relative abundance at age in the data is already averaged over strong and weak year classes. Each trial consisted of drawing a sample of size 80 000 from the canonical age composition of the catch and then generating two random readings of each otolith in the sample according to the estimated misclassification probabilities reported in the results section below. Misclassification estimates were computed with the data grouped by both canonical age and mean assigned age. (For the latter grouping, an mean assigned age that fell midway between two successive ages was rounded up or down with equal probability.) Whenever an estimate failed to provide a very good fit to the simulated distribution of sample differences, the search was repeated several times from randomly chosen starting points to check for multiple maxima.

Estimates computed using the canonical ages were unbiased and quite precise for the more numerous age groups, but they became quite variable and slightly biased when sample size dropped into the low hundreds among the oldest age groups in the simulation (Fig. 2). A few instances of multiple maxima also appeared among these groups. Estimates computed using the mean assigned ages were significantly biased statistically ($t > 10$ for many ages), but as can be seen from the graphs, the size of the bias is negligible. The mean assigned ages produce virtually the same estimates as the canonical ages in this case.

Results

Estimates of misclassification probabilities were computed for each mean assigned age from 6 through 25 in the Pacific halibut data. Both symmetric and asymmetric estimates of $f_A(v)$ were computed to check for evidence of asymmetry. For the youngest fish, the best estimates were asymmetric, but from age 10 onward, both procedures produced the same symmetric estimates.

The symmetric estimates predict very well the sample distributions of differences between paired readings through age 20 (Fig. 3). At the smaller sample sizes after age 20, the fits deteriorate, just as in the simulations. The estimated probability that an age reading will be the canonical age decreases from about 0.8 at age 6 to about 0.5 at age 20, whereas the probabilities of deviations of all sizes increase gradually with age (Fig. 4).

The computed age-specific estimates are satisfactory through age 20 but not for older fish. One way to handle age groups with small sample sizes is to smooth the sample frequencies of differences $g_A(0)$, $g_A(1)$, … over ages and then use the smoothed frequencies to estimate $f_A(v)$ at each age.

A simpler solution is available for Pacific halibut because all of the well-determined estimates of $f_A(v)$ have the same simple form. A plot of the estimated log frequencies of unsigned deviations against the deviations is linear at every age (Fig. 5), meaning that the unsigned deviations follow the geometric distribution $f_A(|v|) = p_A q_A^{|v|}$, where $q_A = 1 - p_A$. The signed deviations are therefore distributed as $f_A(0) = p_A$ and $f_A(v \neq 0) = (p_A q_A^{|v|})/2$.

The value of p_A for any age can be inferred from any well-determined summary statistic of the distribution of readings at that age, e.g., variance. Simulations show that for the Pacific halibut example, the variance of the difference between paired readings is virtually the same whether calculated with the data grouped by canonical age or by mean assigned age. The general trend of the variance of the differences among older age groups (Fig. 6) is clear even though the sample sizes are too small to permit age-specific estimates of $f_A(v)$, and the variance of single readings about the canonical age is just half the variance of the differences. Because of the two

Fig. 5. The logarithms of the nonparametric estimates of the frequencies of unsigned deviations $f(|v|)$ plotted against the deviations. The lines are linear regressions.

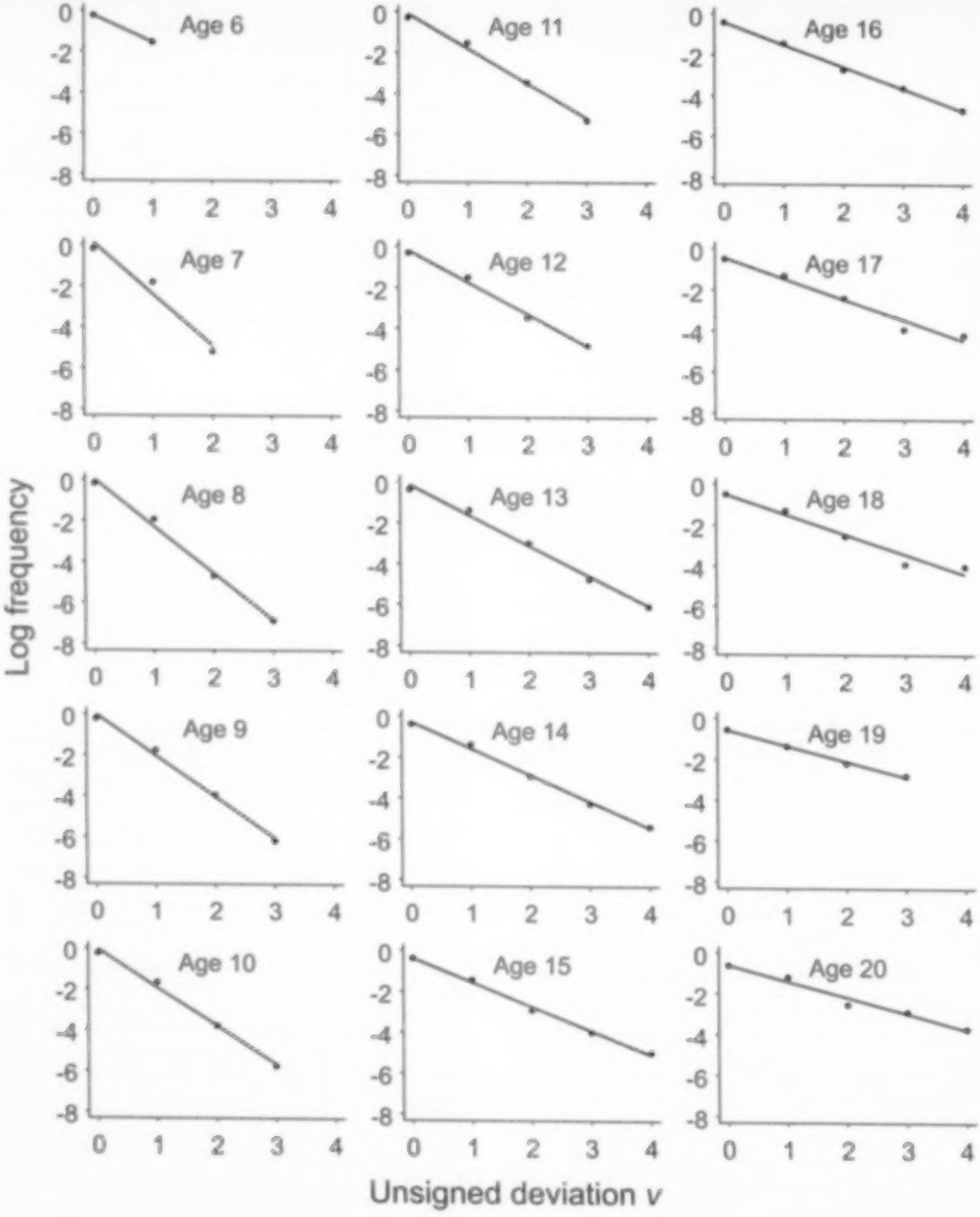

Fig. 6. The standard deviation of the difference between paired readings at each mean assigned age, and the inferred standard deviation of single readings about the canonical age.

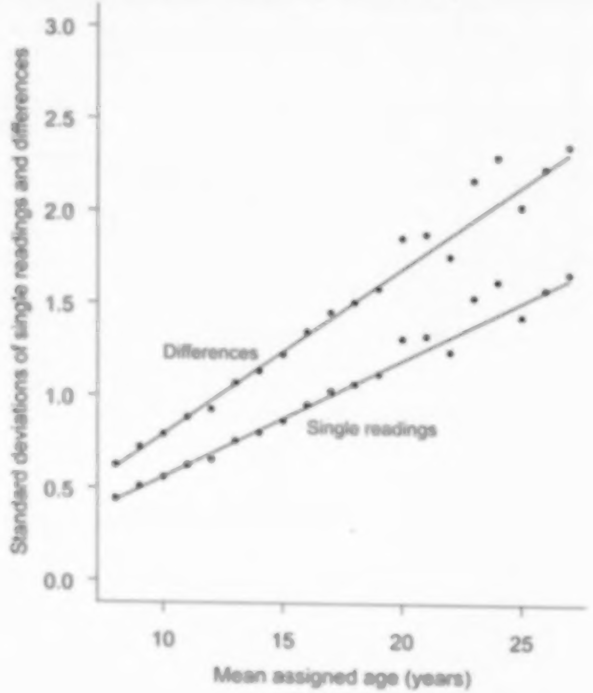

sidedness of the distribution, the variance of the signed deviations is equal to the second moment of the geometric distribution, or (omitting the subscript A for simplicity)

$$\sigma_v^2 = (q + q^2)/p^2$$

whence after some algebra

$$p = \frac{-3 + \sqrt{1 + 8\sigma_v^2}}{2(\sigma_v^2 - 1)}$$

(The value of p at $\sigma_v^2 = 1$ is 2/3.) The standard deviations of single readings (plotted in Fig. 6) all lie on a straight line, so the misclassification probabilities for all ages of Pacific halibut can be specified concisely by saying that the unsigned deviations are geometric and the standard deviation of the signed deviations at canonical age A is $\sigma_v = -0.112 + 0.0668A$. These are the probabilities used in the simulations.

Discussion

This paper has presented a method of estimating age misclassification probabilities without making any assumption about the form of the distribution of readings (apart from symmetry). It was motivated by the large number of paired surface readings available for Pacific halibut, but it could be applied to cases with more than two readings per otolith by simply generating all possible pairs to construct the sample of differences.

A potential weakness of the method is its reliance on grouping the data by mean assigned age rather than by (unknown) canonical age to compute the estimates. This does result in bias, the size of which will depend on the actual variation with age of both abundance and misclassification probabilities. The latter can be expected to vary smoothly, so the real concern is unsmooth variation in abundance. When the data are derived from several years of sampling, the sample age compositions should be smooth and the bias should be demonstrably negligible, as in the case of Pacific halibut. A single year's data from a stock with large variations in year-class strength would be questionable, but the question could and should be answered by simulation.

A more serious limitation of the method is its need for relatively large samples — at least a few hundred pairs of readings for each estimate and preferably at least 500. One way to increase the sample size available for each age-specific estimate is to use a moving data window of 3 or more years to compute the estimate for the central age. This will reduce the variance of the estimates but increase the bias caused by grouping. If that bias is negligible to begin with, there may be little harm done.

In some cases, it may be possible to identify the form of $f_A(v)$ and the way in which it varies with age in the more numerous age groups from nonparametric estimates and thereby choose a parsimonious parametric model that can be fitted to the entire data set. This was true of the IPHC surface readings and is also true for IPHC break-and-burn readings where the available number of paired readings is much smaller. (The break-and-burn readings are also geometric.)

If sample sizes at all ages are too small for nonparametric estimates, one is obliged to assume a parametric model for $f_A(v)$ at each age and fit that, or to fit alternative candidates and choose the best one according to standard model selection criteria. There is no way to know to what extent the estimates are biased by model misspecification.

Richards et al. (1992) provide a detailed account of how to compute maximum-likelihood estimates of the parameters of an assumed misclassification model and, if desired, associated estimates of the canonical age distribution of the sample or the canonical age of each fish in the sample. It is a thorough treatment of the topic except for its lack of any consideration of possible bias, which can be present in maximum-likelihood estimates even when the model is correctly specified. For example, one of the procedures outlined in the paper, and applied to paired readings by Heifetz et al. (1999), is to estimate the canonical age of each fish and use a discrete version of the normal density function to model misclassification. The procedure is easy to apply because with a normal density the maximum-likelihood estimate of the canonical age is simply the mean assigned age, and the associated likelihood is quite simple. But when applied to paired readings, it greatly underestimates their variability because the procedure essentially locates the maximum-likelihood estimates of the mean and variance of the readings of each otolith. In the case of the variance that is $\Sigma(x - \bar{x})^2/n$ rather than the usual unbiased sampling estimate $\Sigma(x - \bar{x})^2/(n - 1)$. When n is large, the difference is unimportant. When the data are paired readings and $n = 2$, the difference is substantial. (Richards et al. (1992) had data with $n = 6$ readings of each otolith.)

This behavior is illustrated (Fig. 7) with simulated paired readings that actually follow the discrete version of the nor-

Fig. 7. Parametric and nonparametric estimates of the distribution of deviations of single readings computed with simulated data that follow the "normal model" described in Richards et al. (1992). Each plotted point is the mean of 100 simulated trials with a sample size of 80 000 paired readings each.

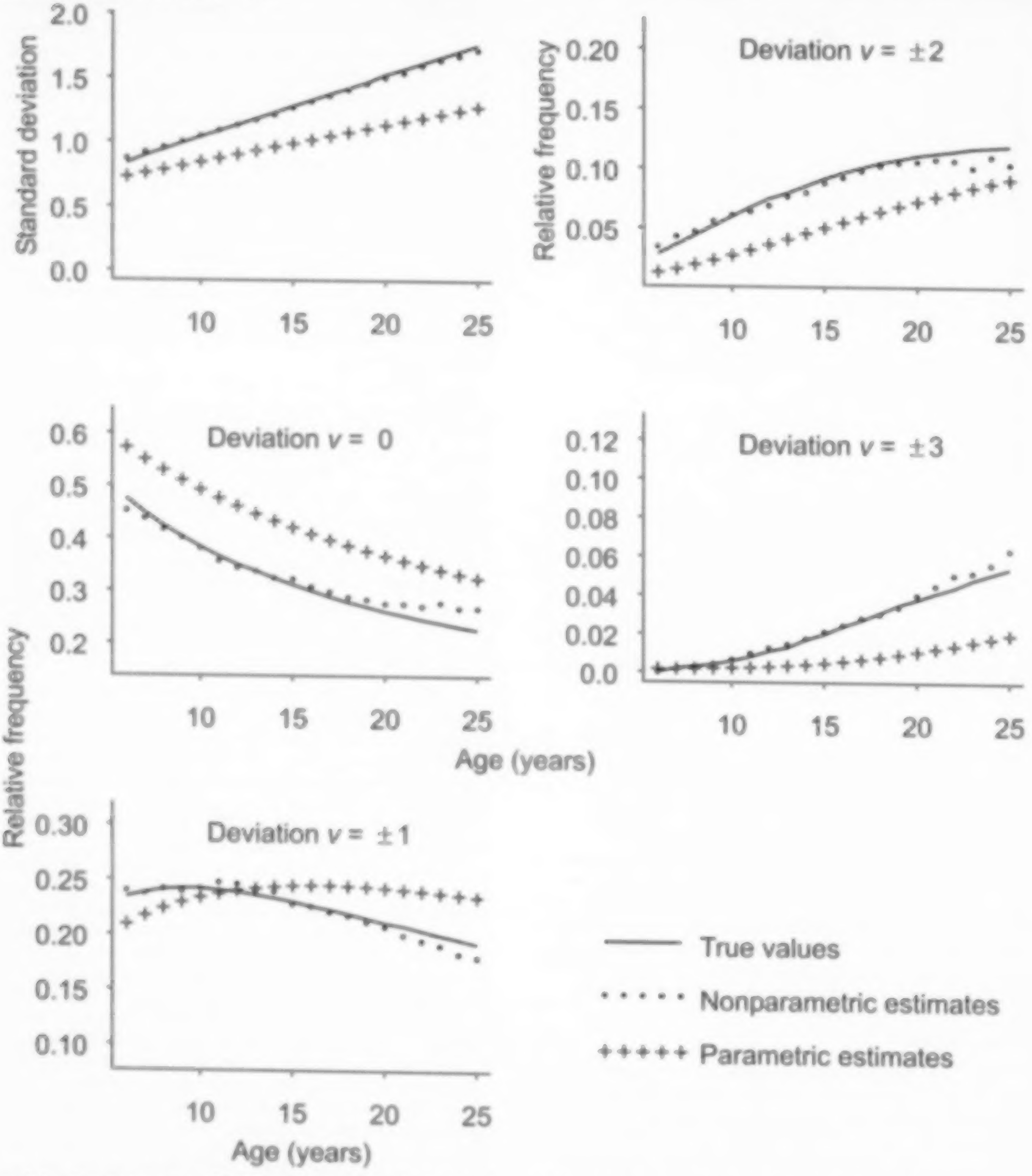

mal density: $f(v) \propto \exp(-v^2/(2\sigma^2))$. The standard deviation of this distribution is equal to the parameter σ for $\sigma \geq 0.6$. Parametric estimates of the standard deviation and the misclassification probabilities were computed with likelihood 4.3 in table 4 of Richards et al. (1992), and nonparametric estimates were computed using the method developed in this paper. Even though the model is correctly specified, almost all of the parametric estimates are very biased. Meanwhile the nonparametric estimates perform quite well without benefit of any knowledge or assumption concerning the form of the distribution.

Heifetz et al. (1999), in fact, knew the true ages of the fish in their sample because they had been marked early in life and later recaptured. The ages assigned by two readers showed considerable variability about the known ages but no bias, so the known age could be taken to be the canonical age and the authors could fit the model to known misclassification frequencies. They did that, and they also applied the procedure from Richards et al. (1992) to the paired readings using the mean assigned age instead of the known age. They were puzzled that the latter estimates of misclassification probabilities were so much lower than the former and attributed the difference to some unknown peculiarity of the paired readings, but it is more likely that the reason was simply bias in the estimation procedure. This example illustrates the importance of conducting simulation trials to verify that a numerical estimation procedure is really working correctly before applying it to real data (Hilborn and Mangel 1997).

Acknowledgements

The large number of age readings described in this paper were done by many readers in the International Pacific Halibut Commission's Age Reading Unit, supervised over the years by Edward Best, Calvin Blood, and presently Joan Forsberg. Dan Kimura and Bruce Leaman kindly read an earlier draft and made a number of suggestions that greatly improved the exposition. Geoffrey Evans' signed review of the submitted paper pointed out a number of places where there was still room for improvement.

References

Campana, S.E. 2001. Accuracy, precision, and quality control in age determination, including a review of the use and abuse of age validation methods. J. Fish Biol. **59**: 197–242.

Forsberg, J.E. 2001. Aging manual for Pacific halibut: procedures and methods used at the International Pacific Halibut Commission. Int. Pac. Halibut Comm. Tech. Rep. No. 46.

Heifetz, J., Anderl, D., Maloney, N.E., and Rutecki, T.L. 1999. Age validation and analysis of ageing error from marked and recaptured sablefish, *Anoplopoma fimbria*. Fish. Bull. **97**: 256–263.

Hilborn, R., and Mangel, M. 1997. The ecological detective. Princeton University Press, Princeton, N.J.

Kimura, D.K., and Lyons, J.J. 1991. Between-reader bias and variability in the age determination process. Fish. Bull. **89**: 53–60.

Press, W.H., Flannery, B.P., Teukolsky, S.A., and Vetterling, W.T. 1988. Numerical recipes in C. Cambridge University Press, Cambridge.

Reeves, S.A. 2003. A simulation study of the implications of age-reading errors for stock assessment and management advice. ICES J. Mar. Sci. **60**: 314–328.

Richards, L.J., Schnute, J.T., Kronlund, A.R., and Beamish, R.J. 1992. Statistical models for the analysis of ageing error. Can. J. Fish. Aquat. Sci. **49**: 1801–1815.

Appendix A. Computing instructions.

Given paired readings of a number of otoliths from fish of canonical age A or in that vicinity (e.g., fish of mean assigned age $\bar{a} = A$), the aim is to estimate the distribution $f_A(v)$ of deviations of age readings from the canonical age. This can be done numerically by predicting and fitting the observed distribution of differences of paired readings $g_A(d)$. The following instructions detail how to tabulate the data, handle the parameter vector, and code the objective function. For simplicity, the subscript A is omitted. Any general-purpose minimizer can be used to locate the estimates.

1. Tabulate the frequencies of absolute differences of paired readings of all otoliths of mean assigned age A (or range of mean assigned ages centered at A). These absolute differences will range from 0 through, say, $d_{\max}$. Denote these frequencies $n_0, n_1, n_2, \ldots, n_{d_{\max}}$.
2. Set the largest absolute deviation (of a single reading from the canonical age) $v_{\max}$ to $d_{\max}/2$ rounded up, e.g., if $d_{\max}$ is 5 or 6, $v_{\max}$ is 3 and $v_{\min}$ is –3.
3. The parameters to be estimated are the probabilities of deviations (from the canonical age) $f(0), f(1), \ldots, f(v_{\max} - 1)$, with the understanding that $f(-v) = f(v)$. The last value $f(v_{\max}) = f(v_{\min})$ is not estimated as a parameter because the probabilities must sum to one. A simple way to handle the working vector of estimates $\hat{f}(v)$ is to specify a parameter vector of unconstrained real numbers $x_0, \ldots, x_{v_{\max}-1}$ and run them through the logistic function $y = 1/(1 + e^{-x})$ so that they are all confined to (0,1). Call those numbers $y_0, \ldots, y_{v_{\max}-1}$ and fill in $\hat{f}(v)$ as follows:

```
$\hat{f}(0) = y_0$
remainder = $0.5(1 - \hat{f}(0))$
for $v$ in 1 to $(v_{\max} - 1)$
        {prop = $y_v \cdot$ remainder
        $\hat{f}(v) = \hat{f}(-v)$ = prop
        remainder = remainder – prop}
$\hat{f}(v_{\max}) = \hat{f}(-v_{\max})$ = remainder
```

4. With this value of $\hat{f}(v)$, calculate the predicted distribution of differences $\hat{g}(d)$

$$\hat{g}(0) = \sum_{v_{\min}}^{v_{\max}} [\hat{f}(v)]^2$$

and

$$\hat{g}(|d|) = 2 \sum_{v_{\min}}^{v_{\max}-d} \hat{f}(v)\hat{f}(v + d) \quad \text{for } |d| > 0$$

5. Compute the multinomial log likelihood of this predicted value as

$$\log L = \text{constant} + \sum_{d=0}^{d_{\max}} n_d \log(\hat{g}(d))$$

With a general-purpose minimizer, the objective function should return $-\log L$ so as to maximize $\log L$.

A genetic perspective on management and recovery of federally endangered trout (*Oncorhynchus gilae*) in the American Southwest

John P. Wares, Dominique Alò, and Thomas F. Turner

Abstract: The native trout of New Mexico and Arizona have been managed for conservation for almost 80 years and are currently listed under the US Endangered Species Act. Management of these populations has improved the outlook for these species. However, because of a history of non-native salmonids being stocked in the region, genetic analysis of the remaining populations is necessary to ensure that each population is as representative as possible of ancestral populations of Gila (*Oncorhynchus gilae*) and Apache (*Oncorhynchus gilae apache*) trout. Here we provide a multilocus genotypic assessment of 19 populations of native southwestern trout that strongly indicates that management has maintained the genetic integrity of these species, while restoring each species to a number of historically occupied streams.

Résumé : Les truites indigènes du Nouveau-Mexique et de l'Arizona ont été aménagées dans un but de conservation depuis presque 30 ans et elles sont actuellement incluses dans la liste dressée d'après la loi américaine sur les espèces menacées (« US Endangered Species Act »). L'aménagement de ces populations a amélioré la perspective d'avenir des espèces. Cependant, à cause de l'ensemencement dans le passé de salmonidés non indigènes dans la région, il faut procéder à une analyse génétique des populations survivantes afin de s'assurer que chaque population représente, autant qu'il est possible, les populations ancestrales de truites Gila (*Oncorhynchus gilae*) et de truites apaches (*Oncorhynchus gilae apache*). Nous présentons un évaluation basée sur plusieurs locus de 19 populations de truites indigènes du sud-ouest qui indique clairement que l'aménagement a préservé l'intégrité génétique de ces espèces, tout en rétablissant chacune des espèces dans un certain nombre de cours d'eau qu'elles ont occupés dans le passé.

[Traduit par la Rédaction]

Introduction

The native trout of New Mexico and Arizona (Gila trout (*Oncorhynchus gilae* Miller) and Apache trout (*Oncorhynchus gilae apache*); see Behnke 1992; Nelson et al. 2004) were among the first species placed under the protection of the US Endangered Species Act of 1973. Propst et al. (1992) and Carmichael et al. (1993) reviewed almost 80 years of work by state and federal agencies and tribal governments to protect these salmonids. These approaches included angling closures, the construction of barriers to prevent invasion of non-native salmonids into their high mountain stream habitats, and replication of remnant populations into similar habitats to guard against extirpation by fire, drought, or flooding. The summer of 1989 illustrated the potential for catastrophic loss of populations, when a combination of factors eliminated the Main Diamond Creek population and over 95% of the South Diamond Creek population of *O. gilae* — just as the species was being proposed by US Fish and Wildlife Service (USFWS) for downlisting from endangered to threatened status (Propst et al. 1992).

Continued management of these populations, including hatchery propagation following strict mating protocols and replication of genetically distinct and historically important lineages throughout the Gila River drainage, has lowered the risk of widespread extirpation of *O. gilae* (USFWS 2003). However, because of a history of non-native salmonids (particularly rainbow trout (*Oncorhynchus mykiss*)) being stocked in these same drainages (Propst et al. 1992; Dowling and Childs 1992; Carmichael et al. 1993), a criterion for delisting either subspecies is the assurance that the recovery process maintains aforementioned genetic distinctiveness and diversity (Propst et al. 1992; USFWS 2003). Previous genetic studies (Dowling and Childs 1992; Carmichael et al. 1993; J.L. Nielsen et al., unpublished[3]) identified populations that contained high percentages of hybrid individuals; such populations are no longer managed, and many were destroyed. These same analyses identified particular drainages as being genetically distinct, for example, genetic data from the Spruce Creek lineage of Gila trout (San Francisco River drainage) are significantly different from data taken in other

Received 14 July 2003. Accepted 18 May 2004. Published on the NRC Research Press Web site at http://cjfas.nrc.ca on 15 December 2004.
J17639

J.P. Wares,[1,2] D. Alò, and T.F. Turner. University of New Mexico, Department of Biology and Museum of Southwestern Biology, Castetter Hall, Albuquerque, NM 87131, USA.

---

[1] Corresponding author (e-mail: jpwares@uga.edu).

[2] Present address: Department of Genetics, University of Georgia, Athens, GA 30602, USA.

[3] Nielsen, J.L., Wiltse, D.S., and Fountain, M.C. Testing for rainbow trout introgression in Arizona Apache trout populations using microsatellites. Technical report submitted Aug. 11, 1999, to Arizona Game and Fish.

Can. J. Fish. Aquat. Sci. **61**: 1890–1899 (2004) doi: 10.1139/F04-124

Gila and Apache trout drainages (Riddle et al. 1998; Leary and Allendorf 1999).

Our objective was to assess extant managed populations of Gila and Apache trout for presence of non-native genetic markers. This task was complicated by the close relationship between these native species and their sister taxon *O. mykiss* (rainbow trout; Stearley and Smith 1993; Riddle et al. 1998). Diagnostic alleles between two species at neutral genetic loci should be rare when the divergence time is recent (Bagley and Gall 1998; Bulgin et al. 2003; Hudson and Turelli 2003). Thus, assessing the likelihood that a particular set of alleles in native trout might represent introgression of rainbow trout, rather than ancestral polymorphism, was an important element of this study.

In particular, we needed to be able to compare populations without assuming a known reference population (Manel et al. 2002). Illustrating that native southwestern trouts are similar to each other and distinct from rainbow trout was not sufficient for identifying historically "pure" populations of trout. We used a group of methods that (*i*) identified distinct historical lineages of salmonids based on multilocus genotypes, (*ii*) estimated the likelihood of inclusion/exclusion of individuals into each analytically defined evolutionarily significant unit (ESU; sensu Ryder 1986; Waples 1991; Moritz 1994), and (*iii*) searched for genotypic patterns that might suggest hybridization, without a priori definitions of what was a pure population of Gila or Apache trout. We also used standard analyses of molecular variance to quantify the distinctiveness of relict lineages of native trout, each of which has been managed separately to retain the full diversity of this species (USFWS 2003).

Here we show multilocus genotypic data for trout from 10 populations of Gila trout (representing all four relict lineages) and nine populations of Apache trout (representing three relict lineages). These data, including mitochondrial haplotypes, nuclear gene sequences, and variation at seven microsatellite loci, strongly indicated that management of both native trout taxa has maintained the genetic integrity of each, while stocking restored each species to a number of historically occupied streams. With continued success in preventing introduction of non-native fishes and the loss of relict lineages, both will be successfully restored to much of their historical range (see USFWS 2003).

Methods

Tissues from trout in 10 populations of *O. gilae* and nine populations of *O. g. apache* (Table 1; Fig. 1) were provided by cooperating state and federal agencies. Small (~1 cm^2) clips were taken from the caudal fin and specimens were returned alive to the stream. Ethanol-preserved tissue samples are held in the Museum of Southwestern Biology, Division of Fishes (University of New Mexico, Albuquerque, NM 87131, USA), along with voucher specimens for most sampled populations (Museum of Southwestern Biology catalogue numbers 49875–49893) of *O. gilae*. Individuals (n = 24) of *O. mykiss* were sampled from Rock Lake Fish Hatchery in New Mexico; this hatchery is the source for most of the rainbow trout stocking in the Gila Wilderness region, and the original lineage is thought to be derived from McCloud River (California) stock. We also compared the New Mexico and Arizona populations with five trout from Brush Creek (Montana), a tributary of the Kootenai River. These trout have additionally been confirmed as *O. mykiss* using protein electrophoresis (P. Spruell, University of Montana, personal communication).

We screened over 30 published microsatellite loci for their ability to reliably amplify in three species (*O. gilae*, *O. g. apache*, and *O. mykiss*) and their ability to distinguish among these taxa. Of those that amplified, we only used loci for which the proportion of shared alleles (PSA; Bowcock et al. 1994) was less than 0.4, providing significant discrimination between the native species and the closely related *O. mykiss* (Table 2). No microsatellite locus was diagnostic for southwestern trout taxa. We only scored alleles with a clearly identifiable phenogram; loci with strong stutter bands were typically only scored if the same allele could be reliably called after two or more amplification reactions. Of the seven loci used, three are believed to be strongly linked to quantitative trait loci (QTL) in the *O. mykiss* genome (Jackson et al. 1998; Sakamoto et al. 1999). These QTL loci are associated with variation in spawning time and upper thermal tolerance, and subsequent analyses compared linked versus "unlinked" markers.

Variation at the nuclear transferrin gene (exon 13; Ford et al. 1999) and mitochondrial control region was assayed using single-stranded conformational polymorphisms (SSCP; Sunnucks et al. 2000). We cloned variant alleles using a Topo TA vector kit (Invitrogen) and cycle-sequenced in both directions. To enable SSCP screening of the mitochondrial control region, two fragments (of approximately 300 nucleotides in length) were chosen that have been screened previously (DL3, Bagley and Gall 1998; S-*Phe*/P2, Nielsen et al. 1994). We directly sequenced 3–6 copies of each variant in both directions.

Assignment tests — baseline

We used standard likelihood-based assignment tests to ensure that native trout populations (Table 1) were free of individuals with *O. mykiss* genetic backgrounds. We assigned trout using a series of different baseline populations in the program WHICHRUN (Banks and Eichert 2000). Because no known lineage or population of *O. gilae* or *O. g. apache* can be assumed representative of the whole taxon, this analysis was repeated using each relict lineage as a baseline for comparison to "unknown" individuals and with hatchery *O. mykiss* (Table 1) representing the "known" rainbow trout baseline.

Bayesian assignment of multilocus genotypes

Analyses of inclusion/exclusion of each trout into Gila, Apache, or rainbow trout groups were performed using only the multilocus microsatellite genotype of each individual, reserving the diagnostic mtDNA and transferrin sequence data for clarification of ambiguous genotypes (see Results). First, we used a Bayesian clustering algorithm (Partition/Analyze 1.1, Belkhir and Dawson 2001) on the individuals that were 100% genotyped (some individuals were not reliably scored at all seven microsatellite loci). This determined how distinct the genotype groupings are without a priori information about

Table 1. Native populations of Gila and Apache trout sampled for this study.

Population	Source lineage	Sample size
Main Diamond (MD)	Relict (Gila, 4)	49
Black Canyon (BC)	Main Diamond (Gila, 4)	44
McKnight Creek (MK)	Main Diamond (Gila, 4)	28
South Diamond (SD)	Relict (Gila, 4)	83
Mogollon Creek (MC)	South Diamond (Gila, 4)	34
Whiskey Creek (WC)	Relict (Gila, 4)	14
Little Creek (LC)	Whiskey (Gila, 4)	23
Big Dry Creek (BDC)	Spruce Creek (Gila, 3)	30
Dude Creek (DC)	Spruce Creek (Gila, 3)	6
Raspberry Creek (RC)	Spruce Creek (Gila, 3)	35
Soldier Creek (SDC)	Relict (Apache, 2)	47
Coleman Creek (CLC)	Soldier Creek (Apache, 2)	32
Coyote Creek (CYC)	Ord Creek (Apache, 1)	42
Mineral Creek (MRC)	Ord Creek (Apache, 1)	42
Hayground Creek (HGC)	East Fork White River (Apache, 1)	35
Home Creek (HMC)	East Fork White River (Apache, 1)	12
Stinky Creek (SKC)	East Fork White River (Apache, 1)	47
W. Fork Black R. (WBR)	East Fork White River (Apache, 1)	39
Wildcat Creek (WDC)	East Fork White River (Apache, 1)	3
McKittrick Creek (MCK)	Putative hybrid (Apache, 3)	31
Domestic Rainbow	Hatchery (NM, MT)	24
Total		711

Note: Source lineage is given for replicate populations of relict lineages, and the subspecies/management unit is also indicated (number corresponds to drainage on Fig. 1). Detailed location information is available from the Museum of Southwestern Biology (University of New Mexico, Albuquerque, New Mexico, USA).

Fig. 1. Region of the southwestern United States where Gila and Apache trout (*Oncorhynchus gilae* and *O. g. apache*, respectively) were collected for this study. Major drainages are indicated by numerals: 1, White River – Little Colorado River; 2, Gila River (Coronado National Forest, Arizona); 3, San Francisco River; 4, Gila River. Gila and Apache trout are found in the moderate- to high-gradient mountain streams above ~1645 m (USFWS 2003). Elevation is indicated by shading (light grey, 1500–2440 m altitude; darker grey, over 2440 m). Map modified from Arizona Geographic Alliance (Department of Geography, Arizona State University, Tempe, AZ 85257, USA).

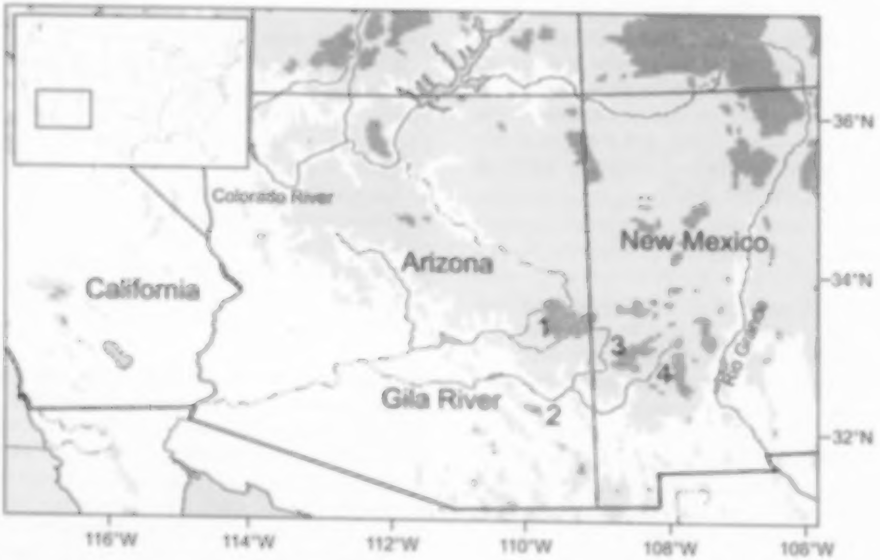

baseline populations of any taxon. These analyses incorporated 10^7 Markov chain observations (each separated by 10 steps) using a uniform prior distribution on the number of source populations and a prior estimate of θ (a coalescent measure of genetic diversity) of 1.0. This analysis estimates the posterior probability of the number of source populations

Table 2. Locus-by-locus comparisons of diversity across native southwestern trout (g, Gila trout; a, Apache trout) and rainbow trout (m, *O. mykiss*) lineages.

Marker	No. of alleles (m/g/a)	*H* (m/g/a)	F_{ct} (among species)
D-loop[a]	6/5/6	0.471/0.098/0.606	0.851 ($p < 0.001$)
Transferrin[b]	1/1/1	n/a	Fixed
*One*μ*11*[c]	3/3/3	0.478/0.094/0.045	0.593 ($p < 0.05$)
Ocl2[d]	7/3/3	0.763/0.414/0.192	0.522 ($p < 0.001$)
Ogo4[e]	9/3/3	0.850/0.223/0.529	0.240 ($p < 0.01$)
Ssa197[f]	2/2/3	0.467/0.306/0.424	0.169 ($p < 0.01$)
OmyFGT12[g]	15/7/7	0.894/0.678/0.637	0.245 ($p < 0.001$)
Omy325[h]	12/9/12	0.858/0.779/0.641	0.089 ($p < 0.01$)
Omy77[i]	7/7/5	0.736/0.707/0.668	0.236 ($p < 0.01$)

Note: Gene diversity (*H*; Nei 1987) for Gila and Apache trout is presented as the average across all populations. Significance values for F_{ct} are based on analysis of molecular variance (AMOVA) results (Excoffier et al. 1992). n/a, not available.

[a] Nielsen et al. (1998), Bagley and Gall (1998).

[b] Ford et al. (1999).

[c] Scribner et al. (1996).

[d] Condrey and Bentzen (1998).

[e] Olsen et al. (1998).

[f] O'Reilly et al. (1996).

[g] Sakamoto et al. (1999).

[h] O'Connell et al. (1997).

[i] Morris et al. 1996.

(*k*) and calculates a Bayes factor to compare hypotheses of $k = 1$ and $k > 1$. This application also computes the posterior co-assignment probabilities for each pair of individuals.

We then included all remaining individuals in an assignment test. Again, without a known baseline population for native trout, we avoided using methods that require a priori designations. We used GeneClass 1.0.2 (Cornuet et al. 1999), a program for assignment and exclusion using multilocus genotypes that incorporates Bayesian estimates of allele frequencies, and an exclusion procedure of assignment, that simulates the appropriate number of individuals by randomly drawing alleles from the population sample: the log-likelihood of a given individual is then simply compared with the distribution based on simulated individuals (Cornuet et al. 1999). We determined each assignment class by the output from the partition analysis, using those groups that had low (<0.50) probabilities of co-assignment into any other group. We simulated 10^5 pseudo-replicate individual genotypes to determine the threshold probability of assignment of each individual to each group. The test assigned individuals to lineages when ratios of posterior probabilities (test lineage *L* / maximum lineage *L*) were greater than 0.01.

Probability of hybrid history

Anderson and Thompson (2002) have implemented a test (NewHybrids 1.1*b*3) that uses deviation from Hardy–Weinberg equilibrium among multilocus genotypes to assess the posterior probability that an individual came from a single (equilibrium) genetic background (i.e., was not hybrid). The strength of this analysis is that it assumes no known baseline genotype or population, but compares allele frequencies among individuals to determine the probability that they belong to one of two pure lineages, or are a hybrid mixture. In this case, we only assessed the likelihood of hybrid history assuming two generations of introgression (F1, F2, and backcross genotypes), because marginal probabilities of further hybrid classes become increasingly difficult to calculate (Anderson and Thompson 2002); this is certainly appropriate for ensuring that there has been no continued non-native stocking or hybridization in the native trout populations.

All individuals were included in pairwise tests of *O. gilae* (Gila River drainage) versus *O. mykiss*, *O. gilae* (Spruce Creek) versus *O. mykiss*, and *O. g. apache* versus *O. mykiss*. Burn-in of the analysis lasted for 10^4 sweeps, Monte Carlo chain averages then were reset, and the total run included 5×10^5 sweeps. We assumed no prior allele frequencies and a uniform prior distribution for diversity at each locus.

Diversification of river drainages

We used analysis of molecular variance (AMOVA; Arlequin 2.001; Schneider et al. 1997) to compare the complete genotype of each individual (including mtDNA and transferrin sequence data) for population structure relating to species divergence and degree of genetic distinction among drainages within each native taxon. Locus-by-locus AMOVA results were obtained for comparisons among species to determine if particular loci provided greater resolution. Geographic partitions were designed within each species analysis based on the relict lineages (i.e., Main Diamond, South Diamond, Whiskey, and Spruce creeks for *O. gilae*; Soldier and Ord creeks and East Fork White River for *O. g. apache*).

Results

Sequence data at exon 13 of the transferrin gene (499 bp; see Ford et al. 1999) were diagnostic for native southwestern trout (*O. gilae* and *O. g. apache*) relative to *O. mykiss* and other salmonids that have been screened. Two fixed nucleotide substitutions (involving a single amino acid substitution) made SSCP scoring of individuals clear. No individual scored from Gila/Apache populations contained a rainbow trout allele (GenBank AF472515), and there was no variation within native populations of the two native species (GenBank AF472516).

Mitochondrial control region sequence data were diagnostic for each species in this study. We recovered seven haplotypes from *O. mykiss* (GenBank AF517756–AF517762, the last one being equivalent to RTDL 14/33 from Bagley and Gall 1998) and used the complete set of sequences from both Bagley and Gall (1998) and Nielsen (Nielsen 1997; Nielsen et al. 1998) for comparison with a broad range of rainbow and cutthroat (*O. clarki*) mitochondrial sequence variants (Wares and Turner, unpublished data). Six haplotypes were recovered from *O. g. apache* (AF517764–AF517767, AY490785, AY490786). Only a single haplotype was found in *O. gilae* populations in the Gila River drainage (AF517763), as in previous studies (Nielsen et al. 1998; J.L. Nielsen et al., unpublished[1]; Riddle et al. 1998), but this haplotype and four others (AY490781–AY490784) were found in the Spruce Creek drainage.

Likelihood-based assignment tests

The results of all assignment tests provided strong support that populations of *O. gilae* and *O. g. apache* that we examined are distinct from *O. mykiss*. Regardless of baseline "native" population chosen, no individual fish had a likelihood ratio (comparing the likelihood of a native southwestern genetic background with the rainbow genetic background) of less than 3.0 (rejecting the "rainbow" hypothesis with $p < 0.001$ for all individuals), with many individuals having likelihood ratios of 10 or higher.

Bayesian assignment of multilocus genotypes

We analyzed all individuals that were genotyped for all seven microsatellite loci ($n = 283$, and all 24 individuals of *O. mykiss* from the Rock Lake Fish Hatchery in New Mexico) for the posterior probability of the pairwise probability of co-assignment. Without a priori categorization of individuals, the probability of co-assignment of any native southwestern trout with rainbow trout was less than 0.43 (less than 0.20 for individuals believed to be Gila trout from New Mexico), whereas the corresponding probabilities within each cluster are greater than or equal to 0.75 (probabilities of co-assignment among individuals of Gila trout are greater than 0.89). Overall, this analysis rejected the co-assignment of all individuals into a single group ($k = 1$), with a posterior probability of 0.754 that there are two or three main historical lineages. However, the Bayes factor of 0.746 (see Goodman 1999) indicated that the likelihood of a single historical lineage could not be strongly rejected because of overall genotypic similarity among populations and species in this study. This problem is typical for studies focusing on closely related ESUs (Bulgin et al. 2003).

Trout from McKittrick Creek (Arizona), believed to be rainbow–Apache hybrids, were co-assigned with rainbow trout with high probability (>0.80). Mitochondrial data also support the inference that this population is primarily of rainbow trout background. Assignment of all remaining individuals was based on the designation of five groups (rainbow, McKittrick hybrid, Apache, Gila, Spruce). The distinction between Gila and Spruce was made not because of statistical separation in the prior Bayesian analysis, but to see if inference of evolutionary distinction between these populations made in earlier studies (Riddle et al. 1998) is supported. Using these five groupings, 91% of the 711 individuals are correctly assigned to group based on their collection locality. Only individuals from McKittrick Creek were reassigned with high probability to *O. mykiss*. Of the 687 native southwestern trout analyzed, 47 could not be excluded from *O. mykiss* and were assigned to both their own lineage and that of rainbow trout. This does not suggest hybrid origin, but a lack of resolution; these doubly assigned trout were only partially genotyped. Difficulty in reliably genotyping some individuals at all microsatellite and sequence-based loci, perhaps because of variation in tissue quality, resulted in ~15% of samples being genotyped at fewer than five microsatellite loci (Fig. 2). None of these individuals was scored for a non-native allele at the mitochondrial control region or transferrin locus. Only a single individual (*O. apache* FMRC45 from Mineral Creek) that had been genotyped at more than four of the seven microsatellite loci was unable to be excluded from *O. mykiss* (and so could be grouped with either *O. mykiss* or *O. g. apache*), yet this individual had native southwestern mtDNA and transferrin alleles.

Fig. 2. Histogram indicating the number of individuals that were able to be scored at a given number of microsatellite loci, including information on the additional scoring of native versus non-native alleles at the mitochondrial control region and the nuclear transferrin (exon 13). The poor allelic resolution of some individuals tended to be associated with particular population samples, suggesting tissue degradation may be the cause. Solid bars, mtDNA/Tf scored; open bars, mtDNA/Tf not scored.

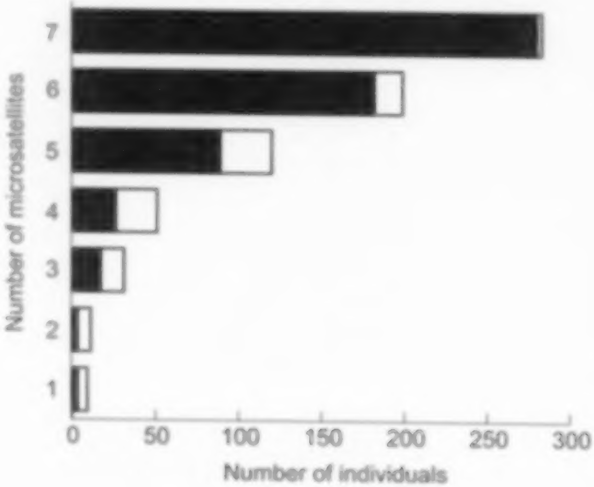

Probability of hybrid history

Bayesian hybrid analysis (Anderson and Thompson 2002) revealed only 27 individuals that had less than 0.99 posterior probability of being pure native southwestern trout (only five individuals at less than 0.95). Of these, only three individuals (all from Hayground Creek, FHGC) were genotyped for more than three microsatellite loci, and all had native mtDNA haplotypes and native transferrin alleles. The ambiguities in our analysis of microsatellite data all appear to be related to problems with reliably scoring alleles in some in-

Table 3. Locus-by-locus analysis of molecular variance (AMOVA) results: (*a*) variation partitions for each locus and (*b*) average variance partitions across all microsatellite loci.

(*a*) Variation partitions for each locus.

	Among species	Among populations	Within populations
_Omy325_*	8.48	9.81	81.71
Ssa197	21.27	4.64	74.08
Ogo4	39.64	2.61	57.74
_OmyFGT12_*	26.06	4.17	69.76
Ocl2	51.79	2.81	45.39
_Omy77_*	18.08	14.14	67.77
Oneμ11	69.67	1.38	28.95

(*b*) Average variance partitions across all microsatellite loci.

Source of variation	Degrees of freedom	Sum of squares	Variance components	Percentage of variation
Among species	2	179.943	0.78419 Va	30.71
Among populations within species	11	71.294	0.16256 Vb	6.37
Within populations	426	684.325	1.60640 Vc	62.92
Total	439	935.561	2.55314	

Note: Analyses only include fully genotyped individuals. Variance components are as in Excoffier et al. (1992). All results are significant ($p < 0.01$; $F_{st} = 0.371$; $F_{sc} = 0.092$; $F_{ct} = 0.307$). Asterisks indicate loci with putative linkages to QTLs.

Table 4. Analysis of molecular variance (AMOVA) results for Gila trout microsatellite variation.

Source of variation	Degrees of freedom	Sum of squares	Variance components	Percentage of variation
Among lineages	4	82.077	0.16885 Va	13.11
Among populations within lineages	7	10.225	0.00701 Vb	0.54
Within populations	602	669.716	1.11248 Vc	86.35
Total	613	762.018	1.28834	

Note: Variation partitions in a locus-by-locus analysis are only significant among lineages for *Omy77*, *Omy325*, and *OmyFGT12* between Spruce Creek and the other Gila River lineages (Main Diamond, South Diamond, Whiskey). Average variance partitions across all loci are shown here. Variance components are as in Excoffier et al. (1992). Only F_{st} (within populations) and F_{ct} (among lineages) are significant ($p < 0.01$; $F_{st} = 0.136$; $F_{sc} = 0.006$; $F_{ct} = 0.131$).

Table 5. Analysis of molecular variance (AMOVA) results for Apache trout.

Source of variation	Degrees of freedom	Sum of squares	Variance components	Percentage of variation
Among lineages	2	77.480	0.15727 Va	13.25
Among populations within lineages	6	37.576	0.08895 Vb	7.50
Within populations	593	557.663	0.94041 Vc	79.25
Total	601	672.719	1.18664	

Note: Analyses only include fully genotyped individuals. Variance components are as in Excoffier et al. (1992). Only F_{st} (within populations) and F_{sc} (among populations) are significant ($p < 0.01$; $F_{st} = 0.207$; $F_{sc} = 0.086$; $F_{ct} = 0.132$); F_{ct} (among lineages) is significant at $p < 0.05$.

dividuals, resulting in a lack of resolution or power, rather than the potential for hybrid history.

Analysis of molecular variance

We address two questions with these analyses: how distinct are native southwestern trout from *O. mykiss*, and how can patterns of variation within species guide management decisions (e.g., how distinct are separate lineages)? Three separate analyses address these questions. Locus-by-locus AMOVA indicates strong isolation of *O. mykiss* from *O. gilae* spp. and illustrates that there is no major difference between QTL-linked and other microsatellite loci for explaining differences between species or among lineages/populations within species (Table 3; similar results were obtained for locus-by-locus estimates within each species, J.P. Wares, unpublished data).

Overall, the highly polymorphic loci used in these analyses indicated strong differentiation among lineages within *O. gilae* and *O. g. apache*, as well as high levels of within- and among-population variation. We present AMOVA results for these two species (Tables 4, 5). In *O. gilae*, only F_{st} (within populations; 0.136) and F_{ct} (among lineages; 0.131) are significant ($p < 0.01$), although F_{sc} (among populations within lineages; 0.006) is marginally significant ($0.01 < p < 0.05$).

In *O. g. apache*, among-lineage variation is lower (F_{ct} = 0.132, $0.01 < p < 0.05$), but within- and among-population variation is significant ($p < 0.01$, $F_{st} = 0.207$, $F_{sc} = 0.086$, respectively). The elevated levels of variation among populations within lineages may suggest that moving larger numbers of individuals between these populations is necessary to maintain cohesion. Overall among-lineage variation is high enough in both species to merit continued attention to each relict lineage.

Although many populations had significantly high F_{st} in pairwise comparisons, Gila trout from the Spruce Creek lineage typically had significantly higher levels of differentiation, with average pairwise F_{st} from Spruce Creek populations to other *O. gilae* populations being 0.252, but average pairwise F_{st} among all other populations being only 0.016. In Apache trout, MRC (see Table 1) is highly different from CYC (both are Ord Creek lineages, Table 1; F_{st} = 0.25). However, SDC is not significantly different from CLC in the Soldier Creek lineage (F_{st} = –0.033), and variation in the East Fork White River group is low (F_{st} = –0.0012). Therefore, all signal of within-lineage variation is due to inclusion of the Ord lineage, and it is possible that inclusion of Ord swamped out among-lineage signal. We detected strong divergence across all loci within the Ord group (MRC, CYC) except at *One*μ11, which is invariant in those populations. Other loci indicate that 12–56% of all genetic variation in the Ord Creek lineage is attributable to differences between replicate populations.

Discussion

Multilocus analysis of single copy nuclear genes, microsatellites, and mtDNA loci indicated that populations of Gila and Apache trout do not harbor individuals with rainbow trout (*O. mykiss*) genetic backgrounds. The probability that rainbow alleles are present in these populations was evaluated using three methods: (*i*) standard likelihood based assignment tests that require a set of "known" genotypes be used for comparisons of all individuals in the study; (*ii*) Bayesian estimates of co-assignment that require no known baseline population (an important distinction for choosing appropriate methods; Manel et al. 2002); and (*iii*) analysis of Hardy–Weinberg disequilibrium among individuals and lineages of trout (Anderson and Thompson 2002). Each method has relative strengths and weaknesses. Likelihood analysis typically rejected the hypothesis that any individual could be assigned to *O. mykiss* with high probability ($p < 0.001$) and correctly assigned all native trout. Concordant results among Bayesian analyses suggest a complete lack of *O. mykiss* genetic background. A number of individuals could not be genotyped at all loci, and for individuals genotyped at fewer than five microsatellite loci (n = 102 out of 704), a lack of power to resolve genetic differentiation may be a problem (Cornuet et al. 1999). However, most of these individuals were scored for native mitochondrial and transferrin alleles; no individuals had ambiguous genotypic backgrounds when all data were considered.

Comparisons were made only between putative native southwestern trout and individuals of a single stock of rainbow trout (from a New Mexico hatchery used for much of the *O. mykiss* stocking in the Gila Wilderness region) for most microsatellite loci. Although this could limit inferential power to assess hybrid status, initial screening of microsatellite loci also used individuals from other rainbow trout stocks (the Brush Creek lineage, see Methods), and no genotypic difference was detected between the New Mexico hatchery stock and other individuals sampled. In fact, overall levels of divergence between the native trout lineages and the Brush Creek rainbow trout were higher than when compared with the Rock Creek (New Mexico) trout. The average F_{st} = 0.458 between *O. gilae* and BC lineage, and the average F_{st} = 0.399 between *O. gilae* and the New Mexico hatchery, only using microsatellites *Ssa*197, *Ogo*4, and *Ocl*2. Another locus, *Omy*0004, was also part of the initial screening process and was discarded because of a low PSA between the Rock Creek rainbow trout and *O. gilae*, but the BC *O. mykiss* are also more divergent at this locus (J.P. Wares, unpublished data).

A number of previous surveys using both allozyme and microsatellite data had already confirmed these remaining lineages of *O. gilae* as being distinct from several other lineages of *O. mykiss* (Dowling and Childs 1992; Carmichael et al. 1993; Leary and Allendorf 1999; J.L. Nielsen et al., unpublished[3]). Additionally, we had no difficulty identifying hybrid lineages (McKittrick Creek, Arizona) as such using both standard and Bayesian assignment tests, though the lineage of rainbow trout introduced to that population is unknown. Finally, we compared our mitochondrial sequence data with a broad survey of published rainbow trout sequences (Nielsen 1997; Nielsen et al. 1998; Bagley and Gall 1998) to ensure that native southwestern sequences represented a unique set of haplotypes (J.P. Wares and T.F. Turner, unpublished data). It is clearly a difficult problem to determine the most appropriate population comparisons between a highly diverse species and a very closely related, low-diversity taxon (Bulgin et al. 2003), particularly at microsatellite loci, which may differ among species in allele frequencies but not in allelic range.

Because there are several distinct lineages in each species studied and management of these lineages has involved the replication of each into other suitable habitats, we can compare genetic divergence among lineages and among replicates within lineages. As expected from previous allozyme work (Leary and Allendorf 1999), there is strong genetic divergence between trout in the Spruce Creek lineage of Gila trout and other members of this species. Trout from Spruce Creek have a number of morphological and genetic differences from other Gila trout (David 1976; Riddle et al. 1998; reviewed in USFWS 2003), and our microsatellite and mtDNA data support the continued management of this lineage as a distinct group of Gila trout.

Variation among the three Gila River lineages of *O. gilae* (Main Diamond, South Diamond, and Whiskey Creek) was minimal. Genetic variation partitions among replicates of all Gila trout lineages were not significant. However, in Apache trout, there is significant signal for among-replicate variation in the Ord Creek lineage. Zimmer (2003) reviews the impacts of "rapid evolution" that may be caused by severe population bottlenecks and may affect the long-term viability of natural populations. Current replication schemes implemented by managers typically involve at most a few hundred fish being moved at a time (J. Brooks, US Fish and Wildlife Service, New Mexico Fishery Resources Office, Albuquerque, NM 87113, USA, personal communication), with no ongoing gene flow or return translocations between the replicates to limit the transmission of introduced disease vectors among replicate populations. Briskie and Mackintosh (2004) suggest that fitness reductions may accompany translocation bottlenecks of fewer than ~150 individuals. However, reciprocal translocations among replicate populations could eliminate the potential for evolutionary divergence of stocked populations within a single relict lineage. These data, and measures of inbreeding such as F_{st}, are interpreted here solely as measures of genetic dissimilarity and not as indicators of gene flow. Neigel (2002) discusses the use of frequency-based estimators of genetic divergence and their drawbacks, but they remain valid for describing levels of distinction among populations.

Earlier trout conservation studies have used the genetic loci discussed here. The mtDNA haplotype data was known to be diagnostic for Gila and Apache trout, along with several allozyme loci (USFWS 2003). We show that exon 13 of transferrin is also diagnostic for these native southwestern trout species, though not variable within or among these populations. Ford et al. (1999) indicates that this gene, which plays a role in resistance to bacterial infection in salmonids, is likely to be diagnostic for most salmonid lineages because of the positive directional selection found in interspecific comparisons. Of the microsatellite loci used here, all have been shown to be consistent with Mendelian inheritance. Ardren et al. (1999) indicated that there may be size homoplasy at the *One*µ11 locus in comparisons among rainbow trout populations, but overall lack of variation at this locus, and high differentiation between rainbow trout and native southwestern trout, made it suitable for this study.

Three of the microsatellite loci screened here are presumed to be tightly linked with quantitative trait loci (QTL) in rainbow trout (Jackson et al. 1998; Sakamoto et al. 1999). These QTL appear to reflect variation in spawning time (*Omy*77; Sakamoto et al. 1999) and upper thermal tolerance (*Omy*325 and *Omy*FGT12; Jackson et al. 1998). Kashi et al. (1997) suggested that highly variable microsatellite markers may contribute to quantitative phenotypic variation, and we find interesting comparisons to be made between those markers that are believed to be linked to quantitative traits and those that are not. "Linked" markers are almost four times as variable as "unlinked" markers in this study (J.P. Wares, unpublished data) and contribute almost all of the among-lineage variation between the Spruce Creek and Gila River lineages of Gila trout. However, the other four loci could also be linked to genomic regions under selection (see Gillespie 2001) and so further analysis of this pattern, considering the rainbow trout linkage map (Sakamoto et al. 2000), is necessary. It should be noted that there is no evidence for variation in the quantitative traits that are believed to be linked to our markers in the trout populations studied. Lee and Rinne (1980) found no significant difference in temperature tolerance for Gila, Apache, rainbow, brown (*Salmo trutta*), and brook (*Salvelinus fontinalis*) trout. There is also little or no apparent variation in spawning time known among these populations or natural populations of *O. mykiss* (Behnke 1992; USFWS 2003).

In conclusion, our multilocus genetic analysis indicates that the management strategies used by the Gila and Apache trout recovery programs have been successful in several ways. As outlined in the recovery plan for Gila trout (USFWS 2003), long-term goals for recovery of native trout species included the replication of all known, nonhybridized, indigenous lineages into suitable habitat. Here we show that these replicated lineages of native southwestern trout species do not contain genes of hybrid origin and that current management practices are maintaining these genetically distinct relict lineages.

The context of this work has been set by previous and ongoing efforts to genetically and ecologically characterize other native salmonid populations in the southwestern United States and northern Mexico (Nielsen et al. 1998; Hendrickson et al. 2003; Ruiz-Campos et al. 2003). Further genetic analysis of historical isolation, introgression, and other demographic parameters should be coordinated for the lineages and species in this region so that similar markers and sampling methods are used. In this way, we can better understand the impacts of climate change and habitat loss on populations at the limits of the geographic distribution of *Oncorhynchus* (Nielsen et al. 1998).

Acknowledgments

The authors would like to thank K. Meier, M. McPhee, A. Snyder, G. Rosenberg, P. Spruell, T. Dowling, J. Nielsen, D. Propst, J. Brooks, and members of the Gila Trout and Apache Trout Recovery Teams for significant technical and intellectual contributions to this report. The authors also thank E. Anderson for providing the native OS X version of NewHybrids. D. Propst and two anonymous reviewers greatly improved this manuscript with their editorial suggestions and technical expertise. Support for this work came from the USDA Forest Service (Agreement No. 00-CS-11031600-028), the New Mexico Department of Game and Fish, and the Arizona Game and Fish Department. JPW would also like to thank R. Toonen, R. Grosberg, and J. Wares for additional support in the writing of this paper.

References

Anderson, E.C., and Thompson, E.A. 2002. A model-based method for identifying species hybrids using multilocus genetic data. Genetics, **160**: 1217–1229.

Ardren, W.R., Borer, S., Thrower, F., Joyce, J.E., and Kapuscinski, A.R. 1999. Inheritance of 12 microsatellite loci in *Oncorhyncus mykiss*. J. Hered. **90**: 529–536.

Bagley, M.J., and Gall, G.A.E. 1998. Mitochondrial and nuclear DNA sequence variability among populations of rainbow trout (*Oncorhyncus mykiss*). Mol. Ecol. **7**: 945–961.

Banks, M.A., and Eichert, W. 2000. WHICHRUN (version 3.2): a computer program for population assignment of individuals based on multilocus genotype data. J. Hered. **91**: 87–89.

Behnke, R.J. 1992. Native trout of western North America. Am. Fish. Soc. Monogr. **6**: 1–275.

Belkhir, K., and Dawson, K.J. 2001. A Bayesian approach to the identification of panmictic populations and the assignment of individuals. Genet. Res. **78**: 59–77.

Bowcock, A.M., Ruiz-Linares, A., Tomfohrde, J., Minch, E., Kidd, J.R., and Cavalli-Sforza, L.L. 1994. High resolution of human evolutionary trees with polymorphic microsatellites. Nature (Lond.), **368**: 455–57.

Briskie, J.V., and Mackintosh, M. 2004. Hatching failure increases with severity of population bottlenecks in birds. Proc. Natl. Acad. Sci. U.S.A. **101**: 558–561.

Bulgin, N.L., Gibbs, H.L., Vickery, P., and Baker, A.J. 2003. Ancestral polymorphisms in genetic markers obscure detection of evolutionarily distinct populations in the endangered Florida grasshopper sparrow (*Ammodramus savannarum floridanus*). Mol. Ecol. **12**: 831–844.

Carmichael, G.J., Hanson, J.N., Schmidt, M.E., and Morizot, D.C. 1993. Introgression among Apache, cutthroat, and rainbow trout in Arizona. Trans. Am. Fish. Soc. **122**: 121–130.

Condrey, M.J., and Bentzen, P. 1998. Characterization of coastal cutthroat trout (*Oncorhynchus clarki clarki*) microsatellites, and their conservation in other salmonids. Mol. Ecol. **7**: 787–789.

Cornuet, J., Piry, S., Luikart, G., Estoup, A., and Solignac, M. 1999. New methods employing multilocus genotypes to select or exclude populations as origins of individuals. Genetics, **153**: 1989–2000.

David, R.E. 1976. Taxonomic analysis of Gila and Gila × rainbow trout in southwestern New Mexico. M.S. Thesis, New Mexico State University, Las Cruces, New Mexico.

Dowling, T.E., and Childs, M.R. 1992. Impact of hybridization on a threatened trout of the southwestern United States. Conserv. Biol. **6**: 355–364.

Excoffier, L., Smouse, P.E., and Quattro, J.M. 1992. Analysis of molecular variance inferred from metric distances among DNA haplotypes: application to human mitochondrial DNA restriction data. Genetics, **131**: 479–491.

Ford, M.J., Thornton, P.J., and Park, L.K. 1999. Natural selection promotes divergence of transferrin among salmonid species. Mol. Ecol. **8**: 1055–1061.

Gillespie, J.H. 2001. Is the population size of a species relevant to its evolution? Evolution, **55**: 2161–2169.

Goodman, S.N. 1999. Toward evidence-based medical statistics. 2. The Bayes factor. Ann. Intern. Med. **130**: 1005–1013.

Hendrickson, D.A., Pérez, H.E., Findley, L.T., Forbes, W., Tomelleri, J.R., Mayden, R.L., Nielsen, J.L., Jensen, B., Campos, G.R., Romero, A.V., Van Der Heiden, A., Camarena, F., and Garcia De León, F.J. 2003. Mexican native trouts: a review of their history and current systematic and conservation status. Rev. Fish Biol. Fish. **12**: 273–316.

Hudson, R.R., and Turelli, M. 2003. Stochasticity overrules the "three-times rule": genetic drift, genetic draft, and coalescence times for nuclear loci versus mitochondrial DNA. Evolution, **57**: 182–190.

Jackson, T.R., Ferguson, M.M., Danzmann, R.G., Fishback, A.G., Ihssen, P.E., O'Connell, M., and Crease, T.J. 1998. Identification of two QTL influencing upper temperature tolerance in three rainbow trout (*Oncorhynchus mykiss*) half-sib families. Heredity, **80**: 143–151.

Kashi, Y., King, D., and Soller, M. 1997. Simple sequence repeats as a source of quantitative genetic variation. Trends Genet. **13**: 74–78.

Leary, R.F., and Allendorf, F.W. 1999. Genetic issues in the conservation and restoration of the endangered gila trout: update. Division of Biological Sciences, University of Montana, Missoula.

Lee, R.M., and Rinne, J.N. 1980. Critical thermal maxima of five trout species in the southwestern United States. Trans. Am. Fish. Soc. **109**: 632–635.

Manel, S., Berthier, P., and Luikart, G. 2002. Detecting wildlife poaching: identifying the origin of individuals with Bayesian assignment tests and multilocus genotypes. Conserv. Biol. **16**: 650–659.

Moritz, C. 1994. Defining evolutionary significant units for conservation. Trends Ecol. Evol. **9**: 373–375.

Morris, D.B., Richard, K.R., and Wright, J.M. 1996. Microsatellites from rainbow trout (*Oncorhynchus mykiss*) and their use for genetic study of salmonids. Can. J. Fish. Aquat. Sci. **53**: 120–126.

Nei, M. 1987. Molecular evolutionary genetics. Columbia University Press, Columbia, NY.

Neigel, J.E. 2002. Is F_{st} obsolete? Conserv. Gen. **3**: 167–173.

Nelson, J.S., Crossman, E.J., Espinosa-Pérez, H., Findley, L.T., Gilbert, C.R., Lea, R.N., and Williams, J.D. 2004. Common and scientific names of fishes from the United States, Canada, and Mexico. 6th ed. American Fisheries Society, Bethesda, Md.

Nielsen, J.L. 1997. Molecular genetics and evolutionary status of the trout of the Sierra Madre. *Edited by* R.E. Gresswell, P. Dwyer, and H.R. Hamre. Montana State University Press, Bozeman. pp. 103–109.

Nielsen, J.L., Gan, C., and Thomas, W.K. 1994. Differences in genetic diversity for mitochondrial DNA between hatchery and wild populations of *Oncorhynchus*. Can. J. Fish. Aquat. Sci. **51**: 290–297.

Nielsen, J.L., Fountain, M.C., Favela, J.C., Cobble, K., and Jensen, B.L. 1998. *Oncorhynchus* at the southern extent of their range: a study of mtDNA control-region sequence with special reference to an undescribed subspecies of *O. mykiss* from Mexico. Environ. Biol. Fishes, **51**: 7–23.

O'Connell, M., Danzmann, R.G., Cornuet, J., Wright, J.M., and Ferguson, M.M. 1997. Differentiation of rainbow trout (*Oncorhynchus mykiss*) populations in Lake Ontario and the evaluation of the stepwise mutation and infinite allele mutation models using microsatellite variability. Can. J. Fish. Aquat. Sci. **54**: 1391–1399.

O'Reilly, P.T., Hamilton, L.C., McConnell, S.K., and Wright, J.M. 1996. Rapid analysis of genetic variation in Atlantic salmon (*Salmo salar*) by PCR multiplexing of dinucleotide and tetranucleotide microsatellites. Can. J. Fish. Aquat. Sci. **53**: 2292–2298.

Olsen, J.B., Bentzen, P., and Seeb, J.E. 1998. Characterization of eight microsatellite loci derived from pink salmon. Mol. Ecol. **7**: 1087–1089.

Propst, D.L., Stefferud, J.A., and Turner, P.R. 1992. Conservation and status of Gila trout, *Oncorhynchus gilae*. Southwest. Nat. **37**: 117–125.

Riddle, B.R., Propst, D.L., and Yates, T.L. 1998. Mitochondrial DNA variation in Gila trout, *Oncorhynchus gilae*: implications for management of an endangered species. Copeia, 1998: 31–39.

Ruiz-Campos, G., Camarena-Rosales, F., Varela-Romero, A., Sáncez-González, S., and De La Rosa-Vélez, J. 2003. Morphometric variation of wild trout populations from northwestern Mexico (Pisces: Salmonidae). Rev. Fish Biol. Fish. **13**: 91–110.

Ryder, O.A. 1986. Species conservation and systematics: the dilemma of subspecies. Trends Ecol. Evol. **1**: 9–10.

Sakamoto, T., Danzmann, R.G., Okamoto, N., Ferguson, M.M., and Ihssen, P.E. 1999. Linkage analysis of quantitative trait loci associated with spawning time in rainbow trout (*Oncorhynchus mykiss*). Aquaculture, **173**: 33–43.

Sakamoto, T., Danzmann, R.G., Gharbi, K., Howard, P., Ozaki, A., Khoo, S.K., Woram, R.A., Okamoto, N., Ferguson, M.M., Holm, L., Guyomard, R., and Hoyheim, B. 2000. A microsatellite linkage map of rainbow trout (*Oncorhynchus mykiss*) characterized by large sex-specific differences in recombination rates. Genetics, **155**: 1331–1345.

Schneider, S., Kueffer, J., Roessli, D., and Excoffier, L. 1997. Arlequin Ver. 1.1: a software for population genetic data analysis. Available at http://lgb.unige.ch/arlequin.

Scribner, K.T., Gust, J.R., and Fields, R.L. 1996. Isolation and characterization of novel microsatellite loci: cross-species amplification and population genetic applications. Can. J. Fish. Aquat. Sci. **53**: 685–693.

Stearley, R.F., and Smith, G.R. 1993. Phylogeny of the Pacific trouts and salmons (*Oncorhynchus*) and genera of the Family Salmonidae. Trans. Am. Fish. Soc. **122**: 1–33.

Sunnucks, P., Wilson, A.C.C., Beheregaray, L.B., Zenger, K., French, J., and Taylor, A.C. 2000. SSCP is not so difficult: the application and utility of single-stranded conformational polymorphism in evolutionary biology and molecular ecology. Mol. Ecol. **9**: 1699–1710.

US Fish and Wildlife Service. 2003. Gila trout recovery plan. 3rd revision. US Fish and Wildlife Service, Albuquerque, N.M.

Waples, R.S. 1991. Pacific salmon, *Oncorhynchus* spp., and the definition of species under the ESA. Mar. Fish. Rev. **53**: 11–22.

Zimmer, C. 2003. Rapid evolution can foil even the best-laid plans. Science (Wash., D.C.), **300**: 895.

Deriving condition indices from standard fisheries databases and evaluating their sensitivity to variation in stored energy reserves

C. Tara Marshall, Coby L. Needle, Nathalia A. Yaragina, Adnan M. Ajiad, and Evgeny Gusev

Abstract: To evaluate interstock differences in condition, it would be advantageous to develop stock-level condition indices from standardized databases on weight and length. This study describes a method for estimating stock-level condition when individual-level observations on length and weight are not easily accessible. For each year in a 56-year time series (1946–2001) for Northeast Arctic cod (*Gadus morhua*), pseudo-observations of weight and length were generated by pairing the Norwegian and Russian values for weight-at-age provided annually to the assessment working group with estimates of length-at-age derived from the same databases. A weight–length relationship fit to each year was then used to predict weight-at-length, i.e., girth, for a range of standard lengths (30–120 cm). This index was uncorrelated with both the liver condition index and the abundance of Barents Sea capelin (*Mallotus villosus*), suggesting that at the stock level, the girth of cod is not necessarily indicative of the magnitude of stored energy reserves. Partitioning body size into length-at-age and girth revealed long-term trends in body size. In particular, large/old cod showed substantially higher values of both length-at-age and girth that could be the result of long-term increases in fishing mortality.

Résumé : Afin d'évaluer les différences de condition physique entre les stocks, il serait avantageux de mettre au point des indices de condition à l'échelle des stocks à partir des banques de données standardisées de masses et de longueurs. Notre étude décrit une méthode pour estimer la condition à l'échelle des stocks dans les cas où aucune observation sur la longueur et la masse à l'échelle individuelle n'est facilement disponible. Nous avons généré des pseudo-observations de masses et de longueurs de *Gadus morhua* pour chacune des années d'une série chronologique de 56 années (1946–2001) en associant deux à deux des données norvégiennes et russes de masses en fonction de l'âge à des estimations des longueurs en fonction de l'âge tirées des mêmes banques de données. Une relation masse–longueur ajustée à chaque année a ensuite servi à prédire la masse en fonction de la longueur, c.-à-d., le tour du corps, pour une gamme de longueurs standard (30–120 cm). Cet indice ne montre pas de corrélation, ni avec l'indice de condition hépatique, ni avec l'abondance de capelans (*Mallotus villosus*) de la mer de Barents, ce qui laisse croire qu'à l'échelle du stock, la circonférence du corps n'est pas nécessairement un bon indicateur de l'importance des réserves énergétiques emmagasinées. La division de la taille du corps en longueur en fonction de l'âge et en circonférence montre les tendances à long terme de la taille du corps. En particulier, les morues grandes/âgées ont des valeurs considérablement plus élevées à la fois de longueur en fonction de l'âge et de circonférence qui peuvent être le résultat de l'accroissement à long terme de la mortalité due à la pêche.

[Traduit par la Rédaction]

Introduction

In fisheries science, condition factors are often used to represent the amount of energy stored within individual fish. However, it is also relevant to estimate condition at the stock level because some fish stocks appear to be especially prone to poor condition (e.g., Dutil and Lambert 2000; Chouinard and Swain 2002). For example, cod stocks in less productive ecosystems have low and highly variable condition values, whereas cod stocks inhabiting more productive (and usually warmer) ecosystems have high and relatively stable condition values (Dutil et al. 1999). Within stocks, spatial gradients in condition result from variability in habitat quality (Lloret and Rätz 2000; Chouinard and Swain 2002), and

Received 6 August 2003. Accepted 2 June 2004. Published on the NRC Research Press Web site at http://cjfas.nrc.ca on 16 December 2004.
J17691

C.T. Marshall[1,2] and A.M. Ajiad. Institute of Marine Research, P.O. Box 1870, N-5817 Bergen, Norway.
C.L. Needle. FRS Marine Laboratory, P.O. Box 101, 375 Victoria Road, Aberdeen, AB11 9DB, Scotland.
N.A. Yaragina and E. Gusev. Polar Research Institute of Marine Fisheries and Oceanography, 6 Knipovich Street, Murmansk, 1837763, Russia.

[1] Corresponding author (e-mail: c.t.marshall@abdn.ac.uk).

[2] Present address: University of Aberdeen, Department of Zoology, Tillydrone Avenue, Aberdeen, AB24 2TZ, Scotland, UK.

Can. J. Fish. Aquat. Sci. **61**: 1900–1917 (2004) doi: 10.1139/F04-128

temporal variation results from fluctuations in prey abundance (Yaragina and Marshall 2000), seasonality in feeding patterns (Schwalme and Chouinard 1999), migration (Comeau et al. 2002), and gonadal maturation (Eliassen and Vahl 1982).

The implications of spatial and temporal variation in condition for population dynamics are manifold. Interannual variation in condition contributes directly to variability in stock biomass and yield. Poor condition can result in increased natural mortality (Dutil and Lambert (2000) and references therein). Fishing mortality could potentially be impacted if fish with lower condition have a lower probability of escapement because of a reduced swimming ability (Martínez et al. 2002, 2003). Condition influences the reproductive potential of a stock via its effects on maturation (Henderson and Morgan 2002), fecundity (Hislop et al. 1978; Kjesbu et al. 1998; Lambert and Dutil 2000), atresia (Ma et al. 1998; Óskarsson et al. 2002; Kurita et al. 2003), egg size (Kjesbu 1989; Chambers and Waiwood 1996; Marteinsdottir and Steinarsson 1998), egg density (Saborido-Rey et al. 2003), yolk volumes (Morimoto 1996), hatching success (Laine and Rajasilta 1999), and larval survival (Marteinsdottir and Steinarsson 1998). Because of the cumulative impact on reproduction, there have been several suggestions that condition can influence recruitment for both pelagic and demersal species (Kawasaki and Omori 1995; Schülein et al. 1995; Marshall and Frank 1999).

The importance of inter- and intra-stock variation in condition for fisheries management has only recently been examined (e.g., Rätz and Lloret 2003; Dutil et al. 2003). Incorporating such information into routine assessment of stock status requires an index of condition that is based on a sufficient number of observations so as to be representative of the stock as a whole. To facilitate cross-stock comparisons, the index should be computed from data that are available for a large number of stocks. In this respect, the weight and length data routinely collected for many stocks are well suited for estimating morphometric condition indices representing the fatness, or girth, of individuals at a given length. The implicit assumption of this approach to estimating condition is that girth reflects the magnitude of stored energy reserves. Commonly used morphometric indices include the following: (*i*) Fulton's condition factor (K), which is calculated as $K = 100(W/L^3)$, where W represents width and L represents length; (*ii*) relative condition factor (Kn), which is calculated as $\mathrm{Kn} = W/\hat{W}$, where W and $\hat{W}$ are, respectively, the observed weight and the weight predicted from an empirical weight–length relationship; and (*iii*) $\hat{W}$ for a standard length ($\hat{W}_l$) (Bolger and Connolly 1989). The first two indices describe the condition of an individual fish relative to either isometric growth (i.e., K) or the body size characteristics of the group (i.e., Kn). The latter index ($\hat{W}_l$) describes the condition of the group of fish for which the weight–length relationship is established. Thus, it is appropriate for comparing among groups (or stocks) but cannot be used for describing individuals within a group.

Condition indices are straightforward to compute when weight and length observations for individual fish are available. However, the computation of condition indices at the stock level can be problematic if individual-level observations on weight and length are not readily accessible. Such a situation typically arises when more than one laboratory or country collects length–weight data for the aggregate stock. Stock weight-at-age (SW_a) is routinely included in assessment reports because it is used to estimate spawning stock biomass (SSB). In some cases, these estimates of SW_a are obtained by averaging weight-at-age (W_a) values provided by more than one country and (or) laboratory. The individual W_a time series used to estimate SW_a may or may not be reported in the assessment. Because the original data used to estimate the W_a values are archived in different locations and (or) formats, it can be difficult to access and collate the original observations for individual fish. Corresponding values of stock length-at-age (SL_a) are not usually included in assessment reports because that information is not used directly in age-based assessments. The net result is that although considerable amounts of weight and length data exist, difficulties in accessing these data, either electronically or via the assessment reports, can impede the estimation of a condition index at the stock level and hinder research into the causes and consequences of variation in condition.

This study illustrates how a condition index for Northeast Arctic cod (*Gadus morhua*) stock can be derived using the W_a time series provided annually to the International Council for the Exploration of the Sea (ICES) Arctic Fisheries Working Group (AFWG) by Norway and Russia. Briefly, the same primary databases that generated these W_a time series were used to develop year-specific age–length keys (ALK) for both countries, and the mean length-at-age (L_a) values were calculated. These L_a values were then paired with the corresponding W_a value to generate a set of pseudo-observations for each year. A fitted weight–length relationship was used to predict stock weight-at-length (SW_l) for each year. Isometric growth was tested by comparing the values of exponent of the year-specific weight–length relationships with 3. To determine whether SW_l accurately reflects the bioenergetic status of the stock, the relationship between the biomass of the preferred prey of Northeast Arctic cod, Barents Sea capelin (*Mallotus villosus*), and SW_l was evaluated against the positive relationship that has been observed between the liver condition index of cod and capelin stock biomass (Yaragina and Marshall 2000). Because estimating SW_l and L_a allowed body size to be partitioned into its two basic constituents (girth and length), the degree of covariance between them was assessed. Several of the factors influencing long-term trends in length and girth were discussed.

Materials and methods

Both Norway and Russia have extensive long-term databases (1946–2001) describing biological characteristics of Northeast Arctic cod. The two countries sample, via commercial fisheries and during research vessel surveys, different subcomponents of the stock with Russian observations representing cod that are younger and possibly slower growing than cod sampled by Norway. Given that differences in body size characteristics between the two countries are known to exist, it was not an aim of this study to test for significant differences. Instead, the intention was to combine the information from both countries in a manner that is as consistent as possible with the procedures used by the

AFWG to estimate SW_a. This has the advantage of making the estimates of SW_i generated in this study directly comparable to SW_a. Although changes to the estimation procedure were possible, and in some respects desirable, they were not implemented because the resulting estimates would not be comparable to SW_a.

Age determinations

Otoliths have been used for age determinations throughout the time period. Similar methodology is used by both countries, and annual exchanges of otoliths have taken place since 1992. To determine whether contemporary ages are in agreement with historical ages, special investigations have recently been undertaken by both countries to re-age otoliths selected at random from Norwegian collection of historical otoliths. Preliminary results for a single year (1967) show that the contemporary ageing by Norwegian readers gave values of mean L_a that were slightly lower (usually less than 3 cm) than values calculated using the historical ages (see fig. 4.2 in ICES ACFM 2003). A more extensive Norwegian investigation re-aged otoliths from a longer time period (1965–1968) and found that the contemporary age agreed with the historical age in 72% of the cases. Russian re-ageing of the Norwegian otoliths from 1967 gave a larger discrepancy in values of mean L_a than Norwegian re-ageing (ICES ACFM 2003). On the basis of these few comparisons, it is premature to draw conclusions regarding likely prevalence and direction of ageing bias. No correction was applied here, particularly as applying a correction would have introduced an unwanted discrepancy between values of L_a estimated here and the values of W_a used by the AFWG to estimate SW_a.

Length-at-age

Norwegian and Russian protocols for measuring length differ slightly in that Norwegian measurements are rounded down (e.g., all fish from 53.1 to 53.9 cm are rounded down to 53 cm), whereas Russian measurements are rounded to the nearest whole centimetre (e.g., all fish from 52.6 to 53.5 cm are rounded to 53 cm). In the most extreme case, a Russian cod of length 52.6 cm and a Norwegian cod of 53.9 cm would have the same length (53 cm) in the database. This systematic difference was not corrected for in the ALK used in this study. However, because the magnitude of the difference is constant, it becomes proportionally smaller with increasing age and length.

Both Norwegian and Russian ALK were constructed using 5-cm length classes. However, there was a 1-cm offset between them such that cod between 50 and 54 cm were grouped in one length class for the Norwegian ALK, whereas cod between 51 and 55 cm were grouped in one length class for the Russian ALK. ALK were constructed for cod ages 3–12. For both Norwegian and Russian ALK, L_a was estimated for each year as

$$(1) \qquad L_a = \sum_l p_{al} z_l$$

where p_{al} is the proportion of the observations in each length class as given in the ALK (a and l index age and length, respectively) and z_l is the midpoint of the length class. Interannual variation in values of L_a was examined relative to the arithmetic average estimated for 1946–2001. The databases used to construct the ALK are described separately for each country in the following sections.

Norwegian ALK

The Norwegian data used to construct the ALK used in this study originated in three different databases with individual-level observations being available for all three. The data for 1946–1972 were obtained from a single flatfile (Åge Fotland, Institute of Marine Research, Bergen, Norway) that was previously used for an analysis of long-term trends in maturation (Jørgensen 1990). The observations originated from sampling of the commercial catch. Data for the 1973–1979 time period were also obtained by sampling the commercial catch but were stored in a slightly different format than that of the earlier time period. Since 1980, data have been stored in a relational database that is continuously updated as new data are collected (Fotland et al. 1997). The observations stored in this database originate from the research-vessel surveys, as well as from sampling of the commercial catch (Jakobsen et al. 1997).

For all three data sources, observations for individual cod were selected so as to exclude Norwegian coastal cod (as identified by otolith type), cod younger than 3 years, and months in the 2nd, 3rd, and 4th quarters. Only observations from the 1st quarter were used because the W_a time series provided by Norway to the AFWG is based on data from this time period. Biologically, this represents the prespawning period. Because the commercial fishery is dominated by mature fish, the number of young fish sampled is low for the first two time periods and there are frequently years having no observations for cod of ages 3 and 4 (Fig. 1*a*). Cod in intermediate age classes (ages 5–10) are the best-represented age classes. The number of observations for the younger age classes increased dramatically for the third time period (1980–2001) because of the addition of survey information (Fig. 1*a*). For this time period, the strong 1975, 1983, and 1989 year classes are evident in the sampling.

Russian ALK

Russia and the former USSR have conducted annual surveys for young cod and haddock in the southern Barents Sea since 1946. In 1957 the geographical coverage of these surveys was expanded to include the Bear Island – Spitsbergen area (Lepesevich and Shevelev 1997). Observations describing the age, length, and weight of individual cod are not presently archived in an electronic form. However, ALK compiled for the 4th quarter in support of the recent reconstruction of historical weights and maturities undertaken by the AFWG (ICES ACFM 2001) were available to this study. To cover the entire length range, the survey data were occasionally supplemented with observations from sampling the commercial catch in the 1st quarter of the next year.

Early years show a high proportion of missing values and there are frequently years having no observations in the Russian ALK for cod age 10 and older (Fig. 1*b*). In contrast to the Norwegian ALK, the youngest age classes (cod ages 3 and 4) are well-represented throughout most of the time period and age 5 is most often the predominant age class. This is consistent with the westward shift in the spatial distribution of the stock with increasing age (Ottersen et al. 1998)

Fig. 1. Contour plots showing the number of observations used to construct the age–length keys for (*a*) Norwegian data and (*b*) Russian data. Open circles indicate years where no observations were recorded.

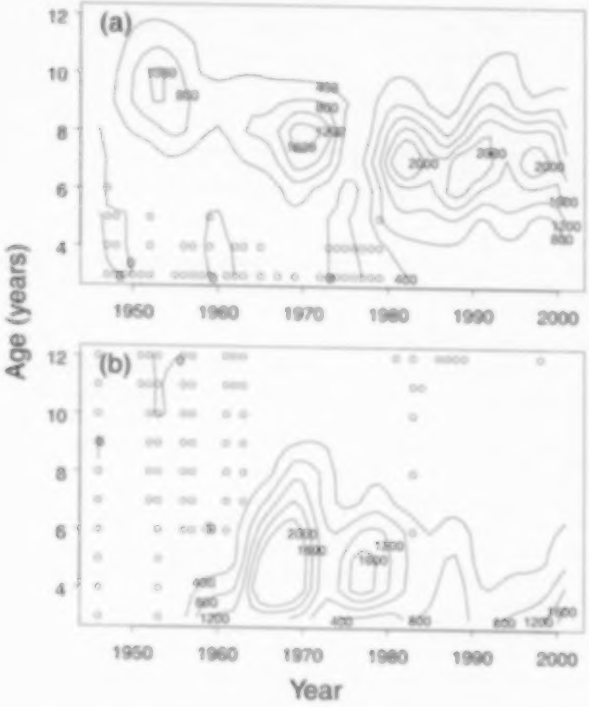

that results in older fish becoming less available to the Russian sampling programs.

Combined ALK

Before they were combined into a single ALK, missing values of p_{al} in both the Norwegian and Russian ALK were interpolated from adjacent years having data to eliminate gaps. Because the Russian ALK apply to the 4th quarter, they were shifted forward by one year and age class to make them consistent with the Norwegian ALK applying to the 1st quarter. The ALK for the two countries were then combined by arithmetically averaging, with equal weight being given to the ALK from both countries. Both the shifting forward of the Russian data and the equal weighting of data for both countries are consistent with how the AFWG combines the W_a estimates from both countries to estimate SW_a (ICES ACFM 2001). The Russian ALK were not adjusted for the growth that would occur between the 4th and 1st quarters because no correction is applied by the AFWG when combining the values of W_a to estimate SW_a. Thus, the arithmetic averaging of the Norwegian and Russian data generates estimates that are composite values for the two quarters (roughly time referenced to 1 January). Values of SL_a were then estimated for each year from the combined ALK using eq. 1. Because the Russian data are shifted forward, only the Norwegian ALK was available for 1946; this precluded estimating SL_a for that year. The long-term trends for the SL_a were summarized using a LOESS smoother with confidence intervals being approximated as twice the standard error of the fitted value.

Weight-at-age

The annual assessment reports contain both Norwegian and Russian estimates of W_a from 1985 onwards only. For this time period, the Norwegian values of W_a are weighted averages of the estimates obtained from the winter survey of the Barents Sea (table A7 in ICES ACFM 2002) and Lofoten survey (table A9 in ICES ACFM 2002). To represent W_a for a given year, these two surveys are averaged with weighting according to the acoustic estimate of abundance-at-age. The Russian values of W_a (table A13 in ICES ACFM 2002) are obtained from the surveys conducted between October and December. The AFWG arithmetically averages the Norwegian and Russian W_a time series to obtain the SW_a time series that is then used to estimate SSB for the stock (ICES ACFM 2001).

Before 2001, constant values of SW_a had been assumed for the period 1946–1984. For the 2001 meeting of the AFWG, both Norway and Russia compiled available historical data to develop year-specific values for W_a for this period, and these were averaged to obtain revised estimates of SW_a (ICES ACFM 2001). The databases and procedures used to estimate W_a for both countries are summarized below.

Norwegian W_a

For the years preceding the survey time period (1946–1984), historical databases from the Lofoten fishery (described above) and the spring fishery around the Finnmark coast were used. Whereas the Lofoten data describe primarily mature individuals undertaking spawning migrations, the Finnmark data include both immature and mature cod. In the case of the Lofoten database, direct weight observations were missing for 1959–1988; however, length and age information were available. The missing W_a values were estimated from the L_a values using the following equation:

$$(2)\qquad \log(W_a) = -5.19 + 3.08\log(L_a)$$

where the regression coefficients were estimated as averages of the year-specific values determined for the years in which both length and weight were available (ICES ACFM 2001). In the case of the Finnmark database, the years 1940–1948 were missing. The missing W_a values were estimated by assuming that the ratio of Lofoten weights to Finnmark weights was constant. To estimate the Norwegian W_a values, the Lofoten and Finnmark databases were combined. The average W_a was calculated by weighting the W_a estimates for the Lofoten and Finnmark areas by the year-specific proportion of mature and immature, respectively. Estimation of these proportions is described in section 10.3.2 of ICES ACFM (2001). Because of missing values for both the Lofoten and Finnmark databases, variation in the Norwegian W_a values for 1940–1948 is derived solely from the Lofoten data, whereas from 1949 to 1984, interannual variation in the Norwegian W_a values was introduced by the Finnmark data only.

Table 1. Summary statistics for observed liver weights measured during the Norwegian winter surveys of the Barents Sea.

Year	No. of observations	Length range	Liver weight range	*a* (SE)	*b* (SE)	PED
1997	1000	9–138	1–2305	–9.37 (0.27)	3.40 (0.063)	0.74
1998	658	24–124	1–1960	–13.70 (0.35)	4.43 (0.084)	0.77
1999	640	14–125	1–2430	–11.21 (0.29)	3.80 (0.070)	0.81
2000	50	40–118	15–1055	–9.34 (1.50)	3.47 (0.35)	0.55
2001	1472	22–131	1–2440	–11.73 (0.22)	3.96 (0.054)	0.73

Note: The ranges in length (cm) and liver weights (g) are given for each year. The *a* and *b* values refer to the coefficients in eq. 6, and the standard error (SE) of each coefficient is in parentheses. The proportion of explained deviance (PED) is given as measure of goodness of fit.

Russian W_a

In the early years of the Russian surveys, there was a tendency to exclude fish longer than 36 cm from the sampling. Thus, it is more likely that mean weights for ages 3–4 are underestimated relative to later data. In 1951, 1955, 1956, 1960, and 1962, there were few observations for fish larger than 36 cm. There were no data for 1952. From 1963, the surveys probably covered the entire length range because of changes in the survey design. Visual inspection of the time series suggested that the weights-at-age for ages 5 and 8 in 1959 were anomalously high. These years also had low numbers of observations (8 and 2 specimens, respectively). Consequently, they were deleted. As a result of missing data and excluded data, the resulting time series had some gaps. These missing observations were replaced by the arithmetic average of adjacent values.

Length–weight regressions

The Norwegian and Russian time series for W_a were paired with the corresponding values of L_a estimated from the Russian and Norwegian ALK (eq. 1) to create a set of pseudo-observations for weight and length. Because of missing values for either W_a or L_a, or both, the number of observations varied considerably across years. Visual examination of the bivariate plots of weight and length for each year indicated that there were two outlying values reflecting gross errors in the database. This resulted in the Norwegian observation for age 11 in year 1991 and the Russian observation for age 10 in year 1976 being omitted from further analysis.

Length–weight regressions were then constructed for each year using the pseudo-observations for weight (in grams) and length. A generalized linear model (GLM)

$$(3)\qquad W = \exp(a + b\log(L))$$

(where a and b are the fitted coefficients of the model) was fit to the pseudo-observations for each year using a log-link function and assuming a gamma error distribution. This model can be re-expressed as

$$(4)\qquad W = \exp(a)L^b$$

making it appropriate for testing the null hypothesis that growth is isometric ($b = 3$). Model fit was evaluated using the proportion of explained deviance (PED) estimated as the difference between the null deviance (the deviance associated with a model having no predictors) and residual deviance for the fitted model expressed as a proportion of the null deviance. These fitted models were then used to generate estimates of SW_l for each year for several standard lengths ranging, in 10-cm intervals, from 30 to 120 cm.

Estimation of liver weight

Russia and the former USSR have monitored the liver weights of cod in the Barents Sea on a monthly basis since 1927 (Yaragina and Marshall 2000). The weights were obtained from the Russian fishing fleet operating in the southern Barents Sea region; although for a few years, observations from the Svalbard area were also used. The database is largely independent of the databases used to generate the Russian W_a and L_a values because it is derived primarily from commercial information rather than survey information.

The liver weight data have been archived as monthly estimates of the liver condition index (LCI = liver weight/total body weight × 100) for several length or weight classes. Consequently, it was not possible to compute liver weight directly. However, liver weight (in grams) at a standard length could be derived by multiplying SW_l (from eq. 4) with the Russian LCI value corresponding to that length class. Thus, the liver weight of a 70-cm cod (LW_{70}) in year t was estimated as

$$(5)\qquad LW_{70} = LCI_{61\text{–}70} \cdot SW_{70}$$

where $LCI_{61\text{–}70}$ is the annual average LCI for the 61- to 70-cm length class in year $t - 1$. Because $LCI_{61\text{–}70}$ is an annual average for the preceding year and SW_{70} averages 4th quarter data from year $t - 1$ and 1st quarter data from year t, the resulting liver weights will not apply to an exact point in the seasonal cycle but instead integrate information obtained across a fairly broad time window. A standard length of 70 cm was chosen partly because the LCI time series was more complete for the 61- to 70-cm length class than for older age classes (see fig. 3 in Yaragina and Marshall 2000). For the 12 years having missing values, $LCI_{61\text{–}70}$ was either assumed to be equal to values observed that year for a corresponding weight class (1946–1953) or interpolated from the adjacent years (1955, 1983, 1985, and 1992).

Since 1997, liver weights of cod have been measured during Norwegian surveys of the Barents Sea and Lofoten regions conducted in February, March, and April. To evaluate the accuracy of the liver weights derived using eq. 5, liver weight data from the Norwegian surveys were used to develop year-specific relationships as

$$(6)\qquad \text{Liver weight} = \exp(a + b\log(L))$$

Fig. 2. Time series of mean length-at-age for ages 3–12 estimated from Norwegian (dotted–dashed lines) and Russian (solid lines) age–length keys. The horizontal broken lines indicate the long-term mean values for both time series. The Russian age–length keys for the 4th quarter were shifted forward by one year and one age class.

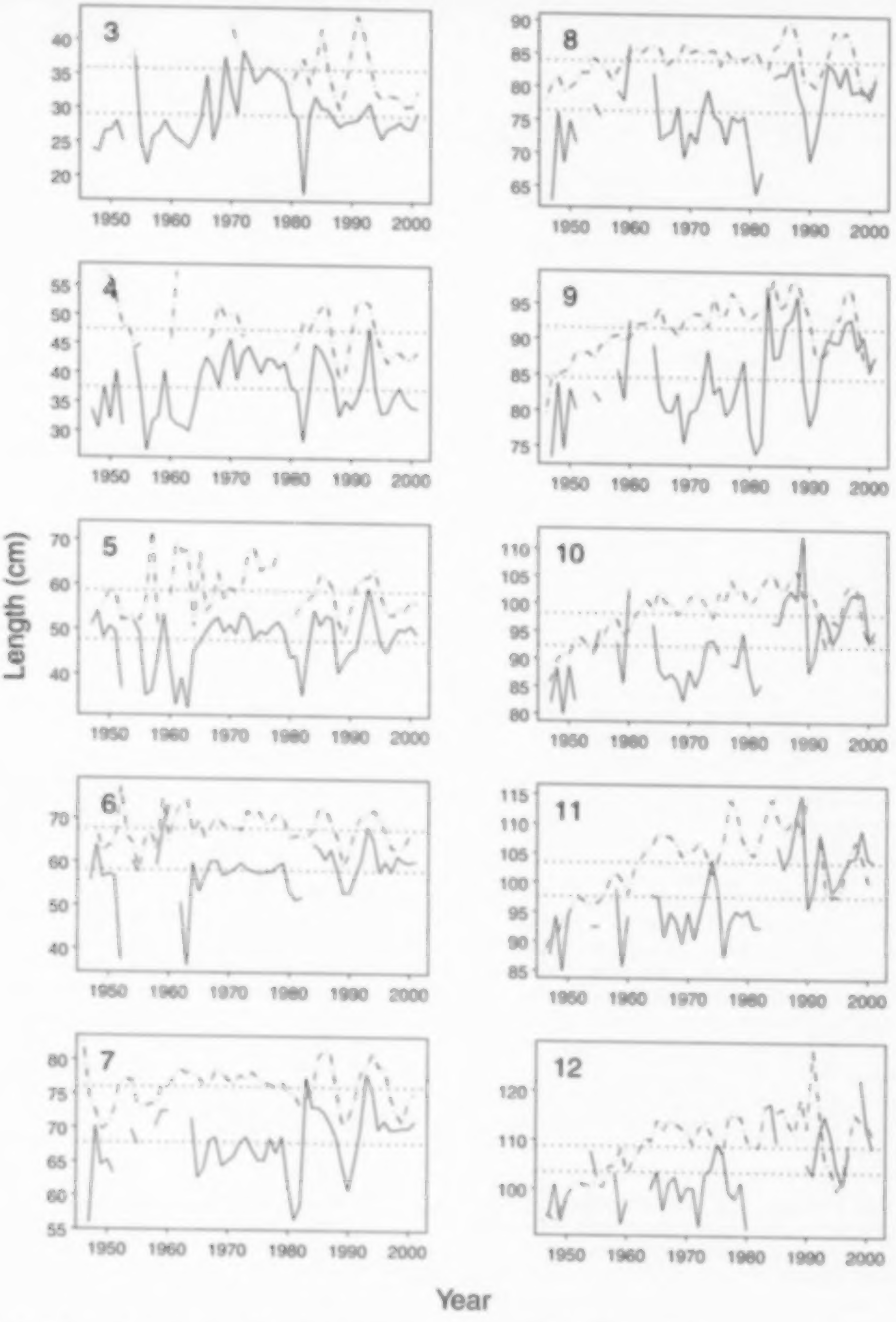

which was fit to data for each year using a log-link function and assuming a gamma error distribution. The resulting models (Table 1) were then used to predict liver weight (in grams) at 70 cm along with the corresponding 95% confidence intervals.

Capelin stock biomass

Acoustic surveys of capelin stock biomass have been conducted annually in the autumn since 1973 (Gjøsæter 1998). For the time period 1973–1996, acoustic estimates of capelin stock abundance in year *t* were significantly ($n = 24$, $p <$

Fig. 3. Time series of mean length-at-age for ages 3–12 estimated for the combined age–length keys (open circles). The LOESS smoothers (solid line) with their approximate 95% confidence intervals (broken lines) are also indicated.

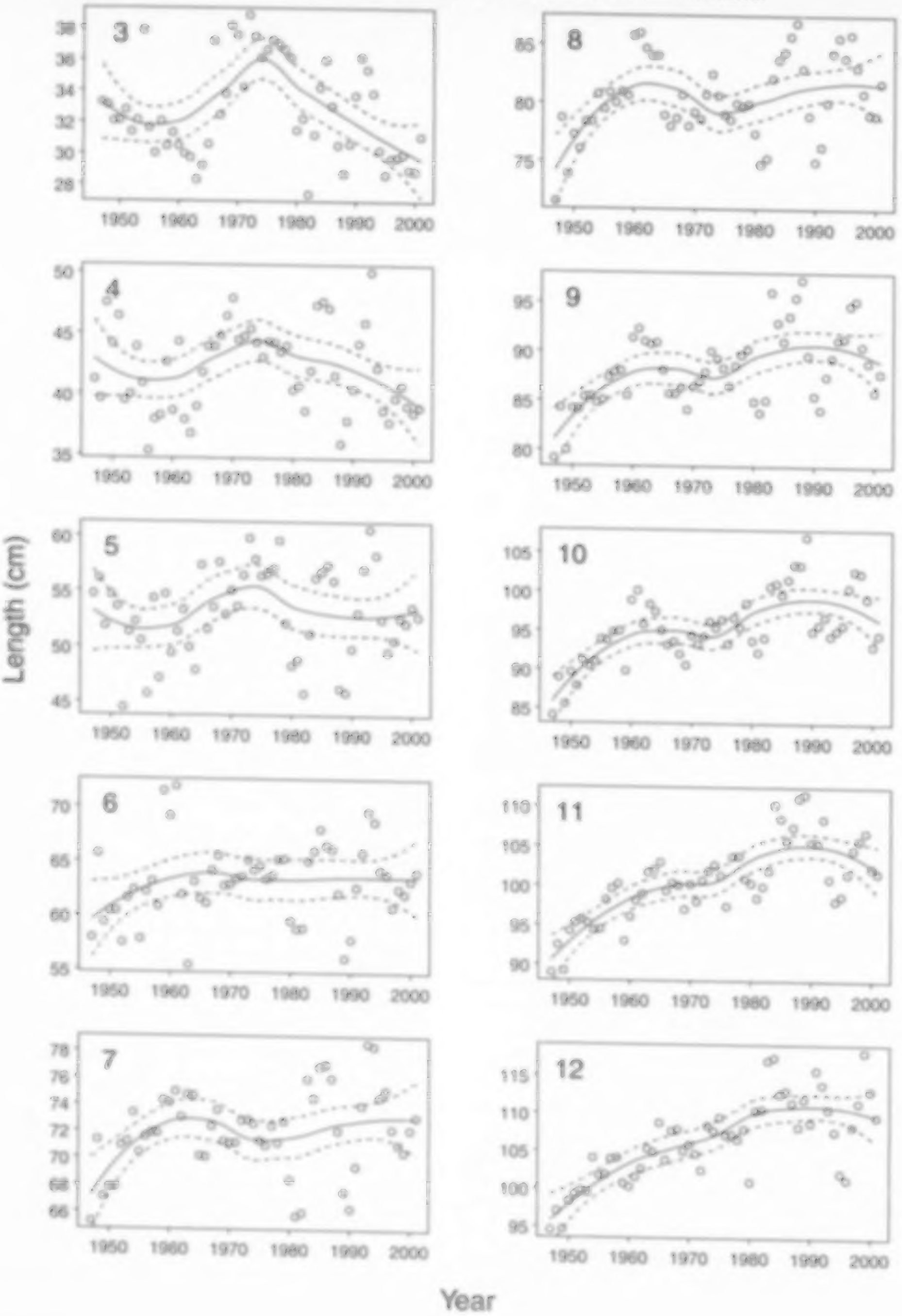

0.001, $r^2 = 0.63$) correlated with the percentage of cod stomachs containing capelin the following year ($P_{\mathrm{cap},t+1}$). To hindcast capelin stock biomass for the preceding time period (1946–1972), it was assumed that the intensity of cod feeding on capelin was linearly related to capelin stock biomass. For the time period 1946–1972, capelin stock biomass in year t (in tonnes (t) × 10^3) was estimated by the following model:

$$(7) \qquad \text{Capelin stock biomass} = 159P_{\mathrm{cap},t+1} - 390$$

Table 2. Minimum, maximum, and mean values of stock length-at-age (in cm), stock weight-at-length (in kg), and stock-weight-at-age (in kg).

Body size metric	Abbreviation	Minimum	Maximum	Mean	CV
Stock length-at-age	SL_3	27.41	38.83	32.72	0.093
	SL_4	35.36	50.04	42.12	0.082
	SL_5	44.46	60.67	53.04	0.074
	SL_6	55.42	71.95	63.12	0.056
	SL_7	65.26	78.58	71.98	0.042
	SL_8	71.59	86.93	80.43	0.042
	SL_9	79.16	97.28	88.27	0.043
	SL_{10}	84.06	107.10	95.45	0.048
	SL_{11}	88.93	111.62	100.65	0.050
	SL_{12}	94.49	118.23	106.37	0.053
Stock weight-at-length	SW_{30}	0.10	0.34	0.22	0.18
	SW_{40}	0.30	0.77	0.53	0.15
	SW_{50}	0.68	1.46	1.04	0.12
	SW_{60}	1.35	2.47	1.81	0.10
	SW_{70}	2.41	3.86	2.88	0.09
	SW_{80}	3.62	5.67	4.32	0.09
	SW_{90}	5.08	7.95	6.18	0.09
	SW_{100}	6.89	10.77	8.51	0.10
	SW_{110}	9.04	14.20	11.37	0.11
	SW_{120}	11.54	19.64	14.81	0.12
Stock weight-at-age	SW_3	0.19	0.52	0.35	0.24
	SW_4	0.40	1.17	0.70	0.26
	SW_5	0.79	1.82	1.26	0.19
	SW_6	1.48	2.82	2.04	0.16
	SW_7	2.14	4.06	3.08	0.15
	SW_8	2.92	5.83	4.40	0.15
	SW_9	3.65	8.93	5.97	0.17
	SW_{10}	4.56	12.15	7.95	0.21
	SW_{11}	5.84	14.29	9.27	0.20
	SW_{12}	7.08	12.09	10.18	0.13

Note: The coefficient of variation (CV) is also given as an index of the variation in the data. Data for 1981–1984 were excluded from the estimation of minimum, maximum, and mean weights-at-length. The data for stock weight-at-age are taken from ICES ACFM (2002).

which is described in further detail elsewhere (Marshall et al. 2000). Because the capelin stock biomass estimates are time-referenced to 1 October each year, they were shifted forward by 1 year before correlating them with the condition indices. Given that the values of SW_l are roughly time-referenced to 1 January, the time lag between the capelin index and SW_l is consistent with the 3- to 4-month time lag that has been observed between the stomach fullness index (i.e., food) and the condition indices (somatic *K* and LCI) for cod in the southern Gulf of St. Lawrence (Comeau et al. 2002).

Results

Trends in L_a and SL_a

As expected, the time series of L_a for both countries show the Norwegian values to be consistently higher than the corresponding Russian values (Fig. 2). The difference between Norway and Russia in long-term mean values of L_a increased from 6.8 cm for age 3 to a maximum of 11.1 cm for age 5. Thereafter, the difference between the long-term means decreased with increasing age to a value of 5.2 cm for age 12. Since the mid-1980s, the difference between Norwegian and Russian values has been relatively small for cod age 9 and older. For cod ages 3–7, there is no strong evidence of a long-term drift towards smaller or larger values of L_a over time for either country. However, for cod age 9 and older, there has been an increase in values of L_a for both countries such that they are currently higher than postwar values. In addition to the long-term trends observed for the older age classes, there was a high degree of short-term variation in both the Norwegian and Russian data. In particular, synchronous reductions in L_a occurred most notably in the late 1980s and early 1990s as a result of the collapse of the Barents Sea capelin stock in 1986 (Yaragina and Marshall 2000).

The long-term trends in SL_a, estimated from the combined ALK, show that for cod ages 3–7, the present values of SL_a are not significantly different from the values at the beginning of the time series (Fig. 3). Since the late 1970s, cod ages 3 and 4 have shown a tendency towards decreasing values of SL_a. That same time period (1970 to present) showed relatively stable values of SL_a for cod ages 5–7 and a tendency for increasing values of SL_a for cod ages 8 to 12 (Fig. 3). This latter trend towards higher SL_a becomes more pronounced with increasing age such that current values of SL_a for cod age 12 are almost 15 cm longer than they were

Fig. 4. A scatterplot matrix showing the relationship between length and weight (all ages combined) for Norwegian (N) and Russian (R) data for the years 1946–2001.

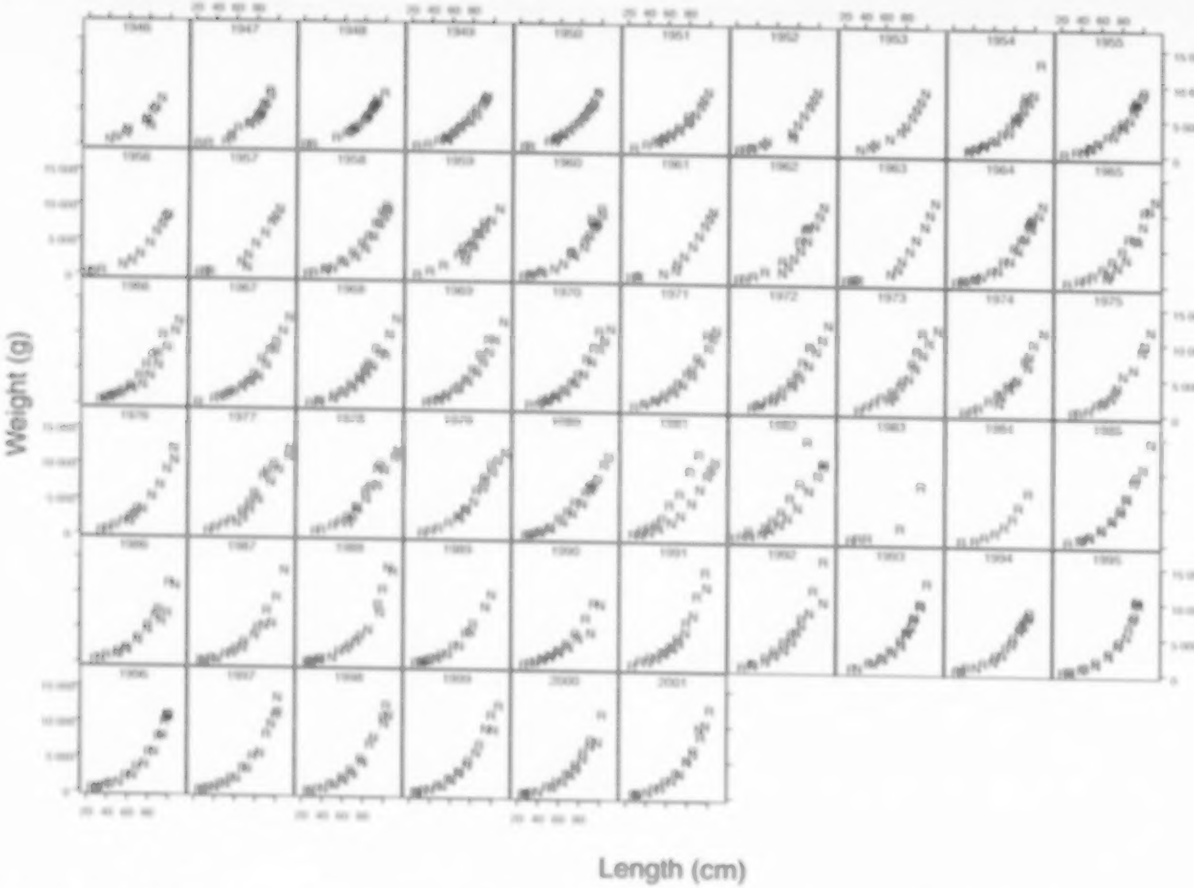

in 1947. The difference in trends over 1970 to 2001 from decreasing (ages 3 and 4) to stable (ages 5–7) to increasing (ages 9–12) suggests that trends in SL_a deviate from the lagged correlations that would be expected if cohort effects were primarily responsible for generating temporal trends in SL_a. When temporal variation is expressed on a relative scale (coefficient of variation), the variation is highest for the youngest age classes (Table 2).

Year-specific weight–length relationships

A scatterplot matrix of the weight–length relationships by year (Fig. 4) shows that the data for the two countries usually spanned a similar length range. There were several years having no overlap between the Norwegian and Russian values of L_a (e.g., 1952, 1956, 1957, 1961, and 1963). For a given length, the Russian weights tend to be slightly higher than the corresponding Norwegian weights with two exceptions (1981 and 1982) when the Russian values were distinctly higher. In combination with differences between Norwegian and Russian L_a values (Fig. 2), this suggests that the cod sampled by Russia are shorter for their age but heavier for their length relative to the cod being sampled by Norway. The model fit is good, with values of PED higher than 0.9 (Table 3) except for 1981 and 1982 when the marked discrepancy between Norwegian and Russian values resulted in low values of PED (less than 0.9; Table 3). The cause of this discrepancy is unknown. The two following years were also problematic in having no Norwegian values and relatively few Russian observations (5 and 8 observations for 1983 and 1984, respectively). Because these 4 years generated condition indices that were anomalous in the full time series, they were omitted from subsequent analyses.

Values of the exponent b from the weight–length relationships (eq. 4) were significantly greater than 3 for 8 years (1948, 1949, 1974–1976, 1985, 1995, and 1998), whereas b values for the years 1951, 1967, and 1971 were significantly less than 3 (Fig. 5). Thus, 11 of the 52 years (21%) had b values that were significantly different from the value of 3 that defines isometric growth. Consequently, Fulton's K cannot be recommended as a measure of stock-level condition for Northeast Arctic cod because the assumption of isometric growth is not valid for a high proportion of years.

Time series of SW_l

Time series of SW_l for standard lengths of 30–120 cm (by 10-cm intervals) reveal differences in the long-term trends exhibited by small cod (<60 cm) compared with large cod

Table 3. Coefficients for the model *W* (in grams) = exp(*a* + *b*log(*L*)) for each year.

Year	*a*	*b*	SE *a*	SE *b*	Residual	Null	df	PED
1946	–4.27	2.85	0.94	0.22	0.29	4.70	8	0.94
1947	–5.87	3.23	0.55	0.13	0.67	15.39	14	0.96
1948	–5.57	3.15	0.19	0.04	0.08	13.92	15	1.00
1949	–5.57	3.17	0.29	0.07	0.19	14.14	17	0.99
1950	–4.63	2.94	0.24	0.06	0.15	14.56	17	0.99
1951	–3.85	2.78	0.35	0.08	0.20	10.98	15	0.98
1952	–5.17	3.06	0.50	0.12	0.51	18.92	11	0.97
1953	–4.44	2.90	0.50	0.12	0.12	7.02	8	0.98
1954	–5.01	3.06	0.28	0.07	0.17	16.27	18	0.99
1955	–4.43	2.92	0.23	0.05	0.14	16.06	17	0.99
1956	–4.59	2.94	0.26	0.06	0.11	16.41	9	0.99
1957	–4.58	2.92	0.66	0.16	0.85	15.13	9	0.94
1958	–4.36	2.91	0.28	0.07	0.23	17.84	17	0.99
1959	–3.85	2.80	0.48	0.11	0.42	9.63	15	0.96
1960	–4.18	2.87	0.33	0.08	0.36	19.46	18	0.98
1961	–4.21	2.84	0.65	0.15	0.81	16.29	10	0.95
1962	–4.38	2.90	0.53	0.12	0.80	16.74	14	0.95
1963	–4.55	2.91	0.49	0.12	0.57	20.22	10	0.97
1964	–4.15	2.86	0.35	0.08	0.41	21.43	18	0.98
1965	–4.35	2.88	0.64	0.15	1.08	16.02	16	0.93
1966	–4.67	2.98	0.45	0.11	0.50	17.67	18	0.97
1967	–4.25	2.87	0.27	0.06	0.18	15.97	17	0.99
1968	–4.66	2.96	0.34	0.08	0.32	17.58	18	0.98
1969	–4.83	3.01	0.33	0.08	0.18	13.95	17	0.99
1970	–5.17	3.09	0.42	0.10	0.41	17.33	18	0.98
1971	–4.07	2.85	0.28	0.07	0.22	16.71	18	0.99
1972	–5.28	3.12	0.44	0.10	0.29	13.65	16	0.98
1973	–5.85	3.25	0.74	0.17	0.72	12.82	15	0.94
1974	–7.02	3.50	0.65	0.15	0.55	14.57	14	0.96
1975	–8.10	3.74	0.40	0.09	0.16	16.27	12	0.99
1976	–7.53	3.62	0.58	0.14	0.35	14.98	12	0.98
1977	–4.88	3.03	0.58	0.13	0.56	13.19	16	0.96
1978	–4.61	2.97	0.50	0.12	0.44	13.02	16	0.97
1979	–4.87	3.02	0.26	0.06	0.10	12.49	15	0.99
1980	–4.72	3.00	0.26	0.06	0.19	20.57	18	0.99
1981	–2.28	2.49	0.78	0.19	1.71	16.15	17	0.89
1982	–1.51	2.30	0.71	0.17	2.08	19.86	17	0.90
1983	–4.66	2.91	1.37	0.35	0.40	9.10	3	0.96
1984	–7.44	3.55	0.77	0.19	0.22	9.67	6	0.98
1985	–5.46	3.18	0.23	0.05	0.09	16.53	15	1.00
1986	–4.63	2.97	0.39	0.09	0.30	15.86	15	0.98
1987	–5.30	3.10	0.38	0.09	0.32	19.43	14	0.98
1988	–4.92	3.04	0.32	0.08	0.32	25.02	15	0.99
1989	–4.49	2.95	0.23	0.06	0.10	17.22	13	0.99
1990	–4.07	2.85	0.36	0.09	0.27	15.20	15	0.98
1991	–4.00	2.89	0.69	0.17	0.77	15.07	15	0.95
1992	–4.49	2.97	0.46	0.11	0.45	16.00	16	0.97
1993	–5.12	3.10	0.35	0.08	0.22	14.45	16	0.99
1994	–4.27	2.88	0.45	0.11	0.47	16.24	16	0.97
1995	–5.30	3.14	0.27	0.07	0.22	21.66	16	0.99
1996	–5.30	3.14	0.29	0.07	0.27	22.98	16	0.99
1997	–5.59	3.22	0.31	0.07	0.24	23.04	15	0.99
1998	–5.40	3.16	0.33	0.08	0.31	22.34	16	0.99
1999	–5.09	3.09	0.24	0.06	0.17	21.76	16	0.99
2000	–5.06	3.07	0.30	0.07	0.25	19.80	16	0.99
2001	–5.13	3.11	0.30	0.07	0.23	19.89	16	0.99

Note: The standard errors (SE) for the model coefficients, the residual and null deviances, residual degrees of freedom (df), and proportion of explained deviance (PED) are indicated. *W*, weight; *L*, length.

Fig. 5. The bivariate relationship between coefficients *a* and *b* for the model $W = \exp(a + b\log(L))$ fit to each year in the time period 1946–2001 excluding 1981–1984. The 95% confidence intervals for the estimates of *a* (horizontal dotted lines) and *b* (vertical solid lines) are indicated. The horizontal solid line indicates $b = 3$, which is assumed for isometric growth.

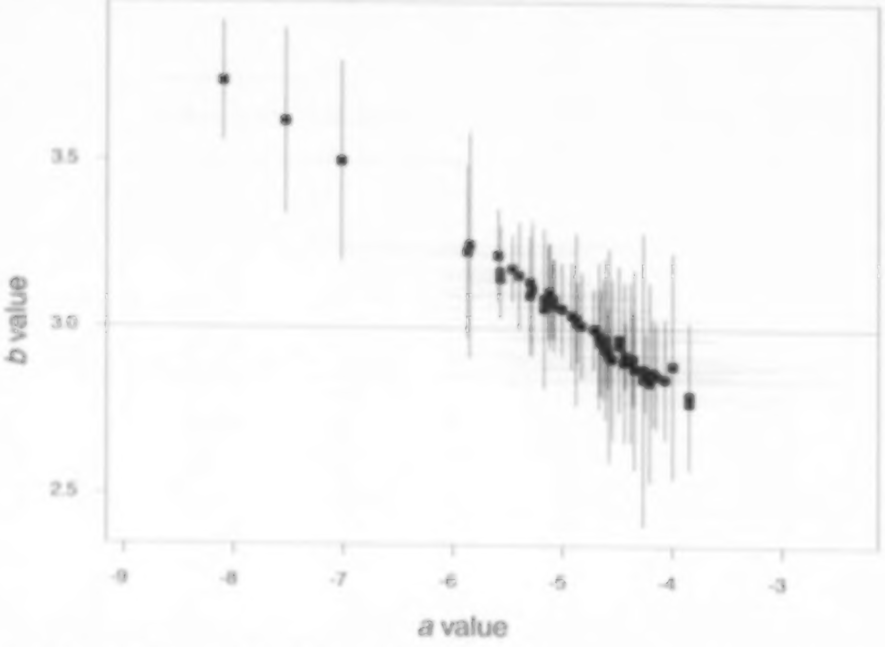

(>70 cm) (Fig. 6). For the smaller length classes (30, 40, and 50 cm), current values of SW_l are not significantly different from the postwar values, suggesting that there has been no long-term change (Fig. 6). However, for cod 70 cm and larger, the current values of SW_l are significantly higher than the postwar values (Fig. 6). The temporal trends differ among these age classes. For example, the SW_l for 80- and 90-cm cod show a near-linear increase over the entire time period, whereas the increase in SW_l of the largest length classes leveled off in the mid- to late 1970s. The magnitude of the increases is substantial. For example, the weight of 120-cm cod in recent years is approximately 2.5 kg higher than it was in the postwar period. Temporal variation expressed on a relative scale (coefficient of variation) in SW_l shows a decrease with increasing length (Table 2).

Comparing trends in SL_a and SW_l

For Northeast Arctic cod, comparisons between age- and length-based body size metrics are facilitated by growth being fairly linear up to approximately age 9. As a simple rule of thumb, the length of a Northeast Arctic cod can be approximated as 10 times their age (Fig. 3). To evaluate whether the long-term trends in the two different body size metrics covary, the LOESS trends in SL_a for ages 3, 5, 7, and 9 (Fig. 3) were contrasted with the LOESS trends in SW_l for lengths of 30, 50, 70, and 90 cm (Fig. 6). To remove scale differences, the LOESS trends were standardized by dividing by the long-term mean of the LOESS values. Cod of lengths 30 cm and 50 cm exhibited an oscillatory pattern in SW_l that was the inverse of the trends in SL_a for ages 3 and 5, respectively (Fig. 7), indicating that cod in this length–age range alternate between a long, lean form and a short, heavy form. Over the entire time period, older, larger cod (age 7, 70 cm, and age 9, 90 cm) exhibit a strong directional trend towards larger values of both SL_a and SW_l (Fig. 7). Thus, large cod have become both longer and heavier over the entire time period.

To evaluate whether the year-specific values of SL_a and SW_l showed significant covariation, the correlations between SL_a (ages 3–9) and SW_l for three of the standard lengths ((10 × age) – 10 cm, (10 × age) cm, and (10 × age) + 10 cm) were examined. None of the correlations between the SL_a and SW_l time series was statistically significant (Table 4), indicating that the long-term trends in length-at-age and girth are essentially decoupled. For the younger/smaller cod, the correlation coefficients are negative, indicating that the SL_a and SW_l time series are negatively related, albeit not significantly (Table 4).

Variation in liver weights

A bivariate plot of the SW_{70} versus capelin stock biomass shows that there is no significant correlation ($n = 50$, $p = 0.66$, $r^2 < 0.01$) between the two variables (Fig. 8*a*). Given that the magnitude of variation in SW_{70} during this time period was substantial (Table 2), the lack of a significant relationship is not due to insufficient contrast in the data. For the same time period, there is a significant, positive correlation between LCI_{61-70} and capelin stock biomass ($n = 54$, $p < 0.001$, $r^2 = 0.44$; Fig. 8*b*). Because of this latter correlation, there is also a significant, positive correlation between LW_{70} and capelin stock biomass ($n = 50$, $p < 0.001$, $r^2 = 0.24$; Fig. 8*c*). Thus, at the stock level, condition indices based on liver weights are more sensitive to variation in prey availability compared with condition indices based solely on total body

Fig. 6. Predicted weight-at-length values for a cod (*Gadus morhua*) of standard lengths ranging (10-cm intervals) from 30 to 120 cm. The LOESS smoothers (solid line) with their approximate 95% confidence intervals (broken lines) are also indicated.

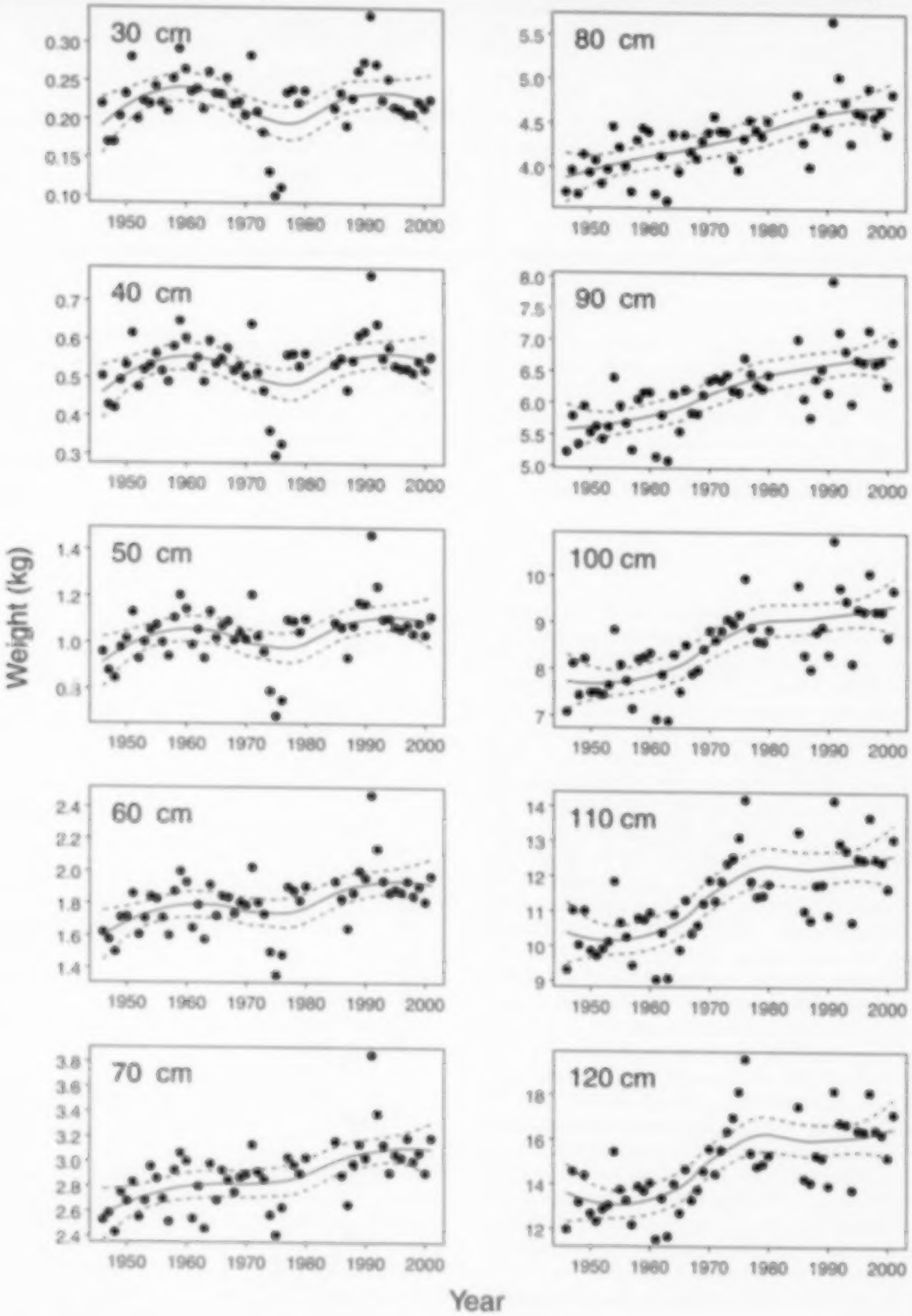

weight. Furthermore, SW_{70} and LCI_{61-70} are uncorrelated (n = 51, $p = 0.095$, $r^2 = 0.06$), indicating that there is no significant relationship between indices representing girth and liver weight of the stock.

When plotted as a time series, the LW_{70} varies by a factor of approximately 2.5 over the entire time period (Fig. 9). There is no evidence of a long-term trend in values; however, there is marked short-term variability in liver weight

Table 4. Correlation coefficients and levels of significance (in parentheses) for correlations between the length-at-age and weight-at-length time series.

	SL_3	SL_4	SL_5	SL_6	SL_7	SL_8	SL_9
SW_{30}	–0.21 (0.13)	–0.03 (0.85)					
SW_{40}	–0.17 (0.23)	0.00 (0.99)	–0.23 (0.11)				
SW_{50}		0.04 (0.79)	–0.19 (0.19)	0.07 (0.65)			
SW_{60}			–0.13 (0.38)	0.09 (0.53)	0.06 (0.69)		
SW_{70}				0.11 (0.42)	0.08 (0.59)	0.04 (0.76)	
SW_{80}					0.09 (0.42)	0.04 (0.75)	0.14 (0.32)
SW_{90}						0.04 (0.78)	0.16 (0.26)

Note: In all cases, the number of observations was 49 as there were no SL_a values for 1946 and the SW_l values for 1980–1983 were excluded.

that seems to have increased in recent years. For example, the LW_{70} varies from a historical low in 1988 (108 g) to a historical high in 1991 (260 g). The Norwegian survey values for 1997–2001 are both higher and lower than the derived liver weights (Fig. 9), which suggests that the derived liver weights are on a similar scale to the values that were measured during surveys conducted in the first quarter.

Discussion

The goals of this study were, firstly, to develop a morphometric condition index for the Northeast Arctic cod stock from stock-level data and, secondly, to evaluate whether this index was an accurate measure of the bioenergetic status of the stock using the liver condition index (Yaragina and Marshall 2000) as a benchmark. The first goal was achieved by generating pseudo-observations of weight and length using the databases underlying the SSB estimates and then calculating a morphometric condition index from these pseudo-observations. Although this approach is undeniably circuitous compared with estimating condition directly from observations made on individual cod, it was necessitated by the practical difficulties in accessing raw data for the entire time period from both Norwegian and Russian sources. Similar difficulties exist for many stocks and particularly those that are sampled by more than one country or institute. Fortunately, ALK were available for both Norway and Russia, enabling a reconstruction of historical trends in L_a for Northeast Arctic cod that could then be matched with the W_a time series used by the AFWG to estimate SW_a. Despite their routine use in the assessment, the accessibility of historical ALK is often as limiting as the accessibility of individual-level observations. The problems encountered in accessing historical fisheries data illustrate the need to evaluate current reporting practices, as well as the archiving of standard fisheries data. One relatively simple change would be to ensure that both L_a and W_a are routinely reported for all of the primary data sources used to estimate SW_a.

The second question that was addressed here was whether the morphometric condition index developed from stock-level data constituted an accurate measure of the energy reserves of the stock. The significant, positive relationship that was observed between the LCI and capelin stock biomass provides strong evidence of the prey effect on the energy reserves of Northeast Arctic cod. However, the lack of sig-

Fig. 7. LOESS curves scaled to the long-term mean LOESS value (1946–2001) for selected ages and lengths: (*a*) stock length-at-age (SL_a) from Fig. 3 for age 3 (solid line), age 5 (dotted line), age 7 (dotted–dashed line), and age 9 (broken line); and (*b*) stock weight-at-length (SW_l) from Fig. 6 for 30 cm (solid line), 50 cm (dotted line), 70 cm (dotted–dashed line), and 90 cm (broken line).

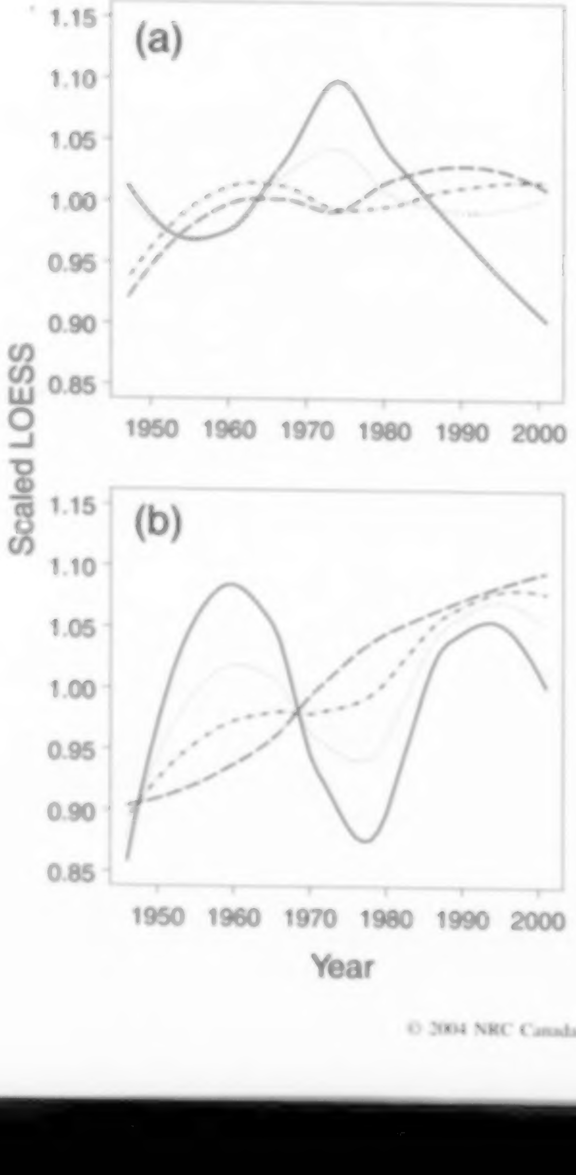

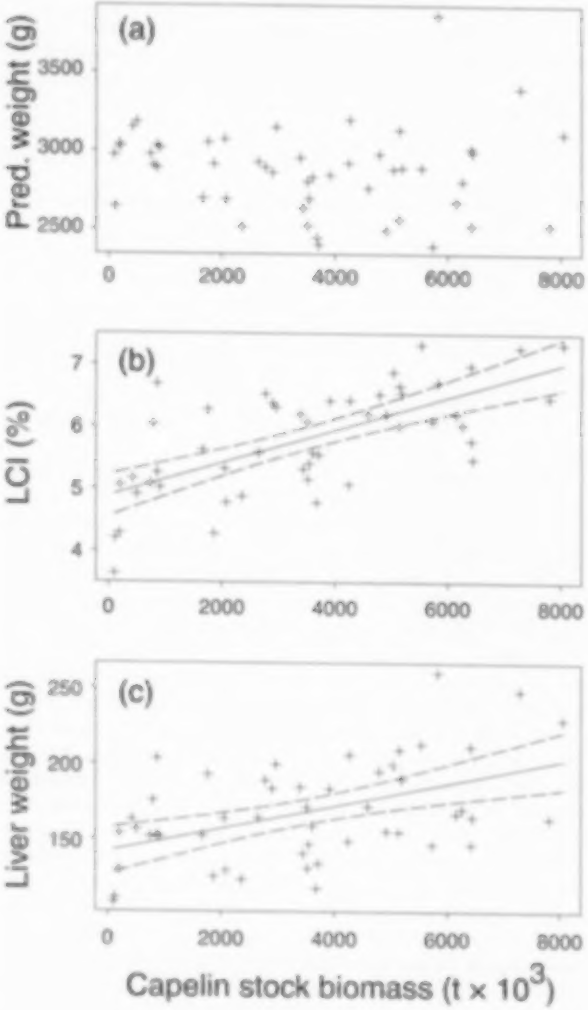

Fig. 8. The bivariate relationships between capelin (*Mallotus villosus*) stock biomass (t × 10^3) and (*a*) predicted (Pred.) weight at 70 cm, (*b*) liver condition index (LCI) of the 61- to 70-cm length class, and (*c*) estimated liver weight at 70 cm. Observations are denoted by year. Solid line indicates the least squares model fit, and broken lines indicate approximate 95% confidence intervals for the estimate. The model fit is not shown in (*a*) because the correlation was not significant.

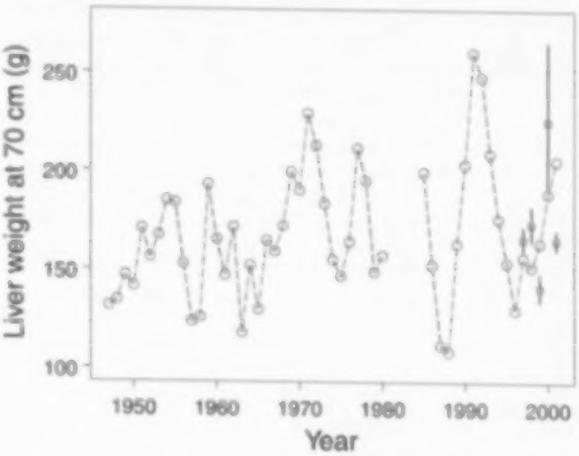

Fig. 9. Time series of estimated liver weight (g) for a 70-cm cod, *Gadus morhua* (broken line, open circles). Values estimated from liver weight observations made during the Norwegian surveys of the Barents Sea and Lofoten regions are indicated by open squares with approximate 95% confidence intervals being represented by the vertical lines.

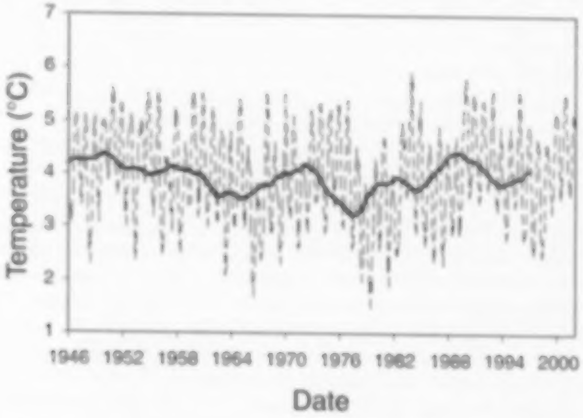

Fig. 10. Monthly temperature values measured at the Kola hydrographic section in the Barents Sea (broken line) and the 5-year running mean temperature for the time series (solid line) representing the long-term trend.

nificant correlations between either SW_l and capelin stock biomass or SW_l and LCI suggests that stock-level condition indices describing girth do not reflect the true magnitude of stored energy reserves. This conclusion is consistent with a study at the individual level, suggesting that total lipid reserves of Arctic char cannot be predicted using a morphometric condition index (Fulton's *K*) alone (Adams et al. 1995). Similarly, weight- and lipid-based condition indices estimated for spawning females differ in their ability to resolve linkages between energy reserves and fecundity. For Icelandic cod, the LCI was more strongly correlated with relative fecundity (potential fecundity / total weight) than Fulton's *K* in each of the 6 study years and, in two of those years, explained more of the variation in relative fecundity than did total length (Marteinsdottir and Begg 2002). For haddock on the eastern Scotian Shelf, the LCI explained a higher proportion of variability in fecundity than did Kn in a model that also included length when data for the 3 years were pooled (Blanchard et al. 2003). Clearly, it is unwise to assume a priori that morphometric condition indices are sensitive indices of condition without independent and preferably bioenergetic evidence supporting this assumption.

Irrespective of whether or not SW_l constitutes a sensitive measure of condition, it can be considered a basic descriptor of fish girth. The lack of temporal correlation between SL_u and SW_l for Northeast Arctic cod suggests that temporal trends in length and girth are decoupled to a greater extent

Fig. 11. Time series (1946–2001) of stock length-at-age (SL_a; solid line) and fishing mortality (F; dotted line) estimated for that age class: (*a*) age 3; (*b*) age 5; (*c*) age 7; and (*d*) age 9.

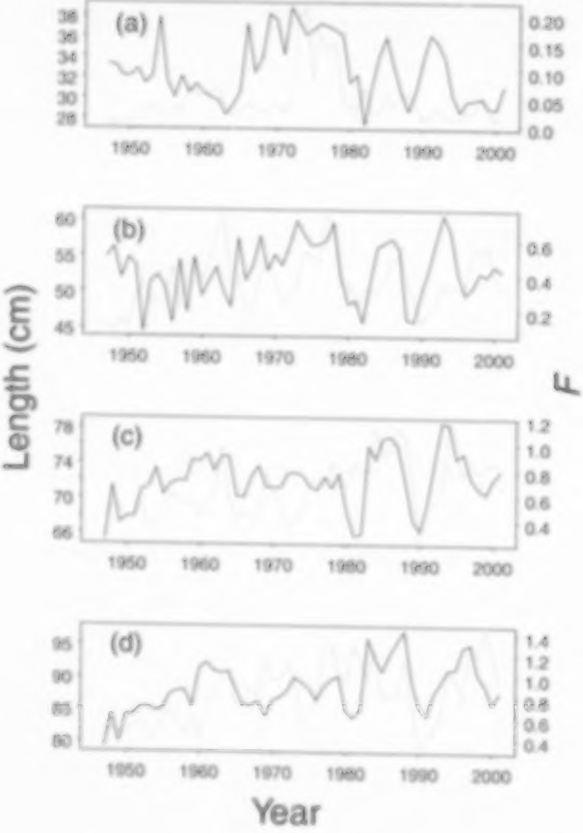

than has been realized. For example, the temporal trends in length and girth described here indicate that young cod alternate between a long, lean form and a short, heavy form. More highly resolved growth models should be developed treating length and girth as separate terms, particularly as the environmental factors affecting length may differ from those affecting girth. For example, variability in condition factor and growth rates for northern cod were explained by food and temperature, respectively (Krohn et al. 1997).

Although the degree to which cod growth is genetically determined is uncertain (Imsland and Jónsdóttir 2002), there have nevertheless been repeated calls for genetic considerations to be included in fisheries management (Heino 1998; Conover and Munch 2002; Kenchington et al. 2003). It has previously been suggested that size- and stage-specific exploitation has resulted in selection for a fast-growing, early-maturing genotype in Northeast Arctic cod (Law and Grey 1989). If true, then a fast-growing genotype should manifest itself at early life history stages. In this context, it was noted that neither the SL_a for cod ages 3 and 4 or SW_l for cod 30 and 40 cm has shown any trend towards either increased or decreased values over the entire 56-year time period. Thus, the observed trends in body size for the youngest/smallest age/size classes are not consistent with the hypothesis that the high levels of fishing mortality experienced by this stock has selected for a fast-growing genotype. In fact, the strongest evidence of a trend towards larger body size was observed for older age classes in which the phenotype had been substantially modified by the cumulative effects of size-selective mortality from fishing.

Table 5. Correlation coefficients and levels of significance for correlations between the length-at-age and fishing mortality (F) for that age class (from ICES ACFM 2002).

Age class	r^2	p
3	0.15	0.0042
4	0.003	0.667
5	0.018	0.32
6	0.0055	0.59
7	0.14	0.0043
8	0.17	0.0017
9	0.17	0.0021
10	0.29	<0.001
11	0.014	0.37
12	0.025	0.24

Note: In all cases, the number of observations was 54 because the SL_a value for 1946 was not available.

The considerable increase in SL_a values that has occurred for the oldest/largest cod is one of the most striking features of the data. This is unlikely to be the result of ageing bias given that the limited data available suggest that discrepancies between contemporary and historical ages result in minor differences in mean length. Furthermore, if historical ages give higher mean lengths than would be calculated for contemporary ages, then correcting the full time series for this possible source of bias would only strengthen the trend towards a long-term increase in SL_a. Temperature in the Barents Sea has not exhibited any directional tendency over the entire time period (Fig. 10), making it unlikely that the long-term increase in SL_a was due to temperature-dependent changes in growth rates of older fish. The long-term trends in SL_a for older age classes occurred at the same time as a substantial long-term increase in fishing mortality (F) estimated for the older age classes (Fig. 11). The older age classes show reasonably simultaneous increases and decreases in both SL_a and F (Figs. 11*c*, 11*d*), with the correlations between the two time series being statistically significant ($p < 0.05$) for cod ages 7–10 (Table 5). Among these four age classes, the degree of correlation increases with increasing age and is strongest for cod age 10. These observations suggest that the temporal trends in F are modifying the size structure of age classes that are fully recruited to the fishery such that larger individuals dominate the age class when F is high. Within an age class, high F could favour the differential survival of large cod that swim faster and have a higher probability of escapement. The cumulative nature of survival probabilities could cause the phenotype to become more prevalent with increasing age, thus explaining why the correlation between SL_a and F increased with increasing age up to age 10 (Table 5). If this interpretation is correct, then the selection gradient being applied to fully recruited age classes by high F (favouring survival of large cod) is opposite to the

Table 6. General recommendations for adapting sampling programs for measuring individual condition, as adapted from Dutil et al. (1995).

Topic	Recommendation
Frequency	Samples should be taken periodically during the year. Monthly samples are required in the spring and the fall to identify the extremes in condition. Given the pronounced seasonal cycle in condition and possible variability in this cycle, one sample taken annually is not sufficient to monitor condition adequately.
Sampling protocol	Samples should contain a minimum of 30 fish. This number should be increased when assessing condition in stocks characterized by a wide range in size, particularly if condition factor and length are correlated. Length-stratified samples would allow for comparisons between size groups and may facilitate comparison of condition between stocks.
Formulation of index	Fulton's condition factor and hepatosomatic index should be calculated using somatic weight, not total weight. Somatic weight provides a more accurate measure of condition and will facilitate both within- and between-stocks comparisons because it is not affected by potential differences in feeding intensity and timing of maturation as will occur when comparing different sites or time periods.
Variables measured	For each fish sampled, the minimum information collected must include total length, total weight, weight of stomach contents, sex, gonad weight, liver weight, and water content of liver and muscle.

selection gradient that is often assumed to apply to partially recruited age classes favouring the survival of smaller, slow-growing cod at high *F* (Kristiansen and Svåsand 1998). The direction of selection gradients is not constant through time (Hanson and Chouinard 1992; Sinclair et al. 2002*a*); therefore, it is possible for the direction of the selection gradient to vary across age/size classes. There could also be a density-dependent basis for the positive correlations between SL_a and *F* given that high *F* reduces the abundance of these age classes, thereby enhancing per capita food availability. The two mechanisms (size-selective mortality favouring the differential survival of large cod and density-dependent growth) are not mutually exclusive. For example, a negative effect of population density on the growth of cod in the southern Gulf of St. Lawrence was detected in addition to the significant effects of size-selective mortality (Sinclair et al. 2002*b*).

The substantial increase in both SL_a and SW_l that has been observed in older/larger age classes in combination with the overall decline in numerical abundance are likely to have had repercussions for the reproductive potential of the Northeast Arctic cod stock. To evaluate the impacts of changes in growth and demography on stock reproductive potential, alternative indices are required given that SSB is likely to be an inaccurate index of total egg production for this stock (Marshall et al. 1998, 2003). Because reproductive traits of Northeast Arctic cod vary according to length rather than age, a length-based approach to quantifying reproductive potential of the stock is warranted. The ALK and year-specific weight–length relationships developed here facilitate this in several important ways. The combined ALK can be used to convert the values of number-at-age given in the annual assessment to number-at-length. These estimates can then be coupled with length-based databases and models, e.g., the year-specific weight–length relationships, the length-based Russian liver condition database (Yaragina and Marshall 2000), or length-based fecundity models (e.g., Kjesbu et al. 1998; Marteinsdottir and Begg 2002), to develop alternative estimates of reproductive potential (e.g., Blanchard et al. 2003). The age-based SSB and the length-based alternative index of reproductive potential would be directly comparable given that the ALK and year-specific weight–length relationships used for estimating the alternative are derived from the same primary databases. A high degree of comparability between SSB and the alternative index is an important attribute when evaluating whether there are substantial differences between them (Marshall et al. 2003).

Although the importance of bioenergetic condition indices for understanding the growth and reproduction of fish is clear (Shulman and Love 1999), relatively few long-term databases exist at the stock level. Adapting existing sampling programs to collect more detailed information on condition has previously been advocated (Dutil et al. 1995). That study provided a series of recommendations for the routine monitoring of condition that are summarized here (Table 6). These recommendations, which were developed in the wake of the collapse of several Canadian cod stocks, have yet to be widely adopted. We concur with their view that the measurement of condition "should be viewed as an original and informative simple-to-measure stock characteristic" that has been largely overlooked. There are signs that sampling programs are being modified so as to collect more detailed measurements. For example, the Norwegian surveys of the Barents Sea began measuring liver weights in 1997, and liver weights of cod in the southern and northern Gulf of St. Lawrence are now monitored regularly through a combination of sentinel and research-vessel surveys (J.-D. Dutil, Institut Maurice-Lamontagne, 850 route de la Mer, Mont-Joli, QC G5H 3Z4, Canada, personal communication). Samples taken annually at a fixed point in time will probably be inadequate given the pronounced seasonal cycle in condition and the possible variability in this seasonal cycle (Dutil et al. 1995, 2003; Yaragina and Marshall 2000). Measurements that are highly resolved in space and time pose a considerable logistical challenge; however, many of the existing high-resolution condition databases were developed in support of or by commercial fisheries. For example, industrial sources of information have been used to derive monthly condition indices for pelagic stocks in the Southern California region (Parrish and Mallicoate 1995) and Benguela system (Schülein et al. 1995).

This study has shown that although it is possible to generate a morphometric index representing the girth of Northeast Arctic cod at the stock level using standardized fisheries databases, the resulting index does not accurately reflect the magnitude of stored energy reserves. It is important to recognize that this conclusion was developed from stock-level data collected over broad spatiotemporal scales and may not necessarily apply to short-term studies conducted at the individual level. Its applicability to other stocks is difficult to gauge given the relatively small number of stocks having long-term data on fish growth (length and girth), lipid reserves, and food availability. The importance of developing time series of condition that accurately track fluctuations in the energy reserves of the stock is increasingly clear given the impact of condition on all major elements of population dynamics, including natural mortality, fishing mortality, growth, and recruitment. For commercially exploited stocks that experience variable environmental conditions, the technical and logistical impediments to monitoring condition should be considered as minor relative to the costs of not monitoring this key variable.

Acknowledgements

Discussions with our colleagues on the ICES Arctic Fisheries Working Group are acknowledged with gratitude. We are grateful to Å. Fotland for his assistance with compiling the Norwegian liver weight data and to J.-D. Dutil for valuable discussions on several aspects of cod growth. Two anonymous referees provided constructive reviews. Funding was provided by the European Community (QL K5-CT1999-01609), the Research Council of Norway (Project No. 130197/130), and the Department of Marine Environment, Institute of Marine Research, Bergen.

References

Adams, C.E., Huntingford, F.A., and Jobling, M. 1995. A non-destructive morphometric technique for estimation of body and mesenteric lipid in Arctic charr: a case study of its application. J. Fish Biol. **47**: 82–90.

Blanchard, J.L., Frank, K.T., and Simon, J.E. 2003. Effects of condition on fecundity and total egg production of eastern Scotian Shelf haddock. Can. J. Fish. Aquat. Sci. **60**: 321–332.

Bolger, T., and Connolly, P.L. 1989. The selection of suitable indices for the measurement and analysis of fish condition. J. Fish Biol. **34**: 171–182.

Chambers, R.C., and Waiwood, K.G. 1996. Maternal and seasonal differences in egg sizes and spawning characteristics of captive Atlantic cod, *Gadus morhua*. Can. J. Fish. Aquat. Sci. **53**: 1986–2003.

Chouinard, G.A., and Swain, D.P. 2002. Depth-dependent variation in condition and length-at-age of Atlantic cod (*Gadus morhua*) in the southern Gulf of St. Lawrence. Can. J. Fish. Aquat. Sci. **59**: 1451–1459.

Comeau, L., Campana, S.E., and Chouinard, G.A. 2002. Timing of Atlantic cod (*Gadus morhua* L.) seasonal migrations in the southern Gulf of St. Lawrence: interannual variability and proximate control. ICES J. Mar. Sci. **59**: 333–351.

Conover, D.O., and Munch, S.B. 2002. Sustaining fisheries yields over evolutionary time scales. Science (Wash., D.C.), **297**: 94–96.

Dutil, J.-D., and Lambert, Y. 2000. Natural mortality from poor condition in Atlantic cod (*Gadus morhua*). Can. J. Fish. Aquat. Sci. **57**: 826–836.

Dutil, J.-D., Lambert, Y., Chouinard, G.A., and Fréchet, A. 1995. Fish condition: what should we measure in cod (*Gadus morhua*)? DFO Atlantic Fisheries Research Document No. 95/11.

Dutil, J.-D., Castonguay, M., Gilbert, D., and Gascon, D. 1999. Growth, condition, and environmental relationships in Atlantic cod (*Gadus morhua*) in the northern Gulf of St. Lawrence and implications for management strategies in the Northwest Atlantic. Can. J. Fish. Aquat. Sci. **56**: 1818–1831.

Dutil, J.-D., Gauthier, Y., Lambert, Y., Fréchet, A., and Chabot, D. 2003. Cod stocks rebuilding and fish bioenergetics: low productivity hypothesis. Canadian Science Advisory Secretariat Res. Doc. No. 2003/060.

Eliassen, J.-E., and Vahl, O. 1982. Seasonal variation in biochemical composition and energy content of liver, gonad and muscle of mature and immature cod, *Gadus morhua* (L.), from Balsfjorden, northern Norway. J. Fish Biol. **20**: 707–716.

Fotland, Å., Borge, A., Gjøsæter, H., and Mjanger, H. 1997. Håndbok for prøvetaking av fisk og krepsdyr. Internal document published by the Department of Marine Resources, Institute of Marine Research, Bergen, Norway. [In Norwegian.]

Gjøsæter, H. 1998. The population biology and exploitation of capelin (*Mallotus villosus*) in the Barents Sea. Sarsia, **83**: 453–513.

Hanson, J.M., and Chouinard, G.A. 1992. Evidence that size-selective mortality affects growth of Atlantic cod (*Gadus morhua* L.) in the southern Gulf of St. Lawrence. J. Fish Biol. **41**: 31–41.

Heino, M. 1998. Management of evolving fish stocks. Can. J. Fish. Aquat. Sci. **55**: 1971–1982.

Henderson, B.A., and Morgan, G.E. 2002. Maturation of walleye by age, size and surplus energy. J. Fish Biol. **61**: 999–1011.

Hislop, J.R.G., Robb, A.P., and Gauld, J.A. 1978. Observations on effects of feeding level on growth and reproduction in haddock, *Melanogrammus aeglefinus* (L.), in captivity. J. Fish Biol. **13**: 85–98.

International Council for the Exploration of the Sea Advisory Council on Fisheries Management (ICES ACFM). 2001. Report of the Arctic Fisheries Working Group. ICES CM 2001/ACFM:19.

ICES ACFM. 2002. Report of the Arctic Fisheries Working Group. ICES CM 2002/ACFM:18.

ICES ACFM. 2003. Report of the Study Group on biological reference points for Northeast Arctic cod. ICES CM 2003/ACFM:11.

Imsland, A.K., and Jónsdóttir, O.D.B. 2002. Is there a genetic basis to growth in Atlantic cod? Fish Fish. **3**: 36–52.

Jakobsen, T., Korsbrekke, K., and Mehl, S., and Nakken, O. 1997. Norwegian combined acoustic and bottom trawl surveys for demersal fish in the Barents Sea during winter. ICES CM 1997/Y:17.

Jorgensen, T. 1990. Long-term changes in age at sexual maturity of Northeast Arctic cod (*Gadus morhua* L.). J. Cons. Int. Explor. Mer. **46**: 235–248

Kawasaki, T., and Omori, M. 1995. Possible mechanisms underlying fluctuations in the Far Eastern sardine population inferred from time series of two biological traits. Fish. Oceanogr. **4**: 238–242.

Kenchington, E., Heino, M., and Nielsen, E.E. 2003. Managing marine genetic diversity: time for action? ICES J. Mar. Sci. **60**: 1172–1176.

Kjesbu, O.S. 1989. The spawning activity of cod, *Gadus morhua* L. J. Fish Biol. **34**: 195–206.

Kjesbu, O.S., Witthames, P.R., Solemdal, P., and Greer Walker, M. 1998. Temporal variations in the fecundity of Arcto-Norwegian cod (*Gadus morhua*) in response to natural changes in food and temperature. J. Sea Res. **40**: 303–321.

Kristiansen, T.S., and Svåsand, T. 1998. Effect of size-selective mortality on growth of coastal cod illustrated by tagging data and an individual-based growth and mortality model. J. Fish Biol. **52**: 688–705.

Krohn, M., Reidy, S., and Kerr, S. 1997. Bioenergetic analysis of the effects of temperature and prey availability on growth and condition of northern cod (*Gadus morhua*). Can. J. Fish. Aquat. Sci. **54**(Suppl. 1): 113–121.

Kurita, Y., Meier, S., and Kjesbu, O.S. 2003. Oocyte growth and fecundity regulation by atresia of Atlantic herring (*Clupea harengus*) in relation to body condition throughout the maturation cycle. J. Sea Res. **323**: 1–17.

Laine, P., and Rajasilta, M. 1999. The hatching success of Baltic herring eggs and its relation to female condition. J. Exp. Mar. Biol. Ecol. **237**: 61–73.

Lambert, Y., and Dutil, J.-D. 2000. Energetic consequences of reproduction in Atlantic cod (*Gadus morhua*) in relation to spawning level of somatic energy reserves. Can. J. Fish. Aquat. Sci. **57**: 815–825.

Law, R., and Grey, D.R. 1989. Evolution of yields from populations with age-specific cropping. Evol. Ecol. **3**: 343–359.

Lepesevich, Yu.M., and Shevelev, M. 1997. Evolution of the Russian survey for demersal fish: from ideal to reality. ICES CM 1997/Y:09.

Lloret, J., and Rätz, H.-J. 2000. Condition of cod (*Gadus morhua*) off Greenland during 1982–1998. Fish. Res. **48**: 79–86.

Ma, Y., Kjesbu, O.S., and Jørgensen, T. 1998. Effects of ration on the maturation and fecundity in captive Atlantic herring (*Clupea harengus*). Can. J. Fish. Aquat. Sci. **55**: 900–908.

Marshall, C.T., and Frank, K.T. 1999. The effect of interannual variation in growth and condition on haddock recruitment. Can. J. Fish. Aquat. Sci. **56**: 347–355.

Marshall, C.T., Kjesbu, O.S., Yaragina, N.A., Solemdal, P., and Ulltang, Ø. 1998. Is spawner biomass a sensitive measure of the reproductive and recruitment potential of Northeast Arctic cod? Can. J. Fish. Aquat. Sci. **55**: 1766–1783.

Marshall, C.T., Yaragina, N.A., Ådlandsvik, B., and Dolgov, A.V. 2000. Reconstructing the stock–recruit relationship for Northeast Arctic cod using a bioenergetic index of reproductive potential. Can. J. Fish. Aquat. Sci. **57**: 2433–2442.

Marshall, C.T., O'Brien, L., Tomkiewicz, J., Marteinsdóttir, G., Morgan, M.J., Saborido-Rey, F., Köster, F.W., Blanchard, J.L., Secor, D.H., Kraus, F., Wright, P., Mukhina, N.V., and Björnsson, H. 2003. Developing alternative indices of reproductive potential for use in fisheries management: case studies for stocks spanning an information gradient. J. Northwest Atl. Fish. Sci. **33**: 161–190.

Marteinsdottir, G., and Begg, G.A. 2002. Essential relationships incorporating the influence of age, size and condition on variables required for estimation of reproductive potential in Atlantic cod, *Gadus morhua*. Mar. Ecol. Prog. Ser. **235**: 235–256.

Marteinsdottir, G., and Steinarsson, A. 1998. Maternal influence on the size and viability of Iceland cod (*Gadus morhua* L.) eggs and larvae. J. Fish Biol. **52**: 1241–1258.

Martínez, M., Gunderley, H., Nelson, J.A., Webber, D., and Dutil, J.-D. 2002. Once a fast cod, always a fast cod: maintenance of performance hierarchies despite changing food availability in cod (*Gadus morhua*). Physiol. Biochem. Zool. **75**: 90–100.

Martínez, M., Guderley, H., Dutil, J.-D., Winger, P.D., He, P., and Walsh, S.J. 2003. Condition, prolonged swimming performance and muscle metabolic capacities of cod (*Gadus morhua*). J. Exp. Biol. **206**: 503–511.

Morimoto, H. 1996. Effects of maternal nutritional conditions on number, size and lipid content of hydrated eggs in the Japanese sardine from Tosa Bay, southwestern Japan. *In* Survival strategies in early life stages of marine resources. *Edited by* Y. Watanabe, Y. Yamashita, and Y. Oozeki. A.A. Balkema, Rotterdam. pp. 3–12.

Óskarsson, G.J., Kjesbu, O.S., and Slotte, A. 2002. Predictions of realized fecundity and spawning time in Norwegian spring-spawning herring (*Clupea harengus*). J. Sea Res. **48**: 59–79.

Ottersen, G., Michalsen, K., and Nakken, O. 1998. Ambient temperature and distribution of north-east Arctic cod. ICES J. Mar. Sci. **55**: 67–85.

Parrish, R.H., and Mallicoate, D.L. 1995. Variation in the condition factors of California pelagic fishes and associated environmental factors. Fish. Oceanogr. **4**: 171–190.

Rätz, H.-J., and Lloret, J. 2003. Variation in fish condition between Atlantic cod (*Gadus morhua*) stocks, the effect on their productivity and management implications. Fish. Res. **60**: 369–380.

Sabarido-Rey, F., Kjesbu, O.S., and Thorsen, A. 2003. Buoyancy of Atlantic cod larvae in relation to developmental stage and maternal influences. J. Plankton Res. **25**: 291–307.

Schülein, F.H., Boyd, A.J., and Underhill, L.G. 1995. Oil-to-meal ratios of pelagic fish taken from the Northern and the Southern Benguela systems: seasonal patterns and temporal trends, 1951–1993. S. Afr. J. Mar. Sci. **15**: 61–82.

Schwalme, K., and Chouinard, G.A. 1999. Seasonal dynamics in feeding, organ weights, and reproductive maturation of Atlantic cod (*Gadus morhua*) in the southern Gulf of St. Lawrence. ICES J. Mar. Sci. **56**: 303–319.

Shulman, G.E., and Love, R.M. 1999. Biochemical ecology of marine fishes. Adv. Mar. Biol. **36**.

Sinclair, A.F., Swain, D.P., and Hanson, J.M. 2002*a*. Measuring changes in the direction and magnitude of size-selective mortality in a commercial fish population. Can. J. Fish. Aquat. Sci. **59**: 361–371.

Sinclair, A.F., Swain, D.P., and Hanson, J.M. 2002*b*. Disentangling the effects of size-selective mortality, density, and temperature on length-at-age. Can. J. Fish. Aquat. Sci. **59**: 372–382.

Yaragina, N.A., and Marshall, C.T. 2000. Trophic influences on interannual and seasonal variation in the liver condition index of Northeast Arctic cod. ICES J. Mar. Sci. **57**: 42–55.

Optimum sampling levels in discard sampling programs

Lisa Borges, Alain F. Zuur, Emer Rogan, and Rick Officer

Abstract: This paper presents optimum sampling levels in discard sampling programs considering cost and precision objectives simultaneously and explores their dependence on both variables. The analysis is based on the Irish discard program: an onboard-observer voluntary sampling scheme aimed at estimating discard rates in trawl fisheries. Multistage analysis was performed to establish the precision levels achieved in the past, and a cost function was determined to estimate the financial cost of the program. Gear, fishing ground, targeted species, and International Council for the Exploration of the Sea (ICES) divisions were the main factors affecting discarding, together with random effects of the three nested groups considered: haul, trip, and vessel. Reductions in the present budget will imply only marginal decreases in precision, although changes in cost variables can have an impact on sampling levels. On the other hand, increasing the target precision by one-half will imply a considerable increase in sampling and associated cost, which will be difficult if not impossible to achieve. Finally, the analysis by fleet components suggests a marked increase in sampling levels, which emphasizes the importance of clearly stated discard sampling objectives.

Résumé : Notre étude détermine les intensités optimales d'échantillonnage dans les programmes d'échantillonnage des rejets, afin de tenir compte à la fois des coûts et de la précision visée, et elle examine la dépendance de ces programmes des deux variables en question. L'analyse se base sur le programme irlandais des rejets qui comporte un plan d'échantillonnage volontaire par un observateur à bord qui vise à estimer les taux de rejet dans les pêches au chalut. Une analyse en plusieurs étapes a permis d'estimer les niveaux de précision atteints dans le passé et une fonction de coût a servi à estimer le coût financier du programme. Les principaux facteurs qui affectent les rejets sont les engins de pêche, les aires de pêche, les espèces recherchées et les divisions du Conseil international pour l'exploration de la mer (ICES); il y a aussi des effets aléatoires des trois groupes emboîtés considérées, soit le trait de chalut, la sortie et le navire. Des réductions du budget actuel n'entraineront qu'une diminution marginale de la précision, bien que des changements dans les variables reliées au coût peuvent avoir un impact sur l'intensité de l'échantillonnage. D'autre part, pour augmenter la précision visée de moitié, il faudrait accroître considérablement l'échantillonnage et les coûts associés, ce qui sera difficile ou impossible à réaliser. Enfin, l'analyse en fonction des composantes des flottes indique un accroissement marqué de l'échantillonnage, ce qui met en lumière l'importance de préciser clairement les objectifs de l'échantillonnage des rejets.

[Traduit par la Rédaction]

Introduction

Discarding fish at sea is an inherent part of fishing, accounting for more than 25% of total worldwide catches (Alverson et al. 1994). However, discarding is not always taken into consideration in fish stock assessments, even when it might account for a high proportion of fishing mortality, especially in younger ages, which may lead to unrealistically optimistic evaluations. In most cases, the reason is the lack of systematic sampling and the associated low precision levels (ICES 2003).

Quantifying discards has become more important in recent years as fisheries management objectives change to include an environmental perspective. In the European Union, this change has resulted in the introduction of the Data Collection Regulation (thereafter called DCR; Council Regulation No. 1543/2000 and Commission Regulation No. 1639/2001), which aims to establish "a community framework for the collection and management of the data needed to conduct the Common Fisheries Policy". These regulations provide funding for sampling in all areas of the fisheries sector, from vessel characteristics and fishing effort to catches and basic biological species parameters. They also establish compulsory discard sampling levels directly by specifying sampling and precision levels and indirectly by the amount of funding made available.

Received 8 July 2003. Accepted 13 April 2004. Published on the NRC Research Press Web site at http://cjfas.nrc.ca on 16 December 2004.
J17625

L. Borges[1,2] **and E. Rogan.** Aquaculture and Fisheries Development Centre, Department of Zoology, Ecology and Plant Science, University College Cork, Lee Maltings, Prospect Row, Cork, Ireland.
A.F. Zuur. Highland Statistics Ltd., Newburgh, UK.
R. Officer. Marine Institute, Galway Technology Park, Parkmore, Galway, Ireland.

[1] Corresponding author (e-mail: lisa.borges@marine.ie).
[2] Present address: Marine Institute, Snugboro Road, Abbotstown, Dublin 15, Ireland.

Can. J. Fish. Aquat. Sci. 61: 1918–1928 (2004) doi: 10.1139/F04-138

Unfortunately, there is little guidance in how to conduct the discard sampling in order to achieve the required sampling and precision levels. Discard sampling is a large-scale process because of the size of the fishing fleet and the numerous factors that may influence discarding practices and hence involves vast human and economic resources and specific methodology. Although some authors have presented methodologies for optimum fisheries sampling programs considering both cost and precision constraints simultaneously (Schweigert and Sibert 1983; Horppila and Peltonen 1992), only precision levels are specified in the literature for discard programs (Tamsett et al. 1999; Allen et al. 2002; Rochet et al. 2002).

Optimum sampling schemes in discard sampling programs require allocation of limited sampling resources among the different hierarchical levels sampled, i.e., number of vessels, trips on a vessel, and hauls within a trip that should be sampled, taking into consideration that each level has different variance and cost. This study presents optimum sampling levels considering precision targets but also budget constraints based on an analysis of the discard sampling program carried out by the Marine Institute in Ireland. Following and further developing the approach detailed in Allen et al. (2002), existing sampling levels and the associated variance and cost of this program where used to predict sampling levels that would achieve desired levels of precision with limited sampling resources. Additionally, a detailed cost function is described for the first time for discard programs, in a form that is applicable to other sampling programs.

Materials and methods

The Irish discard sampling program

The Irish discard sampling scheme is an at-sea observer program, aboard commercial vessels and based on a voluntary participation of fishers. It is carried out by five, and since 2001 by six, technicians (Fisheries Assessment Technician (FAT)) based in the six major Irish fishing ports: Killybegs, Rossaveel, Dingle Castletownbere, Dunmore East, and Howth (Fig. 1). Discard trips are chosen by the FAT according to the trawl fleet activity in each port. In each haul, auxiliary information such as fishing method and location and weather conditions are collected, and also (*i*) total catch (C_{vth}, where vessel (v) = 1, …, v', trip (t) = 1, …, t_v, and haul (h) = 1, …, h_{vt}) is estimated by eye by the skipper and total species landings boxed after sorting (L_{vth}) are recorded and (*ii*) one box (usually 40 kg) is taken randomly from the discards, from as many hauls as possible, and numbers at length per species are determined. Otoliths of target species (cod (*Gadus morhua*), whiting (*Merlangius merlangus*), haddock (*Melanogrammus aeglefinus*), hake (*Merluccius merluccius*), plaice (*Pleuronectes platessa*), megrim (*Lepidorhombus whiffiagonis*), and sole (*Solea solea*)) are collected for age readings and individuals weights are recorded. (*iii*) Landings length frequency is determined proportionally to total landings, and otoliths of target species are collected.

Total discards per haul (D_{vth}) are estimated from the difference between C_{vth} and L_{vth}. The discarded length frequencies are raised to haul level by the ratio of D_{vth} to the sample discard quantity.

The discard data analysed consisted of total numbers of fish discarded per hour towed (hereafter called TDPUE). Species were not considered individually as the objective of the program is to determine a global discard rate, which may differ from a species-specific one. The data collected are highly variable with unbalanced sampling levels (i.e., different number of vessel, trips, and hauls sampled) and show extreme positive skewness. Consequently, the data were normalised by natural log transformation and, in some cases, with the addition of a constant, using the DISTRIBUTION directive of the software GenStat® (Release 6.1, VSN International Ltd., Herts, UK; Payne 2002) to follow the assumptions of the subsequent analyses.

Variance components

When a traditional multiple regression model is used to analyse data with a meaningful multilevel structure, the nested structure of the data often cannot be represented completely by the explanatory variables. This regression can give misleading results as the regression parameters may depend on the nested structure. The best way to analyse multilevel data is an approach that represents within- and between-group relations within a single analysis. In such an analysis, unexplained variation within and between groups is considered random variability, i.e., the partition of unexplained variability over the various levels (Snijders and Bosker 1999).

Because of the actual hierarchical structure of discard data (hauls nested within trips nested within vessels), a multilevel analysis was undertaken to determine the optimum sampling levels. This analysis has the advantage of estimating the variance between and within each level (random effects) that is used to determine the amount of sampling in each level, and in doing so, it also determines the major parameters affecting discards (fixed effects). The variance of a data set, i.e., between vessel (S_v^2), between trips within vessels (S_t^2), and between hauls within trips within vessels (S_h^2), and the effect of underlying factors were estimated by residual maximum likelihood (REML) in a linear mixed model. REML was chosen because it is the most efficient method when estimating variance components based on unbalanced and highly variable data (Snijders and Bosker 1999). The model was fitted using the software GenStat® (Release 6.1, VSN International Ltd.; Payne 2002) under the assumption that the residuals are independent and normally distributed (see Appendix A for a full description of the model).

Several factors were considered a priori to affect discards and were divided by group level as follows: (*a*) trip level (gear, year, quarter, ICES division, port of departure, port of landings, targeted species, and mesh size); and (*b*) haul level (time of day, depth, fishing ground, targeted species, and catch composition). The International Council for the Exploration of the Sea (ICES) division refers to a sea-area division, whereas fishing ground is the area where fishing occurred and may include several substrate types (e.g., sand, mud, etc.). Targeted species were considered to be the species with at least 30% of the landings per haul. Catch composition was considered a function of species richness given by the total number of fish species discarded.

All factors (random and fixed) were included in the preliminary runs of the hierarchical linear (HL) mixed model and were subsequently assessed and included or excluded

Fig. 1. Map of Ireland showing (*a*) the Fisheries Assessment Technician (FAT) base ports and the International Council for the Exploration of the Sea (ICES) divisions and (*b*–*c*) the location of the fishing hauls sampled by gear: (*b*) otter trawl (+), (*c*) beam trawl (▲), and (*d*) Scottish seine (●).

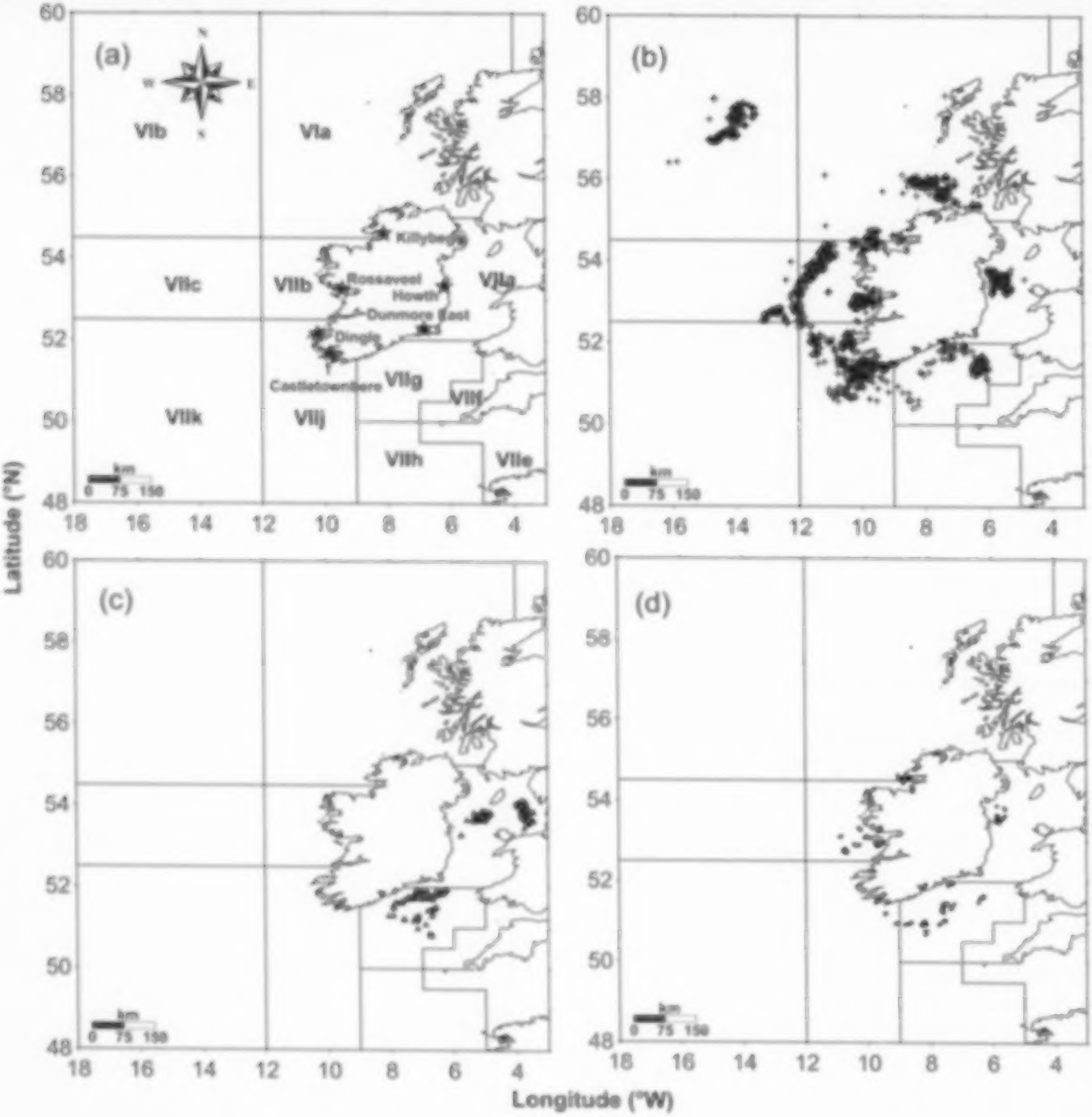
(a)
(b)
(c)
(d)
N
W
E
S
VIb
VIa
VIIc
VIIb
VIIa
VIIg
VIIf
VIIk
VIIj
VIIh
VIIe
Killybegs
Rossaveel
Howth
Dunmore East
Dingle
Castletownbere
km
0 75 150
Latitude (°N)
Longitude (°W)
60
58
56
54
52
50
48
18
16
14
12
10
8
6
4

from the final model according to the proportion of the variance explained by each. This analysis is carried out for random effects by using likelihood ratio test statistics where the importance of each individual term is determined by comparing the full mixed-effects model with a simpler model without the factor of interest. Fixed-effects significance can also be determined by Wald statistics, which test the null hypothesis that the fixed model term is equal to zero, based on the value of the estimated parameter and its variance–covariance matrix. However, Wald statistics are only asymptotically distributed as χ^2 and thus will only be reliable for large samples (Welham and Thompson 1997). Nevertheless, the increase in the final model complexity resulting from the inclusion of a significant fixed effect, given by the Wald test, might not be justified. This final decision is reached using a further likelihood ratio test, as described above.

The variance of the overall sample mean, $V(\bar{\bar{y}})$, was calculated based on the formula given by Cochran (1977, page

Fig. 2. Histogram and plots of residuals of the mixed-models estimated for (*a*) otter trawl, (*b*) beam trawl, and (*c*) Scottish seine.

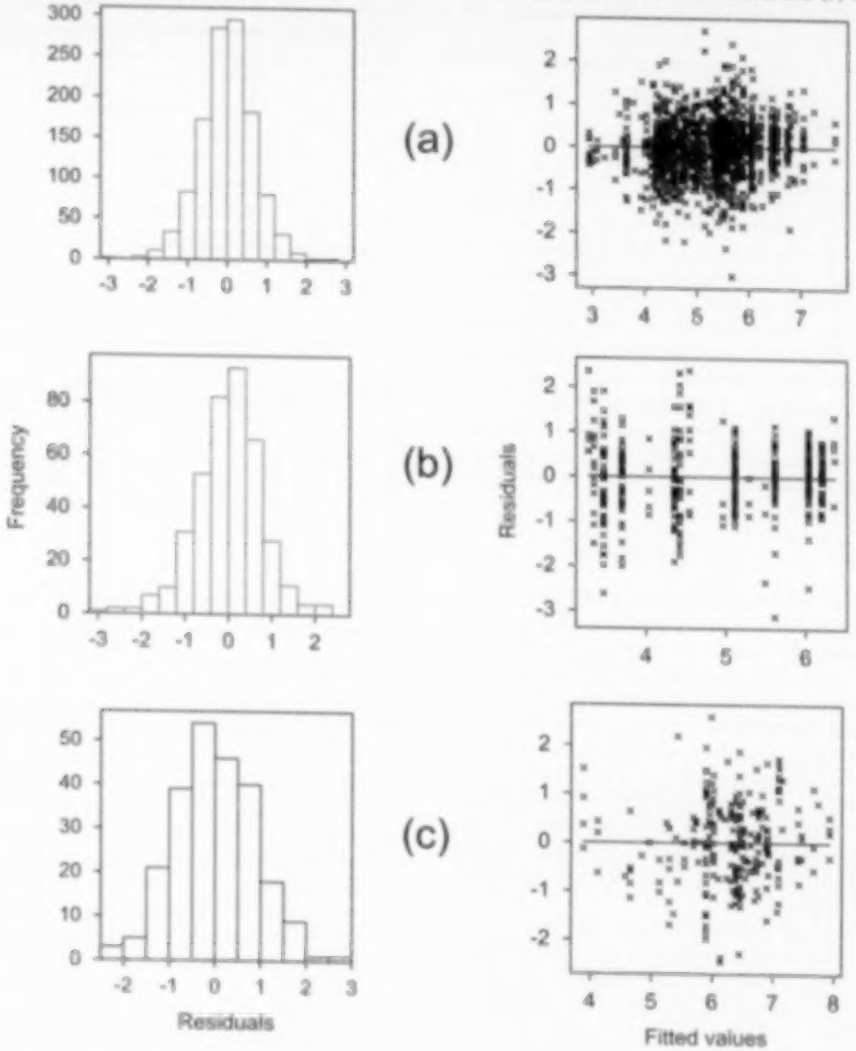

286, eq. 10.34) and specified below, where the partial level/group variances are the variance components estimated for vessel (S_v^2), trip (S_t^2), and haul (S_h^2).

$$(1) \qquad V(\overline{\overline{y}}) = \frac{1 - v'/V}{v'} S_v^2 + \frac{1 - t'/T}{v't'} S_t^2 + \frac{1 - h'/H}{v't'h'} S_h^2$$

where v' is the total number of vessels sampled, t' and h' are the mean number of trips per vessel and hauls per trip sampled, respectively, V is the total number of vessels in the fishery, T and H are the mean number of trips per vessel and hauls per trip in the fishery, respectively, and v'/V, t'/T, and h'/H are the sampling fractions at the three levels.

Preliminary results show that multilevel analysis is applicable because there is significant random variability (likelihood ratio test, $P < 0.01$) in the three nested levels in the three gears and also because the visual inspection of residual plots did not show a clear deviation from the initial assumptions of normality and independence. Also, with regard to fixed effects, gear showed a highly significant effect (Wald test, $P < 0.001$) on the total number of fish discarded per hour and was considered a priori, i.e., the data were divided and the subsequent models were estimated for each gear. The random variability was re-assessed for the three gear-specific data sets, and once again there was a justification to use mixed models (Fig. 2). Moreover, in view the extensive spatial distribution of otter trawl (see Fig. 1*b*), all former analyses were performed considering the different fleet components of the total otter trawl fishery, as defined by the gear used, fishing ground, and ICES division. Fleet components targeting Norway lobster (*Nephrops norvegicus*) were also identified as such.

The final stage of this analysis was to convert the calculated total variance in a comprehensible quantity, like a coefficient of variation (CV), to allow a comparison between the different gears and also to establish precision targets. Because of the data normalisation process, the total variance is in a logarithmic scale, whereas the CV will be in an arithmetic scale, preventing a direct transformation of variance in CV. However, because of the special properties of the log-normal distribution, it can be demonstrated that $\mathrm{var}(\log(x)) = \mathrm{CV}^2$ (Julious and Debarnot 2000).

Cost function

A cost function was estimated based on the knowledge available about the Irish discard sampling scheme and considering three price units (c_v, c_t, c_h), one for each nested sampling level. The financial cost of sampling a gear is described as a function of time spent on different tasks: sampling, data input, age determination, etc. The cost function also reflects fixed costs like consumables, e.g., safety gear and lab materials, and takes into account only the proportion of the technician's time spent in discard sampling, as FATs are not exclusively discard samplers in the studied program. The final cost function, based on the formula given by Cochran (1977, page 288, eq. 10.43), is expressed mathematically as follows:

$$(2) \qquad C_{g_y} = v' c_v + v' t' c_t + v' t' h' c_h + \mathrm{const}_y$$

where C_{g_y} is the cost of sampling a gear g per year y, c_v is the cost of sampling vessel v, c_t is the cost of sampling trip t, c_h is the cost of sampling haul h, v' is the total number of vessels sampled, t' and h' are the mean number of trips per vessel and hauls per trip sampled, respectively, const_y is a constant cost per year y, and also

c_v = FAT's salary × time explaining program to skipper

c_t = FAT's salary × (time asking to board + time inputting data + time at sea + number of otoliths × (time processing otoliths + age reading time)) + sea allowance × time at sea + time checking data × (technician's salary + lab attendant's salary) + scientist salary × time managing data

c_h = FAT's salary × (haul duration + time inputting data + lieu leave) + sea allowance × time at sea + time checking data × (technician's salary + lab attendant's salary)

const_y = consumables + technician II's salary × time managing program

considering three technician career grades (lab attendant, technician, and technician II, in ascending order) and one scientist also working in the sampling program. In practice, the times spent in the different tasks listed above were determined and are presented in Table 1. Note that time inputting and checking data and time at sea have different values between trip and haul. This is because different data and time at sea are associated with each sampling level (for example, fishing port data or time spent travelling to a fishing ground are specific only to trip level, whereas species-specific data and haul duration are specific to haul level). The time spent processing one otolith was considered to be around 4 min, and age reading was calculated to take ~9 min/otolith. Also, it was estimated that it takes 2 work days/month to administer the program. The remaining variables were taken as the mean values based on the observed data (Table 2) and as discussed below.

In sampling programs involving work at sea, there is normally a requirement to compensate observers for working extended hours, especially during weekend days. This compensation usually takes the form of "lieu leave", i.e., time off work, and was considered here as a one to one weekend/working day basis. However, accruing lieu leave as a function of hauls, and thus of time spent at sea, constituted a problem for which we could not determine a satisfactory solution. Consequently, lieu leave accrued (2 work days) was simply divided by the average number of hauls done in a week per gear. Also, the number of otoliths collected was originally considered at the haul level based on the assumption that there is a correlation between the number of hauls and otoliths collected in a fishing trip. However, in the Irish discard sampling program, an average number of otoliths were collected with different trip durations within gears: 55, 97, and 60 for otter trawl, beam trawl, and Scottish seine, respectively. Although this lack of correlation might be a characteristic unique to this sampling program, to our knowledge there are no published data to prove otherwise, and therefore, the cost associated with otolith sampling was considered at trip level. Furthermore, the lack of correlation between the numbers of hauls and otoliths collected prevents an age-related cost unit and thus a cost analysis with four nested levels.

Table 1. Time in working days and in minutes (7.5-h working day) spent per task in each sampled nested level.

Nested level	Task	Time (working days)	Time (min)
Vessel	Explaining to skipper	1	450
Trip	Asking to board	0.5	225
	Data inputting	0.022	10
	Time at sea	1	450
	Data checking	0.011	5
	Data managing	0.133	60
Haul	Haul period	[a]	[a]
	Data inputting	0.2	90
	Data checking	0.067	30
	Time at sea	[a]	[a]
	Lieu leave	[b]	[b]

[a] Haul period, and thus time at sea, is gear-specific: three hauls sampled per day in otter trawlers, four in Scottish seiners, and five in beam trawlers.

[b] Lieu leave, defined as time off work to compensate technicians for extended working hours at sea, per haul was considered to be two working days accrued over a weekend divided by the average number of hauls done in a week per gear.

The total cost of a discard sampling program per year y (C_y) is simply the sum of the cost of sampling each gear g:

$$(3) \qquad C_y = \sum_g C_{g_y}$$

Sampling levels

The calculations of optimal sampling levels involve the determination of the optimal set of the number of vessels, trips, and hauls that minimize the product of variance and trip cost ($V \times C_{g_y}$), i.e., the final values obtained in the two previous sections. The optimal solution will be a compromise between an acceptable level of variance while keeping cost within budget.

The variance components and costs calculated previously were substituted in the formulas given by Cochran (1977, page 288, eq. 10.44), and specified below, to produce opti-

Table 2. Present sampling levels shown as annual mean numbers of vessels, trips per vessel, and hauls per trip per vessel sampled between 1993 and 2002, coefficient of variation (CV), associated total cost ($C_{g,y}$) based on costing of 2002, budget allocation by gear, and total cost of the discard sampling program in year y (C_y).

Gear	CV (%)	No. of vessels	No. of trips per vessel	No. of hauls per trip per vessel	$C_{g,y}$ (€)	Budget allocation (%)
Otter trawl	20	16	1	8	39 730	55.7
Beam trawl	68	1	2	30	16 067	22.5
Scottish seine	29	2	2	10	15 509	21.7
Total C_y					71 306	

Note: 1 € ≈ 1 US dollar.

Table 3. Total numbers of vessels, trips, and hauls sampled by gear and year.

Year	Otter trawl			Beam trawl			Scottish seine		
	Vessels	Trips	Hauls	Vessels	Trips	Hauls	Vessels	Trips	Hauls
1993	3	3	29	1	2	20	—	—	—
1994	15	17	131	3	4	94	2	2	30
1995	5	5	43	2	2	77	—	—	—
1996	28	37	266	2	3	82	6	7	53
1997	33	38	344	1	2	79	3	6	49
1998	22	26	243	1	2	61	3	6	56
1999	16	18	160	1	2	108	1	2	20
2000	13	13	123	—	—	—	—	—	—
2001	15	17	135	1	2	56	—	—	—
2002	11	12	87	—	—	—	1	1	29
Total	161	186	1561	12	19	577	16	24	237

Note: A dash (—) indicates no data.

mum numbers of hauls per trip (h_{opt}) and trips per vessel (t_{opt}) to sample.

$$(4)\qquad h_{\text{opt}} = \frac{S_h}{\sqrt{S_t^2 - S_h^2/H}}\sqrt{c_t/c_h}$$

$$(5)\qquad t_{\text{opt}} = \frac{\sqrt{S_t^2 - S_h^2/H}}{\sqrt{S_v^2 - S_t^2/T}}\sqrt{c_v/c_t}$$

The optimum total number of vessels to sample is derived from the variance (eq. 1) considering either a predefined target variance or total cost. Thus, in the study case presented, the total number of vessels was estimated considering two different scenarios: a CV of 25% for TDPUE, based on the precision target specified per species in the European Union Data Collection Regulation under the minimum program sampling levels, and a hypothetical financial resource, given as a 10% increase in the 2002 spending for discard sampling.

Results

Historical sampling levels

The collection of discard data began in 1993, and over the 10-year period, 229 trips were sampled, corresponding to 2375 sampled tows. The period between 1996 and 1997 had the highest sampling effort, and since then sampling effort has steadily declined. Three different gear types have been sampled: bottom otter trawl, beam trawl, and Scottish seine. The most sampled gear was otter trawl, whereas beam trawl presented more hauls and a better temporal coverage than Scottish seine. However, in recent years, the sampling has been scarce or nonexistent in these two gears (Table 3; Fig. 1). Considering sampling by ICES division, it can be seen that for the majority of the time series, only beam trawls operating in VIIa (Irish Sea) have been sampled, whereas Scottish seine were sampled mainly in VIa (Stanton Bank, no geographical positions available) and in VIIg (Celtic Sea). Otter trawl sampling effort was distributed all around Ireland, showing the general fleet activity (Table 4; Fig. 1).

The gears analysed were sampled at different average yearly levels (only 1 and 2 vessels for beam trawl and Scottish seine, respectively, each with two trips per vessel); whereas otter trawl had 16 vessels sampled, each with one trip. Looking at the number of hauls per trip, beam trawl presents the highest values, with the opposite for otter trawl (Table 2).

Considering the population of the Irish fishing fleet and based on the available logbook fleet activity mean values (1995–2002; Table 5), the annual coverage of the sampling scheme was 0.3%, 4.1%, and 3.5% for otter trawl, beam trawl, and Scottish seine, respectively. The coverage of the Irish discard sampling scheme is higher than the ones achieved in the Scottish discard sampling program (0.1% to 0.2%; Stratoudakis et al. 1998) and of the same order of magnitude as those achieved in the French trawl fleet in the Celtic Sea (0.8%; Rochet et al. 2002).

Variance components

For the three gears studied, the variance increased with increasing hierarchical level, i.e., from between vessels to between hauls within trips within vessels (Table 6).

Table 4. Total number of trips sampled by ICES (International Council for the Exploration of the Sea) division and year for otter trawl, beam trawl, and Scottish seine.

ICES division	1993	1994	1995	1996	1997	1998	1999	2000	2001	2002
Otter trawl										
VIa	2	1		4	4	3	4	1	4	4
VIb	1		2		2	1		1	1	
VIIa		2		8	8	7	4	6	2	1
VIIb		4	1	12	8	5	3	3	6	2
VIIc		1		1	1	2	2			
VIIj		4	2	9	8	6	3	2	3	5
VIIg		5		4	8	5	2	1	3	1
Total	3	17	5	38	39	29	18	14	19	13
Beam trawl										
VIIa	2	1	2	1	2	2	2		2	
VIIg	1	3		2						
Total	3	4	2	3	2	2	2		2	
Scottish seine										
VIa		1		3	1	1				
VIIa				1	1		1			
VIIb				1	1	1				
VIIg		1		1	4	4	1			1
VIIj		1								1
Total		3		6	7	6	2			2

Note: Blank spaces indicate no data.

Table 5. Irish fisheries activity from 1995 to 2002 shown as annual mean numbers of vessels, trips per vessel, and hauls per trip per vessel by gear, based on logbook information.

	No. of vessels		No. of trips per vessel		No. of hauls per trip per vessel[a]	
	Mean	Range	Mean	Range	Mean	Range
Otter trawl	281	231–310	30	29–33	10	9–11
Beam trawl	24	21–30	28	19–38	36	28–45
Scottish seine	27	18–38	34	29–44	11	4–16

[a] Number of hauls were estimated based on the number of hours fished per day divided by the duration of a typical haul per gear: 6 h for otter trawl and 2 h for beam trawl and Scottish seine.

Table 6. Estimated variance components between vessels (S_v^2), between trips within vessels (S_t^2), and between hauls within trips within vessels (S_h^2) and respective standard errors (SE) by gear.

	Vessel		Trip		Haul	
	S_v^2	SE	S_t^2	SE	S_h^2	SE
Otter trawl	0.1638	0.1375	0.5082	0.1219	0.523	0.0231
Beam trawl	0.1946	0.4519	0.5985	0.3118	0.626	0.0454
Scottish seine	0.0408	0.1551	0.2604	0.1490	0.844	0.0839

Note: All random components are significant at the 1% level based on likelihood ratio test statistics.

Table 7. Mixed models as a function of total discards per unit of effort (TDPUE) estimated by gear.

Gear	Model
Otter trawl	Ln (TDPUE + 8.44) = vessel + vessel·trip + vessel·trip·haul + fishing ground
Beam trawl	Ln (TDPUE + 1.18) = vessel + vessel·trip + vessel·trip·haul + fishing ground
Scottish seine	Ln (TDPUE + 25.73) = vessel + vessel·trip + vessel·trip·haul + targeted species haul + ICES division

Note: Only fixed terms significant at the 0.1% level are shown based on Wald test statistics. Also, all models were significant at 1% level based on likelihood ratio test statistics.

Of the factors other than gear that were thought to affect discards, only one, fishing ground, explained a significant proportion (Wald test, $P < 0.001$) of the variance present in the data of otter trawl and beam trawl. ICES division and targeted species at haul level (Wald test, $P < 0.001$) were the main factors in Scottish seine (Table 7). Beam trawl trips in

Table 8. Mixed models as a function of total discards per unit of effort (TDPUE) estimated by otter trawl fleet, as defined by the gear used and fishing area (ICES division and fishing ground).

Otter trawl fleets	Model
VIa Stanton Bank	Ln (TDPUE) = vessel + vessel·trip + vessel·trip·haul + fishing ground
VIb Rockall Bank	Ln (TDPUE + 18.84) = vessel + vessel·trip + vessel·trip·haul
VIIa *Nephrops*	Ln (TDPUE) = vessel + vessel·trip + vessel·trip·haul + catch composition + targeted species haul
VIIb *Nephrops* Aran Isles	Ln (TDPUE) = vessel + vessel·trip + vessel·trip·haul
VIIb West of Achill	Ln (TDPUE) = vessel·trip + vessel·trip·haul
VIIc Porcupine Bank	Ln (TDPUE) = vessel + vessel·trip·haul
VIIg *Nephrops* Smalls	Ln (TDPUE) = vessel + vessel·trip + vessel·trip·haul
VIIj	Ln (TDPUE + 22.54) = vessel + vessel·trip + vessel·trip·haul

Note: Only fixed terms significant at the 0.1% level are shown based on Wald test statistics. All models were significant at 1% and 5% (underlined) level based on likelihood ratio test statistics.

Table 9. Annual optimum sampling levels shown as numbers of vessels, trips per vessel (t_{opt}), and hauls per trip per vessel (h_{opt}) to be sampled for a target precision coefficient of variation (CV) of 25% and the current CV by otter trawl fleet.

Otter trawl fleet	CV (%)	No. of vessels	t_{opt}	h_{opt}
VIa Stanton Bank	52	18	1	2
VIb Rockall Bank	68	5	1	5
VIIa *Nephrops*	59	28	1	2
VIIb *Nephrops* Aran Isles	69	13	1	6
VIIb West of Achill[a]	32	—	4	3
VIIc Porcupine Bank[a]	45	3	—	2
VIIg *Nephrops* Smalls	47	14	1	2
VIIj	24	11	1	2

Note: A dash (—) indicates no data.

[a] Random variability is not statistically significant at vessel and trip level for VIIb West of Achill and VIIc Porcupine Bank fleets, respectively. Consequently, the optimum sampling levels were calculated based on a two-level sampling scheme.

Table 10. Cost of sampling a vessel (c_v), a trip (c_t), and a haul (c_h) by gear based on costing of 2002.

Gear	c_v	c_t	c_h
Otter trawl	178	635	151
Beam trawl	178	846	113
Scottish seine	178	661	127

Note: Cost is expressed in Euros (€), where 1€ = 1 US dollar.

ICES division VIIg were excluded from the final model because of the lack of information regarding fishing ground. Thus, the results obtain showed a significant difference in discarding between the two fishing grounds in the Irish Sea (ICES division VIIa). For different otter trawl fleets, only random effects were the main factors explaining variability in most fleets (Table 8).

The level of variability in the data, given as a coefficient of variation, with the present sampling scheme is 20% for otter trawl and 29% for Scottish seine, whereas in beam trawl, the CV is higher, reaching 68% (Table 2). However, when considering the different fleets that comprise otter trawl, the results show a striking increase in CV in all but one fleet, the otter trawl fleet operating in ICES division VIIj (Table 9).

Cost function

The results show that of the three price units estimated per gear, trip is the most expensive nested level to sample in all gears. This is partly due to the time spent in otolith sampling, but also to the time spent asking to board and at sea (see Table 1). It costs the same to sample a vessel regardless of the gear considered, as it takes the same time to explain the discard program to any skipper. Furthermore, an otter trawl trip is the cheapest to sample, whereas a beam trawl trip is the most expensive; however, at haul level, the opposite is true (Table 10).

Based on the total number of vessels sampled and the average number of trips per vessels and hauls per trip sampled, the total cost of the discard sampling program has been estimated at €71 000 annually. Otter trawl gear was the most expensive gear to sample because of the associated high sampling levels, whereas the two remaining gears had similar costs (Table 2).

Sampling levels

The optimum sampling levels obtained (Table 11) show that it is only necessary to sample one trip per vessel and a much smaller number of hauls per trip compared with the current sampling levels (Table 2). This suggests that a three-stage analysis is unnecessary and that only two nested levels (vessel and haul) should be considered. Also, shorter trips with fewer hauls will be more cost effective.

The number of vessels sampled in the first scenario studied, i.e., as a function of the precision level of 25% for TDPUE, is lower than the present sampling for otter trawl but considerably higher for the remaining gears. A CV of 25% will be difficult to achieve in beam trawl because of the high vessel sampling levels obtained caused by the data variance (Table 11*a*). In this gear, even an increase from the optimum sampling levels to current levels (two trips per vessel) will still involve eight vessels to be sampled and an consequent increase in cost of almost €2000. Nevertheless, regardless of the gear considered, cost does not seem to be a limitation to achieve the 25% precision level as the associated total cost is only slightly higher than the present spending. Furthermore, to obtain the same precision level in all gears studied, considering the price units of the previous section and optimum sampling levels, otter trawl, beam trawl, and Scottish seine must receive, respectively, around 35%, 40%, and 25% of any budget. This fact also shows the need

Table 11. Annual optimum sampling levels shown as numbers of vessels, trips per vessel (t_{opt}) and hauls per trip per vessel (h_{opt}) to be sampled, associated total cost ($C_{g,y}$) based on costing of 2002, and budget allocation by gear and the total cost of the discard sampling program per year y (C_y) for three different scenarios: (*a*) a target precision level of a coefficient of variation (CV) of 25%, (*b*) a target cost of 10% increase in spending for discard sampling, and (*c*) recommended sampling levels based on a re-allocation of the available resources.

Gear	Target CV (%)	No. of vessels	t_{opt}	h_{opt}	$C_{g,y}$ (€)	Budget allocation (%)
(*a*) Precision target						
Otter trawl	25	14	1	2	22 662	35
Beam trawl	25	16	1	3	25 909	40
Scottish seine	25	5	1	5	16 277	25
C_y					64 848	
(*b*) Cost target						
Otter trawl	15	41	1	2	44 100	56
Beam trawl	26	15	1	3	17 834	22
Scottish seine	18	10	1	5	17 215	22
C_y					79 149	
(*c*) Recommended sampling levels						
Otter trawl	25	12	1	>4	>23 814	34
Beam trawl	25	7	2	>6	>30 981	43
Scottish seine	25	5	1	>5	>16 277	23
C_y					>71 072	

Note: 1€ ≈ 1 US dollar.

for the present budget allocation to be restructured to allow a shift of funds from otter trawl to beam trawl.

In the second scenario, a 10% increase in the 2002 spending for discard sampling could increase sampling levels by up to 15 times, with a resulting CV decrease of one-quarter for otter trawl, almost one-half for Scottish seine, and as much as two-thirds for beam trawl (Table 11*b*).

The recommended sampling levels are therefore the result of a compromise between the sampling requirements and available human and financial resources, but also the result of the balance between variability and sampling levels in each nesting level. Hence, a CV of 25% is achieved in all gears by a different budget allocation to achieve a reduction in the vessels sampled in otter trawl to increase those in beam trawl and a slight increase in total budget to increase the number of trips and hauls per trip to sample to reduce vessels in beam trawl (Table 11*c*).

However, when the different otter trawl fleets are considered separately, the total optimum sampling is markedly higher, increasing 10 times the number of otter trawl vessels to be sampled. The number of trips to be sampled per vessel is maintained (Table 9).

Discussion

The variance components obtained show that hauls within trips within vessels have the highest variability in TDPUE. This result was also obtained by Tamsett et al. (1999) and by Allen et al. (2002) based on data collected on several areas and gears, including otter trawlers and beam trawls operating in the Irish Sea. In contrast, Rochet et al. (2002) reported high variability at trip level, but this was the highest sampled level and thus will include the variability associated with vessels. Allen et al. (2002) also found that, in agreement with the present study, variability decreases with hierarchical levels, between hauls to between vessels, which suggests that discarding between vessels is quite consistent.

Of all parameters considered to affect discarding, only gear, fishing ground, targeted species at haul level, and ICES division had a significant effect. Gear has a predictable effect on discarding because of different gear selectivity. The significance of area-related factors such as ICES division and fishing ground has also been reported in several European discard programs (Stratoudakis et al. 1998; Allen et al. 2002; Rochet et al. 2002). This is probably due to the relationship between the distribution of demersal species and ground types. This outcome highlights the fact that different fleets, defined by the gear used and their fishing area, have different discarding patterns and suggests that the different fleets should be considered separately in discarding estimations and sampling level calculations. In the Irish discard program and specifically in the case of beam trawls, both fishing grounds in the Irish Sea are visited on the same fishing trip, hence disabling an area-specific sampling scheme with a consequent decrease in variability. In contrast, in otter trawl, the different fleets can be considered separately, but the total optimum sampling scheme has to be adjusted to higher sampling levels, as a result of low sampling levels, different discard patterns, and population sizes. These results emphasize the importance of clearly stated discard sampling objectives, specifically if discard rates are to be estimated by different variables such as fleet, area, species, or fish stock.

It is interesting to note that year and quarter did not appear to contribute significantly to variability in discards, a result also obtained by Tamsett and Janacek (1999) and Rochet et al. (2002) but not by Stratoudakis et al. (1998) or Allen et al. (2002). This result could be expected considering that this analysis was based on the total number of fish species discarded, and consequently, any species-specific effect, such as year class, might be disguised by changes in abundance of another species. Furthermore, the low quarterly sampling levels cannot be excluded as a reason. Nevertheless, the nonsignificance of these two effects suggests that the data matrix can be pooled in future analyses, thus increasing sampling levels and possibly enabling a fine-temporal scale analysis. Targeted species, at either haul or trip level, does not seem to change discarding patterns in otter and beam trawls. This is probably because discarding occurs mainly in noncommercial species and on undersized fish in otter trawl. Furthermore, targeted species was quite consistent in beam trawl (mainly sole and plaice). In Scottish seine, discard patterns at haul level changes with the main species landed: higher discarding was observed with megrim, hake, and haddock. Rochet et al. (2002) reported that gadoids and *Nephrops* trawling in the Celtic Sea discarded mainly target species, whereas benthic trawlers discarded bycatch species. However, as this study is not species-specific, we cannot confirm these results. Finally, there is little information available concerning mesh size, which may have compromised the significance of this parameter.

The coefficients of variation obtained for otter trawl and Scottish seine are lower than the ones reported for groundfish trawl fisheries in the same areas: West of Scotland (50%–60%) (Stratoudakis et al. 1999) and Celtic Sea (40%) (Rochet et al. 2002), although the otter trawl fleets' CVs range from 24% to 69%. Stratoudakis et al. (1999) argues that the high CVs obtained may be due to low sampling levels and to the larger variability of discarding associated with area and target species. This might also be the case in beam trawl where existent sampling levels are low but there are highly valued target species (plaice and sole) and gadoids are usually discarded in large quantities. Additionally, the precision of the estimations of total catch (C_{ijk}) by the skipper cannot be determined at present, as there is no unbiased estimation of total catch available. This fact may increase the overall variability of the sampling program and thus should be considered in planning future discard programs.

The financial cost of the entire Irish discard program is substantially underestimated, as it only accounts for the actual time spent in discard work (less than half of the FAT's working time) and yet technicians are normally hired on an annual basis. If the working conditions of technicians are changed to work exclusively on discards in order to reduce the discard budget, then other considerations should be taken into account. For instance, extra specialized work effort may be needed in other sampling areas at times when, for example, the fishing fleet is not working because of bad weather conditions.

The optimal sampling schemes obtained are quite sensitive to cost-unit changes, a result also found by Schweigert and Sibert (1983). The high values of cost at trip level forces the level to be two-staged, as it is only necessary to sample one trip per boat. If cost units change by increasing haul costs and decreasing trip costs, then sampling levels will tend to a three-staged scheme. However, even if a relationship between the number of otoliths collected and hauls exists, and thus the cost of sampling otoliths is shifted to haul level, trip would still be the most expensive level to sample and the resulting optimum sampling levels would still indicate one trip per vessel. Changes in staffing costs (e.g., a more generous lieu leave system) would increase the trip and haul costs. As a result, the optimum sampling scheme changes to allow for an increase at vessel level (one more vessel per gear), while maintaining the effort of the remaining sampling levels. Also, changes in the amount of time spent on work related to discard sampling (for example, in age reading, caused by the introduction of new species to be aged, or in inputting data, because of technical reasons such as remote connections to the ports, or in different salary scales) will all imply different cost units and should be taken into consideration when modifying methodologies.

The optimum sampling efforts obtained are in accordance with the ones found by Allen et al. (2001) for trip level, though based only in target precisions. This result suggests that the data can be pooled at haul level in future analyses, for example, for a better understanding of the mechanisms behind discard patterns during the year. However, the discard data are inheritably hierarchical so a three-staged sampling scheme will always be in place. Also, the impossibility of estimating trip variability in the future by adopting a one-trip-per-vessel sampling scheme, should be taken into consideration when planning a discard sampling program. The sampling levels presented are only recommended for the discard program studied and should be seen as illustrative values rather than as absolute. The optimum sampling levels also indicate that the sampling effort in the current sampling scheme should be restructured to allow for shorter trips (3–4 days) while sampling the highest number of vessels possible. This does not mean that longer trips should not be sampled, or that during a trip, when reaching the optimum levels of hauls, sampling should stop: there is always an improvement in precision with higher numbers of hauls sampled. Furthermore, the possibility of shortening the trip (for example, by disembarking after sampling the optimum number of hauls) is often impractical as it implies additional costs because the extra steaming time has to be paid for by the program and requires a willingness of the skipper to come ashore. Additionally, trips with lower than optimum numbers of hauls should also be considered for sampling purposes if the fishing fleet has changed to shorter trips (day trips). However, in this case, more trips per vessel and more vessels should be sampled to obtain the same target precision. In summary, the sampling levels obtained are indicative of what should be sampled, but in no way should they be treated rigidly. Sampling levels should be adaptable to changes in fleet activity without compromising existing fleet sampling coverage. In practice, a compromise between all factors involved in discard sampling should be reached to achieve an optimum sampling scheme. This should include other considerations, such as the resource requirements for sampling landings, fleet activity, state of the stocks, stock importance (national share of fishing quota), discarding levels, etc. In the specific case of the Irish discard program, the sampling scheme will be greatly influenced by the EU DCR specifications in discarding sampling thresholds, precision, and cost targets.

In conclusion, we have shown that optimum sampling levels in a discard sampling program can and should be estimated considering both financial and precision constraints.

In addition, the identification of costing variables and their impact on sampling levels can be a valuable tool in designing and managing sampling programs. Ultimately, our results show that when designing a discard sampling program, it is essential that the objectives of the program be clearly stated, with species, fleets, and (or) areas priorities specified.

Acknowledgements

We wish to thank the skippers who allowed FATs aboard their vessels and the FATs who collected the discard data. We also thank Michelle Allen for helpful comments on an earlier version of the manuscript. This project (Grant-aid Agreement No. PHD/01/002) was carried out with the support of the Marine Institute and the Marine Research, Technology, Development and Innnovation (RTDI) Measure, Productive Sector Operational Programme, National Development Plan 2000–2006.

References

Allen, M., Kilpatrick, D., Armstrong, M., Briggs, R., Perez, N., and Course, G. 2001. Evaluation of sampling methods to quantify discarded fish using data collected during discards project EC 95/094 by Northern Ireland, England and Spain. Fish. Res. **49**: 241–254.

Allen, M., Kilpatrick, D., Armstrong, M., Briggs, R., Course, G., and Perez, N. 2002. Multistage cluster sampling design and optimal sample sizes for estimation of fish discards from commercial trawlers. Fish. Res. **55**: 11–24.

Alverson, D.L., Freeberg, M.H., Murawski, S.A., and Pope, J.G. 1994. A global assessment of fisheries bycatch and discards. FAO Fish. Tech. Pap. No. 339.

Cochran, W.G. 1977. Sampling Techniques. John Wiley & Sons, Inc., New York.

Horppila, J., and Peltonen, H. 1992. Optimizing sampling from trawl catches: contemporaneous multistage sampling for age and length structures. Can. J. Fish. Aquat. Sci. **49**: 1555–1559.

International Council for the Exploration of the Sea (ICES). 2003. Report of the Working Group on the assessment of northern shelf demersal stocks. ICES CM 2003/ACFM:04.

Julious, S.A., and Debarnot, C.A.M. 2000. Why are pharmacokinetic data summarized by arithmetic means? J. Biopharmaceut. Stat. **10**(1): 55–71.

Payne, R.W. (*Editor*). 2002. The guide to GenStat release 6.1. Part 2: Statistics. VSN International, Oxford.

Pinheiro, J.C., and Bates, D.M. 2000. Mixed-effects models in S and S-PLUS. Springer-Verlag, New York.

Rochet, M.-J., Peronnet, I., and Trenkel, V.M. 2002. An analysis of discards from the French trawler fleet in the Celtic Sea. ICES J. Mar. Sci. **59**: 538–552.

Schweigert, J.F., and Sibert, J.R. 1983. Optimizing survey design for determining age structure of fish stocks: an example from British Columbia Pacific herring (*Clupea harengus pallasi*). Can. J. Fish. Aquat. Sci. **40**: 588–597.

Snijders, T., and Bosker, R. 1999. Multilevel analysis. SAGE Publications, London.

Stratoudakis, Y., Fryer, R.J., and Cook, R.M. 1998. Discarding practices for commercial gadoids in the North Sea. Can. J. Fish. Aquat. Sci. **55**: 1632–1644.

Stratoudakis, Y., Fryer, R.J., Cook, R.M., and Pierce, G.J. 1999. Fish discarded from Scottish demersal vessels: estimators of total discards and annual estimates for targeted gadoids. ICES J. Mar. Sci. **56**: 592–605.

Tamsett, D., and Janacek, G. 1999. Sampling trips for measuring discards in commercial fishing based on multilevel modelling of measurements in the North Sea from NE England. Fish. Res. **42**: 103–115.

Tamsett, D., Janacek, G., Emberton, M., Lart, B., and Course, G. 1999. Onboard sampling for measuring discards in commercial fishing based on multilevel modelling of measurements in the Irish Sea from NW England and N Wales. Fish. Res. **42**: 117–126.

Welham, S.J., and Thompson, R. 1997. Likelihood ratio tests for fixed model terms using residual maximum likelihood. J. R. Statist. Soc. B, **59**: 701–714.

Appendix A

The mixed models used in this paper can be expressed generally by the following mathematical formula, based on Pinheiro and Bates (2000):

$$\text{(A1)}\quad y_{vth} = \beta + \alpha X_{vth} + b_v + b_{vt} + \varepsilon_{vth}$$

$$(v = 1, \ldots, v', t = 1, \ldots, t_v, h = 1, \ldots, h_{vt})$$

$$b_v \sim N(0, S_v^2),\ b_{vt} \sim N(0, S_t^2),\ \text{and}\ \varepsilon_{vth} \sim N(0, S_h^2)$$

where β is the intercept of the model, X_{vth} is a variable with a fixed effect on y_{vth}, α is the increment in β due to X_{vth}, b_v is the random variable representing the deviation from the population mean of the mean of total discards per unit of effort (TDPUE) for vessel v, b_{vt} is the random variable representing the deviation from the mean TDPUE for vessel v of the mean TDPUE for the trip t on vessel v, ε_{vth} is the random variable representing the deviation of TDPUE for haul h on trip t on vessel v from the mean TDPUE for trip t, v' is the total number of vessels sampled, t_v is the number of trips sampled per vessel, h_{vt} is the number of hauls sampled per trip per vessel, S_v^2 is the between vessel variability in the population, S_t^2 is the between trip within vessel variability, and S_h^2 is the between haul within trip within vessel variability.

In eq. A1, β and αX_{vth} correspond to the fixed effects, whereas b_v, b_{vt}, and ε_{vth} correspond to the random effects of the mixed model. In this paper, X_{vth} represents fishing ground or targeted species, for example. Also, the designations used to specify the random parameters of the mixed models estimated (vessel, vessel-trip, and vessel-trip-haul) correspond to b_v, b_{vt}, and ε_{vth}, respectively.

Discharge-dependent covariation patterns in the population dynamics of brown trout (*Salmo trutta*) within a Cantabrian river drainage

Javier Lobón-Cerviá

Abstract: Patterns of spatial covariation in the population dynamics of brown trout (*Salmo trutta*) across Rio Esva (northwestern Spain) were explored by using the residuals from stock–recruitment relationships as indices of survival rates of spawner-to-recruit (STR), spawner-to-cohort size (STC), and spawner-to-spawner (STS). Positive correlations in pairwise comparisons among survival rates together with highly significant spatiotemporal variation in STC (74.3%) and STS (51.5%) explained by variation in STR provided evidence for persistent spatial covariation across the river drainage during the whole lifetime. Split-line regressions fitted to the survival rates versus river discharge in March (when trout emerge) highlighted the importance of discharge during, or just after, trout emergence as a major determinant of recruitment whose effects are reflected in the population over the lifetime and emphasized the synchrony between environmental processes and brown trout dynamics. Synchrony in recruitment is caused by hydrological synchrony that, in turn, is determined by climatic synchrony (rainfall) operating at the regional scale. The importance of discharge for recruitment is consistent with studies on native and introduced populations, suggesting its broad effect on the dynamics of stream brown trout across geographical regions.

Résumé : L'analyse des résidus des relations stock–recrutement comme indices de la survie des reproducteurs aux recrues (STR), de la survie des reproducteurs à la taille de la cohorte (STC) et de la survie des reproducteurs aux reproducteurs (STS) a permis d'explorer la structure de la covariation spatiale de la dynamique de population de la truite brune (*Salmo trutta*) dans le Rio Esva du nord-ouest de l'Espagne. Les corrélations positives dans les comparaisons appariées des taux de survie, ainsi que la variation spatio-temporelle très significative de STC (74,3 %) et de STS (51,5 %) qui s'explique par la variation de STR, sont des indices d'une covariation spatiale persistante au sein du bassin versant durant le cycle entier. Des régressions linéaires fragmentées ajustées aux taux de survie en fonction du débit de la rivière en mars (lors de l'émergence des truites) montrent l'importance du débit durant l'émergence des truites ou juste après l'émergence comme un facteur déterminant majeur du recrutement, dont les effets se répercutent durant la vie entière et mettent en lumière la synchronie entre les processus environnementaux et la dynamique de la truite brune. La synchronie du recrutement est causée par une synchronie hydrologique qui, à son tour, est déterminée par une synchronie climatique (précipitations) qui agit à l'échelle régionale. L'importance du débit pour le recrutement est confirmée par des études sur des populations indigènes et introduites, ce qui laisse croire que le débit a un effet étendu sur la dynamique de la truite brune des cours d'eau dans plusieurs régions géographiques.

[Traduit par la Rédaction]

Introduction

Population studies on stream-living salmonids have shown that variability in numerical abundance across spatiotemporal scales is the rule (Heggenes et al. 1999; Gibson 2002; Klemetsen et al. 2003) and that brown trout (*Salmo trutta*) populations are not an exception. Temporal within-site variations in abundance (Crisp 1993; Elliott 1994; Waters 1999) of magnitudes similar to or even greater than variations among nearby sites within a stream or among closely related streams have been described for a variety of stream-living brown trout populations within the natural European distribution (Mann et al. 1989; Milner et al. 1993; Kelly-Quinn et al. 1996) and for populations introduced into lotic environments across distant geographical regions such as North America (Newman and Waters 1989) and New Zealand (Allen 1951; Hayes 1995).

The abundance of spawners and recruits (the juveniles that incorporate into the population) and hydrological factors are thought to play a major role in determining population size (Elliott 1994; Knapp et al. 1998) upon which suites of density-dependent and density-independent factors are likely to operate at different spatiotemporal scales. However, while stock–recruitment relationships for single populations have been shown to explain little variation in the survival rates (Cattanéo et al. 2002; Lobón-Cerviá and Rincón 2004), an increasing appreciation of the importance of recruitment to population size suggested that adult abundance is recruitment dependent (Victor 1983; Freeman et al. 1988; Knapp et

Received 16 October 2003. Accepted 14 April 2004. Published on the NRC Research Press Web site at http://cjfas.nrc.ca on 17 December 2004.
J17792

J. Lobón-Cerviá. Museo Nacional de Ciencias Naturales, Consejo Superior de Investigaciones Científicas, C/José Gutiérrez Abascal, 2, Madrid, 28006 Spain (e-mail: MCNL178@mncn.csic.es).

doi: 10.1139/F04-118

al. 1998). Thus, annual recruitment magnitudes would be reflected in the age structure of the population (Fogarty et al. 1991; Doherty and Fowler 1994; Caley et al. 1996). Moreover, functional links between recruitment and hydrological factors have been described for a variety of stream-living populations of brown trout (Solomon and Paterson 1980; Jensen and Johnsen 1999; Spina 2001) and other salmonids (Clark 1992; Nehring and Anderson 1993; Latterell et al. 1998). The spatiotemporal scales under which suites of factors predominate have yet to be identified.

An approach in recent studies has been to explore patterns of spatial covariation or levels of synchrony in the survival rates. These patterns should provide information on the processes involved at the corresponding spatial scale and could be explored for the operation of synchronous causative factors. Thus, positive spatial covariation in the survival rates of Pacific salmon species revealed that the environmental factors determining recruitment operate over similar spatial scales (Coronado and Hilborn 1998; Peterman et al. 1998; Pyper et al. 2002). If this were the case in stream-living brown trout, patterns of covariation in recruitment across spatial scales would be reflected in the population structure at the corresponding spatial scale (Milner et al. 1993; Cattanéo et al. 2002) and the factors driving recruitment would be reflected, to some extent, in successive life stages (Cattanéo et al. 2003).

In this study, I attempted to (*i*) elucidate patterns of spatial covariation in the population dynamics of brown trout at the spatial scale of a river drainage, namely of Rio Esva, a typical drainage of the Cantabrian corridor of northwestern Spain, and (*ii*) identify the factors responsible for spatial covariation. Earlier studies in one of these streams revealed substantial differences in density among nearby sites but concomitant, discharge-dependent recruitment rates and linear relationships between annual recruitment magnitudes and cohort size (Lobón-Cerviá 2003; Lobón-Cerviá and Rincón 2004). This study is an extension to a substantially broader spatial scale expected to capture the habitat variability that typifies Cantabrian river drainages. The data set encompassed census data of 11–15 successive cohorts at 12 sites of four Rio Esva subbasins. I explored patterns of spatial covariation in the temporal fluctuations (synchrony) in the survival rates of three successive life stages and attempted to identify the relative importance of hydrological factors versus recruitment processes as causative factors of the observed patterns.

Materials and methods

Rio Esva and the study sites

Rio Esva was selected for this long-term, large-scale study because it is safe from major anthropogenic impacts. Stream morphology and hydrology remain natural and no human-induced alterations prevent fish movements or migratory pathways throughout the river network.

Rio Esva is a medium-sized (~500 km^2) coastal river drainage whose waters flow north across the Cantabrian corridor of northwestern Spain (Fig. 1) and is essentially fed by rainfall and runoff with no snow effects owing to the low altitude of the uppermost springs (i.e., 700 m above sea level). Within relatively high rainy conditions (1500 mm annual rainfall), discharge remains low and stable during the driest summer months (July–September), but increased rainfall in spring, autumn, and early winter may lead to strong fluctuations. For any month between October and June, year-to-year variation in total monthly discharge at the main stem of Rio Esva (gauging station, Fig. 1) varied by >10-fold. Overall, monthly discharge ranged from 6 to 160 hm^3 during the study years (1986–2003).

All running waters across the mountainous and rugged Rio Esva landscape flow over quartzite bedrock (Aramburu and Bastida 1995) resulting in a variety of shallow, fast-flowing, and well-oxygenated streams of various size and physiography. These streams whose substratum is essentially composed of pebble, gravel, and boulder are dominated by runs and riffles with a few scattered pools. The latter become deeper in bends where the streams crash against rocky slopes and shallower on runs just behind riffles on stream banks where vegetation grows or where erosive processes predominate. These streams flow through a mosaic of riparian forest alternating with meadowlands. In stream sections dominated by riparian forest, water surface is fully covered by leafy overhanging vegetation (i.e., canopy), preventing isolation, whereas in meadowlands, stream reaches are in full sunlit, with many sections holding intermediate characteristics. A variety of channel structures combine with substratum composition, current velocity, and canopy at the scale of stream sections (of a size ranging from several hundred to a few thousand metres) to conform the stream habitat heterogeneity available for brown trout.

Surveys previous to this study (J. Lobón-Cerviá, unpublished data) revealed a full occupation of Rio Esva by brown trout, reflecting a continuum of individuals from the estuary in the Cantabrian Sea upstream to detectable water reaches. Juveniles and adult individuals showed substantial spatial variation in size and abundance (Lobón-Cerviá 2000, 2003), but all-age individuals thrive at all streams with not even <10-m-long stream sections lacking individuals (J. Lobón-Cerviá, unpublished data).

For the purpose of this study, I attempted to include the environmental patchiness and variability of trout densities. This criterion, however, was mediated by the accessibility and size of the streams or sites and by the sampling efficiency. The aforementioned previous samples identified stream sections of variable densities where the sampling techniques provided highly accurate estimates of all life stages of the population (Lobón-Cerviá 1991, 2003). Accordingly, the study sites were selected to capture a within-site run–riffle–pool succession and the range of among-site variation in density, channel structure, and canopy and to be of a size (length 60–80 m, width 2–7 m, and mean depth <0.5 m) at which the accuracy of population estimates was maximized. Thus, the 12 sites were scattered along four contrasting subbasins, two of them flowing in an east–west direction towards the main stem of Rio Esva and the other two flowing in a west–east direction. In turn, these four streams are representative of the numerous streams flowing across the Cantabrian corridor. The streams and sites (Fig. 1) are Rio Chaballos (four sites, S1–S4), Castañedo (three sites, S8–S10), La Viella, (three sites, S5–S7), and Choudral (two

Fig. 1. Geographical location of Rio Esva (Asturias, northwestern Spain), with the streams and sites examined in this study indicated. GS indicates the location of the gauging station where discharge was recorded. Site numbers (S1–S12) as in Table 1.

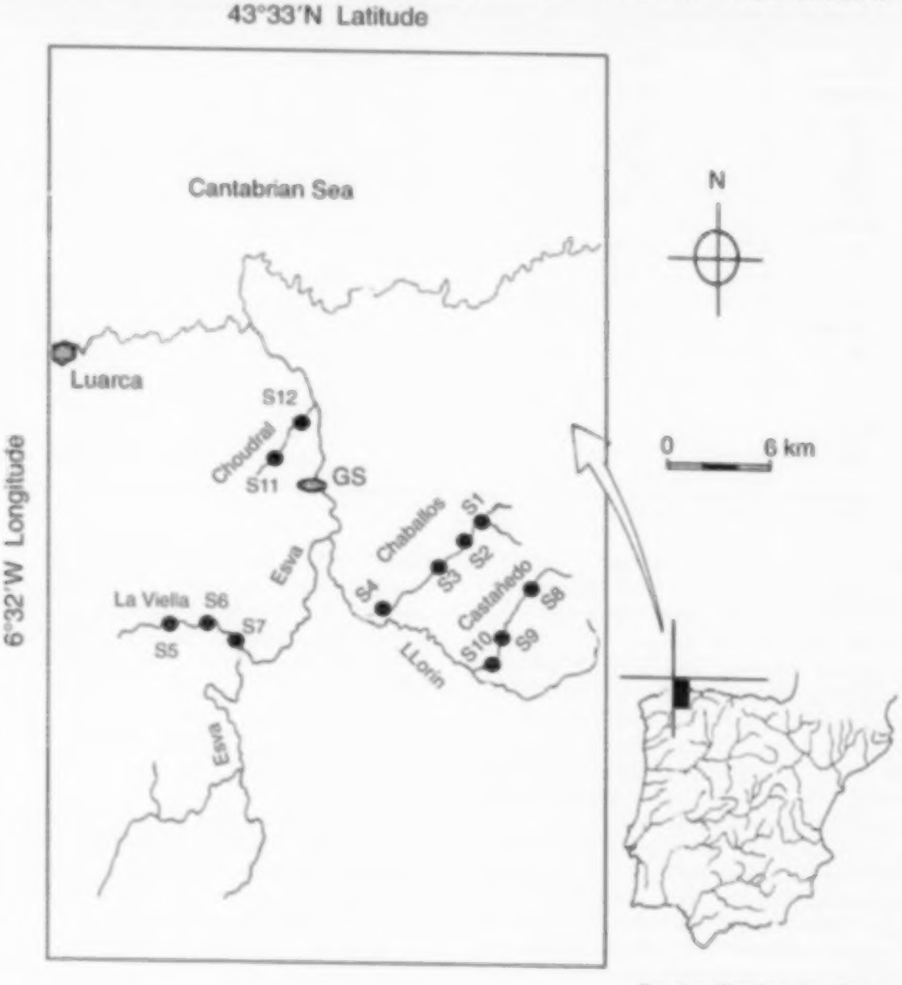

sites, S11 and S12). Major site characteristics are summarized in Table 1. Further details can be found in Lobón-Cerviá et al. (1995) and Lobón-Cerviá (2000).

Brown trout population

Over the whole river drainage, spawning occurs by the end of November to mid-December and emergence occurs by mid-March. Population birthdate was established on 15 March, whereas the maximum age for each cohort and site was assumed to be the age of the individuals in the sample before the total disappearance of that cohort. These stream populations are characterized by a short life span, with slight but persistent differences among sites (30–46 months). For any given site, >80% of the population was age 0 and age 1 with age-2 and a few age-3 individuals being scattered across sites and years (Lobón-Cerviá 2003). Cohort survival patterns assessed for Rio Chaballos brown trout revealed a period of negligible to low mortality prolonged for half the life cycle followed by a second period of heavy mortality of variable intensity depending on the cohort and site (Rincón and Lobón-Cerviá 2002; Lobón-Cerviá 2003). These two-phase mortality patterns were similar for other streams and sites.

Pilot studies based on extensive mark–recapture procedures, supported by the operation of two traps to collect fish moving downstream at the lowermost reaches of Rios Chaballos and La Viella, revealed low mobility and high site fidelity (Lobón-Cerviá 2000, 2003). Moreover, a long-term assessment of the reproductive ecology of these populations indicated a constant 1:1 sex ratio across spatiotemporal scales and that all 21-month-old females >11 cm spawn successfully every year with just a few females surviving to spawn twice (Lobón-Cerviá et al. 1997).

Data collection

Daily discharge ($m^3 \cdot s^{-1}$) in the main stem of Rio Esva was

Table 1. Major characteristics of the 12 sites of Rios Chaballos, La Viella, Castañedo, and Choudral (Rio Esva drainage) examined in this study. Also refer to Fig. 1.

Site	Length (m)	Width (m)	Depth (cm)	Area (m^2)	Volume (m^3)	Velocity ($m\cdot s^{-1}$)	Canopy (%)
Chaballos							
S1	75	2.5	20	240	43	0.25	0
S2	80	3.3	26	250	86	0.36	15
S3	70	3.8	22	220	42	0.31	20
S4	75	3.9	27	370	92	0.18	80
La Viella							
S5	70	3.4	18	260	46	0.20	85
S6	66	2.7	22	160	44	0.23	60
S7	70	3.2	23	190	74	0.30	30
Castañedo							
S8	65	2.9	23	150	54	0.13	40
S9	64	2.9	26	180	73	0.16	40
S10	75	3.9	20	320	79	0.21	70
Choudral							
S11	63	2.3	15	150	18	0.16	92
S12	70	2.5	16	200	26	0.15	95

Note: Data are mean values for each site averaged over the study years.

supplied by the Trevias gauging station located at middistance of the streams studied (Fig. 1). Assumedly, day-to-day variation in discharge in the main stem reflects day-to-day variation in the four streams studied.

Brown trout density was tracked from 1986 (Rio Chaballos), 1989 (Rio Choudral), and 1990 (all other sites). Census data were obtained under base flow conditions in January, May, and September. Sampling was conducted by blocking the sites with nets to apply the three-pass removal method (Seber 1982) with electrofishing techniques (Lobón-Cerviá 1991). These techniques have been shown to be size selective with reduced capture efficiency for smaller individuals (Lobón-Cerviá 1991). To prevent bias in the estimates of the youngest juveniles (i.e., recruits), I conducted sampling by mid-May when 2-month-old individuals have attained a size (4–6 cm) sufficient to be efficiently captured. All fish captured were measured (fork length) and assigned to age-classes easily detectable from length–frequency distributions. Doubtful assignments in larger (older) individuals were confirmed by scale readings. Bathymetric maps were drawn for every site and date just after sampling.

Data analysis

The number of individuals (N) for each site and date was calculated separately for age-0, age-1, and older fish. The values of N were estimated from $N = C_t/1 - q^s$ where q^s was obtained by solving the equation

$$sq^s/(1-q^s) - q/p + \sum_{i=1}^{3}(i-1)C_i/C_t = 0$$

All estimates were tested for the failure condition (Carle and Strub 1978; Otis et al. 1978)

$$\sum_{i=1}^{3}(s-i)C_i \le [(C_t-1)(s-1)/2]-1$$

where $s = 3$ occasions and C_t is the sum of the captures (C_i) obtained on each occasion i. Once the failure condition was assessed, I examined the goodness of fit (i.e., whether the probability of capture remains constant across capture efforts). This was tested with the statistic T_1 (Otis et al. 1978; Seber 1982)

$$T_1 = \sum_{i=1}^{s}(C_i - E_i)^2/E_i$$

where E_i is the number of individuals expected to be captured on each occasion i, which is Np/q^{i-1} and where N is the estimated number of individuals, p is the probability of capture, and $q = p - 1$. The statistic T_1 is distributed as a χ^2 with $s - 2$ degrees of freedom.

This analysis revealed a high capture efficiency for all life stages, seasons, and sites, with 94% of the estimates being significant and an average capturability of 90% for age-1 and older individuals and 75% for age-0 individuals (Lobón-Cerviá 2003). Densities were then referred to the numbers estimated for the area of each site and date (Lobón-Cerviá 2003).

On average, the abundance of each cohort and site was quantified 10 times from emergence to its final disappearance. For the purpose of this study, I selected three cohort traits to summarize the dynamics of each cohort and site as follows. (*i*) Recruitment (R) (individuals per square metre) was measured as the abundance of 2-month-old juveniles. (*ii*) I used the mean cohort size (individuals per square metre) as a measure of the year-class strength. Mean cohort size was calculated as the abundance of a cohort averaged from the second sample (i.e., 6-month-old individuals) to the maximum age observed. (*iii*) Spawner abundance (SA) (individuals per square metre) was measured as the abundance of females about to spawn in September, 19 months after emergence.

The residuals of the nonlinear stock (S) – recruitment (R) model (Ricker 1954)

$$(1) \qquad R = aS^{-bS}$$

were used as indices of survival rates. For each single site, fits of this model to the abundance of recruits, mean cohort size, and spawner abundance over the parental population (i.e., the abundance of female spawners the winter previous to recruitment) were obtained for the cohorts of the years 1987–2001 (sites S1, S3, and S4, Rio Chaballos), 1989–2001 (site S2, Rio Chaballos), 1990–2001 (Rio Choudral), and 1991–2001 (Rios Castañedo and La Viella). Thus, independent sets of survival rates were obtained for spawner-to-recruit (STR), spawner-to-cohort size (STC), and spawner-to-spawner (STS).

Covariation patterns were assessed through Pearson's product moment correlations among pairwise comparisons of the indices of survival rate of STR, STC, and STS. To examine whether the distance among sites influences levels of spatial covariation, Myers et al. (1997) proposed an estimate of the spatial scale as the distance over which the pairwise correlations are reduced by a factor e^{-1}. This can be readily estimated by fitting the covariance function

$$(2) \qquad R_d = R_0 e^{-d/v}$$

where R_0 is the correlation between sites at zero separation, v is the e-folding scale, and d is the distance among sites. The R_0 was constrained to have a value of ≤1. Two-phase or split-line regressions (Perry 1982; Nickerson et al. 1989) were used to fit the trajectories described by the indices of survival rate over hydrological factors. A two-phase regression is defined as

$$(3) \qquad Y = a_1 + b_1 X (\text{for any } X \leq k) + a_2 - b_2 X (\text{for } X > k)$$

with the restriction for continuity $a_1 + b_1 k = a_2 - b_2 k$, at the break point ($k$), where the positive direction of the trajectory described by the dependent variable (Y) switches towards a negative direction. Least squares, iterative quasi-Newton algorithms (Dennis and Schnabel 1983), as offered by the statistical package Statistica 6.0™, were used to fit all linear and nonlinear regressions.

Results

Stock–recruitment relationships

Year-to-year variation in the abundance of parental stocks showed weak potential as a predictor of the abundance of recruits, cohort size, and the subsequent abundance of the parental stock. Fits of the nonlinear Ricker model (eq. 1) revealed poor relationships between the abundance of recruits versus the abundance of female spawners. The only exceptions were site S1 where 63.5% of the variations in recruitment were nonsignificatively ($p = 0.47$) explained by variations in the abundance of female spawners and sites S2, S5, and S6 where the fits were significant ($p < 0.05$) and explained 47.2%, 30.0%, and 20.5% of the recruitment variations, respectively. At all other sites, the fits were nonsignificant and the variance explained ranged from 0.1% (site S9) to 13.5% (site S12). Weaker predictive potentials were yet detected when fitting the nonlinear model to cohort size and to the subsequent parental stock versus the abundance of female spawners. These fits showed an overall lack of significance with the only exceptions being cohort size for site S5 (21.0% of the variance explained, $p = 0.04$), site S6 (7.5% of the variance explained, $p = 0.004$), and site S7 (15.9% of the variance explained, $p = 0.009$).

Patterns of covariation in the indices of survival rates

Pairwise correlations were computed for the indices of survival rates of STR, STC, and STS. All correlation coefficients (66 for each data set) were positive (Table 2). For STR, there were 48 significant correlations ($p < 0.05$), the significance of 10 correlation coefficients was in the range $0.05 < p < 0.10$, and in eight instances, the significance was at $p > 0.10$ (Table 2). For STC, there were 36 significant correlations, 13 correlations were in the range $0.05 < p < 0.10$, and 17 correlations were at $p > 0.10$ (Table 2). For STS, there were 28 significant correlations, eight correlations in the range $0.05 < p < 0.10$, and 30 correlations were at $p > 0.10$ (Table 2).

The amount and magnitude of the correlation coefficients decreased slightly for the older life stages. Yet, numerous sites located in different streams showed consistent significance versus all other sites and revealed no trend to greater magnitudes among nearby sites. Moreover, plots of these coefficients versus stream distance among sites (kilometres) showed no tendency to decreased values with increased distance (Fig. 2), and fits of eq. 2 to the STR, STC, and STS indices of survival rates versus stream distance among sites showed extremely weak relationships with levels of significance at $p = 0.54$ (STR) (Fig. 2*a*), $p = 0.73$ (STC) (Fig. 2*b*), and $p = 0.65$ (STS) (Fig. 2*c*).

Relationships among the indices of survival rates of STR, STC, and STS

An inspection of spatiotemporal variations of the indices of survival rates of STC and STS showed strongly consistent, positive trends versus STR, and linear regressions explained 74.3% and 51.5% of the spatiotemporal variations in STC and STS due to variations in STR indices of survival rates (Figs. 3*a* and 3*b*). Moreover, a linear regression explained 76.5% of the spatiotemporal variations in the STS due to variations in STC (Fig. 3*c*).

The high magnitudes and significance levels of the correlation coefficients observed among sites in combination with these highly significant linear trends offered strong evidence of covariation in the indices of survival rates of recruitment, cohort size, and spawner abundance over the river drainage.

Discharge variations and the patterns of survival

Visual inspections of the trajectories described by the indices of survival rate of STR over total discharge in March (cubic hectometres) when brown trout emerge revealed strongly consistent patterns (Fig. 4*a*). At the 12 sites, these indices increased from the lowest discharge levels recorded during the dry springs of the years 1990, 1997, and 1998 (6.3, 13.6, and 14.8 hm^3, respectively) to attain maximum values in years of average discharge (30–40 hm^3, years 1987, 1988, and 1996) beyond which they reversed to decreased values with increased discharge. Thus, at the 12 sites, these indices of survival rates attained the lowest values at the two extremes of discharge, during the severely drought spring of 1990 (6.3 hm^3) and during the most rainy

Table 2. Pairwise correlation coefficients for the spawner-to-recruit (STR), spawner-to-cohort size (STC), and spawner-to-spawner (STS) indices of survival rates among the 12 sites (S1–S12) examined in Rios Chaballos, La Viella, Castañedo, and Choudral.

	S1 (15)	S2 (13)	S3 (15)	S4 (15)	S5 (11)	S6 (11)	S7 (11)	S8 (11)	S9 (11)	S10 (12)	S11 (12)
Spawner-to-recruit											
S2	**0.72**										
S3	**0.55**	**0.57**									
S4	0.20	**0.64**	0.40								
S5	**0.74**	0.51	**0.68**	**0.72**							
S6	0.26	**0.72**	**0.58**	0.49	0.24						
S7	**0.67**	**0.59**	**0.70**	**0.72**	**0.73**	**0.68**					
S8	**0.69**	**0.56**	**0.71**	**0.70**	0.55	**0.65**	**0.67**				
S9	**0.78**	**0.71**	**0.79**	**0.69**	**0.84**	0.34	0.57	0.56			
S10	**0.60**	**0.90**	**0.69**	**0.77**	**0.69**	**0.71**	**0.65**	**0.66**	**0.81**		
S11	0.49	**0.76**	0.49	**0.60**	0.06	**0.82**	0.53	**0.62**	0.26	0.47	
S12	**0.67**	**0.83**	**0.70**	**0.64**	0.31	**0.85**	**0.59**	**0.83**	0.50	**0.75**	**0.85**
Mean	0.58	0.68	0.64	0.67	0.49	0.68	0.60	0.67	0.52	0.61	0.85
Spawner-to-cohort size											
S2	**0.66**										
S3	**0.58**	**0.60**									
S4	0.48	**0.59**	**0.68**								
S5	**0.77**	**0.59**	**0.69**	**0.93**							
S6	0.14	**0.68**	0.23	0.46	0.26						
S7	0.53	**0.81**	0.57	0.59	0.48	**0.76**					
S8	**0.62**	**0.59**	**0.64**	**0.71**	0.57	0.48	0.36				
S9	**0.76**	**0.82**	**0.73**	**0.84**	**0.80**	0.41	0.57	**0.71**			
S10	**0.75**	**0.85**	**0.70**	**0.78**	**0.74**	0.44	**0.74**	0.54	**0.91**		
S11	0.57	**0.76**	0.40	**0.63**	0.41	**0.83**	**0.63**	0.56	0.60	0.61	
S12	0.43	**0.72**	0.29	0.53	0.29	**0.69**	0.47	0.46	0.59	0.54	**0.92**
Mean	0.57	0.70	0.55	0.68	0.51	0.60	0.55	0.57	0.70	0.58	0.92
Spawner-to-spawner											
S2	**0.56**										
S3	0.46	**0.57**									
S4	0.45	0.50	**0.56**								
S5	0.04	0.31	0.46	**0.74**							
S6	0.29	**0.87**	**0.74**	**0.77**	0.59						
S7	0.09	**0.75**	0.34	0.33	0.11	**0.68**					
S8	0.35	**0.74**	**0.65**	**0.71**	0.44	**0.73**	0.29				
S9	0.48	**0.66**	0.53	**0.67**	**0.75**	**0.64**	0.31	0.56			
S10	0.37	**0.87**	0.38	**0.71**	0.50	**0.83**	**0.76**	0.57	**0.69**		
S11	0.14	**0.75**	0.42	0.43	0.23	**0.65**	**0.83**	**0.61**	0.39	**0.70**	
S12	0.06	0.51	0.02	0.46	0.26	0.44	0.42	0.54	0.32	0.46	**0.74**
Mean	0.30	0.65	0.46	0.60	0.41	0.66	0.52	0.57	0.47	0.58	0.74

Note: The number of data pairs (*i.e.*, cohorts) for each site is provided in parentheses. Levels of significance: $p < 0.05$ (bold); $0.05 \le p < 0.10$ (underlined); $p > 0.10$ (others).

springs of the years 1995 and 2001 (70.3 and 65.5 hm^3, respectively).

Consistent with the highly significant linear relationships previously detected among STC and STS as a function of STR, the indices of survival rates of STC and STS described the very same trajectories over river discharge at the time of brown trout emergence (Figs. 4*b* and 4*c*), and significant fits of two-phase regressions (eq. 3) were obtained between the indices of survival of STC and STS versus discharge for either single site. As well, fits for pooled sites were highly significant for the three life stages. In these fits, river discharge explained 35%, 44%, and 40% of the overall year-to-year variation in the indices of survival rates of STR, STC, and STS, respectively. Constants for the two-phase regressions for single and for pooled sites are shown in Table 3.

These results revealed that despite substantial among-site differences in density and survival rates across life stages, river discharge during brown trout emergence consistently predicted the survival rates of the recruitment of the current year, of the cohort size, and of the abundance of females about to spawn 2 years later (Fig. 4).

Discussion

The results of this study offered strong evidence for positive spatial covariation in the survival rates of successive life

Fig. 2. Magnitude of pairwise correlations among the indices of survival rates of (*a*) spawner-to-recruit (STR), (*b*) spawner-to-cohort size (STC), and (*c*) spawner-to-spawner (STS) as a function of stream distance among sites. Horizontal lines represent mean correlations.

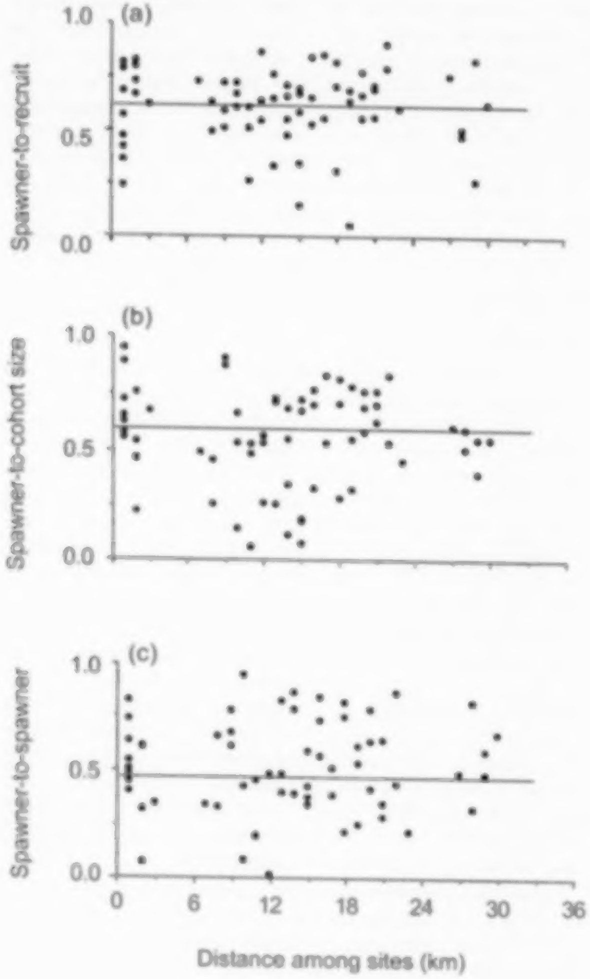

Fig. 3. Positive linear trends of the indices of survival rates of (*a*) spawner-to-cohort size (STC) and (*b*) spawner-to-spawner (STS) as a function of spawner-to-recruit (STR). Regression equations: STC = 0.003 + 0.361STR ($r^2 = 0.744$, $p < 0.0001$) and STS = –0.0001 + 0.092STR ($r^2 = 0.503$, $p < 0.0001$). (*c*) Positive linear trend of the indices of survival rates of STS as a function of STC. Regression equation: STS = –0.0017 + 0.272STC ($r^2 = 0.750$, $p < 0.0001$).

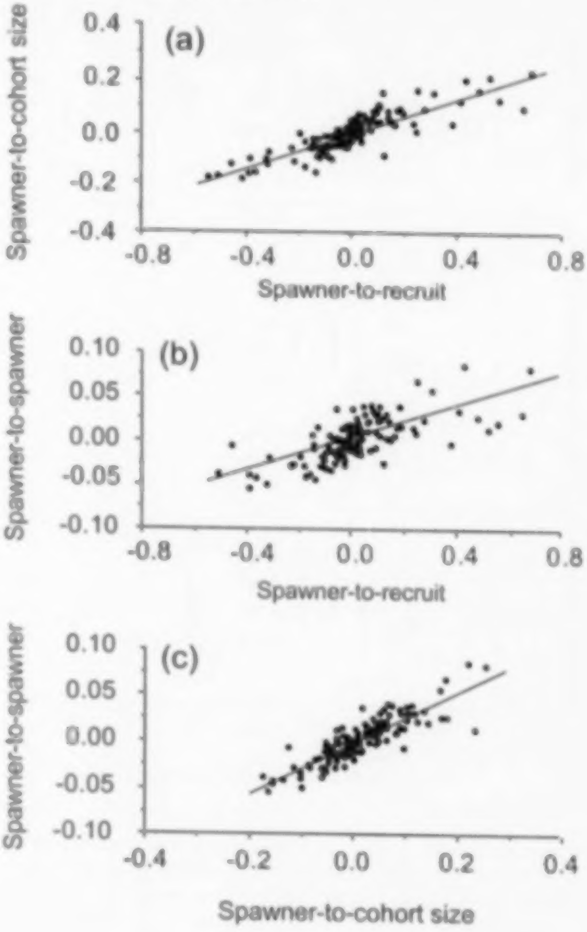

stages of brown trout within an environmentally complex Cantabrian drainage. Similar levels of spatial covariation in recruitment and in the adult components of the population (i.e., STC and STS) and highly significant correlations between the indices of survival rates of STC and STS versus STR and also between STC versus STS revealed persistent synchrony during the whole lifetime. Consistent spatial covariation suggested that a shared environmental factor of temporal variation operates across sites of different streams located over >30 km (maximum separation among sites), a distance slightly smaller than the hypothesized 50-km spatial scale expected to result in recruitment correlations for freshwater fishes (Myers et al. 1997).

Covariation across spatial scales may be caused by several factors. Dispersal or fish movements have been postulated to be a major synchronizing factor (Paradis et al. 1999). If this were the case, levels of covariation would have been stream specific, or grouped for a variety of nearby sites or related to the distance among sites. That is, the trajectories described by the correlation coefficients among survival rates versus distance among sites would have shown consistent trends to increased levels of covariation across fixed spatial scales. No evidence of such trends among the study sites is consistent with the restricted movements and high levels of site fidelity revealed by several-year mark–recapture tagging procedures assessed in Rios Chaballos and La Viella brown trout (Lobón-Cerviá 2000, 2003), and it makes dispersal to be a most unlikely factor determining covariation patterns.

A continuum of biotic–abiotic interactions has been suggested to regulate fish populations along stream gradients (Zalewski and Naiman 1985). Thus, the location of the site

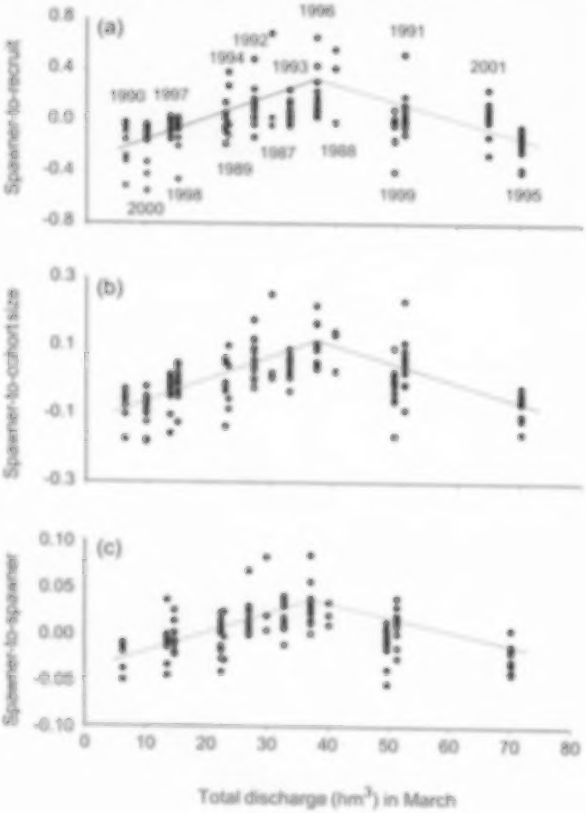

Fig. 4. Two-phase trajectories described by the indices of survival rates of (*a*) spawner-to-recruit (STR), (*b*) spawner-to-cohort size (STC), and (*c*) spawner-to-spawner (STS) over total monthly discharge in March of the year of recruitment. For each life stage, an overall two-phase regression for pooled sites is depicted with indication of recruitment year. Coefficients of two-phase regressions for single and for pooled sites are given in Table 3.

within the stream would determine the predominance and intensity of a particular suite of factors. Reduced hydrological effects and increased biotic interactions would be expected to operate at downstream sites (Zalewski et al. 1985) due to an overall increase in habitat complexity (Horwitz 1978). Owing to the geomorphologic and landscape structures of Rio Esva, streams resemble a mosaic of habitats of heterogeneous quality rather than upstream–downstream gradients of habitat complexity. Therefore, hydrological factors appear to operate in a similar manner at all sites with no evidence of reduced intensity downstream. Linear relationships among the indices of survival rates of STR, STC, and STS across spatiotemporal scales further support this claim.

Discharge appears as a major factor responsible for the high levels of spatial covariation in the population dynamics of brown trout across the Rio Esva drainage. Year-to-year variation in river discharge at the time of emergence (i.e., March) consistently predicted recruitment rates and, at similar levels of significance, the survival rates of mean cohort size and the abundance of females about to spawn. Discharge-dependent survival rates during the lifetime are consistent with the linear relationships shown by the survival rates of recruits, cohort size, and spawner abundance and further imply that the importance of river discharge is limited to the time of emergence but its strength is reflected in the population structure over the years. As a consequence, population size at the scale of the river drainage mainly depends on discharge through its profound effects on the youngest juveniles (Lobón-Cerviá and Rincón 2004) in a manner that the operation of density-dependent or density-independent postrecruitment processes, including natural disturbance such as severe floods and drought (which were recorded during the study period; Lobón-Cerviá 1996, 2003), might not be sufficiently strong to obscure the overwhelming importance of discharge on recruitment. That is, spatial covariation in the adult components of the population depends on the previous synchrony on the youngest juveniles rather than on the operation of synchronizing factors acting on postrecruitment stages.

In a previous study, Lobón-Cerviá and Rincón (2004) highlighted the mechanism operating on recruitment in Rio Chaballos, namely the synchronized discharge-dependent availability of microhabitats suitable for the youngest juveniles soon after emergence. Year-to-year variation in the availability of microhabitats suitable for recruits matches the split-line trajectory described by discharge. In turn, discharge and stream channel structure interact at a site scale to result in site-specific areas suitable for the youngest juveniles and therefore in site-specific recruitment magnitudes.

The large-scale spatial patterns in the survival rates of recruits revealed in this study emphasize the importance of discharge and support the operation of synchronized environmental mechanisms on recruitment throughout the river drainage. The annual rates of recruitment are determined by the availability of microhabitats imposed by discharge that, in turn, is induced by rainfall, a climatic factor operating at a broader, regional scale. Thus, year-to-year variation in March rainfall induces variations in discharge to reset the survival rates of recruits over the river drainage.

Linear relationships among the survival rates of STR, STC, and STS or among the abundance of successive life stages appear to be common in stream salmonids (Beard and Carline 1991; Kennedy and Crozier 1993; Whalen et al. 2000), although more complex and even negative relationships have been described (Elliott 1996; Knapp et al. 1998; Cattanéo et al. 2002). Continuous population growth predicted by linear processes appears to be especially relevant in discharge-driven, short-living populations like the Rio Esva brown trout. Year-class strength is to be maintained from recruitment to spawning, regardless of whether mortality is density dependent, and even under most unfavorable discharge conditions, minor levels of recruitment may yet guarantee survivors to spawn.

Few studies have reported covariation patterns in stream-living brown trout at a drainage scale (Milner et al. 1993; Cattanéo et al. 2003), and still fewer have identified the operation of a common causative factor (Cattanéo et al. 2003). However, temporal variations in discharge have long been recognized to influence recruitment. Discharge-limited survival rates of the youngest juveniles have been described for

Table 3. Coefficients of the two-phase regressions for the indices of survival rates of spawner-to-recruit (STR), spawner-to-cohort size (STC), and spawner-to-spawner (STS) versus total monthly discharge (hm^3) in March for each single site (S1–S12) and for pooled sites over the years.

Site	a_1	b_1	k	a_2	b_2	r^2
Spawner-to-recruit						
S1 (15)	–0.366	0.017	33.4	0.556	–0.011	0.43
S2 (13)	–0.297	0.015	34.5	0.490	–0.007	0.47
S3 (15)	–0.683	0.034	34.5	1.390	–0.026	0.65
S4 (15)	–0.082	0.005	33.3	0.251	–0.005	0.70
S5 (11)	–0.193	0.011	25.5	0.167	–0.003	0.81
S6 (11)	–0.734	0.033	40.3	1.683	–0.027	0.71
S7 (11)	–0.347	0.018	32.9	0.604	–0.011	0.71
S8 (11)	–0.241	0.012	37.3	0.579	–0.103	0.61
S9 (11)	–0.318	0.017	27.1	0.278	–0.005	0.59
S10 (11)	–0.117	0.005	37.3	0.226	–0.004	0.50
S11 (12)	–0.078	0.003	39.6	0.104	–0.001	0.46
S12 (12)	–0.133	0.006	40.5	0.373	–0.006	0.62
Pooled (148)	–0.277	0.013	35.8	0.539	–0.009	0.35
Spawner-to-cohort size						
S1 (15)	–0.146	0.007	31.9	0.179	–0.003	0.60
S2 (13)	–0.128	0.007	35.6	0.370	–0.007	0.80
S3 (15)	–0.226	0.011	33.9	0.469	–0.009	0.53
S4 (15)	–0.057	0.003	37.3	0.212	–0.004	0.49
S5 (11)	–0.120	0.007	27.1	0.135	–0.003	0.50
S6 (11)	–0.154	0.006	51.5	1.030	–0.017	0.75
S7 (11)	–0.098	0.005	35.1	0.169	–0.003	0.50
S8 (11)	–0.178	0.008	37.3	0.293	–0.005	0.68
S9 (11)	–0.225	0.011	34.3	0.348	–0.006	0.63
S10 (11)	–0.227	0.013	25.1	0.175	–0.003	0.75
S11 (12)	–0.047	0.002	43.9	0.199	–0.004	0.55
S12 (12)	–0.060	0.003	45.6	0.278	–0.005	0.48
Pooled (148)	–0.121	0.006	36.8	0.281	–0.005	0.44
Spawner-to-spawner						
S1 (15)	–0.037	0.002	32.9	0.042	–0.001	0.50
S2 (13)	–0.039	0.002	35.4	0.106	–0.002	0.85
S3 (15)	–0.046	0.002	36.0	0.134	–0.003	0.40
S4 (15)	–0.019	0.001	42.8	0.109	–0.002	0.45
S5 (11)	–0.009	0.0005	37.3	0.034	–0.0007	0.17
S6 (11)	–0.035	0.002	38.3	0.113	–0.002	0.87
S7 (11)	–0.016	0.0008	39.5	0.071	–0.001	0.49
S8 (11)	–0.069	0.003	37.3	0.117	–0.002	0.69
S9 (11)	–0.125	0.006	27.1	0.081	–0.002	0.66
S10 (11)	–0.049	0.002	38.1	0.103	–0.002	0.81
S11 (12)	–0.021	0.001	42.2	0.074	–0.001	0.52
S12 (12)	–0.019	0.0007	52.2	0.126	–0.002	0.60
Pooled (148)	–0.032	0.0017	36.5	0.083	–0.0016	0.40

Note: Number of data pairs used to fit each two-phase regression is given in parentheses. k is the break point upon which the trajectories switch the direction of the survival rates and r^2 is the variance explained. All slopes and k values are significant at, at least, $p < 0.05$.

a variety of populations across the European range of brown trout including streams in the United Kingdom (Solomon and Paterson 1980; Milner et al. 1993; Elliott et al. 1997), in northern and boreal latitudes (Jensen and Johnsen 1999; Mäki-Petäys et al. 1999), and in southern Mediterranean latitudes (Cattanéo et al. 2002, 2003). Similarly, numerous introduced populations across geographical (climatic) North American regions appear to be constrained by discharge variations, including Michigan (Nuhfer et al. 1994), Montana (Nelson 1986), Minnesota (Newman and Waters 1989), Colorado (Nehring and Anderson 1993; Latterell et al. 1998), and California (Strange et al. 1992).

These studies provide evidence for the operation of stochastic processes related to rainfall- or snowmelt-induced discharge conditions on the temporal within-site variation of recruitment as a common phenomenon across geographical regions and point out that, similar to Rio Esva, its operation is of major importance during or just after brown trout emergence. Nonetheless, relative to the more complex, two-phase patterns elucidated for Rio Esva, the relationships between recruitment and discharge described by those studies were essentially linear with negative effects of increased discharge. Differences in shape among discharge–recruitment relationships may reflect different ranges of discharge variability among geographical regions or different effects of discharge at a stream scale but also that the data sets examined by those studies might not have been long enough to capture the range of variability needed to detect two-phase patterns. The range of driest versus rainiest springs rarely occurs within short periods of years and the studies above were short-term assessments relative to a 15-year data set examined for Rio Esva.

In conclusion, the results of this study are consistent with recent studies that indicate a predominant role of regional processes in determining survival rates of salmonids including Pacific (Coronado and Hilborn 1998; Peterman et al. 1998; Pyper et al. 2002) and Atlantic–Mediterranean (Cattanéo et al. 2002, 2003) species or populations and emphasize the importance of discharge as a major factor determining spatial covariation in recruitment whose consequences persist during the lifetime. In the light of these results, forecasting the population size of Rio Esva and probably of other nearby river drainages subject of the same climatic conditions (i.e., rainfall-induced discharge conditions) may be readily obtained from stream flow measurements, data that are currently recorded by numerous gauging stations along the Cantabrian range of brown trout.

The operation of discharge as a determinant of recruitment apparently differs among riverine systems or among climatic regions. Research is needed to identify common spatial regions for the operation of discharge and levels of transferability of discharge–recruitment relationships among regions. Further explorations into the complex relationships between stream channel morphology and discharge conditions to arise habitat suitable for recruits at a site scale (Lobón-Cerviá and Rincón 2004) may contribute substantially to the development of models to quantify the impact of a variety of natural processes and anthropogenic activities at local and regional scales.

Acknowledgments

This study was financially supported by three successive Comisión Inter-misisterial para la Ciencia y la Technología (CICYT) (formerly MEC-DGCYT) projects (reference No. PB84-0142, PB89-0048, and PB92-0045) and partially funded by the Municipality of Valdés (Asturias). Permission for fishing was by agreement between the Consejo Superior de Investigaciones Científicas and Principado de Asturias.

References

Aramburu, C., and Bastida, F. 1995. Geología de Asturias. Ediciones TREA, Gijón, Spain.

Allen, R.A. 1951. The Horokiwi stream. A study of a trout population. N.Z. Dep. Fish. Bull. No. 10.

Beard, T.D., Jr., and Carline, R.F. 1991. Influence of spawning and other stream habitat features on spatial variability of wild brown trout. Trans. Am. Fish. Soc. **120**: 711–722.

Caley, M.J., Carr, M.H., Hixon, M.A., Hughes, T.P., Jones, G.P., and Menge, B.A. 1996. Recruitment and the local dynamics of open marine populations. Annu. Rev. Ecol. Syst. **27**: 477–500.

Carle, F.L., and Strub, M.R. 1978. A new method for estimating population size from removal data. Biometrics, **34**: 621–630.

Cattanéo, F., Lamouroux, N., Breil, P., and Capra, H. 2002. The influence of hydrological and biotic processes on brown trout population dynamics. Can. J. Fish. Aquat. Sci. **59**: 12–22.

Cattanéo, F., Hugueny, B., and Lamouroux, N. 2003. Synchrony in brown trout, *Salmo trutta*, population dynamics: a 'Moran effect' on early-life stages. Oikos, **100**: 43–55.

Clark, R.A. 1992. Influence of stream flow and stock size on recruitment of Arctic grayling (*Thymallus thymallus*) in the Chena River, Alaska. Can. J. Fish. Aquat. Sci. **49**: 1027–1034.

Coronado, C., and Hilborn, R. 1998. Spatial and temporal factors affecting survival in coho salmon (*Oncorhynchus kisutch*) in the Pacific Northwest. Can. J. Fish. Aquat. Sci. **55**: 2067–2077.

Crisp, D.T. 1993. Population densities of juvenile trout (*Salmo trutta*) in five upland streams and their effects upon growth, survival and dispersal. J. Appl. Ecol. **30**: 759–771.

Dennis, J.E., and Schnabel, R.B. 1983. Numerical methods for unconstrained optimization and nonlinear equations. Prentice-Hall, Englewood Cliffs, N.J.

Doherty, P., and Fowler, T. 1994. An empirical test of recruitment limitations in a coral reef fish. Science (Washington, D.C.), **263**: 935–939.

Elliott, J.M. 1994. Quantitative ecology and the brown trout. Oxford Series in Ecology and Evolution. Oxford University Press, Oxford, UK.

Elliott, J.M. 1996. The relationship between smolt density and fry density in salmonids. J. Fish Biol. **48**: 1030–1032.

Elliott, J.M., Hurley, M.A., and Elliott, J.A. 1997. Variable effects of droughts on the density of a sea-trout *Salmo trutta* population over 30 years. J. Appl. Ecol. **34**: 1229–1238.

Fogarty, M.C., Sissenwine, M.P., and Cohen, E.B. 1991. Recruitment variability and the dynamics of exploited marine populations. Trends Ecol. Evol. **6**: 241–246.

Freeman, M.C., Crawford, M.K., Barret, J.C., Facey, D.E., Flood, M.G., Hill, J., Stouder, D.J., and Grossman, G.D. 1988. Fish assemblage stability in a southern Appalachian stream. Can. J. Fish. Aquat. Sci. **45**: 1949–1958.

Gibson, R.J. 2002. The effects of fluvial processes and habitat heterogeneity on distribution, growth and densities of juvenile Atlantic salmon (*Salmo salar* L.) with consequences on abundance of the adult fish. Ecol. Freshw. Fish, **11**: 207–222.

Hayes, J.W. 1995. Spatial and temporal variation in the relative density and size of juvenile brown trout in the Kakanui River, North Otago, New Zealand. N.Z. J. Mar. Freshw. Res. **29**: 393–407.

Heggenes, J., Baglinière, J.L., and Cunjak, R.A. 1999. Spatial niche variability for young Atlantic salmon (*Salmo salar*) and brown trout (*S. trutta*) in heterogeneous streams. Ecol. Freshw. Fish, **8**: 1–21.

Horwitz, R.J. 1978. Temporal variability patterns and the distributional patterns of stream fishes. Ecol. Monogr. **48**: 307–321.

Jensen, A.J., and Johnsen, B.O. 1999. The functional relationship between peak spring floods and survival and growth of juvenile Atlantic salmon (*Salmo salar*) and brown trout (*Salmo trutta*). Funct. Ecol. **13**: 778–785.

Kelly-Quinn, M., Tierney, D., Roche, W., and Bracken, J.J. 1996. Distribution and abundance of trout populations in moorland

and afforested upland nursery streams in county Wicklow. Proc. Roy. Irish Soc. **96B**: 127–139.

Kennedy, G.J.A., and Crozier, W.W. 1993. Juvenile Atlantic salmon (*Salmo salar*) — production and prediction. *In* Production of juvenile Atlantic salmon, *Salmo salar*, in natural waters. *Edited by* R.J. Gibson and R.E. Cutting. Can. Spec. Publ. Fish. Aquat. Sci. No. 118. pp. 179–187.

Klemetsen, A., Amundsen, P.A., Dempson, J.B., Jonsson, B., Jonsson, N., O'Connell, F.O., and Mortensen, E. 2003. Atlantic salmon *Salmo salar* L., brown trout *Salmo trutta* L., and Arctic charr *Salvelinus alpinus* (L.): a review of aspects of their life histories. Ecol. Freshw. Fish. **12**: 1–59.

Knapp, R.A., Vredenburg, V.T., and Matthews, K.R. 1998. Effects of stream channel morphology on golden trout spawning habitats and recruitment. Ecol. Appl. **8**: 1104–1117.

Latterell, J.J., Fausch, K.D., Gowan, C., and Riley, S.C. 1998. Relationship of trout recruitment to snowmelt runoff flows and adult trout abundance in six Colorado Mountain streams. Rivers, **6**: 240–250.

Lobón-Cerviá, J. 1991. Dinámica de poblaciones de peces. Pesca eléctrica y los métodos de capturas sucesivas en la estima de abundancias. Monografías No. 3. Museo Nacional de Ciencias Naturales (CSIC), Madrid, Spain.

Lobón-Cerviá, J. 1996. Response of a stream fish assemblage to a severe spate in Northern Spain. Trans. Am. Fish. Soc. **125**: 913–919.

Lobón-Cerviá, J. 2000. Determinants of parr size variations within a population of brown trout *Salmo trutta* L. Ecol. Freshw. Fish, **9**: 92–102.

Lobón-Cerviá, J. 2003. Spatio-temporal dynamics of brown trout production in a Cantabrian stream: effects of density and habitat quality. Trans. Am. Fish. Soc. **132**: 621–637.

Lobón-Cerviá, J., and Rincón, P.A. 2004. Environmental determinants of recruitment and their influence on the population dynamics of stream-living brown trout *Salmo trutta* L. Oikos, **105**: 471–476.

Lobón-Cerviá, J., Utrilla, C.G., and Rincón, P.A. 1995. Variations in the population dynamics of the European eel *Anguilla anguilla* (L.) along the course of a Cantabrian river. Ecol. Freshw. Fish, **4**: 17–27.

Lobón-Cerviá, J., Utrilla, C.G., Rincón, P.A., and Amezcua, F. 1997. Environmentally induced spatio-temporal variations in the fecundity of brown trout *Salmo trutta* L.: trade offs between egg size and number. Freshw. Biol. **38**: 277–288.

Mäki-Petäys, A., Muotka, T., and Huusko, A. 1999. Densities of juvenile brown trout (*Salmo trutta*) in two subarctic rivers: assessing the predictive capability of habitat preference indices. Can. J. Fish. Aquat. Sci. **56**: 1420–1427.

Mann, R.H.K., Blackburn, J.H., and Beaumont, W.R.C. 1989. The ecology of brown trout *Salmo trutta* in English chalk streams. Freshw. Biol. **21**: 57–70.

Milner, N.J., Wyatt, R.J., and Scott, M.D. 1993. Variability in the distribution and abundance of stream salmonids and the associated use of habitat models. J. Fish Biol. **43**(Suppl. A): 103–119.

Myers, R.A., Mertz, G., and Bridson, J. 1997. Spatial scales of interannual recruitment variations of marine, anadromous, and freshwater fish. Can. J. Fish. Aquat. Sci. **54**: 1400–1407.

Nehring, R.B., and Anderson, R.M. 1993. Determination of population-limiting critical salmonid habitats in Colorado streams using the physical habitat simulation system. Rivers, **4**: 1–19.

Nelson, F.A. 1986. Effect of flow fluctuations on brown trout in the Beaverhead River, Montana. N. Am. J. Fish. Manag. **6**: 551–559.

Newman, R.M., and Waters, T.F. 1989. Differences in brown trout (*Salmo trutta*) production among contiguous sections of an entire stream. Can. J. Fish. Aquat. Sci. **46**: 203–213.

Nickerson, D.M., Facey, D.E., and Grossman, G.D. 1989. Estimating physiological thresholds with continuous two-phase regressions. Physiol. Zool. **62**: 866–887.

Nuhfer, A.J., Clark, R.D., Jr., and Alexander, G.R. 1994. Recruitment of brown trout in the South Branch of the Au Sable River, Michigan in relation to streamflow and winter severity. Fish. Res. Rep. 2006. Michigan Department of Natural Resources, Ann Arbor, Mich.

Otis, D.L., Burham, K.P., White, G.C., and Anderson, D.R. 1978. Statistical inference from capture data on closed animal populations. Wildl. Monogr. No. 62.

Paradis, E., Baillie, S.R., Sutherland, W.J., and Gregory, R.D. 1999. Dispersal and spatial scale affect synchrony in spatial population dynamics. Ecol. Lett. **2**: 114–120.

Perry, J.N. 1982. Fitting split-lines to ecological data. Ecol. Entomol. **7**: 421–435.

Peterman, R.M., Pyper, B.J., Lapointe, M.F., Adkinson, M.D., and Walters, C.J. 1998. Patterns of covariation in survival rates of British Columbia and Alaskan sockeye salmon (*Oncorhynchus nerka*) stocks. Can. J. Fish. Aquat. Sci. **55**: 2503–2517.

Pyper, B.J., Mueter, F.J., Peterman, R.M., Blackbourn, D.J., and Wood, C.D. 2002. Spatial covariation in survival rates of northeast Pacific chum salmon. Trans. Am. Fish. Soc. **131**: 343–363.

Ricker, W.E. 1954. Stock and recruitment. J. Fish. Res. Board Can. **11**: 559–623.

Rincón, P.A., and Lobón-Cerviá, J. 2002. Nonlinear self-thinning in a stream-resident population of brown trout (*Salmo trutta*). Ecology, **83**: 1808–1816.

Seber, G.A.F. 1982. The estimation of animal abundance and related parameters. 2nd ed. Griffin Publishers, London, UK.

Solomon, D.J., and Paterson, D. 1980. Influence of natural and regulated stream flow on survival of brown trout (*Salmo trutta* L.) in a chalk stream. Environ. Biol. Fishes, **5**: 379–382.

Spina, A.P. 2001. Incubation discharge and aspects of brown trout population dynamics. Trans. Am. Fish. Soc. **130**: 322–327.

Strange, E.M., Moyle, P.B., and Foin, T.C. 1992. Interactions between stochastic and deterministic processes in stream fish community assembly. Environ. Biol. Fishes, **36**: 1–15.

Victor, B.C. 1983. Recruitment and population dynamics of a coral reef fish. Science (Washington, D.C.), **219**: 419–420.

Waters, T.A. 1999. Long-term trout production dynamics in Valley Creek, Minnesota. Trans. Am. Fish. Soc. **128**: 1151–1162.

Whalen, K.G., Parrish, D.L., Mather, M.E., and McMenemy, J.R. 2000. Cross-tributary analysis of parr to smolt recruitment of Atlantic salmon (*Salmo salar*). Can. J. Fish. Aquat. Sci. **57**: 1607–1616.

Zalewski, M., and Naiman, R.J. 1985. The regulation of riverine fish communities by a continuum of abiotic–biotic factors. *In* Habitat modification and freshwater fisheries. *Edited by* J.S. Alabaster. Butterworths of New Zealand Ltd., Wellington, N.Z. pp. 3–12.

Zalewski, M., Frankiewicz, P., and Brewinska, B. 1985. The factors limiting growth and survival of brown trout, *Salmo trutta* m. fario L. introduced to different types of streams. J. Fish Biol. **27**(Suppl. A): 59–73.

Seasonal changes in the lipids of *Mysis mixta* (Mysidacea) from the hyperbenthos of a cold-ocean environment (Conception Bay, Newfoundland)

Nicole B. Richoux, Don Deibel, Raymond J. Thompson, and Christopher C. Parrish

Abstract: Total lipid (TL) and lipid class composition of *Mysis mixta* Lilljeborg from 240-m depth in a cold-water marine bay were studied throughout 1999 and 2000. The objective was to relate the seasonal lipid dynamics in an abundant and lipid-rich hyperbenthic species to its life cycle and to the annual phytoplankton bloom. *Mysis mixta* accumulated high levels of lipid reserves similar to those reached by other cold-water zooplankton. Greatest accumulation occurred in maturing females and males upon initiation of the spring bloom and continued for 6 months. The lowest TL level was ~5% dry mass (DM) in small juveniles, post-spawned males, and spent females, and the highest level was 32% DM in females approaching full maturity (overall content range 0.3–16 mg·mysid^{-1}). Most females accumulated lipid for 2 years before spawning, although a few females spawned 7 months early with a very low TL content. Seasonal variation in TL resulted primarily from net changes in triacylglycerol, the predominant neutral lipid. Seasonal and interannual variation in TL quantities in individuals and in areal concentrations of lipid in the hyperbenthic population indicates a strong trophic link between *M. mixta* and the pelagic production cycle.

Résumé : Nous avons mesuré les lipides totaux (TL) et la composition des différentes classes de lipides chez *Mysis mixta* Lilljeborg à une profondeur de 240 m dans une baie marine d'eau froide en 1999 et 2000. Notre objectif était de relier la dynamique saisonnière des lipides chez une espèce hyperbenthique commune et riche en lipides à son cycle biologique et au foisonnement annuel du phytoplancton. *Mysis mixta* accumule de grandes réserves de lipides, semblables à celles des autres organismes du zooplancton d'eau froide. L'accumulation la plus forte se produit chez les femelles et les mâles en maturation au début du foisonnement printanier du phytoplancton et elle dure 6 mois. Le contenu le plus faible en TL est de ~5 % de la masse sèche (DM) chez les jeunes de petite taille, les mâles après l'accouplement et les femelles après la ponte; le contenu le plus élevé est de 32 % DM chez les femelles presque complètement arrivées à maturité (étendue globale des concentrations 0,3–16 mg·mysidé$^{-1}$). La plupart des femelles accumulent des lipides pendant 2 années avant la fraye, bien que certaines femelles se reproduisent 7 mois plus tôt avec un contenu très faible en TL. Les variations saisonnières de TL résultent principalement de changements nets de triacylglycérol, le lipide neutre prédominant. La variation saisonnière et inter-annuelle des contenus individuels de TL et des concentrations spatiales des lipides dans la population hyperbenthique indique un fort lien trophique entre *M. mixta* et le cycle de production pélagique.

[Traduit par la Rédaction]

Introduction

Knowledge of the lipid content and composition of zooplankton is essential for understanding the importance of lipids to growth and reproduction and the energetic role of zooplankton within marine food webs. Conception Bay, Newfoundland, is an ideal site for the study of cold-water hyperbenthic species owing to the accessibility of the bay and the year-round influence of an inshore branch of the Labrador Current. The life cycle, growth, and reproductive features of some hyperbenthic animals in this region are more typical of polar than temperate populations (Choe and Deibel 2000; Richoux et al. 2004*a*). The seasonally productive and perpetually cold environment created by the Labrador Current undoubtedly influences the lipid dynamics of populations in this region.

Mysis mixta Lilljeborg exhibits a 2.5-year, semelparous life cycle in the hyperbenthos of Conception Bay (Richoux et al. 2004*a*). Two-year-old adults spawn in late autumn, the females carry broods during the winter, and brood release

Received 30 October 2003. Accepted 31 May 2004. Published on the NRC Research Press Web site at http://cjfas.nrc.ca on 23 December 2004.
J17824

N.B. Richoux,[1] D. Deibel, R.J. Thompson, and C.C. Parrish. Ocean Sciences Centre, Memorial University, St. John's, NL A1C 5S7, Canada.

[1] Corresponding author (e-mail: nrichoux@mun.ca).

Can. J. Fish. Aquat. Sci. **61**: 1940–1953 (2004)   doi: 10.1139/F04-139

Table 1. Life-history stages of *Mysis mixta* and approximate size ranges of mysids and broods collected.

Life-history stage	Body length (mm) or brood size (larvae·brood^{-1})	Dry mass (mg)	Characteristics
Larvae (whole broods)	22–111	3.3–29	Larvae are contained within a brood sac
Juveniles	7.0–15	0.40–6.3	No visible secondary sexual characteristics
Immatures			
Female	14–30	6.1–69	Has developing oostegites
Male	14–30	4.2–41	Has developing penes
Mature females	21–32	19–79	Fully developed brood sac containing larvae
Spent females	25–32	36–57	Fully developed but empty brood sac
Mature males	24–27	23–41	Well developed penes, and 4th pleopods extend beyond the uropods

Note: Free-living juveniles <7 mm were not sampled, probably because they occurred at a different depth. Body length is a measure of rostrum tip to telson tip.

occurs in spring. Mature males disappear from the hyperbenthos earlier than females, presumably because they die following the spawning season (Richoux et al. 2004*a*). Juveniles feed on phytoplankton and other small particles (Richoux et al. 2004*a*), whereas developing and mature individuals consume rotifers, cladocerans, tintinnids, and copepods, in addition to detritus and phytoplankton (*M. mixta* from the Baltic Sea; Rudstam et al. 1989; Hansson et al. 1990). Nightly migrations into the water column increase the variety of prey available to these mysids and create a direct trophic path between the hyperbenthic and pelagic regions.

In Conception Bay, most sedimentation occurs following the spring phytoplankton bloom, which provides the benthos with large influxes of fresh particulate organic matter (Redden 1994). During the remainder of the year, sedimentation input is relatively small, with the exception of a secondary pulse in the fall (Tian et al. 2003). This seasonal pattern of primary production and sedimentation creates variation in the availability of high-quality food for most benthic and hyperbenthic organisms throughout the year. How much of the material originating during the spring bloom is actually consumed by the hyperbenthic organisms, and in what form, remains unclear. Different species are likely to take advantage of this annual influx in different ways, depending on life histories, modes of nutrition, and storage abilities. Of 19 hyperbenthic and benthic macroinvertebrate species in Conception Bay studied during 3 separate years, *M. mixta* exhibited the second greatest mean lipid level (% wet mass) and the highest proportion of neutral lipids (% total lipids) during and following the spring bloom (C.C. Parrish, D. Deibel, and R.J. Thompson, unpublished data).

The purpose of this research was to investigate the role of lipids in the growth and life cycle of *M. mixta* and to establish a trophic connection between the pelagic and benthic regions of a cold-water bay. We hypothesized that lipid content would vary ontogenetically as the mysids matured and reproduced and that lipid levels in individuals would increase following the spring bloom as a result of the increased availability and quality of food. In addition, areal concentrations of lipids in the population were calculated to determine the degree to which the *M. mixta* population accumulates energy from the environment and the quality of the mysids as food for predators. Together with previously reported population dynamics (Richoux et al. 2004*a*), the seasonal lipid data augments our knowledge of the ecological and energetic role of hyperbenthic organisms in a cold-ocean ecosystem.

Materials and methods

Study site and sample collection

Samples of *M. mixta* were collected approximately monthly (December 1998 – November 2000) from the depositional zone at 240-m depth in Conception Bay, Newfoundland. The large fjord-like bay is 100 km long × 30 km wide at the mouth, with a maximum depth of 300 m in the central basin and steep slopes near the shores (deYoung et al. 1993). The Labrador Current supplies Conception Bay with deep water <0 °C throughout the year. Detailed sampling methods for both the hyperbenthos and the water column (physical data) are described elsewhere (Richoux et al. 2004*a*). Briefly, sampling was done during daytime from a 13-m boat equipped with an epibenthic sled (mouth area 0.3 m^2), with tows commencing at 47°30.5′N, 53°07.5′W and ending near 47°32.5′N, 53°07.0′W. Organisms living on the seafloor and those living within 60 cm of the bottom were collected with a 500-µm mesh net tapered to a closed cod end. Tows lasted 20–30 min, with the tow distance ranging from 620 to 930 m.

Specimens

Live, depurated mysids were categorized into life-history stages (Table 1), and up to five straightened, free-living individuals per life stage (depending on availability) were measured to the nearest 0.5 mm under a stereomicroscope (body length measured from the rostrum tip to the telson tip). Larvae were removed from brood sacs and counted, although each brood was processed as a unit. Mysids and whole broods were rinsed with 1-µm filtered seawater and stored in chloroform under nitrogen at −20 °C. Dry mass (DM) of each mysid was calculated from its body length using one of several equations (depending on life-history stage), and DM of whole broods was predicted from brood size (Table 2). Calculated DM of each brood was added to the DM of the corresponding brooding female.

Lipid analyses

Lipids were extracted from each sample using a modified Folch procedure (Parrish 1999). Two or three very small juveniles were pooled on a few occasions to obtain an ade-

Table 2. Equations used to calculate dry mass (DM, mg) of *Mysis mixta* from body length (*L*; mm) and brood DM (mg) from brood size (larvae·brood^{-1}) (Richoux et al. 2004*a*).

Eq. no.	Life-history stage	Equation	r^2	n
1	Juveniles	$DM = 0.00162 \times L^{3.05}$	0.97	187
2	Males (immature and mature)	$DM = 0.00259 \times L^{2.89}$	0.98	102
3	Females (immature and mature)	$DM = 0.00140 \times L^{3.11}$	0.98	124
4	Spent females	$DM = 0.00282 \times L^{2.86}$	0.99	53
5	Broods	$DM = 0.190 \times \text{larvae·brood}^{-1} - 0.137$	0.50	21

quate signal. Samples were ground in 2:1 (*v/v*) chloroform–methanol, 0.5 mL of chloroform-cleaned water added, and the lipid layers removed and combined following each of three chloroform washes. Lipid classes of concentrated extracts were separated by thin-layer chromatography (TLC) on rods coated with silica gel (Chromarods-SIII, Shell USA, Fredericksburg, Virginia) and quantified by flame ionization detection (FID) using an Iatroscan MK V (Mitsubishi Kagaku Inc., Tokyo, Japan) (Parrish 1987). Up to 11 lipid classes were identified and quantified by comparison with FID responses for the following standards (the lipid class represented follows each compound): *n*-nonadecane (hydrocarbon), cholesteryl palmitate (steryl ester), 3-hexdecanone (ketone), tripalmitin (triacylglycerol), palmitic acid (free fatty acid), 1-hexadecanol (alcohol), cholesterol (sterol), 1-monopalmitoyl-rac-glycerol (acetone-mobile polar lipid), and dipalmitoyl DL-α-phosphatidylcholine (phospholipid) (Sigma-Aldrich Canada Ltd., Oakville, Ontario). Methyl esters (ME) were identified by their position between steryl esters – wax esters (SE–WE not separable with this method) and ketones (KET), diacylglycerols (DG) were identified by their position following sterols (ST), and nonlipid material remained at the origin. ME and DG were quantified using the KET and acetone-mobile polar lipid (AMPL) calibration equations, respectively. Frequent peak splitting in the triacylglycerol (TAG) and free fatty acid (FFA) regions made these classes difficult to differentiate. When peak splitting occurred, additional developments using alternative solvent systems separated more saturated from polyunsaturated FFA and TAG (Parrish 1999). These four lipid molecular species were identified by comparison with the standards palmitic acid (C16:0), docosahexaenoic acid (C22:6), tripalmitin (3 × C16:0), and triarachidonin (3 × C20:4). The TAG to FFA ratio was then applied to the pooled TAG + FFA fraction quantified by conventional TLC-FID. Total lipids (TL) were determined by summing all lipid classes. A lipolysis index (LI (%) = [(free fatty acids + alcohols)/(total acyl lipids + alcohols)] × 100; Parrish et al. 1995) was calculated from all samples to assess sample degradation during storage and processing.

Areal concentrations

Following Arts et al. (1992), areal concentrations of reserve (TAG) and TL (mg·m^{-2}) were estimated from the products of TAG or TL·mysid^{-1} and the population density of *M. mixta* in the hyperbenthos on each sampling date. Adjusted (i.e., back-calculated) density values for each life-history stage within a cohort were used (Richoux et al. 2004*a*) because within-cohort density in later samples was frequently higher than that in earlier samples. Densities, and thus areal lipid concentrations, were underestimates of the true population values, since free-living juveniles (length 4 mm at release) were not collected until they reached 7 mm (Richoux et al. 2004*a*).

Statistical analyses

Within-cohort TAG, phospholipid (PL), and TL accumulation or utilization rates were determined from slopes in linear sections of regressions of lipid content·mysid^{-1} against time (least squares regression; linear sections were divided according to pre- and post-bloom start periods). The Durbin–Watson statistic was calculated to detect temporal autocorrelation in the regressions, and the Cochrane–Orcutt procedure was used to remove any autocorrelations (Neter et al. 1996). Analysis of covariance (ANCOVA) was used to determine whether rates of lipid accumulation or utilization differed between sexes within a cohort. Changes in minor lipid classes with development, particularly in cohorts 2 and 3, were determined using regression analyses (spent females were excluded from analyses). Data are reported as means ± 1 standard deviation (SD).

Results

Total lipids

Seasonal life cycle, density, biomass, and growth of *M. mixta* in Conception Bay have been described elsewhere (Richoux et al. 2004*a*). Four discrete cohorts (C1, C2, C3, and C4) were identified during the 2-year sampling period (Fig. 1). Mysids from C2 collected between December 1998 and February 1999 were not sexed and were pooled in an "undifferentiated immatures" category. Mysids from C1, C3, and C4 were adequately staged throughout development. Overall, increases in TL·mysid^{-1} (mg) with DM (mg) were not significantly different in males and females (ANCOVA, $p > 0.05$; analysis included all stages pooled from the four cohorts with the exception of spent females)

$$(1) \qquad TL = 0.0700 \times DM^{1.218}$$

$$(r^2 = 0.85,\ n = 178,\ p < 0.0001)$$

Seasonal changes in lipid content (TL·mysid^{-1}) were similar to changes in TL levels (% DM; Fig. 1). Mature females in December 1998 contained the highest TL of individuals from C1 (29% DM). Lipids in mature females decreased at a rate of 2.5 mg·month^{-1} until broods were released, leaving spent females with a mean lipid level of 15% DM in May 1999 (Table 3; Fig. 1*b*). Mature males in C1 had low TL (5% DM) between December 1998 and March 1999 and

Fig. 1. Calculated dry mass (mg) of lipid samples and changes in total lipid (% dry mass) in (*a*, *b*) cohort 1, (*c*, *d*) cohort 2, (*e*, *f*) cohort 3, and (*g*, *h*) cohort 4 for *Mysis mixta*. JV, juveniles; IU, immatures undifferentiated; IF, immature females; MF, mature females (including brooded larvae); SF, spent females; IM, immature males; MM, mature males. Dotted lines within a cohort represent transition periods between life-history stages; vertical dotted lines represent bloom start and settling times. Error bars are standard deviations around the mean. Superimposed values represent maximum or minimum absolute lipid content (mg·mysid^{-1}) in different stages.

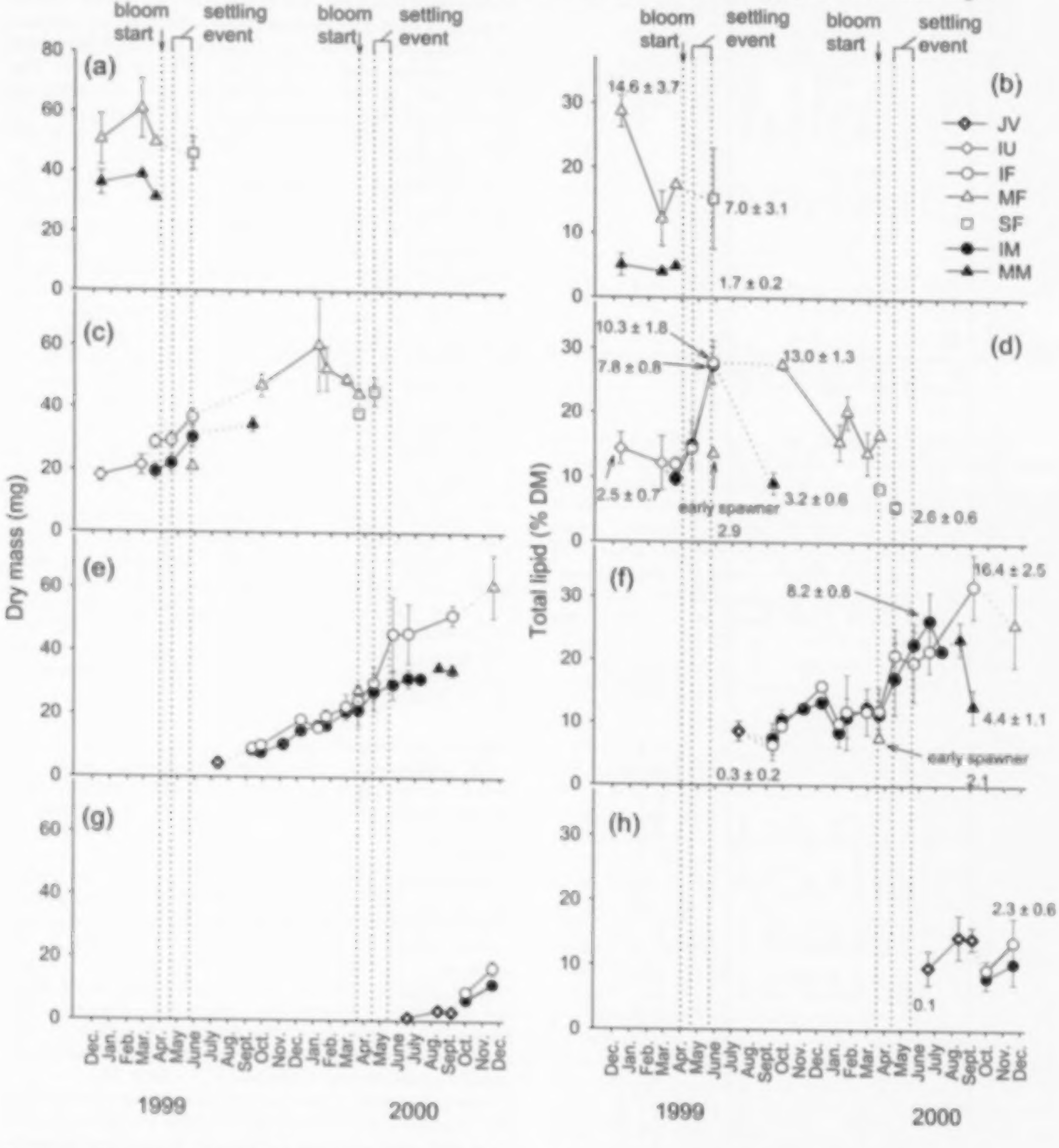

thereafter disappeared from the samples (Tables 3 and 4; Fig. 1*b*).

TL in C2 immature mysids collected between December 1998 and March 1999 remained relatively constant, whereas TL increased at rate of 3.0 mg·month^{-1} in immature individuals between March and May 1999 (Table 3; Fig. 1*d*). The highest lipid level in C2 mysids was recorded in immature females and immature males in May 1999 and in mature fe-

Table 3. Within-cohort total lipid (TL), triacylglycerol (TAG), and phospholipid (PL) accumulation or utilization (rates produced from regression slopes of lipid content·mysid^{-1}).

Cohort	Stages included	Time period	Bloom status	TL (mg·month^{-1})	r^2	TAG (mg·month^{-1})	r^2	PL (mg·month^{-1})	r^2	*n*
1	MF	Dec. 1998 – Mar. 1999	na	–2.5*	0.54	–1.7*	0.56	0.00	na	8
1	MM	Dec. 1998 – Mar. 1999	na	0.00	na	0.00	na	0.00	na	4
2[a]	IU, IF, IM	Dec. 1998 – Mar. 1999	Pre	0.00	na	0.00	na	0.11**	0.34	26
2[a]	IF, IM	Mar. 1999 – May 1999	Post	3.0****	0.72	1.7****	0.73	0.00	na	20
2	MF	Sept. 1999 – Mar. 2000	na	–1.1**	0.52	–0.94***	0.74	0.00	na	12
3	JV, IF, IM	July 1999 – Mar. 2000	Pre	0.30****	0.67	0.15****	0.59	0.091****	0.75	45
3	IF, IM	Mar. 2000 – Sept. 2000[b]	Post	2.3****	0.79	1.4****	0.76	0.32****	0.63	39
3[a]	IM, MM	June 2000 – Sept. 2000	na	0.00	na	–1.6**	0.52	0.00	na	12
4[a]	JV, IF, IM	June 2000 – Nov. 2000	Pre	0.52**	0.37	0.22**	0.38	0.093****	0.68	19

Note: Male and female stages in a cohort were pooled when their rates were not significantly different (analysis of covariance, ANCOVA, $p > 0.05$). Subgroups were created to establish rates before (Pre) and after (Post) the start of the spring bloom, although bloom status was not assigned to mature males or females. Spent females were not included in any calculations. Mysids that exhibited no change ($p > 0.05$) were assigned a rate of 0.00. JV, juveniles; IU, immatures undifferentiated; IF, immature females; IM, immature males; MF, mature females (including brooded larvae); MM, mature males; *, $p < 0.05$; **, $p < 0.01$; ***, $p < 0.001$; ****, $p < 0.0001$; na, not applicable.

[a] Regressions corrected for temporal autocorrelation using Cochrane–Orcutt procedure.

[b] March–June 2000 for IM.

males in September 1999 (28% DM; Fig. 1*d*). In the predominant group of mature females, TL decreased at a rate of 1.1 mg·month^{-1} from September 1999 to March 2000, leaving spent females with low TL (6% DM) in April 2000 (Table 3; Fig. 1*d*). Lipid levels in post-spawned males during September 1999 were very low relative to mature females (Fig. 1*d*; a lipid utilization rate was not calculated owing to the dearth of male samples between May and September 1999); the few other mature males collected between September and December 1999 were damaged, excluding the possibility of lipid analyses. An early spawning female collected in May 1999 had a very low TL level of 14% DM (Fig. 1*d*; Table 5).

In July 1999, C3 juveniles had a TL level of 9% DM (Table 6; Fig. 1*f*). Immature males and females accumulated lipids at the same rate until March 2000 (0.30 mg·month^{-1}; ANCOVA, $p > 0.05$; Table 3). From March to September 2000, TL accumulation increased to 2.3 mg·month^{-1} in the immature mysids, resulting in a maximum mean lipid level (32% DM) in immature females during September 2000 (Fig. 1*f*). An early spawning female in March 2000 had a TL level of 8% DM. TL in immature males peaked at 26% DM in June, after which lipid content (mg·mysid^{-1}) remained constant until September 2000 (Table 3; Fig. 1*f*). TL could not be determined in damaged mature males collected in November 2000. TL in C4 mysids increased slowly at 0.52 mg·month^{-1} from June to November 2000, when sampling was terminated (Tables 3 and 7 ; Fig. 1*h*).

In general, mysids were present in the samples as juveniles in July each year. As the juveniles slowly developed sexual characteristics (usually after September), they accumulated small quantities of lipids prior to the spring bloom (TL range 5%–17% DM) and larger quantities during and following the spring bloom (to a maximum TL of 32% DM in females). Following spawning (main spawning event appears to occur in September), TL decreased significantly in mature females.

Lipid class composition

The predominant lipid classes in most stages were TAG and PL, whereas hydrocarbon (HC), SE–WE, ME, KET, FFA, alcohol (ALC), ST, DG, and AMPL were minor classes.

Females

Highest TAG levels of all life-history stages were recorded in mature females early in the brooding period (up to 16% DM) and in immature females (and immature males) just prior to full maturity (15%–19% DM; Figs. 2*a*, 2*c*, 2*e*). To reach these maximum levels, growing C2 and C3 females (Figs. 1*c*, 1*e*) accumulated TAG at 1.4–1.7 mg·month^{-1} (Table 3; Figs. 2*c*, 2*e*) from the start of the spring bloom in March. Before the bloom, maturing mysids accumulated TAG at slower rates of 0.15 and 0.22 mg·month^{-1} (C3 and C4, respectively) or showed no change (C2) (Table 3).

The lowest TAG level in mature females was recorded in early spawners from May 1999 and March 2000 (5.0% and 1.5% DM, respectively; Figs. 2*c*, 2*e*). These early spawners had lower levels of both neutral and polar lipids than the dominant group of mature females spawning in September or later (Tables 5 and 6). Following spawning, the dominant groups of females utilized TAG at 1.7 mg·month^{-1} (C1) or

Table 4. Lipid class composition of *Mysis mixta* cohort 1.

Class	Mature females (Dec. 1998 – Mar. 1999)		Spent females (May 1999)		Mature males (Dec. 1998 – Mar. 1999)	
	% DM	% TL	% DM	% TL	% DM	% TL
HC	0.18±0.12	0.87±0.21	0.21	1.28	0.00	0.04±0.07
SE–WE	0.83±0.84	3.51±2.48	0.24	1.53	0.14±0.18	2.41±2.89
ME	0.85±1.29	3.21±4.34	0.37	2.14	0.03±0.06	0.54±0.93
KET	0.13±0.11	0.68±0.68	0.09	0.39	0.00	0.00
TAG	9.78±5.36	48.10±6.25	8.20	47.85	0.27±0.17	5.15±3.11
FFA	0.33±0.10	1.93±0.96	1.23	7.93	0.48±0.11	9.74±0.61
ALC	0.00	0.00	0.27	1.22	0.00	0.00
ST	1.09±0.45	6.19±2.80	0.65	4.64	0.49±0.05	10.61±0.89
DG	0.12±0.07	0.64±0.49	0.24	1.71	0.06±0.05	1.10±0.95
Neutral	13.30±7.53	65.13±10.07	11.49	68.69	1.47±0.54	29.60±6.65
AMPL	0.85±0.61	4.19±1.37	0.57	3.63	0.15±0.06	3.03±1.36
PL	5.32±0.44	30.68±10.57	3.30	27.68	3.04±0.06	67.37±6.45
Polar	6.16±0.91	34.87±10.07	3.87	31.31	3.18±0.11	70.40±6.65
TL	19.47±8.44		15.36		4.65±0.56	
TL·mysid^{-1} (mg)	10.24±3.86		7.02		1.65±0.18	

Note: Data are grand means ± SD for stages collected on more than one sampling date. HC, hydrocarbon; SE–WE, steryl ester – wax ester; ME, methyl ester; KET, ketone; TAG, triacylglycerol; FFA, free fatty acid; ALC, alcohol; ST, sterol; DG, diacylglycerol; Neutral, sum of neutral lipids; AMPL, acetone-mobile polar lipid; PL, phospholipid; Polar, sum of polar lipids; TL, total lipid; DM, dry mass.

0.94 mg·month^{-1} (C2; Table 3; Figs. 2*a*, 2*c*). Mean TAG levels in spent females ranged from 1.0% to 8.2% DM (March–April; Fig. 2). TAG in C2 spent females was lower than that in C1 spent females, resulting in lower TL quantities overall.

Females maturing through summer accumulated some PL (up to 0.32 mg·month^{-1}; Table 3) and had maximum PL levels of 6% DM once they became fully mature in autumn (Figs. 2*b*, 2*d*, 2*f*). Otherwise, PL levels fluctuated around 4% DM, with seasonal patterns less pronounced than those of TAG (Fig. 2). The PL levels in mature females remained consistently high throughout the brooding period until the females died following the release of broods in April or May (Table 3; Figs. 2*b*, 2*d*).

The predominant groups of mature females in C1, C2, and C3 contained similar levels of all lipid classes and had higher levels of each lipid class than did spent females and mature males (Tables 4, 5, and 6). The early spawning females in C2 and C3 had lower amounts of all major lipid classes, presumably because they lacked the time and the resources to achieve the higher levels seen in females spawning later in the year. Following release of the broods, females were left with lipid class profiles similar to those in mature males.

Males

Most mature, post-spawned males had very low levels of TAG (mean range 0.07%–14% DM; Figs. 2*a*, 2*c*, 2*e*). The lipid pool of age 2+ males in C1 was not dominated by TAG, unlike that of all other life-history stages including younger mature males in C2 and C3. Low TAG in C1 mature males resulted in consistently higher values for ST and FFA than for any other neutral lipids (Table 4). High TAG accumulation rates in maturing males began in March and continued for several months (1.4–1.7 mg·month^{-1}; Table 3), indicating that males required significant energy reserves for reproduction, as did females. It is unlikely that these energy reserves were utilized for overwintering, since lipid levels dropped during the spawning period in autumn (Figs. 2*c*, 2*e*). Like females, maturing males accumulated TAG at slow rates prior to the initiation of the spring bloom (Table 3). Highest TAG levels in males occurred following spring bloom settlement in May of both years (15%–18% DM; Figs. 2*c*, 2*e*). In general, PL levels remained fairly consistent throughout development (Tables 4, 5, 6, and 7). Small increases in PL were observed in juveniles and immature males prior to the spring bloom (0.091–0.11 mg·month^{-1}; Table 3), and PL accumulation in immature C3 males increased to 0.32 mg·month^{-1} following bloom settlement (no significant change in immature C2 males).

Minor classes and lipolysis index (LI)

HC, KET, ME, and SE–WE all increased with maturation and reached highest levels in mature females and males (Tables 4, 5, 6, and 7). Free fatty acids either remained constant throughout a cohort (C2) or decreased during maturation (C3). Alcohol levels did not change in a predictable manner within cohorts, although they varied among cohorts and were highest in C2 and C3 mature females but absent in adult C1 mysids. ST, AMPL, and DG levels remained constant throughout maturation (Tables 4, 5, 6, and 7; changes in lipid content·mysid^{-1} were determined using linear regressions, significance level 0.05).

Small juveniles in C3 had unusually high LI values, ranging from 10% to 30%, whereas LI values for all other stages remained below 15%. These low LI values indicate that the integrity of the samples was maintained during storage and analysis, and the consistently high LI values in C3 juveniles (20.1% ± 7.6%) probably indicate a physiological change related to rapid allocation of dietary lipids to growth in this life stage, rather than sample degradation.

Areal concentrations

Areal concentrations of TAG and TL varied both seasonally and interannually (Fig. 3). Maxima occurred in Febru-

Table 5. Lipid class composition of *Mysis mixta* cohort 2.

Class	Immatures undifferentiated (Dec. 1998 – Feb. 1999)		Immature females (Mar. 1999 – May 2000)		Immature males (Mar. 1999 – May 2000)	
	% DM	% TL	% DM	% TL	% DM	% TL
HC	0.06±0.05	0.49±0.31	0.08±0.07	0.40±0.34	0.13±0.15	0.51±0.43
SE–WE	0.48±0.12	3.44±0.57	0.22±0.13	1.30±0.33	0.34±0.31	1.65±0.72
ME	0.10±0.04	0.82±0.38	0.23±0.15	1.20±0.38	0.39±0.52	1.44±1.52
KET	0.23±0.18	1.50±1.12	0.14±0.22	0.97±1.52	0.08±0.05	0.45±0.20
TAG	6.05±1.37	43.31±6.33	9.79±4.94	55.66±5.97	8.79±6.05	48.03±17.26
FFA	0.50±0.15	3.85±0.66	0.75±0.36	4.28±0.75	1.11±0.45	6.79±2.34
ALC	0.00	0.00	0.49±0.84	1.97±3.41	0.25±0.43	0.96±1.67
ST	0.72±0.12	5.59±0.01	0.65±0.40	4.52±3.14	0.85±0.31	5.27±1.50
DG	0.18±0.01	1.31±0.09	0.26±0.12	1.48±0.16	0.19±0.14	1.02±0.19
Neutral	8.32±2.02	60.31±9.27	12.61±6.26	71.77±8.72	12.13±8.21	66.12±17.06
AMPL	0.45±0.06	3.34±0.30	0.91±0.60	4.81±2.33	0.76±0.40	4.50±2.19
PL	4.57±0.50	36.36±9.56	3.59±0.73	23.42±10.81	4.18±0.95	29.37±17.89
Polar	5.03±0.43	39.69±9.27	4.51±0.69	28.23±8.72	4.94±0.73	33.88±17.06
TL	13.34±1.59		17.11±6.77		18.18±10.37	
TL·mysid^{-1} (mg)	2.60±0.13		5.62±3.01		4.61±3.45	

Note: Data are grand means ± SD for stages collected on more than one sampling date. Values in square brackets represent an independent, early triacylglycerol; FFA, free fatty acid; ALC, alcohol; ST, sterol; DG, diacylglycerol; Neutral, sum of neutral lipids; AMPL, acetone-mobile polar lipid; PL,

ary 1999 (25 mg TL·m^{-2}, 10 mg TAG·m^{-2}) and June 2000 (55 mg TL·m^{-2}, 39 mg TAG·m^{-2}).

Discussion

This study demonstrates a close relationship between lipid and reproductive dynamics in *M. mixta* and seasonal production in the water column. Lipid content and composition indicate that *M. mixta* in Conception Bay accumulates lipids primarily for reproduction rather than for growth, is a lipid-rich food source for predators, does not experience prolonged periods of starvation, and secures what may be a significant amount of lipid energy from the environment at the population level.

The spring phytoplankton bloom in Conception Bay began in early March in 1999 (bloom start defined as chlorophyll (Chl) *a* > 1 μg·L^{-1}), with a Chl *a* maximum occurring in late April (Richoux et al. 2004*a*). In 2000, the bloom began in late March and the Chl *a* maximum was reached in mid-May. Rapid settlement of this fresh and highly nutritive material to the hyperbenthos was evident in April and May each year (Richoux et al. 2004*a*). A smaller, secondary peak of phytoplankton biomass occurred in July 1999, but no secondary bloom was apparent in 2000. Temperature scarcely deviated from –0.5 °C below 200 m, although surface waters showed a marked seasonal temperature cycle, with values exceeding 14 °C in September each year. Hyperbenthic mysids would have had to migrate within 120 m of the surface to experience temperatures >0 °C. Salinity in the hyperbenthic region remained between 32.0 psu and 34.0 psu in both years (Richoux et al. 2004*a*).

Tian et al. (2003) predicted primary production values of 124–137 g C·m^{-2}·year^{-1} from a model of phytoplankton dynamics in Conception Bay, and Redden (1994) recorded a maximum flux of 600 mg C·m^{-2}·day^{-1} during bloom sedimentation to the benthos in May. Parrish (1998) obtained a range of organic carbon flux (24–1361 mg C·m^{-2}·day^{-1}; derived from nearshore (224 m) and offshore (363 m) stations during spring, summer, autumn, and winter between 1994 and 1997) from Trinity Bay, a nearby fjord, which encompassed the value derived from Conception Bay. Values of primary production in both Newfoundland bays are consistent with total annual phytoplankton production reported for fjords in the Northern Hemisphere (49°N–77°N), which ranges from 100 to 150 g C·m^{-2}·year^{-1} (Falk-Petersen et al. 1990). The proportion of fixed carbon recovered as TL in seston is normally between 10% and 20% (Sargent et al. 1985). The limited information available on the changes in seston lipids within Conception Bay (Ramos et al. 2003; Parrish et al., in press) indicates similarities to seasonal conditions in Trinity Bay (Parrish 1998). In Trinity Bay, TAG levels in diatoms increase substantially during the peak of the spring bloom, particularly as nitrate and silicate are exhausted (Parrish 1998). The TAG increase is followed by increases in PL coinciding with the growth of dinoflagellate and zooplankton populations. Following the bloom, rapid flux results in the arrival of high-quality seston to the benthos of Trinity Bay and Conception Bay, where the fresh organic material is consumed. Up to 70% of the total annual primary production in ice-free temperate and polar regions occurs during the spring phytoplankton bloom (Falk-Petersen et al. 1990), and the spring bloom produces 38%–75% of the annual flux of particulate organic carbon to the Conception Bay hyperbenthos (Redden 1994; Tian et al. 2003).

Choe et al. (2003) determined the seasonal abundance of stage VI female copepods (*Temora* spp., *Metridia* spp., *Pseudocalanus* spp., and *Calanus* spp.) in Conception Bay during 1997 and 1998. High abundance of copepods, important prey of immature and mature mysids (Hansson et al. 1990), coincided with the primary production cycle, albeit with a 3-week time lag similar to the zooplankton increase observed in Trinity Bay (Parrish 1998). Maximum numbers of mature copepods were therefore assumed to occur in early

Mature females (Sept. 1999 – Mar. 2000 [May 1999])		Spent females (Mar. 2000 – Apr. 2000)		Mature males (Sept. 1999)	
% DM	% TL	% DM	% TL	% DM	%TL
0.18±0.04 [0.04]	0.97±0.19 [0.28]	0.01±0.00	0.20±0.13	0.14	1.45
0.74±0.18 [0.30]	4.03±0.80 [2.20]	0.10±0.09	1.33±0.92	0.84	9.21
0.74±0.72 [0.13]	3.79±4.09 [0.93]	0.00	0.00	0.34	3.70
0.36±0.36 [0.15]	2.00±1.74 [1.05]	0.12±0.00	1.67±0.33	0.04	0.47
8.74±4.37 [4.99]	44.47±9.61 [36.34]	1.85±1.28	24.32±11.51	2.85	29.69
0.47±0.34 [0.86]	2.54±2.03 [6.24]	0.35±0.09	4.70±0.20	0.70	7.80
0.96±0.48 [0.68]	5.00±1.48 [4.93]	0.02±0.00	0.28±0.11	0.09	0.89
0.61±0.13 [0.58]	3.46±1.02 [4.19]	0.46±0.07	6.66±0.95	0.59	6.59
0.20±0.10 [0.18]	1.15±0.54 [1.30]	0.11±0.10	1.41±1.05	0.06	0.71
12.99±5.03 [7.90]	67.40±7.19 [57.47]	3.03±1.63	40.57±12.16	5.64	60.51
0.77±0.36 [1.24]	4.14±1.54 [9.05]	0.33±0.18	4.90±3.56	0.19	2.12
5.02±0.43 [4.60]	28.46±7.20 [33.49]	3.72±0.56	54.53±8.60	3.32	37.36
5.79±0.56 [5.85]	32.60±7.19 [42.54]	4.05±0.38	59.43±12.16	3.51	39.49
18.78±5.39 [13.74]		7.07±2.00		9.15	
9.49±2.50 [2.89]		2.92±0.47		3.16	

spawning female in May 1999. HC, hydrocarbon; SE–WE, steryl ester – wax ester; ME, methyl ester; KET, ketone; TAG, phospholipid; Polar, sum of polar lipids; TL, total lipid; DM, dry mass.

or late May in Conception Bay during the present study, with maximum numbers of copepodite stages occurring in late summer and early fall (Davis 1982).

Given high Chl *a* concentrations, copepod abundance, and lipid content in seston associated with the spring bloom, it is likely that lipids in hyperbenthic zooplankton such as *M. mixta* correspond in some predictable way to bloom periods. Although not strictly herbivorous, *M. mixta* can rapidly exploit the high-quality organic material produced during the bloom, presumably in part because of the vertical migrations that bring it into the water column each night (Rudstam et al. 1989). This diel migration provides the mysids with early access to freshly formed aggregates produced in shallower water, whereas nonmigratory hyperbenthic organisms must wait until the material has settled. The commencement of the spring phytoplankton bloom coincides with both the release of broods from mature females (Richoux et al. 2004*a*) and the rapid accumulation of lipids in maturing mysids. Lipid-rich mysids are high-quality prey for demersal and pelagic predators, and organic material consumed by the mysids is repackaged and redistributed through fecal pellet production during diel vertical migrations. The continual process of *M. mixta* "drawing down" organic material within the water column and the seasonal release of juveniles into the hyperbenthos probably have a large influence on the energetics of the hyperbenthos and on the coupling of the benthic and pelagic regions in Conception Bay.

Within-cohort TL in *M. mixta* varied substantially throughout the study period. Some differences were observed among the four cohorts, possibly owing to individual variability and to interannual variation in environmental factors, and general patterns reflected both seasonal food availability and the reproductive cycle. The smallest free-living mysids contained small quantities of TL, and lipids were initially accumulated slowly. Rapid lipid accumulation commenced in maturing mysids concomitantly with the start of the spring phytoplankton bloom in April and continued through the periods of maximum abundance of adult copepods and copepodite stages in summer and autumn. Slower accumulation or rapid utilization of lipids, depending on the life-history stage, occurred at other times of the year. Specifically, once females were fully mature and bearing broods, they began to utilize their lipid stores rapidly, in a manner similar to that of post-spawned males. The apparently comparable net loss of lipids in some groups of mature females and mature males (significant utilization of lipids by C1 and C2 males was assumed owing to the very low lipid content in post-spawned males compared with immature males or mature females) suggests that the process of maintaining broods may not require exceptionally high energy stores. Detailed examination of brood lipids in relation to those of the parent will help to elucidate the energy changes in each constituent.

With the exceptions of spent females, post-spawned males, and late-brood stage females, larger individuals of *M. mixta* generally had higher quantities of lipids than smaller ones, both on a TL·individual^{-1} and a TL·DM^{-1} basis. The smallest juveniles (starting at 0.4 mg DM) had as little as 0.04 mg of lipids (5%–10% DM), whereas the largest females (up to 71 mg DM) had 19 mg of lipids (24%–38% DM). Similarly, TL level in krill *Euphausia superba* from the Antarctic increased with body size (krill up to 30 mg DM had 16% lipid·DM^{-1}, whereas krill between 200 and 300 mg had 35% lipid·DM^{-1}; Ferguson and Raymont 1974). It is common for crustaceans to accumulate lipids in this manner (Adare and Lasenby 1994), as younger stages often invest dietary energy in growth and development rather than in accumulation of energy reserves (Ouellet et al. 1992; Adare and Lasenby 1994; Kattner et al. 1994). In *M. mixta*, increased opportunities to feed on small zooplankton in addition to seston as the mysids matured, as well as increased access to a greater variety of prey items throughout the water column owing to increased swimming ability and dis-

Table 6. Lipid class composition of *Mysis mixta* cohort 3.

	Juveniles (July 1999)		Immature females (Sept. 1999 – Sept. 2000)		Immature males (Sept. 1999 – July 2000)		Mature females (Nov. 2000 [Mar. 2000])		Mature males (Aug. 2000 – Sept. 2000)	
Class	% DM	% TL	% DM	% TL	% DM	% TL	% DM	% TL	% DM	% TL
HC	0.01	0.11	0.14±0.20	0.61±0.71	0.09±0.10	0.51±0.46	0.20 [0.05]	0.82 [0.64]	0.28±0.08	1.51±0.11
SE–WE	0.17	1.79	0.46±0.49	2.54±1.74	0.54±0.46	3.65±2.18	1.76 [0.03]	6.88 [0.35]	1.55±0.42	8.82±1.49
ME	0.06	0.66	0.57±0.73	2.92±2.26	0.22±0.29	1.39±2.11	1.03 [0.00]	4.52 [0.00]	0.41±0.32	1.93±0.80
KET	0.02	0.20	0.34±0.43	1.57±1.80	0.38±0.57	2.16±2.51	1.70 [0.00]	5.87 [0.00]	0.55±0.28	3.00±0.16
TAG	2.43	28.34	8.06±5.55	45.37±15.51	7.28±5.05	44.69±15.01	13.11 [1.45]	50.64 [19.05]	9.28±6.20	48.37±13.87
FFA	1.60	17.70	0.47±0.17	3.93±2.95	0.75±0.25	6.00±3.06	0.09 [0.09]	0.37 [1.18]	0.56±0.15	3.74±2.53
ALC	0.05	0.60	0.24±0.22	1.85±2.01	0.05±0.09	0.37±0.66	1.65 [0.31]	6.07 [4.07]	0.02±0.03	0.10±0.15
ST	0.77	9.01	0.52±0.10	4.30±2.53	0.57±0.11	4.51±1.89	0.38 [0.45]	1.55 [5.91]	0.52±0.01	3.20±1.32
DG	0.12	1.37	0.13±0.05	0.91±0.45	0.12±0.04	0.94±0.33	0.05 [0.09]	0.21 [1.14]	0.10±0.06	0.55±0.15
Neutral	5.22	53.25	10.94±6.96	63.97±13.82	10.01±5.83	64.22±12.14	19.97 [2.45]	76.94 [32.33]	13.27±7.25	71.22±9.68
AMPL	0.75	8.81	0.76±0.47	5.29±2.63	0.61±0.44	4.65±3.34	1.15 [1.01]	4.74 [13.27]	0.33±0.13	1.90±0.14
PL	2.66	31.41	3.87±0.80	30.74±13.28	3.85±0.60	31.12±11.38	4.67 [4.13]	18.32 [54.40]	4.52±0.23	26.87±9.54
Polar	3.41	40.22	4.63±0.99	36.03±13.82	4.46±0.69	35.78±12.14	5.82 [5.14]	23.06[67.67]	4.85±0.35	28.78±9.68
TL	8.62		15.56±7.38		14.51±6.06		25.79 [7.59]		18.11±7.61	
TL·mysid^{-1} (mg)	0.36		4.95±4.91		3.24±2.62		15.38 [2.09]		6.29±2.73	

Note: Data are grand means ±SD for stages collected on more than one sampling date. Values in square brackets represent an early spawning female in March 2000. HC, hydrocarbon; SE–WE, steryl ester – wax ester; ME, methyl ester; KET, ketone; TAG, triacylglycerol; FFA, free fatty acid; ALC, alcohol; ST, sterol; DG, diacylglycerol; Neutral, sum of neutral lipids; AMPL, acetone-mobile polar lipid; PL, phospholipid; Polar, sum of polar lipids; TL, total lipid; DM, dry mass.

Table 7. Lipid class composition of *Mysis mixta* cohort 4.

Class	Juveniles (June 2000 – Sept. 2000) % DM	Juveniles (June 2000 – Sept. 2000) % TL	Immature females (Oct. 2000 – Nov. 2000) % DM	Immature females (Oct. 2000 – Nov. 2000) % TL	Immature males (Oct. 2000 – Nov. 2000) % DM	Immature males (Oct. 2000 – Nov. 2000) % TL
HC	0.11±0.10	0.85±0.86	0.05±0.06	0.43±0.32	0.02±0.02	0.16±0.15
SE–WE	0.76±0.36	5.46±2.42	0.86±0.80	6.91±3.87	0.49±0.39	4.76±2.22
ME	0.47±0.50	3.49±3.56	0.49±0.71	3.70±4.22	0.26±0.29	2.33±2.08
KET	0.36±0.52	2.41±3.11	0.18±0.33	1.54±2.60	0.04±0.04	0.49±0.55
TAG	4.94±1.99	36.24±6.78	4.04±2.71	33.30±14.02	3.16±1.85	31.81±10.95
FFA	1.04±0.38	8.70±5.15	0.65±0.21	6.06±2.23	0.77±0.26	8.75±4.08
ALC	0.02±0.03	0.15±0.22	0.02±0.06	0.17±0.46	0.00±0.01	0.05±0.11
ST	0.56±0.12	4.46±1.24	0.40±0.04	3.80±0.92	0.39±0.06	4.41±1.50
DG	0.11±0.05	0.88±0.47	0.06±0.02	0.58±0.19	0.06±0.04	0.56±0.22
Neutral	8.37±2.67	62.65±6.30	6.75±4.07	56.49±17.21	5.18±2.50	53.31±11.36
AMPL	0.63±0.26	4.74±1.92	0.54±0.20	4.90±1.49	0.43±0.19	4.60±1.73
PL	4.19±0.95	32.61±6.67	3.93±1.33	38.60±17.41	3.84±1.05	42.10±11.98
Polar	4.81±0.98	37.35±6.30	4.48±1.17	43.51±17.21	4.27±1.02	46.69±11.36
TL	13.19±3.13		11.23±3.31		9.45±2.70	
TL·mysid^{-1} (mg)	0.33±0.21		1.48±0.85		0.94±0.43	

Note: Data are grand means ± SD for stages collected on more than one sampling date. HC, hydrocarbon; SE–WE, steryl ester – wax ester; ME, methyl ester; KET, ketone; TAG, triacylglycerol; FFA, free fatty acid; ALC, alcohol; ST, sterol; DG, diacylglycerol; Neutral, sum of neutral lipids; AMPL, acetone-mobile polar lipid; PL, phospholipid; Polar, sum of polar lipids; TL, total lipid; DM, dry mass.

tance travelled during vertical migrations, may have contributed to higher food availability in larger animals. On the other hand, immature Antarctic *E. superba* (Pond et al. 1995) and juvenile *Mysis relicta* (Chess and Stanford 1998) contain higher lipid·DM^{-1} than older and larger stages. These contrasting results emphasize that lipid storage patterns in crustaceans are highly variable, even within the same species, and that it is advantageous to study the general biology concurrently with the lipid dynamics in a population.

Seasonal variability in the lipids of *M. mixta* is similar to that in some deepwater and (or) high-latitude zooplankton species. In general, species whose food is unpredictable or seasonally variable are more likely to store lipids for use when food is scarce (Clarke 1977). Alternatively, an absence of substantial seasonal fluctuations in zooplankton lipids suggests that food availability and quality are consistent year-round. Species that are opportunistic omnivores and that undergo diel vertical migrations may have access to ample food sources in both the hyperbenthic and the pelagic regions throughout the year (Adare and Lasenby 1994), negating any necessity for seasonal storage of energy reserves. Since protein does not usually have a storage function in zooplankton, and carbohydrate levels remain low year-round, species with low lipid levels probably feed consistently throughout the year to survive and reproduce (Clarke 1977; Percy 1979).

Mysis mixta in Conception Bay accumulates substantial amounts of lipids despite its flexible feeding habits and its apparent year-round access to food in both the pelagic and the hyperbenthic realms. This population has probably evolved to mature and spawn using accumulated reserves and to release juveniles during the period of greatest food abundance. The primary storage lipid of *M. mixta* is TAG, which is commonly accumulated in zooplankton species within 1 or 2 months of the spring bloom in preparation for gametogenesis and brooding (Gardner et al. 1985; Hill et al. 1992; Hopkins et al. 1993). TAG is produced in great amounts by diatoms and flagellates (Parrish 1988) and is more prevalent in the water column during phytoplankton blooms. In *M. mixta*, the most rapid accumulation of TAG (up to 1.7 mg·month^{-1} in maturing mysids) occurred in the months following the start of the phytoplankton bloom in March 1999 and 2000. As in the decapod *Pandalus borealis* (Hopkins et al. 1993), TAG levels increased from 20% of TL in smallest juvenile *M. mixta* to 74% of TL in female mysids nearing full maturity (>20% DM in some individuals). Triacylglycerol is mobilized faster than WE, and Sargent and Henderson (1986) noted that copepods not experiencing prolonged periods of starvation deposit storage lipids in the form of TAG rather than the more common WE. *Mysis mixta* may store easily mobilized TAG to take advantage of the higher food availability and quality during the spring bloom, but it may not necessarily require lipid stores to survive and reproduce, as evidenced by low lipid quantities in early spawning females. The few early spawners were much smaller and produced smaller broods (22–56 larvae·brood^{-1}) than the dominant group of large mature females spawning later in the year (up to 111 larvae·brood^{-1}). Although brood sizes differed, larvae from early spawning and late spawning females had similar quantities of TL (~18 μg TL·larva^{-1} and 17–54 μg TL·larva^{-1}, respectively). Since most females postpone spawning until the second year, following accumulation of substantial lipid reserves, there must be a reproductive advantage for individuals that are lipid-rich prior to the production and release of larvae.

In contrast to TAG, PL levels remained relatively low and stable, with very low rates of accumulation occurring in maturing mysids (up to 0.32 mg·month^{-1} in the spring). Highest PL levels were observed in immature and mature females

Fig. 2. Seasonal changes in triacylglycerol and phospholipid (% dry mass (DM)) in (*a*, *b*) cohort 1, (*c*, *d*) cohort 2, (*e*, *f*) cohort 3, and (*g*, *h*) cohort 4 for *Mysis mixta*. JV, juveniles; IU, immatures undifferentiated; IF, immature females; MF, mature females (including brooded larvae); SF, spent females; IM, immature males; MM, mature males. Dotted lines within a cohort represent transition periods between life-history stages; vertical dotted lines represent bloom start and settling times. Error bars are standard deviations around the mean. Superimposed values represent maximum or minimum absolute lipid class content (mg·mysid^{-1}) in different stages.

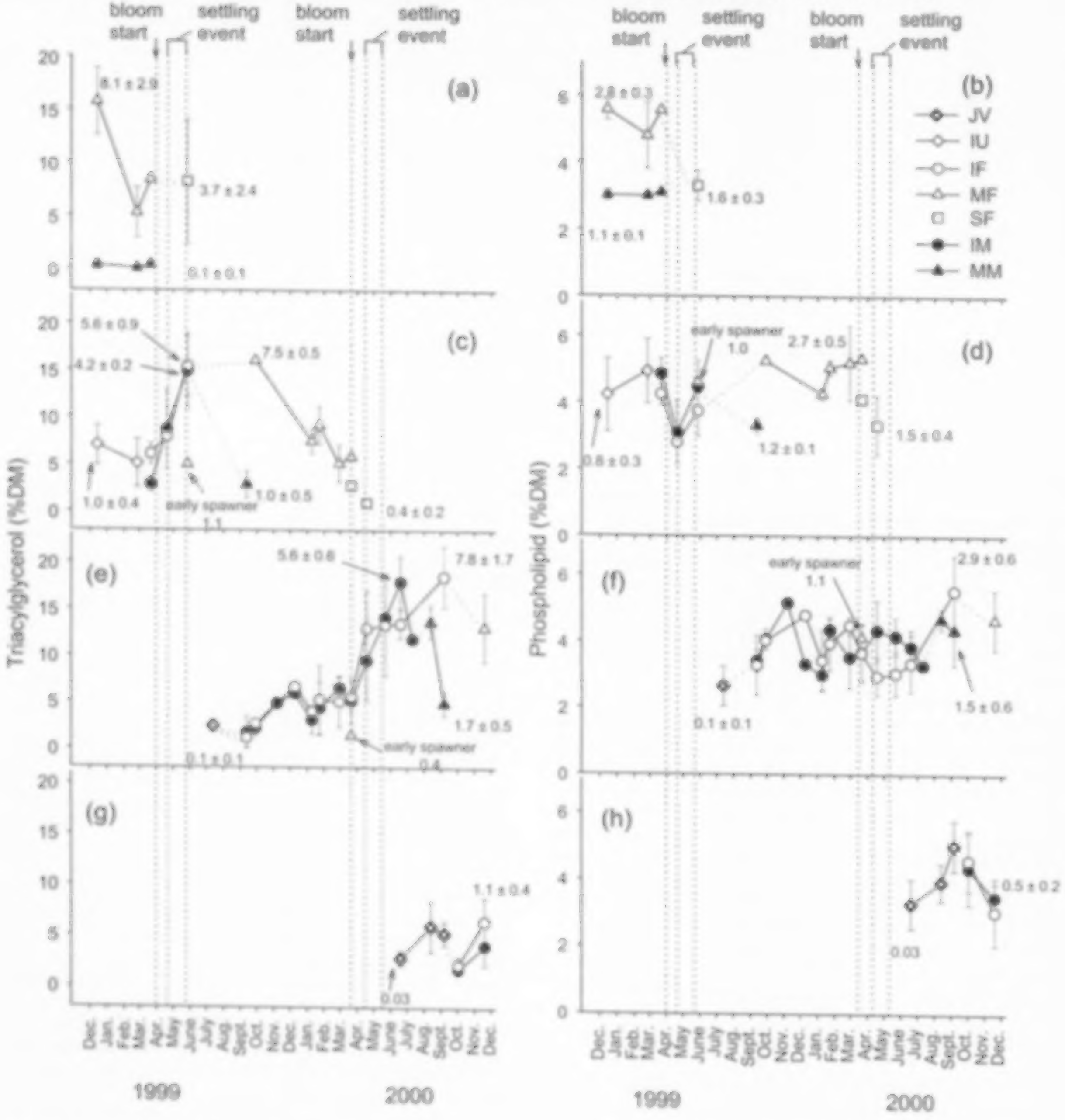

(up to 6.5% DM), and levels in immature males remained below 5% DM. Likewise, PL quantities (mg·mysid^{-1}) in mature males were consistently low relative to those in mature females. The disparity between males and females may have been attributable to the requirement by females to produce egg membranes, as evidenced by low quantities of PL in most spent females. It also suggests that mature males invested much of their PL in the production of sperm, and ac-

Fig. 3. Areal concentrations of total lipid (open circles) and triacylglycerol (filled circles) for *Mysis mixta*. Vertical dotted lines represent spring bloom start and settling times.

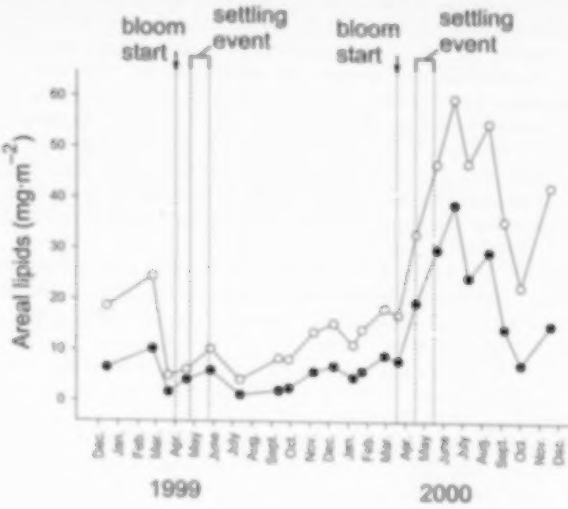

cordingly their PL content was greatly reduced following spawning in autumn. If ingested lipids had been intended solely for growth in *M. mixta*, PL levels would have increased at higher rates during the growth phase of males and females. Increases in PL are normally associated with growth, because PL are major structural and functional components of membranes and organelles (Vanderploeg et al. 1992; Arts 1999).

Seasonal changes in the availability of essential fatty acids may provide a dietary rather than a reproductive influence on seasonal lipid patterns in *M. mixta*, whereby rapid storage of lipids occurs during periods of high abundance of specific fatty acids. Throughout the 1996 bloom in Conception Bay, Parrish et al. (in press) observed high levels (up to 35% of total fatty acids) of polyunsaturated fatty acids even in sediment trap material collected at 220 m. Polyunsaturated fatty acid levels were lower (~20% of total fatty acids) both before and after the spring (Parrish et al., in press). Variation in the swimming activity and daily migrations of the mysids, resulting in higher metabolic requirements at certain times of the year, may also contribute to seasonal variation in lipids. Less active hyperbenthic organisms living in the same region but exhibiting a similar biennial life cycle may have access to fewer resources year-round and may also have lower and less variable metabolic demands. Such populations may accumulate lower and less variable amounts of lipids seasonally, as in the sympatric amphipod *Acanthostepheia malmgreni*, which has lipid levels as high as 15% DM and relatively slow lipid accumulation rates (Richoux et al. 2004*b*). Other than *M. mixta* and *A. malmgreni*, the chaetognath *Parasagitta elegans* is the only hyperbenthic species in Conception Bay for which lipid dynamics have been determined in relation to the reproductive cycle (Choe et al. 2003). The TL content in *P. elegans*, a highly motile and carnivorous species, shows small increases in maturing individuals, with maximum lipid levels reaching 16% DM (Choe et al. 2003).

Female *M. mixta* accumulated higher quantities of TL than all other life-history stages (up to 38% DM or 19 mg·mysid^{-1}). High levels of reserves in females are common in brooding zooplankton (Adare and Lasenby 1994) and reflect the energy requirements of females for brood production and possibly protection. Males accumulated lipids at the same rates but never achieved the high quantities observed in age 2+ mature females (maximum TL in males was 30% DM or 9 mg·mysid^{-1}). With few exceptions, TAG was the most abundant lipid class in *M. mixta* throughout the study period, whereas in other zooplankton species, TAG is predominant only during and following the spring bloom (Gardner et al. 1985; Hill et al. 1992; Hopkins et al. 1993). PL was most abundant in those few instances when TAG was not the major lipid class in *M. mixta*.

TL decreased in mature females, primarily as a result of TAG loss concomitant with larval development from utilization of stored yolk. Females fed while brooding (N.B. Richoux, personal observation), so loss of lipids for maintenance was not the likely cause of the observed decrease. The presence of 1-year-old spawners in both C2 and C3 demonstrates that reproduction is possible in females with lipid concentrations as low as 8% DM, although nothing is known of the survival of early spawned juveniles. Hill et al. (1992) have hypothesized that amphipods not able to store lipids at a level of 20% DM may have to postpone reproduction for an entire year. In *M. relicta*, it appears that body size and TL content, rather than lipid level, are the most important factors determining time of reproduction (Adare and Lasenby 1994). Female *M. relicta* studied in two different lakes required ~1.4 mg TL before they produced broods (Adare and Lasenby 1994). In contrast, early spawning female *M. mixta* in Conception Bay contained 2–3 mg TL, compared with the 7–19 mg TL in 2-year-old females. Release time of larvae by early spawners was estimated as late summer or early autumn, perhaps when the abundance of predators was low.

At the population level, areal concentrations of TL and TAG indicate that *M. mixta* inhabiting the hyperbenthos of Conception Bay can rapidly appropriate organic material produced during a spring phytoplankton bloom. Accumulation of reserves by the population on an areal basis began in March of both years, although markedly higher concentrations occurred following the bloom in 2000. The magnitude, estimated from Chl *a* concentrations, and duration of the diatom bloom in 2000 were notably greater than those in 1999 (Richoux et al. 2004*a*). Maximum areal concentration of TL in 2000 (55 mg·m^{-2}) corresponded to 3% of the integrated input of TL to the hyperbenthos, as measured in 220-m sediment trap material collected throughout the 1996 spring bloom in Conception Bay (1750 g·m^{-2}; Ramos et al. 2003). Unfortunately, similar calculations of areal lipid concentration as a proportion of integrated flux in organisms from other systems are not available for comparison. However, Arts et al. (1992) reported seasonal variation in areal TAG reserves in several small zooplankton species (cladocerans and copepods) from a hypereutrophic lake in Saskatchewan, Canada. Areal lipid energy in the freshwater zooplankton increased 1 month after significant increases in bacterial or algal populations, with maximum concentrations (up to 1200 mg·m^{-2} in dominant populations) reflecting the high productivity of the ecosystem (Arts et al. 1992). In addition to food availability, areal lipids can reflect interactions among numerous factors, including competition, predation, life cycle, and diet (Arts et al. 1992).

Lipid content and composition of zooplankton are influenced by various factors, including location, season, temperature, salinity, food availability, diet, body size, physiology, and reproductive condition. The interactions among these factors can result in substantial and predictable seasonal patterns in lipids, and these patterns can greatly influence the energy flow through an ecosystem. Unfortunately, environmental influences are not easily distinguished from biological effects on the seasonal changes of lipids in an organism. As a hyperbenthic species rich in lipid reserves, *M. mixta* probably serves an important role as an intermediary trophic link in the ecosystem of Conception Bay, and the dependence of *M. mixta* on the seasonal phytoplankton bloom is reflected in a strong seasonality in reproduction and lipid accumulation.

Acknowledgements

We thank M.W. Riehl, J.S. Wells, T.S. Avery, and the captain and crew of the RV *Karl and Jackie II* for assistance in the field and (or) laboratory and two anonymous reviewers for suggestions to improve the manuscript. This study was supported by Natural Sciences and Engineering Research Council of Canada (NSERC) research grants to R.J.T. and D.D. and a graduate student fellowship from Memorial University of Newfoundland to N.B.R.

References

Adare, K.I., and Lasenby, D.C. 1994. Seasonal changes in the total lipid content of the opossum shrimp, *Mysis relicta* (Malacostraca: Mysidacea). Can. J. Fish. Aquat. Sci. **51**: 1935–1941.

Arts, M.T. 1999. Lipids in freshwater zooplankton: selected ecological and physiological aspects. *In* Lipids in freshwater ecosystems. *Edited by* M.T. Arts and B.C. Wainman. Springer-Verlag New York Inc., New York. pp. 71–90.

Arts, M.T., Evans, M.S., and Robarts, R.D. 1992. Seasonal patterns of total and energy reserve lipids of dominant zooplanktonic crustaceans from a hyper-eutrophic lake. Oecologia, **90**: 560–571.

Chess, D.W., and Stanford, J.A. 1998. Comparative energetics and life cycle of the opossum shrimp (*Mysis relicta*) in native and non-native environments. Freshw. Biol. **40**: 783–794.

Choe, N., and Deibel, D. 2000. Seasonal vertical distribution and population dynamics of the chaetognath *Parasagitta elegans* in the water column and hyperbenthic zone of Conception Bay, Newfoundland. Mar. Biol. **137**: 847–856.

Choe, N., Deibel, D., Thompson, R.J., Lee, S.H., and Bushell, V.K. 2003. Seasonal variation in the biochemical composition of the chaetognath *Parasagitta elegans* from the hyperbenthic zone of Conception Bay, Newfoundland. Mar. Ecol. Prog. Ser. **251**: 191–200.

Clarke, A. 1977. Seasonal variations in the total lipid content of *Chorismus antarcticus* (Pfeffer) (Crustacea: Decapoda) at South Georgia. J. Exp. Mar. Biol. Ecol. **27**: 93–106.

Davis, C.C. 1982. A preliminary quantitative study of the zooplankton from Conception Bay, insular Newfoundland, Canada. Int. Rev. Hydrobiol. **67**: 713–747.

deYoung, B., Otterson, T., and Greatbatch, R.J. 1993. The local and nonlocal response of Conception Bay to wind forcing. J. Phys. Oceanogr. **23**: 2636–2649.

Falk-Petersen, S., Hopkins, C.C.E., and Sargent, J.R. 1990. Trophic relationships in the pelagic, Arctic food web. *In* Trophic relationships in the marine environment. *Edited by* M. Barnes and R.N. Gibson. Aberdeen University Press, Aberdeen. pp. 315–333.

Ferguson, C.F., and Raymont, J.K.B. 1974. Biochemical studies on marine zooplankton XII. Further investigations on *Euphausia superba* Dana. J. Mar. Biol. Assoc. U.K. **54**: 719–725.

Gardner, W.S., Nalepa, T.F., Frez, W.A., Cichocki, E.A., and Landrum, P.F. 1985. Seasonal patterns in lipid content of Lake Michigan macroinvertebrates. Can. J. Fish. Aquat. Sci. **42**: 1827–1832.

Hansson, S., Larsson, U., and Johansson, S. 1990. Selective predation by herring and mysids, and zooplankton community structure in a Baltic Sea coastal area. J. Plankton Res. **12**: 1099–1116.

Hill, C., Quigley, M.A., Cavaletto, J.F., and Gordon, W. 1992. Seasonal changes in lipid content and composition in the benthic amphipods *Monoporeia affinis* and *Pontoporeia femorata*. Limnol. Oceanogr. **37**: 1280–1289.

Hopkins, C.C.E., Sargent, J.R., and Nilssen, E.M. 1993. Total lipid content, and lipid and fatty acid composition of the deep-water prawn *Pandalus borealis* from Balsfjord, northern Norway: growth and feeding relationships. Mar. Ecol. Prog. Ser. **96**: 217–228.

Kattner, G., Graeve, M., and Hagen, W. 1994. Ontogenetic and seasonal changes in lipid and fatty acid/alcohol compositions of the dominant Antarctic copepods *Calanus propinquus*, *Calanoides acutus* and *Rhincalanus gigas*. Mar. Biol. **118**: 637–644.

Neter, J., Kutner, M.H., Nachtsheim, C.J., and Wasserman, W. 1996. Applied linear regression models. 3rd ed. Irwin/McGraw-Hill, Chicago.

Ouellet, P., Taggart, C.T., and Frank, K.T. 1992. Lipid condition and survival in shrimp (*Pandalus borealis*) larvae. Can. J. Fish. Aquat. Sci. **49**: 368–378.

Parrish, C.C. 1987. Separation of aquatic lipid classes by Chromarod thin-layer chromatography with measurement by Iatroscan flame ionization detection. Can. J. Fish. Aquat. Sci. **44**: 722–731.

Parrish, C.C. 1988. Dissolved and particulate marine lipid classes: a review. Mar. Chem. **23**: 17–40.

Parrish, C.C. 1998. Lipid biogeochemistry of plankton, settling matter and sediments in Trinity Bay, Newfoundland. I. Lipid classes. Org. Geochem. **29**: 1531–1545.

Parrish, C.C. 1999. Determination of total lipid, lipid classes, and fatty acids in aquatic samples. *In* Lipids in freshwater ecosystems. *Edited by* M.T. Arts and B.C. Wainman. Springer-Verlag New York Inc., New York. pp. 4–20.

Parrish, C.C., McKenzie, C.H., MacDonald, B.A., and Hatfield, E.A. 1995. Seasonal studies of seston lipids in relation to microplankton species composition and scallop growth in South Broad Cove, Newfoundland. Mar. Ecol. Prog. Ser. **129**: 151–164.

Parrish, C.C., Thompson, R.J., and Deibel, D. In press. Lipid classes and fatty acids in plankton and settling matter during the spring bloom in a cold ocean coastal environment. Mar. Ecol. Prog. Ser.

Percy, J. 1979. Seasonal changes in organic composition and caloric content of an Arctic marine amphipod, *Onisimus (= Boeckosimus) affinis*. J. Exp. Mar. Biol. Ecol. **40**: 183–192.

Pond, D.W., Watkins, J.L., Priddle, J., and Sargent, J.R. 1995. Variation in the lipid content and composition of Antarctic krill *Euphausia superba* at South Georgia. Mar. Ecol. Prog. Ser. **117**: 49–57.

Ramos, C.S., Parrish, C.C., Quibuyen, T.A.O., and Abrajano, T.A. 2003. Molecular and carbon isotopic variations in lipids in rapidly settling particles during a spring phytoplankton bloom. Org. Geochem. **34**: 195–207.

Redden, A.M. 1994. Grazer-mediated chloropigment degradation and the vertical flux of spring bloom production in Conception Bay, Newfoundland. Ph.D. thesis, Memorial University of Newfoundland, St. John's.

Richoux, N.B., Deibel, D., and Thompson, R.J. 2004*a*. Population biology of hyperbenthic crustaceans in a cold water environment (Conception Bay, Newfoundland) I. *Mysis mixta* (Mysidacea). Mar. Biol. **144**: 881–894.

Richoux, N.B., Thompson, R.J., Deibel, D., and Parrish, C.C. 2004*b*. Seasonal and developmental variation in the lipids of *Acanthostepheia malmgreni* (Amphipoda) from the hyperbenthos of a cold-ocean environment (Conception Bay, Newfoundland). J. Mar. Biol. Assoc. UK. **84**: 1189–1197.

Rudstam, L.G., Danielsson, K., Hansson, S., and Johansson, S. 1989. Diel vertical migration and feeding patterns of *Mysis mixta* (Crustacea, Mysidacea) in the Baltic Sea. Mar. Biol. **101**: 43–52.

Sargent, J.R., and Henderson, R.J. 1986. Lipids. *In* The biological chemistry of marine copepods. *Edited by* E.D.S. Corner and S.C.M. O'Hara. Clarendon Press, Oxford. pp. 59–108.

Sargent, J.R., Eilertsen, H., Falk-Petersen, S., and Taasen, J. 1985. Carbon assimilation and lipid production in phytoplankton in northern Norwegian fjords. Mar. Biol. **85**: 109–116.

Tian, R.C., Deibel, D., Thompson, R.J., and Rivkin, R.B. 2003. Modeling of climate forcing on a cold-ocean ecosystem, Conception Bay, Newfoundland. Mar. Ecol. Prog. Ser. **262**: 19–25.

Vanderploeg, H.A., Gardner, W.S., Parrish, C.C., Liebig, J.R., and Cavaletto, J.F. 1992. Lipids and life-cycle strategy of a hypolimnetic copepod in Lake Michigan. Limnol. Oceanogr. **37**: 413–424.

Long-term survival of adult Arctic grayling (*Thymallus arcticus*) in the Kuparuk River, Alaska

Karen M. Buzby and Linda A. Deegan

Abstract: In many long-lived species such as Arctic grayling (*Thymallus arcticus*), population growth rate is most sensitive to changes in adult survival probabilities. Understanding the factors that regulate adult survival in this species should provide insight into the population dynamics of this and other long-lived Arctic species. Using the program MARK, we analyzed 17 years of mark–recapture data to estimate survival rates for Arctic grayling in the Kuparuk River, Alaska, from 1985 to 2000. Mean annual survival rates overall ranged from 0.39 to 1.0 and averaged 0.71 ± 0.05 for resident and 0.75 ± 0.05 for nonresident fish. Spending the summer in the more productive fertilized zone of the experimental reach had no influence on survival despite higher productivity on all trophic levels and consistently higher growth rates in Arctic grayling. None of the environmental (stream temperature, discharge, winter severity, and incidence of drought) or population parameters (growth, condition factor, and mean fish size) that we examined explained significant amounts of variance in survival rates. The lack of responsiveness of survival to annual environmental conditions was unexpected and suggests that multiyear factors or life history tactics that maintain survival at the expense of growth and fecundity likely determine survival.

Résumé : Chez plusieurs espèces à forte longévité, telles que l'ombre arctique (*Thymalus arcticus*), le taux de croissance de la population est particulièrement sensible aux changements de probabilité de survie des adultes. La compréhension des facteurs qui contrôlent la survie des adultes chez cette espèce devrait fournir des perspectives sur la dynamique de population de cette espèce et d'autres espèces arctiques qui vivent longtemps. À l'aide du logiciel MARK, nous avons analysé des données de marquage-recapture étalées sur 17 années afin d'estimer les taux de survie des ombres arctiques de la rivière Kurapuk de 1985 à 2000. Les taux moyens annuels de survie varient dans l'ensemble de 0,39 à 1,0; ils sont en moyenne de 0,71 ± 0,05 pour les poissons résidants et de 0,75 ± 0,05 pour les non résidants. Le passage de l'été dans la section enrichie et plus productive de la zone expérimentale n'influence pas la survie, malgré une productivité accrue de tous les niveaux trophiques et des taux de croissance uniformément plus élevés chez l'ombre arctique. Aucune des variables examinées de l'environnement (température du cours d'eau, débit, rigueur de l'hiver, présence de sécheresses) ou de la population (croissance, coefficient de condition, taille moyenne des poissons) n'explique de partie significative de la variance des taux de survie. Ce manque de réaction de la survie aux conditions annuelles du milieu est inattendu et il laisse croire que la survie est déterminée par des variables ou des tactiques démographiques qui agissent sur plusieurs années pour maintenir la survie aux dépens de la croissance et de la fécondité.

[Traduit par la Rédaction]

Introduction

Understanding the factors influencing population growth is critical for fundamental understanding of populations and their impact on ecosystems as well as for managing species. Survival at multiple life history stages, development time, and fecundity all act in concert to determine population growth rates (Stearns 1992). The importance of survival in determining population growth rate has been demonstrated across several taxonomic levels for long-lived species in both modeling (Jonsson and Ebenman 2001) and metapopulation studies (Heppel et al. 2000; Sæther and Bakke 2000).

Survival rates reflect the interplay between changeable environmental conditions, population densities, and a varying population structure. Interannual climatic variation may play a direct or indirect role in survival either by stressing individuals or by affecting the food sources on which they are dependent. Catastrophic events such as floods or droughts often negatively affect survival rates (Lebreton et al. 1992). Overlaying the effects of a changing environment is the influence of the population on its own survival rates. Density-related reduction in survival rates has been attributed to increased competition (De Leo and Gatto 1996), displacement into marginal habitats (Frederiksen and Bregnballe 2000), and increased agonistic interactions (Wildy et al. 2001). Population survival rates may also be affected as the population structure changes owing to shifting sex ratios or the ad-

Received 24 September 2003. Accepted 14 May 2004. Published on the NRC Research Press Web site at http://cjfas.nrc.ca on 23 December 2004.
J17761

K.M. Buzby[1,2] and L.A. Deegan. The Ecosystems Center, Marine Biological Laboratory, Woods Hole, MA 02543, USA.

[1] Corresponding author (e-mail: karen.buzby@mail.wvu.edu).

[2] Present address: Department of Civil and Environmental Engineering, West Virginia University, Morgantown, WV 26506, USA.

Can. J. Fish. Aquat. Sci. **61**: 1954–1964 (2004)   doi: 10.1139/F04-126

vent of strong age-classes owing to sex- or age-specific mortality rates.

In severe environments, climatic conditions are harsh and resources are limited, and we expect a strong influence of environmental conditions on survival rates. Arctic streams on the North Slope of Alaska are severe environments where the growing season is perhaps 3 months followed by a 9-month winter, which includes months of extreme cold and little to no sunlight. While much of the Arctic remains unstudied, the Kuparuk River, Alaska, has been the site of concentrated study over the last 20 years with the Arctic grayling (*Thymallus arcticus*) population under study since 1985. Deegan et al. (1999) have demonstrated high interannual variability in growth of Arctic grayling of the upper Kuparuk River. In addition, the Kuparuk River has been the site of a long-term fertilization experiment that has increased the productivity of the ecosystem and, in most years, has resulted in higher weight gains for Arctic grayling in the fertilized zone (Peterson et al. 1993; Deegan et al. 1999; Slavik et al. 2004). The higher productivity and growth might be expected to result in higher survivorship. This data set provides an excellent opportunity to examine the relative roles that environmental factors and population structure play in survival dynamics of an Arctic fish owing to the length of the study and the breadth of information about the ecosystem.

Methods

Study site

This study was performed in the Kuparuk River (68°38′N, 149°24′W), a meandering tundra stream that originates in the foothills of the Brooks Range, Alaska, and flows north several hundred kilometres to the Arctic Ocean. Much of the study was concentrated in a 5-km experimental reach bisected by the Dalton Highway (Fig. 1). At this point, the Kuparuk River is a fourth-order river consisting of alternating riffles (10–50 cm in depth) and pools (1.5–5 m) with a mean width of 20 m and bottom substrates composed of rocks and cobble (Hershey et al. 1997; Slavik et al. 2004).

The experimental reach of the Kuparuk River has been the site of a long-term phosphorus fertilization experiment initiated in 1983. Each summer, low levels of phosphorus are added to the downstream section of the experimental reach. The location of the phosphorus dripper has changed over the years so that recovery from fertilization could be studied. The original kilometre designations and the locations of the approximately 1.5-km fish capture sections of the reference (–1.3–0.0 km) and fertilized zones (2.0–3.5 km) have remained the same and are referenced to the site of the original 1983 dripper. The phosphorus addition has resulted in increased primary production, macroinvertebrate production, and often fish growth in the fertilized zone of the river (Deegan and Peterson 1992; Peterson et al. 1993). However, environmental factors such as stream temperature and discharge have larger effects on fish growth than phosphorus fertilization (Deegan et al. 1999).

Arctic grayling are the only fish found in the experimental reach of the Kuparuk River as well as further upstream and downstream at least 50 km. Most of the fish in this study spend the winter in Green Cabin Lake about 25 km upstream of the experimental reach, the outlet of which forms the source of the Kuparuk River. After ice-out (mid-May), Arctic grayling leave the lake and spawn and by early July have redistributed themselves to their summer feeding territories where they remain until early to mid-August. In early August, the combination of decreasing day length and high river discharge initiates the overwintering migration to Green Cabin Lake. The migration is usually completed by late September.

Field sampling

Each summer since 1985, fish in the experimental reach have been captured through angling and seining. In most years, there were two 2-week capture periods each year: one in early July and a second in early August focused in 1.5-km sections of each zone. Each year, we attempted to capture at least 100 fish in each zone in July and to recapture at least 50 of these fish again in August. Fish caught in July were considered summer residents, that is, fish that had established feeding territories within the experimental reach. Fish caught in August consisted of summer residents as well as nonresident fish that were migrating through the reach on their way to overwintering sites. For the purposes of the mark–recapture analysis, we made no distinction between capture periods, as they were only 3 weeks apart and treated both as one capture session. Sampling intensity was variable over the years and we never attempted to capture all of the fish in the reach.

Captured fish were held overnight in holding pens close to the capture location. All captured fish were anesthetized with tricaine methanesulfonate (MS 222), weighed (±2 g), and total length (TL) measured (±0.5 cm). Tag information from previously marked fish was recorded and any unmarked fish was given a unique tag. Only fish larger than 29 cm were tagged and therefore constitute the adult population. All fish were released. Tagging methods have changed over the study. From 1985 to 1993, all fish were tagged with an anchor tag. Between 1993 and 1997, many fish were double-tagged with an anchor tag and a passive integrated transponder (PIT) tag, and some fish were tagged with anchor tags only for comparison. Since 1998, we have been tagging fish with PIT tags only based on analysis of the double-tagged fish, which demonstrated higher long-term retention of PIT tags (Buzby and Deegan 1999).

We attempted to prevent fish from leaving the reach before they were recaptured by installing one to four weirs, depending on the year. The weirs remained in place for the entire summer unless large storm events, which occur from zero to four times per summer, knocked down the weirs. The weirs remained down for 24–48 h in most cases or occasionally several days if water levels remained high. If the storm event occurred in early August, the fish often left the reach to migrate upstream to overwintering sites.

In some years (1987, 1989, 1990, 1992, 1995, and 1999), the autumnal migration into Green Cabin Lake, the main overwintering site, was monitored. In 1988 and 1990, the spring out-migration from the lake was also monitored. A weir was placed across the outlet of the lake preventing movement in or out of the lake. The Arctic grayling were captured using a seine as they collected at the weir. Captured fish were anesthetized, weighed, measured, and tagged in the same manner as in the experimental reach. For the pur-

Fig. 1. Map of the study region in Alaska showing the location of the Kuparuk River on the north slope as well as the study site on the Kuparuk River. The Dalton Highway bisects the 5-km (K) experimental reach. The fertilized reach of the river extends from 2.0 through 3.5 km and the reference reach is considered to extend from 0.5 to –1.0 km. Current and historical locations of the phosphorus dripper as well as weir locations are noted. Green Cabin Lake, the main overwintering site, is approximately 25 km from the experimental reach.

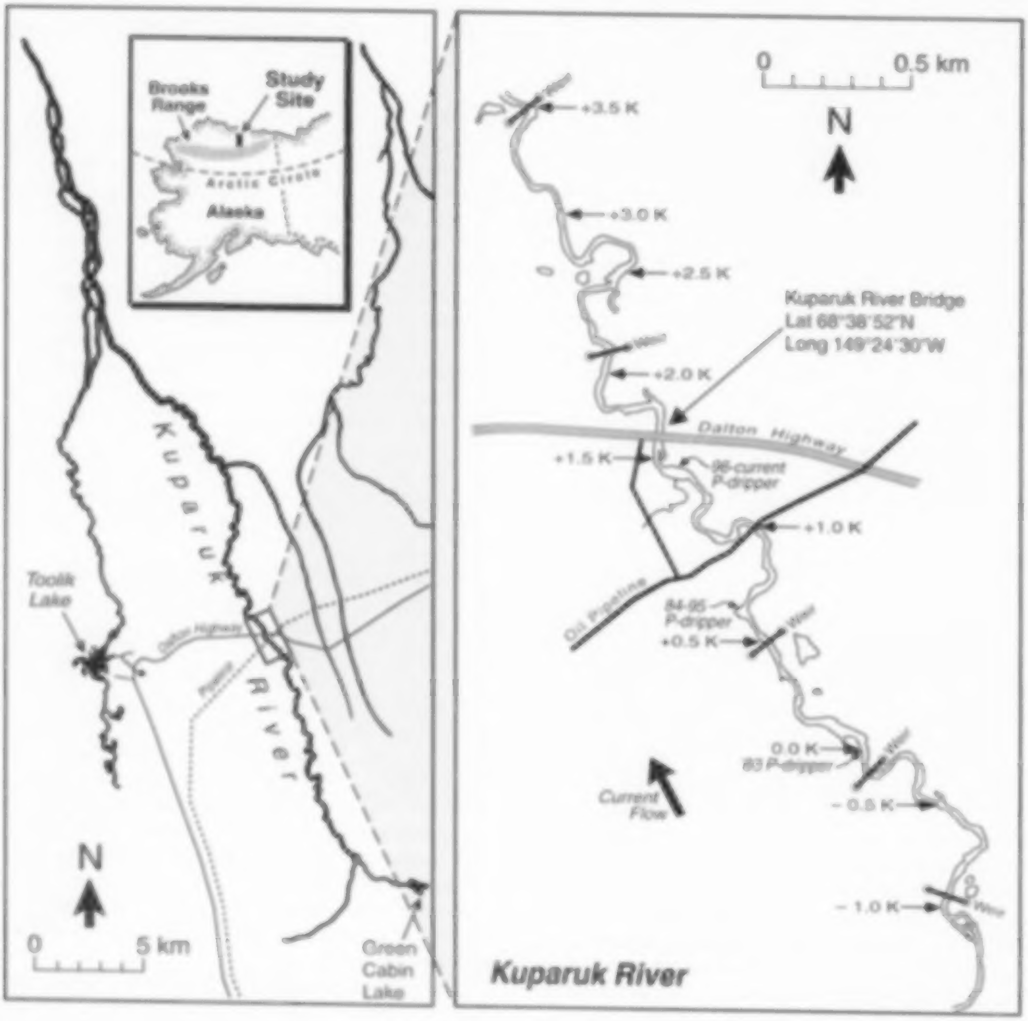
Brooks Range
Study Site
Arctic Circle
Alaska
Kuparuk
River
Toolik Lake
Dalton Highway
Pipeline
N
0
5 km
Green Cabin Lake
0
0.5 km
N
Weir
+3.5 K
+3.0 K
+2.5 K
Kuparuk River Bridge
Lat 68°38'52"N
Long 149°24'30"W
Weir
+2.0 K
Dalton Highway
+1.5 K
96-current P-dripper
+1.0 K
Oil Pipeline
84-95 P-dripper
Weir
+0.5 K
0.0 K
83 P-dripper
Weir
Current Flow
– 0.5 K
– 1.0 K
Weir
Kuparuk River

poses of the mark–recapture analysis, first-time captures within the experimental reach of fish that had been marked at the lake were considered unmarked.

Data analysis

We analyzed the mark–recapture data set with several models available within the program MARK (White and Burnham 1999). All are extensions of the Cormack–Jolly–Seber model, which in its basic form estimates group- and time-dependant survival and recapture rates. A major strength of Cormack–Jolly–Seber models is that unlike other methods used to estimate survival, they are able to separate recapture probabilities from survival estimates (Lebreton et al. 1992). Survival estimates were made using Barker's extension of Burnham's model, which jointly analyzes live recaptures and tag recoveries (Barker 1999). Barker's model incorporates resighting data between capture occasions, which improves the precision of the survival estimates. In addition to estimating survival and recapture probabilities, it also estimates five additional parameters that describe resighting and risk of capture probabilities: r, the probability of resighting a dead fish; R, the probability of being resighted and surviving; R', the probability of being resighted and then dying; F, the probability of being at risk of capture at times t and $t + 1$; and F', the probability of not being at risk of capture at time t but at risk during time $t + 1$.

The r parameter was set to zero because there were no resightings of dead fish. Resighting parameters (R and R') were set to zero (and therefore not estimated) except in years when the autumnal migration into Green Cabin Lake was monitored. Parameters were estimated using numerical maximum likelihood techniques and are reported as estimates ± SE.

We divided the data set into two groups: residents and nonresidents. We believed that residents would have higher recapture rates than nonresidents and that recapture rates might vary depending on when the autumnal migration started. We could not differentiate between resident and nonresident fish once the autumnal migration had started because at that time, they would be captured within the same locations in the river. The start of the autumnal migration, which can be identified because fish alter their behavior and begin to collect behind the weirs, has never begun prior to 1 August. Therefore, we defined residents as those fish that were captured before 1 August and nonresidents as those captured on or after 1 August. Undoubtedly, some fish were misclassified. The most likely misclassification was that resident fish would be classified as migrant. However, since we were most interested in resident fish and the numbers of nonresidents were often an order of magnitude greater than those of the residents, we felt that this criterion would give us the most information about the residents without being overwhelmed by the nonresidents.

Program MARK was used to model survival over a 16-year period. A bootstrap goodness-of-fit test included within program MARK was done to ensure that the general model fit the data. The general model generates estimates for seven parameters for each group and year, many of which are essential to running the model correctly but were of little interest in this study. For this data set, the general model estimates 230 parameters. Once we had determined that the general model fit the data, we used an iterative procedure to determine if all parameters within the general model were group or time dependent. Any that were not group or time dependent could then be condensed to a single parameter. We used Akaike's information criterion (AIC) as the criterion to determine the best fitting model. AIC balances the increased precision of parameter estimates through the reduction in the number of parameters against the reduced fit of the model to the data as the number of parameters are reduced (Burnham and Anderson 1998). The difference in AIC (ΔAIC) between models that are being compared is then used to calculate an Akaike weight ($\exp(-0.5\Delta\text{AIC})$/sum of $\exp(-0.5\Delta\text{AIC})$) for all models. The ratio of the Akaike weight of the model being examined to the Akaike weight of the best model gives the model likelihood (Burnham and Anderson 1998).

Once the best model was found, we examined whether a variety of environmental and population parameters could be used to predict survival better than the reduced general model. We used summer stream temperatures determined as the mean over the period from 1 July to 14 August of each year. Mean, maximum, and minimum summer discharges were determined over the same time period. Drought years were defined as those years with periods of low discharge (below the 25th percentile) for 15 days or longer. At these low discharges, pools become isolated as riffles become dry. In 1988 the mean daily discharge was 0.48 $m^3 \cdot s^{-1}$ for 32 days, in 1993 the daily discharge averaged 0.69 $m^3 \cdot s^{-1}$ for 16 days, in 1990 the daily discharge averaged 0.31 $m^3 \cdot s^{-1}$ for more than 59 days, and in 1998 the daily discharge was 0.61 $m^3 \cdot s^{-1}$ for 25 days. Daily temperature and discharge plots may be found in Deegan et al. (1999) and Slavik et al. (2004). Of all of the environmental conditions that we used, only mean and maximum discharges were correlated (Pearson's correlation coefficient = 0.66, $p < 0.01$). Environmental variables are presented as means ± SE.

We used two measures that evaluate the influence of the summer feeding period: summer growth (calculated as the mean difference in weight for individuals captured in July and August and adjusted for initial weight and time at large, grams per gram per day) and late-season fish condition factor (Fulton-type K_{TL} = 1000(weight (g) × total length (cm)$^{-3}$)). We used a Fulton-type condition factor because the length–weight power regression (n = 9287, 10–45 cm TL) has shown the exponent to be near 3 (±0.03) for Arctic grayling and the size range that we were comparing is small (29–45 cm TL). Because fish condition factor and summer growth were used as indicators of the unfertilized river, they were calculated from data from reference zone fish only. Summer growth is a precise measure of fish performance but was drawn from a small sample of fish (10–20 fish per year) from a relatively restricted section of the river (1.5 km of the reference zone). Condition factor, a less precise measure than summer growth, was calculated from a much larger sample of fish (40–80 fish per year) that ranged over a larger section of river. Late-season condition factor (fish captured after 1 August) was used to assess stream growth conditions for that summer. Mean summer growth and mean late-season condition factor were not correlated (Pearson's correlation coefficient < 0.32, $p > 0.12$, $n = 18$).

As a gauge of winter severity, we used the number of days after 1 May that it took for the snow pack to disappear, which corresponds to the date that flow resumes in the Kuparuk River and Arctic grayling leave their overwintering sites. Early-season condition (fish captured before 11 July) was used as a combined measure of previous winter severity and the previous summer performance. We were missing data for stream temperature and summer growth in 1987, so for these factors, we used only the mark–recapture data from 1988 through 2000. There were notable differences in mean length of residents and nonresidents in many years, so we examined the influence of length on survival for residents and nonresidents separately. The sex or age of Arctic grayling can only be determined on dead fish, so these factors were not included in our analysis.

Survival was estimated for the time between observation periods, from summer to summer. The parameters detailed above were evaluated for their ability to predict survival for the year following the one in which they were measured. That is, a parameter such as stream temperature measured in the summer of 1995 would be evaluated for its ability to predict survival for the year between the summer of 1995 and the summer of 1996. Two parameters, winter severity and early-season condition, were evaluated for their ability to predict survival in the year before the year in which they were measured. For example, winter severity or early-season condition factor measured in the spring of 1996 would be evaluated for its effect on survival from the summer of 1995 to the summer of 1996.

We used the multistrata model (also within program MARK) to assess whether survival differed between the fertilized and reference zones of the experimental reach, as our data were too sparse to use Barker's model. The multistrata model was developed to assess individual site fidelity and the impact that fidelity might have on survival and recapture. It estimates survival, recapture, and transition probabilities. Only resident fish were used in this analysis, as they spent the summer in either the reference or fertilized zone of the river. The multistrata model does not use resighting data; however, it does require information about where the fish was captured. Generally, in any given year, Arctic grayling remained in either the reference or the fertilized zone all summer. In those cases where an individual was caught in both zones in the same year, the first capture site was used as the primary summer residence. The second capture was usually during the autumnal migration.

Results

Of the 5623 individual Arctic grayling used in this analysis, 2901 were captured more than once during the 17 years of the study. We classified 1948 fish as summer residents within the experimental reach and 3675 as nonresidents. Most fish (72%) were in the medium size range (33–38 cm TL) (Fig. 2). Small fish (29–32 cm TL) comprised 11% and large fish (39+ cm TL) 18% of the population. Both residents and nonresidents underwent substantial changes in their population size structure over time. There were two periods (1990–1993 and 1997–1999) during which mean length of the population declined considerably. This corresponded to an increase in fish previously smaller than our cutoff of 29 cm TL recruiting into our target population (Fig. 2). The size change and recruitment were evident in the nonresident population about a year earlier than in the resident population.

Over the 17 years of this study, Arctic grayling were exposed to climatic conditions that varied by 1.5–30 times among years (Table 1). Mean annual stream temperature during the summer varied by a factor of 1.5 (range 8.3–12.9 °C, overall annual average of 9.78 ± 0.32 °C). Minimum discharge varied by a factor of 5 (range 0.20–1.01 $m^3 \cdot s^{-1}$, mean 0.51 ± 0.06 $m^3 \cdot s^{-1}$) among years, while maximum discharge varied by a factor of 30 (range 1.31–38.16 $m^3 \cdot s^{-1}$, mean14.27 ± 2.32 $m^3 \cdot s^{-1}$). As expected, average river discharge (range 0.3–4.4 $m^3 \cdot s^{-1}$, mean 2.52 ± 0.27 $m^3 \cdot s^{-1}$) was less variable (factor of 15) than maximum discharge but more variable than minimum discharge. Winter severity varied between 12 (river flow begins 12 May) and 40 days (10 June) with a mean of 24.9 ± 2.3 days.

Fish growth and condition also differed widely among years (Table 1). Summer growth varied by a factor of 30 (range from a low of 0.3×10^{-3} $g \cdot g^{-1} \cdot day^{-1}$ in 1990 to a high of 4.74×10^{-3} $g \cdot g^{-1} \cdot day^{-1}$ in 1991, mean annual average 2.63 ± 0.43 $g \cdot g^{-1} \cdot day^{-1} \times 10^{-3}$). Early-season condition factor was lower (range 7.56–9.12, mean 8.08 ± 0.09) than late-season condition factor (range 8.09–9.47, mean 8.67 ± 0.08), but variation among years was about the same (factor of 1.2).

Resident fish: fertilized versus reference zone survival

The multistrata model analysis suggested that Arctic grayling that summered in the fertilized zone had a probability of survival similar to that of those that summered in the reference zone (Table 2). The most parsimonious model (i.e., the one that best described the data with the fewest parameters) suggested that survival and recapture probabilities varied among years but not between reference and fertilized groups and transition probabilities varied between years and groups (Table 2). The probability of moving from the reference to the fertilized zone (0.15 ± 0.03) was very similar to that of moving from the fertilized to the reference zone (0.14 ± 0.05) but did vary among years. Because the fertilization did not affect survival rate, all fish, regardless of the zone that they spent the summer in, were combined in subsequent analyses.

Fig. 2. Size distribution of (*a*) residents and (*b*) nonresidents in the experimental reach from 1985 to 2000. The data were divided into small (29–32 cm total length (TL)) (open bars), medium (33–38 cm TL) (hatched bars), and large fish (39+ cm TL) (solid bars). Mean ± SE lengths (circles) of residents and nonresidents in each year are also given.

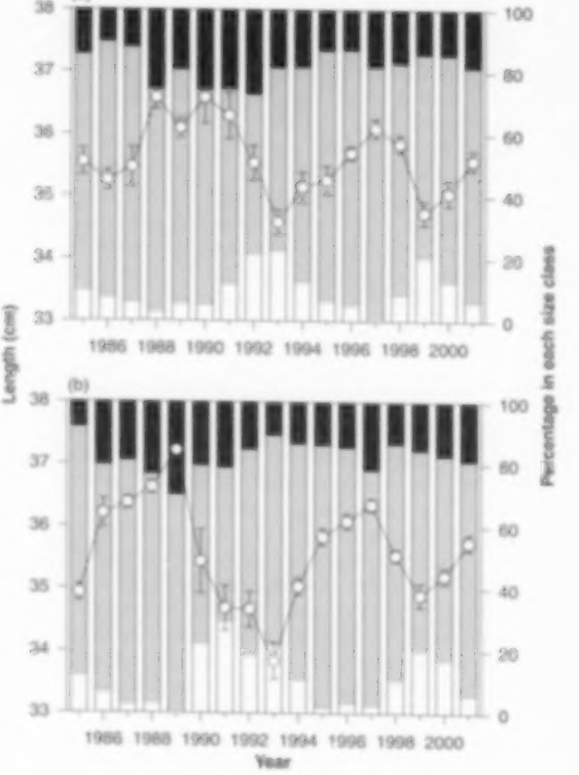

Entire population

The most parsimonious resighting model suggested that annual survival differed among residents and nonresidents (group) and that survival varied annually (year) (Table 3). The resighting parameters *R* and *R′* and the fidelity parameter *F* were also group and year dependent (Table 3). Modeling recapture probabilities as variable between years but not between groups and modeling the fidelity parameter *F′* as constant for residents and variable over time for nonresidents improved model fit.

Table 1. Parameters that were used to assess the influence of environmental variables or fish growth or condition on adult Arctic grayling survival in the Kuparuk River.

Year	Stream temperature (°C)	Average discharge ($m^3 \cdot s^{-1}$)	Minimum discharge ($m^3 \cdot s^{-1}$)	Maximum discharge ($m^3 \cdot s^{-1}$)	Winter severity	Adult growth ($g \cdot g^{-1} \cdot day^{-1}$)	Condition factor	
							Early	Late
1985	8.9	2.1	0.20	12.24	28			8.79
1986	9.2	2.8	0.29	18.59	36	0.00272	7.68	8.35
1987		3.6	0.32	12.93	22			8.43
1988	8.8	1.2	0.32	6.53	12	0.00048	8.13	8.20
1989	10.7	2.5	0.48	11.80	28	0.00396	7.88	8.75
1990	12.9	0.3	0.24	1.31	19	0.00030	9.12	9.08
1991	9.3	1.8	0.36	17.64	14	0.00474	8.30	9.47
1992	9.7	1.7	0.63	25.50	40	0.00163	8.23	8.75
1993	11.2	3.7	0.59	20.08	18	0.00065	8.07	8.19
1994	11.0	2.4	0.75	9.59	14	0.00425	8.02	8.69
1995	9.0	4.4	0.98	28.74	14	0.00389	8.23	8.93
1996	8.3	2.3	1.01	5.61	31	0.00402	8.12	8.85
1997	9.8	3.2	0.57	8.11	28	0.00124	8.14	8.85
1998	10.6	1.1	0.41	4.76	21	0.00051	7.97	8.09
1999	10.3	4.2	0.29	38.16	22	0.00228	7.90	8.65
2000	8.4	2.2	0.62	8.92	38	0.00463	7.56	8.70
2001	8.3	3.3	0.68	12.15	38	0.00414	7.90	8.67

Note: Values for stream temperature and average discharge are summer means (1 July – 14 August). Data were not available for all years.

Table 2. Multistrata model used to generate survival (Φ), recapture (ρ), and transition (Ψ) probabilities for fish in the fertilized and reference zones of the Kupauk River.

Hypothesis tested	Model	AIC[a]	Akaike weight	Model likelihood
Effect of group on survival and recapture	$\mathbf{\Phi}(t)\ \mathbf{p}(t)\ \Psi(g \times t)$	4885	0.880	1.000
Effect of group on survival	$\mathbf{\Phi}(t)\ \rho(g \times t)\ \Psi(g \times t)$	4889	0.116	0.130
Effect of group on recapture	$\Phi(g \times t)\ \mathbf{p}(t)\ \Psi(g \times t)$	4896	0.005	0.005
Time dependent	$\mathbf{\Phi}(t)\ \mathbf{p}(t)\ \mathbf{\Psi}(t)$	4896	0.000	0.000
Fully parameterized	$\mathbf{\Phi}(g \times t)\ \mathbf{p}(g \times t)\ \mathbf{\Psi}(g \times t)$	4904	0.000	0.000
Effect of group on transition between zones	$\Phi(g \times t)\ \rho(g \times t)\ \mathbf{\Psi}(t)$	4909	0.000	0.000

Note: Alternative models were compared with the fully parameterized model (in bold). The parameter or parameters being investigated are in bold. *t*, time; *g*, group. Interaction is denoted with a times symbol (×).

[a]Akaike information criterion.

Overall annual survival rates were very similar between residents (range 0.45 and 1.0, mean 0.71 ± 0.05) and nonresidents (range 0.39 and 1.0, mean 0.75 ± 0.05) over the 15-year period, despite differences in the pattern with year (Fig. 3). In some years, especially between 1995 and 1999, survival rates of both residents and nonresidents were very similar; however, overall there was little correlation in survival rates between the two groups within a year (Pearson's correlation coefficient = 0.18, $p = 0.53$, $n = 15$). Estimates generated with the resighting model were also similar to those generated by the multistrata model, especially in the latter half of the study (Fig. 4).

Recapture rates varied between 1.0 and 0.21, with a steady downward trend over the study period (Fig. 5), but did not differ between resident and nonresident fish. The precision in the estimates has improved throughout the study, especially the period from 1994 to 1999 when fish were tagged with both anchor and PIT tags.

Resighting rates were variable between years and between resident and nonresident fish. The value of *R* (the probability of being resighted and surviving) was higher for all time periods for nonresidents (0.57 ± 0.06) than for resident fish (0.44 ± 0.07). Estimates of *R′* (the probability of being resighted and then dying before the next capture period) were anomalously high in 1987 for residents (1.00) and in 1992 for nonresidents (0.60) but were low (<0.38) for all other time periods.

The fidelity parameters *F* (the probability that an animal is at risk of capture during times *i* and *i* + 1) and *F′* (the probability that an animal not at risk at time *i* is at risk during time *i* + 1) describe migration in and out of the study area. In most years, parameter estimates of *F* approached 1 and *F′* was estimated at 0.12 ± 0.02 for the residents, which is consistent with permanent emigration for that year. Estimates of *F′* were low for the nonresidents; however, estimates of *F* were highly variable. This may reflect variability in sampling effort combined with flood events that knock the weirs down releasing fish before they can be recaptured.

Incorporation of environmental factors (stream temperature and discharge) that strongly influence summer growth (Deegan et al. 1999) did not improve model fit (Fig. 6). Reasoning that perhaps only the most severe conditions affected

Table 3. Resighting models examined to estimate survival rates.

Hypothesis tested	Model	AIC[a]
Group effect in recapture, F' time effect for nonresidents	$\Phi(g \times t)\ \boldsymbol{\rho(t)}\ R(g \times t)\ R'(g \times t)\ F(g \times t)\ \boldsymbol{F'(\cdot,t)}$	19 658
Group effect in recapture	$\Phi(g \times t)\ \boldsymbol{\rho(t)}\ R(g \times t)\ R'(g \times t)\ F(g \times t)\ F'(g \times t)$	19 666
Group effect in F' time effect for nonresidents	$\Phi(g \times t)\ \rho(g \times t)\ R(g \times t)\ R'(g \times t)\ F(g \times t)\ \boldsymbol{F'(\cdot,t)}$	19 674
Fully parameterized model	$\boldsymbol{\Phi(g \times t)\ \rho(g \times t)\ R(g \times t)\ R'(g \times t)\ F(g \times t)\ F'(g \times t)}$	**19 684**
Group effect in fidelity parameters	$\Phi(g \times t)\ \rho(g \times t)\ R(g \times t)\ R'(g \times t)\ \boldsymbol{F(t)\ F'(t)}$	19 698
Group effect in survival	$\boldsymbol{\Phi(t)}\ \rho(g \times t)\ R(g \times t)\ R'(g \times t)\ F(g \times t)\ F'(g \times t)$	19 708
Constant recapture rate by group	$\Phi(g \times t)\ \boldsymbol{\rho(g)}\ R(g \times t)\ R'(g \times t)\ F(g \times t)\ F'(g \times t)$	19 726
Group effect in all parameters	$\boldsymbol{\Phi(t)\ \rho(t)\ R(t)\ R'(t)\ F(t)\ F'(t)}$	19 851
Constant survival rate by group	$\boldsymbol{\Phi(g)}\ \rho(g \times t)\ R(g \times t)\ R'(g \times t)\ F(g \times t)\ F'(g \times t)$	19 869
Discharge effects survival (1988-2000 only)	$\boldsymbol{\Phi(g \times \mathrm{discharge})}\ \rho(g \times t)\ R(g \times t)\ R'(g \times t)\ F(g \times t)\ F'(g \times t)$	19 761
End of summer condition effects survival	$\boldsymbol{\Phi(g \times \mathrm{condition})}\ \rho(g \times t)\ R(g \times t)\ R'(g \times t)\ F(g \times t)\ F'(g \times t)$	19 785
Drought effects survival	$\boldsymbol{\Phi(g \times \mathrm{drought})}\ \rho(g \times t)\ R(g \times t)\ R'(g \times t)\ F(g \times t)\ F'(g \times t)$	19 810
Winter severity effects survival	$\boldsymbol{\Phi(g \times \mathrm{winter})}\ \rho(g \times t)\ R(g \times t)\ R'(g \times t)\ F(g \times t)\ F'(g \times t)$	20 445
Fully parameterized (1988–2000)	$\boldsymbol{\Phi(g \times t)\ \rho(g \times t)\ R(g \times t)\ R'(g \times t)\ F(g \times t)\ F'(g \times t)}$	**15 353**
Summer growth effects survival (1988–2000)	$\boldsymbol{\Phi(g \times \mathrm{growth})}\ \rho(g \times t)\ R(g \times t)\ R'(g \times t)\ F(g \times t)\ F'(g \times t)$	15 412
Stream temperature effects survival (1988–2000 only)	$\boldsymbol{\Phi(g \times \mathrm{temperature})}\ \rho(g \times t)\ R(g \times t)\ R'(g \times t)\ F(g \times t)\ F'(g \times t)$	15 456
Fully parameterized (residents only)	$\boldsymbol{\Phi(t)\ \rho(t)\ R(t)\ R'(t)\ F(t)\ F'(t)}$	**6 326**
Length effects survival	$\Phi(\mathrm{length})\ \rho(t)\ R(t)\ R'(t)\ F(t)\ F'(t)$	6 369
Fully parameterized (nonresidents only)	$\boldsymbol{\Phi(t)\ \rho(t)\ R(t)\ R'(t)\ F(t)\ F'(t)}$	**12 277**
Length effects survival	$\Phi(\mathrm{length})\ \rho(t)\ R(t)\ R'(t)\ F(t)\ F'(t)$	13 286

Note: The resighting model estimates seven parameters: Φ, survival; ρ, recapture; *r*, recovered dead; *R*, resighted and survived; *R′*, resighted and died; *F*, at risk of capture in year *i* and year *i* + 1; *F′*, not at risk of capture in year *i* but at risk in year *i* + 1; *t*, time; *g*, group. Interaction is denoted with a times symbol (×). Alternative models were compared with the fully parameterized model (in bold) using either the entire data set (1985–2000) or a partial data set (1988–2000) when data were lacking. Results are shown for those models that best fit the data. The data set was divided into residents and nonresidents to examine the effect of length because there were significant differences between the populations for this covariate. The parameter or parameters being investigated in the alternative models are in bold.

[a] Akaike information criterion.

Fig. 3. Annual survival estimates (±SE) for residents (solid circles) and nonresidents (open circles). As the capture and release period is during the summer, estimates are for the period from one summer to the next.

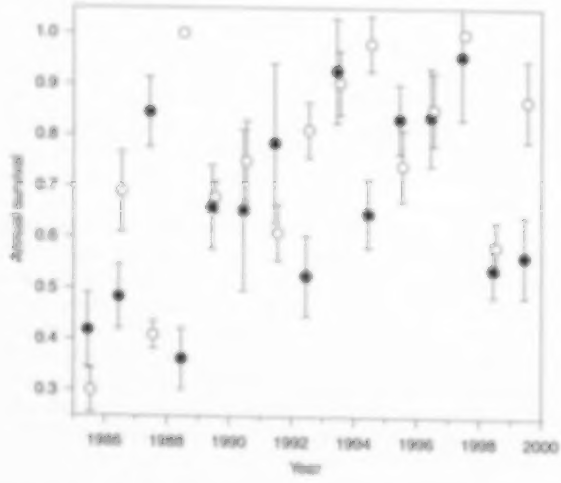

Fig. 4. Comparison of annual survival rate estimates generated by the resighting (solid circles) and multistrata models (open circles).

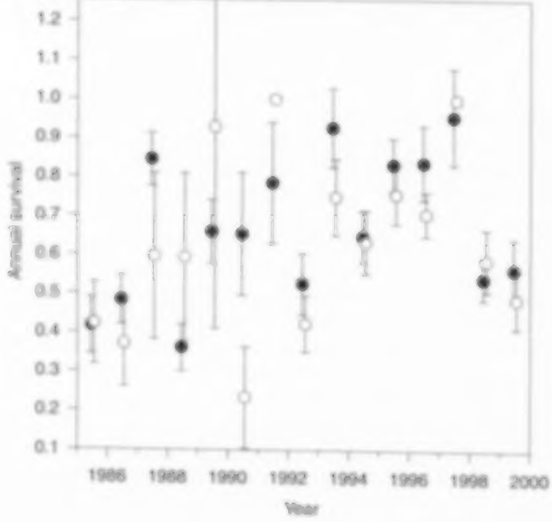

survival, we tested whether drought or nondrought years or winter severity affected survival. Neither of these factors improved our ability to predict survival.

None of the aspects of fish population (growth, early-season or late-season condition, or fish length) improved the fit of the model to survivorship (Table 3). Length was a

Fig. 5. Annual recapture estimates for each year of the study. The combined recapture estimate is given here, since there was no significant difference in recapture rates between residents and nonresidents.

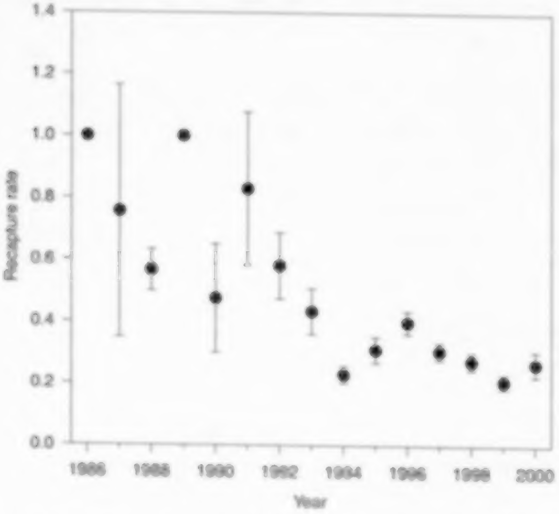

better estimator of survival for residents than for nonresidents; however, it did not fit the data better than the fully parameterized model.

Discussion

Overall, our estimates of annual survival of Arctic grayling (0.71 for residents and 0.75 for nonresidents) are very similar to Clark's (1992) estimate of 0.69 for the more southerly Arctic grayling population in the Chena River, Alaska. None of the parameters used to quantify environmental conditions or the ability of fish to acquire resources were sufficiently important to survival dynamics to improve the fit of the model to the data. In keeping with these results, there was no significant difference in survival between fish that spent the summer in the reference and fertilized zones of the river despite greater food resources and higher weight gain in fish that summered in the fertilized zone.

On an individual basis, larger fish generally have higher survival rates because of their ability to hold better territories (Hughes 1992), evade predation, and have higher energy reserves to withstand overwintering conditions (Cargnelli and Gross 1997; Sogard and Olla 2000). As there were substantial changes in the size structure of the population, we expected there to be a relationship between fish size and survival but were unable to demonstrate this. Our study considered only adult fish (29–42 cm TL, with most fish <40 cm TL) and may not have included a wide enough range of values for size effects to be detected.

Density of fish has been suggested to affect survival rates through competition for resources, increased agonistic interactions, and higher predation risk as individuals are forced into more marginal habitats. Oxygen availability may be a limiting factor in these Arctic lakes that are frozen for 9 months of the year and increased densities may induce hypoxic conditions in overwintering sites. We could not directly assess whether there were density-dependent effects on survival rates because we lack information about fish densities in the river or in the overwintering lake. However, since it takes at least 5 years for young-of-the-year Arctic grayling to recruit into the adult population, we can surmise that in years when survival is poor the population declines and when survival is good the population is constant or increases. There were few years when both survival and recruitment were high; however, a recruitment episode occurred between 1990 and 1994. Resident survival rates were variable over this period; nevertheless, it should be noted that one of the highest survival rates was recorded in 1994. Nonresident survival rates steadily increased during this period. While not conclusive, this indicates that at densities commonly found in the Kuparuk River, it is unlikely that density-dependent factors play a role in survival dynamics.

Surprisingly, there were significant differences in survival rates between fish that were summer residents in the experimental reach and nonresidents that spent the summer downstream of the experimental reach and were caught as they migrated upstream to overwintering sites. Some of this difference may be the result of slight differences in tag loss between the two groups. From 1985 through 1992, fish were tagged with external anchor tags. Retention of these tags is high for the first several years after tagging; however, it decreases dramatically after the tags have been in place for more than 3 years (Buzby and Deegan 1999). The number of resident and nonresident fish tagged in each year was highly variable between the two groups as well as between years, which would lead to differing probabilities in tag loss between the two groups. Mark–recapture methods are unable to differentiate between tag loss and mortality; therefore, differing tag loss probabilities would be superimposed on survival rates. The different tag loss rates between residents and nonresidents are probably causing the perceived differences in survival rate estimates. Bolstering this argument is the convergence in survival rates in the last several years when we were tagging fish with both PIT and anchor tags. The probability that a fish will lose both tags is extremely low, virtually eliminating errors due to tag loss.

The effects of tag loss extend beyond creating variability in survival rate estimates; it undoubtedly caused us to underestimate survival rates. We estimate that in most years, between 10 and 20 fish were not seen because of tag loss. While the uneven distribution of tag loss between residents and nonresidents caused the model to accept the argument that differences between the two groups were significant, the overall effect of tag loss on survival rates was probably minor.

The lack of any single or combination of factors that correlated well with survival may have occurred for several reasons. Our approach evaluated environmental parameters that have been suggested to influence survivorship; however, we may not have used a good surrogate for that factor or we may not have had data pertaining to the critical factor. For example, we lack information on predation rates and on the populations of the predators, one of the major causes of adult mortality identified by Wootton (1998). However, we expected that in years when resources are adequate or plentiful, fish would be less vulnerable to predation and that this might have been reflected in the measures that we used.

Fig. 6. Relationship between environmental variables thought to influence survival and annual survival rates for residents (solid circles) and nonresidents (open circles).

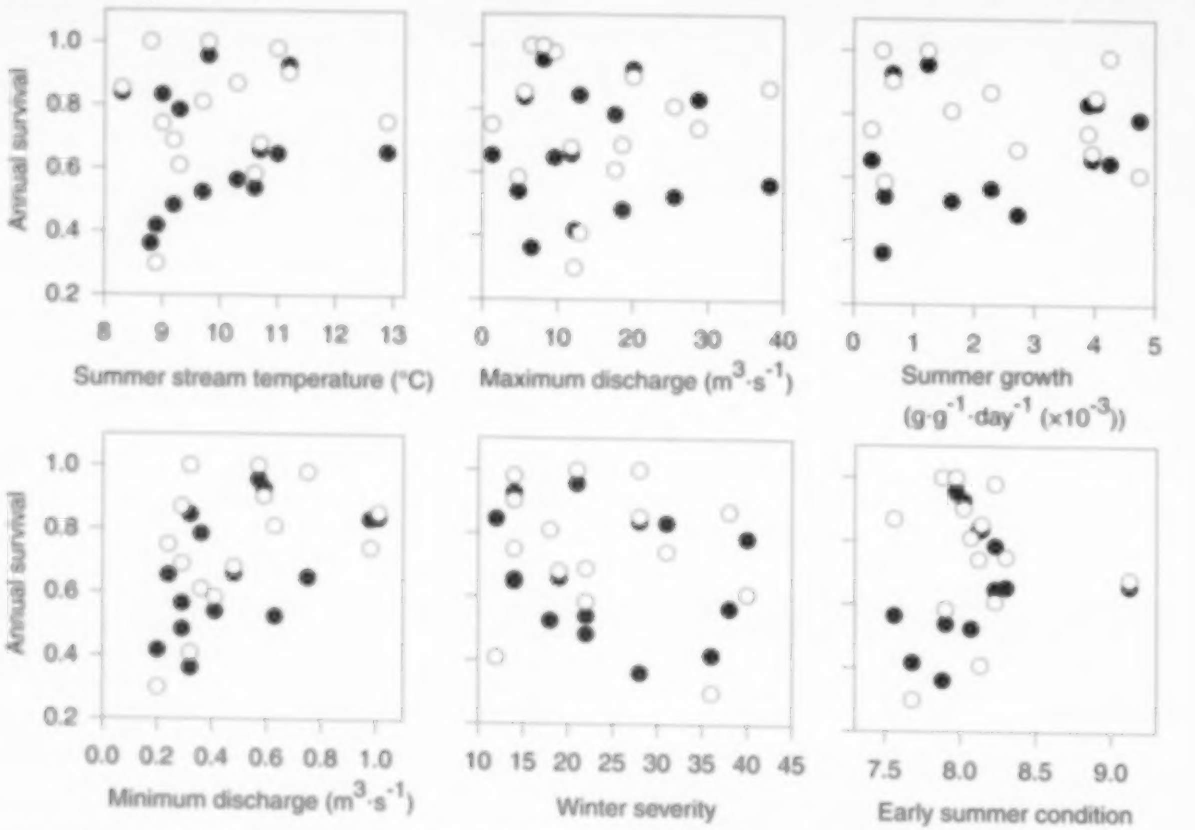

Spawning may be a source of mortality that we could not adequately assess. Arctic grayling are spring spawners and as such are called upon to invest resources in reproduction when body reserves are at a minimum. Adult Arctic grayling typically lose an average of 10% of their body weight (range 0%–20%) over the winter prior to spawning (L.A. Deegan, unpublished data). It might be expected that spawning mortality would occur in fish in the poorest condition and would therefore be included in any relationship between condition and survival. Arctic grayling may instead follow the same strategy as Arctic char (*Salvelinus alpinus*), which do not spawn when they have spent the previous year in unproductive habitats (Dutil 1986). This strategy would not be reflected in any measure that we have available, nor do we know if Arctic grayling use this strategy.

Other reasons that we were unable to find a single or combination of parameters in a year that correlated well with survival may be that there are multiyear effects where the population is capable of withstanding one stressful year but a second or third stressful year would have a disproportionately large effect on survivorship. This type of multiyear conditional mortality cannot be adequately addressed using program MARK.

Another possibility is that survival rates were relatively unresponsive to environmental conditions. The Arctic is a harsh environment with a short growing season and strong nutrient limitation in both aquatic (O'Brien et al. 1992; Peterson et al. 1993) and terrestrial ecosystems (Shaver and Chapin 1995). Most organisms require multiple growing seasons to acquire sufficient biomass and resources to reproduce. In addition, there was considerable interannual variation in environmental conditions. Deegan et al. (1999) demonstrated that conditions favoring adult Arctic grayling growth do not favor growth of young-of-the-year. Within this framework of variability, there is a high likelihood that in any given year there will be poor survival of young-of-the-year or a year-class failure, which is reflected in the observed variability in recruitment into the adult population. Spreading reproduction over several years increases the probability that some offspring will survive to become adults. However, to accomplish this, adult survival rates must remain high and relatively unaffected by resource levels. Life history theory predicts that in long-lived species, resource availability will affect fecundity rather than adult survival (Stearns 1976), and this has been demonstrated in seabirds (Oro et al. 1999). Arctic grayling may be following the same strategy.

This study provides one of the few long-term survival estimates for an Arctic fish. Arctic regions are most likely to experience the greatest degree of warming under all global change scenarios (IPCC 2001). Arctic grayling in streams of Alaska's North Slope face additional challenges as this area becomes more accessible to resource extraction (gravel mining, oil drilling, and transport) and fishing pressure. Owing to the remoteness of the study site and the sampling design, these estimates of survival for the most part exclude anthropogenic effects on the population and as such provide a baseline against which anthropogenic effects may be evaluated.

This study should also sound a note of caution. Arctic grayling are a game fish and they can face substantial fishing pressure. Clark (1992) estimated instantaneous fishing mortality to be 0.45 for Chena River Arctic grayling. Fish stocks are often managed assuming density dependence where natural mortality is substituted for by fishing mortality. With little evidence for density dependence regulating this Arctic population or the subarctic Chena River population, fishing mortality may instead be added to natural mortality. Iteroparous populations with variable survival rates such as Arctic grayling face the greatest risks of local extinction (Jonsson and Ebenman 2001). Care must be taken to avoid depletion of grayling stocks through overfishing or other anthropogenic activities, especially in the Arctic where growth rates are low and recruitment is variable. Stocking efforts by the Alaska Department of Fish and Game have not been successful in replenishing Arctic grayling stocks that have been overfished (Clark 1996). In addition, natural recolonization of areas of local extinction will be slow because of the high site fidelity that Arctic grayling display to their summer feeding locations (Buzby and Deegan 2000). The geographic range of Arctic grayling has been decreasing because of overfishing and extirpation (Kaya 1991; Northcote 1995; Clark 1996). All evidence indicates that it is considerably more difficult to restore Arctic grayling populations than it is to maintain them.

Acknowledgements

This research was supported by National Science Foundation grants OPP-9911278 and DEB-9810222 in conjunction with the Long-term Ecological Research Program. The authors gratefully thank the numerous colleagues for their contribution, especially Carolyn Bauman, Chris Harvey, Heidi Golden, Robert Golder, and Stan Peterson. We thank Rob Gieck of University of Alaska-Fairbanks for his assistance with the Kuparuk River snowmelt data. We also thank the staff of the Toolik Lake Field Station for their logistical support.

References

Barker, R.J. 1999. Joint analysis of mark–recapture, resighting and ring-recovery data with age-dependence and marking effect. Bird Study, **46**(Suppl.): 82–91.

Burnham, K.P., and Anderson, D.R. 1998. Model selection and inference: a practical information-theoretic approach. Springer-Verlag, New York.

Buzby, K., and Deegan, L. 1999. Retention of anchor and passive integrated transponder tags by Arctic grayling. N. Am. J. Fish. Manag. **19**: 1147–1150.

Buzby, K.M, and Deegan, L.A. 2000. Inter-annual fidelity to summer feeding sites in Arctic grayling. Environ. Biol. Fishes, **59**: 319–327.

Cargnelli, L.M., and Gross, M.R. 1997. Fish energetics: larger individuals emerge from winter in better condition. Trans. Am. Fish. Soc. **126**: 153–156.

Clark, R.A. 1992. Influence of stream flows and stock size on recruitment of Arctic grayling (*Thymallus arcticus*) in the Chena River, Alaska. Can. J. Fish. Aquat. Sci. **49**: 1027–1034.

Clark, R.A. 1996. Stock status and rehabilitation of Chena River Arctic grayling during 1995. Alaska Dep. Fish Game Fish. Data Ser. No. 96-2.

Deegan, L.A., and Peterson, B.J. 1992. Whole-river fertilization stimulates fish production in an Arctic tundra river. Can. J. Fish. Aquat. Sci. **49**: 1890–1901.

Deegan, L.A., Golden, H.E., Harvey, C.J., and Peterson, B.J. 1999. Influence of environmental variability on the growth of age-0 and adult Arctic grayling. Trans. Am. Fish. Soc. **128**: 1163–1175.

De Leo, G.A., and Gatto, M. 1996. Trends in vital rates of the European eel: evidence for density dependence. Ecol. Appl. **6**: 1281–1294.

Dutil, J.-D. 1986. Energetic constraints and spawning interval in the anadromous Arctic charr (*Salvelinus alpinus*). Copeia, 4: 945–955.

Frederiksen, M., and Bregnballe, T. 2000. Evidence for density-dependent survival in adult cormorants from a combined analysis of recoveries and resightings. J. Anim. Ecol. **69**: 737–752.

Heppel, S.S., Crowder, L.B., and Caswell, H. 2000. Life histories and elasticity patterns: perturbation analysis for species with minimal demographic data. Ecology, **81**: 654–665.

Hershey, A.E., Bowden, W.B., Deegan, L.A., Hobbie, J.E., Peterson, B.J., Kipphut, G.W., Kling, G.W., Lock, M.A., Merritt, R.W., Miller, M.C., Vestal, J.R., and Schuldt, J.A. 1997. The Kuparuk River: a long-term study of biological and chemical processes in an Arctic river. *In* Freshwaters of Alaska. *Edited by* A.M. Milner and M.W. Oswood. Springer, New York. pp. 107–129.

Hughes, N.F. 1992. Selection of positions by drift-feeding salmonids in dominance heirarchies: model and test for Arctic grayling (*Thymallus arcticus*) in subarctic mountain streams, interior Alaska. Can. J. Fish. Aquat. Sci. **49**: 1999–2008.

Intergovernmental Panel on Climate Change (IPCC). 2001. Climate change 2001: the scientific basis. *Edited by* J.T. Houghton, Y. Ding, D.J. Griggs, M. Noguer, P.J. van der Linden, and D. Xiaosu. Cambridge University Press, Cambridge, UK.

Jonsson, A., and Ebenman, B. 2001. Are certain life histories particularly prone to local extinction. J. Theor. Biol. **209**: 455–463.

Kaya, C.M. 1991. Rheotactic differentiation between fluvial and lacustrine populations of Arctic grayling (*Thymallus arcticus*), and implications for the only remaining indigenous population of fluvial "Montana Grayling". Can. J. Fish. Aquat. Sci. **48**: 53–59.

Lebreton J.D., Burnham, K.P., Clobert, J., and Anderson, D.R. 1992. Modeling survival and testing biological hypotheses using marked animals: a unified approach with case studies. Ecol. Monogr. **62**: 67–118.

Northcote, T.G. 1995. Comparative biology and management of Arctic and European grayling (Salmonidae, *Thymallus*). Rev. Fish Biol. Fish. **5**: 141–194.

O'Brien, W.J., Hershey, A.E., Hobbie, J.E., Hullar, M.A., Kipphut, G.W., Miller, M.C., Moller, B., and Vestal, J.R. 1992. Control mechanisms of arctic lake ecosystems: a limnocorral experiment. Hydrobiologia, **240**: 143–188.

Oro, D., Pradel, R., and Lebreton, J.-D. 1999. Food availability and nest predation influence life history traits in Audouin's, *Larus audouinii*. Oecologia, **118**: 438–445.

Peterson, B.J., Deegan, L., Helfrich, J., Hobbie, J.E., Hullar, M., Moller, B., Ford, T.E., Hershey, A., Hiltner, A., Kipphut, G., Lock, M.A., Fiebig, D.M., McKinley, V., Miller, M.C., Vestal, J.R., Ventullo, R., and Volk, G. 1993. Biological responses of a tundra river to fertilization. Ecology, **74**: 653–672.

Sæther, B.-E., and Bakke, O. 2000. Avian life history variation and contribution of demographic traits to the population growth rate. Ecology, **81**: 642–653.

Shaver, G.R., and Chapin, F.S., III. 1995. Long-term responses to factorial, NPK fertilizer treatment by Alaskan wet and moist tundra sedge species. Ecography, **18**: 259–275.

Slavik, K., Peterson, B.J., Deegan, L.A., Bowden, W.B., Hershey, A.E., and Hobbie, J.E. 2004. Long-term responses of the Kuparuk River to fertilization. Ecology, **85**: 939–954.

Sogard, S.M., and Olla, B.L. 2000. Endurance of simulated winter conditions by age-0 walleye pollock: effects of body size, water temperature and energy stores. J. Fish Biol. **56**: 1–21.

Stearns, S.C. 1976. Life history tactics: a review of the ideas. Q. Rev. Biol. **51**: 3–47.

Stearns, S.C. 1992. The evolution of life histories. Oxford University Press, Oxford, UK.

White, G.C., and Burnham, K.P. 1999. Program MARK: survival estimation from populations of marked animals. Bird Study, **46**(Suppl.): 120–139.

Wildy, E.L., Chivers, D.P., Kiesecker, J.M., and Blaustein, A.R. 2001. The effects of food level and conspecific density on biting and cannibalism in larval long-toed salamanders, *Ambystoma macrodactylum*. Oecologia, **128**: 202–209.

Wootton, R.J. 1998. Ecology of teleost fishes. 2nd ed. Kluwer Academic Publishers, Dordrecht, the Netherlands.

Past and future chemistry changes in acidified Nova Scotian Atlantic salmon (*Salmo salar*) rivers: a dynamic modeling approach

Thomas A. Clair, Ian F. Dennis, Peter G. Amiro, and B.J. Cosby

Abstract: Atlantic salmon (*Salmo salar*) populations have been extirpated from a number of rivers in Nova Scotia, Canada, as a result of acid rain. We applied the model of acidification of groundwater in catchments (MAGIC) to 35 regional rivers to estimate pre-industrial water chemistry conditions and the potential future changes in water chemistry under three acid deposition scenarios for the region. Our model results indicate that water chemistry in the study streams remained relatively unchanged until the 1950s and reached their maximum effects on pH in the mid-1970s. The main effects of acid deposition have been a decrease in pH and an increase in base cations to surface waters, as the ion-exchange processes in soils release soil cations into surface waters. We forecast future water chemistry in the rivers using three deposition scenarios: no change in sulfate deposition from year 2000 and 10% and 20% sulfate reductions per decade. We show that the more rapid the reduction in acid deposition, the faster the recovery. We also show that although stream water acidity will recover within a few decades, in most streams, base cations will not recover to pre-industrial levels within the next 100 years.

Résumé : Plusieurs populations de saumons atlantiques (*Salmo salar*) ont été éliminées des rivières de Nouvelle-Écosse à cause des précipitations acides. Nous avons appliqué le modèle MAGIC (modèle d'acidification des eaux souterraines dans les bassins hydrogéographiques) à 35 rivières de la région pour estimer les conditions chimiques de l'eau avant l'industrialisation et pour prédire les changements futurs de chimie de l'eau dans ces milieux selon trois scénarios de précipitations acides dans la région. Les résultats de la modélisation indiquent que les conditions chimiques de l'eau sont demeurées à peu près inchangées jusqu'aux années 1950 et que les effets les plus importants sur le pH se sont produits au milieu des années 1970. Les effets principaux ont été une baisse du pH et une augmentation des cations basiques dans les eaux de surface, alors que les mécanismes d'échanges ioniques des sols libéraient les cations vers les eaux superficielles. Nous prédisons les caractéristiques chimiques de l'eau dans les rivières selon trois scénarios, soit des précipitations de sulfates inchangées au taux de 2000 et des réductions de 10 % et de 20 % des sulfates par décennie. Plus la réduction des précipitations acides se fera rapidement, plus rapide aussi sera la récupération. Bien que l'acidité de l'eau des rivières puisse se rétablir en quelques décennies, les concentrations de cations basiques ne retrouveront pas leur niveau pré-industriel au cours du prochain siècle.

[Traduit par la Rédaction]

Introduction

Acid rain, in the form of sulfuric (H_2SO_4) and nitric (HNO_3) acids, is deposited in catchments. Some of the hydrogen ions accompanying the acid anions are neutralized, first by calcium and magnesium carbonates and then by alumino-silicate minerals. Increases in acid loadings will then cause increases in the calcium and magnesium (base cations) dissolved from soil minerals and leached into runoff waters. If base cation production from weathering of bedrock and soils cannot keep up with acid leaching, then these will gradually be depleted from catchment ion-exchange sites and replaced by hydrogen and aluminum ions (Kirchner 1992). Large parts of Nova Scotia are underlain by poorly weatherable slates and granites producing soils with naturally low amounts of base cations (Shilts 1981) so that this region is especially vulnerable to acidification effects.

Acid deposition effects were first noticed in Nova Scotia in the 1960s. The pH of surface waters used by fish hatcheries in the region was seen to be decreasing, which caused a number of obvious problems to hatchery managers (Farmer et al. 1979). In the mid-1980s, the region received over

Received 19 March 2004. Accepted 22 October 2004. Published on the NRC Research Press Web site at http://cjfas.nrc.ca on 18 December 2004.
J18033

T.A. Clair[1] and I.F. Dennis. Environmental Conservation Br, Environment Canada – Atlantic Region, P.O. Box 6227, Sackville, NB E4L 1G6, Canada.
P.G. Amiro. Science Branch, Fisheries and Oceans Canada, Bedford Institute of Oceanography, P.O. Box 1006, Dartmouth, NS B2Y 4A2, Canada.
B.J. Cosby. Department of Environmental Sciences, University of Virginia, Charlottesville, VA, 22903, USA.

[1]Corresponding author (e-mail: tom.clair@ec.gc.ca).

Can. J. Fish. Aquat. Sci. **61**: 1965–1975 (2004) doi: 10.1139/F04-196

20 kg·ha^{-1}·year^{-1} of sulfate (SO_4^{-2}), most of which originated in central Canada and the east coast of the United States (Shaw 1979). This deposition clearly had an effect on the fish populations of the region. Watt (1987) showed that formerly viable Atlantic salmon (*Salmo salar*) populations were extirpated in a number of river catchments and were greatly reduced in others. He was also able to make the link between the reduction of fish and increases in acidification.

Since the early 1980s, acid rain controls in both Canada and the United States caused a significant reduction (45%) in SO_4^{-2} deposition in the region (Beattie et al. 2002). However, these reductions have not yet been reflected in positive changes in water chemistry. Clair et al. (2002) examined trends in water chemistry from over 40 lake sites in Nova Scotia from 1982 to 1997. They found that although surface water SO_4^{-2} concentrations decreased along with the deposition, pH and acid neutralization capacity (ANC) did not change. Moreover, they also noted a marked decrease in base cation concentrations ($Ca^{+2} + Mg^{+2} + K^{+} + Na^{+}$) in a number of the sites. A similar situation was noted in biological studies, as the reduced SO_4^{-2} changes occurring were not seen to have helped local fish populations (Watt et al. 2000).

The 16-year data series available for trend analysis is quite good for these kinds of studies, but the results measured tended to present as many questions asked as answered. These changes in water chemistry and fish populations, or lack thereof, emphasized the need to apply geochemical models to the systems to see what kinds of results should be expected. To help answer these questions, we applied the model of acidification of groundwater in catchments (MAGIC) (Cosby et al. 2001) to the rivers in Nova Scotia, which were previously studied by Watt (1987) and which also used to have endemic Atlantic salmon populations.

There were therefore a number of questions that needed to be answered in order to allow us to better manage our responses to the acidification of Nova Scotia's surface waters. First, it was important to determine what were the initial water chemistry conditions at these sites before acidification. Much of our analysis of possible mitigation measures should be moderated by an understanding of what conditions existed in pre-acidification times. We felt that modeling the geochemistry of the catchments might present us with information on earlier conditions and thus produce more realistic management decisions.

Secondly, there was a need to understand where the water chemistry in these ecosystems might be heading under different future acid deposition scenarios. This is most important to managing expectations of stakeholders so that they be aware of the time frames involved in the chemical and ecological recovery of these systems. It is also important that decision makers be made aware of the consequences of the choices they make when they decide on the relative rates of acid emission reductions. To present them with predictions of potential changes, we applied hypothetical acid deposition scenarios to the catchments to determine how water chemistry might change. We used three potential scenarios to provide a range of options: no further decreases in deposition from the year 2000 or 10% or 20% decreases in SO_4^{-2} deposition per decade from the year 2000. We did not address the issue of nitrogen acidification as it currently is not obviously causing problems in this region.

Methods

Study area

The southeastern portion of Nova Scotia is a narrow strip of land draining directly into the Scotian Shelf of the Atlantic Ocean (Fig. 1). Streams and rivers draining this area do not exceed 80 km in length from their headwaters to the estuaries. Beginning in the 1980s, water from 40 streams and rivers containing Atlantic Salmon populations were sampled sporadically by staff of Fisheries and Oceans Canada (DFO) for water chemistry. As the water chemistry varied greatly depending on the years sampled, we use model results normalized for the year 2000 to illustrate the relative water chemistry between the sites (Table 1). Angling catch data extending to 1936 were also available from these sites, so they were known to have had salmon from pre-acidification times. Earlier work by DFO (Watt et al. 2000) related the survival capacity of salmon in these streams to specific 1980 pH ranges. They classified rivers with mean pH values greater than 5.4 as not significantly affected by acidification, and those with pH ranges between 5.4 and 5.0 were identified as having depleted stocks. Sites with pH values between 4.7 and 5.0 still had residual populations, whereas populations at sites with mean annual pHs of less than 4.7 were extirpated. When modeling pH, we will use this classification to place changes in water chemistry into an ecological context.

The area's waters are not only low in natural dissolved ions, but many are also high in natural dissolved organic carbon (DOC), which produces natural organic acids. These originate from littoral wetlands along the water courses and are drained into water courses by runoff. At high concentrations, DOC increases surface water acidity, especially in waters low in basic cations. Clair and Ehrman (1998) have shown that DOC concentrations in this region are controlled by climate. We therefore assume that over the longer term, weather patterns and thus DOC inputs to these catchments will not change, so that their long-term effect on acidity will be constant.

Model description

A number of mathematical models of soil and surface water acidification in response to atmospheric deposition were developed in the early 1980s (e.g., Christophersen and Wright 1981; Cosby et al. 1985). These models were based on process-level acidification information and were built for a variety of purposes ranging from estimating transient water quality responses for individual storm events to estimating chronic acidification of soils and baseflow surface water. The MAGIC model has now been in use for more than 15 years and has been constantly modified and upgraded (Cosby et al. 1985, 2001). It has been applied extensively in North America and Europe to both individual sites and regional networks of sites. The utility of MAGIC for simulating a variety of water and soil acidification responses at the laboratory, plot, hillslope, and catchment scales has been tested using long-term monitoring data and experimental manipulation data. It has been used to reconstruct the history of acidification, to examine current patterns of recovery, and

Fig. 1. Location of Nova Scotia, Canada, and the study rivers relative to the rest of eastern North America. The study rivers are numbered (see Table 1 for descriptions).

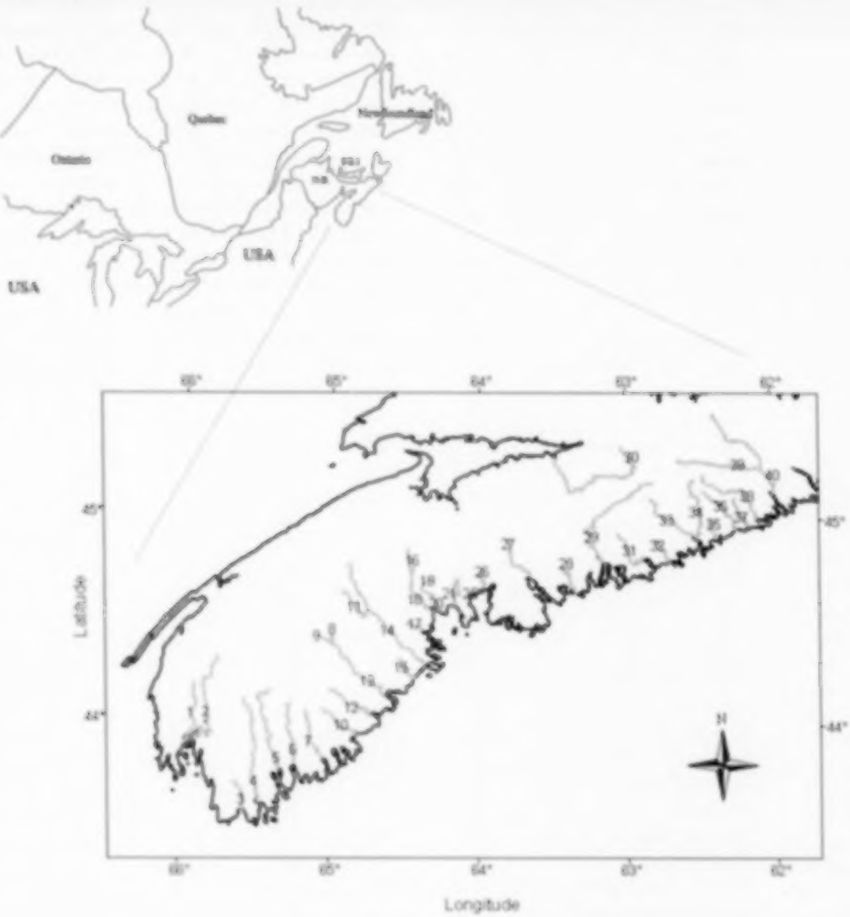

to simulate the future trends in stream water acidity in both individual catchment and regional applications at a large number of sites across North America and Europe (e.g., Wright and Cosby 2003; Clair et al. 2003).

MAGIC is a lumped-parameter model of intermediate complexity developed to predict the long-term effects of acidic deposition on surface water chemistry. The model simulates soil solution chemistry and surface water chemistry to predict the monthly and annual average concentrations of the major ions in these waters. MAGIC consists of (*i*) a section in which the concentrations of major ions are assumed to be governed by simultaneous reactions involving sulfate adsorption, cation exchange, dissolution–precipitation–speciation of aluminum and dissolution–speciation of inorganic carbon and (*ii*) a mass-balance section in which the flux of major ions to and from the soil is assumed to be controlled by atmospheric inputs, chemical weathering, and losses to runoff. At the heart of MAGIC is the size of the pool of exchangeable base cations in the soil. As the fluxes to and from this pool change over time owing to changes in atmospheric deposition, the chemical equilibria between soil and soil solution shift to give changes in surface water chemistry. The degree and rate of change of surface water acidity thus depend on both flux factors and the inherent characteristics of the affected soils.

Atmospheric deposition and net uptake–release fluxes for the base cations and strong acid anions are required as inputs to the model. These inputs are generally assumed to be uniform over the catchment. Atmospheric fluxes are calculated from concentrations of the ions in precipitation and the rainfall volume into the catchment. The atmospheric fluxes of the ions must be corrected for dry deposition of gas, particulates, and aerosols and for inputs in cloud/fog water. The volume discharge for the catchment must also be provided to the model. In general, the model is implemented using average hydrologic conditions and meteorological conditions in annual or seasonal simulations, i.e., mean annual or mean monthly deposition, precipitation, and stream discharge are used to drive the model. Values for soil and surface water temperature, partial pressure of carbon dioxide, and organic acid concentrations must also be provided at the appropriate temporal resolution. For complete details of the model, see Cosby et al. (1985, 2001).

As implemented for the Nova Scotian streams, the model is a two-compartment representation of a catchment. Atmo-

Table 1. River name, location, and modeled pH, acid neutralization capacity (ANC), dissolved organic carbon (DOC, in mmol·m^{-3}), and calcium concentrations (in μequiv.·L^{-1}) for 2000.

River No.	Site	Lat.	Long.	pH	ANC	DOC	Ca^{+2}
1	Carleton R.	43.9	-65.9	5.7	38.7	16.6	61.6
2	Tusket R.	43.9	-65.8	5.0	45.2	42.8	61.5
3	Barrington R.	43.5	-65.5	4.9	20.2	27.4	35.6
4	Clyde R.	43.6	-65.4	5.0	13.9	19.1	32.5
5	Roseway R.	43.7	-65.3	4.7	43.7	59.0	26.0
6	Jordan R.	43.8	-65.2	5.3	16.4	14.4	28.3
7	Sable R.	43.9	-65.1	4.9	14.3	20.9	24.0
8	Westfield R.	44.4	-65.0	5.0	50.1	49.6	32.4
9	Medway R., Caledonia	44.4	-64.9	5.5	56.0	33.0	37.8
10	Broad R.	44	-64.8	4.8	19.4	29.7	24.3
11	West R.	44.5	-64.8	5.1	50.4	44.2	42.7
12	Mersey R.	44.1	-64.8	5.7	27.4	12.0	33.0
13	Medway R., Hwy. 3	44.2	-64.7	5.5	66.7	40.4	45.6
14	Lahave R.	44.4	-64.6	5.8	78.0	34.7	74.9
15	Petite R.	44.3	-64.5	5.7	50.5	25.7	62.4
16	Gold R., New Ross	44.7	-64.4	5.6	90.3	47.9	58.1
17	Mushamush R.	44.5	-64.4	6.4	66.5	15.5	58.0
18	Gold R., Hwy. 3	44.6	-64.4	5.2	68.1	54.4	50.9
19	Middle R., Hennigar L.	44.6	-64.3	4.9	43.6	46.4	24.9
20	Middle R., Chester	44.6	-64.2	5.0	46.0	46.9	39.6
21	Connaught L. outflow	44.6	-64.2	4.8	23.1	33.4	23.6
22	East R., Chester	44.6	-64.1	5.2	46.9	37.4	49.8
23	Officers Camp L.	44.7	-64.2	5.5	127.2	77.4	118.7
24	Timber L. outflow	44.7	-64.1	6.6	135.5	34.2	128.7
25	East R. Wood Road	44.6	-64.1	6.2	115.0	38.1	107.6
26	Ingram R.	44.7	-64.0	5.1	37.3	35.2	35.4
27	Sackville R.	44.8	-63.8	5.1	58.7	48.9	99.2
28	Salmon R., Lake Echo	44.7	-63.4	5.0	13.5	18.6	61.2
29	Musquodoboit R.	44.9	-63.2	6.3	160.8	52.4	345.6
30	Pembroke R.	45.3	-62.9	5.8	83.2	38.1	255.4
31	Ship Harbour R.	44.8	-62.9	6.0	43.1	14.5	50.6
32	Tangier R.	44.8	-62.7	5.4	34.0	22.5	36.9
33	West R. Sheet Harbour	44.9	-62.5	5.5	29.8	18.9	37.5
34	East R. Sheet Harbour	44.9	-62.4	5.7	28.5	13.6	32.9
35	Salmon R., Port	44.9	-62.2	5.8	32.2	13.9	40.9
36	Moser R.	45	-62.3	5.7	31.0	14.5	38.9
37	Ecum Secum R.	45	-62.2	5.8	55.5	24.6	64.4
38	Liscomb R.	45	-62.1	5.5	40.4	23.4	38.1
39	West River, St. Mary's	45.3	-62.1	5.8	52.8	24.0	37.3
40	St. Mary's R.	45.2	-62.0	6.0	82.2	31.7	51.5

Note: The rivers are listed from west to east, as acid deposition is greatest in the western region and is reduced with distance from New England and central Canada. Lat., latitude; Long., longitude; R., river; Hwy., highway.

spheric deposition enters the soil compartment, and the equilibrium equations are used to calculate soil water chemistry. The water is then routed to the stream compartment, and the appropriate equilibrium equations are reapplied to calculate runoff chemistry. In this application, we assumed as a first approximation that the soils were podsols with average depths of 1 m. In the model calibration, this is one variable that is sometimes modified, but this starting assumption generally held for the streams with which we dealt. Once initial conditions (initial values of variables in the equilibrium equations) have been established, the equilibrium equations are solved for soil water and surface water concentrations. These concentrations are used to calculate the stream discharge output fluxes of the model for the first time step. The mass-balance equations are (numerically) integrated over the time step, providing new values for the total amounts of base cations and strong acid anions in the system. These in turn are used to calculate new values of the remaining variables, new stream discharge fluxes, and so forth. The output from MAGIC is thus a time trace for all major chemical constituents for the period of time chosen for the integration.

Calibration procedure

The aggregated nature of the model requires that it be calibrated to observed data from a system before it can be used to examine potential system response. Calibration is achieved by setting the values of certain parameters within the model that can be directly measured or observed in the system of interest (called "fixed" parameters). The model is then run (using observed atmospheric and hydrologic inputs), and the simulated values of surface water and soil chemical variables (called "criterion" variables) are compared with observed values of these variables. If the observed and simulated values differ, the values of another set of parameters in the model (called "optimized" parameters) are adjusted to improve the fit. After a number of iterations, the simulated-minus-observed values of the criterion variables usually converge to zero (within some specified tolerance). The model is then considered calibrated. If new assumptions (or values) for any of the fixed variables or inputs to the model are subsequently adopted, the model must be recalibrated by readjusting the optimized parameters until the simulated-minus-observed values of the criterion variables again fall within the specified tolerance. Further details on model calibration can be found in Clair et al. (2003).

Historical loading

The estimation of the historical changes at the sites requires a temporal sequence of historical anthropogenic deposition. Thus, as part of the model calibration process, the model should be constrained by some measure of historical deposition to the site. However, such long-term, continuous historical deposition data do not exist. We used historical emissions data as a surrogate for deposition (Lefohn et al. 1999). The emissions for each year in the historical period were normalised to emissions from a year for which observed deposition data are available (the reference year). Using this scaled sequence of emissions, historical deposition was estimated by multiplying the total deposition estimated for each site in the reference year by the emissions scale factor for any year in the past to obtain deposition for that year. This procedure was applied for the Nova Scotian streams to provide estimates of past deposition for the historical simulations (Fig. 2). From 1982 onwards, measured data were used to provide model input. From the year 2000, we simulate the scenarios described above until no SO_4^{-2} deposition occurs, either in 2050 or in 2100.

Application to Nova Scotian streams

The MAGIC model was calibrated for 40 of the study streams based on the information collected by DFO (Table 1). For each stream, at least 2 years (but not more than 5 years) of data were averaged to provide calibration inputs for MAGIC. The resultant calibration data periods for the streams ranged from the mid-1980s to the mid-1990s. Soil inputs for the model were based on soil profiles sampled in Kejimkujik National Park located in the middle of the study area, which are typical of the region.

Total deposition inputs used for the calibration period at each stream were based on observed wet deposition at Environment Canada's Canadian Air and Precipitation Monitoring Network (CAPMoN) site at Kejimkujik National Park. This regional wet deposition estimate was adjusted at each site for dry deposition of anthropogenic pollutants and sea salts using mass-balance calculations based on the observed stream exports. Historical simulations for each stream were run using estimates of past deposition described above (Fig. 2).

Fig. 2. Relative regional SO_4^{-2} deposition pattern estimated for eastern North America, as well as three possible future scenarios: no change from the year 2000 (●), 10% decrease per decade (■), and 20% per decade (▲). The broken line represents the estimated historical deposition.

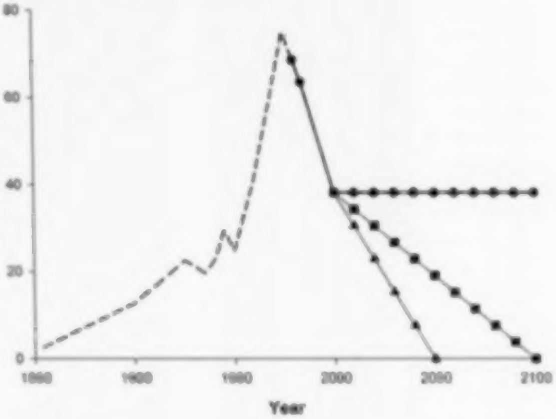

Although MAGIC calculates a number of soil and water variables, we focus this paper on the three most important to the survival of Atlantic salmon. The first is pH, which has been the focus of most of the toxicological studies done on acidification and biota in this region and elsewhere (Lacroix et al. 1985). The second is ANC, which is a measure of the water's ability to neutralize acidity. ANC was estimated as the difference in charge between the sum of the base cations (Ca^{+2}, Mg^{+2}, K^+, Na^+) and the acid anions (SO_4^{-2}, Cl^-, NO_3^-) (Stumm and Morgan 1996). The third parameter on which we focus is the base cation calcium (Ca^{+2}), which is important for a number of osmoregulation and bone maintenance processes in fish (Lacroix et al. 1985), as well as construction of invertebrate shells. It is also the main base cation originating in bedrock found in these waters. The concentrations of the others (K^+, non-sea-salt Na^+, and Mg^{+2}) are usually less than half that of Ca^{+2} and behave somewhat similarly. There are no detectable levels of ammonium (NH_4^+) in these waters, so this ion is not considered in the calculations.

Results

Model hindcast outputs suggest that at the beginning of the 20th century, under pre-acidification conditions, pH in all rivers of the region, except those with high DOC, was higher than the 5.4 threshold for sustainable salmon populations in Nova Scotia (Fig. 3). The data show four regions where rivers are extremely sensitive to acidification. The largest region is in southwestern Nova Scotia (rivers 2 to 14 in Table 1) and shows the greatest sensitivity and reactivity to acid deposition. This region is also the closest to major continental acid pollution sources (Shaw 1979). There is another region of sensitive rivers somewhat to the west of Halifax (rivers 18 to 23, Fig. 1). The sensitivity of rivers draining onto the Scotian Shelf of Nova Scotia is controlled

Fig. 3. Model hindcast pH of study rivers from 1920 to 2000, as well as predictions for future changes with (*a*) 10% and (*b*) 20% decrease in SO_4^{-2} deposition. Green denotes pH > 5.4, which allows sustainable populations; yellow denotes rivers with pH between 5.1 and 5.4 with threatened populations; orange denotes pH between 5.1 and 4.7 and endangered populations; and red denotes pH < 4.7, with extirpated populations.

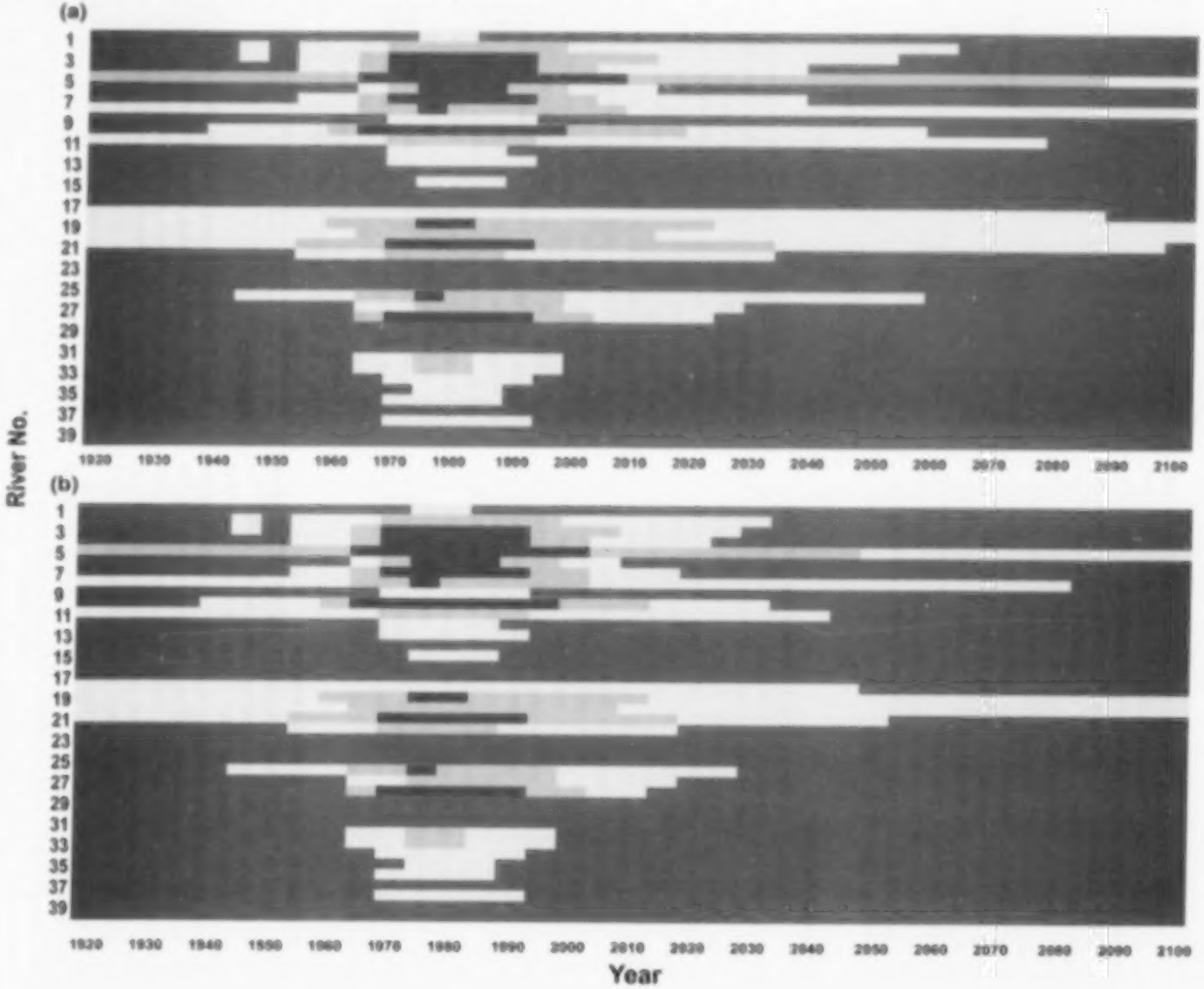

by geology, with slates and granites underlying the sensitive and acidic regions.

The model hindcasts (Fig. 3, here we only show from 1920) suggest that significant changes to the river chemistry only began to be felt in the 1950s. The lowest pH values likely occurred in the mid-1970s to early 1980s when acid rain emissions were at their peak. Since the 1980s (which coincidentally is when ecosystem and acid deposition monitoring began), acidity has been gradually decreasing in regional waters, as has been measured in monitoring programs (Clair et al. 2002). The model simulations show some recovery between 1980 and 2000, with all but one of the sites (Roseway River) having returned to pH levels above extirpation levels for Atlantic salmon by the year 2000.

We then applied the three future deposition forecast scenarios (no change from 2000 (NC) and −10% and −20% SO_4^{-2} reduction per decade) to all stream catchments to see how quickly pH might recover (or not) in the future. Under the NC scenario, the model predicts that stream pH will not change further from the year 2000 values (figure not shown), because in the year 2000, the systems are still receiving acid deposition amounts equal to the natural ability of the catchments to neutralize them.

When we simulate a 10% SO_4^{-2} reduction per decade to the region (see Fig. 2), pH is predicted to rebound to sustainable levels by 2070 in most of the rivers (Fig. 3*a*) except for Roseway River in the southwest, which is very dilute and high in organic acids. By 2100, the model predicts that all rivers should have returned to acidity levels acceptable for sustainable fish populations.

The predictions for the 20% SO_4^{-2} reduction per decade scenario (Fig. 3*b*) provided significantly faster pH recovery times for most rivers. The MAGIC model predicts an almost immediate recovery of pH to levels suitable for salmon within 20 years in most rivers. The difference in recovery time between the two deposition scenarios is striking and indicates that linearity is expected in the response of the rivers to changes in deposition levels.

ANC, estimated as the difference between the base cations and acid anions, should somewhat mirror the pH. The hindcast (Fig. 4) shows ANC in pre-acidification times to be greater than 50 $\mu\text{equiv}\cdot\text{L}^{-1}$ at 75% of the sites before 1920, the lower values being due to the lower buffering capacity caused by the poor geology. Based on historical emissions data and estimated changes in acid deposition, the model suggests that some ANC reductions began in the 1920s in the most sensitive rivers of the region. It shows a decrease in ANC beginning in the 1950s, reaching its lowest values (at or below 0 $\mu\text{equiv}\cdot\text{L}^{-1}$) in the 1970–1980 period in a number of the streams. Reductions in acid deposition from 1980 to 2000 began an improvement in ANC to the point that no streams had ANC values less than 0 $\mu\text{equiv}\cdot\text{L}^{-1}$, as was the case in the 1970s and 1980s. Only a few sites returned to annual levels greater than 50 $\mu\text{equiv}\cdot\text{L}^{-1}$ by 2000.

The ANC forecast for the NC scenario suggests that little further recovery could be expected in this parameter going into the future. The models predict some slight improvement in two or three sites, but overall, most of the sites should have ANC values between 25 and 50 $\mu\text{equiv}\cdot\text{L}^{-1}$, with a few having values below 25 $\mu\text{equiv}\cdot\text{L}^{-1}$. Under the 10% SO_4^{-2} reduction per decade scenario (Fig. 4*a*), approximately two-thirds of the sites will have returned to values of >50 $\mu\text{equiv}\cdot\text{L}^{-1}$ by the year 2050. By the year 2100, when all deposition would have ceased, ANC should have returned to pre-acidification levels. The 20% SO_4^{-2} reduction per decade scenario (Fig. 4*b*) again shows that an accelerated emission control scenario would have a much more rapid effect on ANC. The model predicts that within 10 years of a 20% per decade sulfate reduction, almost all of the sites would have returned to ANC values greater than 50 $\mu\text{equiv}\cdot\text{L}^{-1}$, and that within 50 years, all sites would have their values recovered to pre-acidification levels. These predictions, as with the pH values, emphasize the linearity in catchment response to changes in deposition and emphasize that the faster further emission controls are in place, the faster the ecosystems will recover.

Base cations in waters draining catchments are important for aquatic biota and also provide a good indication of the weathering and ion exchange processes occurring in the basins. There was a wide range of Ca^{+2} values in the rivers sampled (Table 1). Modeling showed changes in absolute values at most of the rivers sampled, though patterns were not easily obvious. To better understand the patterns, we plotted the yearly Ca^{+2} data as the percent difference from pre-industrial conditions (1850 to 1920) (Fig. 5). This allowed us to show how changes in acid deposition would change base cation concentrations relative to the unpolluted state. The hindcasts of absolute values showed changes from pre-acidification beginning at most of the sites in the 1950s. Ca^{+2} values then increased by 5% to 15% at all sites, whereas those in rivers of the far western and Halifax regions increased by more than 15% in the 1960s and 1970s.

As acid deposition decreased from the 1980s, the model predicts a return to pre-industrial concentrations for a few years at all sites. However, continued reductions in deposition cause a continued decrease in dissolved Ca^{+2} everywhere. Under the 10% SO_4^{-2} reduction per decade scenario, Ca^{+2} values decrease between 5% and 15% into the foreseeable future, whereas at some of the most sensitive sites, the decrease will be greater than 15%. The greatest decreases will begin at three sites in the Halifax area from 2020 and should be occurring at some western rivers beginning in the 2070s.

The 20% SO_4^{-2} reduction per decade scenario shows a more rapid arrival of lower Ca^{+2} concentrations in the two most sensitive regions. It also shows the return to pre-acidification levels at three catchments in the late part of the century. Maintenance of SO_4^{-2} deposition at year 2000 levels will not change the relative export of Ca^{+2} from the catchments in the future, as they will remain with ±5% of pre-acidification. However, the constant acidification pressure and thus the constant reduction of soil base cations will continue degrading the soils.

Discussion

These results show a very important feature of acidification effects on these highly sensitive catchments derived from parent materials poor in buffering capacity. Acid precipitation has the effect of titrating catchment soils. Acid protons exchange with base cations and release them to waters leaving the watershed, so the greater the acid precipitated, the greater the loss of base cations. As the titration is reduced through the decrease in acid deposition, the ion exchange leading to cation loss is also reduced, but from a lower soil cation pool. Thus, runoff waters will contain fewer cations.

Fig. 4. Model hindcast acid neutralization capacity (ANC) of study rivers from 1920 to 2000, as well as predictions for future changes with (*a*) 10% and (*b*) 20% decrease in SO_4^{-2} deposition. Dark blue denotes mean annual ANC >50 μequiv.·L^{-1}; light blue denotes ANC between 25 and 50 μequiv.·L^{-1}; yellow denotes values between 10 and 25 μequiv.·L^{-1}; orange denotes values between 0 and 10 μequiv.·L^{-1}; and red denotes ANC values <0 μequiv.·L^{-1}.

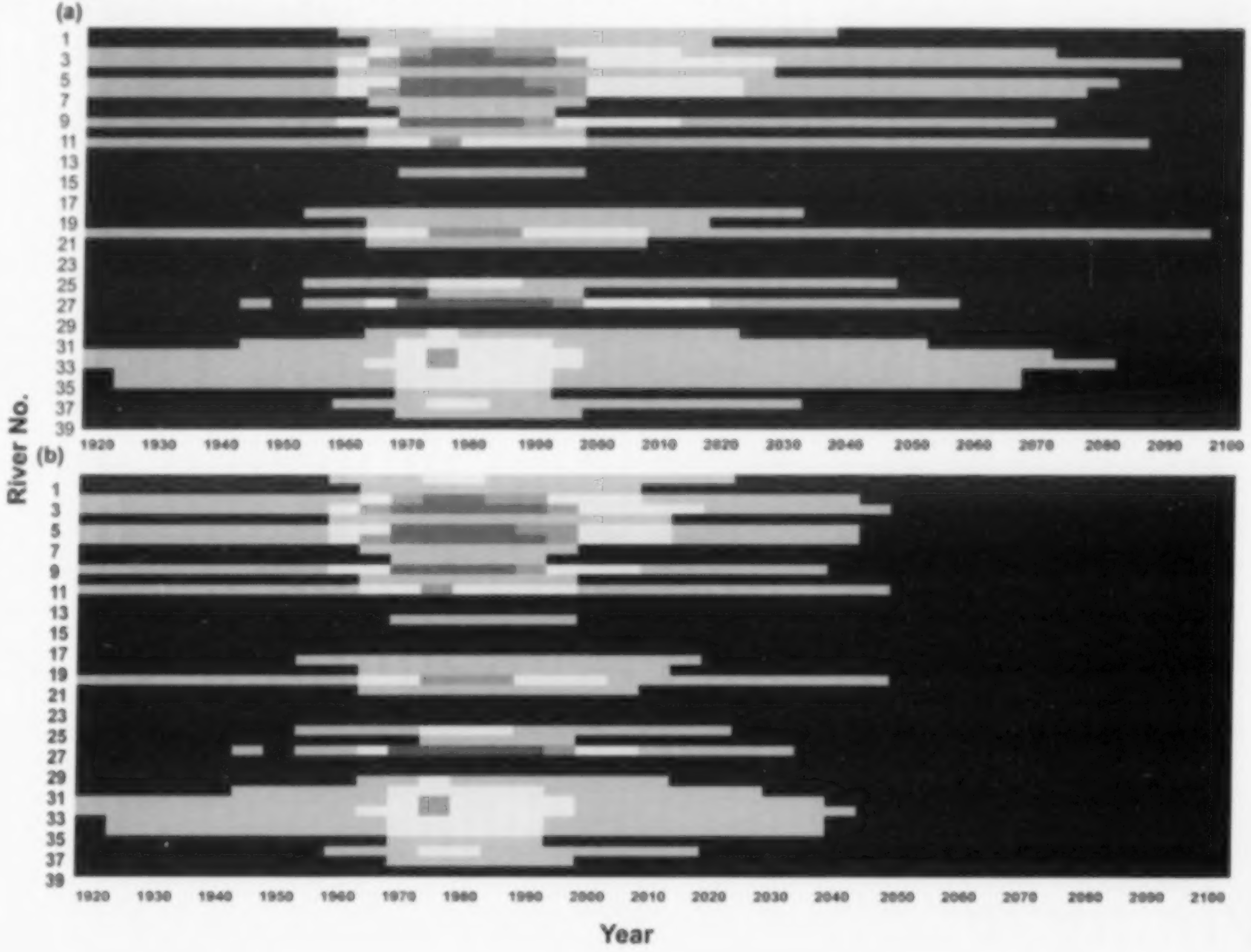

Fig. 5. Model hindcast relative Ca^{+2} of study rivers from 1920 to 2000, as well as predictions for future changes with (*a*) 10% and (*b*) 20% decrease in SO_4^{-2} deposition. Green denotes Ca^{+2} values ±5% of pre-industrial (1850–1920) levels; light blue denotes concentrations between +5 and +15% of pre-industrial and dark blue denotes values greater than +15%; yellow denotes values –5 to –15% of pre-industrial; and red denotes values less than 15% of pre-acidification.

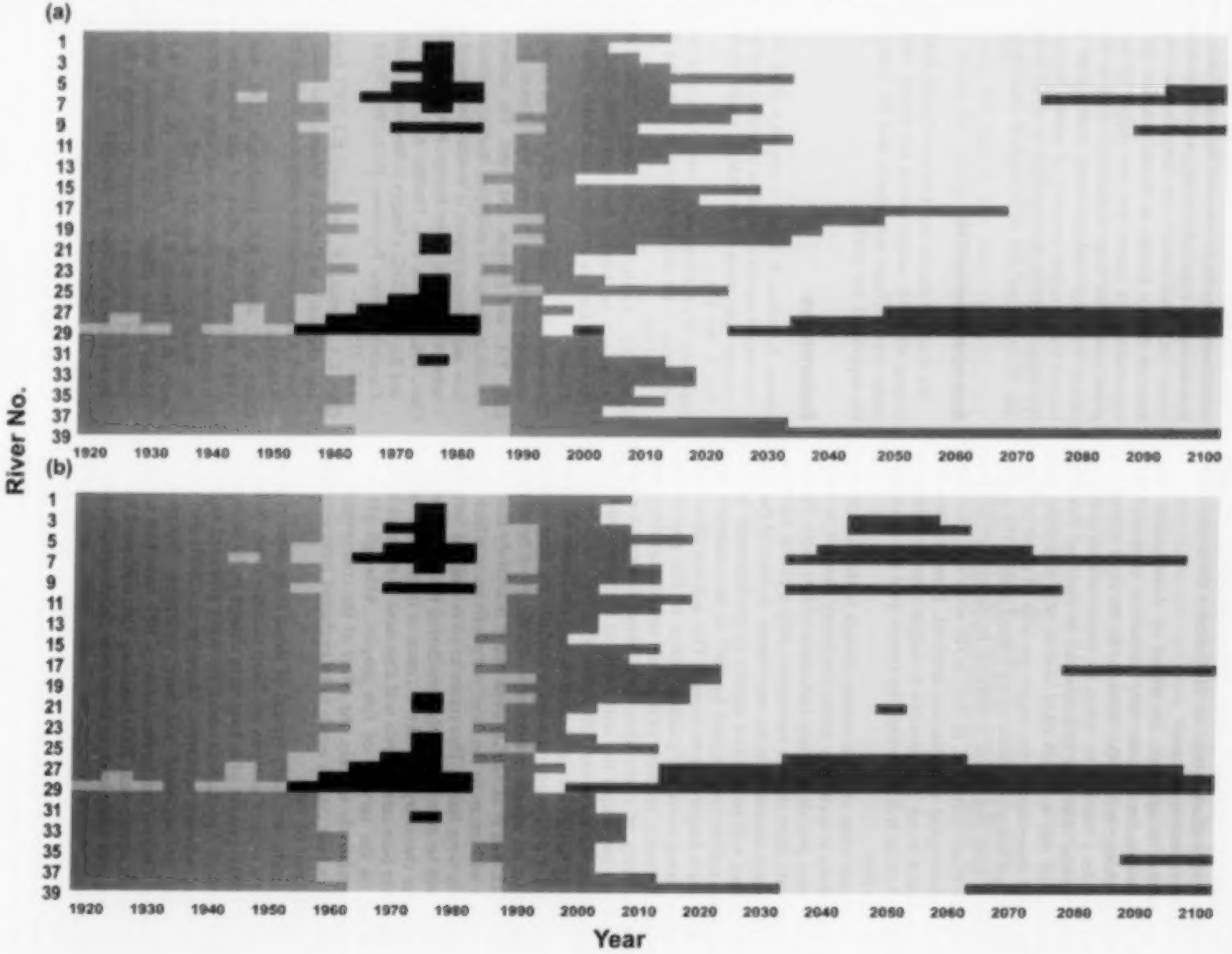

Base cations will only be naturally replenished in the soils through bedrock weathering, which is a very slow process. Our modeling shows only three rivers to have Ca^{+2} recover to pre-acidification levels by 2100 under the more rapid emission reduction scenario.

A number of questions are raised by these results. The first is how realistic are the SO_4^{-2} reduction scenarios? The NC (no change from 2000) seems to be the most unrealistic but provides a baseline by which the improvements achieved under various reduction scenarios can be assessed. Political agreements that will inevitably reduce SO_2 emissions and thus acid deposition to the region are now in place in Canada and are being negotiated in the United States. The actual scope of these reductions is difficult to predict considering the time frames involved, as well as the economic, political, and technological uncertainties involved. However, we believe that it is not unreasonable to suggest that the changes that will occur will fall within the ranges used in our modeling exercise.

The real value of the scenarios though is that despite being unlikely to accurately reflect the future changes in deposition, they provide a strong indication of two facts. Firstly, the models show that we can expect only a partial recovery of the water chemistry in the near future. Acidity of the water courses will be reduced rapidly to pre-industrial levels, but base cations (represented by Ca^{+2} in this analysis) will take a much longer time to recover. This will not allow a return of ecosystems to "pristine" states in this part of the world. Secondly, recovery of river and stream chemistry, and thus recovery of ecosystems, is a linear process, i.e., the faster and the deeper the initial cuts in emissions and thus deposition, the more rapid the recovery.

Pushing further emission controls into the future will seriously delay ecosystem recovery, especially for base cations. The effect on aquatic ecosystems will therefore be difficult to predict. Yan et al. (2003) show that it is unlikely that ecosystems will return to the same compositions in which they originally were found. This return to an ecological "original state" will be even less likely considering the long time that the water chemistry will take to return to its original values. The lower base cation levels will also most likely have direct effects on the survival of fish species. Although pH will recover relatively quickly, the effect of the concomitant reduction in base cations needs to be evaluated from a toxicological point of view.

Our results are fairly typical of those from other regions where this type of analysis has been recently done. Sullivan et al. (2004) predict little long-term change in 50 streams of the southern Appalachian under currently proposed regional emission reduction scenarios. Aherne et al. (2003) also show evidence of continued soil base saturation depletion in southern Ontario catchments under a 50% reduction in acid deposition from a year 2000 baseline. This continued loss of soil ions inevitably leads to lower base cation concentrations of drainage waters. Wright and Cosby (2003) show similar improvements in ANCs of Norwegian lakes, as do we. However, they ascribe this to the result of acid reductions greater than the base cation loss, a situation also similar to ours. All in all, our work and those of others show that in areas with soils low in base cations, recovery of surface waters under current emission reduction regimes will be long and slow.

Our results and those of similar studies show that there is "light at the end of the tunnel" with the reductions of acid deposition. One way of accelerating the recovery of valued ecosystems may be to consider the use of ecosystem mitigation measures, especially liming, which has been used extensively and successfully in Scandinavia (Appelberg and Svenson 2001). Its use in North America has been mostly experimental in nature and not supported or sustained by governments and large landowners such as woodland companies. Now that evidence exists showing the length of time needed for complete recovery of water chemistry, it may be opportune to revisit this approach to assist those streams that may be at greater risk of ecological catastrophe.

Acknowledgments

We thank Fisheries and Oceans Canada field staff for collecting all field samples used for model calibration, often under very difficult conditions, and Dr. Larry Marshall for his support of the work.

References

Aherne, J., Dillon, P. J., and Cosby, B.J. 2003. Acidification and recovery of aquatic ecosystems in southcentral Ontario, Canada: regional application of the MAGIC model. Hydrol. Earth Syst. Sci. **7**: 561–573.

Appelberg, M., and Svenson, T. 2001. Long-term ecological effects of liming — the Iselaw Programme. Water Air Soil Pollut. **130**: 1745–1750.

Beattie, B.L., Keddy, K.N., and Chou, F. 2002. Trends in acid deposition in the Atlantic Provinces (1980–2000). Meteorological Service of Canada, Science Report Series 2002-02, Environment Canada.

Christophersen, N., and Wright, R.F. 1981. A model for streamwater chemistry at Birkenes, Norway. Water Resour. Res. **17**: 377–389.

Clair, T.A., and Ehrman, J.M. 1998. The influence of changing seasonal climates in modifying discharge, dissolved organic carbon and nitrogen export in wetland influenced rivers: a neural network approach. Water Resour. Res., **34**: 447–455.

Clair, T.A., Ehrman, J.M., Ouellet, A.J., Brun, G., Lockerbie, D., and Ro, C.-U. 2002. Changes in freshwater acidification trends in Canada's Atlantic Provinces: 1983–1997. Water Air Soil Pollut. **135**: 335–354.

Clair, T.A., Dennis, I.F., and Cosby, B.J. 2003. Probable changes in lake chemistry in Canada's Atlantic Provinces under proposed North American emission reductions. Hydrol. Earth Syst. Sci. **7**: 574–582.

Cosby, B.J., Wright, R.F., Hornberger, G.M., and Galloway, J.N. 1985. Modelling the effects of acid deposition: assessment of a lumped parameter model of soil water and streamwater chemistry. Water Resour. Res. **21**: 51–63.

Cosby, B.J., Ferrier, R.C., Jenkins, A., and Wright, R.F. 2001. Modelling the effects of acid deposition: refinements, adjustments and inclusion of nitrogen dynamics in the MAGIC model. Hydrol. Earth Sys. Sci. **5**: 499–517.

Farmer, G.J., Goff, T.R., Ashfield, D.M., and Samant, H.S. 1979. Some effects of acidification of Atlantic Salmon rivers in Nova Scotia. Can. Tech. Rep. Fish. Aquat. Sci. No. 972.

Kirchner, J.W. 1992. Heterogeneous geochemistry of catchment acidification. Geochim. Cosmochim. Acta. **56**: 2133–2327.

Lacroix, G.L., Gordon, D.J., and Johnston, D.J. 1985. Effects of low environmental pH on the survival, growth, and ionic composition of postemergent Atlantic Salmon (*Salmo salar*). Can. J. Fish. Aquat. Sci. **42**: 768–775.

Lefohn, A.S., Husar, J.D., and Husar, R.B. 1999. Estimating historical anthropogenic global sulfur emission patterns for the period 1850–1990. Atmos. Environ. **33**: 3435–3444. Data available at www.asl-associates.com/sulfur1.htm.

Shaw, R.W. 1979. Acid precipitation in Atlantic Canada. Environ. Sci. Technol. **13**: 406–411.

Shilts, W.W. 1981. Sensitivity of bedrock to acidification: modification by glacial processes. Geological Survey of Canada. Pap. No. 81-14.

Stumm, W., and Morgan, J.J. 1996. Aquatic chemistry: chemical equilibria and rates in natural waters. 3rd ed. John Wiley and Sons, New York.

Sullivan, T.J., Cosby, B.J., Herlihy, A.T., Webb, J.R., Bulger, A.J., Snyder, K.U., Brewer, P.F., Gilbert, E.H., and Moore, D.L. 2004. Regional model projections of future effects of sulfur and nitrogen deposition on streams in the southern Appalachian Mountains. Water Resour. Res. **40**, W02101, doi:10.1029/2003WR001998.

Watt, W.D. 1987. A summary of the impact of acid rain on Atlantic salmon (*Salmo salar*) in Canada. Water Air Soil Pollut. **35**: 27–35.

Watt, W.D., Scott, C.D., Zamora, P.J., and White, W.J. 2000. Acid toxicity levels in Nova Scotian rivers have not declined in synchrony with the decline in sulfate levels. Water Air Soil Pollut. **118**: 203–229.

Wright, R.F., and Cosby, B.J. 2003. Future recovery of acidified lakes in southern Norway predicted by the MAGIC model. Hydrol. Earth Syst. Sci. **7**: 467–483.

Yan, N.D., Leung, B., Keller, W., Arnott, S.E., Gunn, J.M., and Raddun, G.G. 2003. Developing conceptual frameworks for the recovery of aquatic biota from acidification. Ambio, **32**: 165–169.

Movement of Atlantic bluefin tuna (*Thunnus thynnus*) as determined by satellite tagging experiments initiated off New England

Michael J.W. Stokesbury, Steven L.H. Teo, Andrew Seitz, Ronald K. O'Dor, and Barbara A. Block

Abstract: Pop-up satellite archival tags were attached to 35 Atlantic bluefin tuna (*Thunnus thynnus*) off the New England coast of the United States of America in 1998, 2000, and 2001. The tags provided information on the horizontal and vertical movements and environmental preferences of bluefin tuna. Fish showed movement patterns that can be categorized by age and season. Mature individuals were linked to the Gulf of Mexico breeding grounds based on light level longitude and sea surface temperature latitude estimates of geolocation and a radiosatellite endpoint position. A track based on geolocation indicated that a single individual moved from the tagging release location to the Gulf of Mexico and back to New England waters. Tag-generated water column profiles of depth versus temperature were consistent with fish movement along the shelf and into the Gulf of Mexico. Adolescent fish moved from the New England offshore feeding locations to winter aggregations in the coastal shelf and slope waters of North and South Carolina. Bluefin tuna showed a preference for ambient temperatures that ranged from 14 to 26 °C in autumn and from 18 to 24 °C in winter.

Résumé : Nous avons fixé une étiquette émettrice satellite à déploiement automatique et à archivage à 35 thons rouges (*Thunnus thynnus*) au large de la côte de la Nouvelle-Angleterre des États-Unis d'Amérique en 1998, 2000 et 2001. Les étiquettes fournissent des renseignements sur les déplacements horizontaux et verticaux et sur les préférences de milieux des thons rouges. Les patterns de déplacement des poissons peuvent se caractériser en fonction de l'âge et de la saison. Les individus à maturité sont associés aux aires de reproduction du golfe du Mexique d'après les estimations de la longitude (selon l'intensité lumineuse) et de la latitude (selon la température de surface de la mer) fournies par le géopositionnement et le positionnement extrême par radio-satellite. Un itinéraire basé sur le géopositionnement montre qu'un individu s'est déplacé du point de marquage au golfe du Mexique pour ensuite retourner dans les eaux de la Nouvelle-Angleterre. Les profils d'utilisation des profondeurs de la colonne d'eau en fonction de la température fournis par les étiquettes sont compatibles avec des déplacements le long du plateau continental et dans le golfe du Mexique. Les poissons adolescents se déplacent des aires d'alimentation au large de la Nouvelle-Angleterre vers des aires de rassemblement d'hiver dans les eaux du plateau continental et du talus au large des Caroline du Nord et du Sud. Les thons rouges préfèrent les températures ambiantes qui varient de 14 à 26 °C à l'automne et de 18 à 24 °C en hiver.

[Traduit par la Rédaction]

Introduction

Atlantic bluefin tuna (*Thunnus thynnus*) are large, highly migratory pelagic fish that are distributed in the western Atlantic Ocean from tropical waters off Brazil (Mather et al. 1995) to polar waters off Newfoundland (Caddy et al. 1976) and south of Greenland (Mather et al. 1995). Bluefin tuna conserve metabolic heat and can tolerate ambient temperatures that range from 2.8 to 31.0 °C (Carey and Lawson 1973; Block et al. 2001) while maintaining a relatively constant body temperature (Carey and Teal 1969; Block et al. 2001; Blank et al. 2004). These fish forage in productive cool waters during the summer and return to warm water masses to spawn (Block et al. 1993, 2001; Mather et al. 1995). This gives bluefin tuna the broadest thermal niche of all species of the family Scombridae (Block et al. 1998*a*).

Received 17 October 2003. Accepted 18 June 2004. Published on the NRC Research Press Web site at http://cjfas.nrc.ca on 23 December 2004.
J17796

M.J.W. Stokesbury.[1] Biology Department, Dalhousie University, 1344 Oxford Street, Halifax, NS B3H 4J1, Canada, and Tuna Research and Conservation Center, Stanford University, Hopkins Marine Station, Oceanview Boulevard, Pacific Grove, CA 93950, USA.
S.L.H. Teo and B.A. Block. Tuna Research and Conservation Center, Stanford University, Hopkins Marine Station, Oceanview Boulevard, Pacific Grove, CA 93950, USA.
A. Seitz. Monterey Bay Aquarium, 886 Cannery Row, Monterey, CA 93940, USA.
R.K. O'Dor. Biology Department, Dalhousie University, 1344 Oxford Street, Halifax, NS B3H 4J1, Canada.

[1] Corresponding author (e-mail: mstokesb@dal.ca).

Can. J. Fish. Aquat. Sci. **61**: 1976–1987 (2004) doi: 10.1139/F04-130

Atlantic bluefin tuna are currently managed as two stocks in the Atlantic Ocean and Mediterranean Sea (National Research Council 1994). It is hypothesized that the western Atlantic Ocean stock spawns in the Gulf of Mexico (Richards 1976) and the Straits of Florida (Rivas 1954) and the eastern Atlantic Ocean stock in the Mediterranean Sea (Richards 1976). Larval tows support the hypothesis that these three areas are primary spawning grounds (Richards 1976; McGowan and Richards 1989).

Abundance estimates indicate that the western Atlantic Ocean stock of mature Atlantic bluefin tuna has decreased markedly since the 1970s (Magnuson et al. 2001), in spite of the recovery plan that was put in place by the International Commission for the Conservation of Atlantic Tunas (ICCAT) in the early 1980s. The current management plan assumes that mixing between the two stocks occurs at a low rate (<4%·year^{-1}; National Research Council 1994). However, recent archival and conventional tagging data indicate that fish in the western Atlantic Ocean cross to the eastern Atlantic Ocean at a rate that ranges from 10% to 30% (Block et al. 2001). Increased understanding of the movement patterns and the level of mixing between the two stocks is crucial to improving the management and conservation of bluefin tuna (National Research Council 1994; Sissenwine et al. 1998; Magnuson et al. 2001).

Historically, conventional tag returns from Atlantic bluefin tuna tagged in the northwestern Atlantic Ocean have linked these fish to several regions. Tagging of bluefin tuna with conventional tags in St. Margaret's Bay, Nova Scotia, produced returns from the waters off New England, southwestern Nova Scotia, and the Gulf of St. Lawrence (Burnett et al. 1977). Also, two fish conventionally tagged off Massachusetts were recaptured in the Gulf of Mexico (Mather et al. 1995). Mather et al. (1995) proposed that after spawning, bluefin tuna migrated from the Gulf of Mexico through waters east of the Bahamas and off the southeastern United States. They then followed the eastern edge of the Florida Current to Cape Hatteras. Next, they followed the Gulf Stream northeastward, leaving at varying intervals to make their way north to various feeding grounds (Mather et al. 1995). It was also proposed that some bluefin tuna might follow the Gulf Stream into the northeast Atlantic Ocean to feeding grounds off Norway. The route of the southern return migration of adult bluefin tuna was less clear from the tagging results (National Research Council 1994).

Recently, investigators have used electronic tagging technology to examine the movements of Atlantic bluefin tuna (Block et al. 1998*a*, 2001; Lutcavage et al. 1999). Block et al. (1998*a*, 2001, 2002) reported results from a study using both archival data storage tags and pop-up satellite archival tags (PSATs) that investigated the migration and environmental preferences of electronically tagged fish released off the coasts of North Carolina and New England and in the Gulf of Mexico. Block et al. (2001, 2002) determined that bluefin tuna tagged in the western Atlantic Ocean exhibited four migratory behaviors over 1–3 years after tagging: western Atlantic residency without visiting a recognized spawning ground, western Atlantic residency with visitation to a known western spawning ground, western residency for 1–3 years with visitation to the known eastern spawning ground, the Mediterranean Sea, and transatlantic movement west to east and back. Western residency was the prevalent pattern for adolescent bluefin tuna, as they occupied offshore waters off North Carolina in the winter, the Gulf Stream in spring, and New England waters in summer and autumn.

Atlantic bluefin tuna electronically tagged in the North Carolina winter fishery resided in waters offshore of North and South Carolina and then arrived in summer and autumn in waters off New England. For fish tagged off North Carolina, the most likely place to recover an archival-tagged fish was New England, strongly linking the two groups of fish and the associated fisheries (Block et al. 2001). Also, although many bluefin tuna in New England waters are from a larger more mature component of the population, there remains a large overlap in the adolescent and early-breeding cohorts.

While the waters off New England were clearly important for many Atlantic bluefin tuna tagged in previous studies, some archival and pop-up satellite tagged fish released off North Carolina did not visit this area. Data from Block et al. (2001, 2002) provided strong evidence for a movement of fish from North Carolina waters to the Mediterranean Sea spawning grounds and to the area east of the Flemish Cap and south of Greenland. Fish moving from North Carolina to either the Mediterranean Sea or the Flemish Cap showed no association with waters off New England either on the way to the Flemish Cap or on their way to western or eastern known spawning grounds after residency in feeding areas (Block et al. 2001, 2002).

In a second study, using externally placed pop-up satellite tags, Lutcavage et al. (1999) reported on the movements of Atlantic bluefin tuna tagged in the Great South Channel off Massachusetts. Of 20 satellite tags deployed on fish in the Great South Channel, five reported from the mid-Atlantic east of 45°W, the ICCAT stock management boundary line. Although most of the pop-up satellite tags surfaced on the western side of the stock boundary line, the major conclusion of the paper was that fish from New England travel toward the mid-Atlantic during the winter. The authors raised the possibility, based on these results, that bluefin tuna tagged off New England spawn in the mid-Atlantic.

In the current study, we examine the movements of Atlantic bluefin tuna tagged and released off New England with two types of pop-up satellite tags of increasingly sophisticated software generations. The evolution of the tag software and hardware permitted increased data acquisition during the 3-year period of this study. The results of this study have important implications for bluefin tuna management and conservation and clarify previous data reported from this assemblage in the western Atlantic Ocean.

Materials and methods

Pop-up satellite tags were deployed on Atlantic bluefin tuna in three different years (1998, 2000, and 2001) off the coast of Massachusetts. Tags were secured to the fish using two procedures of capture and release.

In autumn 1998, Atlantic bluefin tuna were captured using a purse seine by the fishing vessel *Sea Rover*. For release, the net was opened enough to permit the release of one bluefin tuna at a time. As the fish swam out of the net, one individual tagged it using a harpoon deployment procedure. A

Table 1. Satellite tag hardware, software, and programing information.

						Type of data				
Tag type	Tag No.	Tag hardware	Tag software	Data summary period (h)	Prerelease program	Ambient temperature (3600S)[a]	Ambient temperature (1800S)[b]	Ambient temperature (120S)	Light (120S)	Pressure (120S)
PAT1	381						×			
	382						×			
	383						×			
	384						×			
	385						×			
PTT100	25171					×				
	8971					×				
	9685					×				
	8836					×				
PAT2	590	2.00	2.03	12				×	×	×
	763	2.00	2.03	24				×	×	×
	764	2.00	2.03	24				×	×	×
	765	2.00	2.03	24				×	×	×
	770	2.00	2.03	24				×	×	×
	760	2.00	2.03	12				×	×	×
	761	2.00	2.03	24				×	×	×
	751	2.00	2.03	24				×	×	×
	753	2.00	2.03	24				×	×	×
	771	2.00	2.03	24				×	×	×
	752	2.00	2.03	24				×	×	×
	772	2.00	2.03	24				×	×	×
	750	2.00	2.03	24				×	×	×
	738	2.00	2.03	24				×	×	×
	1027	2.00	2.06a	24	×			×	×	×
	1024	2.00	2.06a	24	×			×	×	×
	1019	2.00	2.06a	12	×			×	×	×
	1026	2.00	2.06a	12	×			×	×	×
	1018	2.00	2.06a	24	×			×	×	×
	953	2.00	2.06a	24	×			×	×	×
	946	2.00	2.06a	12	×			×	×	×
	1015	2.00	2.06a	24	×			×	×	×
	949	2.00	2.06a	12	×			×	×	×
	871	2.00	2.06a	12	×			×	×	×
	859	2.00	2.06a	12	×			×	×	×
	943	2.00	2.06a	12	×			×	×	×

[a] The first 60 ambient temperature measurements are daily averages derived from hourly measurements from the previous 24-h period. The 61st ambient temperature measurement is the average for the 24-h period prior to the tags' programed report date.

[b] Ambient water temperatures are recorded every 0.5 h and archived for the first 60 days of deployment.

titanium dart anchor with the attached pop-up satellite tag was inserted close to the second dorsal fin. A pop-up satellite tag was secured to the titanium dart by a monofilament leader (136 kg) covered in shrink wrap to increase its stiffness (Block et al. 1998*b*). Two experienced purse-seine vessel captains estimated the sizes of the fish. Of the nine tags deployed, five were first-generation single-point PAT1 tags built by Wildlife Computers and four were single-point Microwave Telemetry PTT100 tags (Table 1). Both types of tags provided an endpoint location based on the Doppler shift of the tags' radio transmission to the Argos satellites (root mean square errors for class 2 and class 3 readings were 350 and 150 m, respectively; Taillade 1992).

In 2000 and 2001, Atlantic bluefin tuna were captured by rod and reel using 120-kg line test and 9/0 to 11/0 Gamakatsu baited circle hooks. Fish were boated using a "lip hook", a short-handled gaff inserted into the lower jaw of the fish to pull it aboard the vessel. The fish were pulled through an opening in the transom of the vessel onto a wet vinyl mat on the deck of the boat using methods previously described by Block et al. (1998*a*, 1998*b*). The curved fork length (CFL) of the fish was measured (centimetres) prior to tagging. Only fish larger than 172 cm CFL were tagged. A titanium dart was inserted into the dorsal musculature at the base of the second dorsal fin so that the tag head was pushed though the pterygiophores, thus providing a solid point of attachment for the tag. The rubber shrink wrap covering the leader of the PSAT had an identification number and telephone contact that provided the opportunity for additional recapture information. A conventional dart tag was also attached on the opposite side of the second dorsal fin from the PSAT. The fish were then released by sliding them off the wet vinyl mat headfirst through the tuna door and into the water. This method was applied to fish as large as 287 cm CFL.

The three types of pop-up satellite tags acquired and transmitted data differently. PTT100 tags acquired ambient temperature data at 1-h intervals for the first 60 days of deployment and the day prior to the tag report. The tag then transmitted the daily mean temperature (calculated from the hourly readings) for the first 60 days and the day prior to the tag report. Wildlife Computer PAT1 tags acquired ambient temperature at 0.5-h intervals for the first 60 days of deployment and transmitted the entire data archive. PAT2 tags acquired data in 60-s intervals for light, ambient temperature, and pressure and archived data in 120-s intervals to memory. Data were summarized into 12- or 24-h bins prior to transmission (Table 1). The summary data for each time period comprised percent distributions of time-at-depth and time-at-temperature and temperature versus depth profiles that were generated by dividing the maximum dive during the interval into eight equally distributed points, inclusive of the surface and maximum depth. A minimum and maximum temperature at each of these depths was stored and transmitted.

In 2000 and 2001, PSATs (PAT2) with two versions of software (2.03 and 2.06a, respectively) were used. The PAT2 tags (software version 2.06a) were equipped with a prerelease program and an auto depth correction in the 2001 deployments. Therefore, if the tag prematurely detached from the fish and floated to the surface, it reported to the satellite 4 days after detachment. PAT2 tags (software version 2.03) deployed in 2000 did not have this program and drifted from the date of detachment from the fish until the preprogramed reporting date. However, the pressure sensor provided direct evidence of the date of tag prerelease from the fish. All PAT2 tags deployed in 2000 and 2001 provided a full archival record at 120-s intervals if recaptured (Table 1).

Tag prerelease software

Early-generation PAT tags had a tendency to release before the scheduled pop-up date (Gunn and Block 2001). Prerelease could be due to a variety of factors, including failure of the titanium dart to remain attached to the monofilament, failure of the stainless steel pin that is the point of attachment of the tag to the leader, and wearing through of the monofilament.

The first step in data analysis was to assess whether individual tags remained attached to the respective Atlantic bluefin tuna for the full duration of the deployment. This was not possible in the case of the Microwave Telemetry PTT100 tags. For Wildlife Computers PAT1 tags, the complete archive of external temperature data at 0.5-h intervals allowed collection of an increased amount of data on external temperature to discern changes in water temperature in association with vertical and horizontal movements. Therefore, it was possible to estimate when the tag prematurely released for those tags that were on the fish for the period of time that the temperature data were archived (60 days after release). The tags for which it was possible to verify whether they remained on the fish and that produced endpoint positions were divided into two groups: (*i*) tags that remained attached, as determined by the temperature and pressure records or temperature alone and (*ii*) tags that were "drifters" for a period greater than 4 days prior to data transmission (the length of time preprogramed into the tag to activate transmission if the tag came prematurely to the surface).

Geolocation

Information on daily movements of Atlantic bluefin tuna was obtained from light-based calculation of longitude using PAT Decoder 7.08.0005 of Wildlife Computers (Hill 1994; Hill and Braun 2001) combined with latitude estimates based on sea surface temperature (SST) (Teo et al. 2004). The accuracy of these geolocation estimates was determined by comparing endpoint positions from pop-up satellite tags and global positioning system (GPS) with geolocation estimates based on light level longitude and SST latitude (Teo et al. 2004). Endpoint data based on radio transmissions at the surface from PAT2s on 49 fish (including 12 from this study) had a root mean square error for geolocation estimates of 1.30° for light-based longitude and 1.89° for SST-based latitude (Teo et al. 2004). Therefore, this geolocation validation provides an ellipse of error estimate around each point.

Results

A total of 35 Atlantic bluefin tuna were tagged with pop-up satellite tags in three seasons of autumn tagging (1998, 2000, and 2001) (Table 2) off New England. The tagged fish ranged from 173 to 287 cm CFL. Radio endpoint locations indicating the last position of the fish prior to tag release were obtained from 14 tags that transmitted within 4 days of tag release. A single tag recapture position of a bluefin tuna recaptured with a pop-up satellite tag attached was provided by the fishers' GPS (Fig. 1). The radio endpoint locations and GPS position indicate the region in which the fish were present at tag detachment, recapture, or, in the case of the engagement of the premature release program, the position of the tag 4 days after detachment. These radio transmission endpoints indicate that most of the tagged fish moved due south from the initial tagging location off Massachusetts. Three tags (381, 382, and 1026) reported endpoints close to the tagging site after short deployments of 10, 12, and 4 days, respectively. Tags 381 and 382 remained attached to the fish for the intended term of deployment. Tag 1026 was attached to a fish that died shortly after tagging and owing to the prerelease program reported 4 days after the death of the fish. One tag (1027) reported an endpoint close to the tagging site after 236 days at liberty. A single tag (859) also reported an endpoint from an area off-shelf south of Halifax, Nova Scotia, after 105 days at liberty. A single tag (383) reported an endpoint off New Jersey. Seven tags (590, 949, 946, 1018, 1019, 1024, and 943) reported endpoint positions from continental shelf and slope waters off the Carolinas (Fig. 1). One tag (1015) reported an endpoint position in the eastern slope waters of the Gulf of Mexico on 3 February 2002 (Fig. 1). Commercial fishers and beachcombers recovered two tags. Tag 770 was returned when a commercial longline vessel captured the fish off the coast of New Jersey, and the fisher provided a GPS position for the recapture point. Tag 763 was found detached from the fish on a beach in the Bahamas. A single tag leader (871) was recovered after tag release by an American purse seiner, providing an endpoint for the tagged fish (Fig. 1).

Table 2. Results of pop-up satellite archival tagging of 35 Atlantic bluefin tuna off Nantucket Island, Massachusetts, during the autumn of 1998, 2000, and 2001.

		Tag deployment date and location			Tag report date and location						
Tag No.	CFL (cm)	Date	Latitude (°N)	Longitude (°W)	Date	Latitude (°N)	Longitude (°W)	Days off fish at time of report	Track length (days)	Distance travelled (km)	Minimum speed (km·day^{-1})
381	229[a]	17 Sept. 1998	41.270	–69.141	29 Sept. 1998	42.008	–69.450	0	12	85.6	7.3
382	272[a]	14 Sept. 1998	41.267	–69.320	24 Sept. 1998	41.668	–69.726	0	10	58.1	6.6
383	245[a]	14 Sept. 1998	41.267	–69.320	17 Nov. 1998	39.416	–73.475	0	64	408.3	6.3
384	252[a]	14 Sept. 1998	41.267	–69.320	13 Dec. 1998	38.191	–71.408	?[b]	90	386.1	4.2
385	238[a]	17 Sept. 1998	41.270	–69.141	29 Jan. 1999	32.524	–77.483	?[b]	134	1221.8	9.1
25171	238[a]	17 Sept. 1998	41.270	–69.141	4 Mar. 1999	36.087	–50.396	?[b]	175	1720.0	9.8
8971	217[a]	17 Sept. 1998	41.270	–69.141	11 Mar. 1999	33.315	–56.560	?[b]	178	1416.8	8.0
9685	Unknown[c]	17 Sept. 1998	41.270	–69.141	Tag did not report						
8836	245[a]	17 Sept. 1998	41.270	–69.141	11 Sept. 1999	34.96	–44.034	?[b]	371	2295.5	6.2
590	173	4 Oct. 2000	41.260	–69.178	15 Dec. 2000	35.22	–75.03	0	72	843.7	11.7
763	221	29 Sept. 2000	41.249	–69.194	15 Apr. 2001	29.49	–67.46	145	198	1316.8	6.7
764	206	30 Sept. 2000	41.258	–69.195	15 May 2001	32.42	–74.10	175	227	1073.5	6.1
765	252	27 Sept. 2000	41.252	–69.175	1 June 2001	39.74	–42.25	195	247	2272.7	9.2
770[d]	191	27 Sept. 2000	41.243	–69.192	15 Oct. 2000	40.00[e]	–70.28[e]	0	18	465.3	25.9
760	287	12 Oct. 2000	41.183	–69.147	Tag did not report						
761	>287	13 Oct. 2000	41.322	–69.076	Tag did not report						
751	218	13 Oct. 2000	41.335	–69.056	1 July 2001	40.18	–33.15	190	261	3002.8	11.5
753	246	12 Oct. 2000	41.261	–69.132	15 June 2001	34.96	–52.85	197	246	1581.6	6.4
771	213	12 Oct. 2000	41.157	–69.157	1 Aug. 2001	40.15	–56.34	123	293	1083.4	3.7
752	279	13 Oct. 2000	41.165	–69.142	1 Aug. 2001	27.59	–55.19	130	292	1974.3	6.8
772	218	12 Oct. 2000	41.157	–69.157	1 Sept. 2001	33.534	–60.368	319	324	1085.2	3.3
750	279	13 Oct. 2000	41.328	–69.059	1 Sept. 2001	40.80	–44.47	296	323	2054.9	6.4
738	218	14 Oct. 2000	41.331	–69.075	1 Sept. 2001	35.20	–53.78	289	322	1495.8	4.6
1027	226	27 Sept. 2001	41.118	–69.025	20 May 2002	40.258	–67.902	0	236	134.3	0.6
1024	237	3 Oct. 2001	41.120	–69.038	21 Jan. 2002	33.84	–76.78	4	110	1058.3	9.6
1019	232	3 Oct. 2001	41.120	–69.038	24 Jan. 2002	36.27	–73.82	4	115	679.9	5.9
1026[f]	231	3 Oct. 2001	41.144	–69.048	7 Oct. 2001	41.14	–69.050	4	4	9.0	2.3
1018	241	15 Oct. 2001	41.168	–69.125	21 Jan. 2002	34.41	–76.76	4	99	1005.1	10.2
953	262	19 Oct. 2001	41.307	–68.927	25 Feb. 2002	Unknown	Unknown	4	130	Unknown	Unknown
946	189	20 Oct. 2001	41.277	–68.962	1 Jan. 2002	35.67	–75.16	4	74	824.4	11.1
1015	267	31 Oct. 2001	41.259	–68.919	3 Feb. 2002	25.16	–83.97	4	95	2263.9	23.8
949	196	31 Oct. 2001	41.291	–68.893	21 Feb. 2002	34.32	–76.11	4	114	999.6	8.8
871	242	31 Oct. 2001	41.277	–68.887	12 Nov. 2001	Unknown	Unknown	4	12	Unknown	Unknown
859	186	29 Oct. 2001	41.211	–68.922	10 Feb. 2002	40.47	–63.67	4	105	449.1	4.3
943	232	1 Nov. 2001	41.293	–68.890	30 Jan. 2002	32.81	–78.53	4	91	1271.5	14.0

[a] Fish were tagged over the side of the tagging vessel; therefore, round weight was estimated and curved fork lengths (CFLs) were calculated.

[b] For PTT100 tags or PAT1 tags that were at liberty for a duration longer than their temperature archive (60 days), it was not possible to discern at what time the tag released from the fish.

[c] Fish CFL was not estimated.

[d] Fish recaptured by American longliner.

[e] Estimate of position reported by recapture vessel.

[f] Mortality at tagging event.

Fig. 1. Position data from pop-up satellite tags deployed on Atlantic bluefin tuna off Massachusetts (green triangle = release location) in 1998, 2000, and 2001 obtained from radio transmission endpoints to the Argos satellite system (yellow squares, $N = 14$), tag recapture (yellow square with ×, $N = 1$), and leader recapture (red square with ×, $N = 1$) positions and geolocation estimates based on light level longitude and sea surface temperature (SST) latitude estimates (white circles, $N = 645$). The endpoint location for tag 1026 is obscured by the symbol representing the release location.

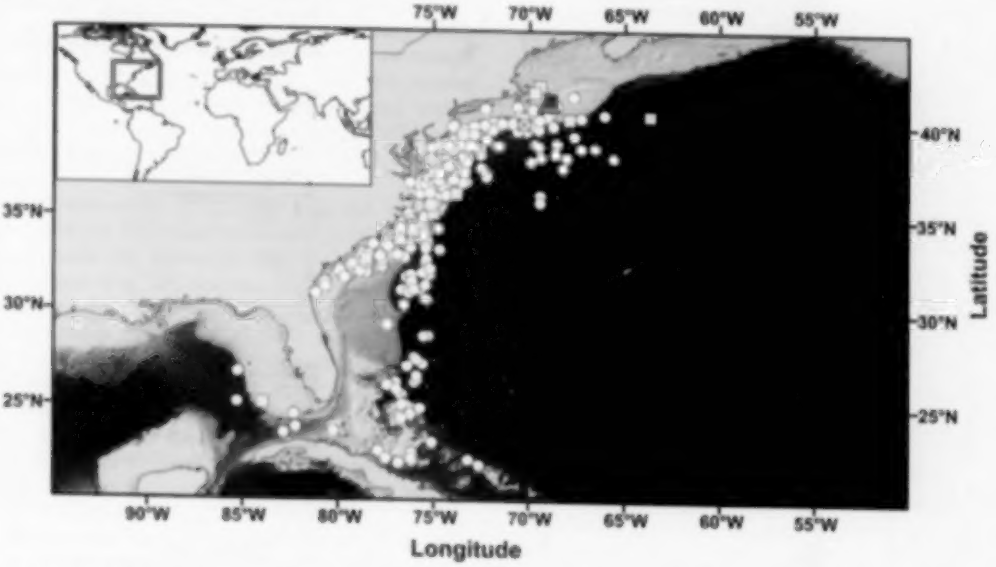

Two mature Atlantic bluefin tuna (1015 and 1027) that were tagged off New England moved into the Gulf of Mexico spawning area. Bluefin tuna 1015 moved south from New England along the continental shelf of the Mid-Atlantic Bight and into North Carolina waters by late November. This bluefin tuna remained in on shelf waters off North Carolina in the winter months and slowly moved into slope waters and then south along the Blake Plateau. This fish traveled south across the Bahama Banks (25°00′N, 75°36′W) into off-shelf waters in December and into the Gulf of Mexico in mid-December. It remained in the Gulf of Mexico until the PSAT reported in early February from slope waters off Florida (Fig. 2*a*). The estimated geolocation track of 1015 is consistent with the water column structure and maximum depth data obtained from the temperature–depth profiles from the PSAT (Fig. 2*b*). The data indicate that this fish was bathymetrically restricted in diving activity while in the shelf waters off New England and North Carolina and then began a period of deeper dives in off-shelf waters. During the portion of the track that the fish was off New England and in the waters of the Mid-Atlantic Bight, the temperatures were cool (16–20 °C). Ambient temperatures increased as the fish moved south along the US continental shelf, corroborating geolocation estimates of southward movement. After a period of residency in winter off North Carolina, the fish moved off the Carolina shelf. It moved into the Straits of Florida and then into the Gulf of Mexico in December. A warm surface water mass and deep thermocline are characteristic of the Straits of Florida and Gulf of Mexico waters. The pop-up endpoint position places the fish in the eastern Gulf of Mexico.

Atlantic bluefin tuna 1027 had a pop-up endpoint position located 171.15 km from the initial deployment location off New England after 8 months at liberty. This indicates that this fish showed fidelity, returning to the region where it was tagged. This is consistent with conventional tagging records from this area. Geolocation estimates indicate that a complex migration occurred between tag deployment and pop-up. Bluefin tuna 1027 displayed a pattern of movement from New England south along the continental shelf in the period from October to March (Fig. 2*c*). A geolocation estimate indicates that the fish moved to the west into a region consistent with the Gulf of Mexico in March. Because of the bluefin tuna's deep diving behavior, and a lack of transmissions, the reported data did not provide many daily light level positions for estimating geolocation. This is consistent with implantable archival tag data from bluefin tuna that entered the Gulf of Mexico and pop-up satellite tag data from the Gulf of Mexico. These data indicated extensive deep diving during the period that the fish enter the Gulf of Mexico (Block et al. 2001, 2002). For 18 days before and 17 days after the single geolocation (9 March 2002) in the Gulf of Mexico, no light level data were reported. The temperature–depth profiles from this tag, which were also limited in number, indicate a period of on-shelf bathymetrically limited diving at the beginning of the track and movement from a cooler water mass through the Gulf Stream and into a warmer water mass consistent with the Gulf of Mexico during March (Fig. 2*d*). This water mass had a 25–26 °C maximum surface water temperature and a 50-m themocline depth, which are consistent with those observed for this period on fish tagged in the western Gulf of Mexico (B.A. Block and S.L.H. Teo, unpublished data). After the fish was in the Gulf of Mexico, it had a period of deep diving and entered water masses cooler than the Gulf of Mexico. This corroborates geolocation estimates that indicate that the fish

Fig. 2. (*a*) Geolocation track for an Atlantic bluefin tuna (1015) tagged with a pop-up satellite archival tag off New England (tag model is PAT2) in autumn 2001 (green triangle = release location; yellow circles = geolocation estimates based on light level longitude and sea surface temperature (SST) latitude; red square = tag radio endpoint location). (*b*) Maximum depth and ambient temperature profiles of the water column (°C) for bluefin tuna 1015. (*c*) Geolocation track for one bluefin tuna (1027) tagged with a pop-up satellite archival tag (PAT2) off New England in autumn 2001 (green triangle = release location; yellow circles = geolocation estimates based on light level longitude and SST latitude; red square = tag radio endpoint location). The broken portion of the yellow line represents a period of 18 days before and 17 days after the estimated geolocation position in the Gulf of Mexico for which there were no geolocation estimates available because of insufficient light data. However, the geolocation position is accompanied by three additional depth temperature profiles in the March period of Gulf of Mexico visitation that show a water column structure consistent with the Gulf of Mexico (refer to panel *d*). (*d*) Maximum depth and ambient temperature profiles of the water column (°C) for bluefin tuna 1027.

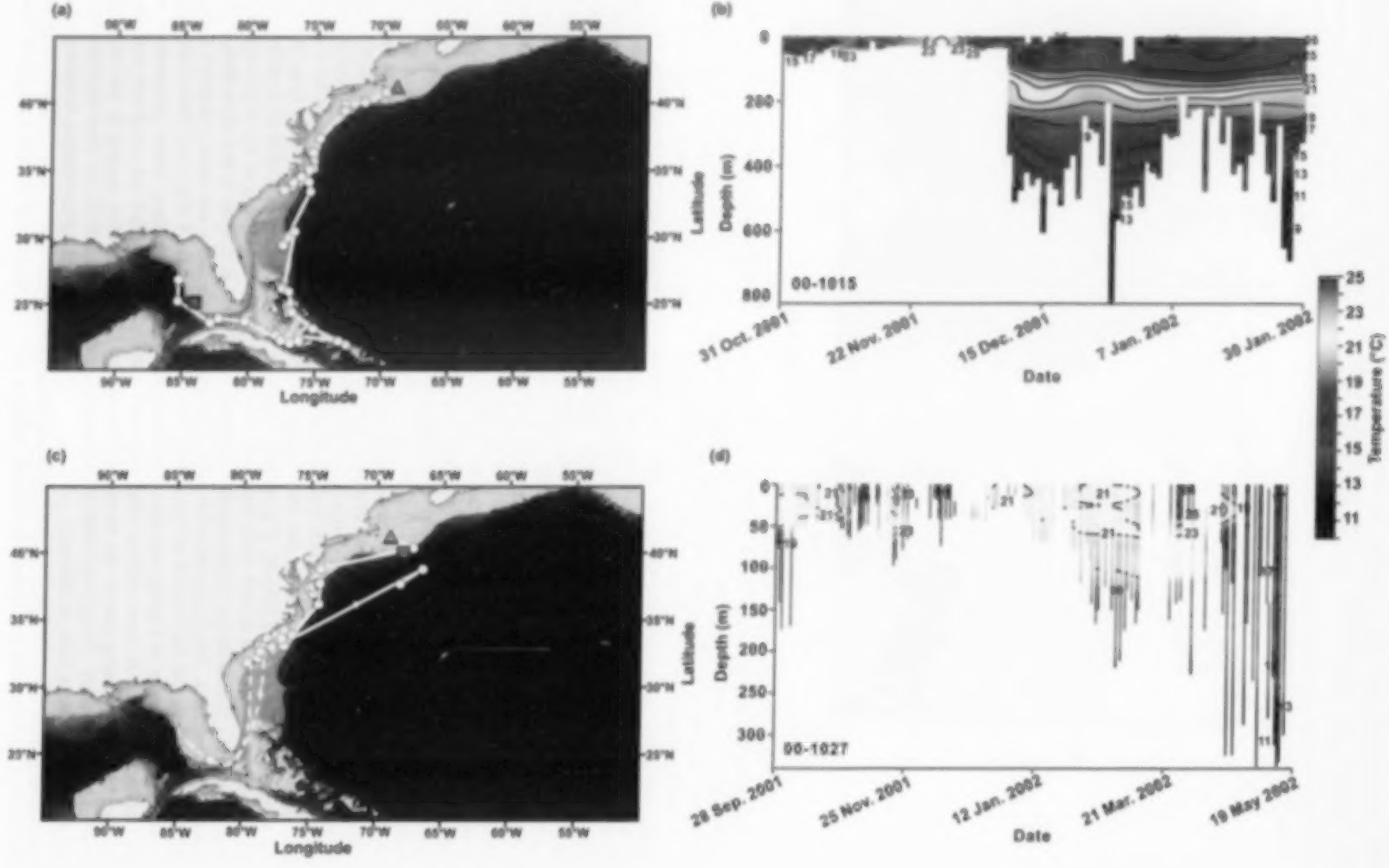

moved to the north. Geolocation estimates indicate that this fish was in the region of the Charleston Bump (29°54′N, 76°18′W) and then moved to waters off the Georgia–Carolina shelf before returning to New England (Fig. 2*a*). One geolocation position (26 March 2002; 32°65′N, 78°66′W) as the fish moved north to the Carolina shelf was 19.49 km from a geolocation position (11 February 2002; 32°74′N, 78°48′W) recorded during the fish's movement south, suggesting fidelity to this location. The fish moved from Carolina waters into the Gulf Stream and spring geolocation estimates place the fish on a cold (9 °C) frontal edge. The tag's endpoint position was 171.15 km from its point of release.

The seasonal movements from New England of potentially mature (>198 cm CFL) and adolescent (<198 cm CFL) Atlantic bluefin tuna are shown in Fig. 3. In the autumn (Fig. 3*a*) and winter (Fig. 3*b*) seasons, based on the autumnal equinox and winter solstice, both adolescent and mature bluefin tuna generally remain aggregated along the North American continental shelf and slope waters between New England and North Carolina. However, in the winter months, bluefin tuna, which are assumed by length measurements to be adolescent, aggregate in the Carolinas. Mature fish also pass through the Carolina shelf waters and move south to Blake's Plateau and to the waters of the Bahamas and the Gulf of Mexico in the winter months.

Atlantic bluefin tuna showed seasonal differences in their ambient temperature preferences (Fig. 4). Ambient water temperatures recorded by the PAT2 tags indicate that the bluefin tuna occupied similar water temperatures during autumn and winter with slightly broader temperatures experienced in autumn. In autumn, bluefin tuna spent 95% of the time in ambient water temperatures from 14 to 26 °C (Fig. 4). In winter, the bluefin tuna had narrower preferences in ambient temperatures spending 93.5% of the time in water from 18 to 24 °C (Fig. 4).

Archival data logged in the memory of two PAT2 tags were recovered from Atlantic bluefin tuna, one upon recapture (770) and one upon recovery of the tag off a beach (763). Bluefin tuna 770 provided 14 days of high-resolution data on diel diving patterns. This fish occupied deeper depths during the night (31.54 ± 35.82 m, mean ± SD) than during the day (20.88 ± 21.44 m). Tag 763 was not analyzed because of a nonlinear depth drift.

Ten PAT2s, which were deployed prior to the development of the prerelease software program, detached from the Atlantic bluefin tuna prematurely (more than 4 days prior to the preprogramed release date) and drifted for from 123–319 days after release (Table 2). These tags were not included in the location analysis above. These tags were attached to fish for 1–23 weeks prior to detachment. The endpoints of these drifting tags provide information on movement of tags that detach early from bluefin tuna. The tags all exhibited a general drift off the continental shelf to the east and northeast following the general path of the Gulf Stream. Several of the tags reported endpoint positions in the mid-Atlantic region (Fig. 5).

Discussion

The pop-up satellite tag positional data sets from three sources (radio endpoints, recovery location, and light level longitude and SST latitude estimations of geolocation) provided a total of 661 days of position data on the assemblage of Atlantic bluefin tuna found off New England. For the Argos radio position data, the quality of the endpoint location was calculated by the Argos system. The restriction of endpoint locations to accuracy class 2 or 3 ensured that the endpoint locations were likely to have an accuracy better than 350 m. If the tag drifted for 1–4 days, it was possible that the tag had moved up to 1.5° from the actual fish location based on drift rates calculated from transmitting tags. The estimated geolocation positions have a reported error estimate that is less than 2° around the geolocation based on comparisons of satellite endpoints, GPS points, and estimated geolocations (Teo et al. 2004). The data sets demonstrate that bluefin tuna from this region, if tagged and tracked for less than a year, are most likely to be found in the western Atlantic Ocean on the North American continental shelf, the North American slope waters, or the Gulf of Mexico. These results are consistent with previously reported implantable archival tag data (Block et al. 2001) but differ in several significant respects to a prior pop-up satellite tag study on this same assemblage of fish (Lutcavage et al. 1999).

The satellite tags placed on Atlantic bluefin tuna in this study remained attached primarily for the autumn and winter seasons (<6 months) and on a single fish into the spring season (approximately 8 months). The position data collectively show a pattern of migration by season where the bluefin tuna leave New England, move southward along the North American continental shelf, and reside in the vicinity of the North Carolina shelf. Data indicate that some fish move into the South Atlantic Bight and that two of the fish entered the Gulf of Mexico. Bluefin tuna 1015 represents the first record of a bluefin tuna being electronically tagged in New England and confirmed by radio endpoint position to visit the Gulf of Mexico breeding ground. Geolocation estimates for this fish indicate that it entered the Gulf of Mexico in December and was in the eastern slope waters of the Florida shelf when the tag popped off on 2 February 2002. Bluefin tuna 1027 entered the Gulf of Mexico in March. Bluefin tunas 1015 and 1027 recorded maximum depth and ambient temperature data consistent with their movements into the Gulf of Mexico. The data were similar to those of an implantable archival tagged bluefin tuna (98-512) previously reported (Block et al. 2001). This fish was tagged off Hatteras, North Carolina, and in 1 year moved to the north of the Gulf Stream in spring and then south along the continental shelf into the Gulf of Mexico and back to the waters of the Mid-Atlantic Bight. In this study, bluefin tuna 1027 moved to the Gulf of Mexico in March and then returned to waters off New England, indicating fidelity to the New England feeding aggregation after migration into the Gulf of Mexico. The tag detached from this fish on 20 May 2002, the preprogramed date of release, 236 days after tag and release. A portion of this 236-day track overlaps the track of a bluefin tuna that was pop-up satellite tagged in the Gulf of Mexico (B.A. Block, unpublished data) and moved into the North Atlantic. Consistent with these tracks is a propensity for deep diving that prevents obtaining light data and estimates of longitude. The release and recapture 334 days later of

Fig. 3. Seasonal movements in (*a*) autumn and (*b*) winter and spring of Atlantic bluefin tuna tagged off New England. Autumn is defined as the period between the autumnal equinox and the winter solstice; winter is the period between the winter solstice and the spring equinox; and spring is the period between the spring equinox and the summer solstice. Maturity was assigned based on curved fork length (CFL) (white circles = adolescent bluefin tuna and are defined as <198 cm CFL; yellow circles = potentially mature bluefin tuna and are define as >198 cm CFL; green triangle = release location; yellow square with × = tag recapture; red square with × = leader recapture; orange = spring locations for one mature bluefin tuna 1027; squares = Argos radio endpoint locations; circles = geolocation estimates based on light level longitude and sea surface temperature (SST) latitude).

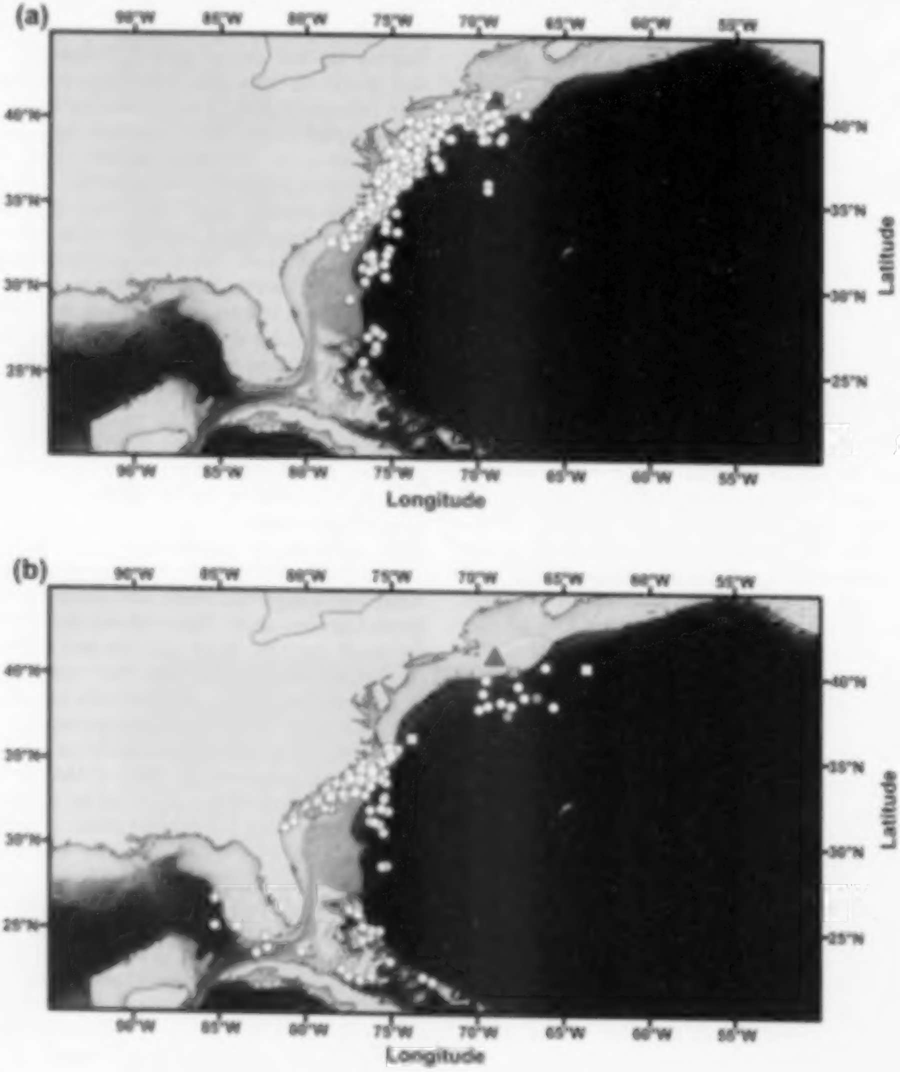

bluefin tuna 871 (leader recapture) indicates that this fish also showed fidelity to the New England feeding aggregation.

Geolocation estimates provide some distinctions between the movements of adolescent and mature Atlantic bluefin tuna. Movements of tagged adolescent bluefin tuna were recorded for durations of 18–114 days postrelease show a general distribution to the south of New England waters. In all but one case, these tuna migrated to the region along the North American continental shelf and remained in shelf waters north of North Carolina. Maximum depth records (28–40 m) from these tags indicated that the dives of the bluefin tuna were depth limited, indicating that they remained in shelf waters. A single tagged adolescent bluefin tuna (tag 859, 186 cm CFL) moved to off-shelf waters south of Halifax in February. This is similar to an off-shelf movement pattern for adolescent bluefin tuna observed by Mather et al. (1995) and Block et al. (2001).

In the first weeks of their autumnal southern migration, mature Atlantic bluefin tuna display movement patterns similar to those of adolescent bluefin tuna moving along the continental shelf and Mid-Atlantic Bight and into Carolina

Fig. 4. Time at temperature distribution of Atlantic bluefin tuna tagged with pop-up satellite tags (PAT2) in 2000 and 2001. Twelve bluefin tuna were tagged and released and provided transmissions that were used to construct the graph. The tags reported ambient temperature data for a total of 293 days ($N = 12$, mean = 24.42, SD = 16.91) during the autumn (solid bars) (autumn equinox (22 September) to winter solstice (21 December)) for 2000 and 2001. Four bluefin tuna were at large, retained their tags, and reported data for a total of 85 days ($N = 4$, mean = 21.33, SD = 14.57) during winter (stippled bars) (winter solstice (21 December) to spring equinox (20 March)) for 2001 and 2002.

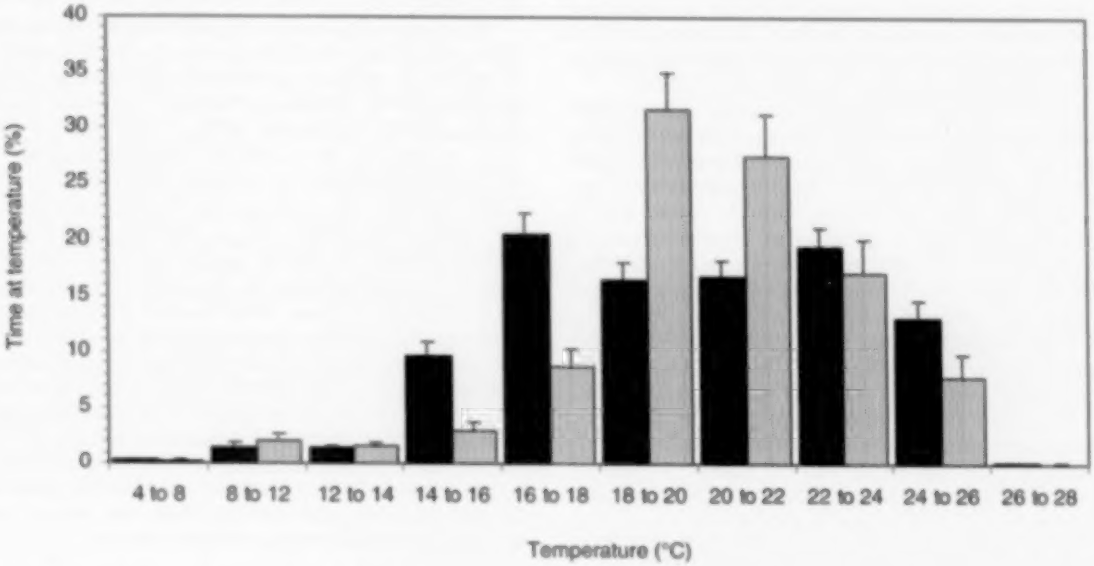

Fig. 5. Argos radio endpoint locations for 10 PAT2 tags that were confirmed by pressure data (2000 and 2001 releases) to have prematurely released from Atlantic bluefin tuna and drifted for from 123–319 days prior to reporting (triangle = release location; squares = Argos endpoints for drifting tags).

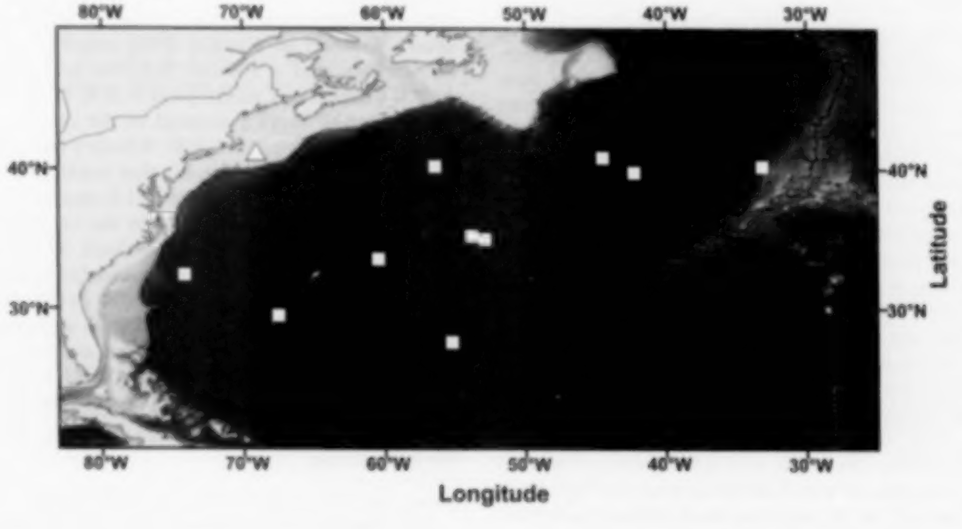

shelf waters. During winter months, however, mature bluefin tuna moved to positions farther south than adolescent bluefin tuna, including the Blake Plateau, Bahamas, and Gulf of Mexico. The passage of fish through the Carolinas region is consistent with previous studies showing that fish tagged in the Carolinas region moved to the south or occasionally into western breeding regions (Block et al. 2001, 2002).

The movements of Atlantic bluefin tuna were seasonal. All fish, whose tags remained on long enough to record a movement to the south, indicated migration along the shelf and toward the Carolinas after a period of autumn residency in the waters off New England. Bluefin tuna with implantable archival tags displayed similar movements south after SSTs cooled to 11–12 °C (Block et al. 2001, supplemental data).

Winter geolocation estimates and pop-up satellite tag end-point positions indicate a winter distribution of bluefin tuna from waters off the Carolinas to the Blake Plateau and Gulf of Mexico.

Atlantic bluefin tuna showed a preference for waters with temperatures from 14 to 26 °C during the autumn. During the winter, bluefin tuna appeared to reside in a narrower temperature range centered on 18–24 °C. In winter off North Carolina, the water column is generally within this temperature range (Block et al. 2001; Boustany et al. 2001).

Pop-up satellite tags of earlier generations that detached prematurely from tagged Atlantic bluefin tuna and were not equipped with prerelease software drifted toward the mid-Atlantic prior to reporting. Four of the 12 free-drifting tags (30%) reported from the eastern Atlantic Ocean ICCAT management zone (east of 45°W). This is in contrast with the pop-up satellite tags that remained attached to the bluefin tuna that showed no movement into the eastern management zone and indicated a western residency period after release. Importantly, this study only covered the 8-month period after tagging and is consistent with Carolinas pop-up satellite tagging studies that suggested western residency for most fish in the first 8 months after release. However, implantable archival tags have shown that 1–3 years after release, bluefin tuna may move into the eastern Atlantic or Mediterranean. While short-term studies indicate western residency of bluefin tuna tagged in the autumn assemblage, it remains possible that bluefin tuna tagged for longer durations will move to the eastern Atlantic Ocean.

The results of this study differ from those of Lutcavage et al. (1999) who used an early generation of pop-up satellite tags that lacked pressure sensors and premature release software. The major contrast between the two studies is that in the current study, tags that remained attached to fish showed positions that were distributed primarily on the North American continental shelf and slope waters due south of New England and, importantly, recorded movements into known western breeding grounds in the Gulf of Mexico and the Florida Straits. Only drifting tags from the current study show agreement with the results of Lutcavage et al. (1999). Several studies have pointed out the challenges of interpreting the results of the earlier generations of pop-up satellite tags that lacked pressure sensors or temperature sensors that recorded significant archival data (Gunn and Block 2001). The lack of archival data makes the determination of when and where the tags released from the bluefin tuna highly challenging to discern (Gunn and Block 2001). Block et al. (2002) reported that results from studies that used single-point pop-up satellite tag technology to track bluefin tuna (i.e., Block et al. 1998*a*; Lutcavage et al. 1999) must be viewed with extreme caution if tags are interpreted beyond the period of the data archive. Clarifying what the New England assemblage of fish do and how much mixing occurs between this assemblage and fish from the eastern Atlantic Ocean is of critical importance. It is up to the electronic tagging community to carefully present the results from electronic tagging studies and qualify any uncertainty in positions.

This tagging study was initiated in the autumn and selected for Atlantic bluefin tuna moving from New England waters toward winter feeding and breeding grounds. These results indicate that fish tagged in the autumn feeding aggregation off New England feed in summer and early autumn in New England waters and in winter in Carolinas waters, consistent with the archival tagging results reported by Block et al. (2001). Also, our results are consistent with prior archival tagging results that tightly link the commercial and recreational fisheries off New England and the Carolinas (Block et al. 2001).

The results of this study represent only a short duration of activity for a long-lived pelagic species. Each Atlantic bluefin tuna is at a distinct period in its life cycle and their behavior might be different if studied for longer durations. Deployment of implantable archival tags that log multiple years of behavior is crucial for understanding the longer term biology and behavior of bluefin tuna (Block et al. 2001, 2002). Tagging data indicate that bluefin tuna movements are complex. Tag prerelease is an ongoing problem for external implantation of pop-up satellite tags. In addition, data compression and uplinking to the satellite are influenced by the state of the antenna, which is often damaged after long durations of attachment. Long-duration tracks spanning multiple years may best be obtained by tagging with implantable archival tags. However, efforts to reduce the size of pop-up satellite tags and improved attachment techniques may help to lengthen their duration of attachment. Efforts to continue electronically tagging bluefin tuna off New England with tags that remain in place for multiple years are necessary to discern the relationship of these fish with eastern assemblages over durations longer than 12 months.

Acknowledgements

This study was supported by grants from the Packard, Disney, and Monterey Bay Aquarium Foundations. M.J.W.S. was supported by a Natural Sciences and Engineering Research Council of Canada IPGS scholarship, a Dalhousie scholarship, and a Natural Sciences and Engineering Research Council of Canada grant to R.K.O. The National Marine Fisheries Service assisted in the recovery of the tags. We thank W. Whippen and R. Whorley for additional financial support and vessel access that made this study possible in New England. L. Ingrande and Captains C. Ingrande and S. Ingrande were instrumental in the tagging effort aboard the F/V *Sea Rover* in 1998. We thank W. Whippen for the donation of his vessel *Tightline* and his expertise in 2000, R. Whorley for providing his vessel *Leslie Anne*, and Captain G. Stuve for providing his skill as a Captain and for his enthusiasm for bluefin tuna and his expertise in 2001. We thank H. Dewar, A. Boustany, and J. Ganong for logistical support and A. Walli for figure preparation.

References

Blank, J.M., Morrissette, J.M., Landeira-Fernandez, A.M., Blackwell, S.B., Williams, T.D., and Block, B.A. 2004. *In situ* cardiac performance of Pacific bluefin tuna hearts in response to acute temperature change. J. Exp. Biol. **207**: 881–890.

Block, B.A., Finnerty, J.R., Stewart, A.F.R., and Kidd, J. 1993. Evolution of endothermy in fish: mapping physiological traits on a molecular phylogeny. Science (Wash., D.C.), **260**: 210–214.

Block, B.A., Dewar, H., Farwell, C., and Prince, E. 1998*a*. A new satellite technology for tracking the movements of Atlantic bluefin tuna. Proc. Natl. Acad. Sci. USA, **95**: 9384–9389.

Block, B.A., Dewar, H., Williams, T., Prince, E., Farwell, C., and Fudge, D. 1998*b*. Archival tagging of Atlantic bluefin tuna (*Thunnus thynnus thynnus*). Mar. Technol. Soc. J. **32**: 37–46.

Block, B.A., Dewar, H., Blackwell, S.B., Williams, T.D., Prince, E.D., Farwell, C.J., Boustany, A., Teo, S.L.H., Seitz, A., Walli, A., and Fudge, D. 2001. Migratory movements, depth preferences, and thermal biology of Atlantic bluefin tuna. Science (Wash., D.C.), **293**: 1310–1314.

Block, B.A., Boustany, A., Teo, S., Walli, A., Farwell, C.J., Williams, T., Prince, E.D., Stokesbury, M., Seitz, A., Weng, K. 2002. Distribution of western tagged Atlantic bluefin tuna determined from implantable archival and pop-up satellite archival tags. SCRS/02/094. ICCAT, Madrid, Spain.

Boustany, A.M., Marcinek, D., Keen, J., Dewar, H., and Block, B.A. 2001. Movements and temperature preferences of Atlantic bluefin tuna (*Thunnus thynnus*) off North Carolina: a comparison of acoustic, archival and pop-up satellite tags. *In* Methods and technologies in fish biology and fisheries. Vol. 1. *Edited by* J. Sibert and J. Neilson. Kluwer Academic Publishers, Dordrecht, Netherlands. pp. 89–108.

Burnett, C.D., Butler, M.J.A., Dickson, C.A., and Iles, T.D. 1977. Canadian tagging and recapture data of large pelagic fish for the period 1970–76. Coll. Vol. Sci. Pap. No. 6. ICCAT, Madrid, Spain. pp. 281–286.

Caddy, J.F., Dickson, C.A., and Butler, J.A. 1976. Age and growth of giant bluefin tuna (*Thunnus thynnus thynnus*) taken in Canadian waters in 1975. Fish. Res. Board Can. MS Rep. No. 1395.

Carey, F.G., and Lawson, K.D. 1973. Temperature regulation in free-swimming bluefin tuna. Comp. Biochem. Physiol. A Comp. Physiol. **44**: 375–392.

Carey, F., and Teal, J.M. 1969. Regulation of body temperature by the bluefin tuna. Comp. Biochem. Physiol. **28**: 205–213.

Gunn, J., and Block, B. 2001. Advances in acoustic, archival, and satellite tagging of tunas. *In* Tuna: physiology, ecology and evolution. *Edited by* B.A. Block and E.D. Stevens. Academic Press, San Francisco, Calif.

Hill, R. 1994. Theory of geolocation by light levels. *In* Elephant seals: population ecology, behaviour and physiology. *Edited by* B.J. Le Boeuf and R.M. Laws. University of California Press, Berkeley, Calif. pp. 227–236.

Hill, R.D., and Braun, M.J. 2001. Geolocation by light-level. The next step: latitude. *In* Methods and technologies in fish biology and fisheries. Vol. 1. *Edited by* J. Sibert and J. Neilson. Kluwer Academic Publishers, Dordrecht, Netherlands. pp. 443–456.

Lutcavage, M., Brill, R., Skomal, G., Chase, B., and Howey, P. 1999. Results of pop-up satellite tagging on spawning size class fish in the Gulf of Maine. Do North Atlantic bluefin tuna spawn in the mid-Atlantic? Can. J. Fish. Aquat. Sci. **56**: 173–177.

Magnuson, J.J., Safina, C., and Sissenwine, M.P. 2001. Whose fish are they anyway? Science (Wash., D.C.), **293**: 1267–1268.

Mather, F.J., Mason, J.M., and Jones, A.C. 1995. Historical document: life history and fisheries of Atlantic bluefin tuna. NOAA Tech. Memo. NMFS-SEFSC-370.

McGowan, M.F., and Richards, W.J. 1989. Bluefin tuna, *Thunnus thynnus*, larvae in the Gulf Stream off the southeastern United States: satellite and shipboard observations of their environment. U.S. Natl. Mar. Fish. Serv. Fish. Bull. No. 87. pp. 613–631.

National Research Council. 1994. An assessment of Atlantic bluefin tuna. National Academy Press, Washington, D.C.

Richards, W.J. 1976. Spawning of bluefin tuna (*Thunnus thynnus*) in the Atlantic Ocean and adjacent seas. Coll. Vol. Sci. Pap. 2. ICCAT, Madrid, Spain. pp. 267–278.

Rivas, L.R. 1954. A preliminary report on the spawning of the western north Atlantic bluefin tuna (*Thunnus thynnus*) in the Straits of Florida. Bull. Mar. Sci. Gulf Caribb. **4**: 302–322.

Sissenwine, M.P., Mace, P.M., Powers, J.E., and Scott, G.P. 1998. A commentary on western Atlantic bluefin tuna assessments. Trans. Am. Fish. Soc. **127**: 838–855.

Taillade, M. 1992. Animal tracking by satellite. *In* Wildlife telemetry remote monitoring and tracking of animals. *Edited by* I.M. Priede and S.M. Swift. Ellis Horwood, New York. pp. 149–160.

Teo, S.L.H., Boustany, A., Blackwell, S., Walli, A., Weng, K.C., and Block, B.A. 2004. Validation of geolocation estimtes based on light and sea surface temperature from electronic tags. Mar. Ecol. Prog. Ser. **283**: 81–91.

Reconstructing the salinity and environment of the Limfjord and Vejlerne Nature Reserve, Denmark, using a diatom model for brackish lakes and fjords

David B. Ryves, Annemarie L. Clarke, Peter G. Appleby, Susanne L. Amsinck, Erik Jeppesen, Frank Landkildehus, and N. John Anderson

Abstract: Diatoms in surface sediments from a data set of 27 brackish lakes and nine fjords in Jutland, Denmark (range 0.2 – 31 $g \cdot L^{-1}$ total dissolved solids (TDS)), were analysed using multivariate methods to determine response to measured parameters (depth, total phosphorus (TP), total nitrogen (TN), TN/TP, salinity, water body type). Water body type, salinity, depth and TP together explained 25.3% of the variation in the diatom data and were all independently significant predictors. A diatom–salinity model (r^2_{jack} = 0.887, root mean square error of prediction = 0.246 log salinity, $g \cdot L^{-1}$) was developed from the 36 sample training set and applied to fossil diatom assemblages in three sediment cores from the east Vejlerne wetland, Denmark, a nature reserve created after the damming of an embayment of the polyhaline Limfjord (~26 $g \cdot L^{-1}$ TDS) in the late 19th century. The diatom-inferred salinity reconstructions reflect the known salinity history of the Limfjord and the freshwater–subsaline Vejlerne lakes, and appear sensitive to documented North Sea storms in the 16th and 17th centuries, which had major impacts on the brackish Limfjord herring fishery. Diatom–salinity models may be useful tools in long-term studies of coastal and estuarine areas to test hypotheses concerning aquatic resources and ecological, hydrographic, and cultural change.

Résumé : Des méthodes multidimensionnelles nous ont permis d'analyser les données sur les diatomées dans les sédiments de surface dans une série de 27 lacs saumâtres et neuf fjords du Jutland, Danemark, (étendue de 0,2–31 $g \cdot L^{-1}$ des solides totaux dissous (TDS)) afin de déterminer la réaction de diatomées à des paramètres choisis (profondeur, phosphore total (TP), azote total (TN), TN/TP, salinité, type de milieu aquatique). Le type de milieu, la salinité, la profondeur et TP expliquent ensemble 25,3 % de la variation des données sur les diatomées; ce sont tous individuellement des facteurs prédictifs significatifs. Nous avons mis au point un modèle des diatomées en fonction de la salinité (r^2_{jack} = 0,887, erreur quadratique moyenne de la prédiction = 0,246 log salinité, $g \cdot L^{-1}$) à partir de ces 36 échantillons expérimentaux et l'avons appliqué aux regroupements de diatomées fossiles dans trois carottes de sédiments prélevées dans la section est des terres humides de Veijlerne, Danemark, une réserve naturelle créée après le barrage d'une baie du Limfjord polyhalin (~26 $g \cdot L^{-1}$ TDS) à la fin du 19^e siècle. Les reconstitutions des salinités basées sur les diatomées correspondent aux salinités connues dans le passé dans le Limfjord et les lacs d'eau douce–subsaline de Vejlerne; elles semblent tenir compte des tempêtes signalées dans la mer du Nord aux 16^e et 17^e siècles, qui ont eu un impact majeur sur la pêche de harengs dans les eaux saumâtres du Limfjord. Les modèles de diatomées–salinités peuvent être des outils utiles pour les études à grande échelle temporelle des régions côtières et estuariennes, afin de vérifier des hypothèses concernant les ressources aquatiques et les changements écologiques, hydrographiques et culturels.

[Traduit par la Rédaction]

Received 18 July 2003. Accepted 24 April 2004. Published on the NRC Research Press Web site at http://cjfas.nrc.ca on 24 December 2004.
J17648

D.B. Ryves[1,2] and N.J. Anderson.[2] Environmental History Research Group, Department of Quaternary Geology, Geological Survey of Denmark & Greenland (GEUS), Øster Voldgade 10, DK-1350 Copenhagen K, Denmark.
A.L. Clarke.[3] School of Geography, Politics and Sociology, University of Newcastle, Newcastle upon Tyne, NE1 7RU, UK.
P.G. Appleby. Department of Mathematical Sciences, University of Liverpool, P.O. Box 147, Liverpool L69 3BX, UK.
S.L. Amsinck and E. Jeppesen. National Environmental Research Institute, Department of Freshwater Ecology, Vejlsøvej 25, 8600 Silkeborg, Denmark, and University of Aarhus, Institute of Biological Sciences, Department of Plant Ecology, Nordlandsvej 68, 8240 Risskov, Denmark.
F. Landkildehus. National Environmental Research Institute, Department of Freshwater Ecology, Vejlsøvej 25, 8600 Silkeborg, Denmark.

[1] Corresponding author (e-mail: d.b.ryves@lboro.ac.uk).
[2] Present address: Department of Geography, Loughborough University, Loughborough, Leicestershire, LE11 3TU, UK.
[3] Present address: National Environmental Research Institute, Department of Marine Ecology, Frederiksborgvej 399, P.O. Box 358, 4000 Roskilde, Denmark.

doi: 10.1139/F04-127

Introduction

At the boundary of offshore (marine) and inland (freshwater) systems, coastal environments are sensitive to changes that affect both environments, for example, fluctuations in freshwater input, sea level, and nutrient supply. As a result, coastal sediments contain important archives of environmental change, recording signals of past changes in salinity, sea level, and nutrient concentrations in sedimentology, geochemistry, and biological remains (Cooper and Brush 1991; Dellwig et al. 1998; Bianchi et al. 2000). Diatoms have been particularly favoured as tools for palaeoenvironmental reconstruction, as many coastal taxa are globally distributed, and their silica frustules tend to preserve well in sediments and are identifiable to species level. A long European tradition of research into contemporary diatom distributions along coasts has produced species classifications according to salinity and habitat preference (e.g., van der Werff and Huls 1976; Snoeijs 1993; Snoeijs and Balashova 1998). This remains the basis for much palaeoenvironmental interpretation of coastal sediments (Cooper 1995; Dellwig et al. 1999; Andrén et al. 2000), despite the growing application of transfer function methodologies in palaeoecology (Birks 1998). Quantitative reconstructions of such important parameters as salinity, sea level, and nutrient concentrations are essential to test ecological hypotheses put forward to explain historical and archaeological variations in aquatic resources (e.g., Holm and Bager 2002; MacKenzie et al. 2002) especially in the context of major climatic and cultural shifts (Rowley-Conwy 1984; Bailey and Milner 2005). Knowledge of long-term variability of coastal environments provides the framework for evaluating recent changes and assessing predictions about future developments.

While much is known about the functioning of maritime, coastal, and freshwater habitats, relatively little research has been conducted in brackish lakes and lagoons across this gradient and how these systems might respond to environmental change (e.g., climate, salinity, eutrophication). Diatom assemblages in surface sediments were analysed as part of an ongoing project examining the ecology and palaeoecology of brackish lakes in Vejlerne, a nature reserve in North Jutland and once part of the marine-brackish Limfjord (Jeppesen et al. 2002; Amsinck et al. 2003). Additionally, diatom assemblages from higher salinity, shallow Danish fjords were added to the lake samples to extend the salinity gradient into the full marine range. As these aquatic environments cover a gradient of salinity and trophic status, we aimed to establish whether these parameters exerted a strong control on diatom communities and therefore could be used to create models for quantitative reconstruction. A resultant diatom–salinity model was then applied to subfossil diatom assemblages from three sediment cores collected from nearby shallow lakes in the east Vejlerne wetlands to reconstruct salinity in the context of major land use change in this area over the last few centuries.

Fig. 1. Location map. (*a*) Training set sites in Denmark. Solid circles are lakes and lagoons (27 sites), and circles with cross are fjords (9 sites). The locations of other sites mentioned in the text are also shown. BB, Bjornsholm Bay. (*b*) East Vejlerne nature reserve with coring sites indicated for the three lakes (Glombak, Han Vejle, and Lund Fjord).

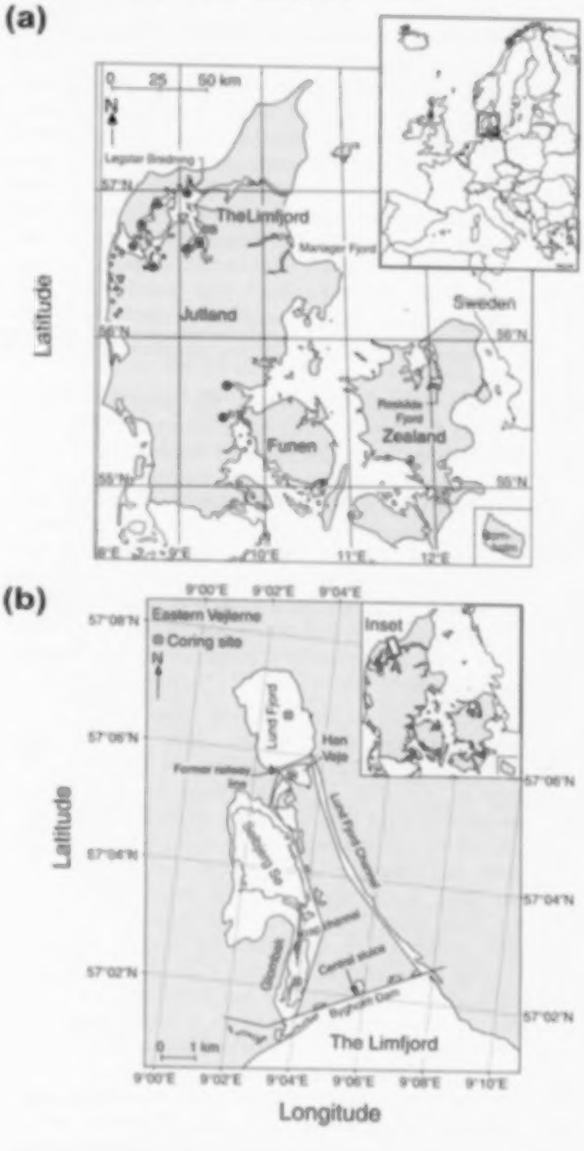

Methods

Study area and fieldwork

The northern part of Jutland, Denmark, contains many small, shallow coastal lakes and lagoons, which exhibit a range of salinity (0.2–18 g·L^{-1} total dissolved solids, TDS) according to their degree of connection to nearby coastal waters or inland fjords (e.g., the Limfjord; Fig. 1). Although much of the region has a relatively low population density and includes areas of seminatural heath and wetland, agricultural land use predominates and has resulted in the enrichment of both N and P of many surface waters. Both salinity and trophic gradients exist among coastal lakes and lagoons today (Table 1). As the salinity gradient does not extend into full marine conditions, a further nine samples collected from nearby Danish fjords were added to the

Table 1. Summary of six parameters measured for lake and fjord groups and the combined data set of 36 sites.

	Salinity ($g \cdot L^{-1}$)	TN ($\mu g \cdot L^{-1}$)	TP ($\mu g \cdot L^{-1}$)	TN/TP	Depth (m)	*F* index (ratio)
All sites (*n* = 36)						
Average	9.0	1724	110	22.4	2.8	—
Maximum	31.1	5600	331	94.0	12.0	—
Minimum	0.2	616	25	3.7	0.5	—
Range	30.9	4984	306	90.3	11.5	—
Lakes (*n* = 27)						
Average	3.6	1972	127	24.3	1.6	0.76
Maximum	17.4	5600	331	94.0	4.2	0.93
Minimum	0.2	850	25	3.7	0.5	0.50
Range	17.2	4750	306	90.3	3.7	0.43
Fjords (*n* = 9)						
Average	25.2	980	59	16.7	6.3	—
Maximum	31.1	1440	83	18.6	12.0	—
Minimum	18.7	616	45	12.2	3.4	—
Range	12.4	824	38	6.3	8.6	—

Note: TN, total nitrogen; TP, total phosphorus. The diatom dissolution index, *F*, was only assessed for the lake samples.

brackish lakes training set, covering the range 19–31 $g \cdot L^{-1}$ (Fig. 1; Table 1). These samples were selected from a larger data set of Danish fjords and estuaries included in an earlier study on diatom distribution in north European coastal waters (Clarke 2001; MOLTEN Project 2003). Combining these samples from the same geographical area allows the full salinity gradient to be covered. While estuarine and fjord habitats are hydrographically different from lake sites, including these environments in inference models provides analogues for reconstructions at coastal sites under changing sea levels in the past. This is especially appropriate for the Vejlerne cores discussed here, which include Limfjord sediments.

East Vejlerne is an artificial wetland created when a shallow embayment on the northern shore of the saline (~26 $g \cdot L^{-1}$) Limfjord was separated by the Bygholm Dam, completed in 1876 (Fig. 1), in an attempt to create agricultural land to offset the loss of Danish territory elsewhere. A series of sluices and drainage canals was set up to regulate water level and salinity within Vejlerne, and in 1906 a railway was built to encourage regional development, which separated Han Vejle from Lund Fjord. Nonetheless, by the early 20th century efforts to reclaim the land for agriculture were proving unsuccessful, and by 1920 land reclamation was finally abandoned (Jakobsen and Sørensen 1998). Since this time, Vejlerne has developed as a mixed wetland of about 6000 ha, consisting of shallow lakes, meadow, and marshland of varying salinity, largely depending on distance from the Limfjord. These varied habitats seasonally attract large numbers of migrating birds, and Vejlerne's international importance for bird conservation was formally recognised by accreditation under the Ramsar Convention in 1977 and the European Union Bird Directive in 1983 (Hald-Mortensen 1998). Changes to the drainage system were made during the 20th century, notably in the 1960s, when self-regulating sluices were replaced by a central sluice on the Limfjord dam (Amsinck et al. 2003).

Surface sediments were collected from the deepest parts of 43 fresh and brackish lakes and lagoons in the northern part of Jutland from June to November 1999, using a simple Kajak-type corer. A subset of 27 lakes selected for diatom analysis (Fig. 1) was chosen to provide approximately equal coverage across the salinity and nutrient range to minimize bias in any one part. Sediments from nine fjord and estuarine sites (Fig. 1) were collected using a HON-Kajak corer (Renberg 1991). Water samples from all sites were analysed for total phosphorus, total nitrogen, and salinity ($g \cdot L^{-1}$ TDS). Lake water total phosphorus (TP) was determined as molybdate-reactive phosphorus (Murphy and Riley 1972) following persulphate digestion (Koroleff 1970). Total nitrogen (TN) was the sum of ammonia, nitrite, and nitrate after potassium persulphate digestion (Solórzano and Sharp 1980) using the phanate method (APHA 1985). Salinity was measured on site using a portable YSI 30 instrument (YSI Environmental Inc., Yellow Springs, Ohio, USA). Lake water samples were analysed at the National Environmental Research Institute, Silkeborg, and were also compared with survey data collated by the Danish counties.

Lake chemistry values are summer means (sampled May to October 1996–2000; median number of measurements per lake = 4.5) for 16 of the 27 lakes; values are based on single samples for the remaining sites collected at the same time as coring. Examining data from the 16 lakes sampled for water chemistry more than once gives some idea of the variability in the abiotic environment in these systems. The coefficient of variation (CV) for both salinity and TP were similar (salinity: mean CV = 20%, range 1%–66%; TP: mean CV = 18%, range 5%–52%; *n* = 16 for both) over the period 1996–2000. For fjords, the uppermost 10 m of the water column was analysed monthly over 5 years as part of the Danish National Monitoring and Assessment Program (Conley et al. 2002), and means for each site were calculated on the basis of 965–4180 individual measurements for salinity and between 65 and 285 measurements for TP and TN, respectively.

Short sediment cores (<1 m long, diameter 5.2 cm) were also taken from several shallow lakes in the east Vejlerne wetlands (including Han Vejle, Glombak, and Lund Fjord; Fig. 1). Cores were taken in October 1998 (Glombak) or June 1999 (Han Vejle and Lund Fjord) with a 1-m Mackereth piston corer (Glombak and Lund Fjord) or a modified Kajak corer (Han Vejle). Only cores with an undisturbed sediment–water interface were kept, and one core was chosen from each site for dating and zooplankton and diatom analysis, while replicate cores were reserved for future analyses. Cores were sectioned in 1-cm intervals and samples stored in dark refrigeration until analysis.

Laboratory methods

All samples for diatom analysis were prepared following the method of Renberg (1990). Diatom analysis was made on surface sediment assemblages from 27 lake sites and nine fjords, and for the sediment core work, counts on 21 levels from Han Vejle, 26 from Glombak, and 18 from Lund Fjord were made. Strewn slides were mounted in Naphrax, and where presevation permitted, at least 300 valves (average 480 for surface sediments) per sample were counted in transects under oil-immersion phase-contrast light microscopy at × 1000 (numerical aperture = 1.4) and identified where possible to species level. Taxa were identified according to a variety of general (e.g., Krammer and Lange-Bertalot 1986–1991; Witkowski et al. 2000) and regional floras (e.g., Snoeijs and Vilbaste 1994; Snoeijs and Potapova 1995; Snoeijs and Kasperovičienė 1996). Diatom taxonomy was harmonized between the lake and fjord samples according to agreements reached by the two analysts during a workshop. Species grouped into aggregate taxa are indicated as "agg.".

Samples from all cores were analysed every 1 cm (Han Vejle and Lund Fjord) or 2 cm (Glombak) for the fraction of dry weight loss-on-ignition at 550 °C (LOI%) after drying overnight at 105 °C (Dean 1974). For Glombak and Lund Fjord, whole core bulk magnetic susceptibility measurements (using a Bartington MS2-C loop; Bartington Instruments Ltd., Oxford, UK) were made before extruding the cores from the Perspex core tubes. Values of magnetic susceptibility are reported in SI units (Système International d'Unités). Homogenized subsamples were analysed for the radionuclides ^{210}Pb, ^{226}Ra, and ^{137}Cs by direct gamma assay using Ortec HPGe GWL series well-type coaxial low background intrinsic germanium detectors (Ortec, Oak Ridge, Tennessee) (Appleby et al. 1986). Dates were calculated using a constant rate of supply ^{210}Pb model (Appleby and Oldfield 1978). Full details of all dating analyses referred to here are available from the authors upon request.

Numerical methods

Environmental data consist of four measured parameters (TN, TP, salinity, and depth) and one derived variable, TN/TP ratio (Table 1). Additionally, a diatom dissolution index (F) was calculated for the 27 lake samples and all core samples. This index is the proportion of all valves counted under light microscopy that are well preserved and varies between 1 (excellent preservation) and 0 (all valves visibly dissolved). It has been previously used to estimate dissolution in diatom studies and permits preservation to be compared between samples (Ryves et al. 2001, 2002). Diatom counts were expressed as relative abundance (percentages) of total counts, and taxa not identified to species level were removed. For multivariate analyses, environmental variables were log transformed to reduce the effect of extreme values. A dummy variable (0/1) was included to take into account the contrast between aquatic system type (lake or fjord) not captured by parameters measured. Ordinations were carried out using CANOCO 4.0 (ter Braak and Šmilauer 1998). Monte Carlo permutation significance tests were carried out with 999 permutations. Downweighting was applied in all unimodal analyses, with detrending by segments (where appropriate).

For model development, detrended correspondence analysis (DCA) of diatom data was used to estimate the species gradient length, values <2 standard deviation (SD) units indicating that most species have monotonic responses to underlying ecological gradients and should thus be modelled using linear methods (ter Braak 1995). Canonical correspondence analysis (CCA) was performed to identify which variables might be suitable candidates for model development, using Bonferroni-adjusted forward selection, inspection of variance inflation factors, and t values of regression coefficients (ter Braak and Šmilauer 1998). Detrended CCA (DCCA) was run to confirm a similar gradient length to that under DCA with any chosen variable (Birks 1995). Candidate parameters should also explain a statistically significant amount of the total species variance in single-variable CCA, where the ratio of the constrained axis (axis 1) to the first unconstrained axis (axis 2) should be >0.5 (Kingston et al. 1992).

A variety of models was investigated using weighted-averaging methods (WA), partial least squares (PLS), and weighted-averaging partial least squares (WA-PLS; ter Braak and Juggins 1993). Both tolerance-downweighting and simple WA were used, with both classical and inverse deshrinking (Birks 1995). All models were internally validated using the leave-one-out jackknife method (Birks 1995) and critically compared according to the root mean square error of prediction (RMSEP). As a rule of thumb, a higher component WA-PLS model should only be accepted if there is >5% improvement in RMSEP over the simpler (lower component) alternative (Birks 1998). Bias (value-dependent error) should be as low as possible. Model building, validation, and reconstruction was carried out using the programs CALIBRATE 0.81 (Juggins and ter Braak 1997) and WAPLS 1.2 (S. Juggins, School of Geography, Politics and Sociology, Newcastle University, UK, and C.J.F. ter Braak, Biometris, P.O. Box 100, 6700 AC Wageningen, The Netherlands, unpublished data), with sample-specific errors calculated using 9999 permutations. Estimates of species richness, E(S), in samples of different count size were made using RAREPOLL (Birks and Line 1992) using $N = 300$ valves.

Results

Environmental and diatom data sets

Environmental data for all sites are summarized in Table 1. While the addition of the fjord sites has extended the salinity range appreciably from 17.4 to 31.1 g·L^{-1} TDS, lakes and fjords also differ in average TN, TP, and depth. Both the range and mean values of TN and TP are greater among lakes than fjords, with mean TN and TP values in lakes (1972 µg·L^{-1} and 127 µg·L^{-1}, respectively) about twice those measured in fjords (980 µg·L^{-1} and 59 µg·L^{-1}, respectively; Table 1). Among the 36 sites, a strong positive correlation ($p = 0.001$, $n = 36$) exists between salinity and depth

(r = +0.799), and weaker, negative correlations (p = 0.01, n = 36) between salinity and TN (r = –0.464), depth and TN (r = –0.447), and TP and TN/TP (r = –0.488). Limnologically, a strong contrast appears between the shallow, nutrient-enriched and lower salinity lakes and the deeper, estuarine fjords, as expected from the varying influence that terrestrial and marine processes have on aquatic systems across a coastal gradient.

After removal of unknown types, 263 diatom taxa could be identified from the 27 lake sites and 240 from the nine fjord samples. This may reflect in part the larger number of valves counted in the fjord data set (average 569 valves) compared with the lake samples (average 424 valves), although fjord assemblages may include valves originating from a greater range of environments and a larger geographical area than the sites on land. Owing to taxonomic difficulties in positive identification of *Chaetoceros* species from the cysts, it was decided to remove these taxa from the merged data set before further analyses. *Skeletonema costatum*, only recorded from the fjord samples, was also removed from the merged data set, as it was considered unlikely to be well preserved in sediments. Removing these taxa reduced the total diatom count by ~5% (by on average 15 and 54 valves per sample for lakes and fjords, respectively).

The combined diatom data set after these deletions consists of 413 taxa, of which about 21% (87) are common to both site types. Many taxa in this diverse flora are rare. In the combined data set, about one third of taxa (137) appear only once among the 36 sites, while only 41% (171) occur at a relative abundance of 1% or above. These proportions are closely mirrored within the lake and fjord data sets individually. However, many of the most important taxa are found in both lake and fjord sites (Fig. 2), supporting the idea that lake and fjord systems are ecologically as well as geographically continuous. Moreover, salinity appears important in structuring the pattern of species' distribution among these varied sites (Fig. 2). While some species (e.g., *Ctenophora* (= *Synedra*) *pulchella* and *Stephanodiscus parvus*) are entirely confined to lakes, and others (e.g., *Eunotogramma dubium* and *Nitzschia distans*) are found only in fjord samples, the majority of important taxa are found in both types, although often with a clear abundance peak in one part of the salinity spectrum. Although diatom preservation is generally good among lake sites (F_{mean} = 0.76, F_{min} = 0.5; Table 1), there is a tendency for diatom dissolution to increase with salinity (Fig. 2).

Multivariate analyses and model development

The gradient length of the first DCA axis (3.98 SD units) of the diatom data confirmed that diatom species' responses were largely unimodal (cf. Fig. 2), with about 11.8% of variation in the species data captured by axis 1 and a further 6.1% along axis 2. Constraining the diatom data by transformed environmental variables revealed that salinity, depth, and TP were all significant in explaining fractions of the species variance, even after accounting for the lake–fjord contrast (Table 2). These four variables explain 25.3% of the diatom data (significant at p = 0.001, n = 999), and each independently explains 3.5% (TP) to 6% (salinity) of total variance when the other three factors are included as covariables in the analysis (Table 2). There is relatively little variance (~8%, 30% of the total explained) shared between two or more factors, despite the large number of combinations involving 2, 3, and 4 factors possible (11 permutations).

Salinity is the most important parameter, explaining 6% of variation uniquely and 10.4% when it is the only constraining variable (axis 1/axis 2 = 1.18; Table 2), with a gradient >3.2 units under DCCA and is thus the most suitable candidate for construction of a diatom model. While both WA and WA-PLS methods produced strong apparent models, the most robust under jackknifing was found to be the second component WA-PLS model (WA-PLS(2); Fig. 3). The improvement in RMSEP under the second component (4.6% smaller than component 1) was accompanied by a reduction in average bias by almost 40% and was deemed a significant improvement overall. The final diatom–salinity model for 36 sites appears robust across the salinity gradient from freshwater to near-full marine conditions (r^2 = 0.977, RMSE = 0.11 log salinity g·L^{-1}), even under internal validation (r^2_{jack} = 0.887, RMSEP = 0.246; Fig. 3).

Application to Vejlerne cores

The diatom–salinity model was applied to sedimentary diatom assemblages from cores collected from three sites in the eastern Vejlerne (Fig. 1; Han Vejle, Glombak, and Lund Fjord). Stratigraphical plots summarizing physical and diatom analyses of these sequences are presented (Figs. 4–6). All three cores contain a striking lithological contrast between uppermost dark, organic-rich, lower density gyttja and grey, organic-poor, higher density clays below, although the relative length of these two sections varies greatly among the three sites. This lithological difference between these sediment types is paralleled by physical and biological analyses (Jeppesen et al. 2002; Amsinck et al. 2003), reflecting sedimentation under marine–brackish (lower unit) and lacustrine conditions (upper unit) following the building of the Bygholm Dam.

Glombak

The 82-cm core from Glombak can be divided into two sections according to lithological, physical, and diatom analyses, the major change occurring at about 54 cm (Fig. 4). Dating results are consistent with this transition occurring in the late 19th century, agreeing with the known age of dam construction. The uppermost 45 cm (post-1915) are characterized by high organic (30%–50% LOI) and water content, low but variable carbonate content, and low bulk magnetic susceptibility (BMS). A transition period from 45 to 54 cm shows declines in LOI, CO_3^{2-}, and water content with increases in magnetic susceptibility. The lower 28 cm of the core consists of low organic, carbonate, and water-poor material, with slight increases in these towards the bottom of the core. A peak in BMS centred on 72 cm is due to a large, rounded 2-cm diameter pebble found in the centre of the core (and so not carried down during coring). Dry mass flux and sedimentation rate show highest values towards the top of the core, where values over 0.06 g·cm^{-2}·year^{-1} flux and 1 cm·year^{-1}, respectively, are recorded. Values decline until a lower peak of 35–45 cm (~1915–1929).

Diatom assemblages also show a major transition across this lithological boundary; taxa with the highest salinity optima (as derived from the modern training set) are generally

Fig. 2. Diatom distributions of selected taxa in surface sediments of 27 lakes and lagoons and nine fjords, plotted as relative abundance (%). All 43 taxa >5% in any sample and found in six sites or more are shown. Sites are ordered in increasing salinity from top to bottom (values shown in g·L^{-1}), and species are ordered according to their weighted average distribution (closely corresponding to salinity optimum, shown in g·L^{-1} in parentheses, increasing from left to right). *Chaetoceros* cysts and *Skeletonema costatum* were excluded from the final counts and are plotted as a proportion of the remaining taxa. Diatom dissolution index (*F*) for the lake samples is also plotted.

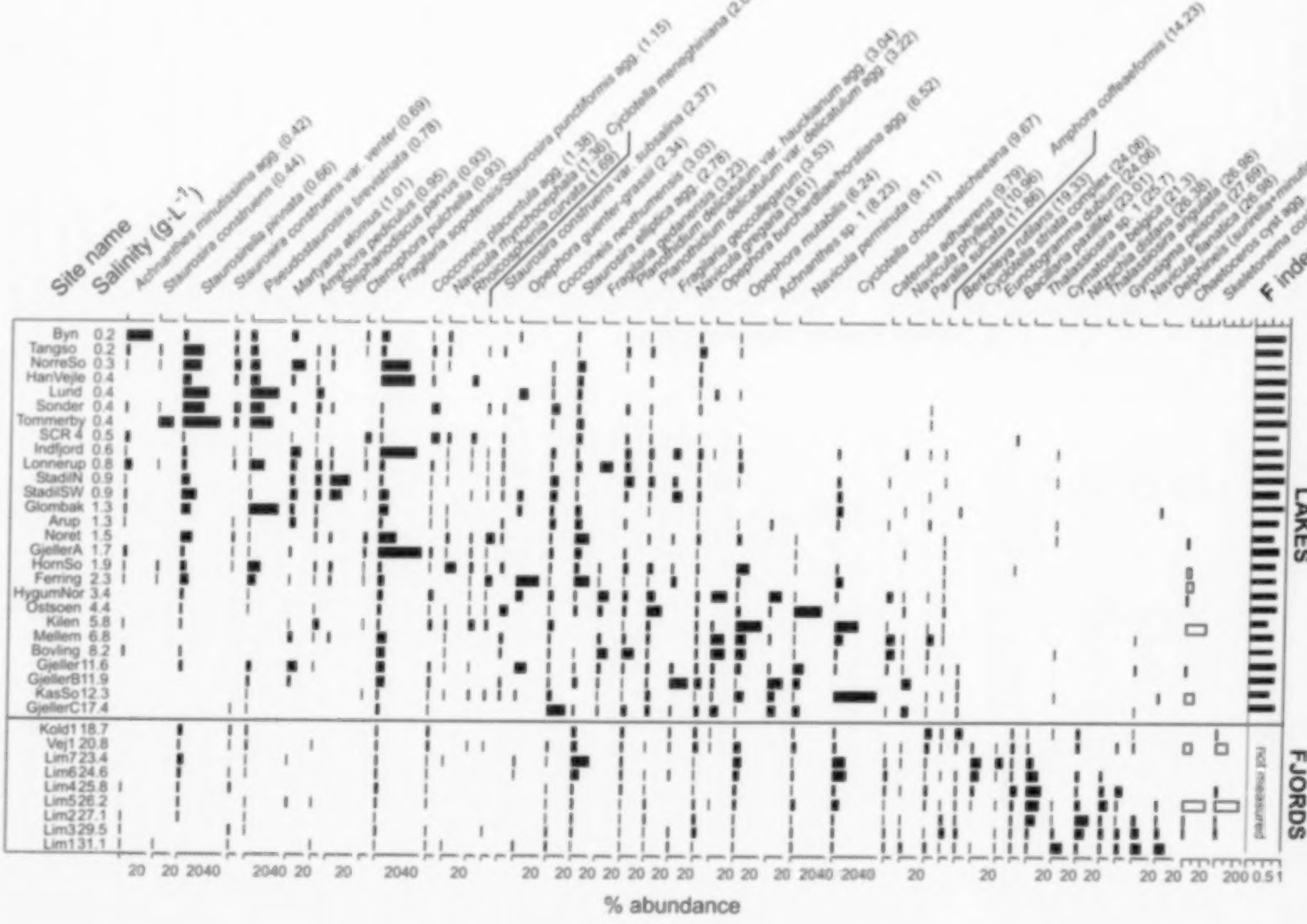

Table 2. Unique variance explained by significant variables during a variance partitioning analysis (using canonical correspondence analysis, CCA) of the 36-site diatom data set.

	Unique explanation		
Variable	λ_{var}	Species variance (%)	p level (n = 999)
Salinity	0.322	6.0	0.001
Lake–Fjord	0.219	4.1	0.002
Depth	0.208	3.9	0.003
Total P	0.189	3.5	0.014
Interactions	0.42	7.8	—
Total explained	1.358	25.3	0.001
Salinity (alone)	0.56	10.4	0.001
$\lambda_{salinity}/\lambda_{axis\ 2}$	ratio = 1.18		

Note: For salinity, results of a single-variable CCA are also given.

replaced by those with lower optima in a stratigraphic sequence from bottom to top. In the lowermost section from 75 to 82 cm, littoral taxa with the highest salinity optima (17.5–29 g·L^{-1}) are important (e.g., *Cocconeis stauroneiformis*, *Cymatosira belgica*, and *Delphineis* spp.). These are gradually replaced by somewhat lower salinity forms (e.g., *Cocconeis scutellum* agg., *Opephora mutabilis* (= *Opephora olsenii*) and *Grammatophora oceanica* (optima 2.5–13 g·L^{-1})). Several other brackish–marine taxa (3–12 g·L^{-1}) are also essentially confined to the lower 30 cm of the core, but show little trend within this part (e.g., *Paralia sulcata*, *Tabularia fasciculata* agg., *Planothidium delicatulum* (= *Achnanthes delicatula*) spp., and *Navicula starmachiodes*).

The transition at 54 cm within the diatom flora is abrupt, with assemblages suddenly dominated by freshwater and subsaline *Fragilaria*, *Staurosira*, *Pseudostaurosira*, *Staurosirella*, and *Martyana* spp. (termed here *Fragilaria* sensu lato). Notably present are several taxa which in this data set have salinity optima <3 g·L^{-1}: *Pseudostaurosira brevistriata*, *Staurosirella pinnata*, *Martyana atomus*, *Fragilaria sopotensis/Staurosira punctiformis* agg., and *Staurosira elliptica* agg., the latter which includes *Staurosira elliptica* and *Pseudostaurosira perminuta* (= *Fragilaria neoelliptica*). Within the freshwater phase, however, there is evidence of ecological and environmental change. Low salinity littoral taxa (*Amphora pediculus* and *Rhoicosphenia curvata*) are important from 35 to 55 cm (late 19th century to 1930). From 25 cm (circa 1960), the higher salinity pelagic species *Cyclotella choctawhatcheeana* (optimum 9.7 g·L^{-1}) appears together with *Achnanthes fogedii*, both maintaining an abundance of 10% or more in all subsequent samples.

Diatom-inferred (DI) salinity accurately reconstructs contemporary conditions (1.3 g·L^{-1}), and species coverage in the model is good, between 83% and 99% (average 93%). There is relatively little change in DI salinity throughout the last century, although values tend to increase in the upper 25 cm (from the 1960s). Across the lithological transition, however, salinity rises consistently to a maximum of 28 g·L^{-1} at 76 cm before dropping to 15 g·L^{-1} at the bottom of the core. Diatom preservation is good in the upper 40 cm (F_{mean} = 0.77) but falls appreciably from 45 to 70 cm (F_{mean} = 0.35), reaching a minimum of F = 0.21 at 60 cm. Preservation improves in the bottom 10 cm, reaching 0.69 in the lowermost sample. The proportion of unidentifiable valves closely follows the dissolution index (r^2 = 0.77, n = 22, p < 0.001).

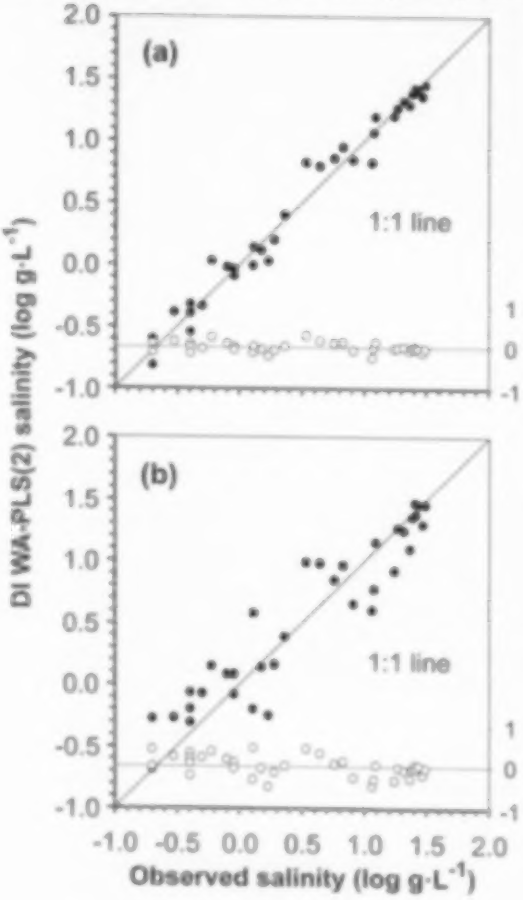
Fig. 3. Diatom–salinity model using weighted-average partial least squares (WA-PLS) (2nd component). Diatom-inferred (DI) salinity for apparent (*a*) and jackknifed (*b*) models is plotted against observed salinity (in log salinity, g·L^{-1}) for 36 sites. Solid circles, DI salinity; open circles, residuals. (*a*) Apparent model: r^2 = 0.977, root mean square error (RMSE) = 0.11 log salinity units; (*b*) jackknifed model: r^2_{jack} = 0.887, root mean square error of prediction (RMSEP) = 0.246 log salinity units.

Han Vejle

This 46-cm core consists almost entirely of gyttja, with the major visible lithological change at approximately 45 cm (Fig. 5). Data from ^{210}Pb and ^{137}Cs analyses suggest that there is a hiatus below 43 cm. Using a constant rate of supply model, the lowest horizon that can be securely dated is 40 cm (1941 ± 12 years), while the sediments below probably predate 1880.

Organic content (as LOI%), which varies between 10% and 40% in the upper 35 cm (~1950) and peaks from 7 to 15 cm (1993–1989) and 20–35 cm (1960–1980), falls below 10% some 3 cm before the lithological boundary, in tandem with a drop in water content. Dry mass flux varies down-

Fig. 4. Stratigraphic diatom analysis from Glombak core, GLOM I. Selected physical parameters, diatom taxa (relative abundance of all taxa >5% in any sample), and diatom indices (diatom-inferred (DI) salinity, % fossil data present in training set, and preservation index, *F*) are plotted. Dotted horizontal line indicates lithological transition from marine (lower) to freshwater (upper) sedimentary units. Age estimates from ^{210}Pb and ^{137}Cs analyses are shown on left. Arrow in DI salinity plot indicates current salinity at site; vertical lines indicate current (1990s) salinity range of Limfjord in Bjornsholm Bay.

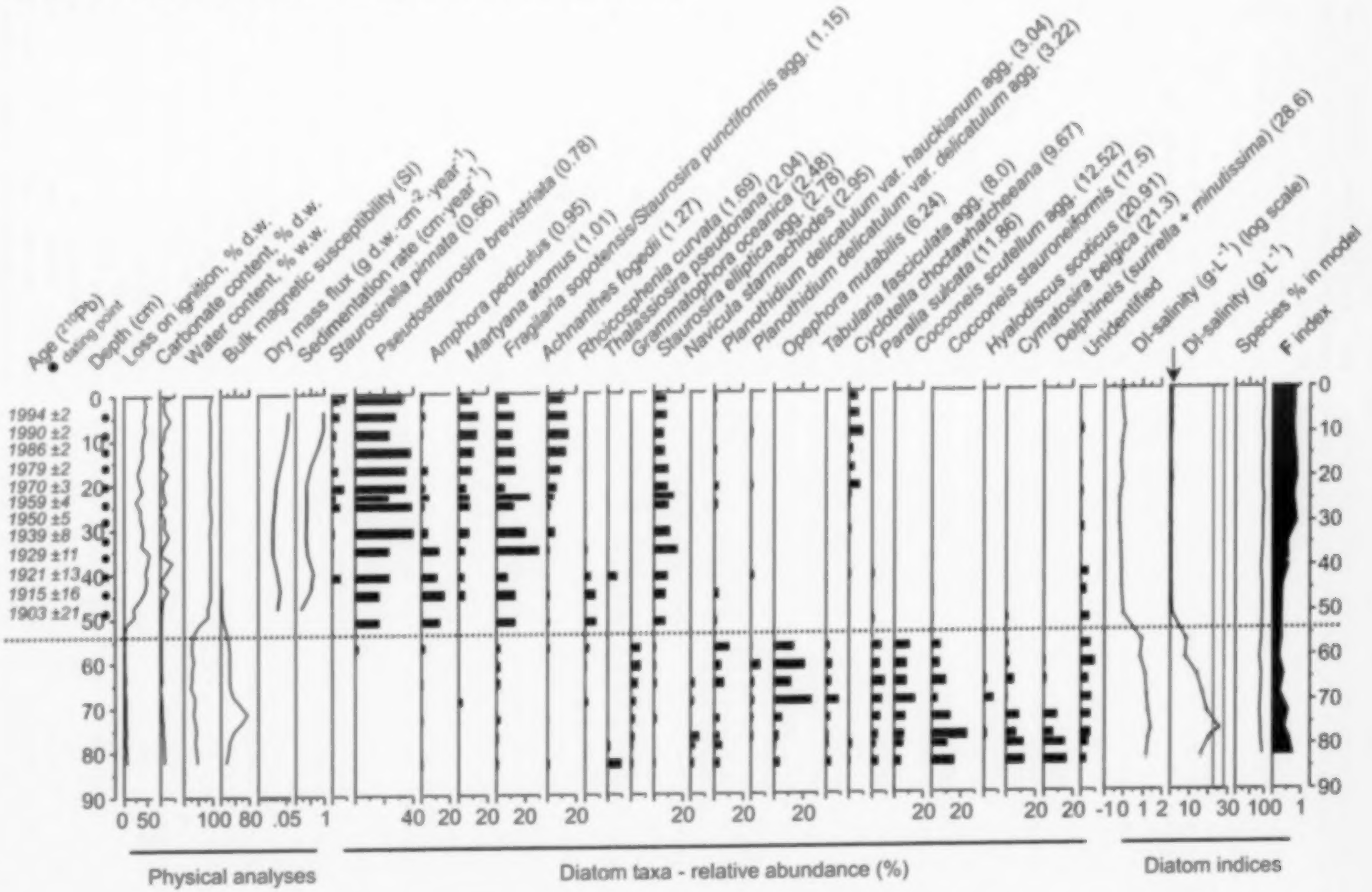

core, with a maximum value at 18 cm (~1983) and a secondary peak below 35 cm (in the 1940s). Sediment accumulation rates rise from a value of 0.4 cm·year^{-1} at 40 cm (dated 1941) to a peak of 2 cm·year^{-1} at 8 cm (~1992), before falling off slightly. Diatom valve concentrations and flux data are available for this core. Concentrations rise unevenly from values <1 × 10^{6} valves·g^{-1} dry weight (d.w.) at the base of the core to maximum values of almost 260 × 10^{6} valves·g^{-1} d.w. in the surface sediment and follow the LOI% curve. Diatom flux, however, is greatest from 15 to 20 cm (in the early 1980s, with a peak of nearly 60 × 10^{6} valves·cm^{-2}·year^{-1}), and at 3 cm (1996), with enhanced values below 35 cm (1940s).

The diatom flora shows only minor changes throughout the sequence, being dominated by many of the same oligosaline *Fragilaria* sensu lato (optima <3 g·L^{-1}) as found in the upper sections of the Glombak core (especially *Staurosirella pinnata*, *Pseudostaurosira brevistriata*, *Fragilaria sopotensis/Staurosira punctiformis* agg., and *Staurosira elliptica* agg.). Littoral taxa (e.g., *Achnanthes* spp., *Amphora pediculus*, *Navicula* spp.) become less abundant above 15–20 cm (from the early 1980s). The lowermost two samples contain few, generally poorly preserved diatoms ($F < 0.5$), and <100 valves could be counted from these levels. *Fragilaria* sensu lato are still important, but valves of polyhaline species appear (e.g., *Paralia sulcata*, *Cymatosira belgica*), indicating a transition to, or a mixture of, marine Limfjord sediments. DI salinity in the surface sediment matches measured values well (0.4 g·L^{-1} in 1998) and remains low throughout the upper 45 cm of the core (<1 g·L^{-1}), with almost 100% species coverage in the model. Even below 45 cm, DI salinity only rises to 1.5 g·L^{-1}, although these values are based on few valves. Diatom preservation is good for all samples above 45 cm ($F_{\text{mean}} = 0.71$).

Lund Fjord

The 80-cm core retrieved from this shallow lake contains the longest section of Limfjord sediments, with the lithological transition at only 6–7 cm below the surface (Fig. 6). Radiometric ^{210}Pb and ^{137}Cs analyses suggest a discontinuity in sedimentation at 5–6 cm, with all sediments above this depth postdating the early 1960s and a hiatus of unknown duration beneath, but spanning at least the first half of the 20th century.

Organic content is lower in this core than that found at Glombak and Han Vejle, fluctuating between 3% and 12% LOI below 5 cm and reaching 20% only in the surface sediment. This trend is repeated by carbonate and water content, with BMS showing the reverse (although values remain below 3 SI units throughout the sequence). Given the dating results, sedimentation rates can only be calculated for the uppermost section. Dry mass flux shows a subsurface peak of 0.04 g·cm^{-2}·year^{-1} at 3 cm (~1978) while accumulation rates are low (always <0.2 cm·year^{-1}) and decline sharply by 4 cm (~1968) to 0.05 cm·year^{-1}. Diatom concentrations fall rapidly within the upper 5 cm from 800 × 10^{6} to 12 × 10^{6} valves·g^{-1} d.w. and remain low throughout the lower section varying between 3 × 10^{6} and 140 × 10^{6} valves·g^{-1} d.w. (average <70 × 10^{6} valves·g^{-1} d.w.). Diatom fluxes, again only available for the uppermost three samples, mirror the concentrations and fall from 20 × 10^{6} to 0.2 × 10^{6} valves·cm^{-2}·year^{-1} by 6 cm. Levels with few diatoms and marked by poor diatom preservation were found in the lower section at 10 cm and from 30 to 35 cm.

As might be expected, the diatom flora shifts almost completely across the lithological transition, from dominance by freshwater *Fragilaria* sensu lato assemblage, with some higher salinity elements (e.g., *Opephora* spp. and *Cocconeis neothumensis*), to assemblages dominated by taxa with a marine affinity (especially *Paralia sulcata*, *Cocconeis scutellum* agg. and *Cocconeis stauroneiformis*, *Fallacia cryptolyra*, *Cymatosira belgica*, and *Delphineis* spp.). There is little systematic stratigraphic pattern within the lower core section, with assemblages dominated by littoral (epiphytic and benthic) taxa throughout. Subtle shifts among species abundance may indicate changes in habitat availability (e.g., patterns within *Navicula perminuta*, *Paralia sulcata*, *Cocconeis stauroneiformis*, *Tryblionella punctata*, and *Tryblionella coarctata*) within a more or less high salinity period.

DI salinity reflects these lithological and ecological transitions. The model predicts present-day salinity accurately (0.4 g·L^{-1}) and changes little within the uppermost post-damming section. The sample below this boundary contains few and very poorly preserved diatom valves ($F = 0.08$) and reconstructs salinity higher than fully marine conditions (45 g·L^{-1}). Inferred values below this point vary between 13 and 24 g·L^{-1}, at or below present-day observations in the Limfjord (23–31 g·L^{-1}), even for other poorly preserved assemblages with low counts. Species coverage is good for all samples throughout the core (on average 88%). Diatom dissolution shows a close correspondence with total diatom abundance (log concentration; $r^2 = 0.41$, $n = 18$, $p < 0.005$) and % unidentified taxa ($r^2 = 0.63$, $n = 18$, $p < 0.001$). While F values are high in the freshwater sediments ($F_{\text{mean}} = 0.79$), preservation falls at the transition to marine conditions and, although lower throughout this part ($F_{\text{mean}} = 0.38$), tends to improve with depth to the core base.

Discussion

Diatom distributions with respect to environmental gradients

Salinity, depth, and nutrient concentration have been shown to be important variables structuring diatom assemblages in surface sediments in Danish coastal areas (Clarke et al. 2003; this study). Covariation of environmental gradients in coastal areas and along estuaries (especially inversely between salinity and nutrients; Underwood et al. 1998) may make it difficult to determine which factors algal communities are primarily responding to, particularly if response to one variable is modulated by another (i.e., dependant effects). Although sophisticated techniques are now available to separate and test the independent effects of different parameters on biological data sets and estimate covariation between them (e.g., Muylaert et al. 2000), there is a need for experimental data to confirm these empirical models and underpin them with physiological and autecological evidence (e.g., Underwood et al. 1998; Saros and Fritz 2002). This is especially evident where biological data sets show strong spatial or temporal structure, which eludes statistical explanation by measured environmental variables (e.g., Lapointe

Fig. 5. Stratigraphic diatom analysis from Han Vejle core, HV I. Selected physical parameters, diatom taxa (relative abundance of all taxa >3% in any sample), and diatom indices (diatom-inferred (DI) salinity, % fossil data present in training set, and preservation index, *F*) are plotted. Dotted horizontal line indicates lithological transition from marine (lower) to freshwater (upper) sedimentary units. Age estimates from ^{210}Pb and ^{137}Cs analyses are shown on left. Arrow in DI salinity plot indicates current salinity at site. Levels where few diatom valves could be counted are shown as open bars or open circles.

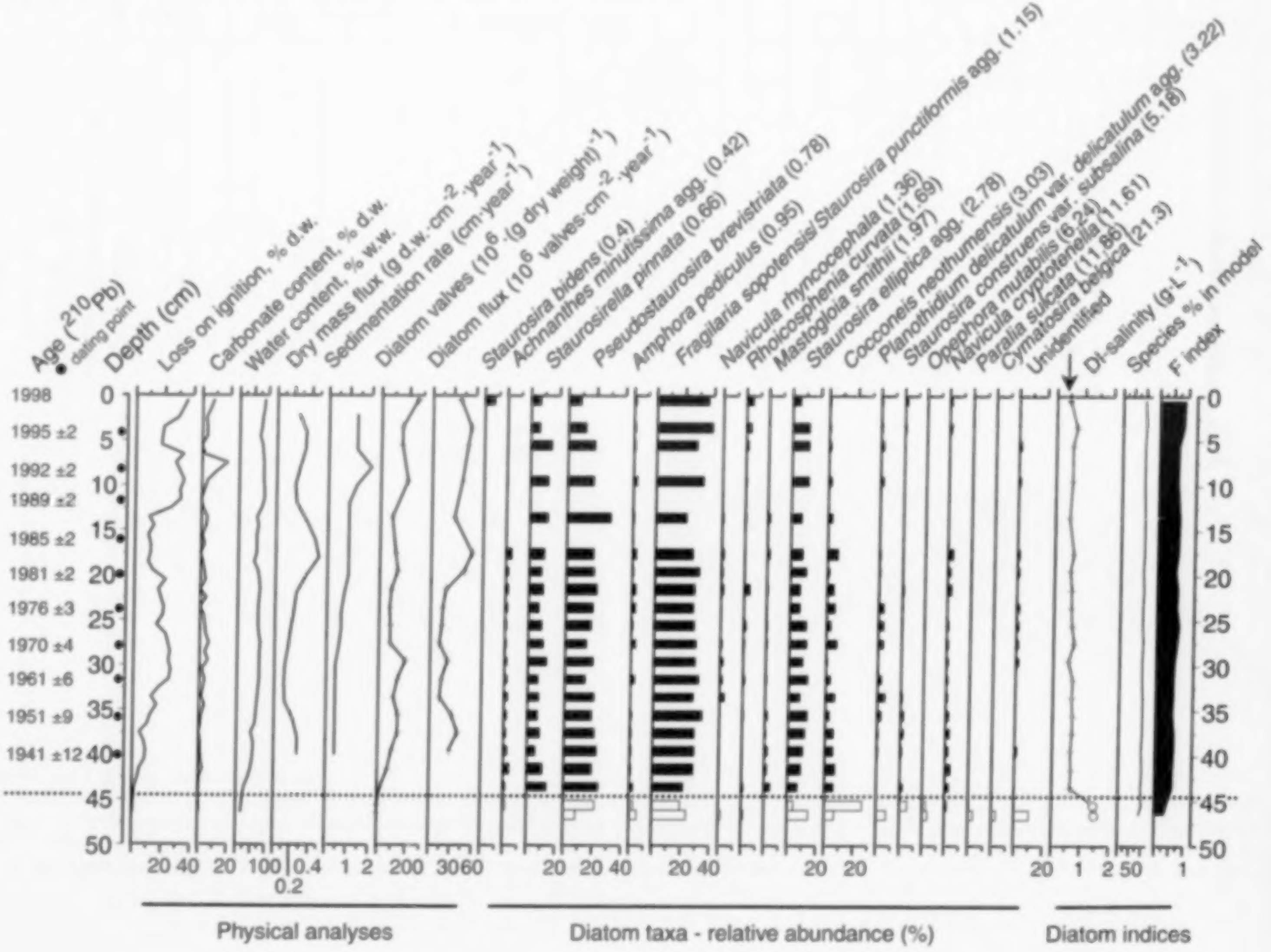

Fig. 6. Stratigraphic diatom analysis from Lund Fjord core, LUND I. Selected physical parameters, diatom taxa (relative abundance of all taxa >4% in any sample), and diatom indices (diatom-inferred (DI) salinity, % fossil data present in training set, and preservation index, *F*) are plotted. Dotted horizontal line indicates lithological transition from marine (lower) to freshwater (upper) sedimentary units. Age estimates from ^{210}Pb and ^{137}Cs analyses are shown on left. Arrow in DI salinity plot indicates current salinity at site; DI salinity at 10.5 cm is 45 g·L^{-1} (circled). Vertical lines indicate current (1990s) salinity range of Limfjord in Bjørnsholm Bay. Levels where few diatom valves could be counted are shown as open bars or open circles.

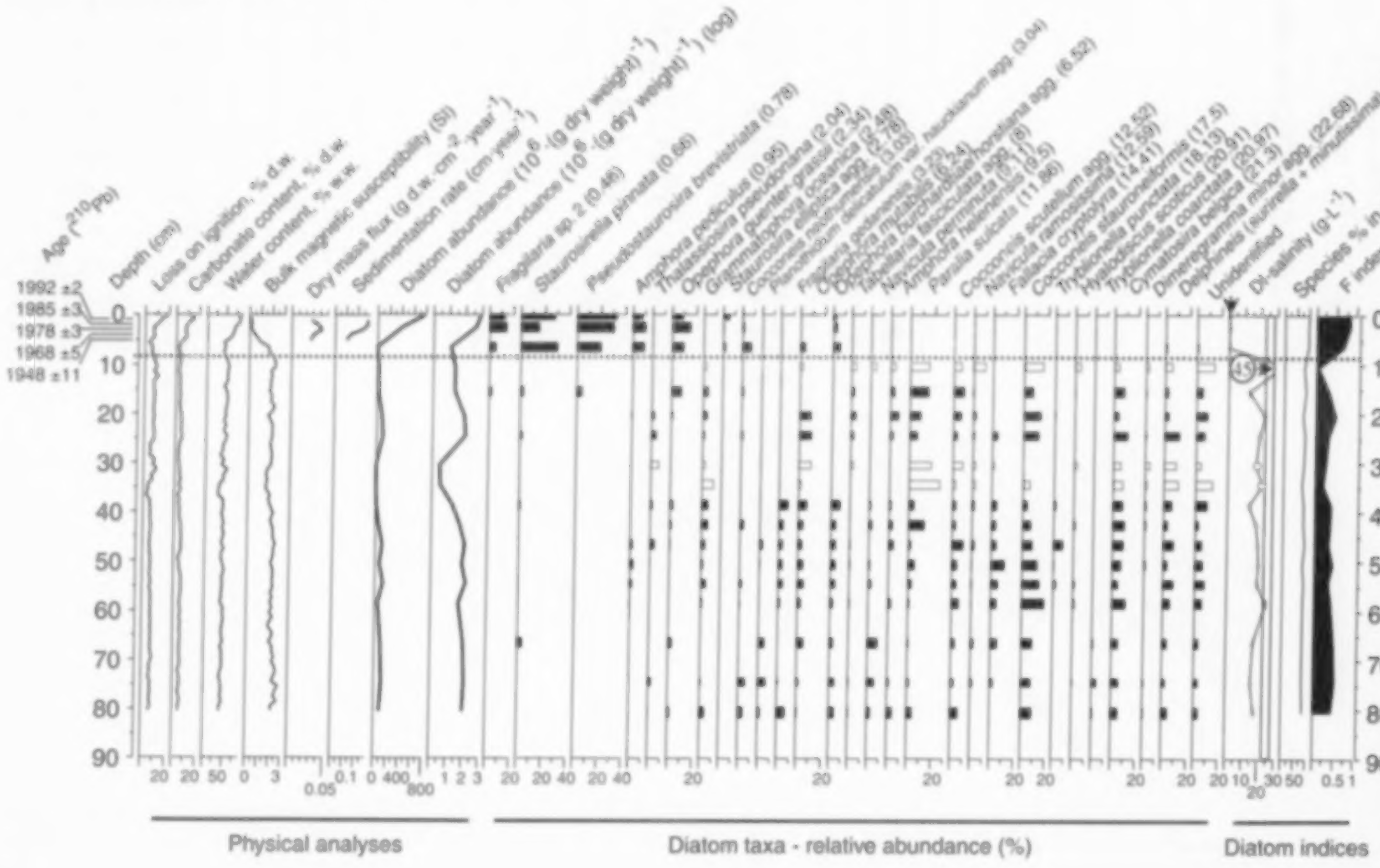

2000), particularly when commonly 60%–80% or more variation in contemporary biological data sets remains statistically unexplained (e.g., Zong and Horton 1999; Muylaert et al. 2000; this study). Part of the problem undoubtedly relates to the quality of the measured environmental data on which the models are based and also to potential mismatches between time-smoothed sedimentary assemblages and discrete, point measurements of the environment. Single water samples (defining the water chemistry for 11 lakes in this study) will fail to integrate temporally the chemical conditions that affect diatom growth, and this has likely contributed to the large amount of unexplained variation in the present data set.

Salinity was found to explain over 10% of species variance within the lake–fjord data set, and of the variables included, salinity accounted for the greatest unique fraction (6%). Studies on estuarine planktonic (Muylaert et al. 2000) and periphytic diatom communities (Juggins 1992; Underwood et al. 1998) and from epilithic habitats in the northern Baltic (Bothnian Bay; Busse and Snoeijs 2002) have demonstrated the importance of salinity in determining diatom distributions. While this is expected given the observed salinity gradient from fresh to fully marine within a freshwater tidal estuary (e.g., within the Schelde, Belgium, where salinity accounted for 18.9% of diatom variance; Muylaert et al. 2000), salinity was important in the northern Baltic where the range was 0.4–3.3 g·L^{-1} (Busse and Snoeijs 2002). Similarly in lakes across large salinity (conductivity) gradients, species assemblages in surface sediments are dominated by salinity (e.g., Fritz 1990; Gasse et al. 1995; Reed 1998*b*), but strong responses have also been demonstrated at low salinity across much smaller gradients similar to that found in the Bothnian Bay (e.g., in West Greenland, Ryves et al. 2002). Approaching marine conditions, Underwood et al. (1998) also demonstrated that algal communities responded to salinity along a saltmarsh creek within the range of 22.5–33 g·L^{-1}, although this co-varied with a nutrient gradient, whereas Jiang (1996) found that sedimentary diatom assemblages varied over a salinity range of 14–35 g·L^{-1} in the shallow Danish coastal waters of the Skagerrak and Kattegat. The physiological stress resulting from changes in osmotic pressure appears sufficient to cause total species turnover several times across a series of thresholds, although as earlier halobian classifications recognised (e.g., van der Werff and Huls 1976), this sensitivity is nonlinear across the salinity gradient, with small differences at the freshwater–brackish part as important as larger changes at higher salinities. Diatoms exhibit similar nonlinear responses to other environmental gradients, e.g., phosphorus (Bennion et al. 1996) and pH (Birks et al. 1990).

Salinity has also been shown to be a major factor affecting zooplankton and fish communities (Jeppesen et al. 1994, 2002), which may have direct effects on diatom communities via grazing and predation on grazers. Indeed, within the same regional data set of lakes and lagoons analysed here (salinity 0.2–17.4 g·L^{-1}, 36 lakes; S.L. Amsinck, unpublished data), variation in zooplankton assemblages in surface sediments was explained by salinity, TP, and planktivorous fish density. Salinity plays an important structural role at all trophic levels, both directly (physiologically) and indirectly on habitat (affecting macrophyte coverage, which appears to be partly independent of nutrients in brackish lakes; Jeppesen et al. 1994, 1997). Potentially, both top-down (via fish-predation effects on zooplankton) and bottom-up (independent importance of TP) effects also exert significant influence on diatom communities, at least in brackish nonfjord systems. Unfortunately, we do not currently have enough information about these aspects within this data set to permit a proper evaluation here.

Water body type (lake–fjord) is also independently important in explaining variation in the diatom data: Species richness was significantly higher in fjords (n = 9, E(S) = 72) than in lakes (n = 27, E(S) = 40; $p < 0.001$) and showed no correlation to salinity within either group ($r^2 < 0.03$), in contrast with a strong decline in zooplankton richness with salinity within the lakes group (S.L. Amsinck, unpublished data). Unsurprisingly, the difference between the lake and fjord sites is not fully captured by the few variables measured here. As salinity and its dependent factors — such as macrophyte and zooplankton communities that exhibit their greatest change below 7–8 g·L^{-1} (i.e., within the lake group; Jeppesen et al. 1994; S.L. Amsinck, unpublished data) — have been factored out, functional differences due to hydrographic settings may be important. As the tidal range is generally small (<1 m) in the western Baltic, tidal effects (depth fluctuations and diurnal turbidity changes) are unlikely to account for this difference. Salinity varies seasonally in both estuaries and coastal lakes, but over 5 years monitoring, seasonal changes in salinity at sites within the Limfjord were muted, varying by only 0.7–2.1 g·L^{-1}, and at Vejle and Kolding by 2.5–3.7 g·L^{-1} (MOLTEN Project 2003). In contrast, some lakes vary from almost fresh to saline from winter to summer. Stratification patterns and duration, ice cover, and other factors such as differences in silica cycling between lake and fjord sites may also be important. Differences in biological structure between these systems may also be relevant; for example, mussels (*Mytilus* spp.) are present in fjords but not in lakes.

Depth and TP also explained significant fractions of diatom species variance, independently accounting for 3.9% and 3.5%, respectively. The role of depth appears to act through the availability of periphytic and littoral habitats compared with pelagic habitats, perhaps mediated through macrophyte cover, and as although the deepest sites are fjords with the highest salinity, this covariation has been factored out. Muylaert et al. (2000) also found that the ratio of maximum to photic depth explained significant amounts of variation among algal communities along the Schelde estuary, which they related to a turbidity maximum in the freshwater tidal part. In a study of benthic diatoms in the Gulf of Riga, Vilbaste et al. (2000) found depth important, both due to deposition of planktonic valves from the overlying water column and the availability of fine-grained substrates for epipelic taxa. Depth in this case was inversely correlated with exposure to wave action, which affects diatom communities by direct hydraulic stress and by allowing epipelic habitats to replace coarser-grained epipsammic habitats. Substrate type may also affect the abundance and types of macrophytes that can colonize benthic areas, which may be more important than nutrient levels (see above) in brackish systems. Exposure to wave action was also found to structure epilithic diatom communities in the Bothnian Bay within an area of similar salinity (~5 g·L^{-1}; Busse 2002). In the present study, depth may reflect the availability of pelagic habitats, as pelagic species (e.g., *Thalassiosira*, *Cyclotella*, *Chaetoceros* spp.) develop in the deeper lake sites (e.g., Kås Sø and Kilen, both ~4 m deep) across a range of salinities, as well as within the fjords.

TP is known to dominate variation within diatom assemblages in freshwater lakes in modern agricultural landscapes (Bennion et al. 1996) and to affect brackish diatom communities from impacted coasts (Cooper 1995). Despite the 10-fold variation in TP values among sites in the present study (25–331 μg·L^{-1} TP), salinity has an overriding effect on diatom distributions. Neither TN nor TN/TP was found to be important in explaining diatom distributions, which may be attributed to high water column TN/TP ratios above Redfield (N:P = 16:1 on a molar basis, 7.23:1 by weight) for all but two sites (both lakes), indicating N enrichment. Coastal waters in the western Baltic often have high N loads from terrestrial human activity (agricultural runoff, sewage, and industrial effluents), funnelled along freshwater estuaries draining large inland areas and also from other point sources along coasts (e.g., sewage treatment works). While large diatom–environmental data sets of freshwater lakes have not shown major responses to TN, brackish diatoms from large regional Baltic data sets exhibit strong responses to both N (Clarke et al. 2003) and P (MOLTEN Project 2003). Such data sets show promise as a means to infer nutrient concentrations from diatom assemblages in coastal areas.

Diatom–salinity model

Several models for inferring tidal level (e.g., Zong and Horton 1999) and salinity (Juggins 1992; Jiang et al. 1998; Parsons et al. 1999) have been developed from sedimentary diatom assemblages in coastal environments. Tidal fluctuations will often be associated with salinity variations, and within a tidal estuary the dominant response may be to salinity rather than to tidal range per se (Juggins 1992). Parsons et al. (1999) used a salinity index to infer salinity changes over the last 300 years in Louisiana coastal marshes based on an empirical relationship between observed salinity (range 2–23 g·L^{-1}) and proportions of freshwater, estuarine, and marine diatoms in dated horizons from sediment cores. As pointed out by the authors, this technique is sensitive to dating errors and performed less well at the ends of the gradient, especially >20 g·L^{-1} (Parsons et al. 1999).

Surface sediment diatom assemblages from the Skagerrak-Kattegat showed strong response to summer and winter sea-surface salinity (Jiang 1996). From this, WA models were created from a 19-sample training set (salinity range 14–35 g·L^{-1}) and used to reconstruct sea-surface salinity over the Holocene (RMSEP = 2–5 g·L^{-1}; Jiang et al. 1998). Similarly, Juggins (1992) used surface sediment diatom assemblages to infer mean half-tide salinity along the tidal Thames estuary (range ~0.1–24 g·L^{-1}) and found WA-PLS methods improved predictive power (ter Braak and Juggins 1993). The salinity model presented here compares well with these other studies, both in terms of model diagnostics (r^2_{jack} = 0.887, RMSEP = 0.246) and the salinity gradient covered. Coherence in the order of modelled salinity optima of major diatom taxa among these three data sets supports the contention that while these empirical models make great ecological assumptions to simplify real-world complexity, the approach captures the strong underlying and ecologically meaningful response to salinity that studies on living diatom communities have shown.

Although it might be argued that inclusion of shallow fjord sites might weaken the model in terms of its application to wetland areas such as Vejlerne, especially as water body type was itself significant, validation is provided both internally (via jackknifing) and by independent comparison to known historical events (see below). Indeed, a model that includes freshwater and brackish lakes and shallow, marine fjord systems is necessary to provide the range of modern analogues for the variety of conditions that sites in the Vejlerne wetlands (and many other shallow, coastal margins) have experienced in the past. While important differences exist between lakes and fjords, the present study suggests an underlying coherence between these shallow, brackish–marine systems.

Recently, other biological groups have shown potential as quantitative salinity indicators. Morphological variations in several dinoflagellate cyst taxa have been related to changes in salinity (Ellegaard 2000), and a predictive model has been developed for the Baltic cyst *Gonyaulax baltica*, which experiments have shown grows longer cyst processes at lower salinity (Ellegaard et al. 2002). Stratigraphic variations in cyst morphology for three taxa (including *Gonyaulax baltica*) have been observed in fossil samples from a 5.5-m sedimentary sequence from the Limfjord, also taken from Bjørnsholm Bay, and two zones were dominated by cysts with aberrant (reduced) processes (Ellegaard 2000) but appeared to overestimate salinity (J.T. Christensen, M. Ellegaard, T. Cedhagen, and J. Hylleberg, unpublished data). As the diatom and historical evidence suggests (see below), salinity may not have been stable within zones, and sample-specific salinity estimates may provide more realistic estimates.

Diatom dissolution

Diatom dissolution is strongly correlated with (log) inferred salinity within the three Vejlerne cores (r^2 = 0.33–0.74, p < 0.025 in all cases) and for all core samples together (r^2 = 0.56, n = 61, p < 0.001), although this might be expected, as dissolution increases with salinity in the lake training set (r^2 = 0.41, n = 27, p < 0.001). Poor diatom preservation has been linked to periods of changing hydrography and salinity during Holocene sequences from the Baltic (e.g., during the Litorina – post-Litorina Sea stage; Andrén et al. 2000) and to increases in salinity (conductivity) in some lake records (e.g., Ryves et al. 2001). Decreasing diatom preservation with increasing salinity has also been observed in other diatom training sets (e.g., Reed 1998*a*; Ryves et al. 2002). Although experimental studies suggest silica dissolution rates increase with increasing NaCl concentration beyond the salinity of seawater (Barker et al. 1994), preservation differences between marine Limfjord and freshwater Vejlerne sedimentary units may owe much to differences in silica cycling between freshwater and marine systems. Silica dissolution in marine systems may be promoted by physico-chemical conditions of higher pH, greater turbulence, and water movement, and Si cycling may alter under eutrophication. Rates of bacterial degradation of organic coatings protecting diatom walls may differ, and more effective bioturbation of upper sediments by marine macrofauna may enhance release of dissolved pore water silica back into the water column.

Dissolution does appear to be an important control on diatom concentration at both Han Vejle and Lund Fjord individually (see previous sections) and combined ($r^2 = 0.36$, $n = 39$, $p < 0.001$). Dissolution thus appears an important taphonomic process affecting the interpretation of diatom accumulation rates as a record of productivity, as has been found in estuarine systems elsewhere (DeMaster 1981, 2002). Differential dissolution of valves biases assemblages towards more robust forms (Ryves et al. 2001), and since many littoral brackish and marine forms are more heavily silicified than littoral freshwater taxa, or contain elements that are easily identifiable even when badly corroded, DI salinity may be overestimated in some assemblages. A dissolution index can thus be a guide to the reliability of qualitative and quantitative inferences made from fossil assemblages.

Recent environmental history of the Limfjord: pre-1880

Documentary and palaeoecological evidence has shown that salinity in the Limfjord has undergone major and dramatic shifts according to the opening or closing of the western end (and in Viking times, perhaps the northern margin) to the North Sea. Based on known salinity ranges of foraminifera, ostracods, molluscs, and other fauna and flora, major trends in salinity have been reconstructed from sediment cores in Bjørnsholm Bay, in the Limfjord south of Vejlerne, over the last 2000 years (Fig. 1; Kristensen et al. 1995) and before (J.T. Christensen, M. Ellegaard, T. Cedhagen, and J. Hylleberg, unpublished data). While these autecological approaches provide a basic framework of salinity and ecosystem-scale change within the Limfjord, the salinity estimates themselves are semiquantitative with wide uncertainty and may not be sensitive to short-term fluctuations. Temporal resolution is reduced by the need for large sample sizes, while the collection of several parallel cores brings with it problems of core correlation, macrofossil patchiness, and site-specific sedimentation rate. A documented low-salinity period, measured at ~8 g·L^{-1} in 1811 by Mr. Jacobsen, a local chemist (Kristensen et al. 1995), began around 1220 and lasted until 1825, when the North Sea broke through the western end of the Limfjord during a storm, a connection that is artificially maintained today. Palaeoecological evidence suggests that the Limfjord has experienced near-marine conditions since then (Kristensen et al. 1995). Presently, salinity within the Limfjord varies from 23–26 g·L^{-1} in the central–east to 31 g·L^{-1} in the west (MOLTEN Project 2003).

Salinity in the Limfjord is known to have varied within this brackish phase (circa 1220–1825). Severe storms caused marine breakthroughs in this period, which lasted for a decade or more, particularly in the late 16th and early 17th centuries (Kristensen et al. 1995), perhaps linked to the deterioration in climate of the Little Ice Age (Andrén et al. 2000). While such major events have been preserved in the sedimentary macrofaunal record, shorter-term changes may leave little trace if there is insufficient time for a new faunal community to develop, especially if dependent on the availability of suitable habitat. Less complex organisms, such as algae and dinoflagellates, will generally respond rapidly, particularly pelagic forms. Diatom stratigraphies can potentially provide sensitive palaeoenvironmental reconstructions at high temporal resolution to test such hypotheses.

Both diatom records that extend significantly into the Limfjord phase of Vejlerne (Glombak and Lund Fjord) show variations in diatom composition and inferred salinity. Diatom assemblages are dominated by littoral taxa indicative of shallow water, principally *Planothidium delicatulum* spp., *Amphora* spp., *Cocconeis* spp., *Cymatosira belgica*, *Delphineis* spp. *Opephora* spp., and benthic *Navicula* and *Fallacia* spp., with stratigraphic change more pronounced at Glombak leading to a distinct trend in DI salinity. *Paralia sulcata*, found in both records and common in coastal sediments across a range of salinity, is found in both plankton and benthic habitats (Zong 1997). While its ecology is poorly known, within the Vejlerne training set ($n = 20$ occurrences) it exhibited unimodal distributions with well-defined optima for depth (3.5 m), TP (63 µg·L^{-1}), and salinity (11.9 g·L^{-1}), although both salinity and depth showed broad tolerances. While *Paralia sulcata* has been seen as an indicator of high productivity (especially when small cell sizes dominate; McQuoid and Nordberg 2003), in sediment cores from the southwestern Baltic, *Paralia sulcata* declines as *Cyclotella choctawhatcheeana* (indicating nutrient enrichment; see below) increases (Andrén et al. 1999). Similarly, in cores from the mesohaline Chesapeake Bay along the eastern seaboard of the USA, *Paralia sulcata* is abundant prior to anthropogenic disturbance (Cooper 1995). McQuoid and Nordberg (2003) found that the relative abundance of *Paralia sulcata* among surface sediments from the Swedish west coast was positively correlated with degree of mixing of the water column and, contrary to expectation, negatively with nitrogen concentration (as both total N and NO_3). Within a similar salinity and depth regime, nutrient enrichment may favour other taxa that are better competitors at lower Si:P (or Si:N) ratios (cf. McQuoid and Nordberg 2003), while increased organic sedimentation may reduce the area of suitable sandy substrates. *Paralia sulcata* valves are generally robust and identifiable even when badly corroded, which may also favour its (over)representation in marine sediments.

Direct comparison of the stratigraphies within the marine period is hampered by a lack of dating, especially as the Lund Fjord record contains a hiatus before the 1940s of unknown duration. The lack of unsupported ^{210}Pb below the organic upper layer in these sites and from another nearby sequence from another lake within Vejlerne (Selbjerg Sø), however, implies that all these sections must predate circa 1880, approximately when Vejlerne was separated from the Limfjord. A dam was first built across the Løgstør Bredning in 1866–1868, and pumping out of salt water from the enclosed area began soon after. Experimental grass planting began on land below what is now Lund Fjord in 1871, and by 1873, ~830 ha were under grass cover (Jakobsen and Sørensen 1998). In January 1874, the main dam failed during a storm, and salt water flooded the area. Vejlerne was abandoned for 2 years until a new dam was built in 1874–1876 and draining began again. Despite minor incursions of salt water later, for example in 1880, pumping allowed grass planting in the north (Lund Fjord) and eastern parts, although the results were poor. Finally soon after 1912, attempts to drain east Vejlerne were abandoned, after which

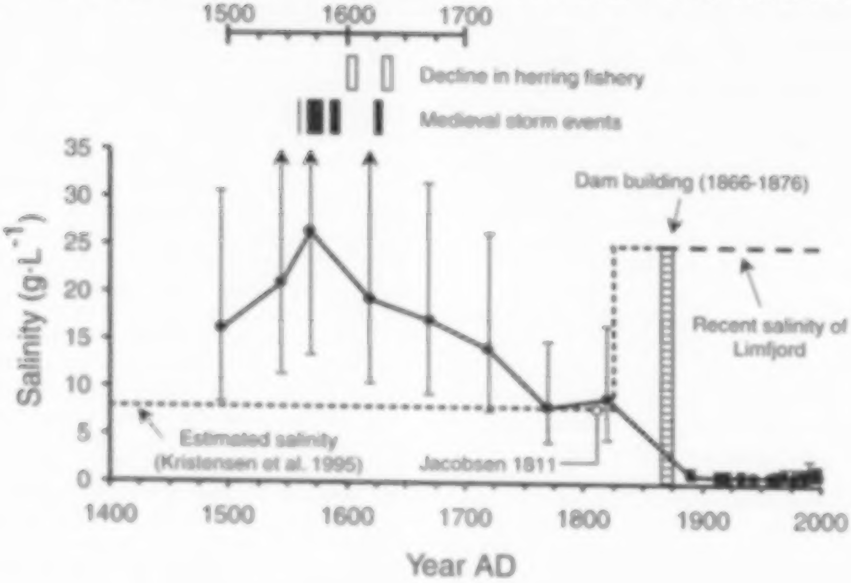

Fig. 7. Diatom-inferred salinity (solid line) for Glombak core, GLOM I, plotted against age (assuming a net sedimentation rate of 0.08 cm·year^{-1}), with sample-specific errors based on 9999 permutations within weighted-average partial least squares (WA-PLS). Values above 35 g·L^{-1} are shown as up arrows. Also shown are documented periods when the western barrier to the North Sea was open in the 16th–17th centuries following storms (solid bars) and periods when the Limfjord herring fishery was in decline (open bars; from Holm and Bager 2002). Estimated salinity fluctuations of the inner Limfjord based on macrofossil evidence (Kristensen et al. 1995) are shown (dotted line), as well as the period of dam construction across the Løgstør Bredning, which created the east Vejlerne wetland. A historical salinity measurement made in 1811 in the inner Limfjord is also plotted (cited in Kristensen et al. 1995).

water levels rose throughout the area. Further disruption occurred when a railway line was built across the southern part of Lund Fjord in 1906, which permanently separated Han Vejle from Lund Fjord (Hald-Mortensen 1998). These historical events may explain why the Lund Fjord and Han Vejle sediment records are disturbed and may both contain hiatuses from before the dam building until well into the 20th century. In contrast, maps from 1883 and throughout the 20th century show that both Glombak and Selbjerg have existed as lakes since the earliest dams were built (Hald-Mortensen 1998; Jakobsen and Sorensen 1998). It is likely that sediment has accumulated more or less continuously at these sites since separation from the Limfjord in the late 19th century, as ^{210}Pb data suggest.

Independent dating controls (e.g., ^{14}C) on the marine sections in Lund Fjord and Glombak cores are not available. A ~2-m sediment sequence, collected further south within the Limfjord at Bjørnsholm Bay from a depth of 10 m, was dated by ^{14}C analyses on foraminifera and molluscs using a constant 400-year reservoir (Kristensen et al. 1995). A linear age–depth model fitted 10 of the 16 dates (within errors), with average net sedimentation rates of ~0.08 cm·year^{-1} throughout the last 2500 years. Using this figure for the Vejlerne cores suggests that the marine section in GLOM I spans ~375 years (30 cm) and LUND I, ~925 years (74 cm). Given the likelihood of extensive stratigraphic disturbance at Lund Fjord and observed poor sample preservation at several levels, it seems unwise to attempt to match the DI salinity in LUND I with that of Kristensen et al. (1995). This comparison may be justified at Glombak, however, if it is accepted that sedimentation has been continuous throughout the sequence (see above). We show DI salinity at Glombak over the last 500 years compared with that in the Limfjord estimated by Kristensen et al. (1995), assuming a net sedimentation rate of 0.08 cm·year^{-1} below 52.5 cm in GLOM I (Fig. 7, ~AD 1870 from ^{210}Pb data).

Kristensen et al. (1995) used biostratigraphical zones (based on foraminifera, ostracods, molluscs, and other aquatic macrofossils) to define high and low salinity phases in the last 2500 years, with salinity estimated semiquantitatively using autecological information from several species. Although they noted biological assemblages vary within these zones, monotonic salinity estimates were applied within zones. From 1220 until 1825, they inferred generally low salinity (brackish) conditions of around 8 g·L^{-1} (Kristensen et al. 1995). Several storms are known to have breached the opening to the North Sea in the west of the Limfjord during this period, however, especially during the mediaeval period, with four separate events from 1560 to 1624, lasting up to 12–14 years (Kristensen et al. 1995), coinciding with the level at which the large pebble was found (72 cm, ~1620). While macrofossil assemblages at these times imply higher salinity excursions (Kristensen et al. 1995; J.T. Christensen, M. Ellegaard, T. Cedhagen, and J. Hylleberg, unpublished data), the DI salinity profile suggests that since the storm breakthroughs of the 16th century, the Limfjord might only have been <10 g·L^{-1} for short periods (Fig. 7).

Rather than being a stable, brackish period in the Limfjord, this phase may have been characterized by wide fluctuations in salinity, with aperiodic marine incursions having major ecological impacts. The Limfjord has supported a herring fishery as early as 1200 (Holm and Bager 2002), relying on the lower salinity waters as a feeding ground before spawning in the higher salinity Kattegat. Historical records from the Limfjord brackish herring fishery from the 16th to early 19th century seem to reflect large, long-term fluctuations in herring stocks rather than changes in economic conditions (Holm and Bager 2002). The herring fishery was depressed in the early 1600s (perhaps in response to the series of breakthroughs in the late 1500s), peaked from 1610 to 1620, and was poor when records continued in 1630, when the westerly opening to the North Sea closed, but thereafter improved. Similarly, the fishery collapsed within a decade of the 1825 breach and did not recover. The DI salinity profile agrees with the known storm history of the Limfjord, the trends in the herring fishery in the late 16th to 17th century, and the measured salinity in 1811, giving confidence in the salinity model and the dating assumptions used in this section of the core (Fig. 7).

Plant and animal macrofossil analyses of a replicate but undated core to GLOM I show a similar trend in increasing salinity below the marine–freshwater transition (Jeppesen et al. 2002). The lowermost sediments contain a near-marine assemblage, including the foraminifer *Ammonia beccarii*, the mussel *Mytilus edulis*, and the marine polychaete *Nereis* sp. This is replaced by a brackish assemblage, including eelgrass (*Zostera* sp.), charophyte algae (*Tolypella* sp.), horned pondweed (*Zannichellia major*), and fennel-leaf pondweed (*Potamogeton pectinatus*), together suggesting a salinity of 12–15 g·L^{-1} (Jeppesen et al. 2002), close to that estimated by the diatom model below the freshwater transition (Fig. 7).

In GLOM I, no samples were analysed in the period between 1825, when present-day salinity (~26 g·L^{-1}) was established, and before the dam building was completed in 1876, when Glombak developed as a freshwater–subsaline lake. It is perhaps possible that the extreme (and overestimated) salinity (45 g·L^{-1}) inferred at Lund Fjord at 10.5 cm represents this high salinity period from 1825 to 1876 (Fig. 7), but given the very poor sample preservation (F = 0.08) and uncertain sedimentation at this site, this remains speculative.

Development of the east Vejlerne wetland and Limfjord: post-1880

Postdamming development of the east Vejlerne area followed that of many shallow Danish freshwater lakes in the 20th century, dominated by periphytic *Fragilaria* sensu lato (e.g., *Pseudostaurosira brevistriata*, *Staurosirella pinnata*) typical of mesotrophic conditions (10–100 μg·L^{-1} TP; Bradshaw et al. 2002). Forms found in slightly elevated salinities are more common (e.g., *Fragilaria sopotensis/Staurosira punctiformis* agg. and *Staurosira elliptica* agg.), and rare mesohaline (e.g., *Cocconeis neothumensis*, *Opephora* spp., or *Planothidium delicatulum* spp.) or polyhaline taxa (e.g., *Navicula cryptotenella* in Han Vejle) attest to continuing saline influences, from direct connection to the Limfjord, storms in the North Sea to the north, or salts leaching out from the marine sediments underlying Vejlerne. Throughout the preserved freshwater record, zooplankton and macrofossil evidence show that Han Vejle has been clear and macrophyte-dominated since at least the 1940s, while Glombak is comparatively macrophyte-poor and more turbid, reflecting a higher TP and salinity (Amsinck et al. 2003). Freshwater Lund Fjord, with a much larger agricultural catchment, is a turbid system with higher levels of TP (~154 μg·L^{-1}) and TN and the lowest macrophyte coverage (Jeppesen et al. 2002). Despite these divergent functional pathways in the 20th century, diatom assemblages seem to reflect local hydrology and perhaps nutrient conditions rather than macrophyte development directly, although the greater importance of littoral–benthic taxa to planktonic taxa in Han Vejle may reflect its lower turbidity.

Changes in the influence of the Limfjord on east Vejlerne are most clearly reflected in the diatom record from Glombak, nearest the Limfjord and directly connected via a drainage canal. At around 22 cm (~1963), there is a marked increase in the mesohaline planktonic *Cyclotella choctawhatcheeana*, coincident with the oligohaline periphytic *Achnanthes fogedii*. *Cyclotella choctawhatcheeana* is common in coastal waters in the Baltic (Snoeijs 1993) and in Chesapeake Bay (as *Cyclotella* cf. *Caspia*, *Cyclotella* cf. *caspia*, Cooper 1995). It has been found to dominate sediment records in the southwestern and central Baltic since the early 20th century (Andrén et al. 1999, 2000), although in Roskilde Fjord it was important in sediments dating pre-1860 (Clarke et al. 2003) and is found sporadically in the marine sections of both Glombak and Lund Fjord cores. In Baltic records *Cyclotella choctawhatcheeana* is linked to increasing nutrient concentrations (Andrén et al. 1999, 2000), while in Chesapeake Bay sediments, it is thought to be an indicator of human disturbance (Cooper 1995). Within the present training set, *Cyclotella choctawhatcheeana* seems to be an indicator of high TP rather than TN (TP optimum 150 μg TP·L^{-1}, n = 22). This is in contrast to its distribution within a larger Baltic–Netherlands surface sediment data set, however, where *Cyclotella choctawhatcheeana* shows its highest abundance in Swedish and Finnish data sets, with relatively low TP and TN optima in both (MOLTEN Project 2003).

The timing of the major appearance of this taxon in the Glombak record agrees with the construction of a new central sluice controlling water outflow from east Vejlerne to the Limfjord, built from 1963 to 1965. This resulted in a 10–15 cm lowering of water level and an increased risk of intrusion of saline Limfjord water (Hald-Mortensen 1998). *Cyclotella choctawhatcheeana* is found in surface sediments from the Limfjord, Mariager Fjord, and other Danish fjords (Clarke 2001; MOLTEN Project 2003). If the dating of the Glombak Limfjord sequence is accepted (Fig. 7), the major increase must postdate 1825, as seen elsewhere in the Baltic (Andrén et al. 1999, 2000). In the Limfjord, its rise is likely to be linked to increasing anthropogenic coastal eutrophication rather than salinity changes, as it has a broad salinity tolerance from subsaline to almost marine conditions, with an optimum of 9.7 g·L^{-1} (this study; MOLTEN Project 2003). A diatom-inferred TN record from Roskilde Fjord on Zealand, Denmark, shows that TN concentrations began to rise ~1900 and accelerated in the postwar period coincident with major increases in the use of artificial fertilizers (Clarke et al. 2003).

Diatom analysis may be a more effective tool for reconstructing salinity in rapidly changing environments, as diatoms respond quickly to changes in salinity, whereas higher organisms need time to establish populations seeded from elsewhere and may be more dependent on habitat constraints.

Oysters (*Ostrea edulis*), for example, were not recorded in the Limfjord until 1849, some 24 years after high salinity conditions returned (Bailey and Milner, in press). Furthermore, as smaller sediment samples are needed, stratigraphic profiles can be analysed at high temporal resolution, and salinity for each assemblage can be quantitatively reconstructed, with sample-specific error estimates. Diatom–salinity models may be very useful tools in studies of coastal and estuarine areas where knowledge of past salinity regimes can test hypotheses about aquatic ecosystem development (Holm and Bager 2002; MacKenzie et al. 2002) and can shed light on cultural, hydrographic, and climatic transitions affecting aquatic resources.

Acknowledgements

We thank Beth Stavngaard and Suzanne McGowan for laboratory work and diatom slide preparation, the MOLTEN group for discussion and support, and the A.V. Jensen Fund for providing financial support and logistical help during fieldwork. EJ and FL were also supported by the CONWOY project (Consequences of Weather and Climate Changes for Marine and Freshwater Ecosystems; www.conwoy.ku.dk). We are grateful to Kaarina Weckström and an anonymous referee for their helpful reviews of the manuscript.

References

Amsinck, S.L., Jeppesen, E., and Ryves, D. 2003. Cladoceran stratigraphy in two shallow brackish lakes with special reference to changes in salinity, macrophyte abundance and fish predation. J. Paleolim. **29**: 495–507.

Andrén, E., Shimmield, G., and Brand, T. 1999. Environmental changes of the last three centuries indicated by siliceous microfossil records from the southwestern Baltic Sea. Holocene, **9**: 25–38.

Andrén, E., Andrén, T., and Kunzendorf, H. 2000. Holocene history of the Baltic Sea as a background for assessing records of human impact in the sediments of the Gotland Basin. Holocene, **10**: 687–702.

American Public Health Association (APHA). 1985. Standard methods for the examination of water and waste water. 16th edition. American Public Health Association, New York.

Appleby, P.G., and Oldfield, F. 1978. The calculation of ^{210}Pb dates assuming a constant rate of supply of unsupported ^{210}Pb to the sediment. Catena, **5**: 1–8.

Appleby, P.G., Nolan, P.J., Gifford, D.W., Godfrey, M.J., Oldfield, F., Anderson, N.J., and Battarbee, R.W. 1986. ^{210}Pb dating by low background gamma counting. Hydrobiologia, **141**: 21–27.

Bailey, G., and Milner, N. The marine molluscs from the Mesolithic and Neolithic deposits of the Norsminde shell midden. *In* The Norsminde "Køkkenmødding" — Archaeology and Environment. Vol. 2. *Edited by* S.H. Andersen. Århus University, Århus, Denmark. In press.

Barker, P., Fontes, J.-C., Gasse, F., and Druart, J.-C. 1994. Experimental dissolution of diatom silica in concentrated salt solutions and implications for paleoenvironmental reconstruction. Limnol. Oceanogr. **39**: 99–110.

Bennion, H., Juggins, S., and Anderson, N.J. 1996. Predicting epilimnetic phosphorous concentrations using an improved diatom-based transfer function and its application to lake eutrophication management. Environ. Sci. Tech. **30**: 2004–2007.

Bianchi, T.S., Engelhaupt, E., Westman, P., Andrén, T., Rolff, C., and Elmgren, R. 2000. Cyanobacterial blooms in the Baltic Sea: natural or human-induced? Limnol. Oceanogr. **45**: 716–726.

Birks, H.J.B. 1995. Quantitative palaeoenvironmental reconstructions. In Statistical Modelling of Quaternary Science Data, Technical Guide 5. *Edited by* D. Maddy and J.S. Brew. Quaternary Research Association, Cambridge. pp. 161–254.

Birks, H.J.B. 1998. D.G. Frey & E.S. Deevey Review #1: Numerical tools in palaeolimnology — progress, potentialities, and problems. J. Paleolim. **20**: 307–332.

Birks, H.J.B., and Line, J.M. 1992. The use of rarefaction analysis for estimating palynological richness from Quaternary pollen-analytical data. Holocene, **2**: 1–10.

Birks, H.J.B., Line, J.M., Juggins, S., Stevenson, A.C., and ter Braak, C.J.F. 1990. Diatoms and pH reconstruction. Philos. Trans. R. Soc. Lond. B Biol. Sci. **327**: 263–278.

Bradshaw, E.G., Anderson, N.J., Jensen, J.P., and Jeppesen, E. 2002. Phosphorous dynamics in Danish lakes and the implications for diatom ecology and palaeoecology. Freshw. Biol. **47**: 1963–1975.

Busse, S. 2002. Benthic diatoms in the Gulf of Bothnia: community analysis and diversity. Ph.D. thesis, Department of Plant Ecology, University of Uppsala.

Busse, S., and Snoeijs, P. 2002. Gradient responses of diatom communities in the Bothnian Bay, northern Baltic Sea. Nova Hedwigia, **74**: 501–525.

Clarke, A.L. 2001. A diatom-based transfer function to infer historical changes in total nitrogen concentration from coastal sediments: a case study from Roskilde Fjord, Denmark. Ph.D. thesis, Department of Geography, University of Newcastle.

Clarke, A.L., Juggins, S., and Conley, D.J. 2003. A 150-year reconstruction of the history of coastal eutrophication in Roskilde Fjord, Denmark. Mar. Poll. Bull. **46**: 1615–1618.

Conley, D.J., Markager, S., Andersen, J., Ellermann, T., and Svensen, L.M. 2002. Coastal eutrophication and the Danish National Aquatic Monitoring and Assessment Program. Estuaries, **25**: 848–861.

Cooper, S.R. 1995. Chesapeake Bay watershed historical land use: impacts on water quality and diatom communities. Ecol. Appl. **5**: 703–723.

Cooper, S.R., and Brush, G.S. 1991. Long-term history of Chesapeake Bay anoxia. Science, **254**: 992–996.

Dean, W.E., Jr. 1974. Determination of carbonate and organic matter in calcareous sediments and sedimentary rocks by loss-on-ignition: comparison with other methods. J. Sed. Petrol. **44**: 242–248.

Dellwig, O., Gramberg, D., Vetter, D., Watermann, F., Barckhausen, J., Brumsack, H.-J., Gerdes, G., Liebezeit, G., Rullkötter, J., Scholz-Böttcher, B.M., and Streif, H. 1998. Geochemical and microfacies characterization of a Holocene depositional sequence in northwest Germany. Org. Geochem. **29**: 1687–1699.

Dellwig, O., Watermann, F., Brumsack, H.-J., and Gerdes, G. 1999. High-resolution reconstruction of a Holocene coastal sequence (NW Germany) using inorganic geochemical data and diatom inventories. Estuar. Coast. Shelf Sci. **48**: 617–633.

DeMaster, D.J. 1981. The supply and accumulation of silica in the marine-environment. Geochim. Cosmochim. Acta, **45**: 1715–1732.

DeMaster, D.J. 2002. The accumulation and cycling of biogenic silica in the Southern Ocean: revisiting the marine silica budget. Deep-Sea Res. (2 Top. Stud. Oceanogr.), **49**: 3155–3167.

Ellegaard, M. 2000. Variations in dinoflagellate cyst morphology under conditions of changing salinity during the last 2000 years in the Limfjord, Denmark. Rev. Paleobot. Palynol. **109**: 65–81.

Ellegaard, M., Lewis, J., and Harding, I. 2002. Cyst-theca relationship, life cycle, and effects of temperature and salinity on the cyst morphology of *Gonyaulax baltica* sp. nov. (Dinophyceae) from the Baltic Sea area. J. Phycol. **38**: 775–789.

Fritz, S.C. 1990. Twentieth-century salinity and water-level fluctuations in Devil's Lake, North Dakota: test of a diatom-based transfer function. Limnol. Oceanogr. **35**: 1771–1781.

Gasse, F., Juggins, S., and Khelifa, L.B. 1995. Diatom-based transfer functions for inferring past hydrochemical characteristics of African lakes. Palaeogeogr. Palaeoclim. Palaeoecol. **117**: 31–54.

Hald-Mortensen, P. 1998. Vejlernes natur — status over reservatets mangfoldighed. A.V. Jensen's Fonde, Thisted, Denmark.

Holm, P., and Bager, M. 2002: The Danish fisheries *c.*1450–1800: medieval and early modern sources and their potential for marine environmental history. *In* Exploited seas: directions for marine environmental history. *Edited by* P. Holm and T. Smith. International Maritime History Association, St. John's, Newfoundland. pp. 97–122.

Jakobsen, I., and Sørensen, S. 1998. Vejlerne, folk og natur i fortid og nutid. A.V. Jensen's Fonde, Thisted, Denmark.

Jeppesen, E., Søndergaard, M., Kanstrup, E., Petersen, B., Eriksen, R.B., Hammershøj, M., Mortensen, E., Jensen, J.P., and Have, A. 1994. Does the impact of nutrients on the biological structure and function of brackish and freshwater lakes differ? Hydrobiologia, **275/276**: 15–30.

Jeppesen, E., Søndergaard, M., Jensen, J.P., Kanstrup, E., and Petersen, B. 1997: Macrophytes and turbidity in brackish lakes with special emphasis on the role of top-down control. *In* The structuring role of submerged macrophytes in lakes. *Edited by* E. Jeppesen, M. Søndergaard, M. Søndergaard, and K. Christoffersen. Springer-Verlag, New York. pp. 369–377.

Jeppesen, E., Søndergaard, M., Amsinck, S., Jensen, J.P., Lauridsen, T.L., Pedersen, L.K., Landkildehus, F., Nielsen, K., Ryves, D., Bennike, O., Krog, G., Christensen, I., and Schriver, P. 2002. Søerne i De Østlige Vejler. National Environmental Research Institute (Silkeborg) Tech. Rep. No. 394.

Jiang, H. 1996. Diatoms from the surface sediments of the Skagerrak and the Kattegat and their relationship to the spatial changes of environmental variables. J. Biogeogr. **23**: 129–137.

Jiang, H., Björck, S., and Svensson, N.-O. 1998. Reconstruction of Holocene sea-surface salinity in the Skagerrak-Kattegat: a climatic and environmental record of Scandinavia. J. Quat. Sci. **13**: 107–114.

Juggins, S. 1992. Diatoms in the Thames Estuary, England: ecology, palaeoecology, and salinity transfer function. (H. Lange-Bertalot). J. Cramer, Stuttgart.

Juggins, S., and ter Braak, C.J.F. 1997. CALIBRATE — A Computer Program for Species–Environmental Calibration by [Weighted-Averaging] Partial Least Squares Regression (0.81). University of Newcastle, UK.

Kingston, J.C., Birks, H.J.B., Uutala, A.J., Cumming, B.F., and Smol, J.P. 1992. Assessing trends in fishery resources and lake water aluminum from paleolimnological analyses of siliceous algae. Can. J. Fish. Aquat. Sci. **49**: 116–127.

Koroleff, F. 1970. Determination of total phosphorus in natural water by means of persulphate oxidation. An. Interlab. Rep. No. 3, Cons. Int. Explor. Mer.

Krammer, K., and Lange-Bertalot, H. 1986–1991. Bacillariophyceae. *In* Süsswasserflora von Mitteleuropa Band 2/1–2/3. *Edited by* H. Ettl, J. Gerloff, H. Heynig, and D. Mollenhauer. Gustav Fisher Verlag, Stuttgart & Jena.

Kristensen, P., Heier-Nielsen, S., and Hylleberg, J. 1995. Late-Holocene salinity fluctuations in Bjørnsholm Bay, Limfjorden, Denmark, as deduced from micro- and macrofossil analysis. Holocene, **5**: 313–322.

Lapointe, M. 2000. Modern diatom assemblages in surface sediments from the Maritime Estuary and the Gulf of St. Lawrence, Québec (Canada). Mar. Micropal. **40**: 43–65.

MacKenzie, B.R., Alheit, J., Conley, D.J., Holm, P., and Kinze, C.C. 2002. Ecological hypotheses for a historical reconstruction of upper trophic level biomass in the Baltic Sea and Skagerrak. Can. J. Fish. Aquat. Sci. **59**: 173–190.

McQuoid, M.R., and Nordberg, K. 2003. The diatom *Paralia sulcata* as an environmental indicator species in coastal sediments. Estuar. Coast. Shelf Sci. **56**: 339–354.

MOLTEN Project 2003. MOnitoring Long-term Trends in Eutrophication and Nutrients in the coastal zone. Available from http://craticula.ncl.ac.uk/Molten/jsp/index.jsp [accessed 10 March 2004; updated 9 November 2004].

Murphy, J., and Riley, J.R. 1972. A modified single solution method for the determination of phosphate in natural waters. Anal. Chem. Acta, **27**: 21–26.

Muylaert, K., Sabbe, K., and Vyverman, W. 2000. Spatial and temporal dynamics of phytoplankton communities in a freshwater tidal estuary (Schelde, Belgium). Estuar. Coast. Shelf Sci. **50**: 673–687.

Parsons, M.L., Dortch, Q., Turner, R.E., and Rabalais, N.N. 1999. Salinity history of coastal marshes reconstructed from diatom remains. Estuaries, **22**: 1078–1089.

Reed, J.M. 1998*a*. Diatom preservation in the recent sediment record of Spanish saline lakes: implications for palaeoclimate study. J. Paleolim. **19**: 129–137.

Reed, J.M. 1998*b*. A diatom-conductivity transfer function for Spanish salt lakes. J. Paleolim. **19**: 399–416.

Renberg, I. 1990. A procedure for preparing large sets of diatom slides from sediment cores. J. Paleolim. **4**: 87–90.

Renberg, I. 1991. The HON-Kajak sediment corer. J. Paleolim. **6**: 167–170.

Rowley-Conwy, P. 1984. The laziness of the short-distance hunter: the origins of agriculture in western Denmark. J. Anthropol. Archaeol. **3**: 300–324.

Ryves, D.B., Juggins, S., Fritz, S.C., and Battarbee, R.W. 2001. Experimental diatom dissolution and the quantification of microfossil preservation in sediments. Palaeogeogr. Palaeoclim. Palaeoecol. **172**: 99–113.

Ryves, D.B., McGowan, S., and Anderson, N.J. 2002. Development and evaluation of a diatom-conductivity model from lakes in West Greenland. Freshw. Biol. **47**: 995–1014.

Saros, J.E., and Fritz, S.C. 2002. Resource competition among saline-lake diatoms under varying N:P ratios, salinity, and brine type. Freshw. Biol. **47**: 87–95.

Snoeijs, P. 1993. Intercalibration and distribution of diatom species in the Baltic Sea. Baltic Marine Biologists Publ. 16a. Opulus Press, Uppsala.

Snoeijs, P., and Balashova, N. 1998. Intercalibration and distribution of diatom species in the Baltic Sea. Baltic Marine Biologists Publ. 16e. Opulus Press, Uppsala.

Snoeijs, P., and Kasperovičienė, J. 1996. Intercalibration and distribution of diatom species in the Baltic Sea. Baltic Marine Biologists Publ. 16d. Opulus Press, Uppsala.

Snoeijs, P., and Potapova, M. 1995. Intercalibration and distribution of diatom species in the Baltic Sea. Baltic Marine Biologists Publ. 16c. Opulus Press, Uppsala.

Snoeijs, P., and Vilbaste, S. 1994. Intercalibration and distribution of diatom species in the Baltic Sea. Baltic Marine Biologists Publ. 16b. Opulus Press, Uppsala.

Solórzano, L., and Sharp, J.H. 1980. Determination of total dissolved nitrogen in natural waters. Limnol. Oceanogr. **33**: 702–724.

ter Braak, C.J.F. 1995. Ordination. *In* Data analysis in community and landscape ecology. *Edited by* R.H.G. Jongman, C.J.F. ter Braak and O.F.R. van Tongeren. Cambridge University Press, Cambridge, England. pp. 91–173.

ter Braak, C.J.F., and Juggins, S. 1993. Weighted averaging partial least squares regression (WA-PLS): an improved method for reconstructing environmental variables from species assemblages. Hydrobiologia, **269/270**: 485–502.

ter Braak, C.J.F., and Šmilauer, P. 1998. Canoco for Windows (4.0). Centre for Biometry, Wageningen.

Underwood, G.J.C., Phillips, J., and Saunders, K. 1998. Distribution of estuarine benthic diatom species along salinity and nutrient gradients. Eur. J. Phycol. **33**: 173–183.

van der Werff, A., and Huls, H. (1957–1974) Reprinted 1976. Diatomeënflora van Nederland. Koeltz Science Publishers, Koenigstein.

Vilbaste, S., Sundbäck, K., Nilsson, C., and Truu, J. 2000. Distribution of benthic diatoms in the littoral zone of the Gulf of Riga, the Baltic Sea. Eur. J. Phycol. **35**: 373–385.

Witkowski, A., Lange-Bertalot, H., and Metzeltin, D. 2000. Diatom flora of marine coasts I. (H. Lange-Bertalot). A.R.G. Gantner Verlag K.G., Ruggell.

Zong, Y. 1997. Implications of *Paralia sulcata* abundance in Scottish isolation basins. Diat. Res. **12**: 125–150.

Zong, Y., and Horton, B.P. 1999. Diatom-based tidal-level transfer functions as an aid in reconstructing Quaternary history of sea-level movements in the UK. J. Quat. Sci. **14**: 153–167.

Slow initial decomposition and fungal colonization of pine branches in a nutrient-rich lowland stream

Bernd Spänhoff and Mark O. Gessner

Abstract: Mass loss, fungal colonization, and chemical changes of submerged pine (*Pinus sylvestris*) branches were monitored in a nutrient-rich lowland stream. Branches retrieved from the stream were analyzed for water-soluble substances to assess mass loss by leaching. Concentrations of substances soluble in hot 1% NaOH were determined in order to detect changes in wood-tissue structure indicating microbial degradative activity, and fungal colonization was estimated as ergosterol concentration. Decomposition of the pine branches was slow, with a mean mass loss of 8.3% within 13 months and an overall decay coefficient, *k*, of 0.074·year^{-1}. Concentrations of water-soluble substances in wood decreased from 2.8% to 1.7% after 5 weeks and in bark from 5.6% to 3.8% within 2 weeks. No further losses were noted, nor were significant changes observed in concentrations of substances soluble in hot dilute NaOH. Fungal biomass in bark increased within the first 5 weeks (14–69 µg ergosterol·g^{-1} dry mass) but was invariably low in wood. These results indicate that decomposition of intact fully corticated pine branchwood in streams proceeds very slowly, with little fungal colonization and no notable changes in wood structure occurring after more than a year even when dissolved nutrients in stream water are readily available.

Résumé : Nous avons suivi la perte de masse, la colonisation par les champignons et les changements chimiques dans des branches submergées de pin (*Pinus sylvestris*) dans un cours d'eau riche en nutriments et situé en basse altitude. Nous avons dosé les substances hydrosolubles dans les branches prélevées dans le cours d'eau afin d'évaluer la perte de masse par lessivage. Les concentrations de substances solubles dans le NaOH 1 % chaud permettent de détecter les changements dans le tissu du bois, ce qui reflète l'activité de la dégradation microbienne, et la concentration d'ergostérol permet d'évaluer la colonisation fongique. La décomposition des branches de pin est lente, la perte moyenne de masse étant de 8,3 % après 13 mois et le coefficient global de décomposition (*k*) étant de 0,074·an^{-1}. Les concentrations de substances hydrosolubles diminuent de 2,8 % à 1,7 % dans le bois après 5 semaines et de 5,6 % à 3,8 % dans l'écorce après 2 semaines. Il n'y a pas de pertes supplémentaire, ni de changements significatifs dans les concentrations de substances solubles dans le NaOH chaud et dilué. La biomasse des champignons dans l'écorce augmente durant les 5 premières semaines (14 à 69 µg ergostérol·g^{-1} de masse sèche), mais elle reste toujours basse dans le bois. Nos résultats indiquent que la décomposition de branches de pin intactes et pleinement munies de leur cortex se fait très lentement, qu'il y a peu de colonisation fongique et qu'il ne se produit pas de changement important dans la structure du bois après plus d'un an, malgré la disponibilité de nutriments dissous dans l'eau du cours d'eau.

[Traduit par la Rédaction]

Introduction

Wood is an important element in stream ecosystems draining forested catchments (Harmon et al. 1986; Bilby and Bisson 1998). It influences channel morphology, hydraulic conditions, and retentive capacity of both particulate and dissolved matter (Hilderbrand et al. 1997; Mutz 2000). In addition, woody debris provides habitat for a range of aquatic organisms including fish (e.g., Fausch and Northcote 1992), food for invertebrates (e.g., Pereira et al. 1982; Anderson et al. 1984), and colonizable surfaces and carbon and energy sources for microorganisms (e.g., Aumen et al. 1983; Tank and Webster 1998; Collier et al. 2004). The amounts of wood supplied to stream channels can be sizeable. They may approach inputs received as leaf litter, which is generally considered to be the major carbon and energy source in forested headwater streams (Anderson and Sedell 1979; Webster et al. 1995). Residence times of wood, particularly large logs, tend to be long (Guyette et al. 2002), since physical retention in the stream channel is efficient (Benke and Wallace 1990). As a consequence, average annual stocks of wood in streams lined by natural riparian vegetation can greatly outweigh those of other types of coarse particulate organic matter (Harmon et al. 1986; Webster et al. 1995).

Received 30 October 2003. Accepted 31 May 2004. Published on the NRC Research Press Web site at http://cjfas.nrc.ca on 24 December 2004.
J17804

B. Spänhoff.[1,2] Department of Limnology, Institute for Animal Evolution and Ecology, University of Münster, Germany.
M.O. Gessner. Department of Limnology, Swiss Federal Institute for Environmental Science and Technology (EAWAG), Limnological Research Center, 6047 Kastanienbaum, Switzerland.

---

[1] Corresponding author (e-mail: bernd.spaenhoff@uni-jena.de).

[2] Present address: Research Group for Limnology, Institute of Ecology, Friedrich Schiller University, Jena, Germany.

Can. J. Fish. Aquat. Sci. **61**: 2007–2013 (2004) doi: 10.1139/F04-145

This suggests that wood decomposition is an important process in forest streams in spite of its recalcitrant nature (Bilby and Bisson 1998; Webster et al. 1999; Gessner and van Ryckegem 2003).

In comparison to the abundant data available on the decomposition of leaf litter in streams, the decomposition of wood has received little attention (Spänhoff and Meyer 2004). Furthermore, most information has been derived from experiments with small artificial substrates such as wood veneer strips, ice-cream sticks, dowels, or cubes (e.g., Melillo et al. 1983; Sinsabaugh et al. 1991; Stelzer et al. 2003). These surrogates of woody debris differ from natural branchwood and logs in size and surface structure, notably the absence of bark. A critical factor determining wood-decomposition rates in streams is the surface to volume ratio, because in contrast to marine and terrestrial invertebrates and decomposers, freshwater organisms are considered unable to penetrate wood much beyond the surface and to colonize it pervasively (Aumen et al. 1983; Anderson et al. 1984). Accordingly, decomposition rates of standardized wood pieces have been found to be higher than those of natural branchwood (Diez et al. 2002). Thus, although they are expedient experimental units for testing specific hypotheses (e.g., Melillo et al. 1983; Tank and Webster 1998; Fisher Wold and Hershey 1999), small artificial substrates may not fully reflect the natural decomposition process. Information on the decomposition of natural intact wood pieces, including bark and ranging in size from twigs to branches to large logs, is therefore critically needed to assess the importance of woody debris in organic-matter dynamics in streams.

Fungi are important wood decomposers in terrestrial (e.g., Rayner and Boddy 1988) and marine (Pointing and Hyde 2000) environments, and their central role in leaf decomposition in streams is also well established (Gessner and Chauvet 1994; Suberkropp 1998). Furthermore, woody debris in streams is known to be colonized by a variety of fungi, primarily Ascomycetes (Shearer 1993; Ho et al. 2002) and aquatic and dematiaceous hyphomycetes (Shearer 1992; Gönczöl and Revay 1997; Gessner and van Ryckegem 2003). Many of these cause soft rot (Zare-Maivan and Shearer 1988; Wong et al. 1998; Yuen et al. 1999). Quantitative evidence indicating the involvement of aquatic fungi in wood decomposition is scarce, however, and where available has mainly been obtained by using surrogates of natural woody debris (Golladay and Sinsabaugh 1991; Tank and Webster 1998; Hendel and Marxsen 2000). For example, only a single study has determined fungal-biomass dynamics in submerged decomposing wood sticks with an intact bark (Diez et al. 2002).

As microorganisms start to degrade the structural polymers of wood tissue, particularly cellulose, short-chained carbohydrates are formed as intermediate products. These are soluble in dilute hot alkaline solution (Farmer 1967; Hoffmann and Parameswaran 1982; Zare-Maivan and Shearer 1988). Increases in the concentration of alkali-soluble matter in wood tissue should therefore be indicative of initial microbial degradative activity. This is the rationale underlying a standardized method to detect early wood degradation by measuring the mass loss of wood after treatment with dilute hot NaOH (Technical Association of the Pulp and Paper Industry 1993*a*).

The goal of this study was to determine mass loss and fungal colonization of intact branchwood decomposing in a nutrient-rich lowland stream and to assess whether they were correlated with changes in the concentration of alkali-soluble matter in the wood as a measure of microbial degradative activity. We chose pine wood for this study because it was expected to decompose slowly and because pines are widely distributed worldwide (e.g., Ho et al. 2002; Berg and McClaugherty 2003) and are often planted for timber production, where they replace native vegetation (e.g., Collier et al. 2004). Our results indicate that decomposition of natural pine branches was indeed exceedingly slow, which is consistent with the poor fungal colonization and few structural changes of the wood tissue that we observed.

Material and methods

The study was carried out in a third-order reach of the Ladberger Mühlenbach, which is located about 30 km northeast of the city of Münster, Germany (52°7′38″N, 7°52′48″E). The Ladberger Mühlenbach is a tributary of the River Ems and is a sand-dominated stream typical of the lowland region of the Westfälische Bucht. Further details on catchment landscape and geology can be obtained from Cleven and Meyer (2003). The woody riparian vegetation along the stream reach consists mainly of alder (*Alnus glutinosa*) and oak (*Quercus robur*), but other species such as pine (*Pinus sylvestris*), willows (*Salix* spp.), and ash (*Fraxinus excelsior*) are also present in the riparian corridor and supply wood to the stream. The predominant substrate is sand with a grain diameter of 165–270 μm (Cleven 1999). Woody debris is the only natural hard substrate in the channel. Discharge during the summer months (June to September) is rather constant at 150 $L \cdot s^{-1}$, whereas high-discharge events with peak flows of up to 1400 $L \cdot s^{-1}$ frequently occur in winter and spring. The maximum daily mean water temperature was 17 °C in summer and the minimum temperature was 0.7 °C in January. Table 1 summarizes additional physical and water-chemical characteristics of the stream.

Branchwood was collected from a Scots pine (*Pinus sylvestris*) forest near the stream immediately after clear-cutting. A total of 60 sticks with similar surface areas (approximately 400 cm^2; lengths ranged from 16 to 47 cm and diameters from 2.5 to 7.8 cm) were cut and stored for 3 months. Branches showing signs of extensive infection by blue-staining fungi were discarded. Wood and bark samples from reference pieces of each branch to be used in the experiment were retained for ergosterol analyses and determination of solubility in water and hot NaOH. The remaining branches were tied to metal rods marked with colour-coded nylon ties that allowed us to identify wood pieces individually. Each rod was fixed to the end of a second metal rod to form a "T". Ten such units, each comprising six branches, were secured at the river bottom by driving the vertical rod into the sediment until the horizontal rod was buried and the branches were lying on top of the sediment surface. All sticks were placed within a single reach on 18 October 2000.

On each of nine sampling occasions (2, 5, 8, 12, 20, 29, 36, 46, and 56 weeks after submergence), five randomly selected branches were cut and transported to the laboratory in plastic bags filled with stream water. Branches were care-

Table 1. Physical and chemical characteristics of the study reach in the Ladberger Mühlenbach during the 13-month study period (18 October 2000 to 14 November 2001).

	Median	Range
Water temp. (°C)	9.6	0.2–25.2
Conductivity (µS·cm^{-1})	580	524–598
pH	7.68	7.35–8.03
Oxygen concn. (mg·L^{-1})	11.1	8.7–13.1
Oxygen saturation (%)	93	84–99
NH_4-N (mg·L^{-1})	0.078	0.005–0.14
NO_2-N (mg·L^{-1})	0.056	0.026–0.105
NO_3-N (mg·L^{-1})	8.19	1.35–9.93
PO_4-P (mg·L^{-1})	0.119	0.090–0.148
Discharge (L·s^{-1})	211	59–1400
Stream width (m)	4.8	3.5–5.5

Note: *N* = 9 (except for temperature and discharge, which were recorded continuously with data loggers).

fully washed with tap water to remove deposited sand and attached invertebrates, and weighed to the nearest 0.1 g. The bark was removed with a scalpel and ground wet in an electric coffee mill. The slurry was passed over a set of nested screens and the particles in the size fractions >63 and <500 µm were used for determining concentrations of water-soluble substances. Ground bark samples were stored at –18 °C for later ergosterol analysis. Wood chips were obtained from the debarked branches with a fixed commercially available electrical drill. One set of wood chips per wood stick was taken from several boreholes drilled to a depth of 1 cm. A second set was taken from a depth of 1–2 cm in the same boreholes. Subsamples of both fractions were stored at –18 °C until analyzed for ergosterol. The remaining wood chips from each fraction were ground to a fine powder and processed separately as described above for bark material. Finally, the branches were carefully washed to remove remaining chips from the boreholes, weighed to the nearest 0.1 g, dried at 105 °C, and reweighed to determine wood water content and total dry mass of the intact wood pieces.

Solubility of wood in hot 1% NaOH was determined according to test method T212 om-93 of the Technical Association of the Pulp and Paper Industry (1993*a*) but using 1 g instead of 2 g of wood dry mass. Samples were extracted for 60 min at 100 °C by adding 100 mL of 1% NaOH to an Erlenmeyer flask and placing it on a hotplate. The flasks were regularly stirred by hand and the suspensions were finally filtered through a glass-fibre filter (GF 6 VG Schleicher & Schüll, Dassel, Germany). The retained wood residue was washed with hot water, then 15 mL of 10% acetic acid was added and it was allowed to soak for 1 min. Finally, the sample was washed with distilled water until it was acid-free, dried at 105 °C, cooled in a desiccator for 24 h, and weighed to the nearest 0.1 mg.

Test method T207 om-93 of the Technical Association of the Pulp and Paper Industry (1993*b*) was used to determine concentrations of water-soluble substances in wood. Wood and bark samples of 1–2 g dry mass were extracted for 48 h at room temperature in Erlenmeyer flasks with 300 mL of distilled water. Samples were continuously shaken during the extraction (reciprocating shaker, type 3016, Gesellschaft für Labortechnik mbH, Burgwedel, Germany). The suspensions were then filtered through a glass-fibre filter, washed with 200 mL of distilled water, dried, cooled in a desiccator, and weighed as above.

Fungal biomass in wood and bark was estimated by determining ergosterol content (Gessner and Newell 2002). Samples were freeze-dried and 50-mg subsamples were weighed (to the nearest 0.1 mg). The ergosterol was extracted in alcoholic KOH (10 mL of 0.8% KOH in methanol for 30 min at 80 °C) with stirring in tightly capped tubes. The resultant extract was cleaned by solid-phase extraction (Gessner and Schmitt 1996) and the ergosterol was purified and quantified by high pressure liquid chromatography (HPLC). A LichroSpher 100 RP-18 column (0.46 cm × 25 cm) (Merck Inc. KGaA, Darmstadt, Germany) connected to a Jasco AS-950 autosampler and PU-980 liquid chromatograph was used. The mobile phase was HPLC-grade methanol at a flow rate of 1.5 mL·min^{-1}. Ergosterol was detected at 282 nm with a Jasco UV-970 UV/VIS detector (R_t = approximately 8 min), and was identified and quantified based on comparison with ergosterol standards (Fluka Chemical Company, Buchs, Switzerland). Ergosterol was converted to fungal dry mass by assuming an ergosterol concentration of 5.5 µg·mg^{-1} fungal dry mass (Gessner and Chauvet 1993).

The exponential decay coefficient, *k*, of pine wood was calculated by regressing the natural logarithm of the percent dry mass remaining of each stick against the exposure time of branchwood in the stream. Possible changes in concentrations of water-soluble and NaOH-soluble compounds in wood were assessed by one-way analyses of covariance with sampling date as factor and wood-stick diameter as covariate. Tukey's test was used for post-hoc pairwise comparisons when overall differences were significant. Reported *p* values refer to untransformed data, but analyses based on arcsine square root transformed data produced virtually identical results. Temporal differences in concentrations of water-soluble compounds and fungal biomass in bark were tested by one-way analysis of variance (ANOVA), followed by Tukey's test. Two-way ANOVA with sampling date and depth of wood boreholes (i.e., 0–1 vs. 1–2 cm) as factors was used to test for differences in fungal biomass. Wood-stick diameter was not used as a covariate in that analysis, because fungal-biomass data refer to defined layers of the wood sticks (0–1 and 1–2 cm depth, respectively) rather than entire branches. However, including wood diameter as a covariate would produce very similar results. Pearson's correlation coefficients were calculated to explore relationships between the above variables. Quantile–quantile plots and Lilliefors' test (adjusted one-sample Kolmogorov–Smirnov test for normality) indicated that the data distributions approximately matched the normal distribution. All statistical analyses were done with SYSTAT® version 10 for Windows (SPSS Inc. 2000).

Results

Pine branches initially lost 2% of ash-free dry mass, but no further loss was observed during the following 3 months (Fig. 1). Subsequently, branchwood decomposed at an exponential rate, which resulted in a total mass loss of 8.3 ± 0.7% (mean ± 1 standard error) after 13 months and an overall decay rate of 0.074 ± 0.007·year^{-1} (r^2 = 0.71, $p < 0.001$).

Fig. 1. Mass loss of fully corticated branchwood of pine (*Pinus sylvestris*) during 13 months of submergence in a nutrient-rich lowland stream. Error bars denote standard errors.

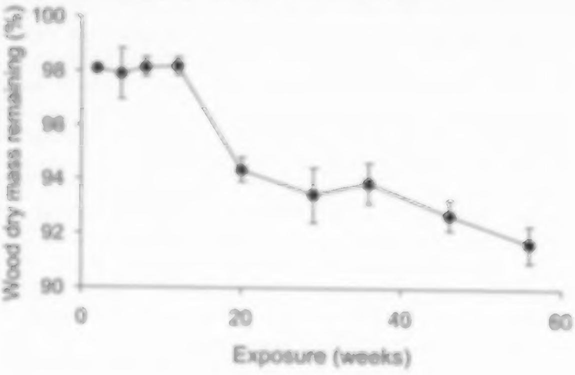

Fig. 2. Changes in concentrations of water-soluble compounds in bark (*a*) and wood (*b*) from the outermost 1 cm of the pine branchwood. Error bars denote standard errors.

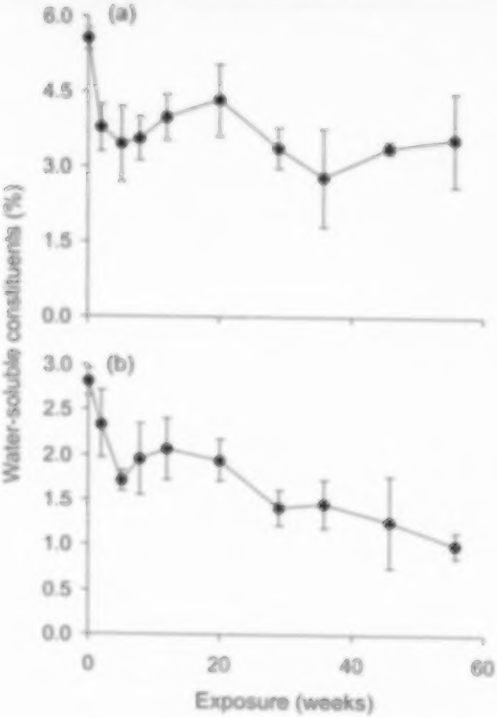

Fig. 3. Concentrations of wood constituents soluble in hot 1% NaOH as an indicator of microbial degradative activity during 13 months' submergence of pine branchwood in a nutrient-rich lowland stream. Error bars denote standard errors.

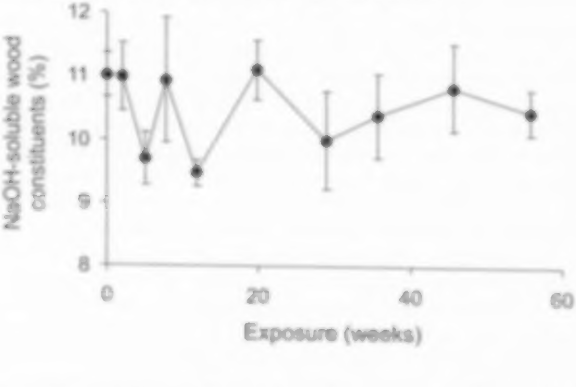

There was no indication of extensive abrasion of bark or feeding activities of invertebrates throughout the study.

Bark initially contained 5.6 ± 0.2% of water-soluble compounds. Within the first 2 weeks of submergence this value decreased to 3.8 ± 0.5% and it varied little over the following 12 months (Fig. 2*a*). Tukey's pairwise comparisons revealed that the overall significant effect of sampling date ($F_{[9]} = 3.46$, $p = 0.003$) was entirely due to differences between initial concentrations of water-soluble compounds and their concentrations after wood exposure in the stream. Concentrations of water-soluble compounds in wood tended to decrease gradually during the study, from initially 2.8 ± 0.2% to 1.0 ± 0.1% after 13 months (Fig. 2*b*). Analyses of covariance followed by Tukey's test showed, however, that as with bark the significant effect of sampling date ($F_{[9]} = 4.10$, $p < 0.001$) was due only to higher concentrations of water-soluble compounds before wood exposure in the stream. Wood diameter had no significant influence ($F_{[1]} = 0.04$, $p = 0.85$)

Submerged branchwood rapidly absorbed water following submergence, resulting in an increase in water content from 8.9% initially to 47.8% after 2 weeks (data not shown). Water content gradually increased further, reaching 60% after 13 months. It was negatively correlated with the concentration of water-soluble compounds ($r = 0.97$, $p < 0.001$). The average concentration of wood constituents soluble in hot 1% NaOH fluctuated between 9.5% and 11% during the study but showed no clear temporal pattern (Fig. 3; $F_{[9]} = 1.09$, $p = 0.39$). Wood diameter had no significant influence ($F_{[1]} = 0.45$, $p = 0.51$).

The ergosterol concentration of bark increased from 14.4 ± 6.0 $\mu g \cdot g^{-1}$ dry mass initially to 68.5 ± 9.8 $\mu g \cdot g^{-1}$ after 5 weeks, but showed no clear trend thereafter, with average values fluctuating between 38.7 and 72.4 $\mu g \cdot g^{-1}$ and standard errors of up to 22.7 $\mu g \cdot g^{-1}$ (Fig. 4*a*). As with the concentration of NaOH-soluble compounds, the significant overall effect of sampling date ($F_{[9]} = 3.97$, $p = 0.002$) was entirely due to the different initial ergosterol concentration compared with several concentrations after exposure of branches in the stream. Given an average conversion factor for various strains of aquatic hyphomycetes (5.5 μg ergosterol$\cdot g^{-1}$ fungal dry mass; Gessner and Chauvet 1993), measured ergosterol concentrations correspond to a fungal biomass of 7–13 $mg \cdot g^{-1}$ bark dry mass.

Ergosterol concentrations in wood from both depths (0–1 and 1–2 cm) were low throughout the study (Figs. 4*b*, 4*c*), with average values fluctuating between 5 and 12 $\mu g \cdot g^{-1}$ dry mass. ANOVA revealed no significant effects of either sampling date ($F_{[9]} = 1.04$, $p = 0.42$) or depth ($F_{[1]} = 1.26$, $p = 0.27$), nor of the interaction between the two factors ($F_{[9]} = 0.26$, $p = 0.98$). Concentrations at the two depths were

Fig. 4. Fungal biomass within bark (*a*) and the outermost wood layers (*b* (0–1 cm depth) and *c* (1–2 cm depth)) during 13 months' submergence of pine branchwood in a nutrient-rich lowland stream. Error bars denote standard errors.

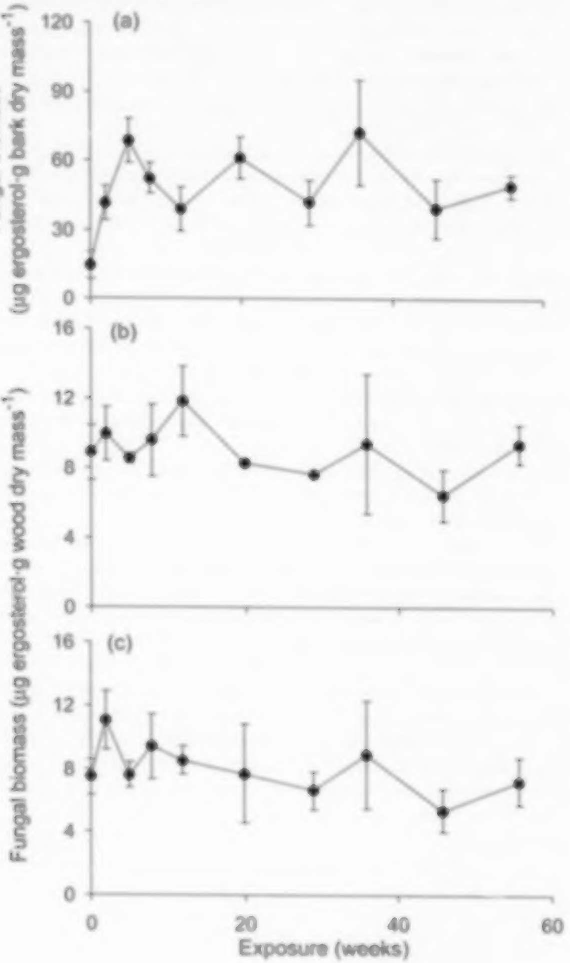

significantly correlated with one another when two outliers were removed ($N = 40$, $p < 0.001$, $r = 0.77$).

Discussion

A range of natural wood types has been found to decompose considerably faster in streams than the pine wood in the present study; these include branchwood with intact bark of tree species such as alder (Chergui and Pattee 1991; Diez et al. 2002), oak (Golladay and Webster 1988; Diez et al. 2002), and maple, poplar, cherry, and sycamore (Shearer and von Bodman 1983). However, the decay rate of pine wood in the lowland stream of the present study corresponds well with the results of Webster et al. (1999), who reported rates between 0.062·year^{-1} for branches (approximately 2.8 cm in diameter) and 0.102·year^{-1} for small twigs (1.5 cm in diameter) of *Pinus strobus* in a headwater stream of the Appalachian Mountains. Diez et al. (2002) found even lower rates for branchwood of *Pinus radiata* in several mountain streams in northern Spain (0.016–0.067·year^{-1}), attributing the variation among streams mainly to differences in streamwater concentrations of phosphate. Given the high concentrations of phosphate and nitrogen species, particularly nitrate, in our study stream, microbial activity associated with wood was unlikely to be limited by nutrients. This suggests that the intrinsic recalcitrance of the wood tissue rather than a shortage of external nutrient supply accounted for the slow decomposition.

The low ergosterol concentration of the outer layers (0–1 and 1–2 cm depth) of the sticks used in the present study reveals that the pine wood was poorly colonized by fungi. This finding is consistent with the slow mass loss and low ergosterol concentrations (23–36 µg·g^{-1} dry mass) of pine branches with bark (J. Pozo, Department of Plant Biology and Ecology, University of Bilbao, Spain, personal communication) that had been submerged in several streams for more than 3 years (Diez et al. 2002). As in the present study, no substantial increase in ergosterol concentration was noted over time by Diez et al. (2002), suggesting that fungal colonization of intact pine branches submerged in streams is greatly restricted even over extended periods.

The ergosterol initially present in the wood sticks in the present study may have been due to blue-staining or other fungi that had colonized the sticks before they were placed in the stream. The slight increase in ergosterol concentration observed shortly after wood submergence suggests that fungal growth may have been boosted when water became readily available. Blue-staining fungi, however, are known to cause discoloration of wood without damaging the cellular structure (Farmer 1967). Consequently, these fungi would be expected not to cause significant mass loss of wood or to colonize it pervasively. This idea is in accordance with the slow decomposition of pine wood that we observed and with the rather constant concentrations of both lignin (Diez et al. 2002) and NaOH-soluble matter in the present study, indicating that structural characteristics of the submerged wood were not notably altered during the 13-month incubation period in the stream.

The limited fungal growth in the above studies contrasts with the gradually increasing ergosterol concentration (up to 60 µg·g^{-1} dry mass) found in submerged wooden cubes of beech (*Fagus sylvatica*) sapwood (Hendel and Marxsen 2000). However, the cubes used in that study were small (1 cm × 1 cm × 1 cm), lacked protecting bark, and offered a large surface area that may have facilitated fungal colonization especially at the ends cut perpendicular to the wood fibres. In other studies on fungal biomass dynamics in submerged wood, ergosterol contents were given per unit wood surface area rather than expressed as mass (Golladay and Sinsabaugh 1991; Tank and Webster 1998; Collier et al. 2004). This makes a direct comparison with the results of the present study difficult. Nevertheless, continuous increases in ergosterol content (up to 4 µg·cm^{-2}) were noted during submergence of ice-cream sticks made of white birch (*Betula papyrifera*) in a stream for 23 weeks (Golladay and Sinsabaugh 1991). In a companion study in the same stream, ergosterol associated with small (10 cm × 10 cm × 1 cm) plates of pine (*P. strobus*) wood increased during the first 54 days only (up to 0.5 µg ergosterol·cm^{-2}) and then declined (Sinsabaugh et al. 1991). This discrepancy indicates that the differences in fungal growth dynamics observed in different studies may be due at least in part to differences in wood quality rather than to protection by bark.

The higher concentrations of ergosterol in bark than in wood may be unexpected given that the bark of various woody plant species contains phenolic compounds with bactericidal and fungicidal effects (Browning 1967). However, these substances are typically water-soluble and would therefore be removed by leaching. Cooke (1984) reported, moreover, that many extractives of wood and bark do not affect fungal growth, and others may even stimulate hyphal extension. Thus, the potentially inhibitory effect of bark constituents on fungal growth should not be overrated, especially as ergosterol concentrations in bark were still considerably lower than some concentrations found in decomposing leaves (e.g., Gessner and Chauvet 1994; Grattan and Suberkropp 2001; Hieber and Gessner 2002).

In conclusion, the results of this study underline the remarkably slow decomposition of intact fully corticated pine branchwood in a sandy lowland stream in spite of high concentrations of dissolved nutrients in the stream water. This finding is consistent with the limited fungal colonization and unnoticeable structural changes of the wood tissue. The primary reason underlying the slow decomposition thus is likely the recalcitrant nature of pine wood. Nevertheless, the temporal pattern of mass loss and the constant concentrations of water-soluble compounds in the wood tissue show that the observed mass loss was not simply a result of leaching.

Acknowledgments

Many thanks are extended to E.I. Meyer for her support during this study, to D. Steiner for ergosterol analyses, and to G. Schulze for water chemistry analyses.

References

Anderson, N.H., and Sedell, J.R. 1979. Detritus processing by macroinvertebrates in stream ecosystems. Annu. Rev. Entomol. **24**: 351–377.

Anderson, N.H., Steedman, R.J., and Dudley, T. 1984. Patterns of exploitation by stream invertebrates of wood debris (xylophagy). Verh. Int. Verein. Limnol. **22**: 1847–1852.

Aumen, N.G., Bottomley, P.J., Ward, G.M., and Gregory, S.V. 1983. Microbial decomposition of wood in streams: distribution of microflora and factors affecting [^{14}C]lignocellulose mineralization. Appl. Environ. Microbiol. **46**: 1409–1416.

Benke, A.C., and Wallace, J.B. 1990. Wood dynamics in coastal plain blackwater streams. Can. J. Fish. Aquat. Sci. **47**: 92–99.

Berg, B., and McClaugherty, C. 2003. Plant litter — decomposition, humus formation, carbon sequestration. Springer-Verlag, Berlin.

Bilby, R.E., and Bisson, P.A. 1998. Function and distribution of large woody debris. *In* River ecology and management: lessons from the Pacific coastal ecoregion. *Edited by* R.J. Naimann and R.E. Bilby. Springer-Verlag, New York. pp. 324–346.

Browning, B.L. 1967. Methods of wood chemistry. John Wiley & Sons, New York.

Chergui, H., and Pattee, E. 1991. The breakdown of wood in the side arm of a large river: preliminary investigations. Verh. Int. Verein. Limnol. **24**: 1785–1788.

Cleven, E.-J. 1999. An improved method of taking cores in sandy sediments. Arch. Hydrobiol. **147**: 65–72.

Cleven, E-J., and Meyer, E.I. 2003. A sandy hyporheic zone limited vertically by a solid boundary. Arch. Hydrobiol. **157**: 267–288.

Collier, K.J., Smith, B.J., and Halliday, N.J. 2004. Colonization and use of pine wood versus native wood in New Zealand plantation forest streams: implications for riparian management. Aquat. Conserv. Mar. Freshw. Ecosyst. **14**: 179–199.

Cooke, R.C. 1984. Ecology of saprotrophic fungi. Longman Group Ltd., New York.

Diez, J., Elosegi, A., Chauvet, E., and Pozo, J. 2002. Breakdown of wood in the Aguëra stream. Freshw. Biol. **47**: 2205–2215.

Fausch, K.D., and Northcote, T.G. 1992. Large woody debris and salmonid habitat in a small coastal British Columbia stream. Can. J. Fish. Aquat. Sci. **49**: 682–693.

Farmer, R.H. 1967. Chemistry in the utilization of wood. Pergamon Press, London.

Fisher Wold, A.K., and Hershey, A.E. 1999. Effects of salmon carcass decomposition on biofilm growth and wood decomposition. Can. J. Fish. Aquat. Sci. **56**: 767–773.

Gessner, M.O., and Chauvet, E. 1993. Ergosterol-to-biomass conversion factors for aquatic hyphomycetes. Appl. Environ. Microbiol. **59**: 502–507.

Gessner, M.O., and Chauvet, E. 1994. Importance of stream microfungi in controlling breakdown rates of leaf litter. Ecology, **75**: 1807–1817.

Gessner, M.O., and Newell, S.Y. 2002. Biomass, growth rate, and production of filamentous fungi in plant litter. *In* Manual of environmental microbiology. 2nd ed. *Edited by* C.J. Hurst, R.L. Crawford, G.R. Knudsen, M.J. McInerney, and L.D. Stetzenbach. ASM Press, Washington, D.C. pp. 390–408.

Gessner, M.O., and van Ryckegem, G. 2003. Water fungi as decomposers in freshwater ecosystems. *In* Encyclopedia of environmental microbiology. *Edited by* G. Bitton. John Wiley & Sons, New York. [Online edition: DOI: 10.1002/0471263397.env314.]

Gessner, M.O., and Schmitt, A.L. 1996. Use of solid-phase extraction to determine ergosterol concentrations in plant tissue colonized by fungi. Appl. Environ. Microbiol. **62**: 415–419.

Golladay, S.W., and Sinsabaugh, R.L. 1991. Biofilm development on leaf and wood surfaces in a boreal river. Freshw. Biol. **25**: 437–450.

Golladay, S.W., and Webster, J.R. 1988. Effects of clear-cut logging on wood breakdown in Appalachian Mountain streams. Am. Midl. Nat. **119**: 143–155.

Gönczöl J., and Revay, A. 1997. Spatial dynamics of fungal populations (Hyphomycetes) on submerged corticated twigs. Nova Hedwigia, **64**: 553–565.

Grattan, R.M., II, and Suberkropp, K. 2001. Effects of nutrient enrichment on yellow poplar leaf decomposition and fungal activity in streams. J. N. Am. Benthol. Soc. **20**: 33–43.

Guyette, R.P., Cole, W.G., Dey, D.C., and Muzika, R.M. 2002. Perspectives on the age and distribution of large wood in riparian carbon pools. Can. J. Fish. Aquat. Sci. **59**: 578–585.

Harmon, M.E., Franklin, J.F., Swanson, F.J., Sollins, P., Gregory, S.V., Lattin, J.D., et al. 1986. Ecology of coarse woody debris in temperate ecosystems. Adv. Ecol. Res. **15**: 133–302.

Hendel, B., and Marxsen, J. 2000. Extracellular enzyme activity associated with degradation of beech wood in a Central European stream. Int. Rev. Hydrobiol. **85**: 95–105.

Hieber, M., and Gessner, M.O. 2002. Contribution of stream detrivores, fungi, and bacteria to leaf breakdown based on biomass estimates. Ecology, **83**: 1026–1038.

Hilderbrand, R.H., Lemly, A.D., Dolloff, C.A., and Harpster K.L. 1997. Effects of large woody debris placement on stream channels and benthic macroinvertebrates. Can. J. Fish. Aquat. Sci. **54**: 931–939.

Ho, W.H., Yanna, W., Hyde, K.D., and Hodgkiss, I.J. 2002. Seasonality and sequential occurrence of fungi on wood submerged in Tai Po Kau Forest stream, Hong Kong. Fungal Divers. **10**: 21–43.

Hoffmann, P., and Parameswaran, N. 1982. Chemische und ultrastrukturelle Untersuchungen an wassergesättigten Eichenhölzern aus archäologischen Funden. Berl. Beitr. Archaeom. **7**: 273–288.

Melillo, J.M., Naiman, R.J., Aber, J.D., and Eshleman, K.N. 1983. The influence of substrate quality and stream size on wood decomposition dynamics. Oecologia, **58**: 281–285.

Mutz, M. 2000. Influences of woody debris on flow patterns and channel morphology in a low energy, sand-bed stream reach. Int. Rev. Hydrobiol. **85**: 107–121.

Pereira, C.R.D., Anderson, N.H., and Dudley, T. 1982. Gut content analysis of aquatic insects from wood substrates. Melanderia, **39**: 23–33.

Pointing, S.B., and Hyde, K.D. 2000. Lignocellulose-degrading marine fungi. Biofouling, **15**: 221–229.

Rayner, A.D.M., and Boddy, L. 1988. Fungal decomposition of wood. John Wiley & Sons, New York.

Shearer, C.A. 1992. The role of woody debris. *In* The ecology of aquatic Hyphomycetes. *Edited by* F. Bärlocher. Springer-Verlag, Berlin. pp. 77–98.

Shearer, C.A. 1993. The freshwater Ascomycetes. Nova Hedwigia, **56**: 1–33.

Shearer, C.A., and von Bodman, S.B. 1983. Patterns of occurrence of Ascomycetes associated with decomposing twigs in a midwestern stream. Mycologia, **75**: 518–530.

Sinsabaugh, R.L., Golladay, S.W., Linkins, A.E. 1991. Comparison of epilithic and epixylic biofilm development in a boreal river. Freshw. Biol. **25**: 179–187.

Spänhoff, B., and Meyer, E.I. 2004. Wood breakdown rates in streams. J. N. Am. Benthol. Soc. **23**: 189–197.

SPSS Inc. 2000. SYSTAT®. Version 10 for Windows. SPSS Inc., Chicago.

Stelzer, R.S., Heffernan, J., and Likens, G.E. 2003. The influence of dissolved nutrients and particulate organic matter quality on microbial respiration and biomass in a forest stream. Freshw. Biol. **48**: 1925–1937.

Suberkropp, K.F. 1998. Microorganisms and organic matter decomposition. *In* River ecology and management: lessons from the Pacific coastal ecoregion. *Edited by* R.J. Naimann and R.E. Bilby. Springer-Verlag, New York. pp. 120–143.

Tank, J.L., and Webster, J.R. 1998. Interaction of substrate and nutrient availability on wood biofilm processes in streams. Ecology, **79**: 2168–2179.

Technical Association of the Pulp and Paper Industry. 1993*a*. One percent sodium hydroxide solubility of wood and pulp. T 212 om-93. Revised form of the official test method 1983. Technical Association of the Pulp and Paper Industry, Atlanta, Ga.

Technical Association of the Pulp and Paper Industry. 1993*b*. Water solubility of wood and pulp. T 207 om 93. Revised form of the official test method 1983. Technical Association of the Pulp and Paper Industry, Atlanta, Ga.

Webster, J.R., Wallace, J.B., and Benfield, E.F. 1995. Organic processes in streams of the eastern United States. *In* Ecosystems of the world 22: river and stream ecosystems. *Edited by* C.E. Cushing, G.W. Minshall, and K.W. Cummins. Elsevier, Amsterdam. pp. 117–187.

Webster, J.R., Benfield, E.F., Ehrman, T.P., Schaeffer, M.A., Tank, J.L., Hutchens, J.J., and D'Angelo, D.J. 1999. What happens to allochthonous material that falls into streams? A synthesis of new and published information from Coweeta. Freshw. Biol. **41**: 687–705.

Wong, M.K.M, Goh, T.-K., Hodgkiss, I.J., Hyde, K.D., Ranghoo, V.M., Tsui, C.K.M., et al. 1998. Role of fungi in freshwater ecosystems. Biodivers. Conserv. **7**: 1187–1206.

Yuen, T.K., Hyde, K.D., and Hodgkiss, I.J. 1999. Soft rot decay in tropical freshwater fungi. Mater. Org. (Berl.), **33**: 155–161.

Zare-Maivan, H., and Shearer, C.A. 1988. Wood decay activity and cellulase production by freshwater lignicolous fungi. Int. Biodeterior. **24**: 459–474.

Coupling of methyl and total mercury in a minerotrophic peat bog in southeastern Sweden

O. Regnell and T. Hammar

Abstract: During most of an annual cycle, we studied the temporal variation of total mercury (Hg_T) and methyl mercury (MeHg) in unfiltered and filtered (0.45 µm) peat water from a minerotrophic peat bog in southeastern Sweden. MeHg in bulk water ($[MeHg_T]$) and total Hg in filtered water in discharge water from the peat bog ($[Hg_D]$) were an order of magnitude higher than in upland runoff water entering the peat bog. At the discharge end, peat-water $[Hg_D]$ and $[MeHg_D]$ ranged from 8 to 54 $pmol \cdot L^{-1}$ and from 1 to 32 $pmol \cdot L^{-1}$, respectively. Whereas the variation of $[MeHg_T]$ was explained by changes in $[MeHg_D]$, the variation of inorganic Hg_T $[IHg_T] = [Hg_T] - [MeHg_T]$ was explained by changes in particle-bound IHg $[IHg_P] = [IHg_T] - [IHg_D]$. Filterable organic matter and sulfide in the water both correlated poorly with $[Hg_D]$. Neither did the amount of Hg_T in precipitation and upland runoff water correlate well with the estimated discharge of Hg_D from the peat bog. However, there was a strong correlation between $[Hg_D]$ and $[MeHg_T]$ in the peat water ($r = 0.96$). Furthermore, a significant fraction of Hg_D was MeHg (mean 28%; range 8–60%). These results suggest that methylation increased the mobility of Hg.

Résumé : Nous avons suivi, sur presque tout un cycle annuel, la variation temporelle du mercure (Hg_T) total et du méthyl-mercure dans l'eau de tourbière filtrée (0,45 µm) et non filtrée, prélevée dans une tourbière minérotrophe du sud-est de la Suède. Les concentrations de méthyl-mercure dans l'eau brute ($[MeHg_T]$) et de mercure total dan l'eau filtrée ($[Hg_D]$) sont de l'ordre de 10 fois plus élevées dans l'eau de drainage de la tourbière que dans l'eau de ruissellement qui coule vers la tourbière en amont. Au point de drainage, $[Hg_D]$ et $[MeHg_D]$ de l'eau de la tourbière varient respectivement de 8–54 $pmol \cdot L^{-1}$ et de 1–32 $pmol \cdot L^{-1}$. Alors que la variation de $[MeHg_T]$ s'explique par les changements de $[MeHg_D]$, la variation de $[IHg_T] = [Hg_T] - [MeHg_T]$ s'explique par les changements de $[IHg_P] = [IHg_T] - [IHg_D]$. Il y a peu de corrélation entre la matière organique filtrable et le sulfite dans l'eau, d'une part, et $[Hg_D]$, d'autre part. Il n'y a pas non plus de bonne corrélation entre la quantité de Hg_T dans les précipitations et dans l'eau de ruissellement d'amont, d'une part, et l'exportation estimée de Hg_D de la tourbière, d'autre part. Il y a cependant une forte corrélation ($r = 0,96$) entre $[Hg_D]$ et $[MeHg_T]$ dans l'eau de la tourbière. De plus, une fraction significative de Hg_D est en fait MeHg (moyenne, 28 %; étendue, 8–60 %). Ces résultats indiquent que la méthylation augmente la mobilité de Hg.

[Traduit par la Rédaction]

Introduction

Several studies indicate that drainage lakes and rivers can receive significant quantities of methyl mercury (MeHg) from hydrologically connected wetlands (e.g., St. Louis et al. 1994; Hurley et al. 1995; Waldron et al. 2000). In contrast to inorganic Hg (IHg), MeHg is biomagnified in aquatic food webs, leading to bioconcentration factors ($[MeHg]_{organism}/[MeHg]_{water}$) of up to 10^7 for predaceous fish (Surma-Aho et al. 1986; Driscoll et al. 1994). Highly neurotoxic MeHg readily passes the blood–brain barrier and the blood–placenta barrier. Furthermore, the human fetus is known to be highly sensitive to MeHg exposure during development (Clarkson 1990; Choi 1991). This has prompted health authorities to issue fish-consumption advisories for a large number of lakes and rivers in Canada, the USA, and Scandinavia (e.g., Sorensen et al. 1990; Johansson et al. 2001).

In wetlands, organic matter (OM) is degraded anaerobically. A large number of studies have shown that net Hg methylation rates are considerably higher under anaerobic than aerobic conditions (e.g., Compeau and Bartha 1984; Regnell and Tunlid 1991; Regnell et al. 1997). More specifically, there seems to be a strong link between dissimilatory sulfate reduction and Hg methylation (e.g., Compeau and Bartha 1985; Gilmour et al. 1992; Branfireun et al. 1999).

A relatively small fraction of the total atmospheric Hg deposition on boreal-forest watersheds may reach surface waters, the remainder being either volatilized or retained in the soil (Swain et al. 1992; Quemarais et al. 1999). Several studies indicate that the retention of Hg in wetlands is lower than in upland soils (e.g., Mierle 1990; Hurley et al. 1995; Waldron et al. 2000). This is a somewhat surprising finding, considering the fact that Hg interacts strongly with surface components of live and dead OM. Notably, inorganic divalent Hg (Hg(II)) has a very high affinity for reduced organic sulfur (Hesterberg et al. 2001). However, several processes can remove Hg(II) from particulate organic matter and other solids and (or) counteract its tendency to sorb to solids. Such processes represent

Received 23 July 2003. Accepted 8 July 2004. Published on the NRC Research Press Web site at http://cjfas.nrc.ca on 24 December 2004.
J17659

O. Regnell.[1] Ecotoxicology, Department of Ecology, University of Lund, Sölvegatan 37, SE-223 62 Lund, Sweden.
T. Hammar. Environmental Unit, Kalmar County Administration, SE-391 86 Kalmar, Sweden.

[1] Corresponding author (e-mail: Olof.Regnell@ecotox.lu.se).

Can. J. Fish. Aquat. Sci. **61**: 2014–2023 (2004)   doi: 10.1139/F04-143

Fig. 1. Locations of the peat bog and the sampling sites for peat water (PW), upland runoff water entering the peat bog (UW), wet deposition (WD), and observation wells for water-level measurements (OW). The river-water samples discussed in the paper were sampled approximately 5 km downstream of the lakes. Depth isopleths (m) are shown for the lakes. The inset map shows the location in Sweden.

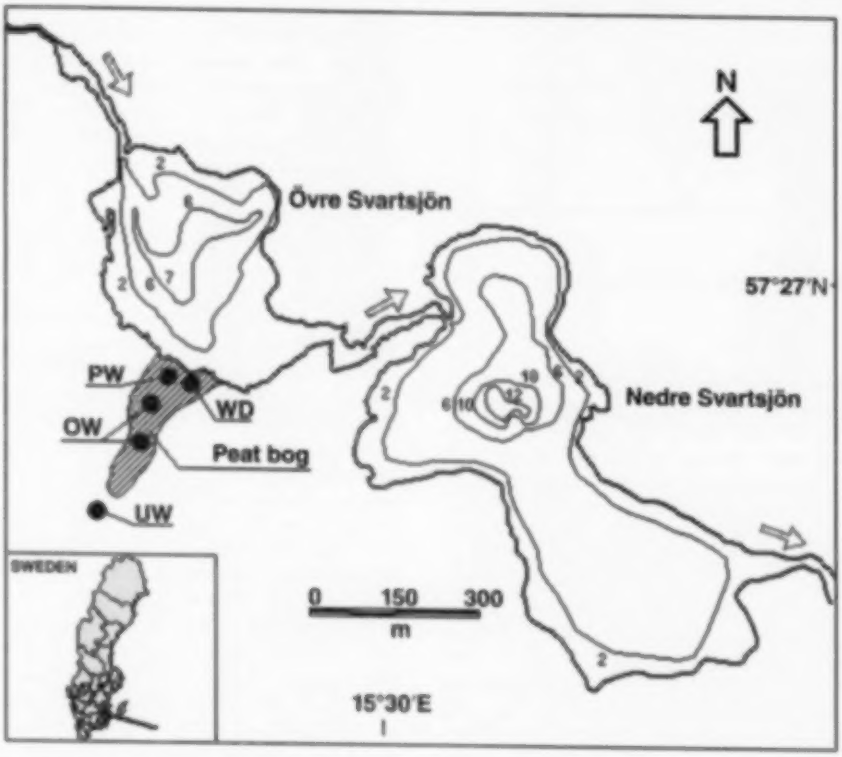

heterotrophic activity leading to degradation of particulate organic matter (Schlüter 1996; Drexel et al. 2002), complexation of Hg(II) by inorganic sulfide and dissolved organosulfur compounds (Benoit et al. 1999), and reductive dissolution of iron and manganese oxides (Regnell et al. 1997, 2001).

In comparison with Hg(II), MeHg has a somewhat lower affinity for reduced-sulfur functional groups because the methyl group withdraws electrons and decreases the covalent character of the Hg–S bonding (Craig 1986). Furthermore, unlike Hg(II), MeHg rapidly exchanges reduced-sulfur ligands (Carty and Malone 1979; Jackson 1998). Hence, methylation can be expected to increase the mobility of Hg. Recently, it was reported that MeHg constituted 60%–80% of total Hg (Hg_T) in water flowing out of an experimentally flooded wetland in northeastern Ontario (St. Louis et al. 2004); the authors stated that methylation probably increased the mobility of Hg.

The present paper is based on data obtained from a minerotrophic peat bog in southeastern Sweden. Our objective was to determine relationships between the release of Hg and environmental conditions, to develop testable hypotheses regarding processes that affect the mobilization of Hg in peat bogs.

Materials and methods

Study site

The study site is a *Sphagnum*-dominated minerotrophic peat bog (1.3 ha) within a watershed (84 ha) dominated by coniferous forest in southeastern Sweden (Fig. 1). The discharge to the peat bog is mainly ground water from a valley that collects surface runoff as well as soil ground water from the surrounding hills. The valley directs these flows to the peat bog, the latter being an exfiltration area for ground water at the mouth of the valley. During most of the year, flow takes place as ground water. However, during periods of high discharge (mainly snowmelt), a surface stream occurs at the bottom of the valley and is spread over the peat bog as diffuse surface water. Hydrological investigations indicate that about 90% of the discharge from the valley takes place in the soil (including occasional surface water) and is directed through the peat bog, while the remaining part leaves the area through fracture zones in the bedrock. At the mouth of the valley, where the soil surface and moraine are overlain by peat, the ground-water level reaches the soil surface. The ground-water discharge and occasional surface runoff from the valley thus pass the peat bog before being discharged to the lake (Övre Svartsjön) (Fig. 1). Basic chemical and physical data from the peat water are given in Table 1.

It is possible that the bog has received Hg from a paper mill located 2.5 km upstream of the lakes shown, which used phenyl Hg as a slimicide until 1965. The lake remains a potential source of Hg, but we found that [Hg_T] in the peat water was typically several times higher than in the epilimnetic lake water. This indicated that the lake is no longer a significant source of Hg to the peat bog. We recently pub-

Table 1. Basic chemical and physical characteristics of the peat water at the discharge end of the peat bog during the study period (May–December 1996).

	Average	Range
Temperature (°C)	9.3	1.8–18.3
Conductivity (mS·m^{-1})	6.6	5.1–7.2
pH	5.7	5.4–6.0
Total organic C (mmol·L^{-1})	2.1	1.4–2.6
Total N (mmol·L^{-1})	0.10	0.06–0.14
Total P (µmol·L^{-1})	2.1	1.1–5.2
Sulfate (µmol·L^{-1})	69	31–150

lished a paper about Hg in the sediment and water of this lake (Regnell et al. 2001).

Sampling

During May–December 1996, we sampled one site for water entering the peat bog from the valley and one site for water flowing out of the peat bog to the lake (Fig. 1). Focusing on these two sites allowed for a sufficiently high number of sampling occasions (17 times) to study the temporal relationships between different environmental variables and the levels and fluxes of Hg_T and MeHg. It also enabled us to study the ratio between MeHg and Hg_T over most of an annual cycle. Admittedly, however, this may limit the applicability of the findings to other peat bogs because a narrower range of conditions were tested than would have been the case if more sites had been sampled. Considering the fact that surface water flow rarely occurs, it was concluded that representative samples of the water flowing into the peat bog were best obtained by sampling ground water in the moraine close to the surface. This was achieved by pumping from a permanently installed piezometer (polyethylene, 5000 mm, inner diameter (i.d.) 50 mm, slit width 0.2 mm). On each sampling occasion, at least one volume of water was withdrawn from the piezometer before the samples were taken. Water flow through the peat bog takes place mainly in the peat layer. Sampling of this water at the lower end of the peat bog took place in the upper part of the peat (0–90 cm), where permeability is highest because of intermittent freezing and thawing. Yet there is probably a decrease in hydrological conductivity with depth within the sampled 0- to 90-cm layer. Hence, fluxes of elements and compounds associated with microbial activity, the latter being highest in the upper portion of the peat, may have been underestimated (e.g., the flux of MeHg). Each sample was obtained by manually inserting a pointed plastic (polyethylene) cylinder with slits (length 1090 mm, i.d. 50 mm, slit width 0.2 mm) into the live moss and peat. Filtered samples from both sites were obtained immediately in the field using acid-washed plastic syringes to which 0.45 µm filters (Millex-HA, Millipore) were fitted. Long gloves were always used when water samples intended for Hg determinations were handled. Samples for Hg determination were transferred to Teflon bottles (120 mL). These were emptied of their content of ultraclean MQ water and 0.5 mL of concentrated HCl, and washed once with sample water. The bottles were then transferred to a refrigerated box and sent to the laboratory less than 24 h after sampling.

Water samples were also taken at turbulent sites in the river that flows through the adjacent lake by immersing Teflon bottles by hand. The reported site was located approximately 5 km below the lakes shown (Fig. 1).

Two wet-deposition collectors were deployed close to the sampling site for peat water (Fig. 1). These were emptied monthly. They consisted of a funnel (i.d. 82 mm) and a sampling bottle made of borosilicate glass. A capillary tube connected the funnel to the sampling bottle. The latter was shielded from light and contained 2.5 mL of HCl (Suprapur) (Iverfeldt 1991).

Chemical analyses

Hg_T samples were wet-oxidized by adding BrCl. $NH_2OH{\cdot}HCl$ was then added prior to reduction of all Hg compounds to Hg^0 by $SnCl_2$. A technique involving double-amalgamation and atomic fluorescence detection was used for quantification. MeHg was extracted by a distillation procedure. After aqueous-phase ethylation, separation by isothermal gas chromatography and pyrolysis, it was quantified using an atomic fluorescence detector. For the peat-water samples, artifact formation of MeHg during distillation could be safely neglected because of the high proportion of Hg_T that was present as MeHg. The detection limits of Hg_T and $MeHg_T$ were 0.25 and 0.1 pmol/L, respectively.

Sulfide was measured colorimetrically using the methylene blue method (Fonselius 1983). The samples were stabilized in the field by addition of NaOH and zinc acetate.

Total organic carbon (TOC) in water was determined using a carbon analyzer (Shimadzu, TOC-500). Particulate organic carbon (POC) was estimated from the concentration of suspended particulate matter (collected on 1.6 µm filters) and the ignition loss (550 °C) of the suspended particulate matter. A factor of 0.5 was used to convert ignition loss to POC. This factor was obtained from settling matter in the river that was determined with respect to both TOC and ignition loss. For these samples, the ratio was in the interval [0.42, 0.53] (n = 32). Dissolved organic carbon (DOC) was calculated as TOC – POC. Color was measured as absorbance (420 nm) after filtration through 0.45 µm filters (Millex-HA, Millipore). This is a measure of the concentration of humic and fulvic matter that is strongly correlated with DOC (Mierle and Ingram 1991).

Water-discharge measurements

The velocity–area method was used to estimate the water discharge of the river. An electromagnetic current meter (Nautilus C 2000) measured the speed of water in different vertical sections of the river. These measurements were used to obtain an integrated average water velocity for the entire cross section.

The discharge from the valley through the peat bog was modelled with Hydrological Evaluation of Leachate Performance (HELP; version 3.05). This model is a quasi-two-dimensional hydrologic model for conducting water-balance analyses of landfills, cover systems, and other solid waste containment facilities. However, the model is also applicable to natural soil profiles, using the same solution techniques as for cover systems. In the model, the soil profile of the valley was represented by two layers, the upper layer having a hydraulic conductivity of 1×10^{-6} m·s^{-1} and the lower layer

Fig. 2. Concentration of (*a*) filterable total Hg (Hg_D; except for wet deposition, for which total Hg in bulk water is shown) and (*b*) methyl Hg (MeHg) in unfiltered water during the study period in runoff water, peat water, and wet deposition. Minimum values (open bars), averages (shaded bars), and maximum values (solid bars) are shown.

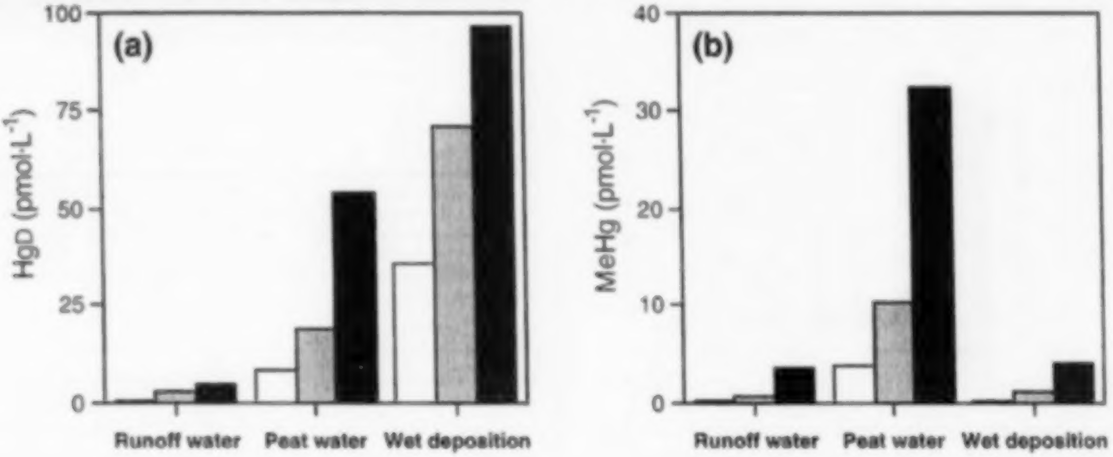

(bedrock) having a hydraulic conductivity of 1×10^{-9} m·s^{-1}, acting as a barrier to vertical percolation. The input of the model consisted of daily data on precipitation, temperature, and solar radiation, mean quarterly humidity, and mean wind speed, together with soil data (hydraulic conductivity, porosity, field capacity, and wilting point) and design data (the geometry of the two-dimensional soil profile, evaporative zone depth, and vegetation intensity). The model was then used to calculate evapotranspiration, surface runoff, ground-water level, lateral ground-water flow in the soil layer, and percolation to deeper ground water in the bedrock.

Calculations were performed for a series of years (1991–1996) to allow comparisons between calculated discharge and regional discharge reported by the Swedish Meteorological and Hydrological Institute. The model resulted in a ground-water table close to that found in the field, and a total discharge (surface runoff and ground-water formation) normalized to the area similar to the total regional discharge as measured in the rivers.

When calculating the discharge of Hg_D ($Hg_{D(flux)}$) and $MeHg_T$ ($MeHg_{T(flux)}$) from the peat bog, we assumed that [Hg_D] and [$MeHg_T$] measured at the lower station represented [Hg_D] and [$MeHg_T$] in the discharge water.

Data analysis

To study covariation between variables, Pearson's product–moment correlation coefficients (r) were computed. Fisher's z test was used to determine the associated significant probability (P). The latter was corrected using a sequential Bonferroni test (Sokal and Rohlf 1995).

Results and discussion

MeHg and Hg_T in rain, in runoff from the watershed, and in the peat water

Average [Hg_D] and [$MeHg_T$] were an order of magnitude lower in the catchment runoff water than in the peat water at the discharge end of the peat bog. In wet deposition, [Hg_T] was higher and [$MeHg_T$] lower, the latter by an order of magnitude than [Hg_T] and [$MeHg_T$], respectively, in the peat water (Fig. 2). These results indicate that most of the MeHg in the discharge water was formed in the peat bog. Branfireun et al. (1996) reported similar results from a peatland study in Ontario. Furthermore, the fact that $Hg_{D(flux)}$ showed no apparent relationship with the wet deposition of Hg_T (Fig. 3) indicated that the amount of Hg_D that was available for export was controlled by partitioning of Hg between the solid phase (live moss and peat) and the water phase. We conclude that processes within the peat bog, together with water-discharge and water levels, controlled the seasonal variation of both [$MeHg_T$] and [Hg_D] in the discharge water. The underlying assumption here is that the difference in water chemistry between the upland site and the lower site was not far from the true difference in water chemistry between the water flowing into and out of the peat bog.

Methylation and release of Hg from the solid phase

The most striking finding was a strong correlation (r = 0.96, $P < 0.0001$) between [$MeHg_T$] and [Hg_D] in the peat water (Fig. 4, Table 2). A comparison of temporal variation between [$MeHg_T$] and [Hg_D] strengthens the impression that these variables were strongly related (Fig. 5*a*, 5*b*). We concluded above that [Hg_D] is a function of solid/water partitioning of Hg in the peat bog and water discharge. Consequently, we claim that the correlation between [$MeHg_T$] and [Hg_D] illustrates a strong relationship between the MeHg levels in the peat water and the release of Hg from the solid phase. Certainly, [$MeHg_T$] and [Hg_D] have the component [$MeHg_D$] in common. This is not a problem as long as the correlation is used to corroborate the hypothesis that methylation of Hg increases the probability that Hg partitions into water. To realize this one can consider the case [Hg_D] = [$MeHg_D$]. However, to test the hypothesis that methylation of Hg is controlled by release of Hg from the

Fig. 3. Temporal variation of atmospheric wet deposition of Hg_T on the peat bog (open bars) and of the flux of filterable total Hg ($Hg_{D(flux)}$) at the discharge end of the peat bog (■).

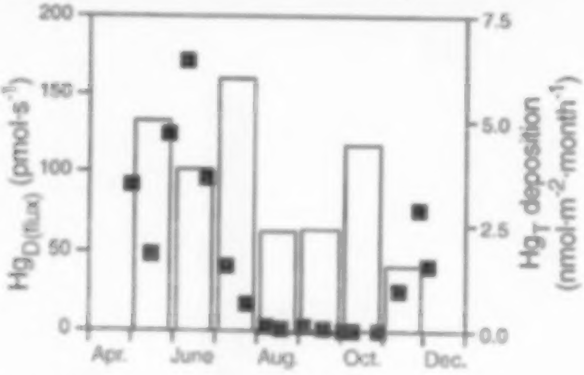

Fig. 4. The MeHg concentration in unfiltered peat water ($MeHg_T$) versus the total Hg concentration in filtered (0.45 μm) peat water (Hg_D) at the discharge end of the peat bog. Each symbol represents one sample. Correlation coefficient (r) = 0.96 ($P < 0.0001$). The significant probability (P) was determined as if $MeHg_T$ and Hg_D were independent variables. A least square fit regression line is also shown.

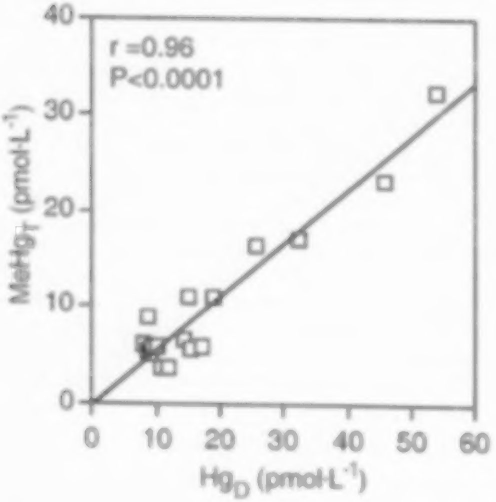

solid phase, it may be more appropriate to study [$MeHg_T$] versus [IHg_D] (e.g., Benoit et al. 2001). Indeed, this correlation was also highly significant (see below).

We did not measure the Hg levels in the solid matrix (peat and live moss). However, we believe that the particles (<0.2 mm diameter) collected by the manually inserted cylinder consisted mostly of fragments, and possibly trapped particles, of the solid matrix. Dividing [$MeHg_P$] by the concentration of suspended solids resulted in an average solid-phase MeHg concentration of 42 ng·g^{-1} dry weight (DW; range 0–98 ng·g^{-1} DW), being close to the 53 ng·g^{-1} DW that Heyes et al. (2000) found in peat from a poor fen in Ontario. A similar calculation for Hg_T suggests an average Hg_T concentration of 410 ng·g^{-1} DW (range 87–1186 ng·g^{-1} DW), being somewhat high in comparison with results from nearby peat bogs (mostly ombotrophic) in Sweden (200–300 ng·g^{-1} DW) (Bindler et al. 2003). Notably, the concentrations of suspended solids and Hg were determined in separate water samples. Also, different filters were used to determine the concentrations of dissolved/particulate Hg and suspended solids (0.45 and 1.7 μm, respectively). This could explain any deviation from the true solid-phase Hg concentration.

Table 2. Correlation matrix with the variables indicated, based on measurements in the peat water at the discharge end of the peat bog (n = 17).

	Hg_D	$MeHg_T$	Color	DOC	Sulfide
Hg_D	1.00				
$MeHg_T$	0.96****	1.00			
Color	0.43	0.51	1.00		
DOC	0.21	0.23	0.72**	1.00	
Sulfide	0.00	0.1	0.71**	0.69*	1.00

Note: Hg_D, filterable total Hg (0.45 μm); color, percent absorbance (420 nm) in water after filtration (0.45 μm); DOC, dissolved organic carbon, i.e., organic carbon after filtration (1.6 μm); $MeHg_T$, MeHg in bulk water; sulfide, sulfide in bulk water; *, $P < 0.05$; **, $P < 0.01$; ****, $P < 0.0001$ (the significance test was treated as if the variables were independent (see the text).

Small-scale spatial variation of solid-phase Hg concentration probably contributed to the rather wide ranges reported above. Considering the probable fact that the particle concentration and composition varied and were affected by sampling, one may find it surprising that the relationship between [$MeHg_T$] and [Hg_D] was so strong. However, this relationship is partly explained by the fact that the variation of [$MeHg_T$] depended almost entirely on the variation of [$MeHg_D$] and was very little affected by the variation of [$MeHg_P$] ([$MeHg_P$] = [$MeHg_T$] – [$MeHg_D$]) (Fig. 6*b*). In contrast, the variation of [IHg_T] was strongly correlated with [IHg_P] and not with [IHg_D] (Fig. 6*a*). Hence, [IHg_T] did not appear to be significantly affected by the release of IHg from the solid phase, whereas [$MeHg_T$] apparently was strongly affected by the release of MeHg from the solid phase, unless MeHg was produced in the liquid phase and stayed there. These relationships suggest that methylation either facilitated the release of Hg from the solid matrix or prevented its sorption to it. Here we assume that the degree of particle association (Fig. 6) can be used to predict the propensity of MeHg and IHg to be released from the solid matrix.

The average [$MeHg_D$]/[IHg_D] ratio of 0.44 (range 0.09–1.49) did not greatly differ from the average [$MeHg_P$]/[IHg_P] ratio of 0.28 (range 0.00–1.21). Hence, one could claim that MeHg and IHg showed similar partitioning behavior. However, this would be misleading considering the fact that a high porportion of MeHg was dissolved at high [$MeHg_T$], whereas a high proportion of IHg was particulate at high [IHg_T] (Fig. 6).

Possible causes of the simultaneous buildup of [$MeHg_T$] and [Hg_D]

MeHg production (or MeHg release) is more related to $MeHg_{T(flux)}$ than to [$MeHg_T$]. Flux and concentration differ

Fig. 5. Temporal variation of total Hg in filtered water (0.45 μm) (Hg_D) and of MeHg in bulk water ($MeHg_T$) at the discharge end of the peat bog, and the temporal variation of MeHg flux ($MeHg_{T(flux)}$) from the peat bog and in the adjacent river. Each symbol represents one sample. (*a*) $MeHg_T$ (●) and $MeHg_D$ (○). In two cases the solid and open symbols coincide. (*b*) Hg_D. (*c*) $MeHg_{T(flux)}$ (▲) and water discharge (—) from the peat bog. (*d*) $MeHg_{T(flux)}$ (▲) and water discharge (—) in the adjacent river.

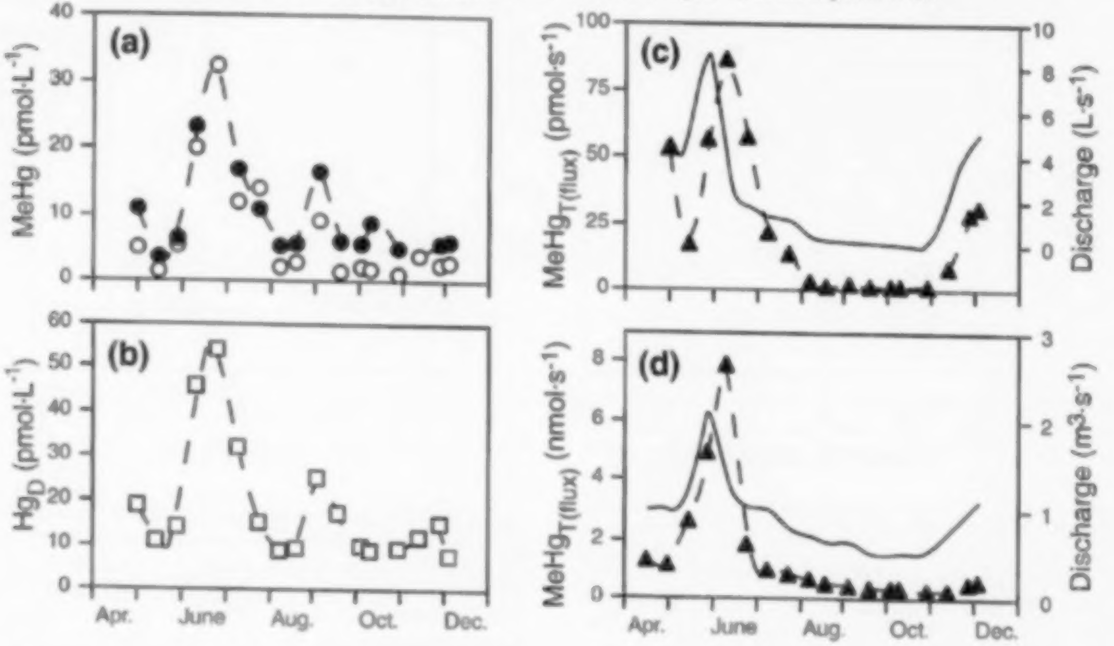

Fig. 6. Relationships between total, particulate (■), and dissolved (□) forms of Hg. Each symbol represents one sample. (*a*) Inorganic Hg (IHg). The regression line is for IHg_T versus IHg_P. (*b*) MeHg. The regression line is for $MeHg_T$ versus $MeHg_D$.

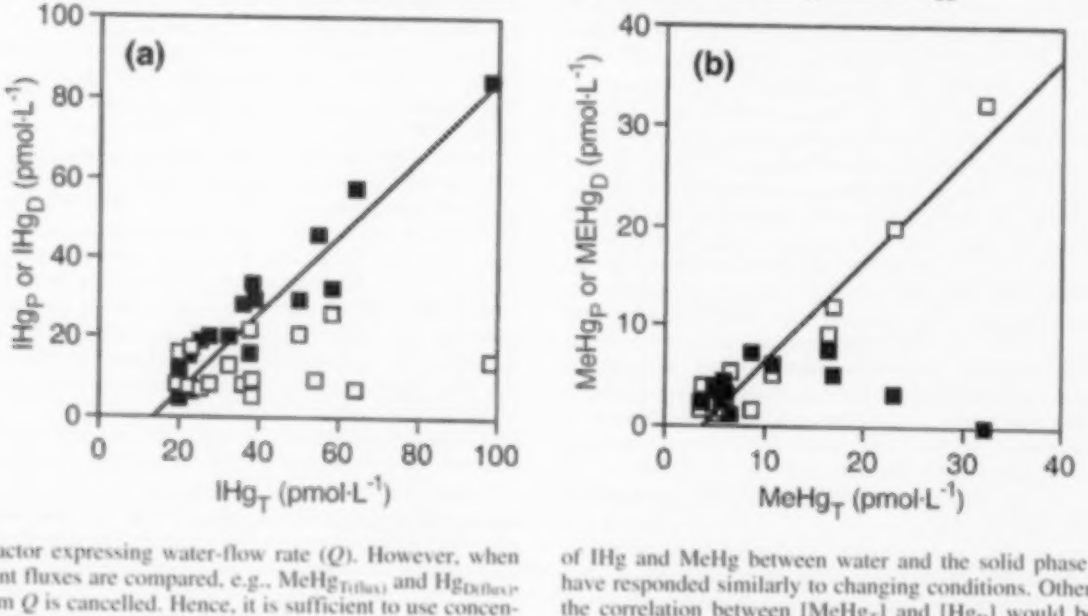

by a factor expressing water-flow rate (*Q*). However, when different fluxes are compared, e.g., $MeHg_{T(flux)}$ and $Hg_{D(flux)}$, the term *Q* is cancelled. Hence, it is sufficient to use concentration data when comparing fluxes.

One hypothesis is that the variation of $MeHg_{T(flux)}$ was due to partitioning, i.e., release from the solid phase to water, rather than to production of MeHg. If so, the partitioning of IHg and MeHg between water and the solid phase must have responded similarly to changing conditions. Otherwise, the correlation between [$MeHg_T$] and [Hg_D] would be less strong (Fig. 4). Both IHg and MeHg could be released from solid OM during decomposition of OM by microorganisms. They could also be released during sulfide production, as free sulfide competes with functional groups on solid OM in

Fig. 7. (*a*) Filterable total Hg (Hg_D) versus the color of filtered (0.45 μm) peat water at the discharge end of the peat bog and (*b*) Hg_D versus sulfide in unfiltered peat water. Each symbol represents one sample.

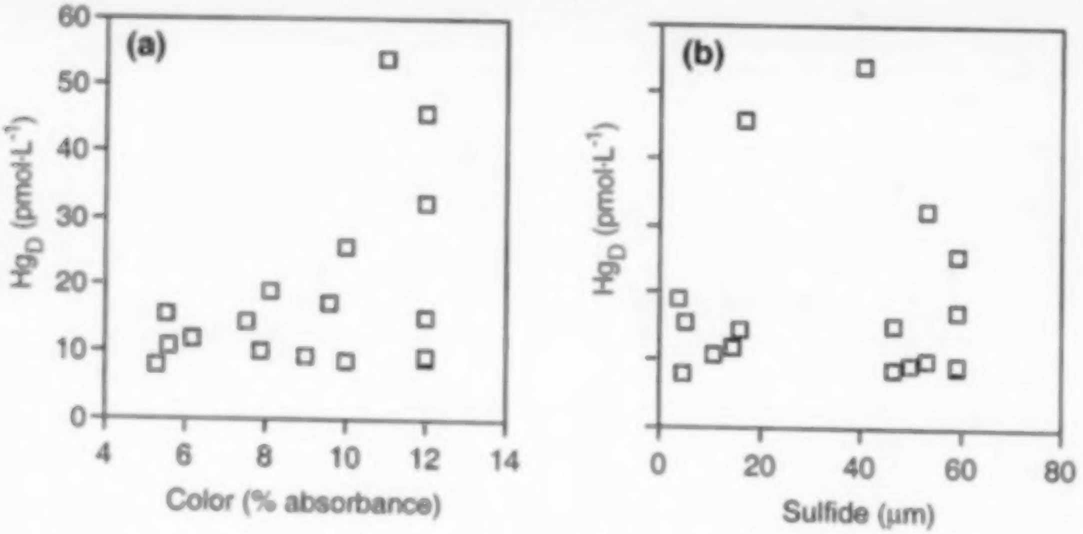

the binding of MeHg and Hg(II) (Hintelmann et al. 1997; Benoit et al. 1999; Drexel et al. 2002). Consequently, one would expect DOC and (or) sulfide to be positively correlated with [Hg_D]. However, neither DOC (color) nor sulfide showed a strong correlation with [Hg_D] (Fig. 7, Table 2). The corresponding partial correlation coefficients (holding [$MeHg_T$] constant) were also low: $r_{\text{color–HgD}} = -0.26$ and $r_{\text{sulfide–HgD}} = -0.31$. These are spurious, however, considering the fact that a significant fraction of Hg_D is $MeHg_D$. More appropriate is to study color and sulfide versus [IHg_D] when [$MeHg_T$] is held constant. These partial correlation coefficients were low, too: $r_{\text{color–HgD}} = 0.04$ and $r_{\text{sulfide–HgD}} = -0.21$.

Moreover, $MeHg_{T(flux)}$ and $Hg_{D(flux)}$ peaked later than the water discharge (Fig. 5*c*). These observations suggest that a simple washout or change in partitioning did not explain the variation of $MeHg_{T(flux)}$ and $Hg_{D(flux)}$. It cannot be ruled out, however, that MeHg and IHg might lag behind water, owing to exchange of Hg between the water and the porous sorbing media in the peat bog. Similarly, DOC and sulfide might not exhibit the same retardation as Hg. This could explain why $MeHg_T$, Hg_D, and IHg_D were poorly correlated with both sulfide and DOC. Furthermore, vertical chemical gradients within the sampled layers could obscure such relationships. Heyes et al. (2000) found that the MeHg concentration in peat pore water from a poor fen in Ontario was highest in the upper layers of the profile, well above the lowest depth (90 cm) sampled in the present study. However, one would expect sulfate reduction and DOC production to coincide with Hg methylation.

Alternatively, the variation of $MeHg_{T(flux)}$ was entirely a result of variation of Hg methylation. In view of the fact that the stability of MeHg might be lower than has previously been assumed (Hintelmann et al. 2000), it seems likely that MeHg levels in most environments are highly dependent on fresh production of MeHg. If Hg methylation takes place in the cytoplasm of dissimilatory sulfate-reducing bacteria, as is currently assumed, only dissolved Hg complexes should be available for methylation. Cells probably do not scavenge Hg directly from solids to a significant extent, given the fact that virtually all particulate Hg(II) is either bound in solid sulfides or strongly bound to OM via thiol groups (Schlüter 1996; Wallschläger et al. 1996; Hesterberg et al. 2001). Hence, the strong correlation between [$MeHg_T$] and [Hg_D] could be explained by cellular uptake of IHg_D followed by intracellular methylation of IHg. Notably, both [$MeHg_T$] and [Hg_D] showed a strong correlation with [IHg_D] ($r = 0.84$ and $r = 0.93$, respectively).

Evidently, intracellular methylation could explain the strong relationship between [$MeHg_T$] and [Hg_D], but could it also account for the [$MeHg_T$]/[IHg_D] ratio of 0.79 (range 0.37–1.49)? In natural waters, any Hg(II) that passes 0.45 μm filters is either complexed by various organic compounds, most of which are of a colloidal nature and too large to pass cell membranes (Stordal et al. 1996; Wallschläger et al. 1998), or is complexed by sulfide (Benoit et al. 1999). Also note that the ability of IHg_D to pass cell membranes would have to be greater than indicated by the [$MeHg_T$]/[IHg_D] ratios if not all of the IHg entering the cells was converted to MeHg, or if some of the MeHg produced was demethylated. It does not seem likely that all cells absorbing IHg were vigorous Hg methylators and that demethylation was negligible. St. Louis et al. (2004) concluded that demethylation had a strong effect on MeHg levels in the wetland system they studied in northwestern Ontario.

The [$MeHg_T$]/([IHg_D] + [$MeHg_T$]) ratio is a more conservative measure of the availability of Hg for methylation. It takes into account that [MeHg] might build up, while [IHg_D] is consumed. This ratio averaged 0.46 (range 0.27–0.93). It is still high enough to raise the question whether intracellular methylation of Hg released from the solid phase could explain the observed MeHg levels.

As already stated, Hg(II) is strongly bound to organic matter via reduced sulfur groups. It seems likely that virtually all Hg entering the peat bog is rapidly sorbed by live

Fig. 8. Water level (—), water temperature (- -), and the flux of MeHg ($\mathrm{MeHg}_{\mathrm{T(flux)}}$; ■). For clarity, the scale of $\mathrm{MeHg}_{\mathrm{T(flux)}}$ is omitted (it is shown in Fig. 4). (*a*) In the river. (*b*) In the peat bog. The water level shown for the peat bog was gauged at the observation well closest to the peat water sampling site. The peat surface at the observation well was at 147.79 m.

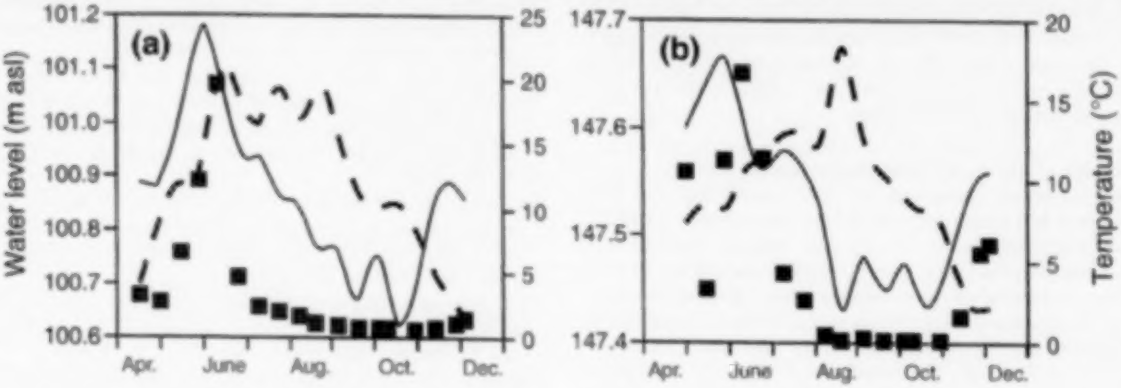

moss and peat (including attached microorganisms), and by free-living cells. An interesting possibility is that the sorbed Hg is released back to the peat water mainly as a result of a weakening of Hg–S bonds by methylation of Hg. Furthermore, Hg passes cell membranes much more rapidly when methylated (Carty and Malone 1979; Mason et al. 1996). Hence, methylation should increase cellular release of Hg. The cause–effect relationship between $[\mathrm{MeHg_T}]$ and $[\mathrm{Hg_D}]$ would then be that methylation causes release of Hg, not vice versa.

A similar possibility in line with a high $[\mathrm{MeHg}]/[\mathrm{IHg_D}]$ ratio is that any IHg released from the solid phase is immediately sorbed by microorganisms (Benoit et al. 2001) and that Hg stays bound to the microbial cells as long as no methylation occurs. In that case, methylation does not cause the initial release of Hg from the solid phase, but causes a secondary release of resorbed Hg.

Notably, methylation being the main cause of Hg release would help to explain the fact that sulfide and DOM levels were poorly correlated with $[\mathrm{Hg_D}]$ (Table 2). Also note that if Hg methylation in the cytoplasm of bacteria is the main cause of Hg release, this would imply that most of the Hg which is released from the solid phase has passed a bacterial cell membrane twice. No effort has been made so far to specifically show that Hg methylation does take place mainly in the cytoplasm of bacteria. We would therefore not rule out the possibility that Hg methylation is at least partly a surface-mediated reaction occurring on cell surfaces, from which MeHg is released as MeHgSH in the presence of free sulfide.

Demethylation inferred?

If methylation was indeed the main cause of Hg release to the water, and if $[\mathrm{Hg_D}]$ was largely explained by Hg release from the solid phase, it would follow that most of the $\mathrm{Hg_D}$ that was not present as MeHg was formed secondarily from MeHg.

MeHg can be degraded by microorganisms (Oremland et al. 1991; Pak and Bartha 1998), photodegraded (Sellers et al. 1996), and consumed in chemical reactions involving sulfide (Craig and Moreton 1984; Baldi et al. 1993; Wallschläger et al. 1995). Hg(II) resulting from demethylation of MeHg could be kept in solution or in a colloidal state by polysulfides and OM (e.g., Paquette and Helz 1997; Ravichandran et al. 1999), or simply stay in solution as HgS or $\mathrm{Hg(SH)_2}$ (Benoit et al. 1999).

However, if methylation and release of IHg occurred simultaneously, demethylation does not have to be inferred to explain the fact that the average $[\mathrm{MeHg_D}]/[\mathrm{Hg_D}]$ ratio did not exceed 0.28 (range 0.08–0.60). The production of strong complexing agents is likely to coincide with MeHg production. (Sulfate-reducing bacteria could be responsible for both Hg methylation and production of sulfide.) Strong complexing agents might also extract Hg(II) from the solid phase. As noted above, the fact that DOC and sulfide levels did not show a strong correlation with $[\mathrm{MeHg_T}]$ and $[\mathrm{Hg_D}]$ (Fig. 7, Table 2) does not exclude the possibility that release of Hg from the solid phase was at least partly a direct result of decomposition of OM and formation of Hg(II)–sulfide complexes.

The rather wide range of $[\mathrm{MeHg_D}]/[\mathrm{IHg_D}]$ ratios (0.09–1.49) is worth noting. The low values within this range seem to argue against the view that methylation had a strong influence on $[\mathrm{Hg_D}]$. However, note that the low values represent time periods of low $[\mathrm{Hg_D}]$ (Figs. 5*a*, 5*b*). Low $[\mathrm{MeHg_D}]/[\mathrm{IHg_D}]$ ratios could be the net result of low methylation rates, high demethylation rates, and a higher uptake of MeHg than of Hg(II) by cells. Low methylation rates can be expected to coincide with high specific cellular uptake of MeHg, since production of both MeHg and reduced sulfur ligands (which will compete with cells for MeHg) can be expected to decrease as a result of lowered anaerobic microbial activity.

Temporal variation of MeHg in the peat water and in the river

The temporal variation of $\mathrm{MeHg}_{\mathrm{T(flux)}}$ in the peat bog was strikingly similar to that in the river passing through the adjacent lake (Figs. 5*c*, 5*d*). Any of the five river stations, some of which were situated upstream of the study peat bog, could have been chosen to show this (data are shown for one station only). Hence, Hg methylation and (or) release of MeHg to the water appeared to be controlled by the same processes along the river as in the study peat bog. Notably, in both the river and the peat bog, the maximum water discharge preceded the maximum $\mathrm{MeHg}_{\mathrm{T(flux)}}$. We believe that a high water table in combination with a rise in temperature favored anaerobic microbial activity that, in turn, caused both increased Hg methylation and increased release of MeHg from the solid phase (Fig. 8). Possibly, $\mathrm{MeHg}_{\mathrm{T(flux)}}$ lagged behind the water discharge because it takes some time for anaerobic conditions to develop.

Dynamics of Hg in minerotrophic peat bogs

Large amounts of live and dead OM should lead to a high retention of Hg in wetlands. However, the retention of Hg in wetlands is often lower than in drier upland soils. Hence, there must be processes in wetlands that cause removal of Hg from solid OM. Such processes could be mineralization of OM, extraction of Hg(II) bound to OM by reduced sulfur compounds, and Hg methylation. In the peat bog we studied, it was clear that MeHg was more mobile than Hg(II). This is possibly explained by the fact that Hg(II) has a higher affinity than MeHg for reduced sulfur groups on OM, and hence is more difficult to remove from such binding sites. We found evidence that methylation, rather than sulfide complexation of Hg(II) and OM mineralization, was controlling the release of Hg. Firstly, $[\mathrm{MeHg}_\mathrm{T}]$ was strongly correlated with $[\mathrm{Hg}_\mathrm{D}]$, whereas sulfide and DOC levels were not. Secondly, MeHg_D comprised a large part of Hg_D, especially when $[\mathrm{Hg}_\mathrm{D}]$ was high (Figs. 5*a*, 5*b*).

We believe that the dynamics of Hg in the studied peat bog were characterized by rapid sorption of Hg entering the peat bog with upland runoff water and precipitation, followed by release of Hg to the water, mainly as a result of methylation of Hg(II) in combination with a high concentration of strong complexing agent in the water. Yet we cannot exclude the possibility that significant quantities of Hg were also released as IHg.

Acknowledgements

The study was supported by the Swedish Environmental Protection Agency. A. Helgée and B. Troedsson helped in the planning and execution of the fieldwork. Dr. P. Elander was in charge of the hydrological investigation. The mercury analyses were carried out at the Swedish Environmental Research Institute, Gothenburg. Mr. K.F.K. Larsson provided linguistic advice. Dr. P. Larsson, Dr. Wen-Qi Wu, Dr. O. Wendt, Dr. B. Wallén, Dr. O. Berglund, and Dr. B. Ekberg provided useful comments.

References

Baldi, F., Pepi, M., and Filipelli, M. 1993. Methylmercury resistance in *Desulfovibrio desulfuricans* strains in relation to methylmercury degradation. Appl. Environ. Microbiol. **59**: 2479–2485.

Benoit, J.M., Gilmour, C.C., Mason, R.P., and Heyes, A. 1999. Sulfide controls on mercury speciation and bioavailability to methylating bacteria in sediment porewaters. Environ. Sci. Technol. **33**: 951–957.

Benoit, J.M., Gilmour, C.C., and Mason, R.P. 2001. The influence of sulfide on solid-phase mercury bioavailability for methylation by pure cultures of *Desulfobulbus propionicus* (1pr3). Environ. Sci. Technol. **35**: 127–132.

Bindler, R. 2003. Estimating the natural background atmospheric deposition rate of mercury utilizing ombrotrophic bogs in southern Sweden. Environ. Sci. Technol. **37**: 40–46.

Branfireun, B.A., Heyes, A., and Roulet, N.T. 1996. The hydrology and methylmercury dynamics of a Precambrian shield headwater peatland. Water Resour. Res. **32**: 1785–1794.

Branfireun, B.A., Roulet, N.T., Kelly C.A., and Rudd, J.W.M. 1999. In situ sulphate stimulation of mercury methylation in a boreal peatland: toward a link between acid rain and methylmercury contamination in remote environments. Global Biogeochem. Cycles, **13**: 743–750.

Carty, A.J., and Malone, S.F. 1979. The chemistry of mercury in biological systems. *In* The biogeochemistry of mercury in the environment. *Edited by* J.O. Nriagu. Elsevier/North-Holland Biomedical Press, New York. pp. 433–479.

Choi, B.H. 1991. Effects of methylmercury on the developing brain. *In* Advances in mercury toxicology. *Edited by* T. Suzuki, N. Imura, and T. Clarkson. Plenum Press, New York. pp. 315–333.

Clarkson, T.W. 1990. Human health risks from methylmercury in fish. Environ. Toxicol. Chem. **9**: 957–961.

Compeau, G.C., and Bartha, R. 1984. Methylation and demethylation of mercury under controlled redox, pH, and salinity conditions. Appl. Environ. Microbiol. **48**: 1203–1207.

Compeau, G.C., and Bartha, R. 1985. Sulfate-reducing bacteria: principal methylators of mercury in anoxic estuarine sediment. Appl. Environ. Microbiol. **50**: 498–502.

Craig, P.J. 1986. Occurrence and pathways of organometallic compounds in the environment — general considerations. *In* Organometallic compounds in the environment: principles and reactions. *Edited by* P.J. Craig. Longman Group Ltd., Harlow, England. pp. 1–64.

Craig, P.J., and Moreton, P.A. 1984. The role of sulphide in the formation of dimethyl mercury in river and estuary sediments. Mar. Pollut. Bull. **15**: 406–408.

Drexel, R.T., Haitzer, M., Ryan, J.N., Aiken, G.R., and Nagy, K.L. 2002. Mercury (II) sorption to two Florida Everglades peats: evidence for strong and weak binding and competition by dissolved organic matter released from peat. Environ. Sci. Technol. **36**: 4058–4064.

Driscoll, C.T., Schofield, C.L., Munson, R., and Holsapple, J. 1994. The mercury cycle and fish in the Adirondack lakes. Environ. Sci. Technol. **28**: 136A–143A.

Fonselius, S.H. 1983. Determination of hydrogen sulfide. *In* Methods of sea water analysis. *Edited by* K. Grasshoff, M. Erhardt, and K. Kremling. Verlag Chemie, Weinheim, Germany, and Deerfield Beach, Fla. pp. 73–80.

Gilmour, C.C., Henry, E.A., and Mitchell, R. 1992. Sulfate stimulation of mercury methylation in freshwater sediment. Environ. Sci. Technol. **26**: 2281–2287.

Hesterberg, D., Chou, J.F., Hutchison, K.J., and Sayers, D.E. 2001. Bonding of Hg(II) to reduced organic sulfur in humic acid as affected by S/Hg ratio. Environ. Sci. Technol. **35**: 2741–2745.

Heyes, A, Moore, T.R., Rudd, J.W.M, and Dugoua, J.J. 2000. Methyl mercury in pristine and impounded peatlands, Experimental Lakes Area, Ontario. Can. J. Fish. Aquat. Sci. **57**: 2211–2222.

Hintelmann, H., Welbourn, P.M., and Evans, R.D. 1997. Measurement of complexation of methylmercury(II) compounds by freshwater humic substances using equilibrium dialysis. Environ. Sci. Technol. **31**: 489–495.

Hintelmann, H., Keppel-Jones, K., and Evans, R.D. 2000. Constants of mercury methylation and demethylation rates in sediments and comparison of tracer and ambient mercury availability. Environ. Toxicol. Chem. **19**: 2204–2211.

Hurley, J.P., Benoit, J.M., Babiarz, C.L., Shafer, M.M., Andren, A.W., Sullivan, J.R. et al. 1995. Influences of watershed characteristics on mercury levels in Wisconsin rivers. Environ. Sci. Technol. **29**: 1867–1875.

Iverfeldt, Å. 1991. Occurrence and turnover of atmospheric mercury over the Nordic countries. Water Air Soil Pollut. **56**: 251–265.

Jackson, T.A. 1998. Mercury in aquatic ecosystems. *In* Metal metabolism in aquatic environments. *Edited by* W.J. Langston and M.J. Bebianno. Chapman & Hall, London. pp. 77–138.

Johansson, K., Bergbäck, B., and Tyler, G. 2001. Impact of atmospheric long-range transport of lead, mercury and cadmium on the Swedish forest environment. Water Air Soil Pollut. Focus, **1**: 279–297.

Mason, R.P., Reinfelder, J.R., and Morel, F.M.M. 1996. Uptake, toxicity, and trophic transfer of mercury in a coastal diatom. Environ. Sci. Technol. **30**: 1835–1845.

Mierle, G. 1990. Aqueous inputs of mercury to Precambrian Shield lakes in Ontario. Environ. Toxicol. Chem. **9**: 843–851.

Mierle, G. and Ingram, R. 1991. The role of humic substances in the mobilization of mercury from watersheds. Water Air Soil Pollut. **56**: 349–357.

Oremland, R.S., Culberstson, C.W., and Winfrey, M.R. 1991. Methylmercury decomposition in sediments and bacterial cultures: involvement of methanogens and sulfate reducers in oxidative demethylation. Appl. Environ. Microbiol. **57**: 130–137.

Pak, K.-R., and Bartha, R. 1998. Mercury methylation and demethylation in anoxic lake sediments by strictly anaerobic bacteria. Appl. Environ. Microbiol. **64**: 1013–1017.

Paquette, K.E., and Helz, G.R. 1997. Inorganic speciation of mercury in sulfidic waters: the importance of zero-valent sulfur. Environ. Sci. Technol. **31**: 2148–2153.

Quemarais, B., Cossa, D., Rondeau, B., Pham, T.T., Gagnon, P., and Fortin, B. 1999. Sources and fluxes of mercury in the St. Lawrence River. Environ. Sci. Technol. **33**: 840–849.

Ravichandran, M., Aiken, G.A., Ryan, N.Y., and Reddy, M.M. 1999. Inhibition of precipitation and aggregation of metacinnabar (mercuric sulfide) by dissolved organic matter isolated from the Florida Everglades. Environ. Sci. Technol. **33**: 1418–1423.

Regnell, O., and Tunlid, A. 1991. Laboratory study of chemical speciation of mercury in lake sediment and water under aerobic and anaerobic conditions. Appl. Environ. Microbiol. **57**: 789–795.

Regnell, O., Ewald, G., and Lord, E. 1997. Factors controlling temporal variation in methyl mercury levels in a seasonally stratified lake. Limnol. Oceanogr. **42**: 1784–1795.

Regnell, O., Hammar, T., Helgée, A., and Troedsson, B. 2001. Effects of anoxia and sulfide on concentrations of total and methyl mercury in sediment and water in two Hg-polluted lakes. Can. J. Fish. Aquat. Sci. **58**: 506–517.

Schlüter, K. 1996. Translocation of ^{203}Hg labelled HgCl$_2$ and CH$_3$HgCl in an iron–humus podzol studied by radio-analytical techniques. Z. Pflanzenernaehr. Bodenkd. **159**: 215–226.

Sellers, P., Kelly, C.A., Rudd, J.W.M., and MacHutchon, A.R. 1996. Photodegradation of methylmercury in lakes. Nature (Lond.), **380**: 694–697.

Sokal, R.R., and Rohlf, F.J. 1995. Biometry. 3rd ed. W.H. Freeman and Co., New York.

Sorensen, J.A., Glass, G.E., Schmidt, K.W., Huber, J.K., and Rapp, G.R., Jr. 1990. Airborne mercury deposition and watershed characteristics in relation to mercury coencentrations in water, sediments, plankton, and fish of eighty northern Minnesota lakes. Environ. Sci. Technol. **24**: 1716–1727.

St. Louis, V.L., Rudd, J.W.M., Kelly, C.A., Beaty, K.G., Bloom, N.S., and Flett, R.J. 1994. Importance of wetlands as sources of methyl mercury to boreal forest ecosystems. Can. J. Fish. Aquat. Sci. **51**: 1065–1076.

St. Louis, V.L., Rudd, J.W.M., Kelly, C.A., Bodaly, R.A. (Drew), Paterson, M.J., Beaty, K.G., Hesslein, R.H., Heyes, A., and Majewski, A.R. 2004. The rise and fall of mercury methylation in an experimental reservoir. Environ. Sci. Technol. **38**: 1348–1358.

Stordal, M.C., Gill, G.A., Wen, L.-S., and Santschi, P.H. 1996. Mercury speciation in the surface waters of three Texas estuaries: importance of colloidal forms. Limnol. Oceanogr. **41**: 52–61.

Surma-Aho, K., Paasivirta, J., Rekolainen, S., and Verta, M. 1986. Organic and inorganic mercury in the food chain of some lakes and reservoirs in Finland. Chemosphere, **15**: 353–372.

Swain, E.B., Engstrom, D.R., Brigham, M.E., Henning, T.A., and Brezonik, P.L. 1992. Increasing rates of atmospheric deposition in midcontinental North America. Science (Wash., D.C.), **257**: 784–787.

Waldron, M.C., Colman, J.A., and Breault, R.F. 2000. Distribution, hydrologic ransport, and cycling of total mercury and methyl mercury in a contaminated river–reservoir–wetland system (Sudbury River, eastern Massachusetts). Can. J. Fish. Aquat. Sci. **57**: 1080–1091.

Wallschläger, D., Hintlmann H., Evans, R.D., and Wilken., R.-D. 1995. Volatilization of dimethylmercury and elemental mercury from River Elbe floodplain soils. Water Air Soil Pollut. **80**: 1325–1329.

Wallschläger, D., Desai, M.V.M., Spengler, M., and Wilken, R.-D. 1996. The role of humic substances in the aqueous mobilization of mercury from contaminated floodplain soils. Water Air Soil Pollut. **90**: 507–520.

Wallschläger, D., Desai, M.V.M., Spengler, M., Windmöller, C.C., and Wilken, R.-D. 1998. How humic substances dominate mercury geochemistry in contaminated floodplain soils and sediments. J. Environ. Qual. **27**: 1044–1054.

Fisheries and Aquatic Sciences
Sciences halieutiques et aquatiques

Photographic Atlas of Fish Otoliths of the Northwest Atlantic Ocean

By / Par Stephen E. Campana

$54.95 CAN. Other countries $54.95 US
54,95 $CAN. À l'étranger 54,95 $US
Softcover / Édition brochée
(*Can. Spec. Publ. Fish. Aquat. Sci. / Publ. spéc. can. sci. halieut. aquat. 133*)
284 pages ISBN 0-660-19108-3 ISSN 0706-6481 NRC / CNRC 46328

Salmonine Introductions to the Laurentian Great Lakes:
An Historical Review and Evaluation of Ecological Effects

By / Par Stephen S. Crawford

$42.95 CAN. Other countries $42.95 US
42,95 $CAN. À l'étranger 42,95 $US
Softcover / Édition brochée
(*Can. Spec. Publ. Fish. Aquat. Sci. / Publ. spéc. can. sci. halieut. aquat. 132*)
215 pages ISBN 0-660-17639-4 ISSN 0706-6481 NRC / CNRC 42734

Marine Protected Areas and Fisheries Closures in British Columbia

By Glen S. Jamieson and Joanne Lessard

$69.95 CAN. Other countries $69.95 US
69,95 $CAN. À l'étranger 69,95 $US
Softcover / Édition brochée
(*Can. Spec. Publ. Fish. Aquat. Sci. / Publ. spéc. can. sci. halieut. aquat. 131)*
414 pages ISBN 0-660-17788-9 ISSN 0706-6481 NRC / CNRC 42846

Workshop on Rebuilding Abalone Stocks in British Columbia

By / Par Alan Campbell

$42.95 CAN. Other countries $42.95 US
42,95 $CAN. À l'étranger 42,95 $US
Softcover / Édition brochée
(*Can. Spec. Publ. Fish. Aquat. Sci. / Publ. spéc. can. sci. halieut. aquat. 130*)
158 pages ISBN 0-660-18292-0 ISSN 0706-6481 NRC / CNRC 42841

To order any of the above titles / Commandez n'importe quel titre ci-dessus à :

Telephone / Téléphone : (613) 990-2254
Fax / Télécopieur : (613) 952-7656
E-mail / Courriel : pubs@nrc-cnrc.gc.ca
Web site / Site web : http://pubs.nrc-cnrc.gc.ca

Order Office / Bureau des commandes
NRC Research Press / Presses scientifique du CNRC
National Research Council / Conseil national de recherches
Ottawa, ON K1A 0R6, Canada

Canadian customers add GST (7%). Prepayment required unless order is accompanied by a purchase order number. Cheques or money orders should be made payable to : "Receiver General for Canada, Credit NRC". For all orders outside Canada, rates are in U.S. Dollars. All sales are final.

Clients du Canada, ajoutez la TPS (7 %). Les commandes doivent être payées d'avance à moins qu'elles ne soient accompagnées d'un numéro de bon de commande. Les chèques ou mandats doivent être libellés au « Receveur général du Canada, crédit du CNRC ». Pour les commandes hors-Canada, les tarifs sont en dollars américains. Toutes les ventes sont finales.

Contents (concluded) / Table des matières (suite et fin)

Nicole B. Richoux, Don Deibel, Raymond J. Thompson, and Christopher C. Parrish 1940–1953 Seasonal changes in the lipids of *Mysis mixta* (Mysidacea) from the hyperbenthos of a cold-ocean environment (Conception Bay, Newfoundland)

Karen M. Buzby and Linda A. Deegan 1954–1964 Long-term survival of adult Arctic grayling (*Thymallus arcticus*) in the Kuparuk River, Alaska

Thomas A. Clair, Ian F. Dennis, Peter G. Amiro, and B.J. Cosby 1965–1975 Past and future chemistry changes in acidified Nova Scotian Atlantic salmon (*Salmo salar*) rivers: a dynamic modeling approach

Michael J.W. Stokesbury, Steven L.H. Teo, Andrew Seitz, Ronald K. O'Dor, and Barbara A. Block 1976–1987 Movement of Atlantic bluefin tuna (*Thunnus thynnus*) as determined by satellite tagging experiments initiated off New England

David B. Ryves, Annemarie L. Clarke, Peter G. Appleby, Susanne L. Amsinck, Erik Jeppesen, Frank Landkildehus, and N. John Anderson 1988–2006 Reconstructing the salinity and environment of the Limfjord and Vejlerne Nature Reserve, Denmark, using a diatom model for brackish lakes and fjords

Bernd Spänhoff and Mark O. Gessner 2007–2013 Slow initial decomposition and fungal colonization of pine branches in a nutrient-rich lowland stream

O. Regnell and T. Hammar 2014–2023 Coupling of methyl and total mercury in a minerotrophic peat bog in southeastern Sweden

NRC Research Press 75th Anniversary

Since the publication of the first issue of the *Canadian Journal of Research* in 1929, the National Research Council has provided scientists and engineers in Canada and elsewhere with a means to communicate with their peers in the international research community through the production of high-quality journals. NRC Research Press is proud to celebrate 75 years of science and technology publishing in Canada.

Le 75^e anniversaire des Presses scientifiques du CNRC

Depuis la parution du premier numéro du *Canadian Journal of Research* en 1929, le Conseil national de recherches du Canada publient des revues savantes de qualité grâce auxquelles les chercheurs et ingénieurs du Canada et d'ailleurs peuvent partager les résultats de leurs recherches avec leurs pairs de la collectivité scientifique internationale. Les Presses scientifiques du CNRC sont fières de célébrer 75 ans d'édition scientifique et technique au Canada.

National Research Council Canada
Ottawa, Canada
K1A 0R6

Conseil national de recherches Canada
Ottawa, Canada
K1A 0R6

Postage paid at Ottawa
Publications mail
Registration No. 40062591

Port payé à Ottawa
Poste-publication
Enregistrement n° 40062591

USPS periodical postage paid at Champlain, NY 12919, USA

Canadian Journal of Fisheries and Aquatic Sciences

Journal canadien des sciences halieutiques et aquatiques

Volume 61, Number 10, October 2004

Volume 61, numéro 10, octobre 2004

ARTICLES		ARTICLES
Michael G. Newbrey and Allan C. Ashworth	**1807–1816**	A fossil record of colonization and response of lacustrine fish populations to climate change
Florian Mermillod-Blondin, Magali Gérino, Sabine Sauvage, and Michel Creuzé des Châtelliers	**1817–1831**	Influence of nontrophic interactions between benthic invertebrates on river sediment processes: a microcosm study
Hazel A. Wright, Robert J. Wootton, and Iain Barber	**1832–1838**	Interpopulation variation in early growth of threespine sticklebacks (*Gasterosteus aculeatus*) under laboratory conditions
Stéphane Gauthier and John K. Horne	**1839–1850**	Acoustic characteristics of forage fish species in the Gulf of Alaska and Bering Sea based on Kirchhoff-approximation models
Steven Y. Litvin and Michael P. Weinstein	**1851–1861**	Multivariate analysis of stable-isotope ratios to infer movements and utilization of estuarine organic matter by juvenile weakfish (*Cynoscion regalis*)
Jukka Horppila, Anne Liljendahl-Nurminen, and Tommi Malinen	**1862–1870**	Effects of clay turbidity and light on the predator–prey interaction between smelts and chaoborids
John T. Lehman, Ali Bazzi, Todd Nosher, and Jerome O. Nriagu	**1871–1880**	Copper inhibition of phytoplankton in Saginaw Bay, Lake Huron
William G. Clark	**1881–1889**	Nonparametric estimates of age misclassification from paired readings
John P. Wares, Dominique Alò, and Thomas F. Turner	**1890–1899**	A genetic perspective on management and recovery of federally endangered trout (*Oncorhynchus gilae*) in the American Southwest
C. Tara Marshall, Coby L. Needle, Nathalia A. Yaragina, Adnan M. Ajiad, and Evgeny Gusev	**1900–1917**	Deriving condition indices from standard fisheries databases and evaluating their sensitivity to variation in stored energy reserves
Lisa Borges, Alain F. Zuur, Emer Rogan, and Rick Officer	**1918–1928**	Optimum sampling levels in discard sampling programs
Javier Lobón-Cerviá	**1929–1939**	Discharge-dependent covariation patterns in the population dynamics of brown trout (*Salmo trutta*) within a Cantabrian river drainage

Continued on inside back cover / Suite au verso

Printed in Canada by / Imprimé au Canada par
NRC Reprographic Services / Service de reprographie CNRC
Page production by / Mise en page par
NRC Research Press / Presses scientifiques du CNRC

0706-652X(200410)61:10;1-1